Université de Montréal

Étude fonctionnelle d'un nouveau complexe multi-enzymatique régulant l'épigénome

par
Salima Daou

Département de Biochimie et de Médecine Moléculaire
Faculté de Médecine

Thèse présentée à la Faculté de médecine
en vue de l'obtention du grade de Philosophiae Doctor (Ph.D)
en Biochimie

04 Septembre 2015

© Salima Daou, 2015

Université de Montréal
Faculté des études supérieures et postdoctorales

Cette thèse intitulée:

Étude fonctionnelle d'un nouveau complexe multi-enzymatique régulant l'épigénome

Présentée par:
Salima Daou

a été évaluée par un jury composé des personnes suivantes :

Benoit Coulombe, président-rapporteur
El Bachir Affar, directeur de recherche
Gerardo Ferbeyre, membre du jury
Luc Gaudreau, examinateur externe
Éric Milot, représentant du doyen de la FES

RÉSUMÉ

L'ubiquitination, une modification post-traductionnelle importante pour le contrôle de nombreux processus cellulaires, est une réaction réversible. La réaction inverse, nommée déubiquitination est catalysée par les déubiquitinases (DUB). Nous nous sommes intéressés dans nos travaux à étudier l'ubiquitination de l'histone H2A (H2Aub), au niveau des résidus lysines 118 et 119 (K118/K119), une marque épigénétique impliquée dans la régulation de la prolifération cellulaire et la réparation de l'ADN. Le régulateur transcriptionnel BAP1, une déubiquitinase nucléaire, a été initialement identifié pour sa capacité à promouvoir la fonction suppressive de tumeurs de BRCA1. BAP1 forme un complexe multi-protéique avec plusieurs facteurs transcriptionnels et sa fonction principale est la déubiquitination de H2Aub. Plusieurs études ont démontré que BAP1 est un gène suppresseur de tumeurs majeur et qu'il est largement muté et inactivé dans une multitude de cancers. En effet, BAP1 émerge comme étant la DUB la plus mutée au niveau des cancers. Cependant, le ou les mécanismes d'action et de régulation du complexe BAP1 restent très peu connus. Dans cette étude nous nous sommes intéressés à la caractérisation moléculaire et fonctionnelle des partenaires protéiques de BAP1.

De manière significative nous avons caractérisé un mécanisme unique de régulation entre deux composants majeurs du complexe BAP1 à savoir, HCF-1 et OGT. En effet, nous avons démontré que HCF-1 est requis pour maintenir le niveau protéique de OGT et que cette dernière est indispensable pour la maturation protéolytique de HCF-1 en promouvant son clivage par O-GlcNAcylation, une signalisation cellulaire nécessaire au bon fonctionnement de HCF-1.

Également, nous avons découvert un nouveau mécanisme de régulation de BAP1 par l'ubiquitine ligase atypique UBE2O. En effet, UBE2O agit comme un régulateur négatif de BAP1 puisque l'ubiquitination de ce dernier induit sa séquestration dans le cytoplasme et l'inhibition de sa fonction suppressive de tumeurs.

D'autre part nous nous sommes penchés sur la caractérisation de l'association de BAP1 avec deux facteurs de la famille des protéines Polycombes nommés ASXL1 et ASXL2 (ASXL1/2). Nous avons investigué le rôle de BAP1/ASXL1/2, particulièrement dans les mécanismes de déubiquitination et suppression de tumeurs. Nous avons démontré que BAP1

interagit directement via son domaine C-terminale avec le même domaine ASXM de ASXL1/2 formant ainsi deux complexes mutuellement exclusifs indispensables pour induire l'activité déubiquitinase de BAP1. De manière significative, ASXM s'associe avec BAP1 pour créer un nouveau domaine composite de liaison à l'ubiquitine. Ces interactions BAP1/ASXL1/2 régulent la progression harmonieuse du cycle cellulaire. De plus, la surexpression de BAP1 et de ASXL2 au niveau des fibroblastes induit la sénescence de manière dépendante de leurs interactions. D'autre part, nous avons identifié des mutations de cancers au niveau de BAP1 le rendant incapable de lier ASXL1/2, d'exercer sa fonction d'autodéubiquitination et de ce fait d'agir comme suppresseur de tumeurs. Ainsi nous avons révélé un lien étroit entre le gène suppresseur de tumeurs BAP1, son activité déubiquitinase et le contrôle de la prolifération cellulaire.

Mots clés : Chromatine, modifications post-traductionnelles des histones, histone H2A K118/K119 monoubiquitination, protéines Polycombes, complexe PR-DUB, ubiquitination, déubiquitination, BAP1, HCF-1, OGT, O-GlcNAcylation, clivage protéolytique, ASXL1, ASXL2, prolifération cellulaire.

ABSTRACT

The reverse reaction of ubiquitination, a crucial post-translational modification, is catalyzed by deubiquitinases (DUBs). BAP1 is an ubiquitously expressed nuclear DUB that recently emerged as an important tumor suppressor highly mutated and inactivated in an increasing number of cancers of diverse origins. Both somatic and germline mutations with loss of heterozygosity were observed in tumors, making BAP1 the most mutated DUB in human malignancies. We previously reported that BAP1 is a component of a large multi-protein complex that includes several transcription regulators. The Drosophila homologue of BAP1, Calypso, forms the Polycomb-repressive DUB (PR-DUB) complex with Additional Sex Comb, ASX. This complex catalyzes the deubiquitination of histone H2A, an essential chromatin modification that regulates gene expression. Despite the ever increasing number of findings describing the occurrence of BAP1 mutations in cancers, few studies investigated the mechanisms of action of this DUB as a tumor suppressor. Therefore, the biological function and the mechanism of action and regulation of BAP1 remains largely uncharacterized.

In the work described in this thesis, we investigated the roles of BAP1 partners in modulating its catalytic activity and tumor suppressor function.

More specifically we discovered a unique mechanism of regulation between two major components of BAP1 complexes, namely HCF-1 and OGT. Indeed, HCF-1 is important for the maintenance of the cellular levels of OGT. OGT, in turn, is required for the proper proteolytic maturation of HCF-1 by promoting its O-GlcNAcylation. This signaling event is required for HCF-1 function as a cell cycle regulator.

On the other hand, we deciphered an intricate mechanism of regulation of BAP1 by the atypical E2/E3 ligase, UBE2O. UBE2O, promote the multi-monoubiquitination of BAP1 on its NLS mediating its cytoplasmic sequestration and thus inhibition of its tumor suppressor function.

Another aspect of modulation of BAP1 H2Aub catalysis is provided by the association of BAP1 with ASXL1 and ASXL2 (ASXL1/ASXL2), two orthologs of ASX. We investigated the role of BAP1/ASXL1/2, particularly in the mechanisms of deubiquitination and tumor

suppression. We have demonstrated that BAP1 interacts directly via its C-terminal domain with the ASXM domain of ASXL1/2, thus forming two mutually exclusive complexes. Significantly, ASXM promote, through assembly with BAP1, the generation of a composite ubiquitin binding domain (CUBI), indispensable for inducing the deubiquitinase activity of BAP1 towards H2Aub. The interactions between BAP1 and ASXL1/2 regulate cell cycle progression. In addition, overexpression of BAP1 or ASXL2 in fibroblasts induces senescence in CTD- and ASXM-dependent manner. We also identified cancer-derived mutation of BAP1 that selectively abolish its interaction with ASXL1 and ASXL2 as well as its H2A deubiquitinase activity. Significantly, this mutant suppressed senescence induced by BAP1 overexpression. Thus we provided a link between the tumor suppressor BAP1, its deubiquitinase activity and the control of cell proliferation.

Key words : Chromatin, histones post-translational modifications, histone H2A K118/K119 monoubiquitination, Polycomb proteins, PR-DUB complex, ubiquitination, deubiquitination, BAP1, HCF-1, OGT, O-GlcNAcylation, proteolytic cleavage, ASXL1, ASXL2, cell proliferation.

TABLE DES MATIÈRES

LISTE DES FIGURES

LISTE DES ABRÉVIATIONS

5hmC:	5-hydroxy-methyl-cytosine
5mC:	5-methyl-cytosine
ADN :	Acide désoxyribonucléique
AR:	Récepteur de l'androgène "Androgen Receptor"
ARN	Acide Ribonucléique
ASX:	Additional Sex Comb
ASXL1/2:	Additional Sex Comb-like 1 and 2
ATP	Adénosine-5′-Triphosphate
BAP1:	BRCA1-Associated Protein 1
BMI1:	B lymphoma Mo-MLV insertion region 1
BRCA1:	Breast cancer-associated 1
CBX :	Protéines à domaine chromo "Chromobox Proteins"
CRPC :	Cellules cancéreuses résistantes aux anti-androgènes
CTD :	Domaine C-terminale, "C-Terminal domain "
dRAF:	Drosophila Ring-associated factors
DSB:	Cassure d'ADN double brins, "DNA double strand break"
dSET1 :	Drosophyl Set
DUB :	Déubiquitinase, "Deubiquitinase"
E1:	Enzyme activatrice de l'Ubiquitine
E2 :	Enzyme conjuguatrice de l'Ubiquitine
E3 :	Ubiquitine Ligase
ES cells:	Cellules Souches Embryonnaires "Embryonic Stem Cells"

ESC or EDD: Extra Sex Combs

EZH1/2: Enhancer of Zeste

FHL2: Four and a Half LIM domain protein 2

FOX : Forkhead transcription factors

FOXK1/2: Forkhead box K1 and K2

H2Aub: Monoubiquitination de H2A sur les lysines K118/K119, “H2A K118/K119

HAT: Histone acétyltransférase

HBM : Domaine de liaison à HCF-1, “HCF-1 Binding Motif”

HCF-1 NC: Non or uncleavable HCF-1

HCF-1: Host-Cell Factor 1

HCF-1C: HCF-1 C-Terminale

HCF-1N: HCF-1 N-Terminale

HDAC: Histone déacéthylases

HECT: Homologous to the E6AP Carboxyl Terminus

HMT: Histones Méthyltransférase

HSV-1: Herpes simplex virus-1

IE: Gènes immédiats précoces “Immediate early genes”

IRIF: Ionizing Radiation Induced Foci

JAMM : JAB1/MPN+/MOV34

JARID: Jumonji- and AT-rich interaction domain

MBLR : Mel18 and Bmi1-like RING finger protein

MCIP: Monocyte Chemotactic Protein-induced Protein

MJD: Machado-josephin domain proteases

MLL: Mixed Lineage Leukemia Protein

MPM: Malignant Pleural Mesothelioma

NLS: Signal de localization nucleaire “Nuclear Localisation Signal”

NSPC: Nervous system Pc1

OBM: Domaine de liaison à OGT “OGT Binding Motif”

OGA: O-GlcNAcase

O-GlcNAc: O-Linked β-N-Acétylglucosamine

OGT: O-linked-N-Acétylglucosamine transférase

OTU: Ovarian tumor domain proteases

Pc: Polycomb

PcG: Protéine polycombe “Polycomb group proteins”

PCGF: Polycomb group ring finger

PCL: Polycomb like

Ph: Polyhomeotic

PHD: C-terminal Plant Homeo Domain finger

Pho-RC: Pho repressive complex

PIP: Phosphatidylinositol (3,4,5)-trisphosphate

PPD: Domaine de clivage protéolytique “Proteolytic processing domain”

PPO: PIP-binding domain of OGT

PRC1/2 : Complexe Polycombe répressif 1/2

PR-DUB : Polycomb repressive deubiquitinase complex

PSC: Posterior Sex Combs

PTMS: Modifications post-traductionnelles “Post Translational Modifications”

Ring: Really Interesting New Gene

SAGA: Spt-Ada-Gcn5-acetyltransferase

SAS: Self-Association Sequences

Sce or RING: Sex Comb Extra

Scm: Sex Comb on Midleg

SET: Su(var)3-9, Enhancer-of-zeste and Trithorax

SIN3: SWI-independent-3

SIN3A: Paired Amphipathic Helix Protein Sin3a

SUMO: Small Ubiquitin-like Modifier

SUZ12 : Suppressor Of Zeste 12

SXC: Super Sex Combs

TET: Ten Eleven Translocation

Trr: Trithorax related

TrxG: Proteines Trithorax “Trithorax group proteins”

Ub: Ubiquitine

UBD: Ubiquitin binding domain

UCH: Ubiquitin C-terminal hydrolases

UDP-GlcNAc: Uridine di-phosphate N-Acetylglucosamine

ULD: Ubiquitin Like Domain

USP: Ubiquitin-Specific Proteases

YY1 : Yin Yang 1

À celui qui a illuminé
Ce parcours de vie
Par sa présence et qui,
En dépit de la distance,
Persiste à briller
Au firmament
De mon cœur.
Je dédie ce
Modeste ouvrage
À celui qui est
et demeurera
L'éternelle étoile qui
Éclairera ma voie,
Mon bien-aimé père,
Rejeb DAOU.

REMERCIEMENTS

Cette partie, incontournable malgré tout, selon les normes habituelles, est une partie-piège car elle peut paraître, aux yeux de certains, trop longue et truffée de noms, et constituer pour d'autres, s'ils n'y sont pas cités, la preuve d'un manque de reconnaissance fatal.

Reconnaissante, je le suis profondément et n'ai pas manqué de l'exprimer de vive voix à tous ceux qui m'ont aidée et, il faut le dire, supportée tout au long de ce parcours.

La seule personne que je ne peux manquer de nommer, et à qui j'exprime mon plus profond respect et mes plus humbles remerciements pour toute l'aide et le soutien sans faille sans lesquels ce modeste travail n'aura jamais vu le jour, c'est mon Directeur de recherche, Docteur El Bachir Affar. Grâce à lui, j'ai pu bénéficier des outils et subventions nécessaires à l'avancement de ce projet; ses conseils précieux, la confiance qu'il m'a accordée, les projets et articles qu'ils a mis à ma portée et fortement cautionnés ont fait de moi le chercheur que je suis aujourd'hui. J'espère qu'il trouvera ici, ainsi que sa femme Diana, l'expression de toute la considération et de toute la gratitude auxquelles ils ont droit.

Je voudrais également remercier tous les membres de mon comité de suivi, comité prédoctoral, pour leur contribution au bon déroulement de mon travail. Ce dernier a gagné en perfectionnement et précision grâce à leurs commentaires, critiques et suggestions, et je leur en suis

redevable. Que les membres du jury d'évaluation de thèse soient aussi assurés de ma reconnaissance pour l'effort qu'ils ont dépensé à la correction de ce projet et aux remarques qu'ils ne manqueront pas de me faire. Je promets d'en tenir compte et d'apporter les corrections indispensables à tout esprit scientifique critique et rigoureux. Ma thèse ne peut que s'enrichir au contact de leurs commentaires. Le personnel du département de biochimie m'a été d'un apport et d'un appui sans faille tout au long de ma recherche et je les remercie vivement d'avoir aplani bien des tracasseries administratives.

Je ne peux oublier ceux qui, au fil des ans, de collègues sont devenus amis, de membres de laboratoire sont devenus, à force de générosité, une famille dont l'assistance m'a été inestimable. Ceux qui m'ont particulièrement appuyée dans mes articles et ma recherche se reconnaîtront. Merci!

Bien évidemment, je tiens à rendre un ultime hommage à mes proches. Je remercie mon père, ange-gardien permanent à mes côtés, qui a consenti à tous les sacrifices pour me garantir quiétude et confort; ma mère, pigeon voyageur et protecteur, trésor inépuisable de patience, d'abnégation et de réconfort; ma sœur Salma, mon âme-sœur et alter ego, pour l'immense secours qu'elle a constitué pour moi, pour tous les encouragements et toutes les marques d'affection qu'elle n'a cessé de me prodiguer; mon frère Amine, grâce à qui les pièges de la technologie ont pu être déjoués et enfin ma Sœur Sonia qui a fait qu'une terminologie assez ardue se réconcilie avec la langue de Molière.

CHAPITRE 1

1. Introduction

1.1 Structure de la chromatine et régulations épigénétiques

Ce qui démarque le développement des organismes multicellulaires, est leur capacité à pouvoir former spécifiquement des types de tissus cellulaires distincts. Malgré la similarité au niveau des séquences génétiques, différents types cellulaires se caractérisent par des profils d'expression géniques distincts et leurs identité cellulaire doit être conservée durant les divisions somatiques. Cette spécificité cellulaire est maintenue grâce à l'épigénétique qui se définie comme étant l'information de l'épigénome qui est indépendante de l'information génétique au niveau de l'ADN et qui est stable et se transmet de manière héréditaire[1,2].

L'épigénome est organisée au sein des cellules eucaryotes de manière très spécifique afin de permettre une expression harmonieuse des gènes et ce dépendamment du contexte physiologique, du tissu ou de l'organe dans lequel la cellule se situe.

1.1.1 Structure et fonctions de la chromatine :

La chromatine est la structure fondamentale qui caractérise l'assemblage de l'ADN avec les histones. Elle représente ainsi un échafaudage permettant de condenser tout le génome en entier plusieurs milliers de fois à l'intérieur du noyau. L'organisation spatio-temporelle du génome favorise une structuration hautement ordonnée et contrôlée de la chromatine ainsi qu'une accessibilité adéquate aux gènes. À cette fin, plusieurs processus très dynamiques au niveau de l'ADN sont conjointement agencés à savoir, la transcription, la réplication et la réparation de l'ADN. Ceci est assuré par la collaboration étroite entre les histones, les facteurs responsables du recrutement ou de l'éviction des histones au niveau de l'ADN, les enzymes qui modifient spécifiquement les histones et l'ADN (on parle dans ce cas précis de la méthylation de l'ADN) et les complexes protéiques de remodelage de la chromatine [1,3-7].

Le nucléosome est l'unité fondamentale de la chromatine. Il est composé de deux copies d'un octamère des quatre histones principales (H2A, H2B, H3, H4) enroulé de 147 paires de bases d'ADN constituant ainsi le premier niveau de compaction de l'ADN. On y retrouve un tétramère de H3-H4 et un dimère de H2A-H2B. Les nucléosomes sont séparés par des

séquences d'ADN qui permettent de faire le lien entre les différentes particules de ce dernier. Ces petites séquences d'ADN nommées, séquences de liaison de l'ADN (*DNA linker*), peuvent être liées par l'histone H1 rajoutant ainsi un autre niveau de compaction à la structure de la chromatine. La structure du nucléosome est globulaire. Des extensions terminales des histones de structure indéfinie, appelés les queues des histones (pour *histones tails*) se prolongent à travers le nucléosome. Le domaine globulaire des histones ou encore appelé, *histone fold* est un domaine basique formé de trois hélices α et présente ainsi une affinité hautement élevée pour l'ADN[1,6-10]

1.1.2 Modifications post-traductionnelles des histones :

Les nucléosomes assurent la mise en place et la coordination d'évènements moléculaires impliquant les histones [11]. De manière plus spécifique, les queues des histones constituent des déterminants majeurs pour la régulation de la fonction de la chromatine. En effet, les extensions terminales des histones représentent une plateforme qui héberge différents évènements de signalisations ainsi que des modifications post-traductionnelles (PTMs) [12,13] (**Figure 1.1**). Néanmoins des modifications post-traductionnelles ont toutefois été identifiées au niveau de la région globulaire du nucléosome [13]. À ce jour, plus de 100 sites de modifications ont été détectés par spectrométrie de masse ou grâce à l'utilisation d'anticorps spécifiques. Ceci inclue d'une part les modifications communément connues et qui ont été largement étudiées comme la phosphorylation au niveau des résidus sérines/thréonines, l'acétylation et l'ubiquitination au niveau des lysines, la méthylation des résidus lysines/arginines, l'ADP-ribosylation au niveau de l'acide glutamique et d'autre part les modifications nouvellement identifiées ou peu caractérisées comme la O-GlcNAcylation sur les sérines/thréonines, la crotonylation sur les lysines et la déamination au niveau des arginines [13-22].

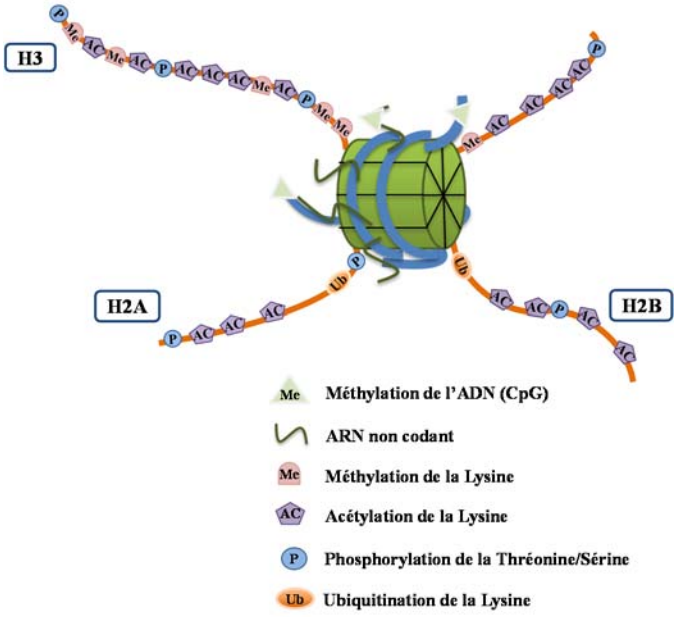

Figure 1.1 : Représentation du nucléosome et des modifications post-traductionnelles des histones : (A) Schéma du nucléosome présentant les quatre histones et autour duquel s'enroule l'ADN. **(B)** présentation des majeurs modifications post-traductionnelles (PTMs) des histones qui se produisent au niveau des queues N- et C-terminaux des histones. Modifiée de Susana Gonzalo, Department of Biochemistry & Molecular Biology, Saint Louis University School of Medicine.

Vue la complexité de régulation au niveau de la chromatine, le nombre de résidus modifiés au sein des histones est probablement sous-estimé. L'identification des multiples modifications des histones, dont les unes corrèlent avec l'activation de l'expression des gènes et d'autres avec la répression transcriptionnelle a contribué à l'émergence de la théorie du « code de l'histone », « *histone code* ». Ce n'est que dans les années 1960 que les histones ont été identifiées comme étant modifiées de manière post-traductionnelles. Depuis ce temps, il a fallu presque une trentaine d'années de recherches pour que les scientifiques commencent à révéler la fonction biologique de ces événements dans la régulation épigénétique. En fait tout a commencé par la découverte des premières acéthyltransférases et déacéthylases nucléaires et leur rôle majeur comme régulateurs transcriptionnels [23,24]. Ainsi, les acéthyltransférases et les déacéthylases ont été révélées comme étant respectivement des coactivateurs et des corépresseurs transcriptionnels. Peu de temps après, le premier complexe coactivateur d'acéthyltransfeérases (SAGA, ADA, NuA4, et NuA3) modifiant les histones a été identifié et purifié. De même, le premier complexe épigénétique de déacéthylases (contenant Rpd3 et

HDAC1) a été caractérisé [25]. De plus, les PTMs des histones se concrétisent sur différents niveaux puisque les lysines peuvent être mono-, di- ou tri-méthylés aboutissant à de variables réponses cellulaires. Un autre aspect de complexité par rapport à ces modifications est le fait qu'il peut s'agir aussi d'une mono- ou d'une di-méthylation symétrique ou asymétrique au niveau des arginines. Les PTMs des histones sont respectivement ajoutées, lues et enlevées à l'aide de facteurs associés à la chromatine qu'on appelle respectivement, les *writers*, *readers* et *erasers* (**Fig 1.2**). Ces complexes sont classifiés selon leurs spécificités envers certains acides aminés au niveau des queues des histones ou de la région globulaire du nucléosome ainsi que des séquences nucléotidiques au niveau de la chromatine [12,13,17,26-30]. Ils sont généralement associés en complexes multi-protéiques stables permettant de former de

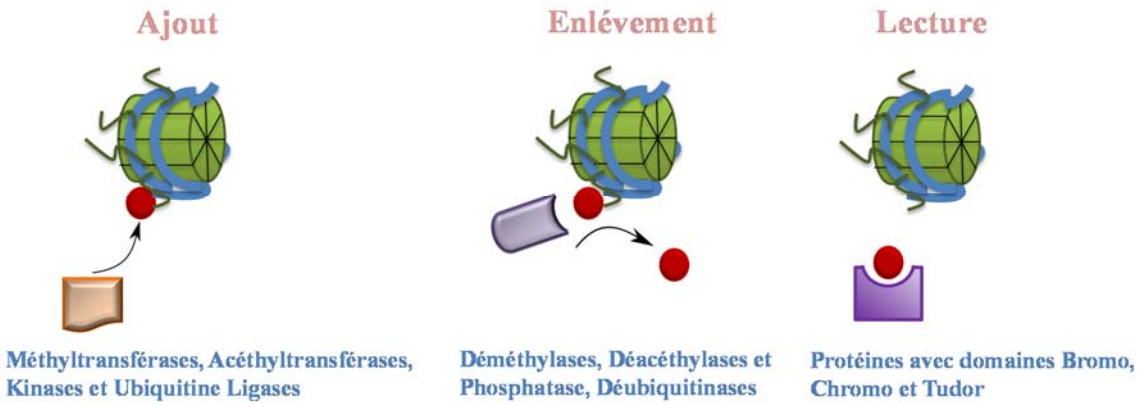

variables complexes épigénétiques multi-fonctionnels et de ce fait contribuent au maintien de la mémoire épigénétique[31].

Figure 1.2 : Description des fonctions des régulateurs épigénétiques au niveau de la chromatine : Les modifications postraductionnelles des histones peuvent être ajoutées au niveau de l'ADN ou les protéines par l'action d'enzymes qu'on appelle les ''*writers*'', ou enlevées par des enzymes spécifiques, les ''*erasers*'', pour permettre l'ajout d'autres PTMs, ou lue par des enzymes possédants des domaines spécifiques pour la reconnaissance des PTMs. Ces derniers sont les ''*readers*'' et se retrouvent généralement dans de larges complexes protéiques. Modifiée de Nature. 2013 Oct 24;502(7472):480-85 [32].

1.2 Régulations épigénétiques par les complexes Thritorax et Polycombes

Toutes les cellules d'un organisme multicellulaire contiennent la même information génétique. La régulation différentielle et spatio-temporelle du même gène procure à la cellule

une identité et une destination spécifique [33]. En effet, l'établissement et le maintien de l'identité cellulaire requiert la mise en place d'une signature d'expression génétique spécifique qui assure la production de la lignée cellulaire adéquate [33]. La mémoire épigénétique, est le moyen central qui permet de maintenir l'identité cellulaire. Cette mémoire est requise pour assurer une transmission stable de l'état transcriptionnel active ou réprimé des gènes au cours des divisions cellulaires sans qu'il y ait un changement au niveau de la séquence d'ADN [31].

Deux groupes de gènes de régulation épigénétiques dont leur rôle fondamental est de procurer la mémoire épigénétique ont été identifiés et largement étudiés et qui sont, les protéines du groupe Trithorax, TrxG (*Trithorax group (TrxG) proteins*) et les protéines du groupe Polycombes, PcG (*Polycomb group (PcG) proteins*). Ces groupes protéiques coordonnent le maintien de la mémoire épigénétique tout au long de plusieurs générations de divisions cellulaires [34]. L'analyse biochimique des protéines TrxG et PcG a révélé que celles-ci forment généralement des complexes multi-protéiques associés aux régulations des évènements de modification de la chromatine et ce en coordonnant respectivement l'activation et la répression de l'expression des gènes [34-36 37 38 39]. Les complexes protéiques TrxG et PcG sont très conservés au sein des organismes multicellulaires[33,40,41]. Ils admettent un rôle crucial dans la régulation du développement de l'organisme et ce par le contrôle de l'état transcriptionnel dynamique des gènes et le maintien des états cellulaires différentiés[42-45].

Ces régulateurs épigénétiques ont été identifiées suite à des études génétiques chez la *Drosophile*. Ainsi, les gènes initialement reconnus pour être des cibles des protéines PcG et TrxG sont les gènes de développement *Hox* [46]. Les gènes codant pour les PcG ont été initialement découverts grâce à l'identification de mutations chez la *Drosophile* qui provoquaient une induction anormale des gènes *Hox* à l'extérieure de leur domaine d'expression approprié, aboutissant à des transformations homéotiques [47]. Peu de temps après, l'identification de la protéine, TRX, a permis d'accorder pour la première fois aux protéines de la famille des Trithorax le rôle de régulateurs positifs des gènes *Hox* [48,49]. De plus, ce qui est très intéressant, c'est qu'au lieu d'être requis pour initier l'expression de ses gènes cibles, TRX a été caractérisée comme ayant pour fonction de maintenir l'état actif des gènes *Hox* au sein de leur domaine d'ADN et ce tout au long du processus du développement de l'organisme [49,50]. Des études ultérieures de génétique, également chez la *Drosophile,* ont permis l'identification

d'autres protéines du groupe TrxG et ce en se basant sur des expériences de perte de fonction de gènes *Hox* ou à la suite d'un criblage génétique en vue de dépister des protéines TrxG pouvant contrecarrer le phénotype de suppression d'expression médié par les protéines PcG. Ainsi, les protéines TrxG sont des antagonistes fonctionnels des protéines PcG vue que ces deux groupes de protéines permettent chez la *Drosophile* de maintenir respectivement un profil d'expression actif et réprimé des gènes *Hox* au sein de leurs régions de clusters appropriées [51] [34,52]. Cependant, il n'est pas établi si ces complexes épigénétiques maintiennent à long terme au niveau des vertébrés, le profil d'expression de leurs gènes cibles [45,53]. Il est maintenant de plus en plus admis que ces deux groupes de protéines régulent en plus des gènes *Hox* un nombre élevé de gènes qui contrôlent de nombreux processus cellulaires indiquant ainsi que le maintien épigénétique des états actifs ou réprimés des gènes semble être un mécanisme fondamental de régulation au cours du développement des organismes [41,54].

1.2.1 Description brève des complexes Trithorax :

- **Les protéines Trithorax et leur fonctions:**

Les protéines Trithorax forment des complexes épigénétiques qui peuvent être regroupés dans trois principales classes de régulateurs selon les fonctions qu'ils exercent au niveau de la chromatine. On y retrouve une première catégorie de TrxG qui inclue des facteurs ayant un domaine SET (*Su(var)3-9, Enhancer-of-zeste and Trithorax*) responsable de la méthylation des queues des histones. La deuxième classe contient des facteurs de remodelage de la chromatine qui agissent de façon dépendante de l'ATP. À l'intérieure de ce même groupe on identifie des protéines capables de lire les modifications post-traductionnelles catalysées par les protéines de la première classe. La troisième catégorie des protéines TrxG comprend des facteurs qui peuvent se lier directement à des séquences spécifiques au niveau de l'ADN et inclue également des enzymes de modification des histones, des facteurs de remodelage de la chromatine ainsi que d'autres protéines qui n'ont pas été insérées parmi les deux premières classes. [33,55]. Les TrxG catalysent l'instauration de modifications post-traductionnelles spécifiques, à savoir la tri-méthylation de H3K4 (H3K4me3), l'acétylation de H3K27 (H3K27ac) et la di-méthylation de H3K36 (H3K36me2) [33]. À l'issue de cette classification, les protéines TrxG admettent un rôle majeur dans la régulation de plusieurs processus cellulaires.

Ainsi, de par leur implication dans le maintien de la mémoire épigénétique et plus spécifiquement un état d'expression génique actif, les protéines TrxG assurent le contrôle des processus de tumorigenèse et l'auto-renouvèlement des cellules souches embryonnaires [56], le choix du destin cellulaire et la prolifération [57], l'inactivation du chromosome X [58], l'apoptose [59], la régénération tissulaire, la réponse cellulaire aux différents stimuli de stress, l'activation de la sénescence et la réponse aux dommages à l'ADN [60,61,62,63].

- **Diversité des complexes de protéines Trithorax:**

Les protéines TrxG ayant le domaine SET sont responsables de la mise en place de la méthylation de H3K4. La première méthyltransférase des histones (HMT) à être identifiée est la protéine Set1 faisant partie du complexe macromoléculaire COMPASS chez la levure (complexe de protéines associées avec Set1). Le complexe COMPASS est responsable de l'introduction des trois formes de méthylation, mono, di- et tri-méthylation de H3K4 chez la levure [17,33,64-66]. Chez la *Drosophile*, le génome code pour plusieurs protéines ayant le domaine SET incluant la la protéineTrx qui est la première protéine TrxG à être identifiée au sein de cet organisme, la protéine Trr (*Trithorax related*) et la dSet1. Toutes ces méthyltransférases font partie du complexe ''*COMPASS-related complex*'' et catalysent également la méthylation de l'histone H3K4 [33,67]. Chez les mammifères, on compte au minimum six complexes ''*COMPASS-related complex*'' avec des fonctions non redondantes et qui catalysent la méthylation de H3K4 puisque les enzymes qui y sont associées comportent le domaine SET. Il s'agit des complexes SED1A, SETD1B, MLL1, MLL2, MLL3, MLL4 et MLL5. À nos jours une multitude de complexes MLL, sont défini comme étant des ''*COMPASS-like complex*'', ont été identifié au niveau des plantes et des mammifères démontrant la présence d'une spécificité de régulation génomique médiée par ces complexes. SETD1A et SETD1B sont les homologues de dSet1 et les complexes formés par ces deux protéines sont les plus similaires au complexe COMPASS de la levure. Ces complexes contiennent spécifiquement la sous-unité protéique WDR82 et assurent une H3K4me3 globale du génome chez les cellules de mammifères et de *Drosophile*. MLL1 et MLL2 sont les équivalents chez les mammifères de Trx alors que MLL3-5 sont les homologues de Trr [55,68]. Pour affiner beaucoup plus le mécanisme d'activation transcriptionnel, des événements de coopérations entre des modifications post-traductionnelles des histones sont procurés par les

complexes MLL. En effet, comme exemple, on peut citer l'acétylation de l'histone H4 au niveau de la lysine 16 qui est catalysée par la protéine MOF. MOF fait partie du complexe MLL1 et appartient à la famille MYST des acétylases des histones (HAT) [69]. De ce fait, la méthylation et l'acétylation ont été associées pour promouvoir une régulation spécifique de la transcription. D'autre part, les complexes méthyltransférases MLL3 et MLL4 contiennent une démethylase, UTX (KDM6) qui est spécifique à l'élimination de la marque répressive H3K27 tri-méthylée (H3K27me3) [70,71].

1.2.2 Les complexes Polycombes

Les protéines Polycombes forment des complexes multi-protéiques composés principalement d'enzymes qui modifient la chromatine. Des études biochimiques et génétiques ont révélés que les protéines Polycombes peuvent être regroupées en deux complexes majeurs, nommés *Polycomb repressive complexe 1* pour PRC1 et *Polycomb repressive complexe 2* pour PRC2. Des analyses ultérieures ont permis de découvrir que les protéines Polycombes composent plusieurs variantes et subdivisions de complexes PRC1 et PRC2 [35,39,72,73]. En plus des complexes Polycombes classiques, PRC1 et PRC2, d'autres complexes Polycombes ont été identifiés à savoir, le complexe Pho-RC (*Pho repressive complex*) [74], le complexe dRAF (*Drosophila Ring-associated factors*) [75] et le nouveau complexe récemment identifié, le complexe PR-DUB (*Pc-repressive deubiquitinase complex*) également connue pour le complexe BAP1 chez les mammifères [76-79] (**Figure 1.3**).

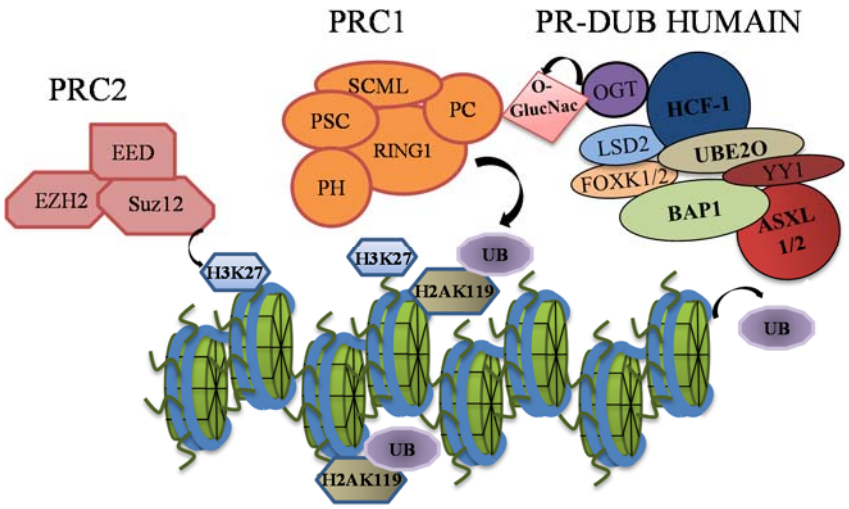

Figure 1.3 : Régulations épigénétiques par les complexes Polycombes : La signature épigénétique de répression H3K27me3 est catalysée par le complexe Polycombe PRC2. Cette marque répressive est reconnue par le complexe PRC1 qui est ainsi recruté au niveau de la chromatine et contribue à la répression par la monoubiquitination de H2A. Cette modification est reversée par le complexe PR-DUB qui est représenté chez l'humain par le complexe BAP1. La OGT, composante du complexe BAP1, participe à la signalisation épigénétique via la O-GlcNAcylation de la protéine PC. (Modifiée de Nature Reviews Cancer 13, 153-159 (March 2013)) [77].

1.2.3.1 Les complexes PRC2

Au niveau moléculaire, la fonction principale de ce complexe est la mise en place des marques épigénétique répressives, di-et tri-méthylation de H3K27 (H3K27me3) [35,37,80,81]. Cette catalyse est assurée grâce à la présence du domaine SET au niveau de la sous-unité catalytique du complexe PRC2, l'histone méthyltransférase E(z) (*Enhancer-of-zeste*) chez la *Drosophile* ou EZH1 et EZH2 chez les mammifères. Les autres composants du complexe sont SUZ12 (*Suppressor Of Zeste 12*), PCL the (*Polycomb like*) (PLC1, 2 and 3 dans les mammifères), ESC (*Extra sex combs*) (EED chez les mammifères) et le facteur de remodelage de la chromatine Nurf 55 (RbAp46/48 chez les mammifères). Cependant, E(z) et EZH2 ne sont catalytiquement actives que lorsqu'elles sont en association avec d'autres composantes du complexe. En effet, E(z) et EZH2 se lient avec SUZ12 et ESC ou EED respectivement. EED joue un rôle important dans le maintien de l'intégrité du complexe PRC2 et de son recrutement sur la chromatine, de l'induction de l'activité méthyltransférase de EZH2 et de la propagation de la marque répressive H3K27me3 [82,83]. De plus, une investigation récente a démontré un rôle inédit de EED comme étant une sous-unité intégrale des deux complexes PRC1 et PRC2. Ainsi, EED semble être requise aussi bien pour la triméthylation de H3K27 que pour l'activité d'ubiquitine ligase de PRC1 [84].

- **Mécanisme d'action des complexes PRC2:**

Chez les mammifères, les complexes PRC2 sont plus diversifiés. Les protéines EZH1 et EZH2 sont codées par deux gènes différents et un épissage alternatif au niveau de l'ARN de EED aboutit à la génération de quatre isoformes distincts de cette protéine et la formation de variables complexes PRC2 [85]. Également, il a été démontré que certains isoformes de EED admettent une activité catalytique et peuvent *in vitro* méthyler l'histone H1 et H3K27. Néanmoins, l'existence de la méthylation de H1 a été prouvée *in vivo* mais son rôle dans la

répression épigénétique médiée par les protéines Polycombes n'a toujours pas été élucidée [86]. De plus, les complexes PRC2 chez les cellules mammifères contiennent également le facteur transcriptionnel JARID2 (*Jumonji- and AT-rich interaction domain (ARID)-domain-containing protein 2*) qui interagie directement avec SUZ12. JARID2 joue un rôle important dans la régulation du développement embryonnaire et est requise pour le recrutement de PRC2 au niveau de la chromatine. Il s'agit d'une déméthylase (KDM) inactive qui agit en modulant l'activité des méthyltransférases et plus particulièrement en inhibant la méthylation H3K27me3 de PRC2 [87,88]. Des études récentes ont démontrés que PRC2 pouvait s'associer avec d'autres régulateurs transcriptionnels comme des facteurs de remodelage de la chromatine, des déacéthylases ou des déméthylases (HDACs et KDMs) [89,90] ainsi qu'une multitude d'ARN non codants (*non-coding RNAs*, ncRNAs) et ce afin d'assurer son bon recrutement et la répression transcriptionnelle des gènes cibles [91-93].

Sur le plan biochimique, les complexes EZH1 et EZH2 ont des activités catalytiques différentes. Ainsi, contrairement à EZH2, EZH1 semble agir la plupart du temps de manière indépendante de son activité catalytique. En effet, le complexe PRC2-EZH1 à la capacité de promouvoir la compaction de poly-nucléosomes *in vivo* alors que PRC2-EZH2 est exempt de cette activité [94]. Ainsi, le niveau de méthylation sur les promoteurs peut varier selon la présence de l'une ou de l'autre composante de PRC2. EZH2 semble être requise pour l'établissement du niveau global de la méthylation de H3K27 tandis que EZH1 permet de remettre suite à la déméthylation, les niveaux de H3K27me sur des sites spécifiques. De plus, les cellules souches embryonnaires déficientes en EZH1 ne présentent pas une perte de leur niveau global de H3K27me alors que les knockout en EZH2 sont incapable de maintenir cette modification [94,95]. Des études récentes ont établis que le complexe PRC2-EZH2 modifie d'autres substrats cibles autres que les histones. Ainsi, il a été démontré que EZH2 catalyse la méthylation du facteur de transcription GATA4 sur la lysine 299 et ce afin de réduire son activité transcriptionnelle et son habilité à recruter l'acéthyltransferase p300 [96]. De plus, EZH2 interagi au niveau des cellules cancéreuses résistantes aux anti-androgènes (CRPC), avec le récepteur des androgènes (AR) et promouvait son activité transcriptionnelle. Ceci suggère que dans différents contextes cellulaires, EZH2, pourrait interagir avec d'autres substrats et être impliquée dans l'activation génétique [97].

Un autre aspect inhabituel de régulation par les complexes PRC2 est le fait que EZH2 a été identifiée comme un nouveau régulateur de la réponse cellulaire aux dommages d'ADN doubles brins (DSB, *DNA double strand break*). En effet, le recrutement de EZH2 ainsi que la H3K27me3 sont enrichis au niveau des sites de dommages, IRIF (*Ionizing Radiation Induced Foci*) [98]. Toutefois, il n'est toujours pas compris comment un composant d'un complexe Polycombe pourrait contrôler des évènements liés à la chromatine lorsque celle-ci se présente dans un état relaxé [99,100].

1.2.3.2 Les complexes PRC1

Le complexe PRC1 a été a été initialement identifié chez la *Drosophile* par la présence des protéines suivantes : protéine *Pc* (*Polycomb*), *Posterior Sex Combs (PSC)*, *Polyhomeotic (Ph)*, *Sex Comb Extra (Sce* or *RING)* et *Sex Comb on Midleg (Scm)*. Ces protéines Polycombes forment des sous-complexes stables et constituent le noyau du complexe PRC1 du fait qu'elles admettent des propriétés biochimiques et fonctionnelles caractéristiques de ce complexe [101,102].

- **Les différents complexes PRC1:**

En plus de ses sous-unités principales, le complexe PRC1 peut se former à partir de plusieurs sous-unités alternatives. Ainsi, plusieurs variantes stables et fonctionnelles du complexe PRC1 ont été identifiées et ce plus particulièrement au sein des cellules mammifères. A nos jours, il est bien connu que chacune des protéines formant le noyau du complexe PRC1 admet plusieurs homologues chez les espèces de mammifères. On compte trois homologues de la protéine *Ph* chez l'humain : PH1, PH2 et PH3 et deux homologues de *Sce* : Ring1A (Ring1) et Ring1B. BMI1 (*B lymphoma Mo-MLV insertion region 1*) qui forme avec Ring1B (aussi connu pour RNF2) le noyau du complexe PRC1 chez les mammifères, est l'homologue de PSC. On définit au minimum trois paralogues de BMI1 à savoir, MBLR (*Mel18 and Bmi1-like RING finger protein*), NSPC1 (*nervous system Pc1*) et MEL18. Ces protéines sont également connues pour *Polycomb group ring finger* (PCGF) protein 6, PCGF1 and PCGF2, respectivement. Six complexes Polycombes différents formés par les protéines PCGF (PCGF1-PCGF2) existent chez les mammifères. Ces facteurs épigénétiques forment des complexes distincts avec d'autres protéines Polycombes mais qui restent fonctionnellement reliés. Les homologues de la protéine Pc de la *Drosophile* chez les mammifères sont

représentés par les protéines Chromobox (*Cbx*) qui sont généralement les unités protéiques qui reconnaissent les marques répressives di-et tri-méthylation de H3K27 catalysées par les complexes PRC2. Ainsi, une multitude de complexes PRC1 différents peuvent se former dans les cellules de mammifères [103-107].

Ce qui définit d'avantage la diversité des complexes PRC1 est la formation de complexes *Polycombes-like complexes* par une combinaison entre des protéines du noyau de PRC1 et d'autres régulateurs épigénétiques. Cette variabilité confère aux complexes PRC1 des activités enzymatiques différentes. Comme exemple, MBLR fait partie du complexe PRC1-E2F6 (E2F-6.com-1) contenant Ring1B, et une méthyltransférase qui modifie l'histone H3K9 (il peut s'agir soit de l'enzyme Eu-HMTase1 (EHMT1) ou NG36 (G9a ou EHMT2)). Un autre complexe *PcG protein-like complex* a été identifié contenant MBRL, et une déméthylase de l'histone H3K4, JARID1D (KDM5D). De plus, NSPC1 a été co-purifiée avec Ring1A, Ring1B et RYBP, en association avec le complexe co-répresseur BCOR qui contient FBXL10 (KDM2B), une déméthylase de l'histone H3K36 [75,104].

- **Principales fonctions des complexes PRC1:**

La grande diversité des complexes PRC1 démontrent qu'ils admettent plusieurs fonctions au niveau de la chromatine. Même si le mécanisme de répression n'est pas complètement élucidé, la répression génique médié par ces complexes se concrétise par le biais d'une inhibition directe de la machinerie transcriptionnelle ou un changement de la structure de la chromatine. En effet, il a été démontré que les complexes PRC1 qu'ils soient purifiés à partir des cellules ou reconstitués *in vitro*, sont capable de réprimer la transcription, inhiber les complexes de remodelage de la chromatine et d'assurer la compaction des nucléosomes [108-110].

- **La monoubiquitination de H2A:**

La fonction enzymatique principale du complexe PRC1 est de catalyser la monoubiquitination de l'histone H2A au niveau de la lysine 119 (K118 chez la *Drosophile*). Chez l'humain, cette activité a était initialement attribuée au moins à deux ubiquitine ligases E3, Ring1B et 2A-HUB [38,39,105,111]. Le complexe PRC1 est constitué de trois protéines ayant chacune un domaine Ring (*Really Interesting New Gene*), soit Ring1B, Ring1A et BMI1 [112].

Malgré la présence de trois domaines Ring au sein de ce complexe, seulement Ring1B possède une activité ubiquitine ligase envers H2A *in vitro*. En effet, le domaine Ring interagi avec une enzyme E2 conjugatrice de l'ubiquitine, UbcH5c afin de promouvoir la monoubiquitination de H2A [113]. Néanmoins, l'activité catalytique de Ring1B est grandement augmentée en présence de Ring1A et BMI1. De plus, BMI1 est également requis pour stimuler l'activité catalytique de Ring1B *in vivo* [39,105,106,114]. De manière similaire à d'autres complexes d'ubiquitine ligases, Ring1B et BMI1 forment un hétérodimère à travers leurs domaines Ring. Cette interaction permet la formation d'un domaine basique (*basic patch*) responsable de la reconnaissance directe du nucléosome [113]. De plus, un résidu au niveau du domaine ring de Ring1B (K93) a été identifié comme étant suffisant pour assurer aussi bien la liaison à l'ADN et l'activité catalytique [115]. Récemment, un travail du groupe de Green a identifié une nouvelle ubiquitine ligase pour H2A, le facteur TRIM37 contenant un domaine Ring. Les auteurs ont démontré que TRIM37 monoubiquitine H2A au niveau des résidus K118/K119. Contrairement à ce qui est classiquement connu, TRIM37 s'associe avec le complexe PRC2 afin de catalyser la répression des gènes cibles [116].

L'histone H2A a été la première protéine à être identifiée comme étant ubiquitinée. De plus, l'ubiquitination de cette histone représente la forme ubiquitinée la plus abondante dans la cellule (5 à 15 % de la totalité de H2A dans les cellules eucaryotes est modifiée par ubiquitination) [117]. L'ubiquitination de H2A se présente de façon majoritaire sous la forme monoubiquitiné. Il a toutefois été révélé une proportion très faible de la polyubiquitination de H2A [118]. Cette modification semble être régulée au cours de la division cellulaire. En effet, la monoubiquitination de H2A disparaît presque en totalité au cours des premières étapes de la mitose et est restaurée immédiatement après la formation de l'enveloppe nucléaire [119-121].

Plusieurs évidences soulignent que la monoubiquitination de H2A (H2Aub) médiée par les complexes PRC1 est étroitement liée à la répression épigénétique. En effet, des expériences d'immunoprecipitation de la chromatine ont démontrées que Ring1B et BMI1 sont conjointement recrutés en présence de H2Aub sur des sites spécifiques des geènes cibles des protéines Polycombes et plus particulièrement sur les gènes *Hox* [105]. D'autre part, des mutations touchant le domaine Ring de Ring1B provoquent une de-répression des gènes *Hox* malgré la présence de H3K27me3 au niveau des promoteurs de ces gènes [79,122,123]. Le mécanisme de répression médié par H2Aub reste toutefois très peu connu. Plusieurs études

suggèrent que H2Aub interfère avec l'initiation de la transcription. En effet, la mise en place de H2Aub inhibe, *in vitro*, la di-et tri-méthylation de H3K4 médiée par MLL et ce durant l'initiation mais pas l'élongation de la transcription [124].

Un autre aspect de régulation transcriptionnelle est reflété par le fait que le niveau de H2Aub semble moduler la libération de la polymérase II phosphorylée au niveau de la sérine 5 (*poised RNA pol II*) à partir des gènes bivalents. Ainsi, il a été reporté que la déplétion de Ring1B par knockout dans les cellules souches embryonnaires (*ES cells*) induit une perte significative de H2Aub de manière concomitante à la libération de de la pol II, l'initiation de l'élongation et de ce fait la de-répression des gènes bivalents [125]. De plus, il a été reporté qu'au niveau des promoteurs des gènes bivalents, H2Aub empêche l'éviction des dimères de H2A-H2B à partir des nucléosomes ce qui inhibe également l'élongation [111].

Le complexe PRC1 est également requis pour maintenir l'inactivation du chromosome X puisque le recrutement de H2Aub et de Ring1B est enrichi au niveau du chromosome X inactivé (Xi). Dans la même optique, la déplétion de Ring1B et BMI1 par un double knockout dans les cellules ES s'associe à une diminution de H2Aub au niveau du Xi [126,127].

- **Modes de répressions épigénétiques non-canoniques par les complexes PRC1:**

La fonction du complexe PRC1 a été initialement déterminée comme étant dépendante de l'action de PRC2. En effet, Il a été longuement admis que la tri-méthylation de H3K27 sert de site de recrutement du complexe PRC1 et ce grâce au domaine chromodomaine dont les protéines CBX possèdent [35,39,72,128]. Toutefois, de nombreuses études ultérieures sont venues mettre en question cette théorie. Ainsi, le complexe PRC1 peut exercer ses fonctions de manière indépendante de la présence de H3K27me3. En effet, les cellules knockout en EED, présentent un niveau significativement élevé en H2Aub même si H3K27me3 est totalement perdue. De plus le recrutement de PRC1 et l'établissement de H2Aub au niveau de Xi peut être indépendant de H3K27me3 [129]. Cette fonction de répression qui se trouve indépendante de la contribution de PRC2 a été également retenue pour deux autres complexes PRC1, les complexes RYBP et YAF2. Même si ces complexes sont dépourvus de la sous-unité protéique CBX, ils permettent le recrutement de Ring1B sur la chromatine et de ce fait la monoubiquitination de H2A [130,131]. Également, le complexe FBXL10-BCOR (dRAF chez la

Drosophile) composé de YAF2, CK2α, Skp1, HP1γ, CBX8, NSPC1, Bmi-1, BCOR, et FBXL10/KDM2B, semble être requis pour l'activation de la catalyse de H2Aub suggérant que ce complexe atypique de PRC1 pourrait avoir *in vivo*, une activité d'ubiquitination de H2A [132,133]. D'autre part, le complexe Ring1B/E2F6.com-1 est requis pour la répression des gènes cibles de E2F et de Myc dans les cellules en quiescence. Il n'est pas connu si le mécanisme de répression entrepris par ce complexe requiert ou pas la monoubiquitination de H2A [134].

Des études récentes ont contribuées à la caractérisation d'une nouvelle cascade de recrutement des complexes PRC1 et PRC2 au niveau de la chromatine. En effet, les travaux de Blackledge et Cooper ont révélé que le complexe PRC1, KDM2B/RING1A/RING1B se lie au niveau des sites CpG non méthylés et catalyse au niveau des nucléosomes la monoubiquitination de H2A, ce qui permet donc le recrutement du complexe PRC2 et par la suite la triméthylation de H3K27 qui serait reconnu par le complexe canonique de PRC1 grâce au chromodomaine des protéines CBX. Ces résultats démontrent alors que le complexe PRC2 est capable de lier H2Aub [135,136]. À la lumière de ceci, le groupe de Kalb et ses collègues ont défini que le complexe PRC2, contenant AEBP2 et JARID2, est capable de lier des nucléosomes présentant H2Aub. Ce complexe catalyse la formation de H3K27me3 qui deviendra un site de recrutement du complexe PRC1 [137].

Une autre fonction médiée par le complexe PRC1 et qui est aussi importante que la régulation transcriptionnelle, est la réparation des dommages d'ADN double brins [138]. En effet, il a été reporté que le complexe PRC1 est recruté au niveau des sites de DSB afin d'assurer la monoubiquitination de H2A et de sa variante l'histone H2AX. Cette action est requise pour garantir une réparation efficace des dommages à l'ADN et la survie cellulaire [139,140].

Plusieurs études ont mis en évidence que le complexe PRC1 est capable de favoriser une compaction du nucléosome et une répression génique de manière indépendante de son activité ubiquitine ligase [102,109,141,142]. En effet, dans des essais *in vitro*, le complexe PRC1 était capable de promouvoir une condensation des nucléosomes et une répression des gènes *Hox* de façon indépendante de H3K27me3 et de H2Aub. De plus, très récemment, le groupe de Müller a dévoilé que les gènes cibles de PRC1 pouvaient être maintenus dans un état répressif même si Ring1B et H2A étaient mutés respectivement au niveau du site catalytique et du résidu d'ubiquitination. Encore plus surprenant, les mutants de *Drosophile* qui présentent un niveau

très bas de H2Aub arrêtent de proliférer sans développer des phénotypes typiques de la déplétion des protéines Polycombes. Il semblerait ainsi que la fonction primaire de PRC1 était de réprimer les gènes sans avoir recours à développer une activité d'ubiquitine ligase envers H2A [143].

1.3 L'Ubiquitination

Les régulations cellulaires impliquent de manière très abondante les modifications post-traductionnelles des protéines. Ceci permet de finement contrôler la localisation ainsi que la fonction des substrats modifiés. La découverte de l'ubiquitine il y a maintenant plus de 30 ans comme modulateur important de plusieurs processus cellulaires, a fait de l'ubiquitination une modification critique requise pour assurer la protéolyse intracellulaire des protéines. À nos jours, l'ubiquitination et sa réaction inverse, la déubiquitination, sont des modifications post-traductionnelles impliquées dans la régulation de quasiment la totalité des voies de signalisation cellulaires [144-147]. Toutefois, l'identification et la compréhension des mécanismes permettant d'intégrer les différents types d'ubiquitination au sein du processus cellulaire adéquat, nécessitent encore de plus amples investigations.

L'ubiquitination est une modification post-traductionnelle qui consiste en l'attachement d'une petite protéine de 76 acides aminés nommée ubiquitine (Ub), sur les lysines des protéines cibles [148-150]. L'Ub est une protéine très stable et est conservée parmi les espèces eucaryotes. Elle admet une structure globulaire avec une queue C-terminale requise pour favoriser les interactions avec les protéines [151,152]. Dans les cellules de mammifères, l'Ub est codée par quatre gènes différents, UBB, UBC, UBA52 et RPS27A. Les deux derniers gènes codent pour une seule molécule d'Ub fusionnée aux protéines ribosomales L40 et S27a, alors que UBB et UBC permettent la génération du précurseur d'Ub qui se présente sous forme d'une chaîne linéaire de poly-ubiquitines [153-156]

1.3.1 Cascade enzymatique de l'ubiquitination :

La conjugaison de l'Ub est un processus à plusieurs étapes impliquant principalement trois enzymes. L'Ub est d'abord activée grâce à la formation d'une liaison thioester avec l'enzyme activatrice de l'Ub, E1 de manière dépendante de l'ATP. Il s'agit dans ce cas d'une adénylation entre la glycine 76 (G76) de l'Ub et la cystéine 632 (C632) de l'enzyme E1. Par la

suite, l'Ub activée est transférée à l'enzyme conjugatrice de l'Ub, E2 qui elle aussi forme une liaison thioester entre la G76 de l'Ub et la cystéine du site catalytique de la E2. Finalement, l'Ub est livrée de l'enzyme E2 vers les substrats cibles et ce grâce à l'action spécifique des enzymes, Ub ligase, E3 [157-161]. Ainsi, dépendamment du type de la E3 impliquée dans la réaction, les E3s peuvent soit participer directement à la livraison de l'Ub sur les groupements ε-amines des résidus lysines des protéines cibles (on parle dans ce cas des HECT E3s), soit agir comme un adaptateur entre les substrats et les E2s afin de permettre le transfert de l'Ub sur les lysines des substrats (il s'agit dans ce cas des RING E3s ou les E3s avec les domaines U-box) [157,161] (**Figure 1.4**). Cette modification est très régulée et se réalise de manière hautement spécifique. En effet, dans le génome des mammifères on compte deux enzymes E1 (UBA1 et UBA6), à peu près 40 E2s et 600 E3s [157,161-163]. Les E2s diffèrent par leur habilité à catalyser des chaînes spécifiques d'ubiquitines. Toutefois, une seule classe de E2, contenant par exemple UBCH5 a été reportée comme étant impliquée dans l'amorçage de l'ubiquitination et ce en catalysant la monoubiquitination (l'ajout de la première ubiquitine) des substrats [164]. Les autres types de E2 sont donc responsables de l'extension des chaînes d'ubiquitines en fonction des liens spécifiques qu'elles favorisent entre ces molécules [164,165]. Par exemple, Cdc34 assiste la polyubiquitination en chaînes d'ubiquitines liées par la lysine 48 (K48) [166], alors que le complexe Mms2-Ubc13 catalyse la polyubiquitination en chaînes K63 [167]. La spécificité de la réaction de l'ubiquitination est attribuée à l'action des E3s ce qui explique leur nombre élevé dans le génome humain [168].

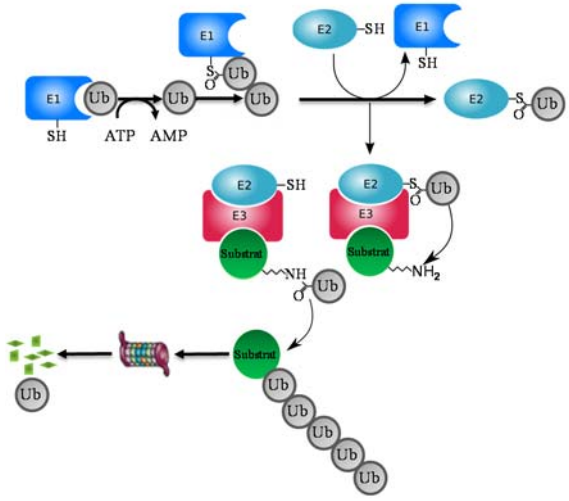

Figure 1.4 : Cascade enzymatique de l'ubiquitination. Illustration de la signalisation de l'ubiquitination des substrats au niveau des résidus lysines. Cette modification post-traductionnelle implique la participation de trois enzymes, l'enzyme activatrice de l'ubiquitine, E1, l'enzyme conjugatrice de l'ubiquitine, E2 et l'ubiquitine ligase, E3 qui assure le transfert de l'ubiquitine sur les substrats. La polyubiquitination est généralement reconnue

comme un signal de dégradation protéasomale des protéines modifiées (Modifiée de Wikepedia).

D'autres types d'ubiquitination dont le mécanisme d'action et le rôle biologique sont similaires à l'ubiquitination classique ont été récemment identifiés. Il s'agit de la modification des protéines par Sumoylation (en utilisant les *ubiquitin-like proteins* SUMO (*small ubiquitin-like modifier*), par Neddylation (via la Nedd8 (*neural precursor cell expressed, developmentally downregulated 8*) [158,169] ou par ISGylation (suite à l'ajout de la molecule de ISG15, *interferon-induced 15 kDa protein*) [169].

1.3.2 Rôles des différents types d'ubiquitination:

En plus de la monoubiquitination qui est une forme de modification très abondante dans les cellules, un nombre élevé de substrats reçoivent d'autres molécules d'Ubs qui sont spécifiquement attachées entre-elles permettant l'obtention de protéines polyubiquitinées. De façon plus spécifique, l'Ub elle-même, contient 7 lysines (Lys6, Lys11, Lys27, Lys29, Lys33, Lys48, ou Lys63) qui sont utilisés pour la formation des différents types de chaînes de polyubiquitines [170]. Ainsi, les protéines cibles peuvent être multi-monoubiquitinées ou polyubiquitinées. La polyubiquitination consiste en la formation de chaînes d'ubiquitines de structures variables. Il peut s'agir de chaînes homotypiques (polyubiquitination en utilisant la même lysine de l'ubiquitine), hétérotypiques (mélange de polyubiquitination et de sumoylation) ou aussi un mélange de chaîne de polyubiquitination en adoptant différentes lysines de l'ubiquitine) [171-174]. De ce fait, en fonction du type de la modification, l'ubiquitination définit le destin fonctionnel du substrat [175,176] (**Figure 1.5**).

L'ubiquitination des protéines a été initialement associée à la dégradation des protéines par le protéasome. Néanmoins, durant la dernière décennie, de multiples fonctions de l'ubiquitination dans la régulation d'une panoplie de voies de signalisations cellulaires ont été révélées. En effet, il est maintenant clairement définit que l'ubiquitination influence l'activité, la stabilité et la fonction des substrats [175,177,178] et de ce fait joue un rôle primordiale dans le remodelage de la chromatine, le contrôle du cycle cellulaire, la différentiation, la sénescence, la transcription, la réponse des cellules aux dommages à l'ADN, l'endocytose, l'apoptose, la voie de signalisation des kinases et la réponse immunitaire. Il n'est donc pas surprenant que la

dérégulation du système de l'ubiquitine est un déterminant majeur de développement de nombreuses maladies humaines malignes [179-184]. Toutes les variétés des chaînes de polyubiquitines sont retrouvées au niveau des cellules humaines. Toutefois, Le mécanisme de formation et la signification biologique des chaînes autres que celles liées par les K48 et K63 restent très peu connus [171,185,186].

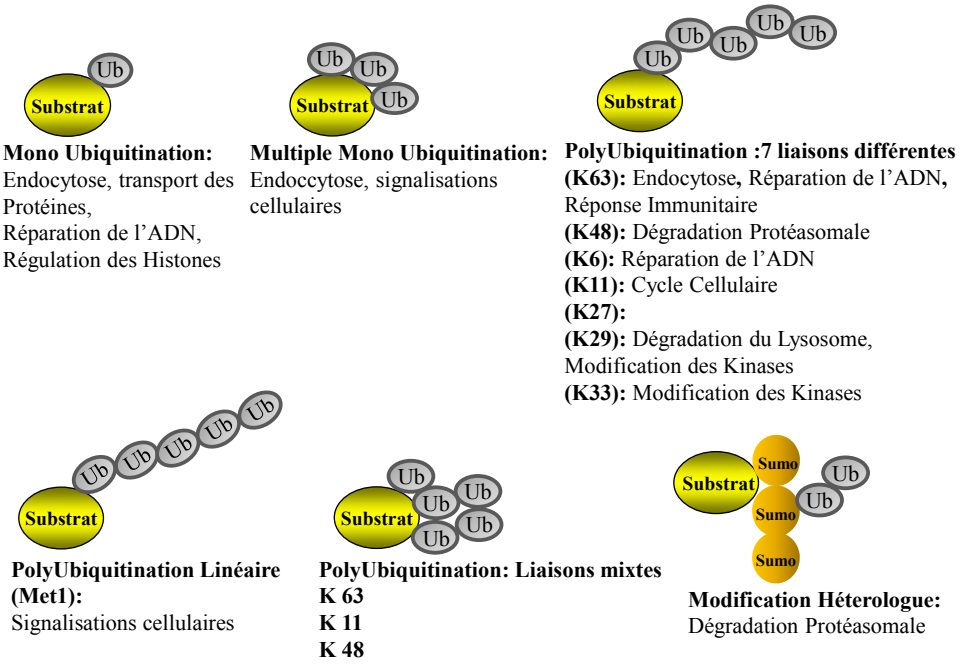

Figure 1.5 : les différents types d'ubiquitination : Représentation schématique des différents types de monoubiquitination et des chaînes de polyubiquitines. Les voies majeures de signalisations cellulaires régulées par ces types d'ubiquitination sont également présentées (Modifiée de Annu Rev Biochem. 2012;81:291-322) [187].

1.3.3 Les domaines de liaison à l'ubiquitine:

L'ubiquitination est une modification qui est aussi abondante que la phosphorylation. De manière similaire à la reconnaissance des protéines phosphorylées, les enzymes du système de l'ubiquitine sont amenées à reconnaître de manière spécifique soit l'ubiquitine sous forme libre ou les substrats modifiés par mono- ou polyubiquitination. Cette spécificité enzyme-substrat est guidée par la présence au niveau de ces enzymes de domaines spécifiques de liaison à l'ubiquitine (UBD, *Ubiquitin binding* domain) ou de récepteurs à l'ubiquitine qui

eux-mêmes contiennent également au niveau de leur structure un ou deux domaines UBD [177]. À nos jours, une multitude de mécanismes d'interaction avec l'ubiquitine ont été déterminés impliquant au moins 20 types de domaines UBD [177]. Quatre surfaces d'interactions protéines/Ub se retrouvent au niveau de l'Ub. La région la plus communément reconnue par les UBDs est le domaine hydrophobe (*hydrophobic patch*). On définit trois domaines hydrophobes. Le patch hydrophobe Ile44 est constitué des acides aminés Ile44, Leu8, Val70 et His68 et est lié par le protéasome et la plupart des UBDs. Il a été démontré que le maintien d'une interaction propre entre les protéines et le patch Ile44 est essentiel pour le bon déroulement des divisions cellulaires [177,188,189]. Le domaine hydrophobe représenté par le patch Ile36 est composé des acides aminés Leu8, Ile36, Leu71 et Leu73. Ce domaine permet de favoriser les interactions entre des chaînes de polyubiquitines et les HECT E3s, les déubiquitinases et certains UBDs [190-192]. Le troisième domaine hydrophobe est le patch Phe4 qui est formé par les acides aminés Gln2, Phe4 et Thr12 [189]. Ce patch est impliqué dans la régulation du transport protéique et est spécifiquement reconnu par les protéines ayant un UBD du type UBAN [191] et les déubiquitinases de la famille des USP [193]. Les deux patchs, Ile36 et Phe4 semblent être indispensables pour assurer des fonctions cellulaires vitales chez les levures [190]. Finalement, une autre région d'interaction avec les protéines est définie par le TEK box, utilisé lors de la formation des chaînes d'Ub K11. Ce domaine qui comprend, les acides aminés Thr12, Thr14, Glu34, Lys6, et Lys11, est requis pour l'assemblage des chaînes de polyubiquitines K11 catalysé par le complexe d'ubiquitine ligase APC/C afin d'initier la dégradation protéasomale des substrats au cours de l'exécution de la mitose [194].

1.4 Les Déubiquitinases

L'ubiquitination est parmi les modifications post-traductionnelles les plus dynamiques et complexes. De ce faite une régulation fine de cette modification est nécessaire afin d'exécuter les évènements de signalisations cellulaires et de garder le pool d'Ub dans les cellules. En effet, comme toute modification post-traductionnelle, l'ubiquitination est une réaction réversible et la réaction inverse de cette modification est catalysée par une famille de protéases, nommées les déubiquitinases (DUB). On compte à présent à peu près 100 DUBs

codées par le génome humain [154,195]. Les DUBs font partie de la superfamille des protéases. Les protéases sont regroupées en cinq familles selon leurs mécanismes de catalyse. Ainsi, on retrouve chez l'humain, les : aspartiques-protéases, métalloprotéases, sérine-protéases, thréonine-protéases et cystéine-protéases [196,197]. Les DUBs appartiennent aux cystéine-protéases et métalloprotéases avec une abondance plus importante pour les cystéine-protéases. Six familles de DUBs sont repertoriées selon la structure de leur domaine catalytique : (i) les cystéine-protéases incluant quatre familles et qui sont les *ubiquitin-specific proteases* (USP), les *Ubiquitin C-terminal hydrolases* (UCH), les *Ovarian tumor domain proteases* (OTU) et les *Machado-josephin domain proteases* (MJD) (ii) les métalloprotéases est représentée par l'unique famille des JAB1/MPN+/MOV34 (JAMM) et (iii) la toute nouvelle famille des DUBs récemment identifiée, la *Monocyte Chemotactic Protein-induced Protein* (MCIP) [154,195,198,199].

1.4.1 Rôles des déubiquitinases:

Les déubiquitinases admettent plusieurs rôles dans la régulation de la signalisation de l'Ub. En effet, (i) des déubiquitinases spécifiques comme l'enzyme USP5/IsoT permettent la maturation de l'ubiquitine et ce en générant des monomères libres d'Ub à partir soit de précurseurs d'Ub ou soit des fusions des monomères d'Ub avec les protéines ribosomales. De plus, les DUBs favorisent l'activation de l'Ub produite sous forme de précurseur et ce en éliminant le résidu additionnel au niveau de l'extension C-terminale de l'Ub. (ii) Les DUBs assurent le recyclage de l'Ub et ce en libérant des monomères d'Ub à partir des chaînes de polyubiquitines générées suite à la dégradation protéasomale des protéines (grâce à l'action des DUBs associées au protéasome comme USP14, UCHL5 et POH1). (iii) De manière similaire à la signalisation de la phosphorylation/déphosphorylation, la déubiquitination agit principalement pour contrecarrer l'action des ubiquitine ligases et donc renverser une signalisation dégradative ou non dégradative de l'ubiquitination. (iiii) De plus, certaines DUBs peuvent catalyser un changement de l'état de l'ubiquitination du substrat et ce en remplaçant une monoubiquitination par une chaîne de polyubiquitines [154,200] (**Figure 1.6**).

Comme l'ubiquitination, la déubiquitination est une voie de signalisation hautement contrôlée et est impliquée dans la régulation de plusieurs processus cellulaires à savoir, le contrôle du cycle cellulaire [201], la dégradation protéasomale et lysosomale des protéinées [202-

[204], la régulation de l'expression génique [205], la réponse aux dommages à l'ADN [206], la différentiation, la sénescence [207,208] [209]. De ce fait, des mutations de DUBs ont été reportées dans plusieurs maladies malignes incluant plusieurs types de cancer et les maladies neurodégénératives [77,210-212]. Depuis quelques années, les études se multiplient afin de mieux comprendre les rôles biologiques des DUBs dans la signalisation cellulaire. Néanmoins, nos connaissances quant aux mécanismes d'action, la reconnaissance spécifique du substrat et le rôle fonctionnel des DUBs restent à nos jours restreintes [154].

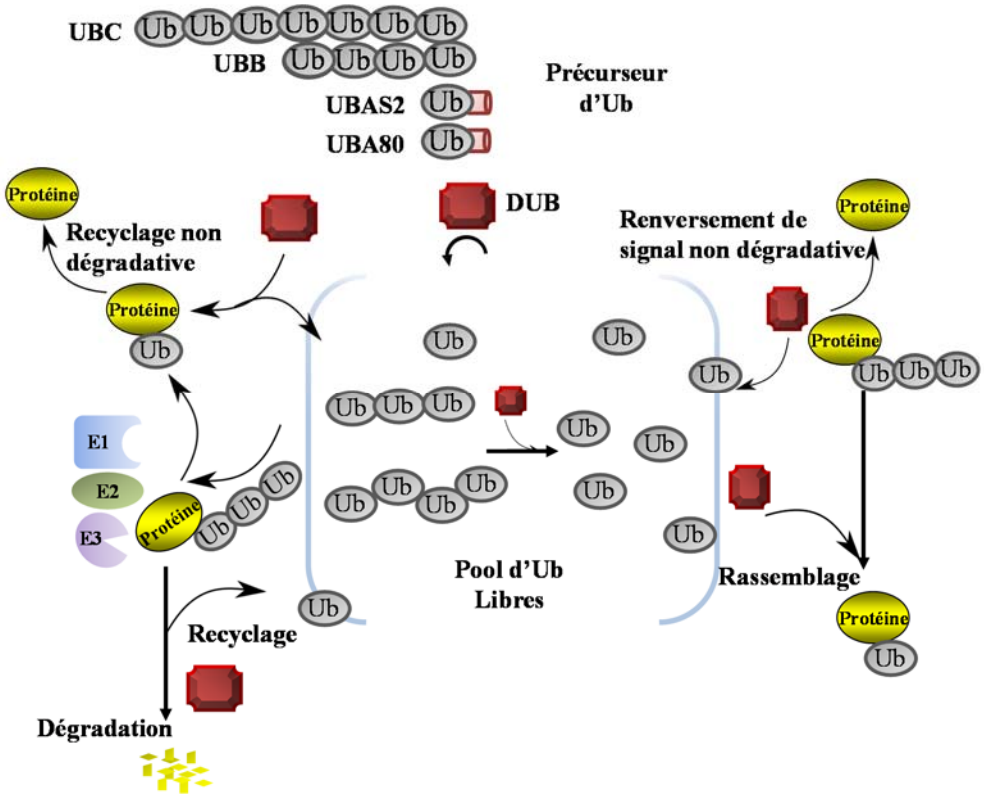

Figure 1.6 : Rôles des déubiquitinases au sein du système de l'ubiquitine : Représentation schématique des principales fonctions des DUB : génération d'Ub libres, renversement de signal dégradatif et non dégradatif, maintien du pool d'Ub, recyclage de l'Ub, maintien de l'homéostasie de l'Ub, changement de type de chaines d'Ub et de ce fait échanger un signal par un autre. (Modifiée de *Nature Reviews Molecular Cell Biology* **10**, 550-563 (August 2009)) [154].

1.4.2 Spécificité des déubiquitinases :

De par le nombre élevé de DUBs dans le génome humain, ces enzymes sont caractérisées par des spécificités élevées envers leurs substrats. En effet, les DUBs reconnaissent de manière

spécifique soit des monomères d'Ub ou des chaînes de polyubiquitines et ce grâce à leur domaines UBD [154].

Les DUBs ont une structure modulaire. En effet, en plus de leur domaine catalytique, elles contiennent des extensions N-terminales et C-terminales et des insertions de domaines requis pour la reconnaissance du substrat et la régulation de leur activité catalytique, de leur localisation subcellulaire ainsi que leurs interactions protéines/protéines [213]. Nous pouvons évoquer comme exemple, la DUB USP7 qui interagie directement avec ses substrats p53 et MDM2 par l'intermédiaire d'une séquence précise [214]. Comme exemple d'interactions indirectes avec le substrat, USP22 s'associe au complexe d'acétyltransférase SAGA (*Spt-Ada-Gcn5-acetyltransferase*) afin de pouvoir être recrutée sur la chromatine et assurer la déubiquitination de l'histone H2B qui est nécessaire pour l'initiation de l'élongation [215-217].

Les DUBs de la famille des JAMM, incluant la DUB associée au protéasome, POH1 (PSMD14), la DUB associée à la réparation des cassures doubles brins de l'ADN, BRCC36 et les DUBs régulatrices de l'endocytose, AMSH et AMSH-LP, présentent une préférence très élevée envers les chaînes d'ubiquitines liées via K63 [218,219]. Les chaînes d'ubiquitines K48 peuvent être reconnues par la DUB associée au protéasome, USP14 et la DUB appartenant à la famille des OTU, OTUB1 [220,221]. Un autre aspect unique de reconnaissance de chaînes de polyubiquitines est médié par USP5 (IsoT). En effet, grâce à son domaine UBP-ZnF, USP5 permet le désassemblement des chaînes de polyubiquitines K48 et K63 libres du fait qu'elle se lie particulièrement au niveau de la région C-terminale de l'ubiquitine non conjuguée à un substrat [192].

L'enlèvement de la monoubiquitination des substrats peut être catalysé par les DUBs de la famille des UCH comme BAP1 et UCH37 ainsi que la DUB USP16 appartenant à la famille des USP [222,223]. De plus, la monoubiquitination des substrats peut être sujette à une extension en chaînes d'ubiquitines par l'action de ligases E3 ou E4. Ce qui est aussi intéressant est que la DUB A20 se présente comme une hybride E3/DUB et est capable de catalyser un changement du type des chaînes d'ubiquitines et renverser ainsi le signal d'une ubiquitination non-dégradative (chaînes K63) vers un signal menant à la dégradation protéasomale (chaînes K48)

[224]. De plus, certaines DUBs peuvent avoir une dualité de spécificité. Comme exemple, USP21 est capable de cliver aussi bien NEDD8 que l'Ub [225].

1.5 Le gène suppresseur de tumeurs BAP1 (BRCA1 Associated Protein1)

BAP1 (*BRCA1 associated protein 1*) fait partie de la super-famille des DUBs et plus spécifiquement de la famille UCH des cystéines protéases.

BAP1 a été découvert pour la première fois pour son interaction avec le gène suppresseur de tumeurs BRCA1 (*Breast cancer-associated* 1) [226]. Cette étude a révélé suite à des expériences d'interactions double hybride chez la levure, que BAP1 interagi avec le domaine RING de BRCA1 par l'intermédiaire de son extension C-terminale. Dans cette même investigation, il a été proposé pour la première fois que la déubiquitinase BAP1 est un nouveau gène suppresseur de tumeurs. En effet, les auteurs ont identifié des mutations homozygotes au niveau du gène *bap1* dans une lignée cellulaire de cancer de poumons, NCI-H226 et ont également démontré que la surexpression de BAP1 augmentait l'activité suppressive de tumeurs de BRCA1 qui consistait à inhiber la prolifération cellulaire de cellules MCF7 du cancer du sein. De plus, une mutation de cancer L691P introduite au niveau du domaine C-terminale de BAP1 induit une diminution de l'interaction de BAP1 avec BRCA1 [226]. De manière plus significative, BAP1 interagi également avec BARD1 un partenaire majeur de BRCA1 requis pour l'activité ubiquitine ligase de BRCA1 [227]. En fait, BAP1 se lie avec BARD1 via une région qui se trouve adjacente à son domaine catalytique, UCH, au niveau N-terminale de la protéine. Depuis la découverte de BAP1 comme partenaire majeur de BRCA1/BARD1, aucune étude jusqu'à nos jours n'a élaboré la signification biologique de l'interaction BAP1/ BRCA1 à l'exception du groupe de Nishikawa et al., qui ont démontré que BAP1 interfère avec l'activité enzymatique de BRCA1/BARD1 et ce en dissociant la formation de l'hétérodimère de ce complexe ubiquitine ligase et que cette inhibition est indépendante de l'activité catalytique de BAP1 [227]. Sachant que le complexe BRCA1/BARD1 a une activité d'autoubiquitination, BAP1 est incapable de contrecarrer cette ubiquitination *in vitro*, mais aucune étude n'a montré cet effet *in vivo*. De ce fait, la relation BAP1/BRCA1 est

restée énigmatique. Néanmoins, la déplétion de BAP1 par shRNA bloque la mise en place d'une réponse cellulaire aux dommages à l'ADN et rend les cellules HeLa sensibles aux radiations ionisantes provoquant ainsi un retard au niveau de la progression du cycle cellulaire à travers la phase S, un phénotype typique de la déplétion de BRCA1. Une hypothèse peut ainsi en découler de ce phénotype est que l'ubiquitination médiée par le complexe BRCA1/BARD1 et la déubiquitination catalysée par BAP1 peuvent être deux phénomènes conjointement établis pour la régulation de la signalisation cellulaire suite aux dommages à l'ADN [228,229].

BAP1 est une protéine nucléaire qui se retrouve en association avec des complexes multi-protéiques ce qui suggère que BAP1 régule plusieurs voies de signalisations cellulaires. En effet, divers travaux récents ont spécifié que BAP1 est impliqué dans la régulation transcriptionnelle, la suppression de tumeurs, la régulation de la prolifération cellulaire [76,78,79,230-236], ainsi que la réparation des dommages de l'ADN par recombinaison homologue [229,237,238] (**Voir Annexe 1 et 3**).

1.5.1 Description du complexe BAP1 :

Plusieurs travaux incluant la première étude de notre groupe sur BAP1, ont identifié la composition du complexe BAP1 [78,233,234,239]. En effet nous avons démontrés par des expériences de filtration sur gel que BAP1 assemble plusieurs complexes multi-protéiques migrant à une taille de 1.6 MDa. En procédant par une purification d'affinité en tandem (TAP) suivie d'une analyse par spectrométrie de masse (MS), nous avons établis que BAP1 s'associe principalement à une multitude de facteurs transcriptionnels et de régulateurs de la chromatine (**Voir Annexe 1**). Les composants majeurs du complexe BAP1 sont le facteur transcriptionnel HCF-1 (*Host Cell Factor-1*), la OGT (*O-linked N-acetylglucosamine transferase*), les protéines Polycombe ASXL1 et ASXL2 (*polycomb group proteins additional sex combs like 1 and 2*), la démethylase d'histones LSD2 (*histone demethylase KDM1B*), les facteurs de transcription FOXK1 et FOXK2 (*forkhead transcription factors*) et l'histone acéthyltransferase HAT1 (*histone acetyl transferase 1*) [78,233,234,239]. Les composants les moins abondants mais qui ont été tout de même séquencé d'une manière consistante, sont le facteur

de transcription YY1 (*Yin Yang 1*) qui est aussi connu comme étant une protéine Polycombe et finalement l'ubiquitine conjugatrice hybride E2/E3, UBE2O [78,239].

Comme la plupart des déubiquitinases et malgré l'avancement de la recherche pour élucider de plus près les fonctions de ces enzymes, le rôle physiologique et les mécanismes d'actions de BAP1 restent très peu connus.

1.5.2 Structure de BAP1 :

En plus de BAP1, la famille des DUBs UCH contient les membres UCHL-1, UCHL-3 et UCHL-5 (UCH37). De manière similaire à toutes les UCHs, BAP1 possède au niveau de son extrémité N-terminale son domaine catalytique, le UCH. Ce domaine est très conservé et contient une triade d'acides aminés qui sont une cystéine, une histidine et un acide aspartique [240]. D'autre part, la région C-terminale de BAP1 s'avère d'une importance élevée pour la régulation fonctionnelle de celui-ci. En effet, on y retrouve au sein de son domaine CTD (C-terminal domain) des régions spécifiques d'interaction avec ses partenaires [78,241 209]. De plus, plusieurs modifications post-traductionnelles se retrouvent au niveau du CTD et du signal de localisation nucléaire, le NLS de BAP1 afin de moduler d'avantage la fonction de BAP1 [229,241] (**Figure 1.7**).

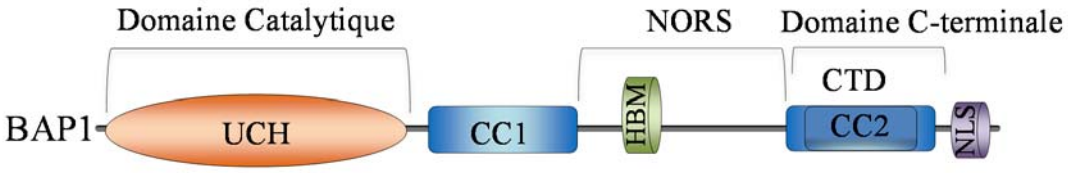

Figure 1.7 : représentation schématique de la structure de BAP1 : Les principaux domaines fonctionnels de BAP1, UCH, CC1, HBM et CTD ainsi que son signal de localisation cellulaire, le NLS sont présentés.

1.5.3 Relation fonctionnelle entre BAP1 et HCF-1 :

L'interaction BAP1/HCF-1 a été initialement déterminée grâce à une analyse par spectrométrie de masse des partenaires de BAP1 obtenus par immunoprecipitation suite à une surexpression de cette DUB [234]. Plus spécifiquement, BAP1 s'associe fortement avec HCF-1

au niveau de son domaine Kelch. Cette interaction est favorisée par la présence au niveau de BAP1 du motif de liaison à HCF-1, le HBM (*HCF-1 binding motif*) [78]. Par la suite d'autres études ont confirmés la présence abondante de HCF-1 dans le complexe BAP1 suggérant un rôle fonctionnel étroit entre BAP1 et HCF-1[78,233,239]. De plus, dans notre étude nous avons démontrés par des expériences d'immunodéplétion que tout BAP1 dans les cellules est complexé à HCF-1 alors qu'une faible proportion de ce dernier est associée avec BAP1 [78]. Ceci peut-être expliqué par le fait que HCF-1 est une protéine très abondante qui s'associe à la chromatine et est en complexe avec plusieurs facteurs et régulateurs transcriptionnels.

Sur le plan fonctionnel, il a été également suggéré que HCF-1 est un substrat de BAP1. En effet, deux groupes ont reporté qu'en surexprimant HCF-1 dans les cellules en présence de HA-Ub, celui-ci est poly-ubiquitiné au niveau de lysines spécifiques à l'intérieur de son domaine Kelch et que BAP1 est capable de reverser plus spécifiquement les chaînes K48 [233,239]. Ce qui est intriguant est que la modulation du niveau protéique de BAP1 par surexpression ou par déplétion en utilisant des RNAi, n'affecte pas la stabilité protéique de HCF-1 [234]. Néanmoins, les auteurs ont mis en place pour la première fois la relation fonctionnelle entre BAP1 et HCF-1. Ils ont pu démontrer que BAP1 régule la prolifération cellulaire de façon dépendante de son interaction avec HCF-1. En effet, la déplétion de BAP1 par RNAi provoque un retard de la prolifération cellulaire. Cet effet est également observé en surexprimant le mutant de BAP1 catalytique inactive, C91S, mais est aboli en présence du mutant de BAP1 C91S ΔHBM démontrant que l'interaction avec HCF-1 est essentielle pour la fonction de BAP1 dans la régulation de la prolifération cellulaire [234]. HCF-1 est requis pour promouvoir la progression du cycle cellulaire à la transition G1/S et ce en recrutant des méthyltransférase qui modifient H3K4 au niveau des promoteurs des gènes cibles de E2F1. De ce fait, il est plausible de dire que BAP1 agit pour accomplir cette fonction en régulant avec HCF-1 la transcription des gènes cibles de E2F à la barrière G1/S.

1.5.4 Rôle de BAP1 entant que régulateur transcriptionnel :

À l'issue de notre première investigation sur BAP1, nous avons pu élucider une partie du rôle fonctionnel de cette déubiquitinase. De manière mécanistique, nous avons démontré que BAP1 forme un complexe tertiaire avec HCF-1 et YY1 [78]. En effet, BAP1 interagi avec le

domaine à doigt de Zinc de YY1 via son domaine coiled coil qui se retrouve au niveau de son extension C-terminale. Même si l'interaction entre BAP1 et YY1 semble être transitoire, il a été possible de pêcher ce facteur de transcription par des expériences de co-immunoprecipitation. De plus, HCF-1 se lie avec YY1 au niveau d'une région riche en glycines et lysines et cette association est requise pour maintenir la formation du complexe tertiaire BAP1/HCF-1/YY1.

D'autre part, notre groupe a défini le profil d'expression des gènes (transcriptome) suite à une déplétion de cette DUB [78]. En effet, nous avons entrepri la technique de microarray afin d'analyser l'expression des ARNm en présence ou en absence de BAP1 (RNAi). Nous avons ainsi identifié une multitude de gènes dont le niveau d'expression a été dérégulé suite à la déplétion de BAP1. On compte des gènes requis pour la régulation du cycle cellulaire, la réponse aux dommages à l'ADN, l'apoptose, la survie cellulaire ainsi que le métabolisme cellulaire [78] (**Voir Annexe 1**).

Pour définir de plus près le rôle de BAP1 entant que régulateur transcriptionnel, nous avons pris comme exemple un gène dont l'expression a été grandement réduite lors de la déplétion de BAP1. Le gène *cox7c*, qui favorise le transport terminal des électrons au niveau de la mitochondrie, a été choisi du fait que YY1 est connu pour être impliqué dans la contrôle du métabolisme cellulaire à différents niveaux et intervient également dans la régulation de notre gène cible [242]. La déplétion de BAP1 ou de HCF-1 induit une diminution du niveau protéique de cox7c alors que le RNAi de YY1 provoque une activation de l'expression de ce gène. De manière plus significative, la déplétion de YY1 diminue la présence de BAP1 et de HCF-1 sur le promoteur du gène *cox7c* indiquant que YY1 est requis pour le recrutement du complexe de régulation transcriptionnel BAP1/HCF-1 sur les gènes cibles [78] (**Voir Annexe 1**). Il faut aussi noter que le complexe BAP1 contient d'autres facteurs de transcription comme FOXK1, FOXK2, NRF-1, la famille ETS des facteurs de transcription qui sont Elf-1, Elf-2 et Elf-3 [78]. Ces régulateurs transcriptionnels qui possèdent des séquences spécifiques de liaisons à l'ADN, peuvent avoir un rôle crucial dans la coordination du recrutement du complexe BAP1 sur des régions promotrices particulières du génome.

1.5.5 BAP1 est un gène suppresseur de tumeurs :

Depuis sa découverte et plus particulièrement durant les quinze dernières années, plusieurs évidences ont été établies démontrant que *BAP1* est un gène suppresseur de tumeurs [77,243]. BAP1 a été identifié comme étant une déubiquitinase qui interagit avec BRCA1. Le locus du gène *BAP1* se localise au niveau du chromosome 3p21.3, une région fréquemment déletée et remaniée au niveau des cellules cancéreuses [244]. En effet, il a été rapporté que des délétions au sein de cette région surviennent dans approximativement 30 à 60 % des cancers de mésothéliome, 85 % des cas de tumeurs de l'œil au stade de métastase et que des pertes d'hétérozygotie se produisent dans 80 % des carcinomes de sein, 90 % des carcinomes des poumons ainsi que la plupart des carcinomes rénaux [226,245]. Dans l'étude décrivant linteraction entre BAP1 et BRCA1, il a été identifié pour la première fois la perte des deux copies du gène *BAP1* [226]. D'autre part, BAP1 peut aussi agir indépendamment de BRCA1 [236]. Cette activité de suppression de tumeurs est toutefois dépendante de son activité catalytique et de sa localisation nucléaire [236,241]. De manière plus intéressante la déplétion de BAP1 par RNAi affecte de manière négative la prolifération cellulaire [227,233,234]. Toutefois, le mécanisme de régulation de cet effet reste inconnu.

- **L'inactivation de BAP1 prédispose au développement du ''syndrome de cancer de BAP1'' :**

De nombreuses autres études sont venues confirmer que BAP1 est un gène suppresseur de tumeurs majeur. BAP1 est muté et inactivé dans plusieurs types de cancers sporadiques et héréditaires [77,243]. En effet, de plus en plus, de nouvelles mutations somatiques et germinales de BAP1 sont diagnostiquées dans le mésothéliome, le mélanome de l'œil, les tumeurs melanocytiques de la peau, le carcinome rénale et les cancers du sein et des poumons. Ainsi, BAP1 représente la DUB la plus mutée et inactivée dans les cancers [226,230,231,235,246-250]. Il a été également reporté que BAP1 possède une activité anti-métastatique. En effet, une prévalence de mutations homozygotes de BAP1 se trouve dans 84 % des échantillons des tumeurs métastatiques de mélanomes de l'œil analysés. La déplétion de BAP1 dans ces cancers provoque un changement de la signature transcriptionnelle de ces cellules tumorales en phase I et permet de les ramener au stade II caractéristique des cellules en métastase. Plus particulièrement, le profil d'expression des ARNm révèle une augmentation de l'expression des gènes impliqués dans l'induction de l'invasion cellulaire à savoir CDH1 ainsi que

l'activation transcriptionnelle du proto-oncogène KIT, deux protéines généralement associés à l'invasion agressive des mélanocytes. Également, l'expression des gènes requis pour la différentiation normale des mélanocytes comme les gènes CTNNB1, EDNRB, et SOX10 étaient grandement diminuée [231].

Toutes ces études qui décrivent les mutations de BAP1 dans les différents cancers démontrent que le dysfonctionnement de cette DUB prédispose au développement du ''syndrome de cancer BAP1''. En effet, dans le but d'identifier les mutations qui seraient à l'origine du développement de mésothéliome, celles de BAP1 étaient parmi les altérations conférant un haut risque de développer la maladie. De plus, la chance de développer d'autres types de cancers est très élevée chez les patients porteurs de ces mutations. Ainsi, des mutations germinales hétérozygotes de BAP1 qui sont à l'origine de la production d'une forme prématurée et non fonctionnelle de BAP1 favorisent le développement ultérieur de cancers agressifs de mésothéliome, de mélanome de l'œil, de mélanome de la peau, d'un carcinome rénal et possiblement d'autres types de tumeurs [235]. De plus, les mêmes individus dépistés pour ces types de mutations présentent également une perte du deuxième allèle de BAP1 au niveau de ces tumeurs [235,249,251]. Des observations similaires ont été révélées par une autre étude soulignant l'incidence élevée de mutations de BAP1 dans des cas de cancers sporadiques de mésothéliome pleural malin (MPM). En effet BAP1 était inactivé dans 23 à 60 % des échantillons de tumeur analysés avec également une perte du deuxième allèle [235,247,252,253].

- **Inactivation de la fonction suppressive de tumeurs de BAP1 dans les malignités myéloïdes :**

Le rôle de BAP1 comme gène suppresseur de tumeurs dans les malignités myéloïdes a été récemment élucidé. En effet, un knockout constitutive chez la souri provoque une létalité précoce de l'embryon. Néanmoins, un knockout conditionnel de BAP1 à l'âge adulte induit par la recombinase *Cre*, sous ajout de tamoxifene, pouvait être généré. Les animaux développant une perte de BAP1, souffraient d'une anémie aigüe accompagnée après 4 semainees de l'injection du tamoxifene, de syndromes myélodysplasiques (SMD) et de leucémies myélomonocytaires chroniques (LMMC). Ceci était à l'origine de dérégulations de l'érythropoïèse et de thrombopoïèse [230].

- **Les différents types de mutations de BAP1 :**

BAP1 est sujet à de multiples types d'altérations génétiques. Ces mutations incluent des mutations faux-sens qui résultent de la substitution d'un nucléotide par un autre, des mutations non-sens provoquant l'apparition d'un codant stop, des insertions/délétions qui causent un décalage du cadre de lecture et de ce faite la production prématurée de la protéine, et des mutations dans des sites d'épissages [77,231,246,249,250,253-255]. Dépendamment du type de mutations ponctuelles et de l'endroit dans lequel elles se produisent, différentes conséquences fonctionnelles en découlent. Les mutations ponctuelles les plus caractérisées de BAP1 se produisent particulièrement au niveau du UCH, du CTD ou encore au niveau du signal de localisation nucléaire (NLS) (**Figure 1.8**). Pour ce qui est du UCH, les mutations affectent soit les acides aminées qui composent la triade catalytique (C91, H169, D184) ou des acides aminés dans le voisinage immédiat du site catalytique (F81, A95, S172) [77,231,246,249-251,253-255]. Les mutations au niveau du CTD pourraient affecter l'interaction de BAP1 avec ses partenaires et de ce fait son habilité à intégrer des complexes multi-protéiques. De point de vue fonctionnel, nous avons démontré récemment qu'une délétion de quatre acides aminées au niveau du CTD de BAP1, R666-H669 [231], abolie spécifiquement son interaction avec les deux protéines Polycombes du complexe, ASXL1 et ASXL2. La perte d'interaction entre BAP1 et ces deux protéines inhibe son activité catalytique envers son substrat H2A K119 monoubiquitiné. Ceci a pour conséquence de perturber la fonction suppressive de tumeurs de cette DUB entant que régulateur de la prolifération cellulaire [209]. Les mutations ponctuelles au niveau du NLS de BAP1 auraient ainsi pour conséquence sa rétention dans le cytoplasme. À la lumière de ceci nous avons établi que des délétions/insertions au niveau du domaine C-terminale de BAP1 (Δ631-634 et Δ637-638InsN), favorisaient sa séquestration cytoplasmique. De manière plus intéressante, ces mutations ne semblent pas affecter l'activité catalytique de BAP1 envers H2A ubiquitiné démontrant que la perte de la fonction suppressive de tumeurs de BAP1 peut être causée par une localisation subcellulaire non appropriée de BAP1 [241] (**Voir Annexe 2**).

Il est également aussi important de signaler la présence d'autres mutations de BAP1 au niveau de son large domaine présent entre le UCH et le CTD. Cette région ne possède pas une caractéristique structurelle bien définit (NORS) mais contient le domaine HBM requis pour sa

liaison avec HCF-1. Ainsi, des mutations au niveau du HBM ont été reportées au sein d'un carcinome rénal aboutissant à la perte de l'interaction de BAP1 avec HCF-1 et de ce faite de son activité anti-prolifération[250].

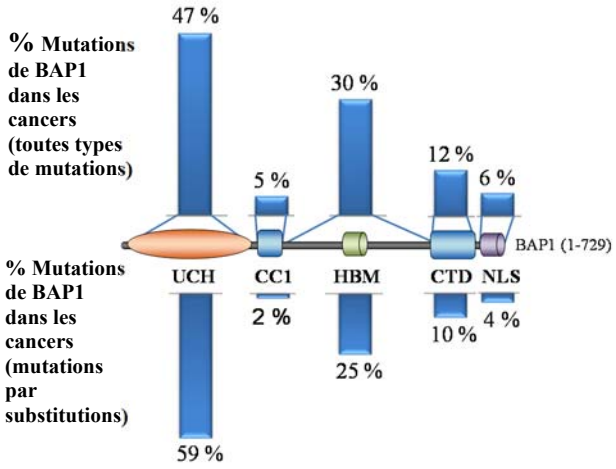

Figure 1.8 : Fréquence des mutations de cancer de BAP1 répertoriées au sein de ses domaines fonctionnels : Les mutations ont été prises à partir de la base de données COSMIC (Catalog of Somatic Mutations in Cancer) et alignées avec les domaines de BAP1.

1.6 Le cofacteur transcriptionnel HCF-1 (Host Cell Factor 1)

Il y a maintenant à peu près une vingtaine d'années depuis la découverte de HCF-1, la protéine la plus abondante dans le complexe BAP1. HCF-1 a été initialement isolée comme étant un cofacteur transcriptionnel du *herpes simplex virus-1 (HSV-1) transactivation factors VP16* et le facteur cellulaire POU2F1. HCF-1 joue un rôle crucial dans l'induction de l'expression virale des gènes immédiats précoces (*immediate early genes*) *(IE)*. En effet, HCF-1 s'associe à la chromatine avec différents complexes de remodelage de la chromatine et permet ainsi de recruter plusieurs facteurs transcriptionnels au niveau des promoteurs des gènes IE afin de moduler leur potentiel transcriptionnel [256-259]. En plus de son rôle comme activateur virale, HCF-1 est maintenant bien identifié comme un régulateur majeur de

plusieurs voies de signalisation cellulaires à savoir, la progression du cycle cellulaire, le métabolisme, l'épissage de l'ARN et la coordination du rythme circadien [258-269].

1.6.1 Caractéristiques de la structure de HCF-1 :

La structure de HCF-1 est très particulière. Plusieurs régions structurales et fonctionnelles distinctes peuvent être définies. Le domaine N-terminale de HCF-1 contient le domaine Kelch qui est composé de cinq régions répétitives de *β-propeller-like*. Ce domaine qui participe à établir des interactions protéines/protéines permet de spécifiquement lier HCF-1 à ses partenaires via leur domaine de liaison à HCF-1, le motif de liaison à HCF-1 (*HCF-1 binding motif*), HBM. Cette petite région d'acides aminés contient une séquence consensus, [E/D]-H-X-Y et se retrouve au sein de plusieurs facteurs de transcription et régulateurs épigénétiques dont le coactivateur de la réponse HSV virale VP16, les facteurs de transcription PGC-1, LZIP, E2F1/3/4, THAP1-4, Krox20, la méthyltransférase MLL5, et BAP1 [258,264,270-274]. Un autre domaine requis pour favoriser des interactions protéines/protéines, est le domaine Basic adjacent au domaine Kelch. En plus, des interactions intramoléculaires, ce domaine favorise l'interaction de HCF-1 avec la protéine SIN3A (*SIN3 Transcription Regulator Family Member A*), la O-linked N-acétylglucosamine transférase (OGT) [259,275], et les facteurs de transcription GABP2 [267] et ZBTB17 [276].

Entre les régions N-terminale et C-terminale, HCF-1 contient un domaine unique de clivage protéolytique nommé, PPD (*proteolytic processing domain*). Ce domaine critique permet, en plus des interactions protéines/protéines, d'assurer la maturation protéolytique de la protéine, un mécanisme indispensable pour la fonction biologique de HCF-1. Les protéines connues pour interagir avec le PPD sont le co-activateur/co-represseur *four-and-a-half LIM domain-2* (FHL2) et la OGT [275,277]. L'extension C-terminale de HCF-1 comprend la région acidique et un tandem de domaines de fibronectine de type 3 : FN3-1 et FN3-2. Des travaux ont révélé que le domaine C-terminale est impliqué dans les interactions avec la protéine phosphatase 1 (PP1) [260] et la protéine PDCD2 qui sont deux régulateurs négatifs de la prolifération cellulaire [278] (**Figure 1.9**).

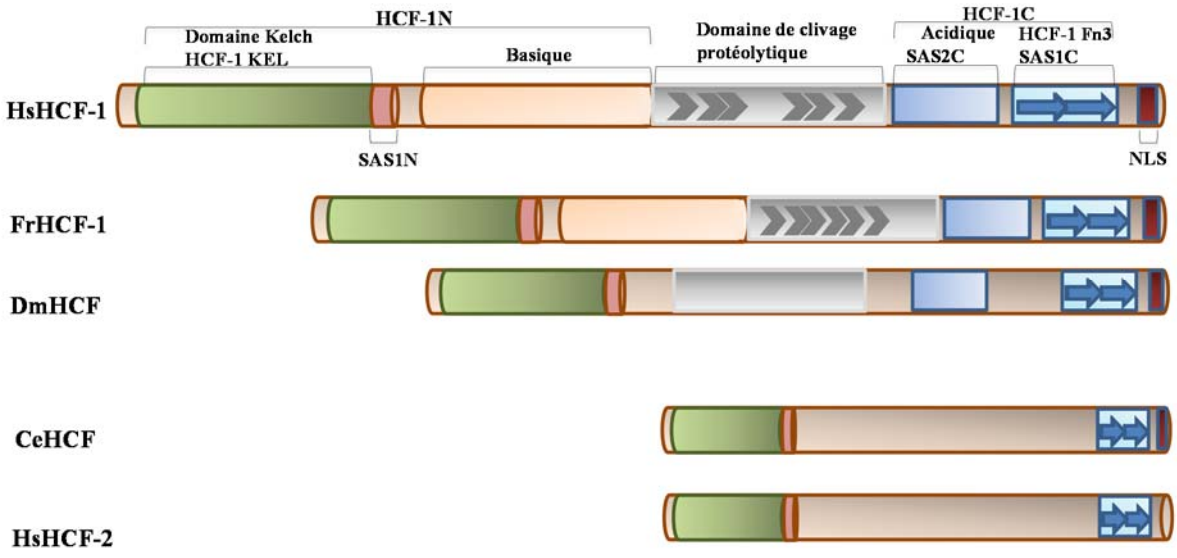

Figure 1.9 : Représentation schématique de la structure de HCF-1 de différentes espèces : Description des domaines qui sont conservés au niveau des protéines de la famille de HCF. HsHCF-1 (Human HCF-1), FrHCF-1 (fish Fugu rubripes HCF-1), DmHCF (Drosophila melanogaster DmHCF), CeHCF (Caenorhabditis elegans CeHCF), HsHCF-2 (Human HCF-2). (Modifiée de Trends Biochem Sci. 2003 Jun;28(6):294-304) [259].

1.6.2 Processus de maturation protéolytique de HCF-1 :

HCF-1 est synthétisé sous forme d'un long précurseur de 300 KDa qui par la suite subit rapidement un processus de protéolyse au niveau de son domaine centrale, le PPD [258,271,277,279]. Ce domaine contient 8 réitérations de 20 acides aminés. Six de ces répétitions sont des sites de clivage actifs et permettent la génération de plusieurs fragments N-terminaux et C-terminaux de différents poids moléculaires [258,271,277,279]. Suite à ce processus de maturation, il s'est avéré que les fragments polypeptidiques N-terminaux et C-terminaux de HCF-1 restent fortement associés. Cette interaction est contribuée par les séquences, *self-association sequences* (SAS). Le SAS-N au niveau N-terminale de HCF-1 se retrouve adjacent au domaine Kelch alors que le C-terminale SAS-C se localise au niveau du domaine FN3-1. Le mécanisme de l'auto-association entre les domaines SAS-N et SAS-C a été récemment identifié et démontre que cette interaction est requise à la bonne formation du complexe de transactivation Oct1/VP16/HCF-1 [280].

Tous les domaines fonctionnels de HCF-1, le domaine Kelch, les motifs SAS, les domaines FN3 et les domaines Basic et acidic sont très conservés au sein des espèces des métazoaires. Ce qui est intéressant est que le processus de maturation protéolytique de HCF-1 est spécifique à tous les ortologues de HCF-1 à l'exception de HCF-1 de *Caenorhabditis elegans* (CeHCF) [281]. De plus, le mécanisme de clivage protéolytique de HCF-1 semble être différent parmi les métazoaires. En effet, HCF-1 de la *Drosophile*, dHCF-1 subit un processus de maturation différent de celui de HCF-1 des cellules de mammifères. dHCF-1 ne comporte pas un domaine PPD mais plutôt un site de clivage spécifique à la taspase-1 requis pour sa protéolyse [282]. Le clivage protéolytique de HCF-1 est une modification post-traductionnelle indispensable pour l'établissement de la fonction biologique de la protéine. En effet, il est bien défini que la maturation de HCF-1 est critique pour assurer le rôle de ce cofacteur transcriptionnel comme régulateur transcriptionnel et pour garantir une progression adéquate du cycle cellulaire à travers la mitose [266,275] . De manière plus spécifique, nous avons contribué à la découverte d'un mécanisme de régulation unique entre HCF-1 et OGT qui met en évidence un rôle indispensable de la O-GlcNAcylation dans le clivage protéolytique propre de HCF-1 [275,283,284] (**Voir Discussion**).

1.6.3 HCF-1 est un régulateur majeur du cycle cellulaire :

HCF-1 est une protéine nucléaire très abondante dans les cellules. Pour exercer ses fonctions biologiques, HCF-1 s'associe avec des activateurs transcriptionnels comme les complexes MLL1, MLL5, SETD1, les complexes d'acétyltransférase MOF-NSL, les 5-méthylcytosine hydroxylase TET2/3 (*Ten-Eleven Translocation*), les histones déméthylases LSD1 et JMJD2 et le complexe de remodelage de la chromatine CHD8. D'autre part HCF-1 se retrouve également au sein de complexes répresseurs à savoir, les complexes de déacethylases SIN3A/HDAC1/2 et THAP1/HDAC3 [270,272,285-289]. De plus, HCF-1 admet un rôle dans le maintien de la structure de la chromatine et ce en recrutant au niveau de l'ADN des facteurs d'assemblage de la chromatine et des chaperonnes (les chaperonnes des histones H3/H4 Asf1a et Asf1b) [290]. Il est important de signaler que tous les complexes multi-protéiques propres à HCF-1 contiennent des quantités importantes de OGT qui constitue un élément crucial pour maintenir la stabilité et la fonction de ces complexes [78,286-288,291].

De point de vue fonctionnel, HCF-1 joue un rôle principal dans la régulation du cycle cellulaire. En effet, il est bien établi que HCF-1 coopère avec les facteurs de transcription E2F pour le control de la progression du cycle cellulaire notamment au cours de la transition G1/S. Les facteurs de transcription E2F jouent un rôle crucial dans la modulation de la transcription de leurs gènes cibles lors de l'initiation et la progression de la phase S du cycle cellulaire [270,288]. Ces facteurs transcriptionnels incluent des activateurs comme E2F1 et E2F3 et des répresseurs comme E2F4. Afin d'exécuter sa fonction, HCF-1 permet le recrutement de complexes transcriptionnels spécifiques sur les gènes cibles des E2Fs. En effet, HCF-1 s'associe avec les complexes MLL/SETD1 afin de promouvoir H3K4me3 sur les promoteurs des gènes cibles de E2F1/3 durant l'initiation de la phase S. Pour agir comme répresseur transcriptionnel, HCF-1 interagi avec E2F4 afin de permettre le recrutement du complexe répresseur HDAC/Sin3A sur les promoteurs des gènes cibles [270,288].

1.7 La O-linked N-acétylglucosamine transférase, OGT

La O-linked N-acétylglucosamine transférase (OGT), est une enzyme essentielle qui s'exprime de manière ubiquitaire au niveau des cellules eucaryotes est qui catalyse la O-GlcNAcylation. Cette modification post-traductionnelle correspond à l'addition d'une seule molécule de monosaccharide de N-acétyl glucosamine (O-GlcNAc) au niveau des groupements hydroxyles des résidus thréonines et sérines des protéines [292-294] (**Figure 1.10**).

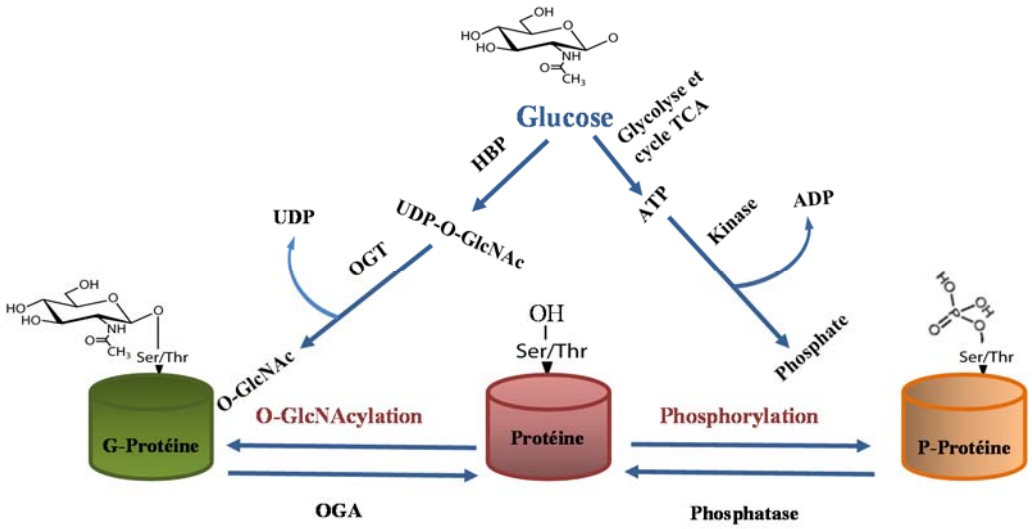

Figure 1.10 : O-GlcNAcylation et phosphorylation des protéines. : La OGT et les kinases modifient respectivement, par O-GlcNACylation et phosphorylation les mêmes résidus sérines et thréonines des protéines. G-protéine (*O-GlcNAcylated protein*). Glc (glucose), HBP (*Hexosamine Biosynthetic Pathway*), UDP (*Uridine di-phosphate N-Acetylglucosamine*), O-GlcNAc (*O-Linked N-acetylglucosamine*), P- protéine (*phosphorylated protein*), TCA (*tricarboxylic acid*). (Modifiée de Proc Natl Acad Sci U S A. 2012 Oct 23;109(43):17319-20) [295].

Les réactions de glycosylation ont été largement définies comme étant des réactions complexes contribuant à l'ajout de chaînes d'hydrate de carbones au niveau des résidus sérines et thréonines des protéines (il s'agit dans ce cas de la O-glycosylation) ou des acides aminés arginines (pour la N-glycosylation). Ces modifications ne sont pas réversibles et ne se produisent que dans certains compartiments cellulaires à savoir, le réticulum endoplasmique ou l'appareil de Golgi. La O-GlcNAcylation, contrairement aux réactions de glycosylation classiques, modifie les protéines nucléaires et cytoplasmiques. Elle n'implique pas une extension en chaînes du monomère d'O-GlcNAc et de ce fait représente une sorte de modification unique [296-298].

De nos jours plus des milliers protéines nucléocytoplasmiques ont été répertoriées comme étant des substrats de la OGT. Ceci démontre que la O-GlcNAcylation est étroitement impliquée dans la régulation de pratiquement tous les processus cellulaires [292-294,299-304] (**Figure 1.11**). Il a été longtemps admis que la OGT est la seule et unique enzyme capable de catalyser la O-GlcNAcylation. Récemment, une étude a révélé l'existence d'une nouvelle enzyme, la e-OGT, qui est également responsable de la modification par O-GlcNAcylation des

protéines de la matrice extracellulaire [305]. Cependant, la OGT reste l'unique enzyme capable de catalyser la O-GlcNAcylation des protéines intracellulaires [292,293,301-304].

La plupart des sites modifiés par O-GlcNAcylation sont également des sites de phosphorylation indiquant que la O-GlcNAcylation joue un rôle majeur dans le contrôle de la cascade de signalisation des kinases [306-308] (**Figure 1.10**).

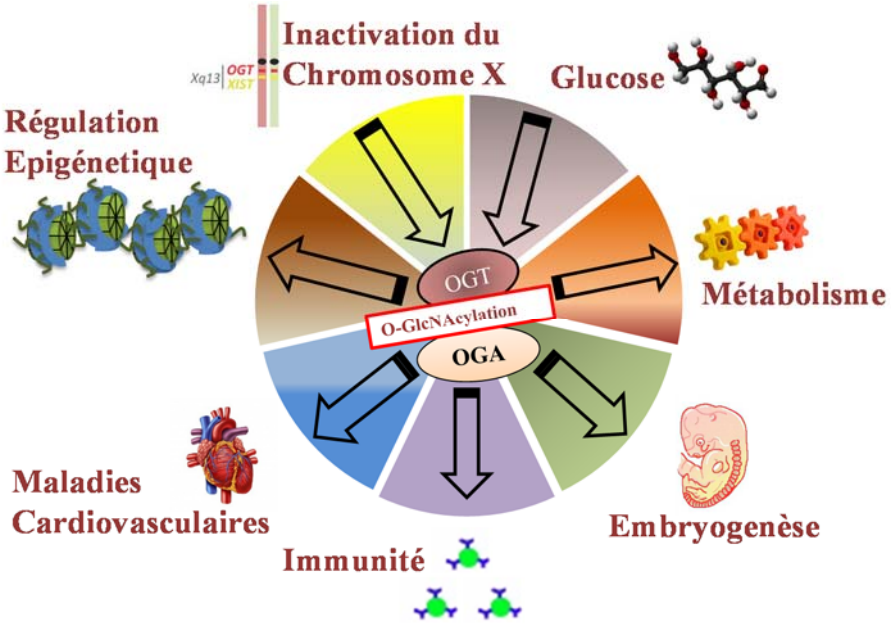

Figure 1.11 : La O-GlcNAcylation est impliquée dans la régulation de tous les processus cellulaires : Les fluctuations de la balance énergétique dans les cellules permet de lier la O-GlcNAcylation à la régulation d'une multitude de voies de signalisation cellulaires incluant la dégradation des protéines, la régulation des réponses immunitaires, la régulation de la mémoire épigénétique, la modulation du rythme circadien et la transcription génique. Des défauts métaboliques lies à des variations du niveau de O-GLcNAC cellulaire sont à l'origine de développement de plusieurs maladies malignes. (Modifiée de J Genomics 2014; 2:77-88. doi:10.7150/jgen.8123) [309].

1.7.1 Structure de la OGT :

OGT est une enzyme très conservée et est retrouvée chez tous les organismes métazoaires. Une enzyme similaire a été aussi identifiée chez les bactéries [310]. Chez l'humain, OGT est traduite sous forme d'un polypeptide de 1028 acides aminés comprenant 11.5 séquences répétitives de tétratricopeptides (TRP) au niveau de son domaine N-terminale et un multi-domaine catalytique au niveau de sa région C-terminale (CDI et CDII) (**Figure 1.12**). Le domaine TRP représente une plateforme pour des interactions protéines/protéines et assure la détermination de la sélectivité envers les substrats [311-315]. OGT a été prédite comme étant une glycosyltransférase appartenant à la superfamille des glycosyltransférase GT-B. La particularité de la OGT est qu'elle est l'unique enzyme parmi les GT-B à être capable de catalyser la O-GlcNAcylation de substrats polypeptidiques [316]. La région catalytique de OGT contient trois domaines distincts, un domaine N-terminale (N-Cat), un domaine C-terminale (C-Cat) et un domaine intermédiaire (Int-D). Ce dernier est un domaine de 120 acides aminés dont la structure est indéterminée [317]. De plus, ce qui distingue OGT, est la présence au niveau de sa région catalytique d'un domaine PPO (*PIP-binding domain of OGT*) de liaison au phosphatidylinositol (3,4,5)-trisphosphate (PIP3) permettant ainsi sa translocation à la membrane plasmique suite à l'induction de la voie de signalisation de l'insuline [318].

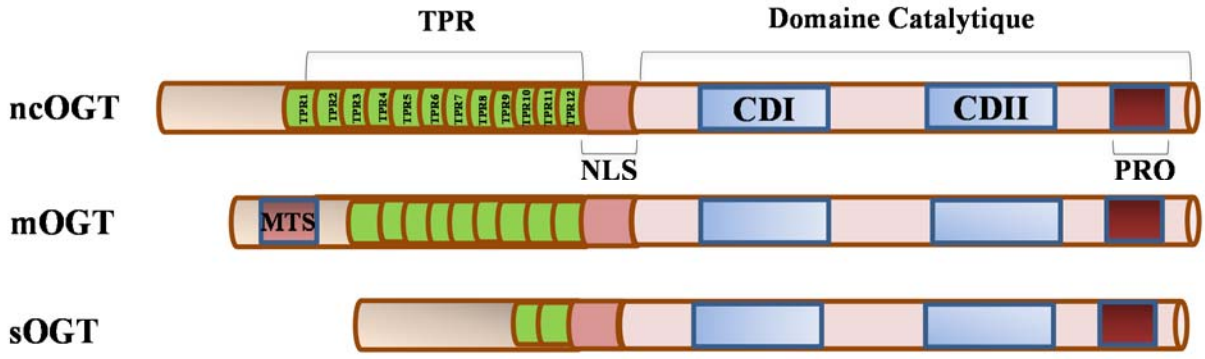

Figure 1.12 : Les différents isoformes de la OGT : Les trois isoformes de la OGT qui sont produits dans la cellule diffèrent selon la longueur des séquences de TRP. La forme nucléaire (ncOCT) comprend 12 TRP, la OGT mitochondriale (mOGT) en contient 9 et la forme la plus courte (sOGT) comprend uniquement 3 TRP. TRP (Tétratricopeptides), MTS (Séquence de ciblage mitochondrial) CD (domaine catalytique). (Modifiée de Nature Reviews Molecular Cell Biology 13, 312-321 (May 2012) et de Trends Endocrinol Metab 24 (6):301-9 Juin 2013) [319,320]

1.7.2 La O-GlcNAcylation est un régulateur majeur du métabolisme

La O-GlcNAcylation joue un rôle primordial dans la régulation des interactions protéines/protéines, la modulation de l'activité enzymatique, la stabilité protéique ainsi que la localisation subcellulaire des protéines [302-304]. De plus, cette modification est une modification très dynamique. Ainsi, la O-GlcNAcylation est sujette à plusieurs types de régulations gouvernées par une multitude des signalisations extracellulaires et intracellulaires incluant la signalisation des facteurs de croissance, la fluctuation intracellulaire de la concentration en glucose et de nutriments ainsi que la réponse cellulaire aux différents stress [302-304,321]. En effet, une fraction de 2 à 5% de la quantité cellulaire en glucose est directement acheminée vers la voie de biosynthèse de l'hexosamine (HBP, *Hexosamine Biosynthetic Pathway*) pour la production de l'UDP-N-Acétyl-glucosamine (UDP-GlcNAc), substrat de la OGT [304,321,322]. Cette signalisation incorpore plusieurs voies métaboliques majeurs à sa voir, le métabolisme du glucose, des acides gras, des acides aminés et des nucléotides [304,321,322]. L'UDP-GlcNAc se place ainsi comme étant un « senseur métabolique » qui participe à la modification des protéines en fonction du changement métabolique en glucose (**Figure 1.10** et **Figure 1.13**).

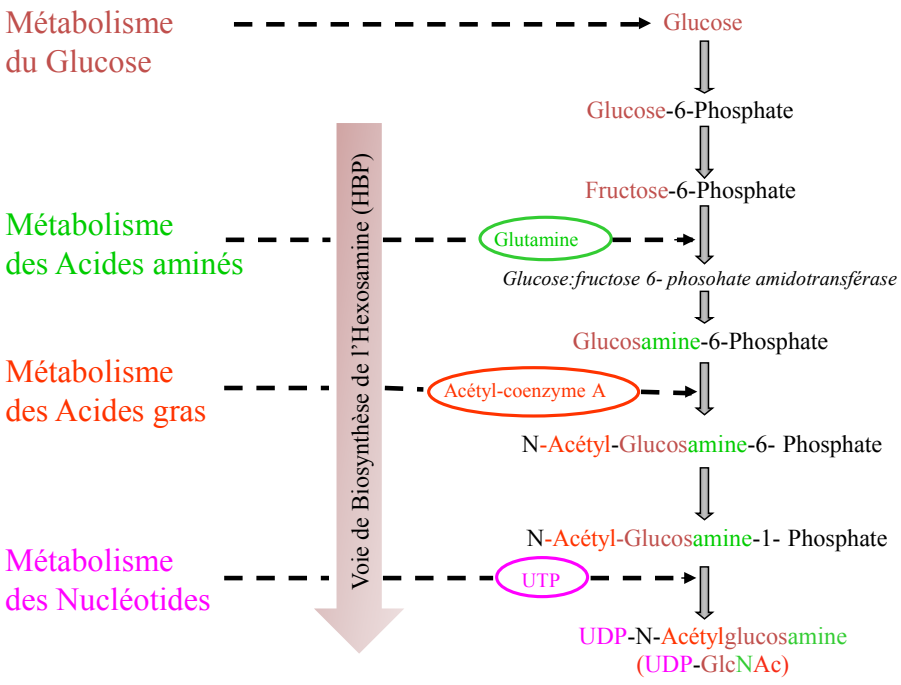

Figure 1.13. La O-GlcNAcylation des protéines et la voie de synthèse de l'hexosamine HBP : La voie de HBP incorpore les voies métaboliques majeures (métabolisme du glucose, des acides gras, des acides aminés et des nucléotides) pour la production de l'UDP-GlcNAC, substrat de la OGT. (Modifiée de Annu. Rev. Biochem, 2011. 80:825-858) [304].

De ce fait, cette relation étroitement régulée entre la disponibilité de l'UDP-GlcNAc et la O-GlcNAcylation des protéines cibles, peut engendrer des réponses cellulaires différentes allant de la modulation de la signalisation au niveau des membranes plasmiques jusqu' à la régulation des réponses immunitaires, la dégradation des protéines, la régulation de la mémoire épigénétique, ainsi que la modulation du rythme circadien et de la transcription génique [303,304,316,318,321,323] (**Figure 1.11)**. De ce fait, des défauts dans les mécanismes de régulation de la O-GlcNAcylation ont été reporté dans de nombreuses maladie humaines malignes comme les maladies neurodégénératives, le diabète et différents types de cancer [308,318,323-331]. Pour justifier davantage l'implication de la O-GlcNAcylation dans la modulation du métabolisme, il a été démontré qu'une hyper O-GlcNAcylation des protéines cellulaires catalysée par la OGT se produit au niveau des cellules cancéreuses caractérisées par une absorption excessive de glucose ou suite à l'hyperglycémie survenant lors du diabète [307,320,321,327,332-335]. De ce fait, il devient urgent de penser à développer des stratégies thérapeutiques basées sur la modulation de l'activité catalytique de la OGT et ce afin d'améliorer le diagnostic et le traitement de cancers et d'autres pathologies sévères.

1.7.3 La O-GlcNAcylation est une réaction réversible :

La O-GlcNAcylation est une modification réversible, et cette réaction hydrolytique est catalysée également par une enzyme unique, la N-Acétyl-β-D glucosaminidase (O-GlcNAcase ou OGA). La OGA est également une enzyme très conservée et présente une structure très particulière. En effet, en plus de son domaine catalytique, le domaine glucosaminidase (GlcNAcase) au niveau N-terminale, OGA possède un autre domaine distinct au niveau de son extension C-terminale qui ressemble au domaine catalytique de l'histone acétyltransférase GCN5 [336-339]. Ceci suggère que OGA possède une activité bi-fonctionnelle du fait qu'elle pourrait en plus de son activité glucosaminidase, promouvoir l'acétylation des protéines cibles.

Cependant malgré cette dualité enzymatique, les mécanismes d'action de la OGA reste encore peu connus.

1.7.4 OGT est un facteur essentiel de la régulation transcriptionnelle :

De nombreuses études ont défini que la O-GlcNAcylation joue un rôle primordiale dans la régulation de l'épigénome [292,340]. En effet, plusieurs facteurs et co-régulateurs transcriptionnels ainsi que des enzymes de modification de la chromatine sont des substrats de la OGT. Ceci a pour effet de moduler leur recrutement au niveau de la chromatine, leur stabilité, leur activité ainsi que leur assemblage au sein de complexes régulateurs fonctionnels [302,341-343]. Plus spécifiquement, OGT s'associe avec HCF-1 à des complexes activateurs comme les complexes MLL1, MLL5, SETD1, les complexes des 5-méthyl cytosine désoxygénasses TET1/2/3 et les complexes d'acétyltransférase MOF-NSL. OGT peut aussi se retrouver au sein de complexes répresseurs comme le complexe de la déacethylase d'histones, SIN3A [285-287,342-344].

1.7.5 OGT et la régulation épigénétique:

Récemment, il a été révélé que la OGT chez la *Drosophile* est codée par le gène exprimant la protéine Polycombe Super Sex Combs (SXC) [345,346]. SXC est recrutée au niveau des clusters des gènes *Hox* pour permettre la répression de la transcription. De plus, la perte d'expression de la protéine SXC engendre une de-répression des gènes *Hox* résultant à une transformation homéotique de multiples segments durant le développement précoce de la *Drosophile* [347]. De même, des mutations hétérozygotes du gène *sxc*, contribuent à des transformations homéotiques sévères aboutissant à une létalité tardive des mutants au stade pupe [345,346]. De plus, le knockout de la OGT dans la souris cause une létalité embryonnaire précoce délignant l'importance critique de cette enzyme au cours du développement de l'organisme vivant [348,349]. Ce qui est très intéressant est que les phénotypes observés suite aux mutations du gène *sxc* peuvent être reversés par une réintroduction de la OGT humaine, soulignant ainsi la conservation fonctionnelle de celle-ci durant l'évolution [348,349]. Les évidences se succèdent pour démontrer le rôle de la OGT comme régulateur épigénétique. Des données relativement récentes suggèrent que trois protéines Polycombe du complexe PRC1 peuvent être des

substrats potentiels de OGT chez la *Drosophile* [345]. Il a été aussi établi que OGT interagit directement avec le complexe Polycombe PRC2 par l'intermédiaire de EZH2. De plus, OGT joue un rôle primordial dans le maintien de la fonction et la stabilité protéique de EZH2 en assurant sa O-GlcNAcylation. En effet, la déplétion de OGT engendre une déstabilisation protéique de la forme non modifiée de EZH2 ainsi qu'une diminution du niveau global de H2K27me3 dans les cellules [350].

Un autre aspect de régulation transcriptionnelle médié par OGT est défini par sa relation fonctionnelle avec la famille des protéines TET. TET1, TET2 et TET3 sont les seules enzymes connues pour catalyser la déméthylation de l'ADN et ce par la conversion du 5-methyl-cytosine (5mC) en 5-hydroxy-methyl-cytosine (5hmC) [68]. Ainsi, de nombreuses études ont rapporté que OGT interagit avec et modifie par O-GlcNAcylation TET1/2/3. Cette modification ne semble toutefois pas affecter l'activité catalytique de ces déméthylases de l'ADN. En contrepartie, TET1/2/3 sont requises pour le recrutement de OGT sur la chromatine, qui elle, permet de réguler l'expression de TET1 et de maintenir le niveau du 5hmC au niveau des promoteurs des gènes cibles [285,351-355].

- **La O-GlcNAcylation et le code de l'histone:**

Ce qui a augmenté d'avantage la popularité de la OGT dans le domaine de l'épigénétique, est le fait d'avoir intégré la O-GlcNAcylation dans le « code de l'histone ». En effet, plusieurs études récentes ont reporté que OGT pouvait directement cibler les histones et de ce fait catalyser une nouvelle marque épigénétique au niveau de la chromatine [20,21,351,356,357]. L'implication de la OGT dans la modification des histones a été suggérée pour la première fois avec le travail de Sakabe et Hart qui ont proposé que H2A, H2B et H4 seraient modifiées par O-GlcNAcylation au niveau des sites Thr101, Ser36, et Ser47 respectivement [21,358]. D'autres études ont également reportées la modification des quatre histones au niveau des cellules HEK293 [68,351,359]. En outre, la O-GlcNAcylation de H3S10 a été également présentée. Cette modification semble rentrer en compétition avec la phosphorylation de H3 sur le même résidu. Il a été ainsi suggéré que la O-GlcNAcylation de H3 pourrait réguler l'état transcriptionnel de la chromatine durant la progression du cycle cellulaire [68,360]. Il est aussi éminent de signaler que la plupart des sites de O-GlcNAcylation des histones se retrouvent dans la région

globulaire du nucléosome suggérant que ces modifications pourraient avoir un rôle dans le maintien de la structure de la chromatine [357]. Ultérieurement, Fujiki et ses collègues ont reporté trois nouveaux sites de O-GlcNAcylation de H2B, Ser91, Ser112 et Ser123. Plus particulièrement, ils ont suggeré que la O-GlcNAcylation de H2B Ser112 promouvait la monoubiquitination de H2B au niveau de la lysine K120 (H2B K120ub) proposant ainsi une possible association de cette modification avec l'activation de la transcription [20]. De plus, un des travaux a reporté que l'interaction entre TET2 et OGT pouvait être requise pour favoriser la O-GlcNAcylation de H2B au niveau de la Ser112 [351].

1.7.6 Le complexe OGT/HCF-1/BAP1 est un régulateur de la gluconéogenèse:

Concernant la relation fonctionnelle entre OGT et le complexe BAP1, Ruan et ses collègues ont révélés que le complexe OGT/HCF-1/BAP1 est un ‘‘senseur’’ métabolique et un facteur important pour le contrôle de la gluconéogenèse. En effet, la modulation du niveau de glucose permet à HCF-1/OGT/BAP1 de se lier au coactivateur transcriptionnel PGC1α, un régulateur majeur de la biogenèse mitochondriale et la gluconéogenèse hépatique. L'action conjointe de OGT et de BAP1 permet la stabilisation protéique de PGC1α et ce en catalysant son O-GlcNAcylation et sa déubiquitination afin de prévenir sa dégradation protéasomale [261]. Une autre étude de Dey et ses collègues, a pu mettre en évidence qu'il existe une régulation protéique entre BAP1 et HCF-1/OGT du fait que le knockout de BAP1provoque une diminution du niveau protéique de HCF-1 et de OGT. De plus, dans cette même étude il a été révélé pour la première fois que OGT est un substrat de BAP1 puisque le complexe de déubiquitinase BAP1/ASXL1 purifié à partir des cellules Sf9 catalyse *in vitro* la déubiquitination de OGT [230]. Ces résultats suggèrent qu'il y aurait une régulation concertée au sein du complexe BAP1/HCF-1/OGT du fait que par le biais de la stabilisation protéique de OGT celle-ci serait en mesure de catalyser l'activation du clivage protéolytique de HCF-1.

1.8 Les régulateurs épigénétiques AXL1 et ASXL2

Chez la *Drosophile*, La protéine ASX (*Drosophila additional sex combs*) est d'un intérêt très particulier puisqu'elle se classifie parmi les rares protéines Polycombes qui sont atypiques

[361]. En effet, ASX a été initialement identifiée pour sa fonction comme répresseur et activateur transcriptionnel du fait que la délétion de *ASX* provoque l'apparition conjointe des phénotypes homéotiques caractéristiques de la délétion des deux classes de gènes codants pour les protéines Polycombes et Thritorax [361-364]. Ainsi, ASX maintient par une dualité fonctionnelle, une expression balancée des gènes *Hox* [361,365-368]. Au cours de l'évolution, le gène de *ASX* a évolué pour diverger en trois gènes paralogues codants au niveau des cellules de mammifères pour les protéines Polycombes ASXL1, ASXL2 et ASXL3 [369-371]. Des études récentes ont établis que de manière similaire à ASX, ASXL1/2 coordonnent leurs fonctions en s'associant avec divers répresseurs et co-activateurs transcriptionnels notamment la déméthylase KDM1/LSD1, le complexe Polycombe PRC2 et certaines protéines Thritorax [372-376]. Néanmoins, le rôle biologique des ASXLs est très peu connu. ASXL2 régule le développement cardiovasculaire, l'ostéogenèse, l'ostéoclastogenèse et l'adipogenèse [366,376,377]. ASXL1 et ASXL2 semble avoir un rôle antagoniste dans la régulation de l'adipogenèse et ce en agissant respectivement comme répresseur et activateur des gènes cibles [374].

1.8.1 Structure des protéines ASXLs :

ASXL3 est la protéine la plus large parmi les trois membres de la famille des protéines ASXLs. Elle compte 2248 acides aminés (aa) pour 1541 aa pour ASXL1 et 1435 aa pour ASXL2 [371]. Ces trois protéines sont caractérisés au niveau de leur extension N-terminale par la présence de deux régions conservées nommées, les domaines ASXN et ASXM (ou aussi ASXH) [367,370,372] (**Figure 1.14**). Le domaine ASXN a été identifié comme étant très conservé parmi tous les vertébrés [370]. ASXN a la particularité d'avoir un domaine unique, le domaine HARE-HTH. Ce domaine est structuralement similaire au domaine FOX (*Forkhead-box*) qui est aussi connu comme étant le domaine *winged helix-turn-helix* retrouvé chez les protéines de la famille des FOX à savoir FOXA3, FOXK1, FOXO1 et FOXO4 [378]. Le domaine FOX est le domaine requis pour permettre la liaison à l'ADN des FOXs afin de réguler la transcription et la réparation de l'ADN [379]. Ainsi, d'après les prédictions émis par SanchezPulido et ses collègues, le domaine ASXN serait requis pour favoriser la liaison à l'ADN des protéines ASXL [378]. Le domaine ASXM de ASXL1 est une région d'interaction protéines-protéines qui lie directement des régulateurs épigénétiques comme BAP1 et KDM1/LSD1 [79,373]. De plus, ASXL1 contient d'autres domaines conservés se situant au milieu de la protéine dont un se

retrouve au niveau de la région de liaison de NCOA1 (SRC1) et un deuxième domaine qui contient un motif LVxxLL, requis pour favoriser des interactions avec des récepteurs nucléaires (NHRs), comme RARα, RARβ, RXRα, RXRβ, ER, AR, GR and TR [372].

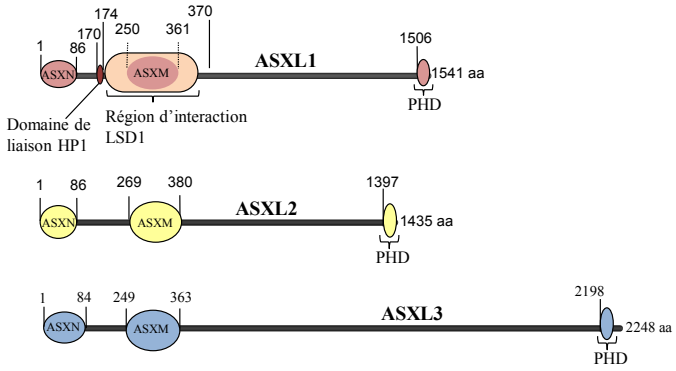

Figure 1.14. Représentation schématique de la structure des protéines de la famille ASXL : Les trois principaux domaines fonctionnels ASXN, ASXM et PHD sont conservés au sein de ASXL1, ASXL2 et ASXL3.

Étant des régulateurs épigénétiques, les protéines ASXLs ont la spécificité de pouvoir se lier sur la chromatine par l'intermédiaire de leurs domaines PHD (*C-terminal Plant Homeo Domain finger*). Les domaines PHD sont des petits modules de signalisation versatiles caractérisés par un motif composé de quatre cystéines, une histidine et trois cystéines (C_4HC_3) [380-383]. La majorité des PHD sont nommés des ''lecteurs'' (*readers*) du fait qu'ils reconnaissent spécifiquement des modifications post-traductionnelles au niveau des queues N-terminales des histones. Les PHD sont des motifs de liaison de lysines acétylées, méthylées ou même non modifiées et de ce fait contribuent de façon majeure à la coordination de plusieurs évènements associés à la régulation de la chromatine [384-392]. Il est également important de signaler que de plus en plus, on s'aperçoit que le mécanisme de reconnaissance entreprit par les domaines PHD est plus complexe de ce qui est déjà compris. En effet, il a été révélé que ces domaines peuvent notamment lier soit l'ADN ou des résidus au niveau du domaine globulaire du nucléosome [382]. Le rôle exacte du domaine PHD des ASXLs reste à notre jour inconnu. Mais des études d'analyses comparatives bio-informatiques prédisent que ce domaine pourrait être spécifique à des lysines internes méthylées de l'histone H3 ou même être capable de se lier a des séquences spécifiques au niveau de l'ADN [393]. De par la spécificité de leurs domaines ASXN, ASXM et PHD, les trois membres de la famille ASXL, seraient donc impliqués dans le

recrutement spécifique de régulateurs épigénétiques et de facteurs transcriptionnels au niveau de la chromatine.

1.8.2 Rôle de ASXL1/2 dans la régulation de la fonction biologique de BAP1 :

Récemment, un nouveau complexe polycombe composé de ASX et de Calypso, l'homologue de BAP1 chez la *Drosophile* a été découvert. Ce complexe a été nommé ''Complexe Polycombe de Déubiquitinase Répressif'', PR-DUB (*Polycomb repressive deubiquitylase (PR-DUB) complex*). Il a été ainsi décrit que ASX/Calypso catalyse la déubiquitination de H2Aub pour réguler l'expression des gènes *Hox*. Chez l'humain, le complexe PR-DUB est composé de BAP1 et de ASXL1. En effet, de manière similaire à Calypso/ASX, il a été démontré que BAP1 interagi avec une séquence minimale de ASXL1 composée de 337 acides aminés se trouvant au niveau de son domaine ASXM. Dans cette même étude, il a été établi pour la première fois la relation fonctionnelle entre BAP1 et ASXL1. Ainsi, la fonction de BAP1 envers H2A est conservée chez les vertébrés puisque la reconstitution de complexes recombinants PR-DUB de la *Drosophile* (ASX/Calypso) ou humain (BAP1/ASXL1) est suffisante pour l'obtention d'un complexe catalytiquement actif envers H2Aub [79]. Ce qui est contre-intuitif est que cette réaction de déubiquitination, contrairement à ce qui serait attendu, promouvait la répression transcriptionnelle des gènes cibles [79]. Depuis, sa découverte, le mécanisme de répression médié par le complexe Polycombe PR-DUB est resté non élucidé. Toutefois, il est plausible d'accorder à ce complexe le rôle de bien contrôler l'expression des gènes cibles et ce en maintenant un niveau harmonieux de l'ubiquitination de l'histone H2A et de prévenir son hyper-ubiquitination par le complexe Polycombe PRC1 [394].

Afin d'élucider le rôle fonctionnel de BAP1/ASXL1/2, nous avons révélé un nouveau mécanisme par lequel l'activité de déubiquitination de BAP1 envers H2A ainsi que sa fonction de suppresseur de tumeurs sont coordonnés par ces facteurs épigénétiques. En effet, nos résultats démontrent qu'il existe une co-régulation protéique étroite entre BAP1 et ASXL2. Plus spécifiquement, le maintien des niveaux protéiques de ASXL2 est strictement dépendant de BAP1. Ainsi, nous présentons l'importance d'assurer un assemblage adéquat du complexe BAP1/ASXL2 afin de permettre le bon fonctionnement de BAP1 comme gène suppresseur de

tumeurs. De plus, ASXL1/2 sont requis pour induire l'activité déubiquitinase de BAP1 envers H2A, De manière significative, ASXM s'associe avec BAP1 pour créer un nouveau domaine composite de liaison à l'ubiquitine. Ces interactions BAP1/ASXL1/2 régulent la progression harmonieuse du cycle cellulaire. De plus, la surexpression de BAP1 et d'ASXL2 au niveau des fibroblastes induit la sénescence de manière dépendante de leurs interactions. D'autre part, nous avons identifié une mutation de cancer au niveau de BAP1 le rendant incapable de lier ASXL1/2 et agir comme suppresseur de tumeurs [209].

1.8.3 ASXL1/2 et le cancer :

Depuis quelques années et grâce au développement imminent des techniques de séquençages génomiques, de nombreuses études sont venues souligner l'implication directe des protéines de la famille des ASXLs dans le développement de maladies humaines malignes notamment le cancer. En effet, de plus en plus on découvre que ASXL1 et ASXL2 sont mutées dans une panoplie de cancers qu'ils soient solides ou leucémiques. Toutefois, ASXL1 semble être sujet de manière plus fréquente aux différents types de mutations que ASXL2 [395-403]. ASXL1 se retrouve dans la région chromosomique 20q11 proche du gène DNMT3B et est exprimé dans toutes les cellules hématopoïétiques. ASXL1 est muté dans la plupart des maladies myéloïdes malignes incluant les syndrome myélodysplasique (SMD), le désordre myéloproliferatif (MPF), le néoplasme myéloproliferatif (MPN), les leucémies myéloïdes aiguës (AML) et les leucémies myélomonocytaires chroniques (LMMC) [396,397,400,404-410]. La plupart de ces mutations sont hétérozygotes et se produisent soit au milieu ou au niveau de l'extension C-terminale de la protéine aboutissant à une perte du domaine PHD de ASXL1 [400,404-407]. Des études de séquençages génomiques révèlent la présence de mutations ponctuelles au niveau des domaines ASXN ou ASXM de ASXL1/2. Plus particulièrement, une mutation somatique ponctuelle au niveau du domaine ASXM de ASXL1 a été reportée chez des patients atteints de leucémie myélomonocytaire chronique (LMMC) [396].

1.9 Hypothèse et objectifs de la thèse :

Depuis quelques années, BAP1 retient beaucoup l'attention des chercheurs en tant que gène suppresseur de tumeurs. La première percée dans la compréhension du mécanisme d'action de BAP1 a débuté par l'identification des partenaires de celui-ci. En effet, d'autres groupes et nous même, avons révélé que BAP1 forme un complexe multi-protéique composé principalement de facteurs et régulateurs transcriptionnels.

Nous nous sommes donc intéressés à définir comment les partenaires de BAP1 coordonnent son activité catalytique, son interaction avec ses substrats ainsi que sa fonction biologique en tant que suppresseur de tumeurs.

De ce fait, notre hypothèse de travail était, que BAP1 définit des complexes épigénétiques distincts qui régulent de manière dynamique et coordonnée différents évènements au niveau de la chromatine assurant ainsi sa fonction suppressive de tumeurs.

Ainsi, nos objectifs étaient de:

1) Caractériser la relation fonctionnelle entre deux composantes majeures du complexe BAP1 à savoir, OGT et HCF-1.
2) Définir le rôle de la O-GlcNAcylation dans la régulation d'évènements cellulaires liés à la chromatine.
3) Déterminer le rôle et le mécanisme d'action de ASXL1/2 dans la modulation de l'activité catalytique de BAP1 envers H2Aub ainsi que sa fonction suppressive de tumeurs.

CHAPITRE 2

Article : Crosstalk Between O-GlcNAcylation And Proteolytic Cleavage Regulates The Host Cell Factor-1 Maturation Pathway

Publié dans: PNAS, 2011, Feb 15;108(7)

Salima Daou[1]*, Nazar Mashtalir[1]*, Ian Hammond-Martel[1], Helen Pak[1], Helen Yu[1], Guangchao Sui[2], Jodi L. Vogel[3], Thomas M. Kristie[3] and El Bachir Affar[1]

1 Maisonneuve-Rosemont Hospital Research Center, Department of Medicine, University of Montréal, Montréal, Canada

2 Wake Forest University School of Medicine, Winston-Salem, NC, USA.

3 Laboratory of Viral Diseases, National Institute of Allergy and Infectious Diseases, National Institutes of Health, Bethesda, MD, USA.

Running title: O-GlcNAcylation regulates HCF-1 proteolysis

*Equal contribution to this work

Introduction à l'article :

Le chapitre 2 de ce travail est réservé à présenter les résultats relatifs à l'objectif 1 de la thèse. De ce fait, comme HCF-1 et OGT représentent des partenaires majeurs de BAP1, nous nous sommes donc intéressés dans cet article à étudier la relation fonctionnelle entre ces deux protéines. Ceci nous permettrait de comprendre d'avantage comment des régulations protéiques au sein du complexe BAP1 pourraient contribuer à moduler la fonction biologique et à élucider le mécanisme d'action de ce gène suppresseur de tumeurs.

Nous avons contribué à caractériser un mécanisme nouveau de régulation entre HCF-1 et OGT. En effet, ce travail représente la première étude décrivant que la O-GlcNAcylation de HCF-1 est une signalisation cellulaire requise pour induire son clivage protéolytique, un processus de maturation finement régulé, et le contrôle de sa fonction comme facteur transcriptionnel.

Contribution : Comme co-premier auteur, ma contribution a consisté à la conception et l'exécution de 50% des expériences de l'article, à l'interprétation des résultats et la préparation des figures ainsi qu'à la rédaction du manuscrit

2.1 Abstract

Host Cell Factor 1 (HCF-1) plays critical roles in regulating gene expression in a plethora of physiological processes. HCF-1 is first synthesized as a precursor, and subsequently specifically proteolytically cleaved within a large middle region termed the proteolytic processing domain (PPD). Although the underlying mechanism remains enigmatic, proteolysis of HCF-1 regulates its transcriptional activity and is important for cell cycle progression. Here we report that HCF-1 proteolysis is a regulated process. We demonstrate that a large proportion of the signaling enzyme O-linked-N-acetylglucosaminyl transferase (OGT) is complexed with HCF-1 and this interaction is essential for HCF-1 cleavage. Moreover, HCF-1 is, in turn, required for stabilizing OGT in the nucleus. We provide evidence indicating that OGT regulates HCF-1 cleavage via interaction with and O-GlcNAcylation of the HCF-1 PPD. In contrast, although OGT also interacts with the basic domain in the HCF-1 amino-terminal subunit, neither the interaction nor the O-GlcNAcylation of this region are required for proteolysis. Moreover, we show that OGT-mediated modulation of HCF-1 impacts the expression of the herpes simplex virus immediate early genes, targets of HCF-1 during the initiation of viral infection. Together the data indicate that O-GlcNAcylation of HCF-1 is a signal for its proteolytic processing and reveal a novel crosstalk between these post-translational modifications. Additionally, interactions of OGT with multiple HCF-1 domains may indicate that OGT has several functions in association with HCF-1

2.2 Introduction

HCF-1 is a ubiquitously expressed chromatin-associated protein and a major transcriptional regulator controlling numerous cellular processes including cell cycle progression (reviewed in (Kristie et al. 2009)).

HCF-1 undergoes a unique mode of limited proteolysis involving a series of 20 aa reiterations within the central proteolytic processing domain (PPD) (Kristie and Sharp 1993; Wilson et al. 1995). Although the mechanism of cleavage remains to be fully defined, previous

studies suggested that HCF-1 might possess an autoproteolytic activity (Vogel and Kristie 2000). HCF-1 cleavage occurs at one or more reiterated sites at the PPD, generating several N-terminal and C-terminal subunits that form stable heterodimers via two corresponding pairs of motifs, termed self association sequences (SAS) (Wilson et al. 2000).

Earlier studies indicated that proteolytic processing of HCF-1 is required to coordinate two major functions of HCF-1 in cell cycle progression (Julien and Herr 2003). The HCF-1 N subunit is necessary and sufficient to promote the G1 to S transition, while the C subunit is required for progression through mitosis (Julien and Herr 2003). However, the molecular properties that characterize the functions of the precursor versus the mature forms of HCF-1 remain unclear. It is likely that the gain or loss of specific protein interactions is one major consequence of HCF-1 processing. For instance, the coactivator/corepressor FHL2 interacts with the HCF-1 precursor via a motif located in the central region of the PPD. HCF-1 processing removes this motif, thus decreasing the activation of an HCF-1-dependent target gene (Vogel and Kristie 2006).

OGT is a highly conserved enzyme that participates in critical nuclear and cytoplasmic signalling events (Butkinaree et al. 2010; Slawson et al. 2010). Similar to phosphorylation, OGT modifies S/T residues of target proteins with a single N-acetylglucosamine (O-GlcNAc); regulating protein function by influencing protein interactions, enzymatic activity, and subcellular localization. Furthermore, O-GlcNAc modification is highly dynamic and ample evidence indicates the existence of extensive crosstalk between O-GlcNAcylation and phosphorylation in controlling biological processes (Butkinaree et al. 2010; Slawson et al. 2010). The reversibility of O-GlcNAcylation is ensured by a unique beta-N-acetylglucosaminidase (OGA) which is also highly conserved (Hu et al. 2010). OGT interacts with numerous cellular proteins, most notably transcription factors and regulators. Significantly OGT was previously shown to interact with and glycosylate the HCF-1 N subunit (Wang et al. 2010; Wysocka et al. 2003). However, the biological significance and mechanism of this O-GlcNAcylation remain unknown. Here, we reveal a novel physical and functional link between O-GlcNAcylation and limited proteolysis.

2.3 Results

2.3.1 HCF-1 regulates the stability of nuclear OGT.

HCF-1 possesses a unique modular structure consisting of an amino-terminal Kelch domain followed by: (i) a region rich in basic residues; (ii) the PPD containing the 20 aa reiterations that are the sites of specific proteolysis; (iii) an acidic activation domain; (iv) and a set of fibronectin repeats (Fig 2.1A). HCF-1 was previously shown to interact with OGT (Wysocka et al. 2003). However the abundance of nuclear OGT stably associated with HCF-1 relative to the entire nuclear pool was not known. To address this, we immunodepleted HCF-1 from HeLa nuclear extracts (Fig 2.1B). Quantification of OGT levels in the HCF-1 complexes fraction (IP) and the flow through (FT) revealed that nearly 50% of the total nuclear OGT is stably associated with HCF-1. The association of a large proportion of OGT with HCF-1 suggests important roles of this complex. Strikingly, depletion of HCF-1 in HeLa cells by shRNA induced a corresponding dose-dependent decrease of OGT (Fig 2.1C). This result was confirmed by a pool of 4 siRNA oligonucleotides targeting HCF-1 (Fig 2.1C).

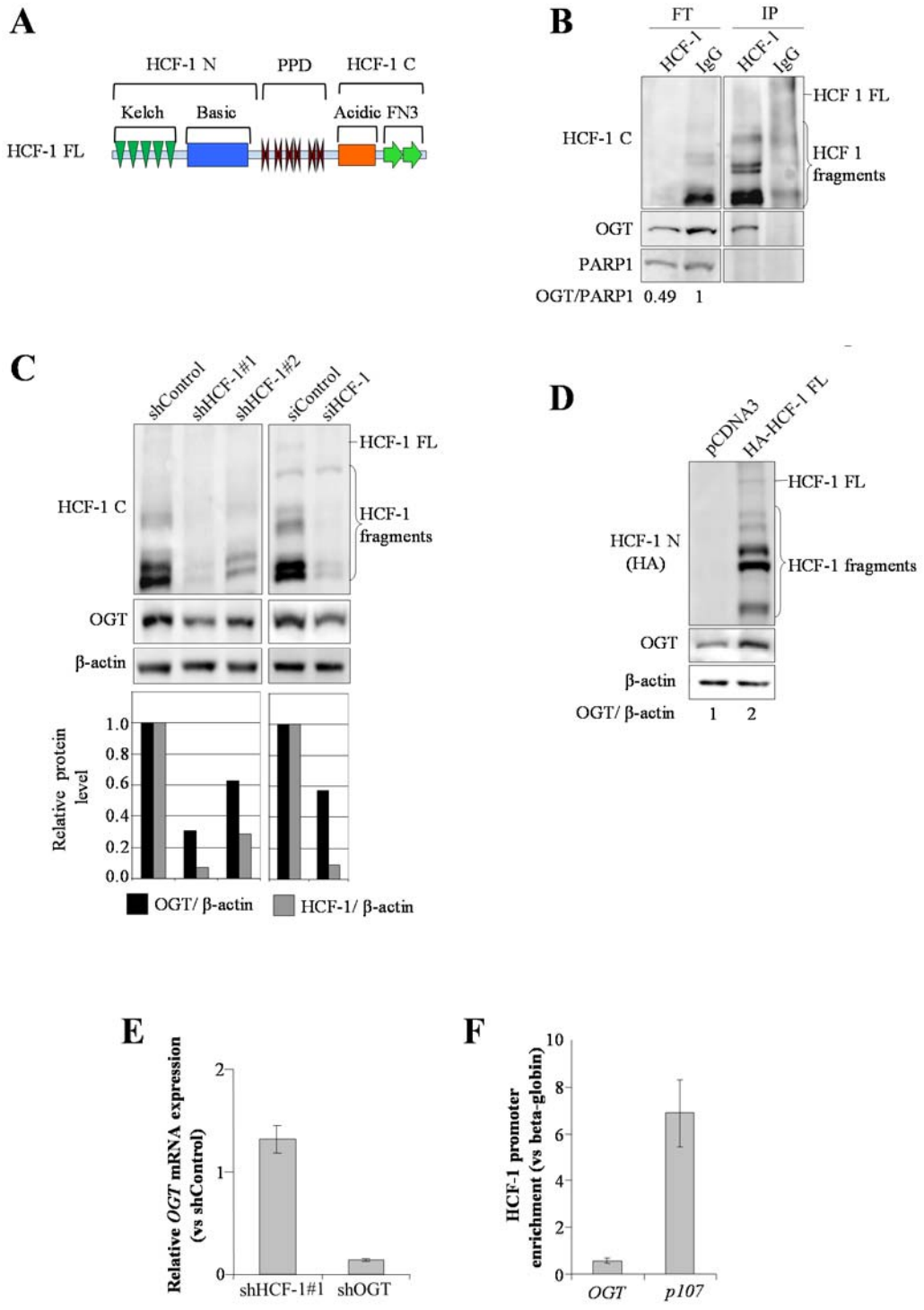

Figure 2.1.HCF-1 is required for the maintenance of proper OGT levels.

(A) Schematic representation of the domains of the human HCF-1. (B) Immunodepletion of HeLa nuclear extracts using anti-HCF-1. OGT and HCF-1 were detected in the HCF-1 immunoprecipitate (IP) and flow through (FT) by western blot. The nuclear protein PARP1 was used as a negative control. Quantification of OGT was done relative to PARP1. (C) Depletion of HCF-1 using shRNA plasmids or

siRNA oligonucleotide pools induces OGT downregulation. Quantification of OGT or HCF-1 was done relative to β-actin. (D) Overexpression of HCF-1 increases OGT protein levels. HeLa cells were transfected with HCF-1 FL and 2 days post-transfection, cells were harvested for immunoblotting. (E) OGT mRNA is not affected by HCF-1 depletion. U2OS cells mRNAs were isolated and cDNAs were quantitated by qRT-PCR relative to GAPDH. shRNA for OGT was included as an internal control. All experiments were repeated at least 3 times and the data are presented as mean ± SD. (F) Promoter occupancy by HCF-1. ChIP assays were done using U2OS cell chromatin and anti-HCF-1 or IgG control. The enrichment of factors was calculated relative to the occupancy of the β-globin promoter. All experiments were repeated at least 3 times and data are presented as mean ± SD.

Conversely, overexpression of HCF-1 induced an increase in OGT protein levels (Fig 2.1D). The reduction in OGT levels in the absence of HCF-1 were not due to a reduction in *OGT* mRNA levels (Fig 2.1E). Moreover, no detectable HCF-1 was found to be associated with the *OGT* promoter (Fig 2.1F). In contrast, HCF-1 was readily detected on the promoter of *p107* RB family member (Fig 2.1F), a known HCF-1 target gene (Tyagi et al. 2007).

The above results suggested that HCF-1 regulates OGT stability via a post-transcriptional mechanism. Since OGT is distributed in both the cytoplasm and the nucleus while HCF-1 is primarily localized in the nucleus, we determined whether the nuclear pool of OGT was preferentially stabilized by HCF-1. Subcellular fractionation showed that the nuclear pool of OGT is significantly reduced relative to the corresponding cytoplasmic pool following depletion of HCF-1 (Fig 2.2A). These results were confirmed by immunostaining following knockdown of HCF-1 where a significant reduction of nuclear OGT could be observed in the HCF-1 depleted cells (Fig 2.2B). To determine whether OGT is regulated by proteasomal degradation, we transfected expression plasmids for OGT and ubiquitin, followed by treatment with the proteasome inhibitor MG132. After OGT immunoprecipitation, we observed a typical ubiquitination smear, which was increased by MG132 treatment (Fig 2.2C). We note that MG132 has a minor effect on OGT protein levels. This is due to the relatively long half-life of OGT (~ 12 hours) (Marshall et al. 2005). We also observed an increase in the ubiquitination of endogenous OGT following extended treatment with MG132 (Fig S2.1). Next, we conducted a cycloheximide chase upon HCF-1 knockdown and found that OGT was slightly reduced overtime while no change or even a small increase was observed for the shControl transfected cells (Fig 2.2D).

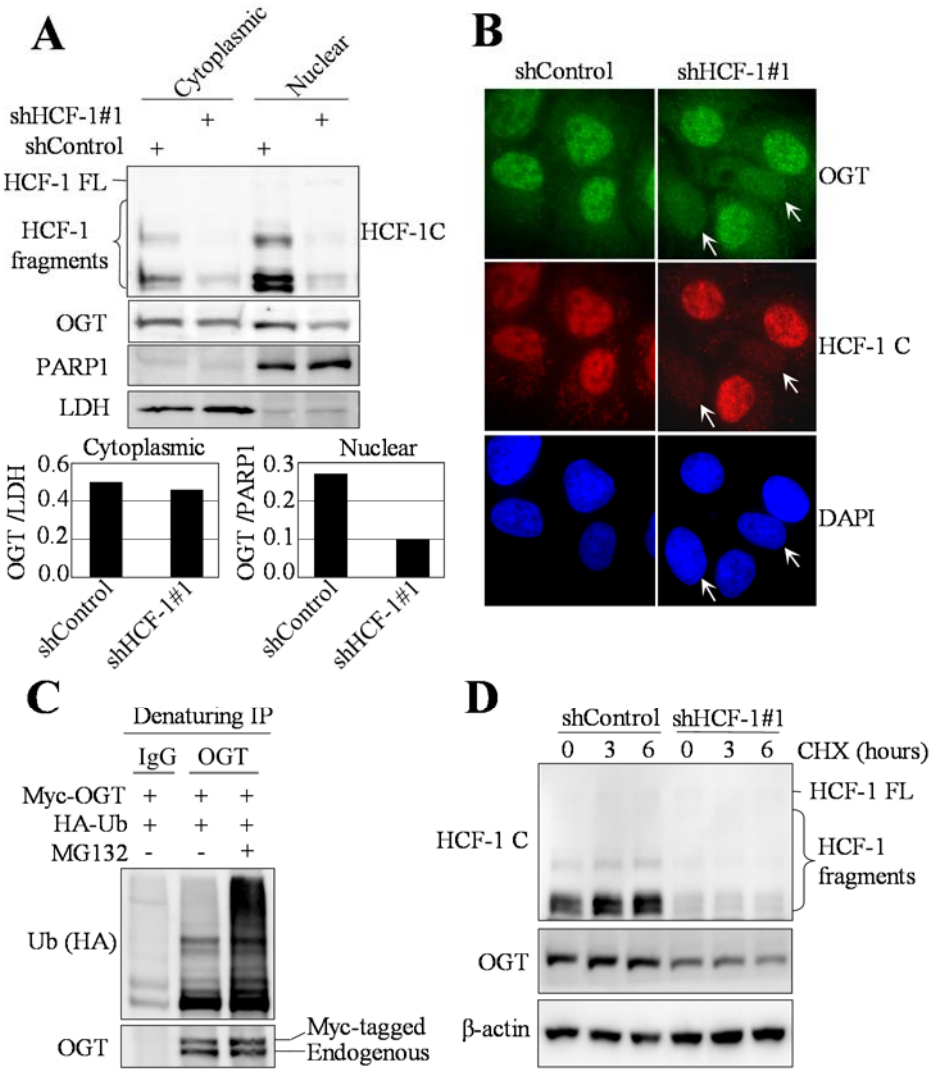

Figure 2.2 .HCF-1 regulates the stability of OGT.

Nuclear OGT is preferentially downregulated following HCF-1 depletion (A-B). (A) Biochemical fractionation of nuclear and cytoplasmic compartments following HCF-1 knockdown in U2OS. PARP1 and LDH, which are localized in the nucleus and cytoplasm, respectively, were used as controls for fractionation. Quantification of cytoplasmic versus nuclear OGT was done relative to LDH or PARP1, respectively. (B) Immunofluorescence detection of OGT in U2OS cells following HCF-1 knockdown. (C) OGT is ubiquitinated and regulated by proteasomal degradation. 293T cells were transfected with Myc-OGT and HA-ubiquitin (HA-Ub). Two days post-transfection, cells were treated with 20 μM MG132 for 4 hours prior to harvesting for immunoprecipitation and western blotting. (D) OGT protein stability is decreased following HCF-1 depletion. U2OS cells were transfected with HCF-1 shRNA plasmids. Three days later, cells were treated with CHX (100 μg/ml) and harvested for western blotting.

2.3.2 OGT is required for HCF-1 proteolytic processing.

It was previously reported that OGT interacts with and glycosylates HCF-1 (Wysocka et al. 2003), suggesting an important reciprocal regulation. Strikingly, depletion of OGT induced an accumulation of the HCF-1 precursor with a corresponding decrease in the HCF-1 cleavage products (Fig 2.3A). Quantification indicated that shRNA constructs, which depleted OGT to different extents, correlated in an inverse manner with the ratio of HCF-1 cleavage products (HCF-1 FL/HCF-1 cleaved forms).

As expected, the extent of OGT knockdown also correlated with a proportional decrease of global O-GlcNAc modification. Transfection of siRNA oligonucleotide pools, which induced a substantial knockdown of OGT, also resulted in a significant accumulation of HCF-1 FL (Fig 2.3A). OGT knockdown also inhibited HCF-1 cleavage in other cell types indicating that this inhibition is not cell-type specific (Fig 2.3A). Conversely overexpression of OGT along with HCF-1 FL resulted in: (i) an increase in global protein O-GlcNAcylation levels; (ii) a decrease in HCF-1 FL levels; and (iii) an increase in the levels of HCF-1 N and C polypeptides (Fig 2.3B). The effect on HCF-1 cleavage was dependent on OGT catalytic activity (FigS2.2).

O-GlcNAc modification is dynamic and cycling is ensured by the concerted action of OGT and OGA (Hurtado-Guerrero et al. 2008; Love et al. 2010). We reasoned that overexpressed OGA would shift the equilibrium toward O-GlcNAc removal with a concomitant effect on HCF-1 cleavage. Although no significant changes were seen on the cleaved forms of HCF-1 following overexpression of OGA, a noticeable increase in the level of HCF-1 precursor was observed (Fig 2.3C). The decrease of global O-GlcNAc with overexpressed OGA was considerably less significant than with OGT RNAi (Fig2 .3C).

Components of the nuclear pore complex are known to be heavily glycosylated by OGT suggesting that O-GlcNAc modification might be required for the nuclear import of proteins (Davis and Blobel 1987; Hanover et al. 1987; Jinek et al. 2004). Although not firmly established, HCF-1 appears to be cleaved in the nucleus (Wilson et al. 1995). We reasoned that depletion of OGT might induce cytoplasmic sequestration of HCF-1 FL from accessing factors required for its cleavage in the nucleus. However, in the absence of OGT, most of the HCF-1 FL is in the nucleus, indicating that the lack of HCF-1 cleavage was not due to a defect in nuclear import (Fig 2.3D). To further confirm these results, cells were stained for HCF-1

following shRNA knockdown of OGT. While substantial depletion of OGT was achieved, no noticeable cytoplasmic accumulation of HCF-1 was observed (FigS2.3). Interestingly, in contrast to HCF-1 cleavage, no effect of OGT knockdown was observed on the histone methyltransferase and transcription regulator MLL1, which is also subjected to specific proteolytic cleavage (Hsieh et al. 2003) (FigS2.4). We concluded therefore that OGT is required for HCF-1 cleavage.

2.3.3 OGT interacts with and glycosylates full length HCF-1.

To investigate the mechanism of HCF-1 maturation, we sought to characterize the OGT interaction with HCF-1. First, we cotransfected HA-HCF-1 FL or HA-HCF-1 N (1-1010aa) with Myc-OGT, and found that significantly more OGT is immunoprecipitated with HA-HCF-1 FL than HA-HCF-1 N (Fig S2.5A), suggesting that the major determinants of OGT/HCF-1 interaction are contained within HCF-1 sequences that are not present in the HCF-1 N protein.

Next we used the WT or an uncleavable form of HCF-1 mutant (NC) in which the critical glutamic acid of each repeat had been mutated to alanine (Vogel and Kristie 2006). Immunoprecipitation assays revealed that the uncleavable HCF-1 mutant was even more efficient in co-immunoprecipitation of OGT than the WT HCF-1 (Fig S2.5B). These effects were also observed following co-expression of HCF-1 WT or the uncleavable mutant with OGT. In this case, OGT expression induced processing of the HCF-1 WT but not the HCF-1 NC mutant (Fig S2.5C). Of note, Myc-OGT was substantially stabilized in cells co-transfected with HCF-1 NC accounting partly for the more efficient co-immunoprecipitation. However, the ratio of the IP/Input supported the conclusion that OGT interacts more efficiently with the uncleaved HCF-1 than the HCF-1 WT (Fig S2.5C). Next, *in vitro* GST-pull down assays using recombinant GST-OGT and various *in vitro* translated forms of HCF-1 (FL, N and C subunits) indicated that the GST-OGT interacts more efficiently (~10 fold) with the HCF-1 precursor than the HCF-1 N subunit (Fig S2.6). No interaction was observed with the HCF-1 C (Fig S2.6). To determine whether HCF-1 FL is O-glycosylated, we immunoprecipitated HCF-1 and found that the precursor reacts with the anti-O-GlcNAc antibody, suggesting that O-GlcNAcylation of HCF-1 precedes its processing (Fig S2.7). We also note that large C-terminal fragments corresponding most likely to processing intermediates are O-glycosylated,

however the most processed forms of HCF-1 C-terminal subunits appear to be very poorly O-glycosylated.

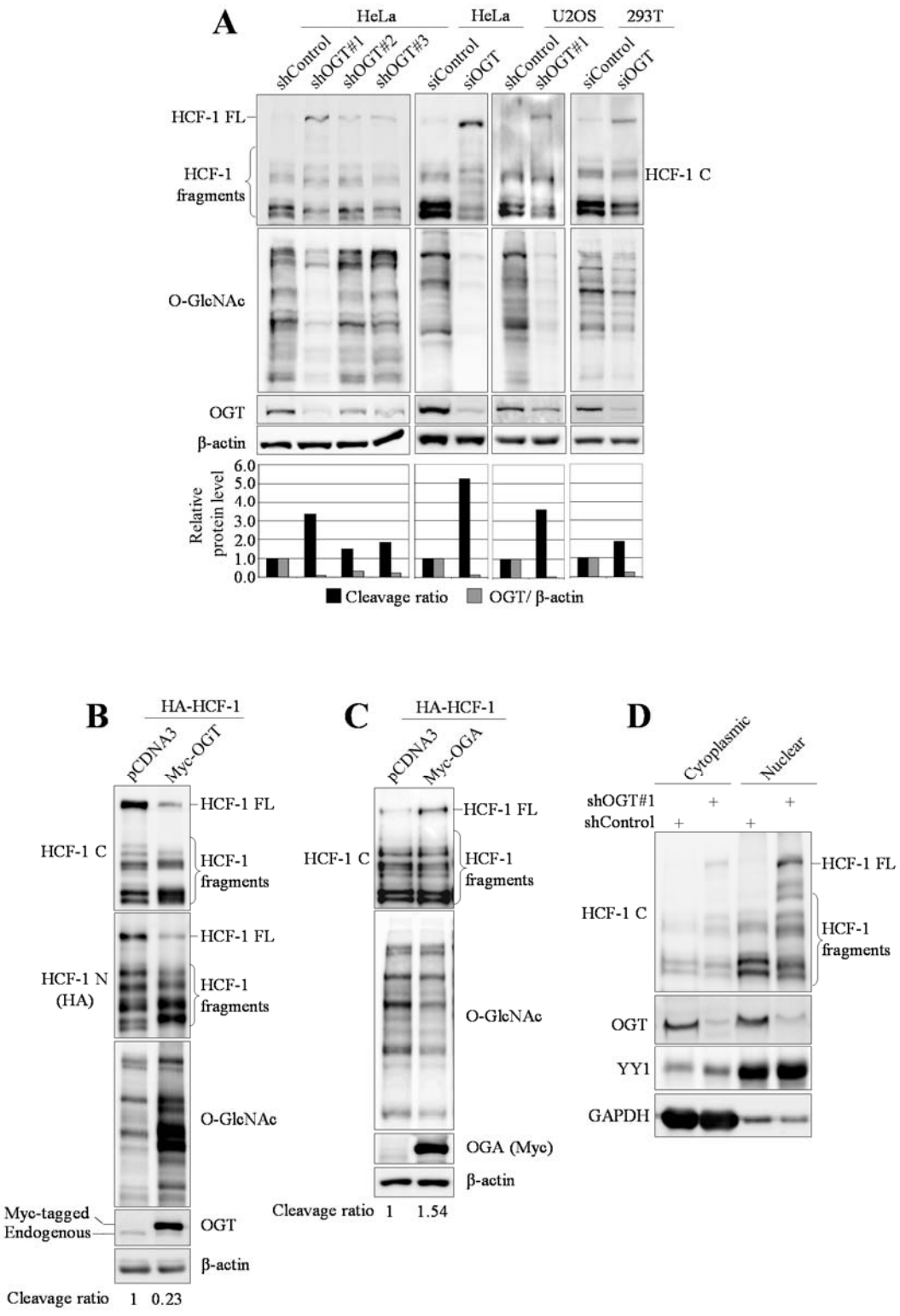
A
HeLa
HeLa
U2OS
293T
shControl
shOGT#1
shOGT#2
shOGT#3
siControl
siOGT
shControl
shOGT#1
siControl
siOGT
HCF-1 FL
HCF-1 fragments
HCF-1 C
O-GlcNAc
OGT
β-actin
Relative protein level
6.0
5.0
4.0
3.0
2.0
1.0
0.0
Cleavage ratio
OGT/ β-actin
B
HA-HCF-1
pCDNA3
Myc-OGT
HCF-1 FL
HCF-1 C
HCF-1 fragments
HCF-1 FL
HCF-1 N (HA)
HCF-1 fragments
O-GlcNAc
Myc-tagged
Endogenous
OGT
β-actin
Cleavage ratio 1 0.23
C
HA-HCF-1
pCDNA3
Myc-OGA
HCF-1 FL
HCF-1 C
HCF-1 fragments
O-GlcNAc
OGA (Myc)
β-actin
Cleavage ratio 1 1.54
D
Cytoplasmic
Nuclear
shOGT#1 + +
shControl + +
HCF-1 FL
HCF-1 C
HCF-1 fragments
OGT
YY1
GAPDH

Figure 2.3. OGT is required for HCF-1 proteolytic cleavage.

(A) OGT depletion induces accumulation of the HCF-1 precursor with a decrease in the levels of the cleaved forms. Cells were transfected with either OGT shRNA or OGT siRNA oligonucleotide pools and harvested for western blotting. Quantification of OGT is relative to β-actin. The HCF-1 cleavage ratio was estimated by dividing the signal value of the precursor by the sum of the signal values of the cleaved forms. (B) Overexpression of OGT promotes HCF-1 cleavage. 293T cells were transfected with either pcDNA3 control or Myc-OGT along with HA-HCF-1 FL. Two days post-transfection, cells were harvested for western blotting. (C) Overexpression of OGA inhibits HCF-1 cleavage. 293T cells were transfected with either pcDNA3 control or Myc-OGA along with HA-HCF-1 FL. Two days post-transfection, cells were harvested for western blotting. (D) Subcellular fractionation following knockdown of OGT. HeLa cells were transfected with OGT shRNA plasmids and harvested for fractionation and western blotting. YY1 and GAPDH were used as markers for nucleus and cytoplasm, respectively.

2.3.4 OGT interaction with and O-GlcNAcylation of the HCF-1 N-terminal subunit are not required for HCF-1 proteolytic cleavage.

To determine the role of O-GlcNAc in the proteolytic processing of HCF-1, we utilized two approaches. We first conducted GST-pulldown assays with subdomains of the HCF-1 N subunit and observed that the HCF-1 basic region interacts with OGT (Fig S2.8A). We further determined that a region between 500 and 550 aa of HCF-1 is sufficient for this interaction (Fig S2.8A). Therefore, we generated a mutant of HCF-1 lacking this domain (Δ500-650 aa) (HA-HCF-1 ΔOBM) (FigS2.8B). Interestingly, this mutant was cleaved as efficiently as the WT HCF-1 (Fig S2.8C, left panel). Moreover, the interaction of this HCF-1 mutant with OGT was almost unchanged in comparison to the WT HCF-1 (FigS2.8C, left panel). Next, we analysed the O-GlcNAcylation levels of this HCF-1 mutant and observed that while a significant decrease in the O-GlcNAcylation of the cleaved forms of HCF-1 was evident, there was no substantial change in the overall O-GlcNAcylation of the uncleaved FL HCF-1 (Fig S2.8C, right panel). The data indicate that neither the interaction of OGT with the N subunit nor its O-GlcNAcylation is responsible for the OGT mediated proteolysis of HCF-1. To confirm these results, we mutated all of the known O-GlcNAcylation sites located in the HCF-1 N subunit (Wang et al. 2010) (HA-HCF-1 ΔO-Glc) (Fig S2.8B). Similar to the HCF-1 ΔOBM mutant, a substantial decrease in HCF-1 O-GlcNAcylation was observed for the cleaved forms while no major changes in the O-GlcNAcylation levels of the uncleaved HCF-1 were seen (Fig S2.8C, right panel). Importantly the extent of HCF-1 cleavage remained

essentially similar to the WT form suggesting that O-GlcNAc modification of the basic region within the HCF-1 N is not required for processing (Fig S2.8C, left panel).

2.3.5 OGT interacts with, O-glycosylates, and promotes the cleavage of the PPD.

To provide further mechanistic insights into the role of OGT in HCF-1 processing, we investigated the role of the PPD in promoting the OGT/HCF-1 interaction. First we transfected cells with the uncleavable HCF-1 FL (HCF-1 NC) or HCF-1 lacking the PPD (HCF-1 Δ PPD) and compared the interaction with OGT. As shown in Fig 2.4A, the HCF-1 lacking the PPD interacted less efficiently (~ 20-fold less) with OGT than the uncleavable form suggesting that the PPD is the major OGT-interacting domain. Previously it was demonstrated that the PPD was sufficient for cleavage in cells, although it is very poorly processed (Wilson et al. 1995). Therefore, we generated PPD expression constructs with and without a Nuclear Localization Signal (NLS) (Fig S2.9A).In contrast to the PPD without the NLS (Myc-PPD), which was moderately cleaved, the PPD with the NLS (Myc-NLS-PPD) was dramatically cleaved and only a faint band of residual uncleaved PPD could be detected (Fig S2.9B). Of note, the Myc-NLS sequences (~3 kDa) enabled us to detect the smallest cleaved form of the Myc-NLS-PPD (PPD repeat 1-2).

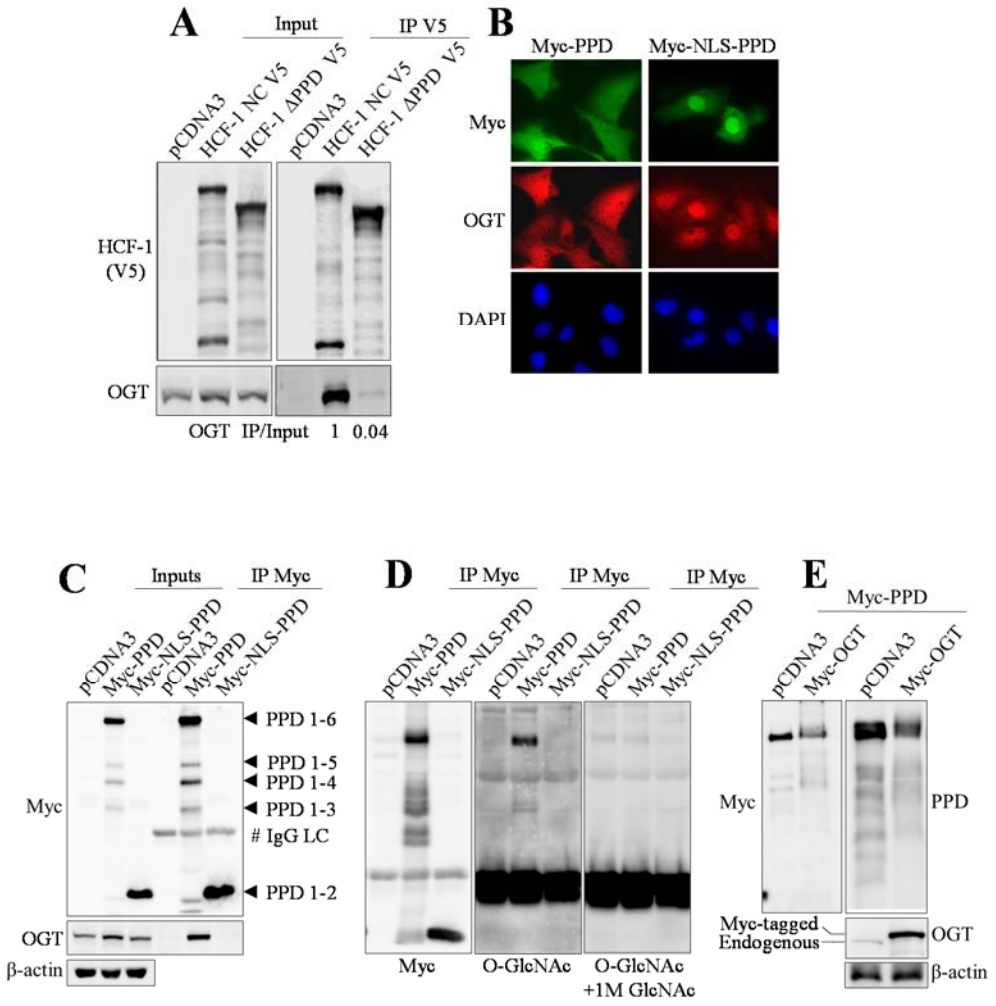

Figure 2.4. OGT interacts with HCF-1 PPD and mediates its cleavage.

(A) Interaction of OGT with HCF-1 lacking PPD or HCF-1 FL. 293T cells were transfected with either HCF-1 NC V5 or HCF-1 ΔPPD V5. Two days post-transfection, total cell extracts were used for immunoprecipitation using an anti-V5. (B) Immunofluorescence localization of PPD with or without a nuclear localization signal. U2OS cells were transfected with either Myc-PPD or Myc-NLS-PPD. Two days post-transfection, cells were used for immunostaining using an anti-Myc. (C) Interaction of PPD with OGT. 293T cells were transfected with either Myc-PPD or Myc-NLS-PPD. Two days post-transfection, total cell extracts were used for immunoprecipitation using an anti-Myc. (D) O-GlcNAcylation of PPD with OGT. 293T cells were transfected with either Myc-PPD or Myc-NLS-PPD and Myc-OGT. Two days post-transfection, total cell extracts were used for immunoprecipitation under denaturing conditions using an anti-Myc. To ensure the specificity of signal, the O-GlcNAc antibody was pre-incubated for 1 H with 1 M of N-acetylglucosamine before being applied to the membrane. (E) Overexpression of OGT promotes PPD proteolytic cleavage. 293T cells were transfected with Myc-PPD along with pCDNA3 or Myc-OGT. Two days post-transfection, total cell extracts were used for immunoblotting.

As detected by immunofluorescence, the Myc-PPD was distributed in the cytoplasm and nucleus (Fig 2.4B). In contrast, the Myc-NLS-PPD accumulated in the nucleus (Fig 2.4B). Interestingly, cells expressing Myc-NLS-PPD exhibited a typical pronounced nuclear OGT staining (Fig2 .4B), similar to mock transfected cells (Fig 2.2B). However, in cells expressing Myc-PPD, OGT was distributed evenly between cytoplasm and nucleus (Fig 2.4B), suggesting that this form of the PPD directly interacts with OGT and interferes with its nuclear localization. This result was confirmed by subcellular fractionation, i.e., cells expressing Myc-PPD exhibit significantly higher OGT levels in the cytoplasm (Fig S2.10). Next, we found that the HCF-1 PPD (Myc-PPD) was sufficient to co-IP OGT (Fig 2.4C). In contrast, the smallest cleaved form of PPD does not interact with OGT indicating that this set of reiterations (R1-2) is not sufficient to mediate the association with OGT. Since the Myc-NLS-PPD appears to be dramatically cleaved, we reasoned that this domain might interact with OGT and be a target of OGT mediated O-GlcNAcylation prior to its cleavage. In support of this, the Myc-PPD was modified by O-GlcNAc in an OGT-dependent manner (Fig 2.4D and Fig S2.11). To further characterize the role of OGT in promoting HCF-1 cleavage, we took advantage of the PPD without the NLS, which localizes in both cytoplasm and nucleus (Fig 2.4B), interacts with OGT, and is moderately cleaved (Fig 2.4C). Following over-expression of OGT, we observed a decrease in the levels of both the FL Myc-PPD and the cleavage products (Fig 2.4E). Conversely, knockdown of OGT induced an accumulation of FL Myc-PPD (Fig S2.12). These results indicate that OGT directly promotes the cleavage of the HCF-1 PPD and intermediate processing forms.

2.3.6 Depletion of OGT enhances HCF-1 target gene expression.

Since we observed a significant accumulation of HCF-1 FL in the nucleus following depletion of OGT, we first determined whether it associates with chromatin. The chromatin/nuclear matrix fraction of HeLa cells was prepared from control and OGT-depleted cells and treated with MNase (Sanders 1978). As shown in Fig 2.5A, HCF-1 was released into the soluble fraction following MNase treatment, indicating its association with chromatin.

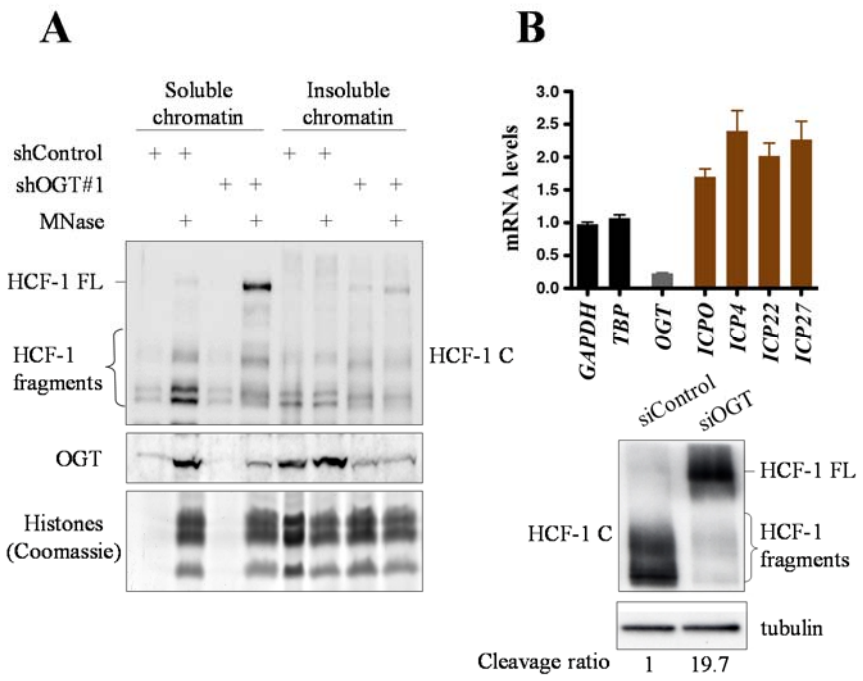

Figure 2.5.Uncleaved HCF-1 associates with chromatin and enhances HCF-1-mediated viral gene expression.

(A) HCF-1 precursor is associated with chromatin. HeLa were transfected with either non-targeting control or OGT shRNA plasmids. Three days post-transfection, cells were harvested for cell fractionation. The chromatin/nuclear matrix fraction was treated with micrococcal nuclease (MNase) to release nucleosomes. Proteins were detected in the soluble and pellet fractions by immunoblotting or coomassie blue staining. (B) HFF cells were transfected with control or OGT siRNAs. Three days post transfection, cells were infected with 0.1 PFU HSV-1 and harvested for mRNA analysis (top panel) and immunoblotting (bottom panel). Levels of control cellular (GAPDH and TBP), OGT, and viral IE mRNAs in OGT depleted cells are shown relative to levels in control siRNA transfected cells. All experiments were repeated at least 3 times and data are presented as mean ± SD.

Finally, to determine the biological consequences of OGT mediated regulation of HCF-1 cleavage, we assessed the impact of OGT depletion on HCF-1 mediated gene expression using the well characterized model of HCF-1-dependent activation of the herpes simplex virus (HSV) IE genes (Kristie et al. 2009). HFF cells transfected with control or OGT siRNAs were infected with HSV and the levels of viral and control cellular mRNAs were determined by qRT-PCR. As shown in Fig 2.5B, depletion OGT (~80%) resulted in a substantial increase in the ratio of HCF-1 precursor to the HCF-1 cleavage products as compared to cells transfected with control siRNAs. Importantly, depletion of OGT also resulted in a consistent increase

(~1.5 to 2.5-fold) in viral IE gene expression (Fig 2.5B). In contrast, no impact was seen on expression of the control *GAPDH* or *TBP* mRNA levels. As factors such as the Sp1 transcription factor, a known component of the viral HSV IE gene expression regulatory circuit, as well as RNA polymerase II can be regulated by O-GlcNAcylation (Kelly et al. 1993; Yang et al. 2001), we also analyzed the expression of a set of Sp1 target genes in cells depleted of OGT. In contrast to the impact on HSV IE gene expression, we did not detect any significant changes in the expression of these Sp1 target genes (Fig S2.13). Thus, although we can not exclude possible effects resulting from O-GlcNAcylation of other cellular factors, the loss of Sp1 or RNA polymerase II O-GlcNAcylation does not likely account for the observed increase in HSV immediate-early gene expression. The results are consistent with previous data indicating that the full-length, non-processed form of HCF-1 was more efficient in induction of viral IE reporter genes (Vogel and Kristie 2006).

2.4 Discussion

Site-specific limited proteolytic cleavage is exploited as a signaling mechanism in nearly all living organisms. Moreover, the importance of this post-translational modification is emphasized by the fact that, in mammals, numerous physiopathological processes have evolved elaborate protein cleavage machineries.

Mammalian HCF-1 is subjected to proteolytic cleavage via limited site-specific proteolysis within unique reiterations of the PPD. Interestingly, *C elegans* HCF does not have a domain homologous to PPD and is not cleaved (Liu et al. 1999). The *Drosophila* HCF, although also cleaved, does not contain cleavage sites homologous to the mammalian HCF-1 PPD (Mahajan et al. 2003). This suggests that a need developed for HCF-1 proteolytic processing, although distinct mechanisms of cleavage have apparently evolved. Indeed, it has been shown that the *Drosophila* HCF is cleaved by the protease taspase 1, while human and mouse HCF-1 are cleaved in a taspase 1-independent manner (Capotosti et al. 2007).

Here, we demonstrate that OGT is required for HCF-1 cleavage. Interestingly O-GlcNAcylation is shown here to promote proteolytic cleavage, protein phosphorylation also impacts proteolytic cleavage by either stimulation or inhibition (Kurokawa and Kornbluth 2009), thus highlighting the importance of post-translational modifications in tightly regulating limited proteolysis. In addition to the previously established role of OGT in inhibiting proteasomal degradation via O-GlcNAcylation of the proteasome or its substrates (Cheng and Hart 2001; Han and Kudlow 1997; Zhang et al. 2003), we have here uncovered an additional role for this enzyme in signalling limited proteolysis. Since both proteolytic cleavage and O-GlcNAcylation modulate the function of several transcription regulators, it would be interesting to determine whether this crosstalk represents a more global signaling event.

The role of OGT in association with HCF-1 is likely to have several functions. With respect to the regulation of HCF-1 cleavage, it is possible that the PPD encodes a dormant protease that is stimulated by O-GlcNAcylation, following a significant conformational change. This model would provide a level of control that prevents promiscuous and untimely autocleavage of HCF-1. Alternatively, O-GlcNAcylation of the PPD may provide a signal for

recruitment of an, as yet unidentified, protease. Importantly, the PPD is not simply a domain containing proteolytic cleavage sites but is also a domain that interacts with HCF-1 binding partners. OGT mediated O-GlcNAcylation of the PPD or PPD interacting partners could result in an enhancement of cleavage via disruption of protective interactions. Thus, OGT-mediated cleavage of HCF-1 can provide a mechanism for controlling the dosage and functional competency of HCF-1 and its processed subunits. In support of this, depletion of OGT results in accumulation of the full-length HCF-1 and a stimulation of HCF-1 dependent transcriptional activation of the HSV IE genes. Finally, an additional implication of the interaction of OGT with HCF-1 is the reciprocal impact of HCF-1 on OGT stability. Thus, as OGT interacts more efficiently with the HCF-1 precursor, it may therefore modulate its own stability.

In addition to modulating HCF-1 cleavage, OGT is also likely to have additional functional roles in association with HCF-1. In addition to its interaction with the HCF-1 PPD, OGT also interacts with the basic domain of HCF-1 and remains associated with the cleaved HCF-1 subunits. Thus, OGT might modulate HCF-1 interactions with chromatin-associated regulators. Notably, OGT is a metabolic sensing enzyme. It would be of continued interest to investigate whether changes in metabolic conditions impact HCF-1 processing and/or function, which in turn would affect cell growth and cell cycle progression. Thus, as HCF-1 is a major regulator of cellular metabolism (Dejosez et al. 2008; Vercauteren et al. 2008), O-GlcNAcylation of HCF-1 might provide a link between cellular metabolism and cell proliferation.

2.5 Materials And Methods

2.5.1 Plasmids and Antibodies

shRNA constructs, expression plasmids, and antibodies used in this study are described in supplemental information.

2.5.2 Cells and virus

HeLa, U2OS, HFF (human foreskin fibroblast), and 293T cells were maintained according to standard protocols. Infections of HFF cells with HSV-1, cell transfections, and western blotting were done as described in supplemental information.

2.5.3 Immunodepletion and Immunoprecipitation

Immunodepletion of HeLa nuclear extracts with anti-HCF-1 or control IgG were done as described in supplemental information.

2.5.4 Biochemical fractionation of subcellular compartments

Nuclear and cytoplasmic fractions were obtained using a hypotonic lysis buffer as described (Nakatani and Ogryzko 2003). Chromatin fractions and digestion with MNase were conducted as described (Groisman et al. 2003).

2.5.5 In vitro GST-pulldown assays

Recombinant GST-OGT fusion protein was purified using glutathione agarose beads and used for pull down assays as described in the text and supplemental information.

2.5.6 Immunofluorescence

Cells were fixed with paraformaldehyde and stained with the appropriate antibodies as detailed in the supplemental information.

2.5.7 mRNA expression analysis and chromatin immunoprecipitations

mRNA was prepared according to standard procedures and cDNAs were used for real time qRT-PCR analysis of cellular and viral mRNA levels. Chromatin immunoprecipitation (ChIP) was done essentially as previously described (Bottardi et al. 2009) with minor modifications as described in supplemental information.

2.6 Acknowledgments

This work was supported by grants to E.B.A. from the Terry Fox Foundation (grant#018144). Work in T.K's laboratory was supported by the Laboratory of Viral Diseases, Division of Intramural Research, National Institute of Allergy and Infectious Diseases, NIH. E.B.A. is a scholar of Le Fonds de la Recherche en Santé du Québec. S.D. is a PhD Scholar of the Islamic Bank for Development. N.M. is a PhD Scholar of Le Fonds Québécois de la Recherche sur la Nature et les Technologies. H. Y. is a PhD Scholar of the Canadian Institutes for Health Research. We are grateful to Winship Herr for his generous gift of HCF-1 constructs and antibodies and to James J.D. Hsieh for his kind gift of MLL1 construct. We thank Elliot Drobetsky for the critical reading of the manuscript.

The authors declare no conflict of interest.

2.7 References

Bottardi, S., et al. (2009), 'Ikaros and GATA-1 combinatorial effect is required for silencing of human gamma-globin genes', *Mol Cell Biol,* 29 (6), 1526-37.

Butkinaree, C., Park, K., and Hart, G. W. (2010), 'O-linked beta-N-acetylglucosamine (O-GlcNAc): Extensive crosstalk with phosphorylation to regulate signaling and transcription in response to nutrients and stress', *Biochim Biophys Acta,* 1800 (2), 96-106.

Capotosti, F., Hsieh, J. J., and Herr, W. (2007), 'Species selectivity of mixed-lineage leukemia/trithorax and HCF proteolytic maturation pathways', *Mol Cell Biol,* 27 (20), 7063-72.

Cheng, X. and Hart, G. W. (2001), 'Alternative O-glycosylation/O-phosphorylation of serine-16 in murine estrogen receptor beta: post-translational regulation of turnover and transactivation activity', *J Biol Chem,* 276 (13), 10570-5.

Davis, L. I. and Blobel, G. (1987), 'Nuclear pore complex contains a family of glycoproteins that includes p62: glycosylation through a previously unidentified cellular pathway', *Proc Natl Acad Sci U S A,* 84 (21), 7552-6.

Dejosez, M., et al. (2008), 'Ronin is essential for embryogenesis and the pluripotency of mouse embryonic stem cells', *Cell,* 133 (7), 1162-74.

Groisman, R., et al. (2003), 'The ubiquitin ligase activity in the DDB2 and CSA complexes is differentially regulated by the COP9 signalosome in response to DNA damage', *Cell,* 113 (3), 357-67.

Han, I. and Kudlow, J. E. (1997), 'Reduced O glycosylation of Sp1 is associated with increased proteasome susceptibility', *Mol Cell Biol,* 17 (5), 2550-8.

Hanover, J. A., et al. (1987), 'O-linked N-acetylglucosamine is attached to proteins of the nuclear pore. Evidence for cytoplasmic and nucleoplasmic glycoproteins', *J Biol Chem,* 262 (20), 9887-94.

Hsieh, J. J., et al. (2003), 'Proteolytic cleavage of MLL generates a complex of N- and C-terminal fragments that confers protein stability and subnuclear localization', *Mol Cell Biol,* 23 (1), 186-94.

Hu, P., Shimoji, S., and Hart, G. W. (2010), 'Site-specific interplay between O-GlcNAcylation and phosphorylation in cellular regulation', *FEBS Lett,* 584 (12), 2526-38.

Hurtado-Guerrero, R., Dorfmueller, H. C., and van Aalten, D. M. (2008), 'Molecular mechanisms of O-GlcNAcylation', *Curr Opin Struct Biol,* 18 (5), 551-7.

Jinek, M., et al. (2004), 'The superhelical TPR-repeat domain of O-linked GlcNAc transferase exhibits structural similarities to importin alpha', *Nat Struct Mol Biol,* 11 (10), 1001-7.

Julien, E. and Herr, W. (2003), 'Proteolytic processing is necessary to separate and ensure proper cell growth and cytokinesis functions of HCF-1', *EMBO J,* 22 (10), 2360-9.

Kelly, W. G., Dahmus, M. E., and Hart, G. W. (1993), 'RNA polymerase II is a glycoprotein. Modification of the COOH-terminal domain by O-GlcNAc', *J Biol Chem,* 268 (14), 10416-24.

Kristie, T. M. and Sharp, P. A. (1993), 'Purification of the cellular C1 factor required for the stable recognition of the Oct-1 homeodomain by the herpes simplex virus alpha-trans-induction factor (VP16)', *J Biol Chem,* 268 (9), 6525-34.

Kristie, T. M., Liang, Y., and Vogel, J. L. (2009), 'Control of alpha-herpesvirus IE gene expression by HCF-1 coupled chromatin modification activities', *Biochim Biophys Acta,* 1799 (3-4), 257-65.

Kurokawa, M. and Kornbluth, S. (2009), 'Caspases and kinases in a death grip', *Cell,* 138 (5), 838-54.

Liu, Y., Hengartner, M. O., and Herr, W. (1999), 'Selected elements of herpes simplex virus accessory factor HCF are highly conserved in Caenorhabditis elegans', *Mol Cell Biol,* 19 (1), 909-15.

Love, D. C., Krause, M. W., and Hanover, J. A. (2010), 'O-GlcNAc cycling: emerging roles in development and epigenetics', *Semin Cell Dev Biol,* 21 (6), 646-54.

Mahajan, S. S., Johnson, K. M., and Wilson, A. C. (2003), 'Molecular cloning of Drosophila HCF reveals proteolytic processing and self-association of the encoded protein', *J Cell Physiol,* 194 (2), 117-26.

Marshall, S., Okuyama, R., and Rumberger, J. M. (2005), 'Turnover and characterization of UDP-N-acetylglucosaminyl transferase in a stably transfected HeLa cell line', *Biochem Biophys Res Commun,* 332 (1), 263-70.

Nakatani, Y. and Ogryzko, V. (2003), 'Immunoaffinity purification of mammalian protein complexes', *Methods Enzymol,* 370, 430-44.

Sanders, M. M. (1978), 'Fractionation of nucleosomes by salt elution from micrococcal nuclease-digested nuclei', *J Cell Biol,* 79 (1), 97-109.

Slawson, C., Copeland, R. J., and Hart, G. W. (2010), 'O-GlcNAc signaling: a metabolic link between diabetes and cancer?', *Trends Biochem Sci,* 35 (10), 547-55.

Tyagi, S., et al. (2007), 'E2F activation of S phase promoters via association with HCF-1 and the MLL family of histone H3K4 methyltransferases', *Mol Cell,* 27 (1), 107-19.

Vercauteren, K., Gleyzer, N., and Scarpulla, R. C. (2008), 'PGC-1-related coactivator complexes with HCF-1 and NRF-2beta in mediating NRF-2(GABP)-dependent respiratory gene expression', *J Biol Chem,* 283 (18), 12102-11.

Vogel, J. L. and Kristie, T. M. (2000), 'Autocatalytic proteolysis of the transcription factor-coactivator C1 (HCF): a potential role for proteolytic regulation of coactivator function', *Proc Natl Acad Sci U S A,* 97 (17), 9425-30.

--- (2006), 'Site-specific proteolysis of the transcriptional coactivator HCF-1 can regulate its interaction with protein cofactors', *Proc Natl Acad Sci U S A,* 103 (18), 6817-22.

Wang, Z., et al. (2010), 'Extensive crosstalk between O-GlcNAcylation and phosphorylation regulates cytokinesis', *Sci Signal,* 3 (104 ra2), 1-22.

Wilson, A. C., Peterson, M. G., and Herr, W. (1995), 'The HCF repeat is an unusual proteolytic cleavage signal', *Genes Dev,* 9 (20), 2445-58.

Wilson, A. C., et al. (2000), 'HCF-1 amino- and carboxy-terminal subunit association through two separate sets of interaction modules: involvement of fibronectin type 3 repeats', *Mol Cell Biol,* 20 (18), 6721-30.

Wysocka, J., et al. (2003), 'Human Sin3 deacetylase and trithorax-related Set1/Ash2 histone H3-K4 methyltransferase are tethered together selectively by the cell-proliferation factor HCF-1', *Genes Dev,* 17 (7), 896-911.

Yang, X., et al. (2001), 'O-linkage of N-acetylglucosamine to Sp1 activation domain inhibits its transcriptional capability', *Proc Natl Acad Sci U S A,* 98 (12), 6611-6.

Zhang, F., et al. (2003), 'O-GlcNAc modification is an endogenous inhibitor of the proteasome', *Cell,* 115 (6), 715-25.

2.8 Supporting Information

2.8.1 SI Materials And Methods

Plasmids and Antibodies

shRNA constructs for human OGT or HCF-1 were generated as described previously (Sui et al. 2002). The cDNAs of human OGT and OGA were cloned from HeLa cell RNA by RT-PCR. GST-OGT was generated by subcloning the OGT cDNA into pGEX-4T1 vector. Mammalian constructs to express N-terminal Myc-tagged OGT or OGA were generated by subcloning into the pDEST-N-Myc Gateway® plasmid (Invitrogen). The Myc-OGT D925A catalytic inactive mutant (Clarke et al. 2008) was generated by site-directed mutagenesis. The HCF-1 N (1-1010 aa) containing mutations in the O-glycosylation sites (S/T to A) was generated by direct gene synthesis (Biobasic Inc), and introduced into pCDNA3 (HA-HCF-1 FL ΔO-Glc). The HCF-1 lacking the OGT-binding motif (HA-HCF-1 ΔOBM) was generated by PCR-based subcloning into pCDNA3. The plasmids pCGN-HCF-1 FL and pCGN-HCF-1 N1011 were generously provided by Dr. Herr (Wilson et al. 1993; Wilson et al. 2000). The Myc-PPD and Myc-NLS-PPD expression constructs were generated by PCR-based subcloning of HCF-1 sequence (3028-4305 bp) into pDEST-N-Myc. The expression vectors V5-tagged wildype HCF-1 and the uncleavable HCF-1 have been described (Vogel and Kristie 2006). The HCF-1 ΔPPD V5 containing a deletion of the PPD (998-1456 aa) was derived from the WT HCF-1 (23). A plasmid containing the full length MLL1 was kindly provided by Dr. Hsieh (Hsieh et al. 2003). The anti-HCF-1 PPD antibody has been described (Kristie et al. 1995; Kristie 1997). Additional antibodies were as follows: anti-HCF-1 (A301-400A) and anti-MLL1-N300 (A300-086A), Bethyl Laboratories; anti-βactin (MAB1501) and GAPDH (MAB374), Millipore; anti-OGT (H300, sc-32921)**,** anti-OGT (A6, sc-74547), anti-ubiquitin (P4D1, sc-8017), anti-PARP-1 (F2, sc-8007), anti-YY1 (H10, sc-7341) and rabbit IgG (sc-2027), Santa Cruz Biotechnology; anti-O-Linked N-Acetylglucosamine (RL2, GTX22739), GeneTex; anti-HA (16B12, MMS-101P), anti-c-Myc (MMS-150P), Covance; anti-V5 (SV5, ab27671), Abcam.

Cell culture, RNAi and immunoblotting

HeLa, U2OS and HEK293T (293T) cells were maintained according to standard culture protocols. Cells were transfected with either 5 μg of non-targeting control or RNA interference plasmids (shRNA) along with 0.2 μg pBABE puromycin resistance-encoding vector using Lipofectamine 2000 (Invitrogen). The transfected cells were selected after 1 day by adding 2 μg/ml of puromycin for HeLa and 3 μg/ml for U2OS and 293T, for 2 additional days as described (Affar et al. 2006). For siRNA, cells were transfected with either 200 pmol of non-targeting control, *hOGT* (L-019111-00) or *hHCF-1* (L-019953-00) siRNAs ON-TARGETplus SMARTpool (Dharmacon). Three days post-transfection, cells were harvested for western blotting. HFF cells were transfected with control or OGT siRNAs. Three days post-transfection, cells were infected with 0.1 PFU HSV-1 and harvested for mRNA analysis and western blotting. Total cell extracts were prepared in lysis buffer (50 mM Tris-HCl, pH 7.3; 5 mM EDTA; 50 mM KCl; 0.1% NP-40; 1 mM phenylmethylsulfonyl fluoride (PMSF); 1 mM dithiothreitol and protease inhibitors cocktail (Sigma), and protein concentration was determined by Bradford assay. SDS-PAGE and Western blotting were done according to standard procedures. The band signals were acquired with a LAS-3000 LCD camera coupled to MultiGauge software (Fuji, Stamford, CT, USA). Densitometric analysis of protein bands and radioautographs were done using Gel-Pro Analyzer 3.1 (Media Cybernetics Inc).

Immunodepletion and Immunoprecipitation

Immunodepletion of nuclear extracts was conducted using HeLa nuclear extracts (~100 μg of proteins) incubated overnight at 4 ºC with 2 μg of anti-HCF-1 (A301-400A) or control IgG in IP buffer (50 mM Tris, pH 7.3; 150 mM NaCl; 5 mM EDTA; 10 mM NaF; 1% Triton X-100; 1 mM PMSF and protease inhibitors cocktail (Sigma)). The immuno-complexes were collected on protein A agarose beads which were saturated with 1% BSA in IP buffer. Immuno-complexes were washed twice with the IP buffer supplemented with 1% BSA. Bound proteins were eluted and subjected, along with the flow through fractions, to western blotting. Co-immunoprecipitations to determine proteins interactions and O-GlcNAc protein modification levels were conducted essentially as described above using 2 mg of total cell lysates prepared in lysis buffer (50 mM Tris, pH 7.3; 150 mM NaCl; 5 mM EDTA; 10 mM

NaF; 1% Triton X-100; 1 mM PMSF, protease inhibitors cocktail (Sigma) and 10 µM *PUGNAc* (*Toronto* Research Chemicals). Denaturing immunoprecipitations were done using the same lysis buffer containing 300 mM NaCl and 1% SDS. After boiling for 3 mins, the samples were diluted 10 fold with the same buffer used above without SDS prior to immunoprecipitation.

In vitro interaction assays

Recombinant GST-OGT fusion protein was purified using glutathione agarose beads (Sigma) and 2 to 3 µg of beads containing bound proteins were incubated with 10 µl of *in vitro* translated *methionine-^{35}S* labelled HCF-1 (*TNT*® T7 Quick Coupled Transcription/Translation System, Promega) for 6 to 8 hours at 4 ºC in 50 mM Tris, pH 7.5; 50 mM NaCl; 0.02% Tween 20; 1 mM PMSF and 500 µM dithiothreitol). The beads were extensively washed with the same buffer, and bound proteins eluted in Laemmli buffer and subjected to autoradiography or western blotting. The primers used for the amplification of HCF-1 fragments used IVT assays are provided below.

Immunofluorescence

Cells were fixed for 20 min using 3 % paraformaldehyde in phosphate-buffered saline (PBS), permeabilized in PBS containing 0.5 % NP-40 for 20 min. Following incubation in blocking solution (PBS containing 0.1% NP-40 and 10% FBS), cells were stained with the polyclonal anti-HCF-1 (A301-400A)**,** the monoclonal anti-OGT (A6) or the monoclonal anti-c-Myc (MMS-150P). Anti-mouse Alexa Fluor® 594 or Alexa Fluor® 488, and Anti-rabbit Alexa Fluor® 488 or Alexa Fluor® 594 (Invitrogen) were used as secondary antibodies. Nuclei were stained with 4', 6-diamidino-2-phenylindole (DAPI). Images were acquired using Leica DMRE microscope, HCX PL APO 63X/ 1.32-0.6 OIL CS objective and Retiga Ex (Qimaging) camera.

mRNA expression analysis

RNA was prepared using Trizol reagent (Invitrogen) and the RNeasy kit (QIAGEN). Total mRNA was used for reverse transcription using the Superscript III reverse transcriptase

and oligo(dT)$_{12-18}$ primers (Invitrogen). The obtained cDNAs were subjected to Real time PCR using SYBR Green detection kit (Invitrogen) to determine levels of individual mRNAs. PCR was conducted on an iCycler iQ apparatus (Bio-Rad). The primers used are listed below.

Chromatin immunoprecipitation analysis

Chromatin immunoprecipitation (ChIP) experiments were done essentially as previously described (Bottardi et al. 2009) with the following modifications. U2OS cells (5 X 10^6) were incubated with EGS (ethylene glycolbis [succnimidyl succinate], Sigma-Aldrich) as described (Nowak et al. 2005; Zeng et al. 2006) and were cross-linked with 1% formaldehyde in PBS for 10 min. Following quenching with glycine, cells were scraped in cold PBS, washed with buffer A (50 mM Tris-HCl, pH 8.0; 0.1% NP40; 2 mM EDTA; 10% glycerol; 1 mM PMSF and protease inhibitors cocktail, Sigma) and then sonicated in Buffer B (50 mM Tris-HCl, pH 8.0; 1% SDS; 10 mM EDTA; 1 mM PMSF and protease inhibitors cocktail). After centrifugation and pre-clearing, the suspension was incubated with anti-HCF-1 **(A301-400A)** or an IgG control. DNA was purified from immunocomplexes and quantitated by qPCR using the $2^{-\Delta\Delta CT}$ method, where $\Delta\Delta$CT is calculated as follows: (ChIP CT– input CT of the control antibody) – (ChIP CT – input CT of the target antibody). The results are shown as a ratio of target gene promoter to a reference gene promoter. The primers are listed below.

2.8.2 Supporting References

Affar, E. B., et al. (2006), 'Essential dosage-dependent functions of the transcription factor Yin Yang 1 in late embryonic development and cell cycle progression', *Mol. Cell Biol.,* 26 (9), 3565-81.

Bottardi, S., et al. (2009), 'Ikaros and GATA-1 combinatorial effect is required for silencing of human gamma-globin genes', *Mol Cell Biol,* 29 (6), 1526-37.

Clarke, A. J., et al. (2008), 'Structural insights into mechanism and specificity of O-GlcNAc transferase', *EMBO J,* 27 (20), 2780-8.

Hsieh, J. J., Cheng, E. H., and Korsmeyer, S. J. (2003), 'Taspase1: a threonine aspartase required for cleavage of MLL and proper HOX gene expression', *Cell,* 115 (3), 293-303.

Kristie, T. M. (1997), 'The mouse homologue of the human transcription factor C1 (host cell factor). Conservation of forms and function', *J Biol Chem,* 272 (42), 26749-55.

Kristie, T. M., et al. (1995), 'The cellular C1 factor of the herpes simplex virus enhancer complex is a family of polypeptides', *J Biol Chem,* 270 (9), 4387-94.

Nowak, D. E., Tian, B., and Brasier, A. R. (2005), 'Two-step cross-linking method for identification of NF-kappaB gene network by chromatin immunoprecipitation', *Biotechniques,* 39 (5), 715-25.

Sui, G., et al. (2002), 'A DNA vector-based RNAi technology to suppress gene expression in mammalian cells', *Proc. Natl. Acad. Sci. U. S. A.,* 99 (8), 5515-20.

Vogel, J. L. and Kristie, T. M. (2006), 'Site-specific proteolysis of the transcriptional coactivator HCF-1 can regulate its interaction with protein cofactors', *Proc Natl Acad Sci U S A,* 103 (18), 6817-22.

Wilson, A. C., et al. (1993), 'The VP16 accessory protein HCF is a family of polypeptides processed from a large precursor protein', *Cell,* 74 (1), 115-25.

Wilson, A. C., et al. (2000), 'HCF-1 amino- and carboxy-terminal subunit association through two separate sets of interaction modules: involvement of fibronectin type 3 repeats', *Mol Cell Biol,* 20 (18), 6721-30.

Zeng, P. Y., et al. (2006), 'In vivo dual cross-linking for identification of indirect DNA-associated proteins by chromatin immunoprecipitation', *Biotechniques,* 41 (6), 694, 96, 98.

2.8.3 SI Figures

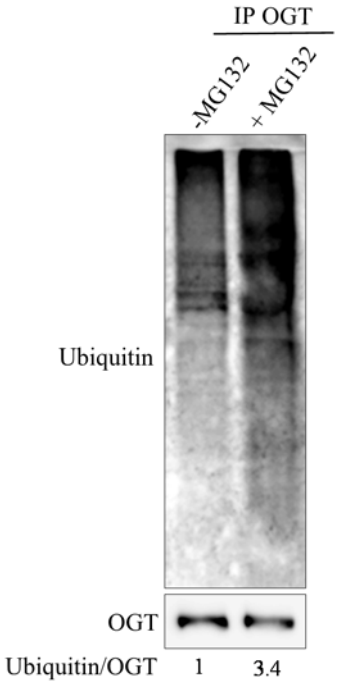

Figure S2.1. Endogenous OGT is ubiquitinated and degraded by the proteasome. 293T cells were treated with 20 μM MG132 for 10 hours. Denatured whole cell extracts were used to immunoprecipitate OGT which was subjected to immunoblotting with the indicated antibodies.

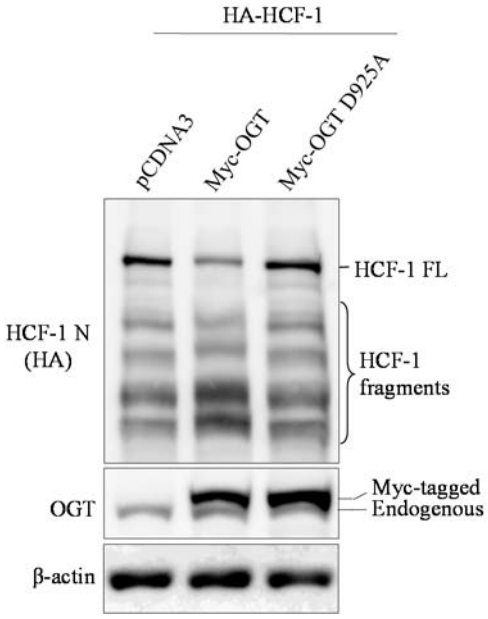

Figure S2.2. OGT regulates HCF-1 cleavage in catalytic activity-dependent manner.

293T cells were transfected with HA-HCF-1 FL expression plasmid along with pCDNA3, Myc-OGT or Myc-OGT D925A. Two days post-transfection, total cell extracts were used for immunoblotting with the indicated antibodies.

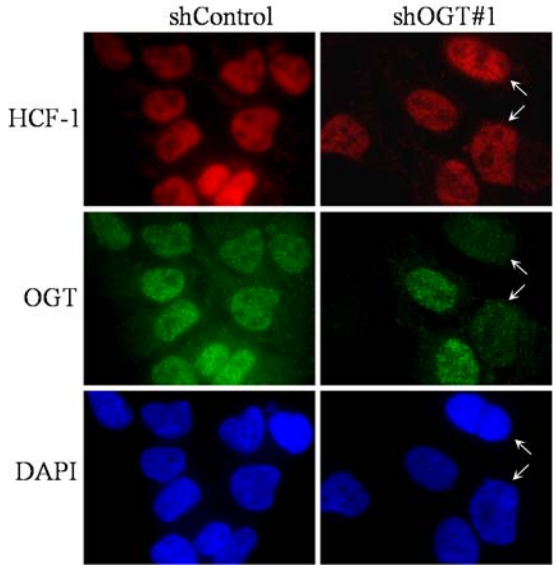

Figure S2.3.Depletion of OGT does not interfere with HCF-1 nuclear import.

Immunofluorescence detection of HCF-1 following knockdown of OGT. U2OS cells were transfected with either non-targeting control or OGT shRNA plasmid for 3 days prior to fixation and immunostaining. Arrows indicate cells depleted for OGT.

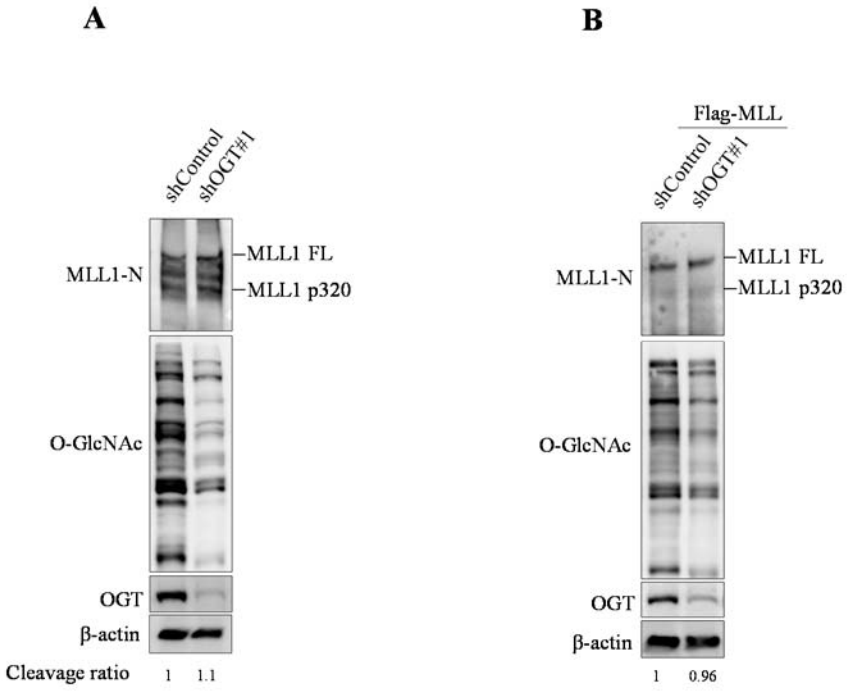

Figure S2.4. OGT is not required for proteolytic cleavage of mixed lineage leukaemiaMLL1.

(A)HeLa cells were transfected with either non-targeting control or OGT shRNA plasmids. Three days post-transfection, cells were harvested for immunoblotting.(B) HeLa cells were transfected with either non-targeting control or OGT shRNA plasmids along with Flag-MLL1 expression plasmid. Three days post-transfection, cells were harvested for western blotting.

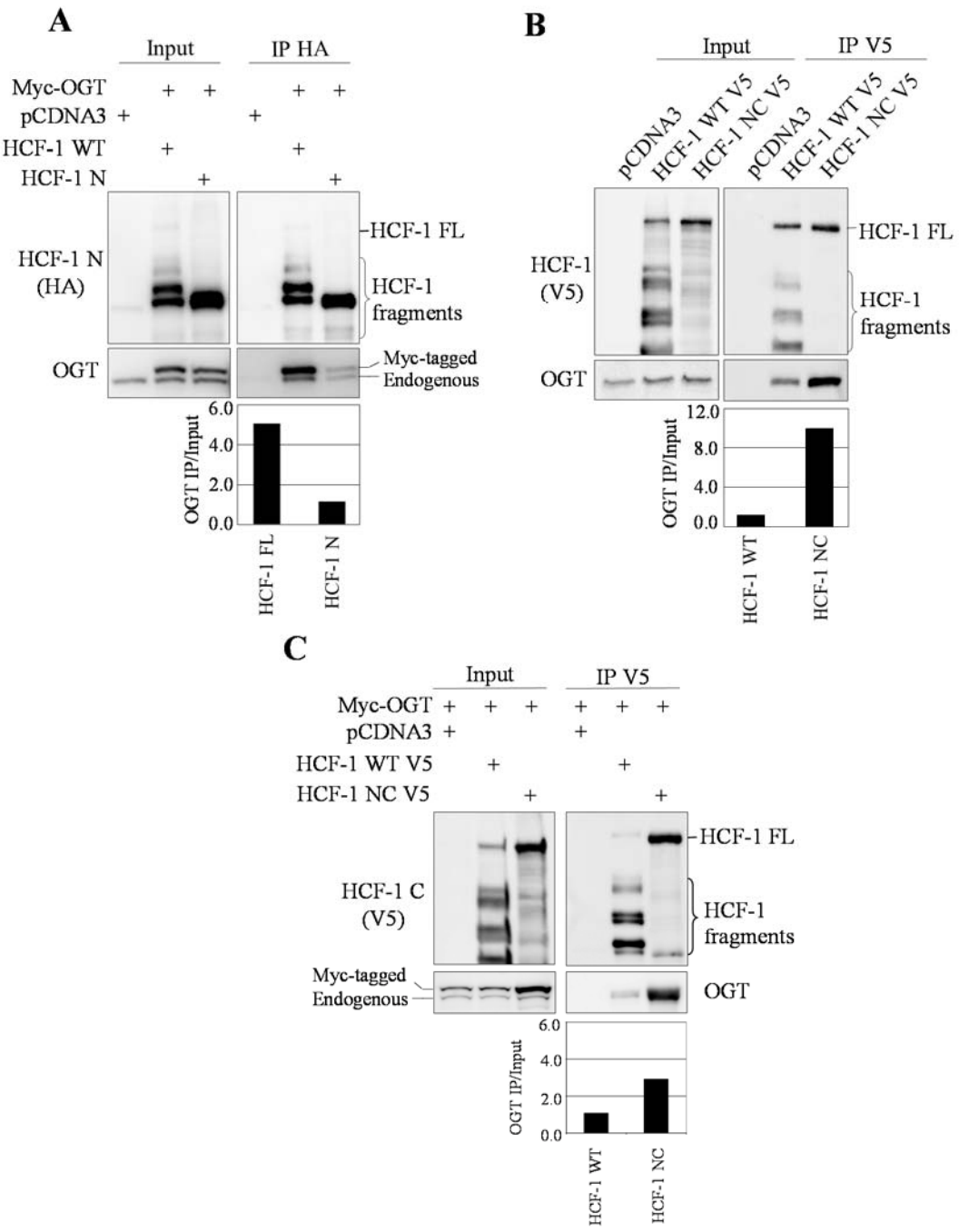

Figure S2.5. OGT interacts more efficiently with the HCF-1 precursor.

(A) Interaction of OGT with HCF-1 N subunit or HCF-1 FL. HeLa cells were transfected with either HA-HCF-1 FL or HA-HCF-1 N (1-1010 aa) along with Myc-OGT. Two days post-transfection, total cell extracts were used for immunoprecipitation using anti-HA and immunoblotting using the indicated antibodies. The efficiency of interaction was determined by densitometry quantification of OGT in the

IP fraction versus OGT in the input cell extract for each condition. Note that transfected cells with both Myc-OGT and HCF-1 show a substantial increase in the levels of transfected OGT. In contrast, the signal of endogenous OGT is not significantly changed between control and HCF-1 conditions as the ratio of non-transfected cells versus transfected cells is high. **(B)** Interaction of OGT with uncleaved HCF-1 or HCF-1 FL. 293T cells were transfected with either HCF-1 FL V5 or HCF-1 NC V5 and used for immunoprecipitation using anti-V5. The efficiency of interaction was determined as in panel A. **(C)** Interaction of overexpressed OGT with uncleaved HCF-1 or HCF-1 FL. 293T cells were transfected with either HCF-1 FL V5 or HCF-1 NC V5 expression plasmids along with Myc-OGT. Two days post-transfection, total cell extracts were used for immunoprecipitation using an anti-V5. The immunocomplexes were subjected to western blotting. The efficiency of interaction was determined as in panel A. We note that: (i) large HCF-1 fragments containing portions of PPD interact more with OGT than HCF-1 N terminal subunit (ii) the uncleaved full length HCF-1 containing intact PPD interacts more efficiently with OGT than HCF-1 cleaved fragments**.**

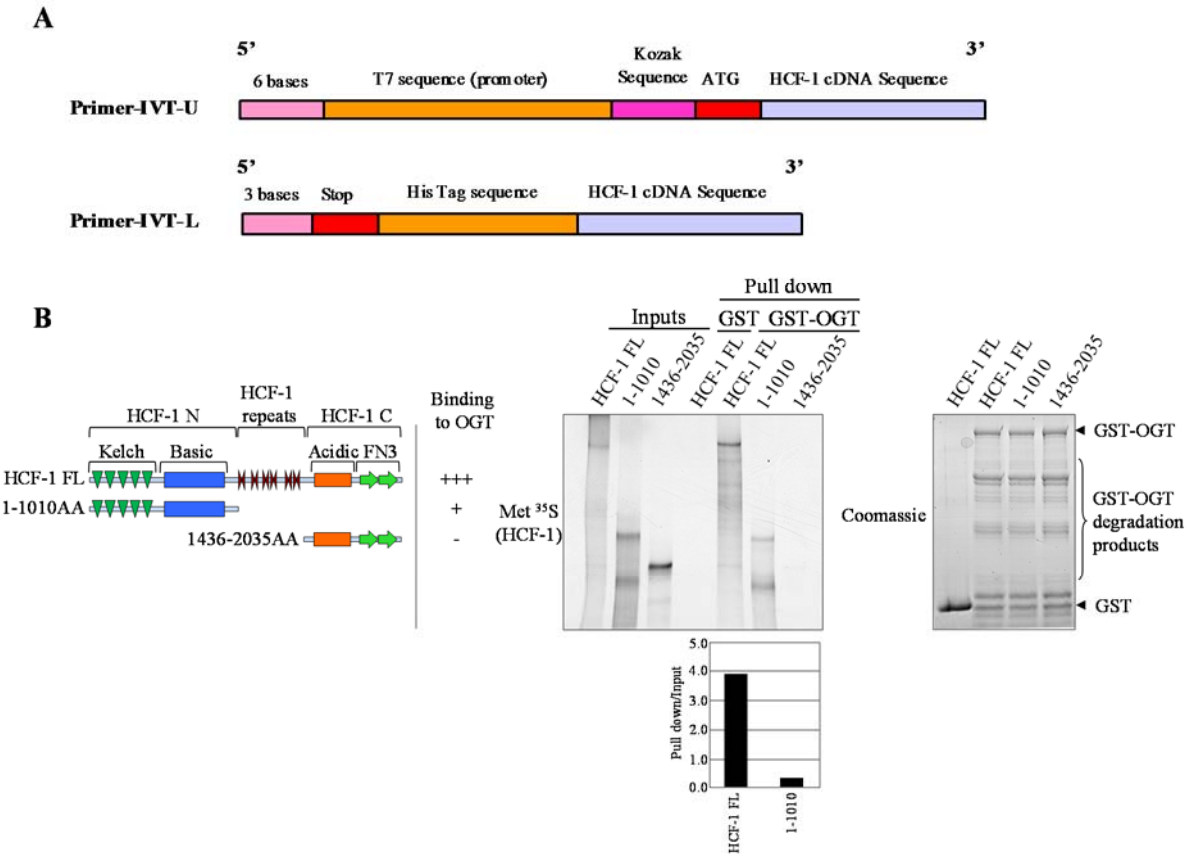

Figure S2.6. Interaction in vitro between OGT and HCF-1 FL, HCF-1 N or HCF-1 C subunits.

(A) Schematic representation of primers design for IVT of HCF-1 fragments. **(B)** HCF-1 full length interacts more efficiently with OGT than HCF-1 cleaved fragments. GST-tagged OGT bound to GSH beads was incubated with various fragments of in vitro translated 35S labeled-HCF-1 for 8 hours. Following extensive washes, the bead-associated complexes were analyzed by coomassie blue staining for GST-OGT and autoradiography for HCF-1. The efficiency of interaction was determined by

densitometry quantification of OGT in the pull down fraction versus OGT in the input fraction for each interaction. These in vitro studies indicate that OGT interacts with the N-terminus subunit of HCF-1. We note that the full-length HCF-1 (with intact PPD) interacts more strongly with OGT comparatively to HCF-1 N subunit.

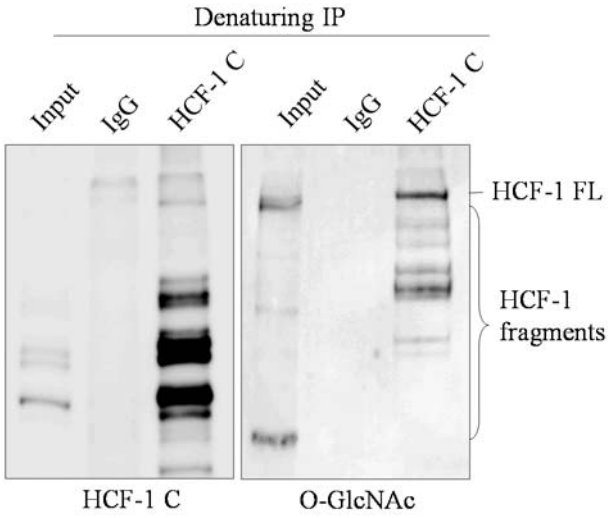

Figure S2.7. The HCF-1 precursor is O-glycosylated

U2OS cell extracts were used for immunoprecipitation under denaturing conditions with an anti-HCF-1 C-terminal antibody. The immunocomplexes were used for western blotting with the indicated antibodies.

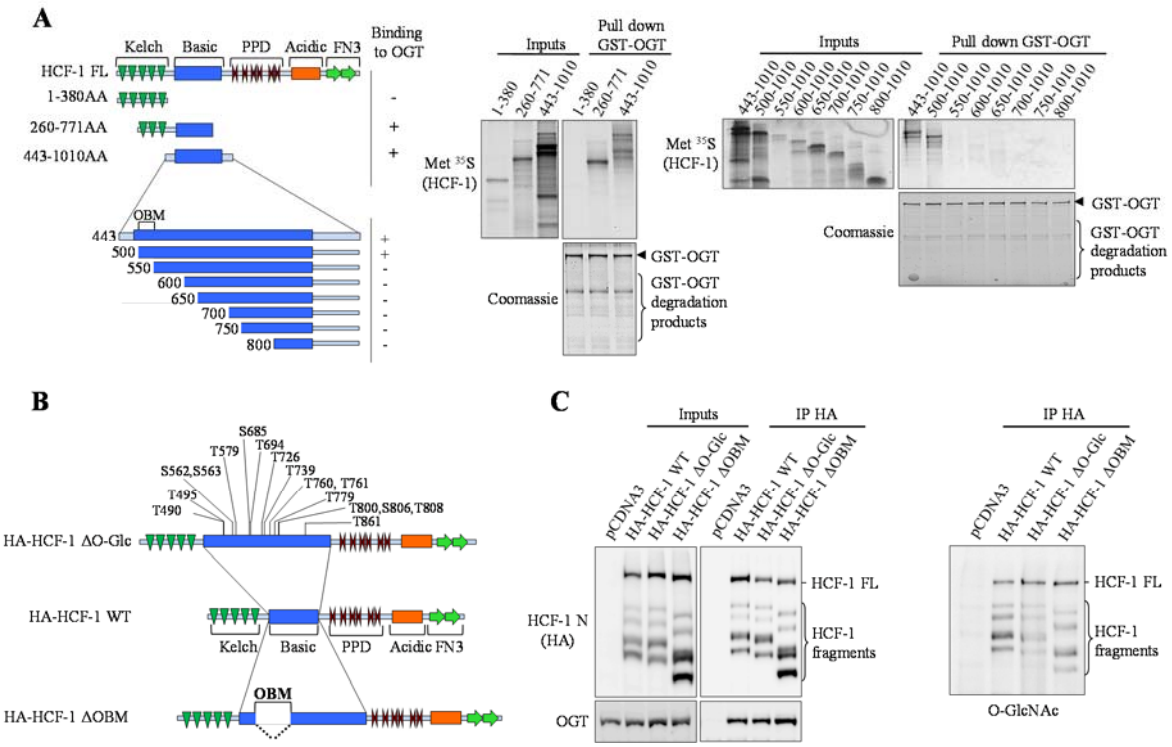

Figure S2.8. HCF-1 N-terminal subunit interaction with OGT or its O-GlcNAcylation are not required for HCF-1 proteolytic cleavage.

(A) Identification of OGT-binding domain in HCF-1 N. GST-tagged OGT bound to GSH beads was incubated with various fragments of in vitro translated 35S labeled-HCF-1. The bead-associated complexes were analyzed by coomassie blue staining for GST-OGT and HCF-1 was analyzed by autoradiography. **(B)** Schematic representation of the S/T O-GlcNAcylation residues mutated in HCF-1 (HA-HCF-1 ΔO-Glc) and the deleted OGT-binding motif OBM in HCF-1 (HA-HCF-1 ΔOBM). **(C)** O-GlcNAcylation status, proteolytic processing and interaction of HCF-1 mutants with OGT. 293T cells were transfected with HA-HCF-1 WT, HA-HCF-1 ΔOBM or HA-HCF-1 ΔO-Glc. Two days post-transfection, cells were harvested for immunoprecipitation using an anti-HA. We note that O-glycosylation of HCF-1 N subunit does not appear to play a role in HCF-1 cleavage since (i) mutation of multiple glycosylation sites in the N-terminal subunit or (ii) deletion of the OGT-interacting motif in this subunit does not affect HCF-1 maturation. Thus the N-terminal subunit, although it provides a distinct domain of interaction with OGT, is dispensable for HCF-1 cleavage. It remains possible that the interaction of the HCF-1 N-terminal subunit with OGT is important for other HCF-1 functions that are distinct from the role of OGT in HCF-1 proteolytic processing.

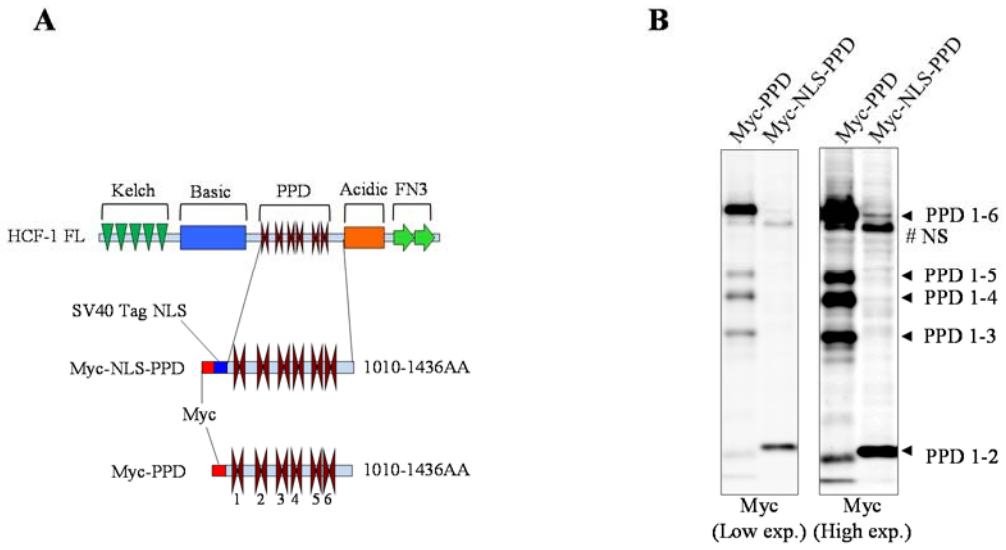

Figure S2.9.Expression of HCF-1 PPD with or without a nuclear localization signal.

(A) Schematic representation of human HCF-1 showing the PPD with the designed constructs**.(B)** 293T cells were transfected with either Myc-PPD or Myc-NLS-PPD expression plasmids. Two days post-transfection, total cell extracts were used for immunoblotting with anti-Myc antibody. NS, non specific band.

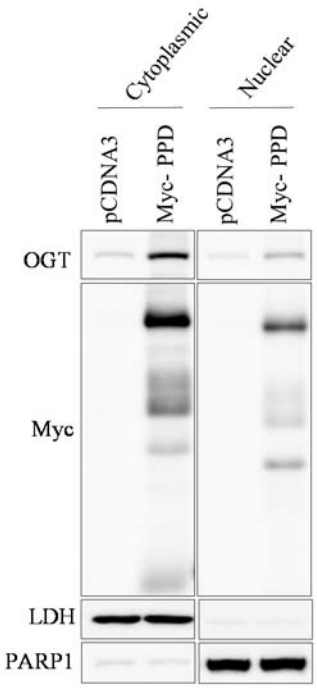

Figure S2.10. HCF-1 PPD stabilizes OGT in the cytoplasm.

293T cells were transfected with Myc-PPD or Myc-NLS-PPD expression plasmids along with Myc-OGT expression plasmid. Forty-eight hours later, cells were homogenized using a dounce homogenizer to separate cytoplasm and nuclei. Homogenates was centrifuged at 3500 g for 15 min, and the cytoplasmic fraction (supernatant) and nuclear fraction (pellet) were collected. Fractions were subjected to immunoblotting with the indicated antibodies. PARP1 and LDH, which are localized in the nucleus and cytoplasm, respectively, were used as controls for fractionation.

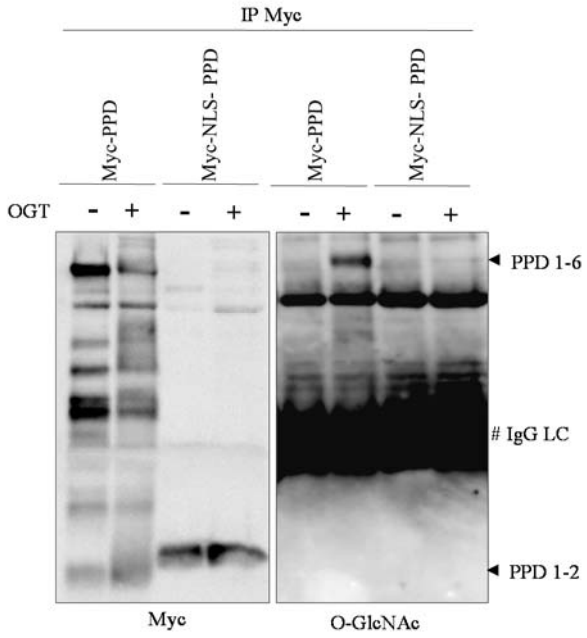

Figure S2.11. O-GlcNAcylation of HCF-1 PPD is dependent on OGT.

293T cells were transfected with Myc-PPD or Myc-NLS-PPD expression plasmids along with OGT expression plasmid or pCDNA3. Forty-eight hours later, extracts of the cells were subjected to IP in denaturing conditions with anti-Myc antibody. Samples were analyzed by immunoblotting with the indicated antibodies.

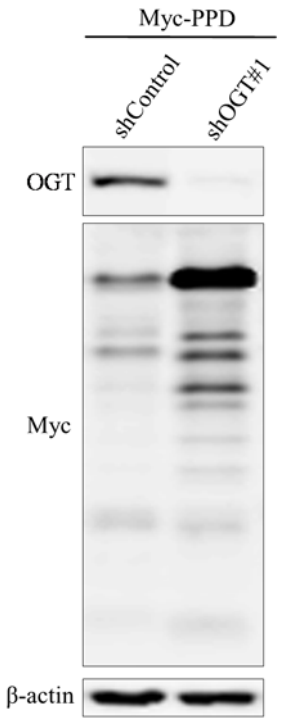

Figure S2.12. RNAi of OGT inhibits cleavage of HCF-1 PPD.

HeLa cells were transfected with the indicated shRNA constructs along with Myc-PPD plasmid and pBABE-puro. The next day, the cells were selected with 2 μg/ml of puromycin for 48 hours. Following selection, the cells were harvested and subjected to immunoblotting with the indicated antibodies.

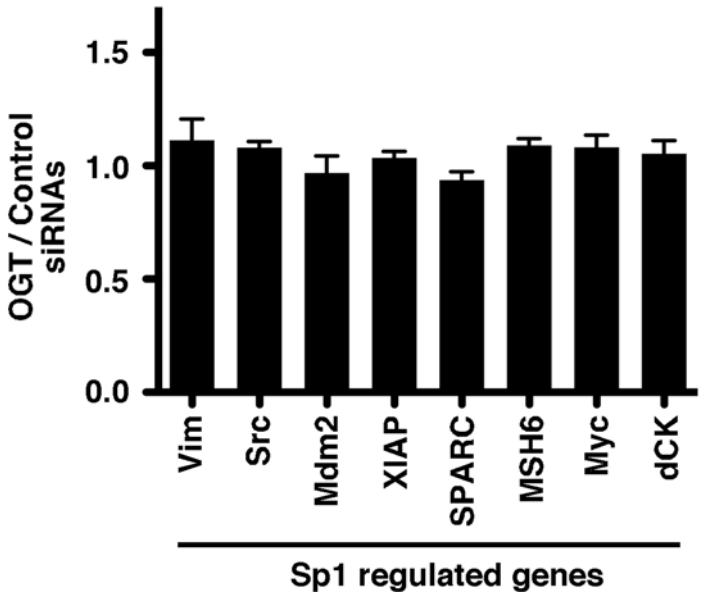

Figure S2.13. Depletion of OGT does not affect Sp1 target gene expression.

HFF cells were transfected with control or OGT siRNAs. Three days post transfection, cells were infected with 0.1 PFU HSV-1 and harvested for mRNA analysis. Levels of Sp1 target gene mRNAs in OGT-depleted cells are shown relative to levels in control siRNA transfected cells. All experiments were repeated at least 3 times and data are presented as mean ± SD.

CHAPITRE 3

Article : Undetectable Histone O-GlcNAcylation in Mammalian Cells

Publié dans: Epigenetics. 2015 Aug 3;10(8):677-91.

Jessica Gagnon[1],†,Salima Daou[1],†,Natalia Zamorano[1],Nicholas VG Ianantuono[1],Ian Hammond-Martel[1], Nazar Mashtalir[1], Eric Bonneil[2], Hugo Wurtele[1], Pierre Thibault[2] and El Bachir Affar[1],#

1 Maisonneuve-Rosemont Hospital Research Center and Department of Medicine, University of Montréal, Montréal H3C 3J7, Québec, Canada

2 Institute for Research in Immunology and Cancer, University of Montréal, Montréal H3C 3J7, Québec, Canada

†Equal contribution

Introduction à l'article :

Dans ce chapitre 3, nous élaborons les résultats qui se rattachent à l'objectif 2 de la thèse.

Comme la OGT est un partenaire intégral de BAP1 et que de nombreux régulateurs transcriptionnels y compris les enzymes de modification de la chromatine, les facteurs et co-facteurs de transcription sont des cibles de la O-GlcNAcylation, indiquant que cette modification est centrale pour les processus associés à la chromatine, nous nous sommes demandés si la O-GlcNAcylation et la déubiquitination de H2Aub peuvent collaborer pour coordonner des évènements cellulaires au niveau de la chromatine.

Récemment, il a été reporté que les histones sont modifiées par O-GlcNAcylation, suggérant un rôle potentiel de cette modification dans la coordination de la structure et la fonction de la chromatine. En revanche, en ayant recours à l'utilisation de plusieurs approches biochimiques, nous rapportons que la O-GlcNAcylation des histones n'est pas détectable dans les cellules de mammifères.

Notre présente étude soulève des doutes quant à l'occurrence et l'abondance de la O-GlcNAcylation comme une modification des histones dans les cellules de mammifères et révèle des complications techniques concernant la détection spécifique de la O-GlcNAcylation.

Contribution: Ma contribution comme co-premier auteur a consisté à la conception et la réalisation de 50% des expériences de l'article ainsi qu'à la préparation des figures, l'interprétation des résultats et la rédaction du manuscrit.

3.1 Abstract

O-GlcNAcylation is a post-translational modification catalyzed by the O-Linked N-acetylglucosamine (O-GlcNAc) transferase (OGT) and reversed by O-GlcNAcase (OGA). Numerous transcriptional regulators including chromatin modifying enzymes, transcription factors and co-factors are targeted by O-GlcNAcylation indicating that this modification is central for chromatin-associated processes. Recently, OGT-mediated O-GlcNAcylation was reported to be a novel histone modification, suggesting a potential role in directly coordinating chromatin structure and function. In contrast, using multiple biochemical approaches, we report here that histone O-GlcNAcylation is undetectable in mammalian cells. Conversely, O-GlcNAcylation of the transcription regulators Host Cell Factor-1 (HCF-1) and the Ten-Eleven Translocation protein 2 (TET2) could be readily observed. Our study raises questions on the occurrence and abundance of O-GlcNAcylation as a histone modification in mammalian cells and reveals technical complications regarding the detection of genuine protein O-GlcNAcylation. Therefore, the identification of the specific contexts in which histone O-GlcNAcylation might occur is still to be established.

3.2 Introduction

O-GlcNAcylation is a widespread post-translational modification corresponding to the addition of a single O-Linked N-acetylglucosamine (O-GlcNAc) moiety to nuclear and cytosolic proteins.[292,293,301] Similar to other post-translational modifications, O-GlcNAcylation regulates protein function by influencing protein-protein interactions, enzymatic activity and sub-cellular localization.[320,411] In mammals, this modification is coordinated by two enzymes, the O-Linked β-N-acetylglucosamine transferase (OGT) which catalyzes the attachment of the O-GlcNAc moiety on serine and threonine residues of target proteins, while the O-GlcNAcase (OGA) ensures its removal through hydrolysis.[412,413] O-GlcNAcylation signaling is dependent on the availability of the donor substrate, Uridine Diphosphate N-Acetylglucosamine (UDP-

GlcNAc), which is produced via the Hexosamine Biosynthetic Pathway.[321] O-GlcNAcylation is a highly dynamic modification, being regulated by a plethora of intracellular and extracellular cues, including growth factor signaling, fluctuation of nutrient levels, as well as stress responses.[319,411,414] Indeed, O-GlcNAcylation signaling acts as a metabolic sensor that links changes in the cellular metabolism to downstream regulation of numerous cellular pathways.[320,325,334] Moreover, recent studies have shown that direct competition between phosphorylation and O-GlcNAcylation can occur for the same amino acid residue, thus adding another layer of complexity to the outcome and regulation of this post-translational modification.[360,415] The physiological importance of O-GlcNAcylation is further emphasized by the fact that defects in its regulation have been associated with human pathologies such as diabetes, neurodegenerative diseases and cancer.[308,328,329,331,416]

O-GlcNAcylation signaling was proposed to play important roles in regulating the epigenome.[292,340] Indeed, several transcriptional regulators and chromatin-modifying enzymes are modified by O-GlcNAcylation, thus impacting their recruitment to chromatin, assembly into functional transcription regulatory complexes, stability and activity.[302,341,343,353] For instance, we and others have identified a non-canonical mechanism of OGT-mediated transcriptional regulation which involves the O-GlcNAcylation of the Host Cell Factor 1 (HCF-1) transcriptional regulator inducing its proteolytic maturation.[275,283,284]

Recent studies have also reported that histones are modified by O-GlcNAcylation, suggesting an interesting possibility of crosstalk with other well-established histone marks.[21,356,357] Moreover, it was suggested that the methylcytosine dioxygenase Ten Eleven Translocation 2 (TET2) enzyme directly interacts with OGT to stimulate histone H2B S112 O-GlcNAcylation (H2B S112O-GlcNAc) and gene expression.[351] Several methods were used to detect histone O-GlcNAcylation, including mass spectrometry, immunodetection with O-GlcNAc-specific antibodies and affinity binding to Wheat Germ Agglutinin lectin (WGA).[20,21,415] However, discrepancies regarding the occurrence and the identity of the histones being modified were also reported. For instance, some studies suggested that histones H2A and H2B might be the principal targets for O-GlcNAcylation while others have shown that histone H3 would be the main substrate.[20,357,360,415] Upon further characterization, it was reported that histone H2B S112 O-GlcNAcylation promotes H2B monoubiquitination on

lysine 120 (H2B K120ub), an event associated with transcriptional activation.[20,359] On the other hand, histone H3 serine 10 was also reported to be O-GlcNAcylated, and this appears to compete with the phosphorylation of this site as well as modulate the transcriptional state of chromatin.[360,415] Other O-GlcNAcylation sites were reported within the globular domains of histones suggesting that they may function in maintaining higher-order chromatin structure.[357] Strikingly, during our investigation on the role of OGT in chromatin function; we were unable to reproduce the previous findings regarding histone O-GlcNAcylation in mammalian cells, whereas modification of other known OGT substrates was readily detected. Our results raise questions about the occurrence of histone O-GlcNAcylation and its proposed function in chromatin regulation.

3.3 Results & discussion

3.3.1 Undetectable histone O-GlcNAcylation using various extraction techniques.

OGT interacts with the TET family of methylcytosine dioxygenase enzymes, notably TET2, which appear to be required for the chromatin association of OGT and this was suggested to promote histone O-GlcNAcylation.[351,352] To further investigate the potential biological significance of histone O-GlcNAcylation, we initially sought to reproduce previously published results on the modification of histones H2B and H2A.[20,21,351,359,415] We co-expressed Flag-H2B or Flag-H2A with either Myc-OGT or the D925A catalytic inactive mutant (Myc-OGT CD).[314] Coexpression of Myc-TET2 with Myc-OGT was also included since their association was expected to significantly increase OGT-mediated histone O-GlcNAcylation.[351,354] We conducted an immunoprecipitation of Flag-H2B or Flag-H2A under denaturing conditions to determine their potential O-GlcNAcylation levels by using the widely employed anti-O-GlcNAc antibodies RL2 and CTD110.6 (Figure 3.1 and Figure S3.1). We did not detect a specific signal at the molecular weight region corresponding to histones Flag-H2B or Flag-H2A using the two anti-O-GlcNAc antibodies. However, using similar conditions, we were able to detect HCF-1 and TET2 O-GlcNAcylation, two known substrates of OGT (Figure S3.2).[275,353] Of note, as expected, OGT-mediated HCF-1 proteolytic cleavage also confirmed the activity of OGT in our co-transfection conditions (Figure S3.2).[275,283,284] Next, using the

same transfection conditions indicated above, we performed several established extraction methods in order to enrich endogenous histones for O-GlcNAcylation detection. Chromatin and Histones were isolated using both high salt extraction/detergent (300 mM NaCl- 1% NP-40) (Figure 3.2A and Figure S3.3A) and acid extraction (0.2 N HCl) (Figure 3.2B and Figure S3.3B) methods, respectively. First, immunoblotting with RL2 or CTD110.6 antibodies was conducted on the soluble fractions to detect global O-GlcNAcylation levels (Figure 3.2 and Figure S3.3, Left panels). As expected, we observed an increase of cellular O-GlcNAcylation levels following OGT overexpression. However, chromatin fractions revealed faint signals between 10 and 20 kDa when the blots probed with RL2 antibody were overexposed. On the other hand, the CTD110.6 antibody occasionally produced more pronounced signals at the levels of histones (Figure 3.2 and Figure S3.3 Right panels). Overall, we did not observe increasing signals following overexpression of OGT or TET2, regardless of the O-GlcNAc antibody used, the quantity of proteins loaded or the method of extraction performed (Figure 3.2 and Figure S3.3). On the other hand, upon OGT overexpression, we detected increased O-GlcNAcylation of certain chromatin-associated proteins corresponding to bands $\geq$ 37 kDa. Based on these results, we concluded that the faint and inconsistent signals produced between 10 and 20 kDa by the RL2 or CTD110.6 antibodies are not indicative of histone O-GlcNAcylation.

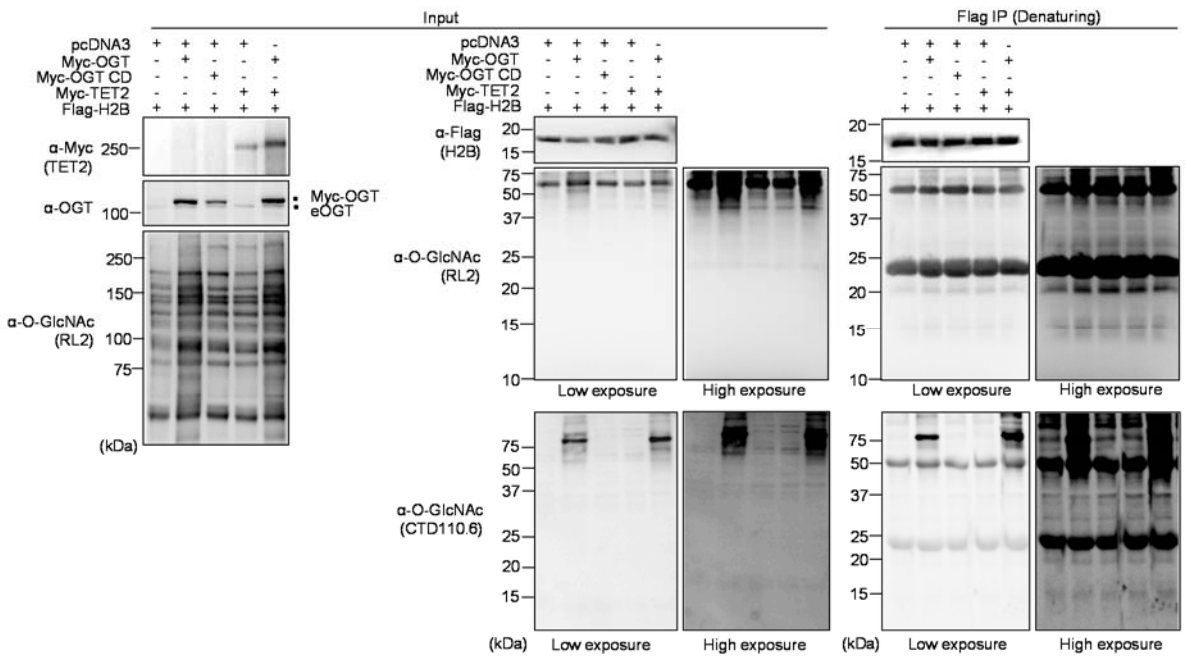

Figure 3.1. Undetectable Histone O-GlcNAcylation following OGT and TET2 overexpression.

(A) HEK293T cells were transfected with Flag-H2B along with pcDNA3 empty vector, Myc-OGT or Myc-OGT catalytic dead (CD), as well as Myc-TET2 alone or in combination with Myc-OGT. Three days post-transfection, cells pellets were harvested and immunoprecipitation (Flag-IP) following protein denaturation was conducted to obtain purified Flag-H2B. The immuno-purified histones were subjected to western blotting analysis using the indicated antibodies. Dots indicate Myc-OGT and endogenous OGT (eOGT).

3.3.2 Modulation of O-GlcNAc levels does not result in the detection of specific histone O-GlcNAcylation

We reasoned that if the signals detected by RL2 or CTD110.6 around 10-20 kDa correspond to histone O-GlcNAcylation, then it might be possible to modulate these signals by depleting endogenous OGT. Thus, we conducted siRNA knockdown of OGT in U2OS cells and performed cellular fractionation to separate the soluble and histone-containing chromatin fractions. As shown in figure 3.3A (Right panel), the signals detected with RL2 or CTD110.6 antibodies around 10-20 kDa, did not decrease following OGT depletion suggesting that these signals are unspecific. In contrast, using both antibodies, we detected a significant decrease in global O-GlcNAcylation in the soluble fraction upon siRNA treatment (Figure 3.3A, Left panel). Again, we noted that while the signal obtained with RL2 antibody in the 10-20 KDa region can be seen only upon overexposure of the membrane, the CTD110.6 antibody

produced a much more readily detectable signal in this region. As RL2 and CTD110.6 are respectively IgG and IgM isotypes, we sought to determine if the signal detected at the level of histones with CTD110.6 could be due to the peroxidase-coupled secondary anti-IgM antibody.

This is particularly relevant as high quantities of histones were probed with anti-O-GlcNAc antibodies. Thus, we incubated the blots with a non-relevant anti-rhodamine IgM antibody prior to incubation with the same anti-IgM antibody or with this secondary antibody alone (Figure 3.3A, Right panel). Interestingly, both combinations displayed a similar signal pattern as that obtained using the CTD110.6, suggesting that the non-specific signal originates from the combination of secondary anti-IgM antibody and high protein density of histone bands. In addition, probing the membranes with a non-relevant anti-BAP1 antibody also resulted in background signals at molecular weights corresponding to histone bands (Figure 3.3A, Right panel). These data indicate that the high abundance of histones present on membranes renders the detection of O-GlcNAcylation amenable to false-positive immunoblotting signals. Of note, previous studies questioned the specificity of CTD110.6 towards O-GlcNAc and revealed cross-reactivity with N-GlcNAc2-modified glycoprotein and GlcNAcylated O-mannose modified proteins.[417,418] Consequently, we used the RL2 antibody to continue our investigation since it was not shown to cross react with other GlcNAc modifications. Nonetheless, our data suggested that the faint signal obtained with RL2 corresponds to a non-specific background caused by high amounts of histones. To further support our data, we extracted endogenous histones from HeLa cells for comparison with purified yeast H2B (yH2B) and recombinant human H2B (hH2B) produced in bacteria. We reasoned that if the faint signal produced by RL2 corresponds to histone O-GlcNAcylation, then this signal should not be detected for histones purified from yeast or bacteria which are not O-GlcNAcylated. We observed that the RL2 antibody produced low signals following overexposure of the blot, and these signals increased proportionally with the amount of histones loaded, irrespective of the species from which the histones were isolated (Figure S3.4, panels A, B). Next, we conducted competition assays and found that, as expected, N-Acetylglucosamine (GlcNAc) inhibited RL2 binding to high molecular weight O-GlcNAcylated proteins present in the soluble fraction or associated with the chromatin fraction (Figure S3.4C). However, GlcNAc also strongly reduced the signal produced by RL2, in the

region of histone bands, for both mammalian chromatin and recombinant human H2B (Figure S3.4C). These results are not surprising as a non-specific and low affinity binding of the RL2 antibody to histone fraction could also be potentially blocked by GlcNAc. Thus, these results further suggest that the RL2 antibody recognizes non-specifically antigenic determinants on histones through its paratope.

To further investigate potential histone O-GlcNAcylation, we sought to determine if inhibiting O-GlcNAcase (OGA), the enzyme responsible for O-GlcNAc removal, with O-(2-acetamido-2-deoxyglucopyranosylidene) amino N-phenylcarbamate (PUGNAc) would increase the signal of histone O-GlcNAcylation above background levels. Treatment of HeLa and HEK293T cells with PUGNAc promoted the accumulation of O-GlcNAcylated proteins but not of the background signal at the level of histones (Figure 3.3B, Left and Right panel). We also conducted a nutrient starvation in C2C12 myoblasts, and analysed global protein and potential histone O-GlcNAcylation. As expected, AMPK phosphorylation progressively increased and decreased with starvation and medium replenishment (R) respectively (Figure 3.3C, Left panel).[86] We observed that while chromatin-associated high molecular weight protein O-GlcNAcylation was reduced upon starvation, only weak and inconsistent background signals were detected for histones (Figure 3.3C, Right panel).

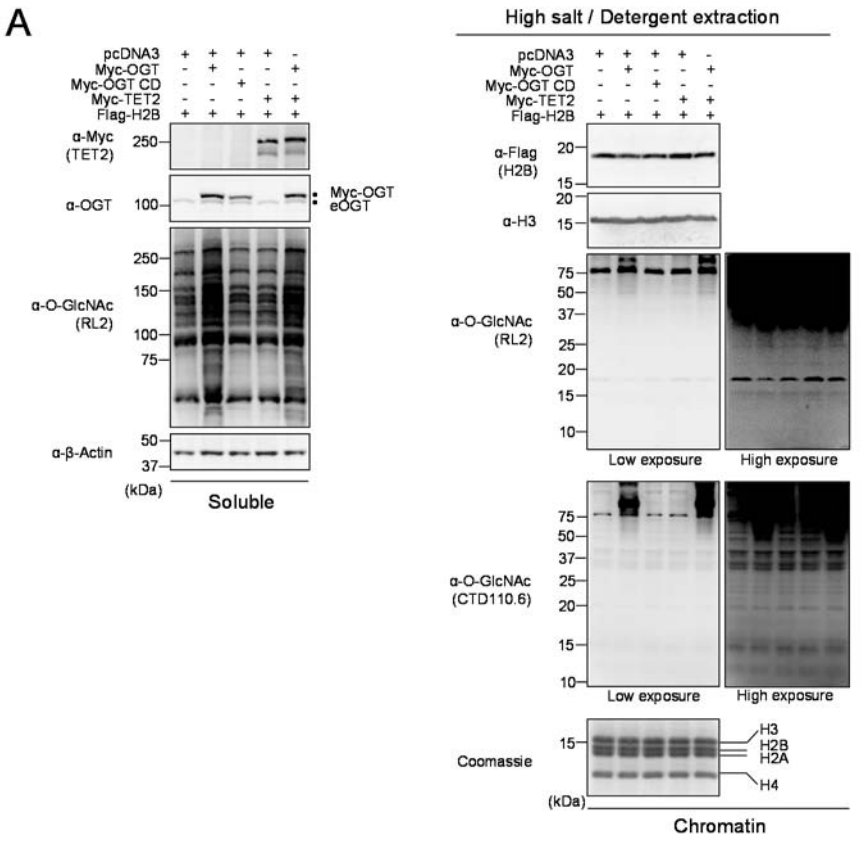
A
pcDNA3
Myc-OGT
Myc-OGT CD
Myc-TET2
Flag-H2B
α-Myc (TET2)
α-OGT
Myc-OGT
eOGT
α-O-GlcNAc (RL2)
α-β-Actin
(kDa)
Soluble
High salt / Detergent extraction
α-Flag (H2B)
α-H3
α-O-GlcNAc (CTD110.6)
Low exposure
High exposure
Coomassie
H3
H2B
H2A
H4
Chromatin

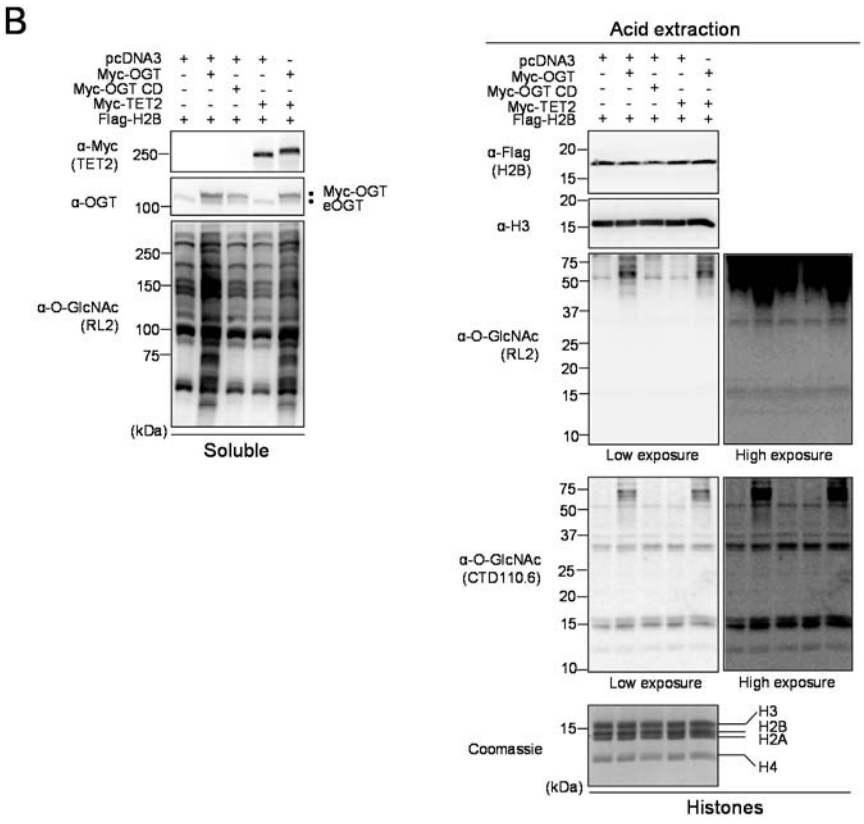
B
pcDNA3
Myc-OGT
Myc-OGT CD
Myc-TET2
Flag-H2B
α-Myc (TET2)
α-OGT
Myc-OGT
eOGT
α-O-GlcNAc (RL2)
(kDa)
Soluble
Acid extraction
α-Flag (H2B)
α-H3
α-O-GlcNAc (CTD110.6)
Low exposure
High exposure
Coomassie
H3
H2B
H2A
H4
Histones

Figure 3.2. Undetectable histone O-GlcNAcylation following various extraction procedures.

(A) HEK293T cells were transfected with Flag-H2B along with either pcDNA3 empty vector, Myc-OGT, Myc-OGT catalytic dead (CD) or Myc-TET2, as well as the combination of Myc-OGT with Myc-TET2. Three days post-transfection, cells pellets were collected for subsequent high salt/detergent extraction and cellular extracts were then analysed by western blotting with the indicated antibodies. (Left panel) Soluble fraction showing global increase of O-GlcNAcylation following OGT overexpression. (Right panel) Immunodetection of histone O-GlcNAcylation by RL2 and CTD110.6 antibodies on chromatin fraction. β-Actin and histone H3 were used as loading controls. **(B)** HEK293T cells were transfected as in (A). Three days post-transfection, cells were harvested and histones were extracted. The samples were analysed by western blotting with the indicated antibodies. (Left panel) Soluble fraction showing global O-GlcNAcylation levels. (Right panel) Histones fraction detected with both RL2 and CTD110.6 anti-O-GlcNAc antibodies. Coomassie Brilliant Blue staining indicates abundance of histones loaded. Histone H3 was use as a loading control. Dots indicate Myc-OGT and endogenous OGT (eOGT). kDa; Molecular weight marker in Kilodalton.

Taken altogether, our results indicate that the immunoblot signal detected by RL2 in the region corresponding to histones, is a non-specific O-GlcNAcylation-independent background signal.

3.3.3 Histone O-GlcNAcylation was undetectable in different cell lines and during cell cycle progression.

Although our data did not reveal constitutive histone O-GlcNAcylation, we could not exclude that this post-translational modification might occur on histones in specific cell types. Thus, we investigated potential histone O-GlcNAcylation in a variety of previously used cell lines including mouse Embryonic Fibroblast (MEF) as well as mouse Embryonic Stem Cells (mESCs).[351,354,359] We also included the mouse pre-adipocyte 3T3-L1 cell line often used in differentiation studies as well as several multiple myeloma cell lines, RPMI8-226, JJN-3, NCI-H292 cells, that we had in culture at the time of our investigation. We find that this cell line panel is representative of multiple tissue-origins as well as primary and cancer cells. When immunoblotting the insoluble chromatin fraction for O-GlcNAcylation, we detected a very faint signal at the level of histones (Figure 3.4A, Top panel). This signal, obtained only following extended exposure of the blot, does not correlate with the cell-specific levels of endogenous O-GlcNAcylation detected for high molecular weight proteins. Instead, by probing total H2A levels, it can be noticed that the RL2 signal follows the trend of histones abundance (Figure 3.4A, Bottom blot).

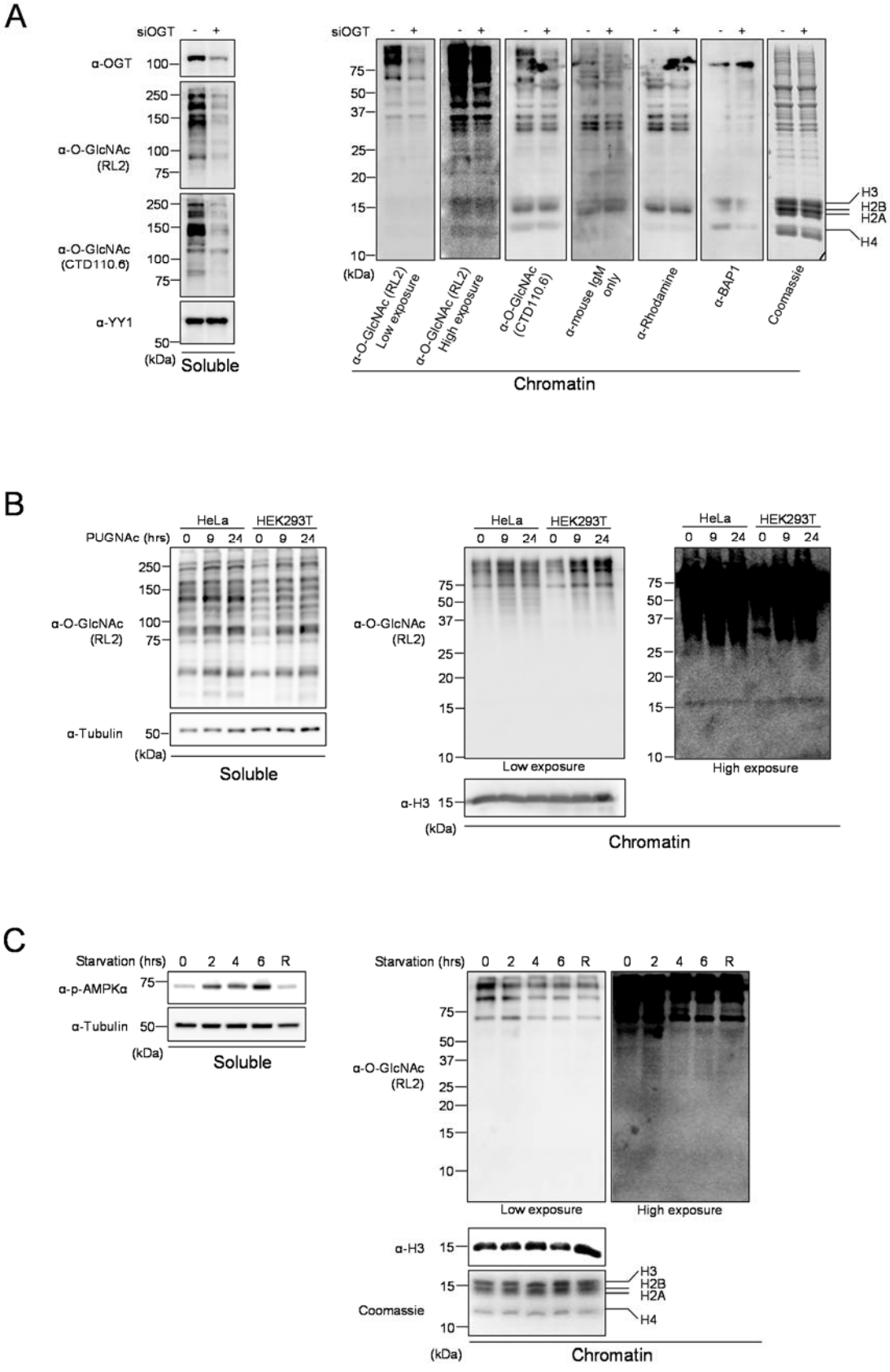
A
siOGT - +
α-OGT
α-O-GlcNAc (RL2)
α-O-GlcNAc (CTD110.6)
α-YY1
(kDa)
Soluble
α-O-GlcNAc (RL2) Low exposure
α-O-GlcNAc (RL2) High exposure
α-O-GlcNAc (CTD110.6)
α-mouse IgM only
α-Rhodamine
α-BAP1
Coomassie
H3
H2B
H2A
H4
Chromatin
B
PUGNAc (hrs) 0 9 24 0 9 24
HeLa
HEK293T
α-O-GlcNAc (RL2)
α-Tubulin
Soluble
Low exposure
High exposure
α-H3
Chromatin
C
Starvation (hrs) 0 2 4 6 R
α-p-AMPKα
α-Tubulin
Soluble
α-O-GlcNAc (RL2)
α-H3
Coomassie
Chromatin

Figure 3.3. Modulation of O-GlcNAcylation does not result in detectable histone O-GlcNAcylation.

(A) U2OS cells were transfected twice with OGT siRNA and three days post-transfection, cells were harvested. Chromatin fraction was isolated and protein levels were analysed by western blotting with the indicated antibodies. (Left) U2OS soluble fraction showing OGT depletion and decrease of global O-GlcNAcylation levels. YY1 was used as a loading control. (Right) Chromatin fraction showing O-GlcNAcylation background detection of histones using various antibodies. (B) HeLa and HEK293T cells that were treated with 100 μM PUGNAc for 0, 9 and 24 hours. The soluble and chromatin fractions were blotted with RL2 antibody. Histone H3 and tubulin were used as loading controls. (C) C2C12 mouse myoblast cell line were starved by incubation in HBSS buffer, and harvested at the indicated times for cellular fractionation. R; 4 hours of starvation followed by 2 hours of replenishment with complete culture medium. (Left) Western blot analysis of the soluble fraction showing increasing levels of phosphorylated AMPKα (α-p-AMPKα) as a control of the starvation treatment. Tubulin was used as a loading control. (Right) The chromatin fraction was analysed by western blotting using the indicated antibodies. Histone H3 was used as a loading control and Coomassie Brilliant Blue staining indicates the abundance of histones loaded. kDa; Molecular weight marker in Kilodalton.

To further determine whether histone O-GlcNAcylation might be enriched in a specific phase of the cell cycle, U2OS cells were synchronized at the G1/S boundary with a double thymidine block and released to progress through the cell cycle.[419] These cells were also treated with the CDK1 inhibitor (RO-3306) to enrich for late G2 cells (Figure 3.4B, Top panel).[420] The chromatin fraction was isolated from cells at different phases of the cell cycle and histone O-GlcNAcylation was monitored by western blotting using the RL2 antibody. We noticed the expected faint signal at the level of histones and that this signal did not change during cell cycle progression. However, high molecular weight chromatin-associated proteins show significantly increased O-GlcNAcylation at G1/S transition. Therefore, we concluded that fluctuating histone O-GlcNAcylation could not be observed during cell cycle. Moreover, along with our previous data, these results strengthen the notion that the signal detected by RL2 at the level of histones following blot overexposure corresponds to background.

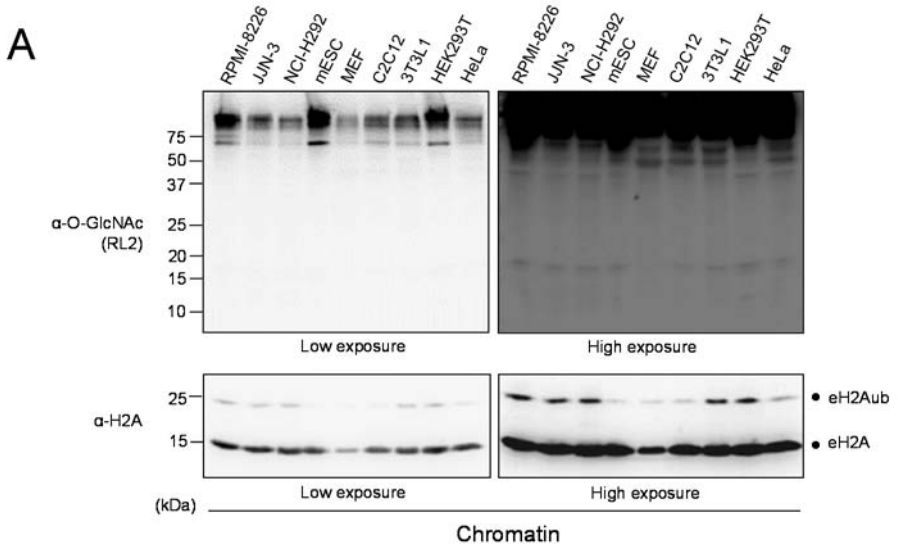
A
RPMI-8226
JJN-3
NCI-H292
mESC
MEF
C2C12
3T3L1
HEK293T
HeLa
α-O-GlcNAc (RL2)
75
50
37
25
20
15
10
Low exposure
High exposure
α-H2A
eH2Aub
eH2A
(kDa)
Chromatin

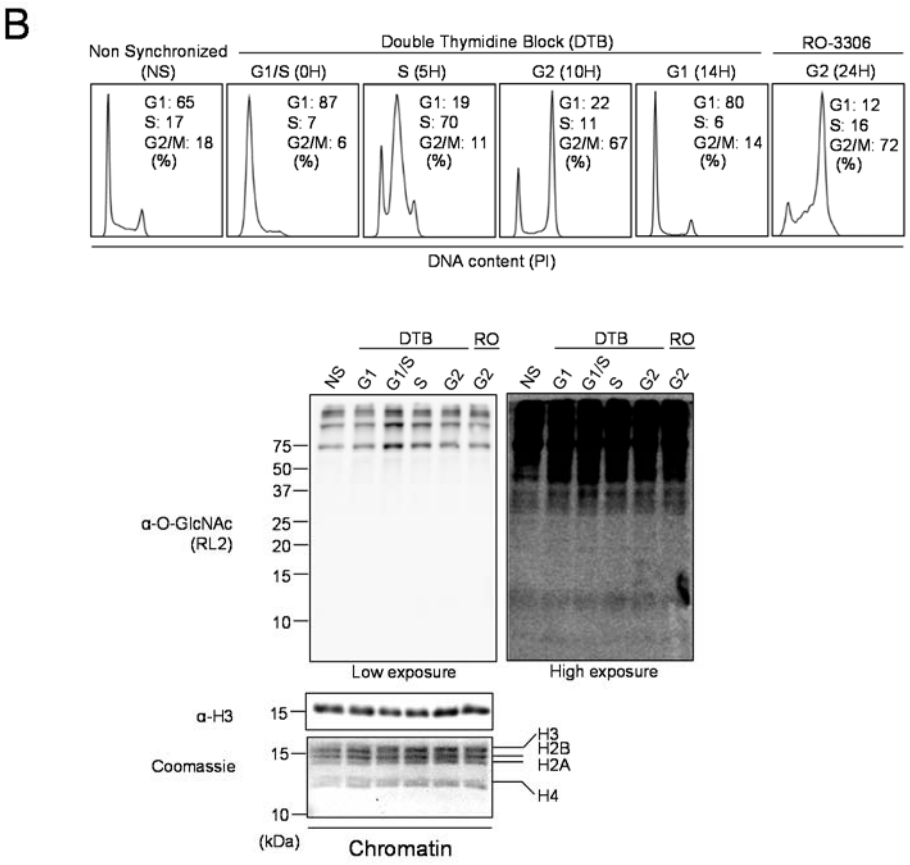
B
Non Synchronized (NS)
Double Thymidine Block (DTB)
RO-3306
G1/S (0H)
S (5H)
G2 (10H)
G1 (14H)
G2 (24H)
G1: 65 S: 17 G2/M: 18 (%)
G1: 87 S: 7 G2/M: 6 (%)
G1: 19 S: 70 G2/M: 11 (%)
G1: 22 S: 11 G2/M: 67 (%)
G1: 80 S: 6 G2/M: 14 (%)
G1: 12 S: 16 G2/M: 72 (%)
DNA content (PI)
DTB
RO
NS
G1
G1/S
S
G2
G2
α-O-GlcNAc (RL2)
75
50
37
25
20
15
10
Low exposure
High exposure
α-H3
Coomassie
H3
H2B
H2A
H4
(kDa)
Chromatin

Figure 3.4. Unspecific signal detected at the level of histones in various cell lines and during cell cycle progression.

(A) Various cell lines were cultured and harvested to perform chromatin extraction. The chromatin fraction was analysed by western blotting with the indicated antibodies. Total histone H2A was used as a loading control. Dots indicate endogenous H2A ubiquitination (eH2Aub) and total H2A (eH2A). (B) Histones O-GlcNAcylation analysis of synchronized U2OS cells. Cells were blocked in G1/S boundary by double thymidine block (DTB) and then released to progress through the cell cycle. U2OS cells were also treated with the CDK1 inhibitor, RO-3306, for 24 hours to block cells in late G2. Cells were harvested at the indicated times for FACS analysis (Upper panel) and for chromatin extraction (Bottom panel). The chromatin fraction was analysed by western blotting with the indicated antibodies and by Coomassie Brilliant Blue staining. Histone H3 was used as a loading control. NS; Non-Synchronized, DTB; Double Thymidine Block. kDa; Molecular weight marker in Kilodalton.

3.3.4 Lack of evidence supporting H2B S112 O-GlcNAcylation and its link with H2B Lys120 monoubiquitination

It was reported that H2B S112 is O-GlcNAcylated (H2B S112O-GlcNAc), an event that appears to promote the monoubiquitination of H2B Lys120 (H2B K120ub) thus coordinating gene expression.[20] It was also described that AMPK-mediated OGT Thr444 phosphorylation hindered its ability to associate with chromatin, and this was shown to reduce the reported H2B S112O-GlcNAc signal.[411] In turn, this effect was proposed to inhibit monoubiquitination of H2B K120, thus repressing gene expression in MEF cells.[359] As an anti-O-GlcNAcylated H2B S112 is commercially available[359], we first inquired about the specificity of this antibody. Since H2B S112O-GlcNAc was shown to decrease dramatically following knockdown of OGT by RNAi, we used a similar approach to deplete OGT by siRNA in HeLa cells (Figure 3.5A).[20,359] As expected, OGT knockdown resulted in the accumulation of the precursor form of HCF-1, as its proteolytic maturation is O-GlcNAcylation-dependent (Figure 3.5A, Left panel).[275,283,284].

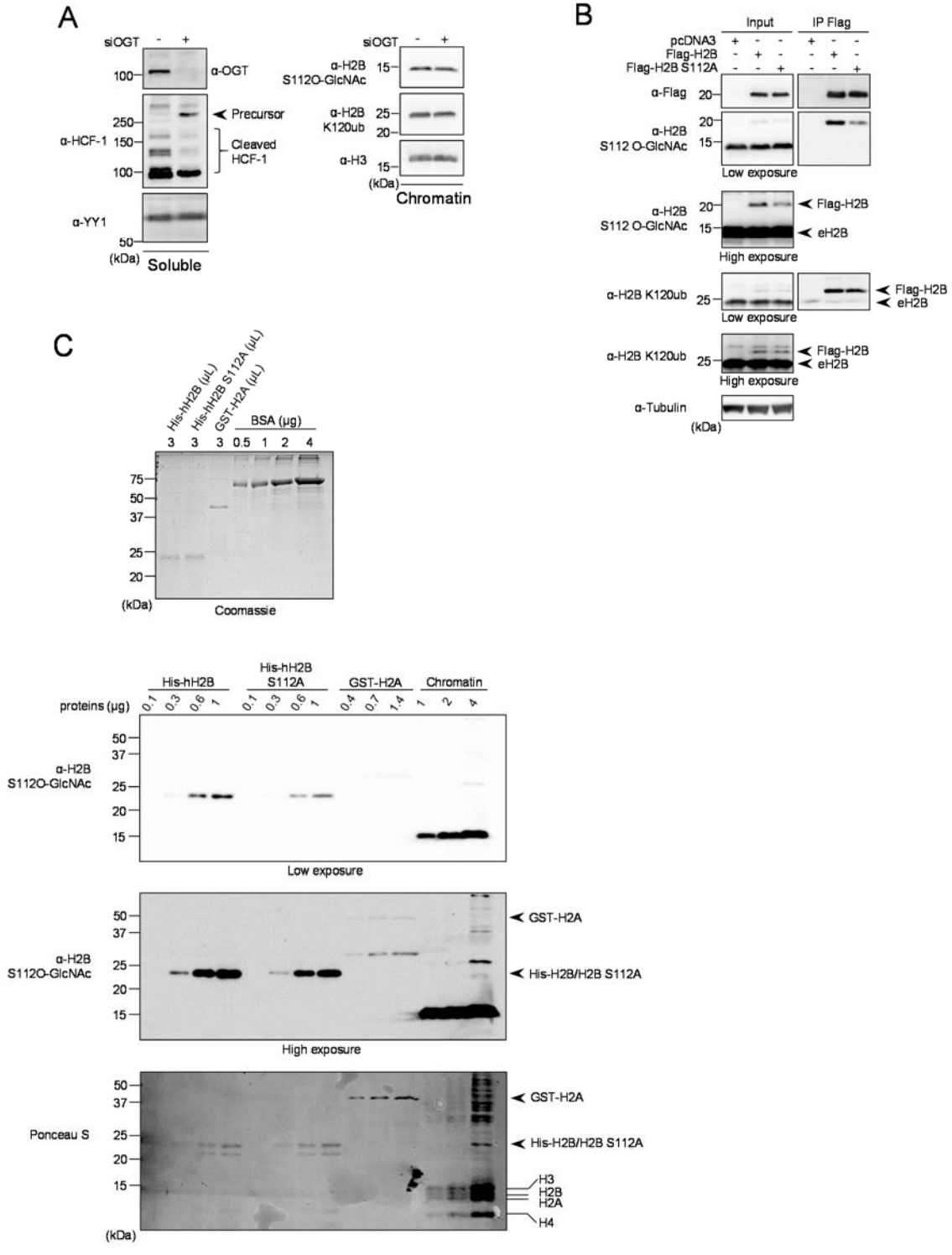
A
siOGT - +
α-OGT
100
Precursor
250
α-HCF-1 150
Cleaved HCF-1
100
α-YY1
50
(kDa)
Soluble
siOGT - +
α-H2B S112O-GlcNAc 15
α-H2B K120ub 25 20
α-H3 15
(kDa)
Chromatin
B
Input
IP Flag
pcDNA3 + - - + - -
Flag-H2B - + - - + -
Flag-H2B S112A - - + - - +
α-Flag 20
α-H2B S112 O-GlcNAc 20 15
Low exposure
α-H2B S112 O-GlcNAc 20 15
Flag-H2B
eH2B
High exposure
α-H2B K120ub 25
Flag-H2B
eH2B
Low exposure
α-H2B K120ub 25
Flag-H2B
eH2B
High exposure
α-Tubulin
(kDa)
C
His-hH2B (μL)
His-hH2B S112A (μL)
GST-H2A (μL)
BSA (μg)
3 3 3 0.5 1 2 4
75
50
37
25
20
(kDa)
Coomassie
His-hH2B
His-hH2B S112A
GST-H2A
Chromatin
proteins (μg)
0.1 0.3 0.6 1 0.1 0.3 0.6 1 0.4 0.7 1.4 1 2 4
50
37
α-H2B S112O-GlcNAc
25
20
15
Low exposure
50
37
α-H2B S112O-GlcNAc
25
20
15
GST-H2A
His-H2B/H2B S112A
High exposure
50
37
Ponceau S
25
20
15
GST-H2A
His-H2B/H2B S112A
H3
H2B
H2A
H4
(kDa)

Figure 3.5. H2B S112O-GlcNAc antibody is not specific and S112 O-GlcNAcylation is not linked to H2B K120 monoubiquitination.

(A) HeLa cells were transfected twice with OGT siRNA and three days post-transfection, cells were harvested to perform cellular fractionation. Protein levels were analysed by western blotting with the indicated antibodies. HeLa soluble fraction was analysed for HCF-1 proteolytic cleavage. YY1 was used as a loading control (Left panel). Chromatin fraction was analysed for H2B S112O-GlcNAc and H2B K120ub levels (Right panel). (B) HEK293T cells were transfected with Flag-H2B or Flag-H2B S112A. Three days post-transfection, cells were harvested and total cell lysates were subjected to protein denaturation and immunoprecipitation (IP) using α-Flag antibody. Input as well as IP fractions were subjected to immunoblotting analysis using the indicated antibodies. Arrows indicate Flag-H2B and endogenous H2B (eH2B). Tubulin was used as a loading control for the input fraction. (C) Relative quantification of eluted purified recombinant histones detected by Coomassie Brilliant Blue staining. Known amounts of BSA protein were used as standards for relative quantification (Top panel). Increasing amounts of recombinant His-hH2B, His-hH2B S112A mutant, GST-H2A as well as chromatin extract from HEK293T cells were analysed by western blot using the indicated antibodies. Red Ponceau S staining of the membrane used for subsequent western blotting showing the loading of purified proteins (Bottom panel). Arrows and lines indicate the position of recombinant and endogenous histones respectively. kDa; Molecular weight marker in Kilodalton.

However, neither the signal generated by the anti-H2B S112O-GlcNAc nor that for anti-H2B K120ub changed following OGT depletion (Figure 3.5A, Right panel). In addition, we expressed Flag-H2B WT and Flag-H2B S112A mutant in HEK293T cells and conducted anti-Flag immunoprecipitation under denaturing conditions (Figure 3.5B). Unexpectedly, the anti-H2B S112O-GlcNAc signal decreases by only ~3-fold in the H2B S112A mutant, instead of completely disappearing. In addition, we observed no change in H2B K120ub levels. Our results could not validate the reported link between H2B S112 O-GlcNAc and H2B K120ub and moreover further suggest that the anti-H2B S112O-GlcNAc antibody might not confer specific detection for H2B O-GlcNAcylation. Next, we sought to further investigate the anti-H2B S112O-GlcNAc antibody specificity by producing recombinant human histones H2B (His-hH2B) and H2B S112A (his-hH2B S112A) purified from bacteria (Figure 3.5C). We also used a GST-H2A construct as a negative control. Following relative quantification of recombinant histones shown by Coomassie Brilliant Blue staining (Figure 3.5C, Top panel), we subsequently probed increasing quantities of these proteins by immunoblotting using the anti-H2B S112O-GlcNAc antibody. We found that purified recombinant proteins are detectable using this antibody and this signal decreased by about two to three folds when the serine was mutated to alanine (His-hH2B S112A) (Figure 3.5C, Middle panel). Moreover, the H2B S112O-GlcNAc signal detected for the recombinant His-hH2B protein is comparable to that detected for a similar amount of mammalian endogenous H2B in the chromatin fraction

(Figure 3.5C, Bottom panel). Thus, these results indicate that this antibody recognizes the H2B backbone itself rather than O-GlcNAc moiety and that unmodified S112 is a major determinant in epitope recognition by this antibody.

3.3.5 Undetectable binding of mammalian histones to the Wheat Germ Agglutinin (WGA) lectin.

It was previously reported that HeLa cell nucleosomes obtained by micrococcal digestion can be enriched with a WGA lectin resin which is known to strongly bind O-GlcNAcylated proteins.[20] However, the extraction procedure does not preclude histone binding to the WGA column as a consequence of interaction of histones with O-GlcNAcylated proteins associated with nucleosomes. Thus, we sought to use an acid extraction procedure to separate the soluble histones from all other proteins that remain in the insoluble fraction. Moreover, acid treatment ensures denaturation of proteins, thereby preventing potential interactions of histones with O-GlcNAcylated proteins associated with chromatin. We cultured HEK293T cells with PUGNAc for 24 hours and also included this inhibitor during the extraction steps to exclude the possibility of losing protein O-GlcNAc modification.[288] Moreover, to ensure that acid treatment does not influence detection of O-GlcNAc modification, we also analyzed the ability of chromatin-associated-proteins in the acid extraction mixture to bind the WGA column (Figure 3.6). Importantly, HCF-1 and several chromatin-associated proteins were enriched approximately 5 to 10 times compared to the input signal, thus confirming that the WGA resin strongly and efficiently binds O-GlcNAcylated proteins (Figure 3.6, Left panel). This result also indicates that acid treatment did not covalently modify or disrupt the O-GlcNAc moiety. In contrast, immunoblotting with RL2, anti-H2B S112 O-GlcNAc or anti-H2A revealed that histones were found only in the input and the flow through fractions (Figure 3.6, Right panel). Consistently, staining of histones with Coomassie Brilliant Blue did not reveal histones binding to WGA-agarose. Note that the background signal produced by the RL2 antibody at the level of histones was observed in the input and the flow through fractions. To further exclude the possibility that only a small fraction of histones are modified in proliferating human cells, and that such limited amounts of modified histones are below immunoblotting detection thresholds, we carried out a WGA pull-down experiment in conditions that would allow for the total depletion of HCF-1 from the cell

lysate (Figure S3.5, Left panel). Even in these conditions, histones were again only detected in the inputs and the flow through fractions by immunodetection and silver staining (Figure S3.5, Right panels). Altogether, these data support our findings that histone O-GlcNAcylation is undetectable in mammalian cells.

3.3.6 Histone O-GlcNAcylation is not detected by Click-it biotin-alkyl chemistry, mass spectrometry or following in vitro O-GlcNAcylation reactions.

To further corroborate our observations, we sought to use other methods for O-GlcNAcylation detection. We first used the commercially available in vitro Click-it chemistry system. This procedure consists in modifying O-GlcNAcylated proteins with an azido sugar (GalNAz), which can then react with biotin-alkyne thus becoming detectable via streptavidin-conjugated HRP.[394]

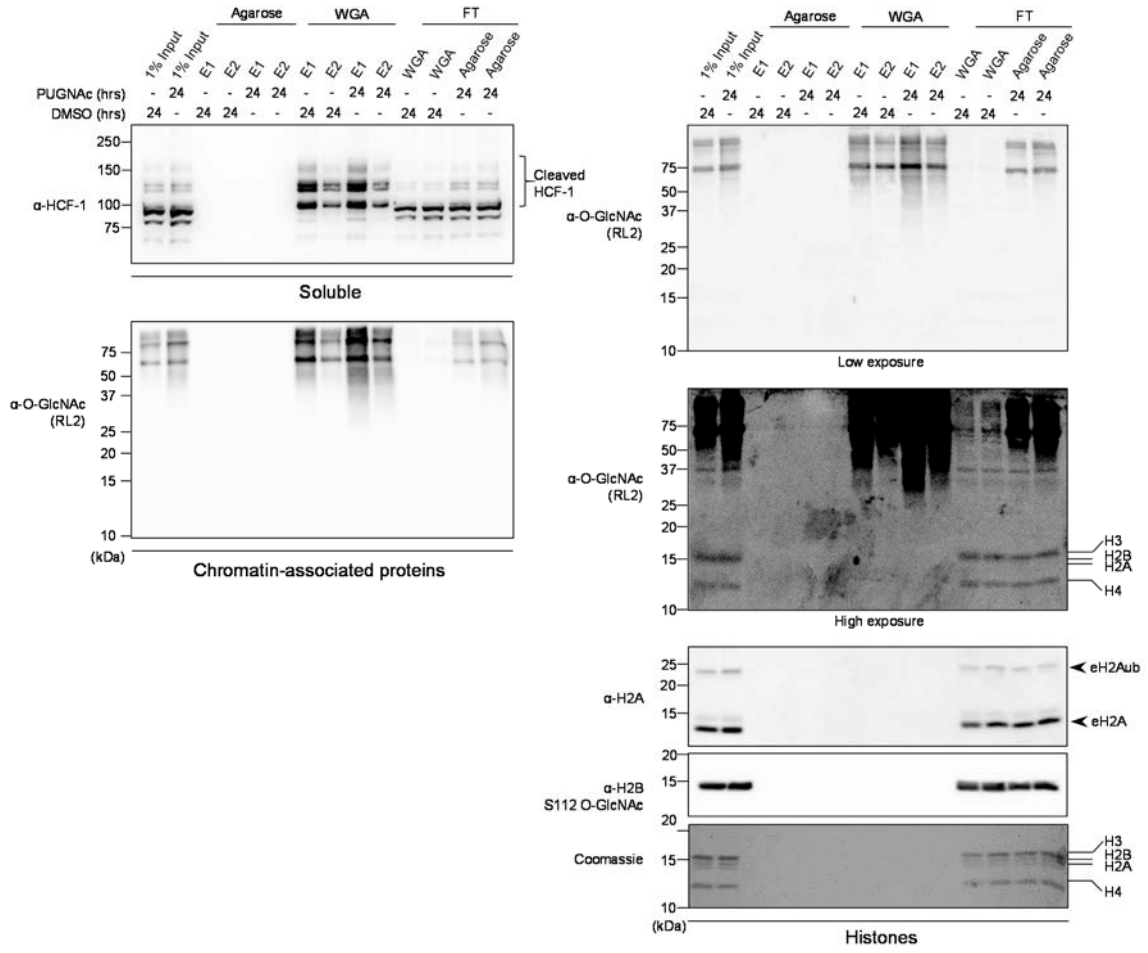

Figure 3.6. HCF-1 and several chromatin-associated proteins but not histones bind to WGA lectin.

HEK293T cells were treated with 100 μM PUGNAc or equal volume of DMSO for 24 hours as indicated and harvested to perform acid extraction of histones. The indicated soluble and chromatin-associated-proteins fractions (Left panels), and histones fraction (Right panels) were incubated for 2 hours with agarose bound WGA lectin or with agarose resin to control for non-specific binding. Two elutions (E1 and E2) of agarose and WGA bound proteins as well as the flow through (FT) fractions were analysed by western blot using the indicated antibodies. The Coomassie Brilliant Blue staining and the anti-H2A antibody indicate that histones are found in the input and the FT fractions. Arrows indicate endogenous H2A ubiquitination (eH2Aub) and total H2A (eH2A). kDa; Molecular weight marker in Kilodalton.

This approach is highly sensitive since it allows for the detection of the O-GlcNAcylation of α-crystallin, a lens protein that was reported to be O-GlcNAcylated at a very low stoichiometric ratio.[394,421] Thus, we performed the Click-it chemistry reaction on histones

extracted from HeLa cells, as well as on α-crystallin, used as the positive control. As shown in Figure 3.7A, although similar amount of both purified histones and α-crystallin were used (Figure 3.7A, Right panel), we could only detect O-GlcNAcylation of α-crystallin in these conditions (Figure 3.7A, Left panel). Moreover, O-GlcNAcylation of co-purified high molecular weight proteins could be readily observed, thus demonstrating the efficiency of GalNAz labeling in the same reaction conditions as histones.

Next, we sought to determine, by performing ETD-MS/MS analysis, if we could recapitulate the reported histone O-GlcNAcylation sites using acid extracted histones from HeLa cells. We also purified HCF-1 from HEK293T cells and included it as a positive control. Mass spectrometry analysis by HCD and ETD for proper glycan localization was conducted.[422] As shown in Figure S3.6 and Table 1, in addition to several novel sites, we were able to identify 6 of the reported HCF-1 O-GlcNAcylation sites.[275,283,350,423-426] However, we were unable to detect O-GlcNAcylation of the core histones. Indeed, even though the MS analysis revealed the presence of histone peptides that were reported to be modified (e.g., H2B S112, H2A T101, H3 S10 and H4 S47), we did not detect their corresponding O-GlcNAcylated forms (Figures S3.7 and S3.8).

Previous studies reported that histones can be modified by OGT in vitro.[20] Thus, we performed in vitro O-GlcNAcylation reactions using purified recombinant human His-hH2B and purified mammalian nucleosomes.

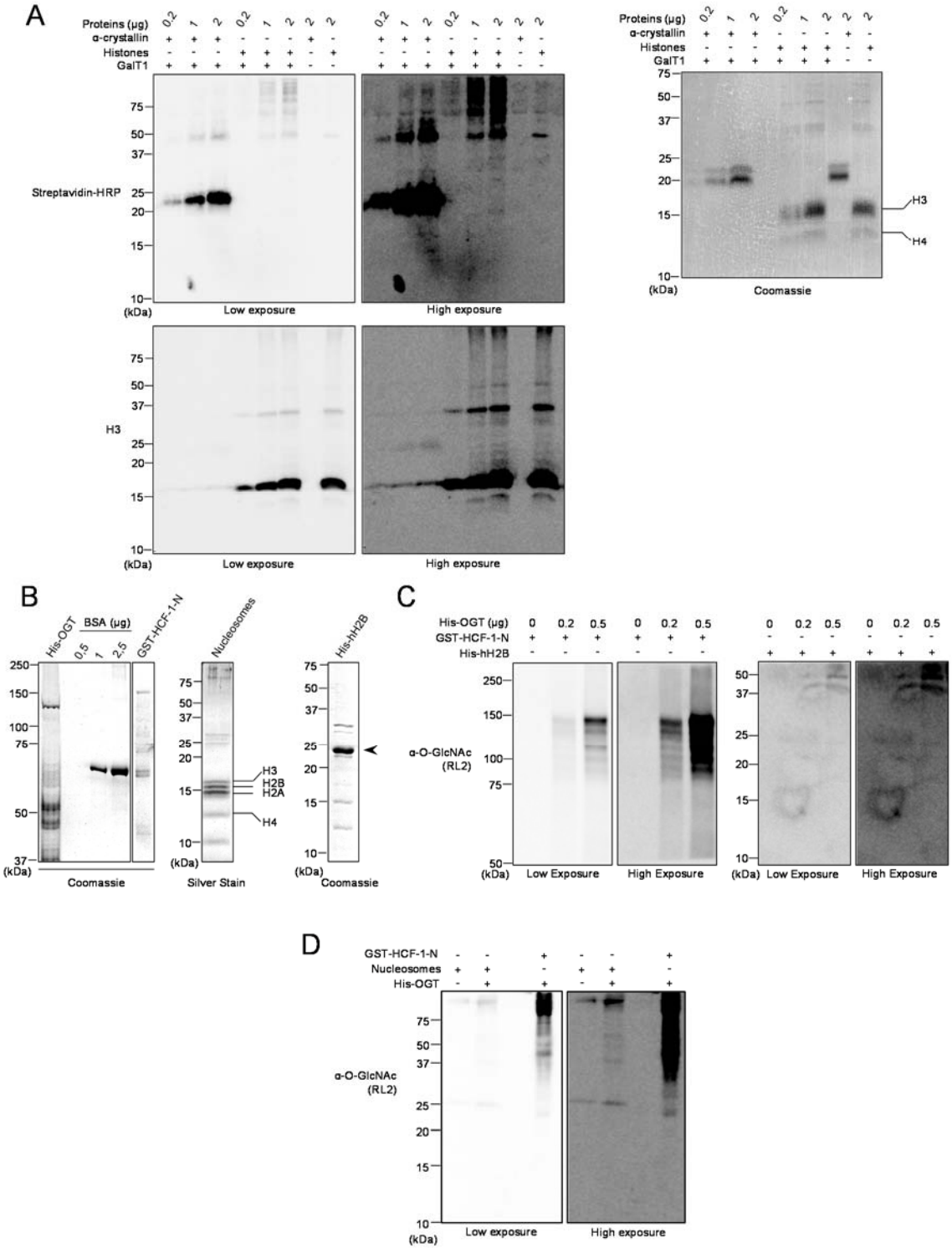

Figure 3.7. Histones are not modified by Click-it biotin-alkyl chemistry or by in vitro OGT-mediated O-GlcNAcylation.

(A) The poorly O-GlcNAcylated α-crystallin is detected with the click-it biotin-alkyl chemistry but not histones. HeLa cells were harvested and acid extraction followed by acetone precipitation was performed to purify histones. The GalNAz labeling reaction was carried out for a minimum of 16 hours and the biotin-alkyl reaction was performed in the presence or absence of the GalT1 enzyme. (Left panel) O-GlcNAcylation was analysed by blotting with streptavidin-HRP. (Right panel) Coomassie Brilliant Blue staining shows the indicated amounts of used purified proteins. (B-D) Histones are not O-GlcNAcylated in vitro by OGT. (B) Purified proteins analysed by Coomassie Brilliant Blue or silver staining as indicated. (Left panel) Relative quantification of purified recombinant His-OGT and GST-HCF-1-N to known amounts of BSA. (Middle and Right panels) Integrity of Flag-H2A-purified mammalian nucleosomes and recombinant His-hH2B. (C) In vitro O-GlcNAcylation reaction of the purified recombinant His-hH2B. GST-HCF-1-N and recombinant His-hH2B were incubated with increasing amounts of recombinant His-OGT for 4 hours. O-GlcNAcylation was detected by western blotting using the anti-O-GlcNAc antibody (RL2). (D) In vitro O-GlcNAcylation reaction of the purified mammalian nucleosomes by OGT. GST-HCF-1-N and nucleosomes were incubated in the absence or presence of His-OGT for 11 hours. The O-GlcNAcylation was detected as in (C). kDa; Molecular weight marker in Kilodalton.

As a positive control, we also used purified recombinant GST-HCF-1N (for N-Terminal HCF-1)[288] as this domain is a well-established substrate of OGT.[275,283,288] The relative quantity and integrity of the purified proteins were assessed by Coomassie Brilliant Blue staining or silver staining as indicated (Figure 3.7B). As shown in Figures 3.7C and 3.7D, we detected a strong O-GlcNAcylation of HCF-1-N, but not of the recombinant His-hH2B (Figure 3.7C) or nucleosomal histones (Figure 3.7D).

In summary, using various approaches, we were unable to detect histone O-GlcNAcylation. Thus, our study provides strong evidence that histone O-GlcNAcylation, if occurring, must be present at levels below detection limits of commonly available tools, while O-GlcNAcylation of other known proteins including HCF-1 and TET2 can be observed. We emphasize that histones are hundreds- to thousands-folds more abundant than the majority of cellular proteins and their modifications, even in relatively low abundance, are in general easily monitored. On the other hand, detection of histone modifications can be prone to false-positive signals, especially when analyzing a large amount of proteins by immunoblotting.

3.4 Material & Methods

3.4.1 Plasmids and mutagenesis

The cDNA of human of OGT and TET2 were cloned from HeLa total RNA by reverse transcription and inserted into pENTR D-Topo plasmid (Life Technologies). Expression construct of Myc-TET2 was generated by recombination using LR clonase kit (Life

Technologies) into pDEST-Myc construct. pCGN-HCF-1 FL was previously described.[257,258] Myc-OGT, Myc- OGT D925A catalytic inactive mutant (Myc-OGT CD) were also previously described.[275] GFP-OGT and GFP-OGT CD were generated by recombination into pDEST-GFP expression construct. pcDNA3-Flag-H2A and pcDNA3-Flag-H2B were obtained from Dr. Moshe Oren. [427] H2B and H2A were generated using gene synthesis (BioBasic) and then subcloned into modified pENTR D-Topo plasmid. H2B S112A construct was generated by site direct mutagenesis using Q5 High-Fidelity DNA Polymerase. The Primers used are: Forward primer: CACGCCGTGGCGGAGGGCACCAAGGCCGTCA; Reverse primer: TGCCCTCCGCCACGGCGTGCTTGGCCAGCTC. HCF-1N was amplified from pCGN-HCF-1 FL and inserted into pENTR D-Topo plasmid. The T antigen NLS coding sequence was added in the primers. His-OGT was generated by subcloning the OGT cDNA into pET30a+ vector. Expression constructs of H2B and H2B S112A were generated by recombination using LR clonase kit into pDEST-Flag or pDEST-6xHis constructs. Expression constructs of H2B and HCF-1N were generated by recombination into pDEST-Flag or pDEST-GST constructs. All DNA constructs were sequenced.

3.4.2 Immunoblotting and antibodies.

Total cell lysates were prepared by harvesting cells with buffer containing 25 mM Tris pH 7.3 and 1% sodium dodecyl sulfate (SDS). Cell extracts were boiled at 95°C for 10 min and sonicated. Quantification of total proteins was conducted using the bicinchoninic acid (BCA) assay.[428] Total cell extracts as well as chromatin fractions and immunoprecipitation samples were diluted in 2X or 4X Laemmli buffer. SDS-PAGE and immunoblotting were conducted according to standard procedures. The band signals were acquired with a LAS-3000 LCD camera coupled to MultiGauge software (Fuji, Stamford, CT, USA).

Mouse monoclonal anti-BAP1 (C4, sc-28383), rabbit polyclonal anti-YY1 (H414, sc-1703), rabbit polyclonal anti-OGT (H300, sc-32921), mouse monoclonal anti-Tubulin (B-5-1-2, sc-SC-23948), were from Santa Cruz. Rabbit polyclonal anti-HCF-1 (A301-400A) was from Bethyl Laboratories. Mouse monoclonal anti-Flag (M2) was from Sigma-Aldrich. Mouse monoclonal anti-MYC (9E10) was from Covance. Rabbit polyclonal anti-H2B K120ub (D11 XP) was from Cell Signaling. Rabbit polyclonal anti-H2B S112O-GlcNAc (ab130951), rabbit polyclonal anti-H2A (ab18255) Rabbit polyclonal anti-H3 (ab1791) and mouse monoclonal

anti-O-Linked N-acetylglucosamine (RL2, ab2739) were from Abcam. The mouse monoclonal anti-O-Linked N-acetylglucosamine (CTD110.6) was kindly provided by Dr. Gerald Hart.[429] Mouse monoclonal anti-β-Actin (MAB1501, clone C4) was from Millipore. Anti-rhodamine (IgM) was a generous gift from Dr. Li-Huei Tsai. Peroxidase Affini-Pure Goat anti-mouse IgM μ chain specific secondary antibody was from Jackson Laboratories.

3.4.3 Cell culture and cell transfection

U2OS osteosarcoma, HeLa, human embryonic kidney HEK293T, 3T3-L1 mouse preadipocytes, C2C12 mouse myoblasts, mouse embryonic fibroblasts (MEF) cell lines were grown in Dulbecco's modified Eagle's medium (DMEM) supplemented with 10 % of foetal bovine serum (FBS), L-glutamine and penicillin/streptomycin. Multiple myeloma cell lines (JJN-3, RPMI-8226, NCI-H292) were cultured in RPMI-1640 medium supplemented with 10 % of foetal bovine serum (FBS), L-glutamine and penicillin/streptomycin. Mouse embryonic stem cells (mESCs) were maintained in DMEM medium supplemented with 15% of embryonic stem cells qualified FBS (Gibco), L-glutamine, penicillin/streptomycin, 0.1 mM β-mercaptoethanol, 0.1 mM MEM (Non-essential amino acids), 1 mM sodium pyruvate and 1000 U/ml of leukemia inhibitory factor (LIF) (Life technologies).

HeLa or HEK293T cells were treated with 100 μM of PUGNAc or equal volume of DMSO for 0, 9 and 24 hours and were subjected to sub-cellular fractionation (soluble and chromatin) or histones extraction. HEK293T cells were transfected with mammalian expressing vectors using polyethylenimine (PEI) (Sigma-Aldrich). Three days post-transfection, cells were harvested for immunoblotting using total cell extracts or following cellular fractionation and histones extraction. Prior to immunoblotting, histones were also immunoprecipitated using anti-Flag antibody following denaturation of cell extracts. HeLa or U2OS cells were transfected using Lipofectamine 2000 (Life technologies) with 200 pmol of either ON-TARGET plus Non-targeting pool (D-001810-10-50) or ON-TARGET plus SMARTpool OGT (L-019111-00-0050) (Thermo Scientific, Dharmacon). Cells were transfected in a serum-free DMEM medium for 16 hours, then changed with DMEM complemented with 5 % FBS, 1 % Glutamine and 1 % Penicillin-Streptomycin and 8 hours later, cells were transfected again as described above. Three days following the first

transfection, cells were harvested in PBS and soluble and chromatin extractions were conducted and used for immunoblotting.

3.4.4 Histone and chromatin extraction

For histone extraction, HEK293T cells were transfected with Flag-H2A or Flag-H2B with or without Myc-OGT, Myc-OGT CD, Myc-TET2 or with the combination of Myc-OGT and Myc-TET2 and harvested three days post-transfection. For high salt/detergent chromatin extraction, cells were lysed in 300 mM NaCl, 1% NP-40, 2 μM PUGNAc, 1 mM PMSF and 1 X protease inhibitors (Sigma). Samples were kept on ice for 15 min and then centrifuged at 6000 rpm for 10 min. The supernatant was kept as the soluble fraction for western blotting analysis. The pellet was washed 2 times with the previous buffer and resuspended in 1% SDS for protein quantification. For the histones acid extraction, cells were lysed in 50 mM Tris pH 7.4, 300 mM NaCl, 2 mM

EDTA and 2 μM PUGNAc. The lysate was centrifuged at 6000 rpm for 10 min and the supernatant was kept as the soluble fraction. The pellet was washed 2 times with the same buffer and treated with 0.2 N HCl (1 volume of buffer for 1 volume 0.4 HCl) for 1 hour on ice. After centrifugation at 14000 rpm for 5 min, the supernatant containing histones was neutralized by adding equal volume of 100 mM Tris pH 8.8. The pellet was also resuspended in 1% SDS. To quantify proteins, part of the histones fraction was precipitated using 100% acetone at -20°C for 2 hours, centrifuged at 14000 rpm for 10 min and resuspended in 1% SDS. Proteins were then quantified using the BCA assay. For chromatin extraction, the cell pellet was resuspended in 50 mM Tris-HCl pH 7.3, 300 mM NaCl, 5 mM EDTA, 1% Triton, 2 μM PUGNAc, 1X protease inhibitors (Sigma) and 1 mM PMSF and kept on ice for 30 min. The chromatin was pelleted by centrifugation at 10 000 rpm for 10 min at 4^0C, the supernatant was kept (soluble fraction) and the chromatin pellet was resuspended in 25 mM Tris pH 7.3 and 1 % SDS. Both fractions were quantified using the BCA protein quantification method.

3.4.5 Wheat Germ Agglutinin lectin Pull-Down

HEK293T cells were either treated with 100 μM PUGNAc or DMSO for 24 hours. Cells were then harvested in 1X PBS and the cell pellet was lysed with 0.25 M sucrose, 3 mM CaCl2, 1 mM Tris-HCl pH 8.0, 0.5 % triton, 2 μM PUGNAc and 1X protease inhibitors

(Sigma). The chromatin was pelleted by centrifugation at 3900 rpm for 5 minutes at 4°C and the supernatant was kept (soluble fraction). Next, the pellet was washed with 300 mM NaCl, 5 mM MgCl2, 1% Triton, 50 mM Tris-HCl pH 8.0, 5 mM DTT and 2 μM PUGNAc and centrifuged at 3900 rpm for 5 min at 4°C. Supernatant was discarded and the pellet was very quickly resuspended in 3 volumes of acid extraction buffer containing 0.5 M HCl, 10% glycerol and 0.1 M β-mercaptoethanol and left on ice for 30 min. The sample was centrifuged at 14 000 rpm for 5 min at 4°C, the supernatant containing the histones was transferred in a new tube and 10 volumes of acetone were added to both the pellet (chromatin-associated proteins) and the supernatant (histones) fractions and were left at -20 °C overnight. The next day, protein precipitates were pelleted at 14 000 rpm for 1 hour at 4°C, resuspended in 25 mM Tris pH7.3 and 1 % SDS, sonicated and diluted in 10 volumes of EB300 Buffer containing 50 mM Tris-HCl pH7.5, 300 mM NaCl, 5 mM EDTA, 1% Triton X-100, 1X protease inhibitors (Sigma), 1 mM PMSF, 1 mM DTT and 2 μM PUGNAc. The samples were incubated for 2 hours with WGA lectin resin (Vector Laboratories, #AL-1023) or agarose beads, washed with EB300 buffer and eluted with 500 mM N-acetylglucosamine. Sample were then analysed by western blotting.

3.4.6 Immunoprecipitation

For histone immunoprecipitation following denaturation, HEK293T cells were transfected with Flag-H2A or Flag-H2B with pcDNA3 empty vector, Myc-OGT or Myc-OGt CD, Myc-TET2 or the combination of Myc-OGT with Myc-TET2 using PEI. Three days post-transfection, cells were harvested and the cell pellets were lysed in 20 mM Tris pH 8.0, 600 mM NaCl, 0.5% NP-40, 0.5% SDS, 0.5% sodium deoxycholate, 1 mM EDTA and 2 μM PUGNAc. Samples were sonicated and centrifuged at 14000 rpm for 10 min. The lysate was then diluted in 5 volumes of 50 mM Tris pH 7.4, 2 mM EDTA and 100 mM NaCl. For TET2 and HCF-1 immunoprecipitation, HEK293T cells were transfected with Myc-TET2 or HA-HCF-1 FL with and without GFP-OGT or GFP-OGT CD. Three days post-transfection, cells were harvested to perform denaturing immunoprecipitation. Briefly cells pellets were lysed using 300 mM NaCl containing buffer (5 mM Tris pH 7.5, 300 mM NaCl, 1% Triton, 1% SDS, 10 mM NaF, 5 mM EDTA 1 mM PMSF, 2 μM PUGNAc and 1X protease inhibitors (Sigma)). After boiling for 3 min in the lysis buffer, cell lysate was sonicated and samples

were diluted 10 folds with the same buffer but without SDS prior to immunoprecititation using anti-Myc or anti-HA antibodies. For mutant histones, HEK293T cells were transfected with PEI with either FLAG-H2B or FLAG-H2B S112A. Three days post-transfection, cells were harvested for denaturing immunoprecipitation in 25 mM Tris pH 7.3 and 1.5 % SDS. Next, suspensions were diluted 10 times with dilution buffer containing 50 mM Tris-HCl pH7.5, 100 mM NaCl, 1% Triton, 1 mM EDTA, 1 mM DTT, 1 mM PMSF, 1X protease inhibitors (Sigma), 2 μM PUGNAc and 20 mM N-Ethylmaleimide (NEM, Sigma). Suspensions were mixed with anti-FLAG M2 resin (Sigma Aldrich #A2220) overnight at 4 ^{0}C. Next day, beads were washed 5 times with the dilution buffer. Proteins were then eluted from the beads by adding Laemmli Buffer 2X and analysed by western blotting.

3.4.7 Recombinant proteins

pDEST-6xHis-H2B, pDEST-6xHis-H2BS112A, pDEST-GST-HCF-1-N and pET30a+ OGT were transformed into RIL bacteria. Following induction with 400 μM IPTG, recombinant proteins were purified either under native or denaturing conditions. For the denaturing immunopurification, the bacterial pellets were lysed in 50 mM Tris pH 8, 8 M urea and 3 mM DTT and left on ice for 30 min. After incubation, suspensions were sonicated and centrifuged at 16 000 rpm for 20 min. Supernatants were incubated with Ni-NTA Agarose resin (Invitrogen #R901-15) overnight at 4 ^{0}C and the resin was then washed with 50 mM Tris-HCl pH 8.0, 500 mM NaCl, 3 mM DTT and 20 mM imidazole and transferred into a Bio-Spin Disposable Chromatography columns (Bio Rad #732-6008). Proteins were eluted with 200 mM imidazole. For the native purification of His-H2B, His-H2B S112A and His-OGT, cell pellets were lysed in 50 mM Tris pH 8, 500 mM NaCl and 3 mM DTT, 1 mM PMSF, 1X protease inhibitors (Sigma) and left on ice for 30 min. After incubation and sonication, the purified proteins were obtained as described above except for His-OGT which was kept on the Ni-NTA Agarose resin in order to use it for the in-vitro O-GlcNAcylation reaction. The OGT Ni-NTA Agarose resin beads were washed 6 times and kept in 50 mM Tris-HCl pH 7.5, 12.5 mM MgCl2, 3 mM DTT, 10% glycerol, 1 mM PMSF, 1X protease inhibitors (Sigma). The induction of GST-H2A expression in bacteria was done in the same manner as indicated above. Pellets of cells were lysed on ice in 50 mM Tris-HCl pH 8, 150 mM NaCl, 1 mM EDTA, 1 % Triton, and 1 mM PMSF, 1 mM DTT, 1X protease inhibitors (Sigma). The lysates

were sonicated, centrifuged at 16000 rpm for 20 min and supernatants were incubated with GSH-Agarose (Sigma Aldrich #A8580) overnight at 4 ^{0}C. Then, the resin was washed with 50 mM Tris-HCl pH 7.5, 150 mM NaCl, 1 mM EDTA, 0.1% Tween20, 1 mM PMSF, 200 µM DTT and 1X protease inhibitors (Sigma)). Proteins were eluted with the same buffer containing 250 mM reduced gluthatione. GST-HCF-1-N was purified in the same manner as GST-H2A. Elutions of His-H2B, His-H2B S112A, GST-H2A and GST-HCF-1N were loaded on SDS-PAGE for Coomassie Brilliant Blue staining using BSA for relative quantification.

3.4.8 Purification of the nucleosomes

For mammalian nucleosomes purification, HEK293T cells were transfected with 7 µg of pCDNA-Flag-H2A using PEI in serum free media. Three days post-transfection, cells were harvested and chromatin fraction extraction and nucleosomes were purified using anti-Flag beads as previously described.[229] For yeast Flag-H2B nucleosomes purification, 2 liters of cells expressing Flag-H2B were grown under standard conditions and 4 grams of cell pellet were used for the purification. Briefly, cells were resuspended in the SP Buffer (20 mM HEPES 7.4, 1.2 M sorbitol, 10 mM DTT) supplemented with 5 mg/ml of Zymolyase 20T. When the spheroplasting in completed, the cell pellet is washed again with the SP buffer and then resuspended in the Buffer L (20 mM HEPES 7.4, 18% Ficoll 400, 20 mM KCl, 5 mM MgCl2, 1 mM EDTA, protease inhibitors (1 µg/ml leupeptin, pepstatin, aprotinin), 3 mM DTT, 1 mM PMSF) prior to the dounce homogenization. The extract was then diluted with the Buffer S (buffer L supplemented with 2.4 M sorbitol instead of Ficoll) and chromatin fraction was recovered by centrifugation at 11 000 rpm for 20 min. The chromatin pellet was washed with the IP buffer (20 mM HEPES 7.6, 150 mM KCl, 5% glycerol, 5 mM MgCl2, 1 mM CaCl2, 0.1% NP-40, protease inhibitors, 1 mM PMSF prior to the MNase treatment. After MNase treatment (15KU/ml for 30 min at room temperature), the reaction was stopped with 1 mM EDTA and 5 mM EGTA. Following centrifugation at 20,000g for 5 min at 4°C, the soluble chromatin fraction was incubated 1 hour at 4°C with anti-Flag M2 beads. The beads were washed four times with the IP2 buffer (same as IP buffer but with 1 mM EDTA, 1 mM EGTA and without CaCl2). Bound nucleosomes were then eluted with 200 µg/ml of Flag peptides (Biobasic Inc.)

3.4.9 Click-it chemistry

HeLa cells were harvested and acid extraction was performed to purify histones as described for the WGA pull-down. Following acetone precipitation the histones were resuspended in 1% SDS, 20mM HEPES pH 7.9 and quantified using the BCA assay. The GalNAz labeling reaction was performed following the manufacturer's instructions using the Click-iT® GalNAz metabolic glycoprotein labeling reagent kit (Life Technologies). α-crystalline was included as a positive control. Following labeling of histones and α-crystalline, the detection was carried out with the Click-iT® Biotin Glycoprotein Detection Kit (Life Technologies) and the reaction was loaded on SDS-PAGE for blotting analysis using streptavidin-HRP (Cell Signaling #3999S) affinity detection.

3.4.10 In-vitro O-GlcNAcylation reaction

Purified GST-HCF-1-N (0.2 µg) and recombinant His-H2B (0.4 µg) were incubated with purified His-OGT (0.2 to 0.5 µg) in the presence of UDP-GlcNAc (1 mM) at 37°C overnight for 4 or 11 hours. The reaction was carried out in 50 mM Tris-HCl pH 7.5 containing 12.5 mM MgCl2 and 3 mM DTT. Purified nucleosomes were also included in the O-GlcNAcylation reaction as described above. The reaction was stopped by adding Laemmli buffer and analysed by immunoblotting.

3.4.11 Synchronization and cell cycle analysis

U2OS cells were synchronized at the G1/S border using the method of thymidine (2 mM) double block as previously described.[419] Cells were then released into new media to follow the progression through S and G2/M phases. U2OS cells were also arrested in late G2 by treating them with 10 µM of the CDK1 inhibitor RO-3306 for 24 hours.[420] Cell cycle analysis was carried out as described.[419]

3.4.12 Cell starvation.

C2C12 cells were incubated for 6 hours in the Hanks Balanced Salt Solution (HBSS) medium completed with 10 mM HEPES pH 7.5 and penicillin/streptomycin. After 4 hours of treatment, a separate plate dish of cells was replenished with fresh media and released for another 2 hours. Cells pellets were harvested at the indicated times for chromatin extraction.

3.4.13 Mass spectrometry analysis

Reduction of histone and HCF-1 samples was performed by adding 5 mM DTT in 50 mM ammonium bicarbonate. Alkylation was performed with chloroacetamide 50 mM with ammonium bicarbonate 50 mM. The digestion with trypsin was performed for 8 h at 37°C. Samples were loaded and separated on a homemade reversed-phase column (150 µm i.d. x 150 mm) with a 106-min gradient from 0–40% acetonitrile (0.2% FA) and a 600 nl/min flow rate on an Easy nLC-1000 (Thermo Fisher Scientific) connected to an LTQ-Orbitrap Fusion (Thermo Fisher Scientific). Each full MS spectrum acquired with a 70,000 resolution was followed by 10 MS/MS spectra, where the 10 most abundant multiply charged ions were selected for MS/MS sequencing. Tandem MS experiments were performed using high-energy C-trap dissociation (HCD) and electron transfer dissociation (ETD) acquired in the Orbitrap. Peaks were identified using a Peaks 7.0 (Bioinformatics Solution Inc.) and peptide sequences were blasted against the human Uniprot database (74,530 sequences). Tolerance was set at 10 ppm for precursor and 0.01 Da for fragment ions during data processing and with carbamidomethylation (C), oxidation (M), deamidation (NQ), and Hex-N-acylation (ST) as variable modifications.

3.5 Acknowledgements

We thank Haider Dar and Diana Adjaoud for technical assistance. This work was supported by grants from the Canadian Institutes of Health Research (CIHR) (MOP-115132) and the Natural Sciences and Engineering Research Council of Canada (NSERC) (355814-2010) to E.B.A and (435636-2013) to H.W.. E.B.A. is a scholar of the Fonds de la Recherche du Québec - Santé (FRQ-S) and the CIHR. H.W is a scholar of the FRQ-S, J.G. has a M.Sc. scholarship from the FRQ-S. The Proteomics facility at The Institute for Research in Immunology and Cancer (IRIC) receives infrastructure support from IRICoR, the Canadian Foundation for Innovation, and the Fonds de Recherche du Québec- Santé (FRQS).

3.6 Supplemental Figures

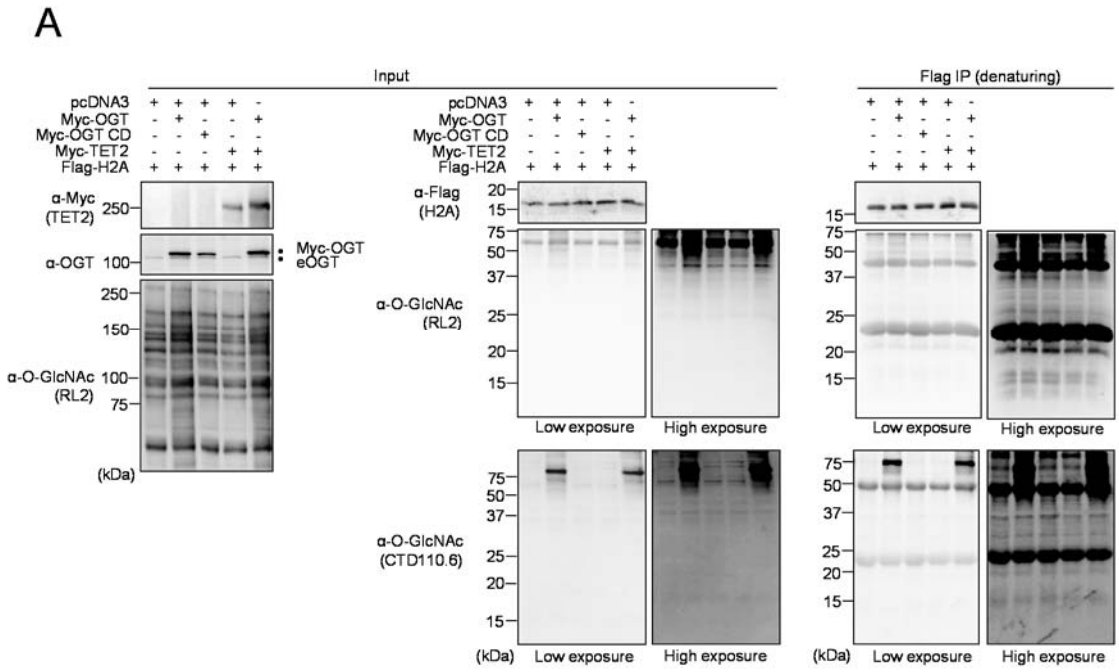

Supplemental Fig.S3.1. Undetectable O-GlcNAcylation of histone H2A.

HEK293T cells were transfected with Flag-H2A along with either pcDNA3 empty vector, Myc-OGT, Myc-OGT catalytic dead (MYC-OGT CD) or Myc-TET2, as well as the combination of Myc-OGT with Myc-TET2. Three days post-transfection, cells were harvested and analysed for Flag-H2A O-GlcNAcylation as conducted for Flag-H2B (see Fig.3.1). Flag immunoprecipitation (Flag-IP) of exogenous H2A was conducted following sample denaturation. Dots indicate Myc-OGT and endogenous OGT (eOGT). kDa; Molecular weight marker in Kilodalton.

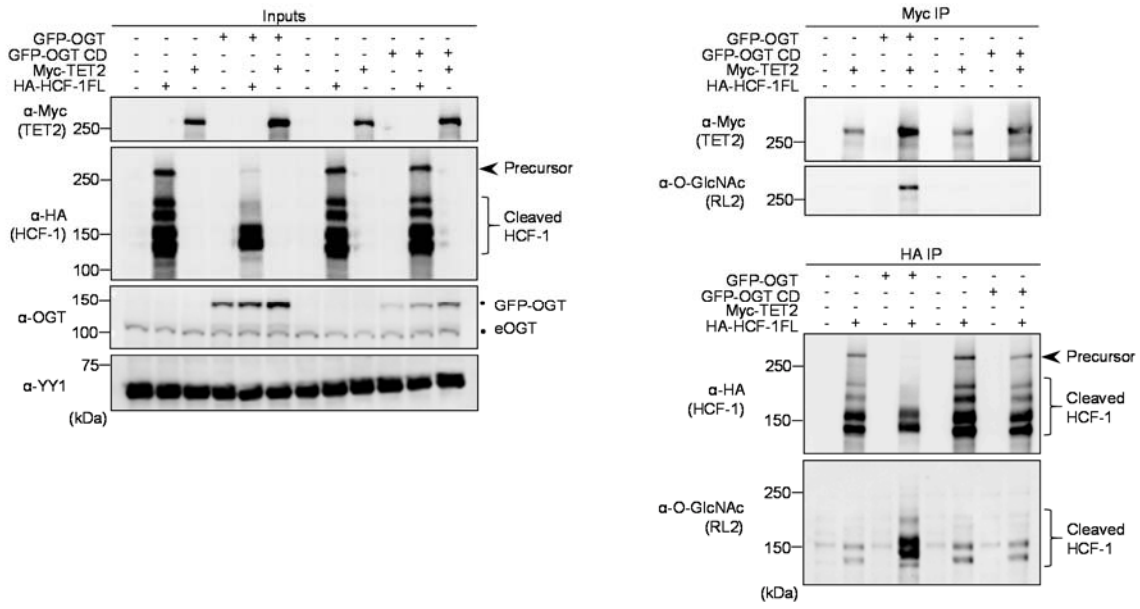

Supplemental FigS3.2. OGT O-GlcNAcylates both TET2 and HCF-1 and modulates HCF-1 cleavage.

HEK293T cells were transfected with either GFP-OGT or GFP-OGT catalytic dead (CD) in the presence of HA-HCF-1 full length (FL) or Myc-TET2 expression vectors. Three days post-transfection, cells were harvested and total cell lysates were subjected to immunoprecipitation (IP), following sample denaturation, using anti-Myc or anti-HA antibodies to purify TET2 and HCF-1 respectively. Total cell lysates (Input fractions) as well as immunopurifications were subjected to western blotting analysis using the indicated antibodies. Arrow indicates the full length (precursor) form of HCF-1 and brace indica thecleaved forms of HCF-1. Dots indicate GFP-OGT and endogenous OGT (eOGT). kDa; Molecular weight marker in Kilodalton.

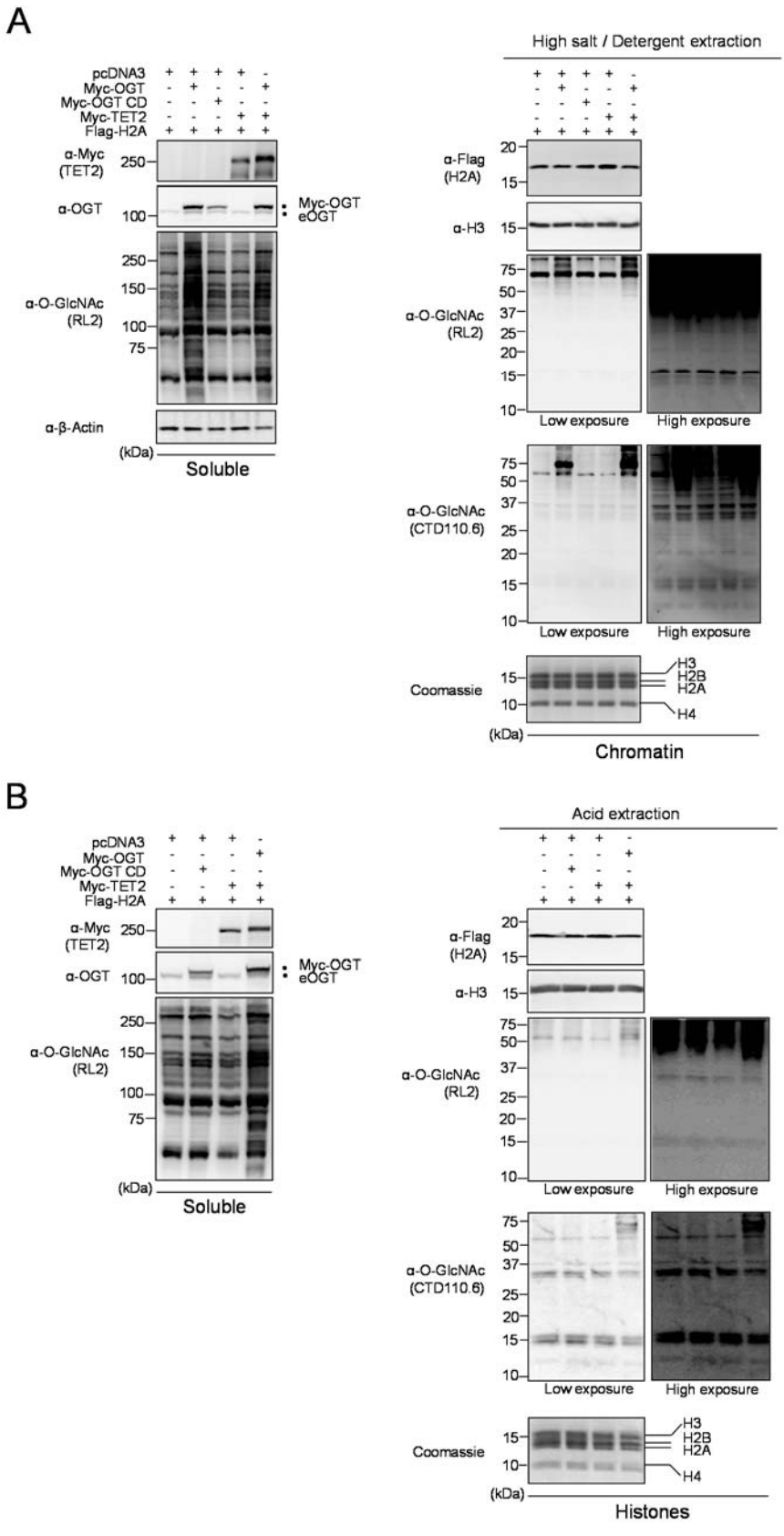
A
pcDNA3
Myc-OGT
Myc-OGT CD
Myc-TET2
Flag-H2A
α-Myc (TET2)
α-OGT
Myc-OGT
eOGT
α-O-GlcNAc (RL2)
α-β-Actin
(kDa)
Soluble
High salt / Detergent extraction
α-Flag (H2A)
α-H3
α-O-GlcNAc (RL2)
Low exposure
High exposure
α-O-GlcNAc (CTD110.6)
Coomassie
H3
H2B
H2A
H4
Chromatin
B
Acid extraction
Histones

Supplemental FigS3.3. Undetectable O-GlcNAcylation of endogenous histones.

HEK293T cells were transfected as in Supplemental Fig 3.1. Three days post-transfection, cells pellets were collected for subsequent high salt /detergent extraction as well as histones acid extraction and cellular extracts were analysed by western blotting with the indicated antibodies. (A) Chromatin high salt extraction. (Left) Soluble fraction showing global increase of O-GlcNAcylation following OGT overexpression. (Right) Detection of O-GlcNAcylation using RL2 and CTD110.6 antibodies on chromatin fraction. (B) Histone acid extraction showing (Left) the soluble fraction and global O-GlcNAcylation levels and (Right) the histone fraction detected with both O-GlcNAc antibodies. β-Actin and histone H3 were used as loading controls. Coomassie Brilliant Blue staining indicates abundance of histones loaded. Dots indicate Myc-OGT and endogenous OGT (eOGT). kDa; Molecular weight marker in Kilodalton.

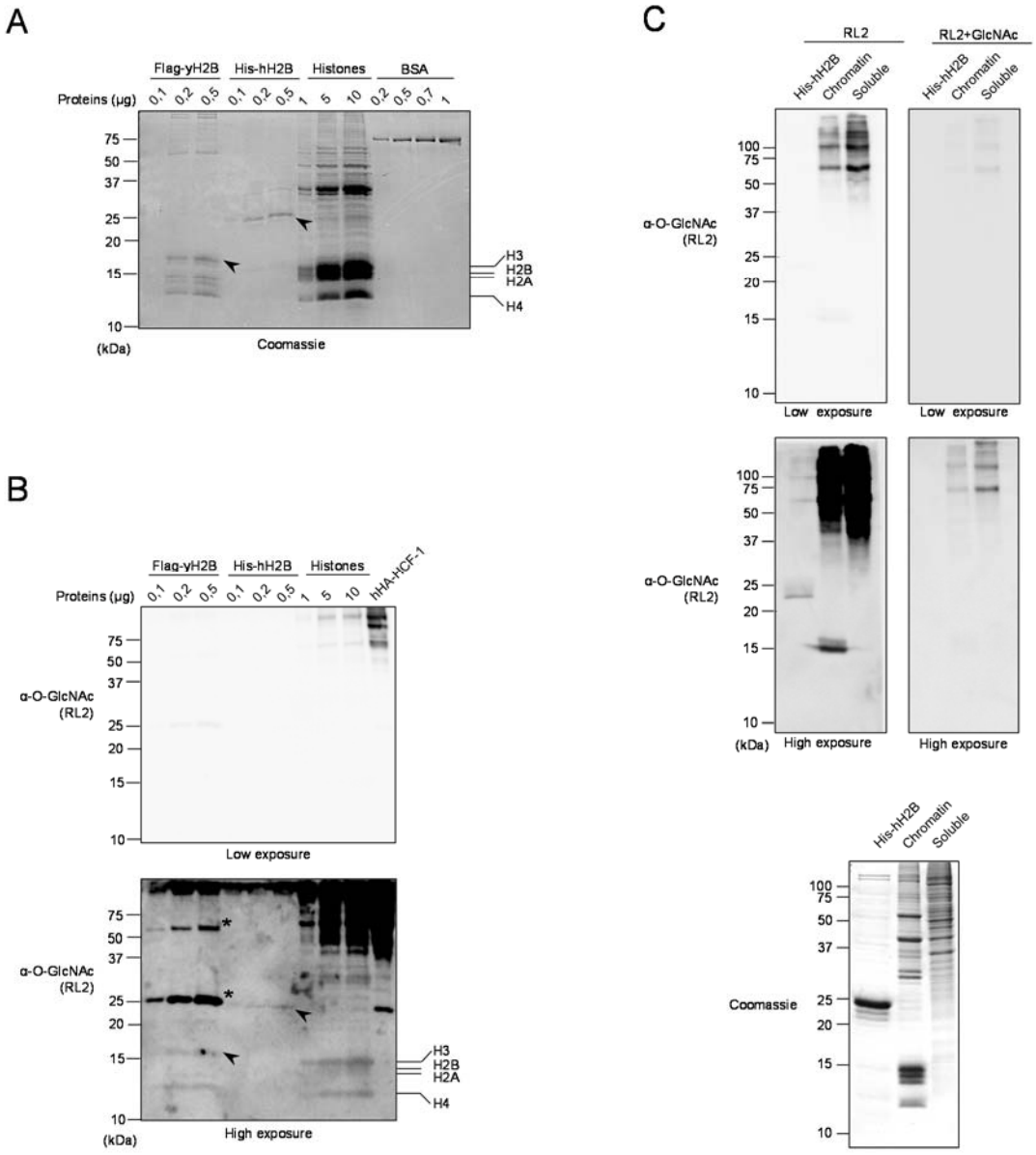

Supplemental FigS3.4. Detection of background signals by anti-O-GlcNAc RL2 antibody following immunoblotting of mammalian, yeast or recombinant histones.

(A) Coomassie Brilliant Blue staining showing molecular weight and relative quantification of purified recombinant yeast Flag-H2B (Flag-yH2B), human His-H2B (His-hH2B) and acid extracted histones purified from HeLa cells relative to bovine serum albumin (BSA). (B) Increasing amounts of recombinant Flag-yH2B, His-hH2B and acid extracted histones from HeLa cells quantified in (A) were analysed by western blot using α-O-GlcNAc (RL2) antibody. Purified human HCF-1(hHA-HCF-1) from HEK293T cells was used as a control for RL2 detection. Lines indicate purified endogenous histones from HeLa cells and Flag-yH2B. Arrows indicate Flag-yH2B and His-hH2B position. Asterisks indicate non-specific signal from the heavy and light chains of Flag antibody respectively. (C) N-Acetyl-D-Glucosamine competition with RL2 antibody. RL2 antibody was incubated with 1 M of N-acetylglucosamine (GlcNAc) for 1 hour. Antibody mixture was then used to immunoblot recombinant human His-hH2B, chromatin and soluble fractions from U2OS cells. Coomassie Brilliant Blue staining was used as a loading control. kDa; Molecular weight marker in Kilodalton

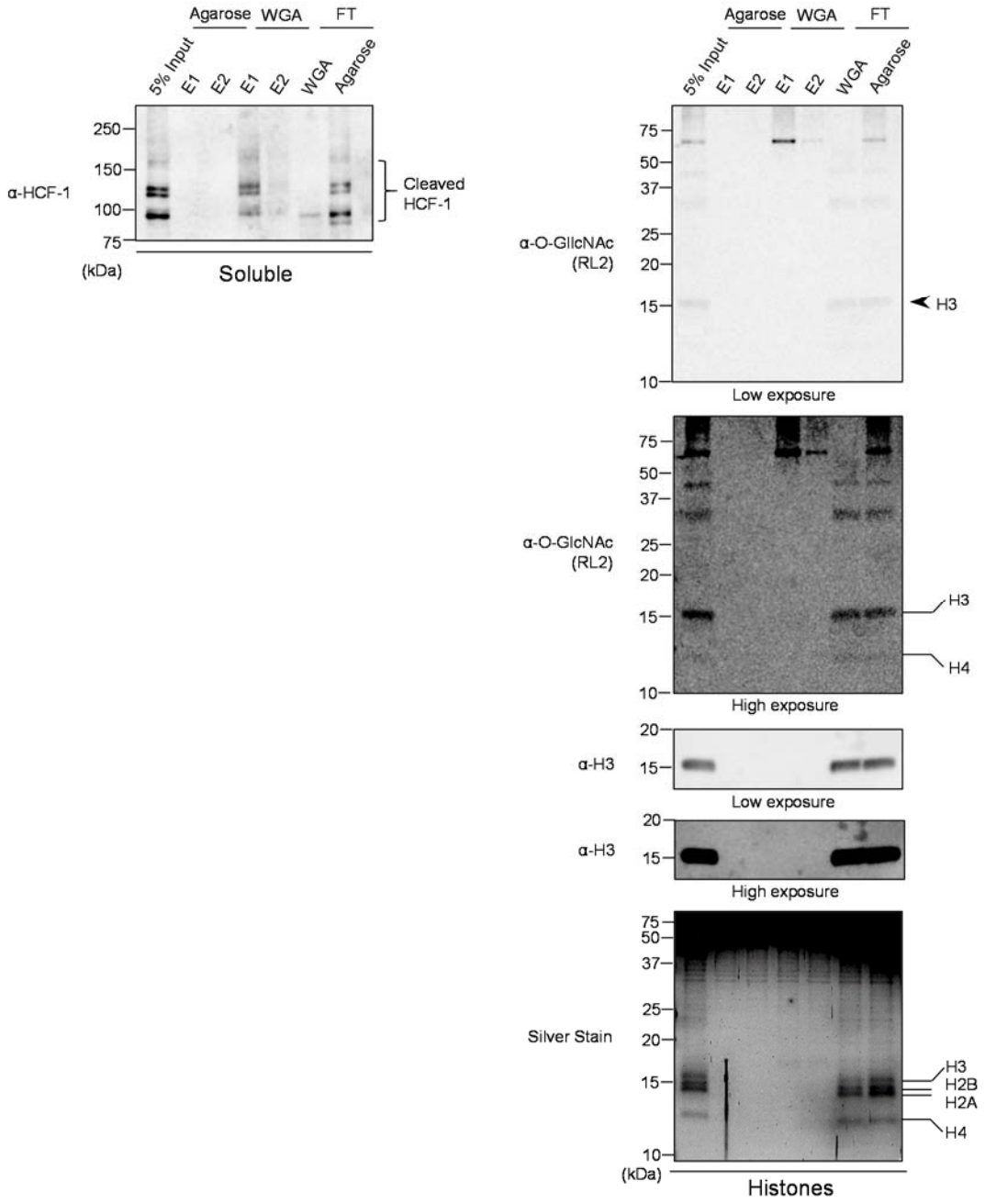

Supplemental FigS3.5. The core histones are not enriched by WGA lectin resin in conditions that ensure complete HCF-1 depletion from extracts.

HeLa cells were harvested and acid extraction of histones was performed. The indicated soluble (Left panel) and histone fractions (Right panel) were incubated overnight with the agarose bound WGA lectin resin or with the agarose resin to control for non-specific binding. The flow through (FT) was kept and the proteins were eluted from the resins (E1 and E2) with N-acetylglucosamine (GlcNAc). Soluble fraction showing depletion of HCF-1 on the WGA lectin resin (Left panel) . Western blot and silver stain analysis of the collected elutions revealed no

interaction between the core histones and the WGA lectin resin (Right panel). Arrows and lines indicate histones molecular weight. kDa; Molecular marker in Kilodalton.

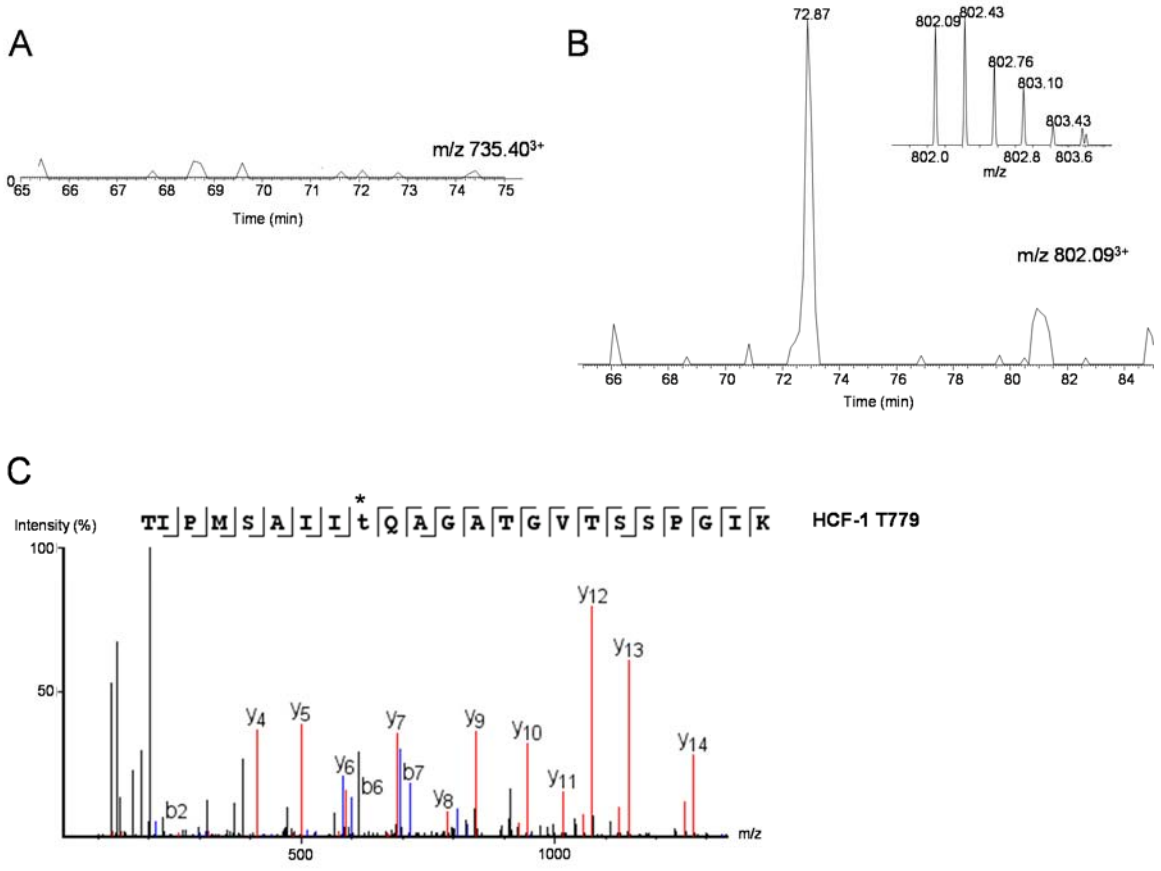

Supplemental FigS3.6. HCD MS/MS spectra for HCF-1 O-GlcNAcylated peptide containing T779 modification site.

(A) Extracted ion chromatogram for the HCF-1 peptide TIPMSAIITQAGATGVTSSPGIK at m/z 735.402+ showing that the peptide was not detected. (B) Extracted ion chromatogram for the HCF-1 peptide TIPMSAIIT(GlcNAc)QAGATGVTSSPGIK at m/z 802.092+ with the corresponding MS spectrum at 72.87 min. (C) MS/MS spectrum showing that the Thr9 indicated with the star is modified with the GlcNAc moiety.

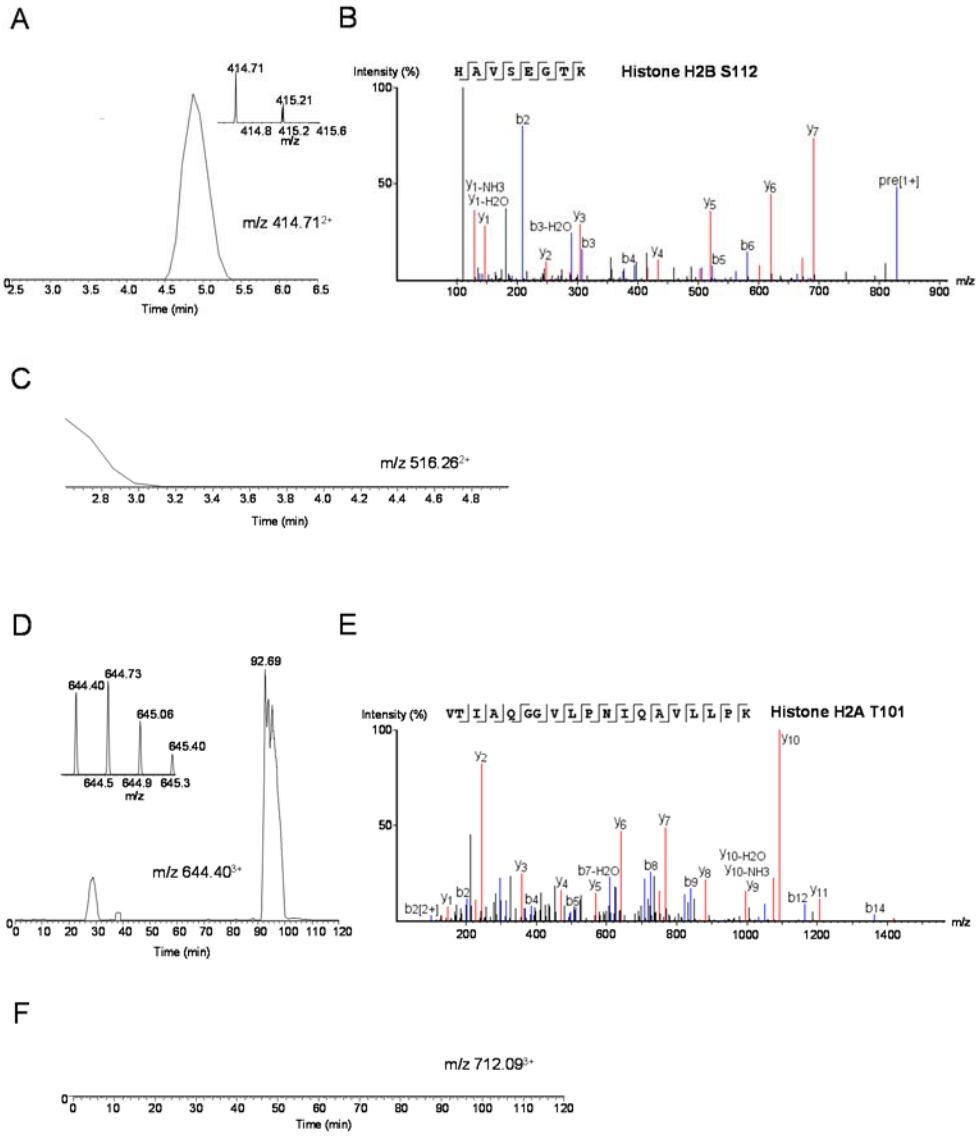

Supplemental FigS3.7. HCD MS/MS spectra for H2B and H2A peptides containing Ser112 and Thr101 respectively.

(A-C) HCD MS/MS spectra for H2B. Extracted ion chromatogram for the H2B peptide HAVSEGTK at m/z 414.712+ showing that the peptide was detected (A) along with the corresponding MS spectrum at 4.9 min and its MS/MS spectrum (B). (C) Extracted ion chromatogram for m/z 516,262+ corresponding to the expected peptide HAVSEGTK with a GlcNAC moiety. The absence of signal at m/z 516,262+ indicates that the corresponding glycopeptide was not detected. (D-F) HCD MS/MS spectra for H2A. Extracted ion chromatogram for the H2A peptide VTIAQGGVLPNIQAVLLPK at m/z 644.403+ showing that the peptide was detected (D) along with the corresponding MS spectrum at 92.69 min and its MS/MS spectrum (E). (F) Extracted ion chromatogram at m/z 712.093+ corresponding to the expected peptide VTIAQGGVLPNIQAVLLPK bearing a GlcNAC moiety. The absence of a signal at m/z 712.093+ indicates that the corresponding glycopeptide was not detected

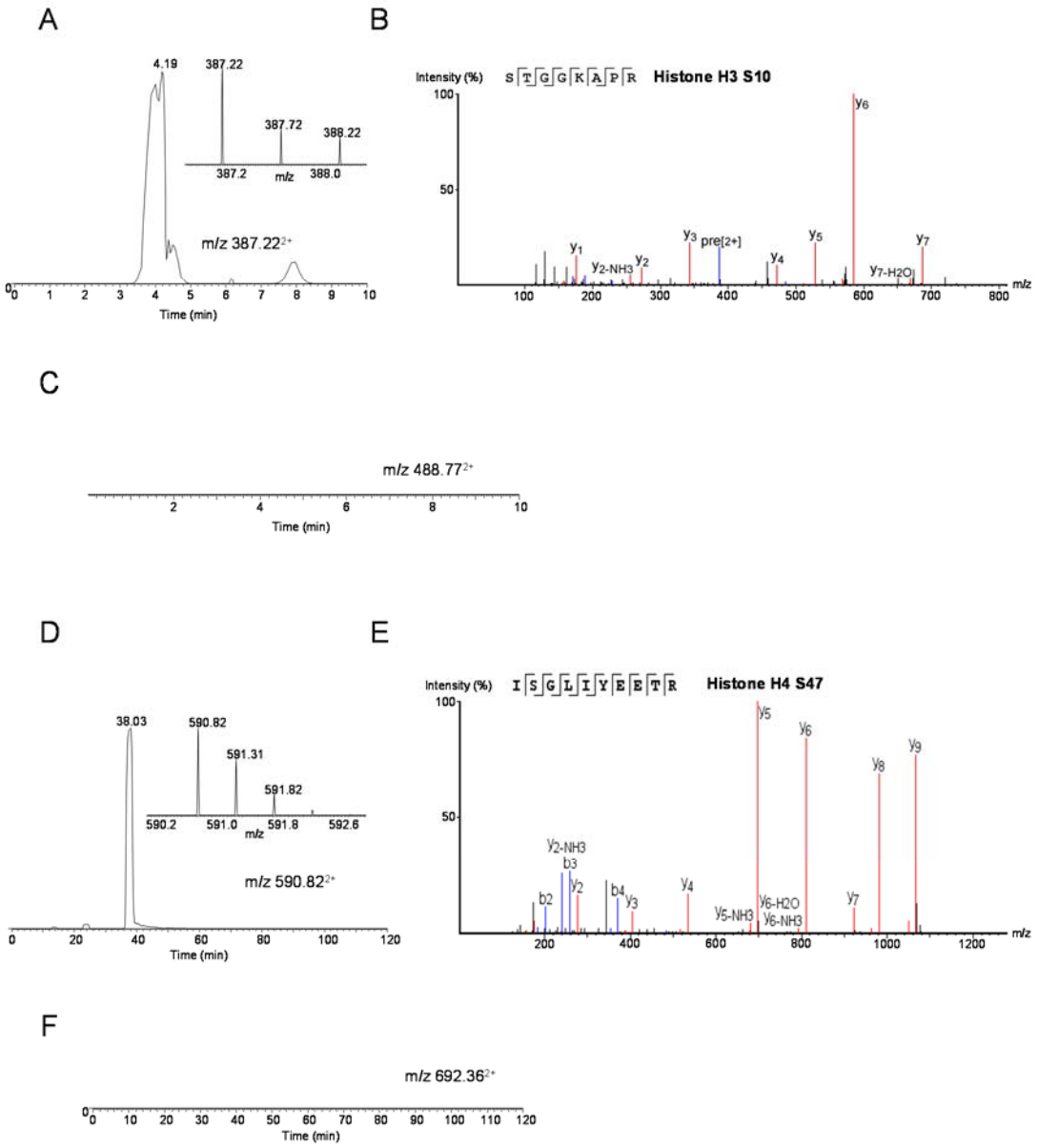

Supplemental FigS3.8. HCD MS/MS spectra for H3 and H4 peptides containing Ser10 and Ser47 respectively.

(A-C) HCD MS/MS spectra for H3. Extracted ion chromatogram for the H3 peptide STGGKAPR at m/z 387.222+ showing that the peptide was detected as evidenced from its (A) corresponding MS spectrum at 4.01 min and its MS/MS spectrum (B). (C) Extracted ion chromatogram for the expected peptide STGGKAPR bearing a GlcNAC moiety at m/z 488.773+, the absence of a signal indicates that the corresponding glycopeptide was not detected. (D-F) HCD MS/MS spectra for H4. Extracted ion chromatogram for the H4 peptide ISGLIYEETR at m/z 590.822+ showing that the peptide was detected as evidenced from the corresponding (D) MS spectrum at 39.03 min and its MS/MS spectrum (E). (F) Extracted ion chromatogram for the expected peptide ISGLIYEETR bearing a GlcNAC moiety at m/z 692.362+, the absence of signal indicates that the corresponding glycopeptide was not detected.

CHAPITRE 4

Article : The BAP1/ASXL2 Histone H2A Deubiquitinase Complex Regulates Cell Proliferation and is Disrupted in Cancer

Publié dans : Journal of Biological Chemistry (JBC). 2015 Nov 27; 290(48):28643-63. doi: 10.1074/jbc.M115.661553. Epub 2015 Sep 28

Salima Daou[1], Ian Hammond-Martel[1], Nazar Mashtalir[1], Haithem Barbour[1], Jessica Gagnon[1], Nicholas V.G. Iannantuono[1], Nadine S. Nkwe[1], Alena Motorina[1], Helen Pak[1], Helen Yu[1], Hugo Wurtele[1], Eric Milot[1], Frédérick A. Mallette[1], Michele Carbone[2] and El Bachir Affar[1]

1 Maisonneuve-Rosemont Hospital Research Center and Department of Medicine, University of Montréal, Montréal H3C 3J7, Québec, Canada
2 University of Hawaii Cancer Center, BSB200, 701 Ilalo Street, Honolulu, Hawaii 96813, USA.

Running title: Inactivation of BAP1/ASXL DUB activity in cancer.

keywords: Histone H2A ubiquitination; epigenetics; deubiquitylation (deubiquitination); Polycomb Group Proteins; BAP1; Calypso; ASXL; cancer biology; cell proliferation; cellular senescence.

Introduction à l'article :

Ce chapitre de la thèse est relié à l'objectif 3.

Nous savons que BAP1 catalyse la déubiquitination de H2Aub et régule la prolifération cellulaire. Néanmoins, l'implication des partenaires de BAP1 dans le contrôle de son activité catalytique et de sa fonction suppressive de tumeurs reste très peu définie. De ce fait, nous nous sommes intéressés à investiguer le rôle de BAP1/ASXL1/ASXL2 dans la modulation des mécanismes de déubiquitination.

Dans cette étude nous avons révélé un mécanisme de régulation de BAP1 par ASXL1 et ASXL2. En effet, les interactions BAP1/ASXL1/ASXL2 sont requises pour induire la liaison de BAP1 à l'ubiquitine et de stimuler son activité déubiquitinase. Plus important encore, nous avons identifié une mutation de cancer de BAP1 qui empêche sa liaison avec ASXL1/2 et perturbe sa fonction de régulateur de la prolifération cellulaire.

Nos résultats dévoilent un lien unique entre l'activite catalytique de BAP1 et sa fonction suppressive de tumeurs.

Contribution : Ma contribution comme premier auteur se résume à la conception et la réalisation de 75% de la totalité des expériences, la préparation de toutes les figures de l'article, la rédaction du manuscrit ainsi qu'à la réalisation de toutes les expériences requises pour les révisions et la finaliseation des figures et du manuscrit.

Background: The relevance of ASXL2 to the function of the histone H2A deubiquitinase (DUB) BAP1 remains unknown.

Results: ASXL2 promotes the assembly by BAP1 of a composite ubiquitin-binding interface (CUBI) required for DUB activity and coordination of cell proliferation.

Conclusion: Cancer-associated mutations of BAP1 disrupt BAP1-ASXL2 interaction and function.

Significance: Novel insights into BAP1 tumor suppressor function.

4.1 ABSTRACT

The deubiquitinase (DUB) and tumor suppressor BAP1 catalyzes ubiquitin removal from histone H2A K119 and coordinates cell proliferation, but how BAP1 partners modulate its function remains poorly understood. Here, we report that BAP1 forms two mutually exclusive complexes with the transcriptional regulators ASXL1 and ASXL2, which are necessary for maintaining proper protein levels of this DUB. Conversely, BAP1 is essential for maintaining ASXL2, but not ASXL1 protein stability. Notably, cancer-associated loss of BAP1 expression results in ASXL2 destabilization and hence loss of its function. ASXL1 and ASXL2 use their ASXM domains to interact with the C-terminal domain (CTD) of BAP1 and these interactions are required for ubiquitin binding and H2A deubiquitination. The deubiquitination promoting effect of ASXM requires intramolecular interactions between catalytic and non-catalytic domains of BAP1 which generate a composite ubiquitin binding interface (CUBI). Notably, the CUBI engages multiple interactions with ubiquitin involving, (i) the ubiquitin carboxyl hydrolase (UCH) catalytic domain of BAP1 which interacts with the hydrophobic patch of ubiquitin and (ii) the CTD domain which interacts with a charged patch of ubiquitin. Significantly, we identified cancer-associated mutations of BAP1 that disrupt the CUBI, and notably an in frame deletion in the CTD that inhibits its interaction with ASXL1/2, DUB activity and deregulates cell proliferation. Moreover, we demonstrated that BAP1 interaction with ASXL2 regulates cell senescence and that ASXL2 cancer-associated mutations disrupt BAP1 DUB activity. Thus, inactivation of BAP1/ASXL2 axis might contribute to cancer development.

4.2 Introduction

Covalent attachment of ubiquitin on lysine or N-terminal residues of target proteins can influence substrate stability and function, and as such exerts major roles in diverse cellular processes including intracellular trafficking, protein quality control, cell cycle progression, transcription, DNA replication and repair [175,182,183,430,431]. Ubiquitination is catalyzed by the concerted action of E1-ubiquitin activating, E2-ubiquitin conjugating and E3-ubiquitin ligases

and generally results in the attachment of one or several ubiquitin molecules, i.e. mono- or poly-ubiquitination, respectively [175,432]. Ubiquitination events are tightly coordinated by DUBs, which are responsible for reversing this modification [198,433]. Proteins containing ubiquitin-binding domains (UBDs) are responsible for the specific and non-covalent recognition of free ubiquitin and of mono- or poly-ubiquitinated substrates. UBDs can be categorized into several families based on structural characteristics such as the presence of single or multiple α-helices, zinc fingers or pleckstrin-homology fold, which constitute interfaces of low affinity interaction with one or multiple molecules of ubiquitin. UBD-containing proteins are thus widely involved in the proper and timely initiation, propagation or termination of ubiquitin-mediated signaling events [175,187]. The nuclear DUB BAP1 is a tumor suppressor deleted and mutated in an increasing number of cancers of diverse origins [77,243]. Indeed, somatic or germinal inactivating mutations in BAP1 are found in mesothelioma, uveal melanoma, cutaneous melanocytic tumors, clear cell renal cell carcinoma, breast and lung cancers, thereby making BAP1 the most frequently and widely mutated DUB-encoding gene in cancer [226,230,231,235,247-250,434]. Previous studies indicated that BAP1 tumor suppressor function requires DUB activity and nuclear localization [236]. Consistent with its role in tumor suppression, BAP1 was shown to act as a positive or a negative regulator of cell proliferation [229,234,236,435]. Moreover, genetic ablation of BAP1 in mice inhibits embryonic development, while selective inactivation of BAP1 in the hematopoietic system induces severe defects in the myeloid cell lineage, recapitulating key features of myelodysplastic syndrome [230]. At the molecular level, BAP1 acts as a chromatin-associated protein that is assembled into large multi-protein complexes containing several transcription factors and co-factors including the Host Cell Factor 1 (HCF-1), the O-linked N-acetyl-Glucosamine Transferase (OGT), the Lysine Specific Demethylase KDM1B/LSD2/AOF1, the Additional Sex Comb Like proteins ASXL1 and ASXL2 (ASXL1/2), the forkhead transcription factors FOXK1 and FOXK2 as well as the zinc finger transcription factor Yin Yang 1 (YY1) [239,435,436]. BAP1 is recruited at gene promoter regions to activate transcription, and has been shown to regulate the expression of genes involved in cell proliferation [247,436,437]. BAP1 is also recruited to sites of DNA double strand breaks to promote repair by homologous recombination [229,438], and is implicated in DNA replication-associated processes [237,439]. Moreover, BAP1 functions appear to be regulated by post-translational

modifications including phosphorylation and ubiquitination [229,237,241]. Nonetheless, the mechanism by which BAP1 function is coordinated by its partners remains poorly defined.

Calypso, the *Drosophila* ortholog of BAP1 is a Polycomb Group (PcG) protein that interacts with the transcriptional regulator ASX and assembles the Polycomb Repressive-DUB (PR-DUB) complex which deubiquitinates histone H2A K118 (H2A K119 in vertebrates, hereafter H2Aub) and promotes PcG target gene repression [79]. While the exact mechanism of repression remains unknown, it is interesting to note that the Polycomb Repressive Complex 1 (PRC1), which catalyzes H2A ubiquitination, is also required for PcG target gene repression [39]. *Drosophila* ASX protein is an atypical PcG factor, since it is involved in both transcriptional silencing and activation [365,368]. ASXL1 and ASXL2 (hereafter ASXL1/2) are paralogs that appear to have diverged from ASX during evolution, and are reported to function with a number of co-repressors and co-activators, notably the Lysine-Specific Demethylase KDM1A/LSD1, the PcG complex PRC2 and the Trithorax Group (TrxG) epigenetic regulators [372-375]. Similar to PR-DUB complex, a minimal complex containing mammalian BAP1 and the N-terminal region of ASXL1 was shown to deubiquitinate H2A *in vitro,* indicating the requirement of ASX or ASXL1 for DUB activity [79]. The DUB activity of BAP1 toward histone H2A K119 was also observed in vivo [229,250,437,440]. BAP1 was also shown to deubiquitinate and stabilise some of its interacting partners including HCF-1 and OGT indicating the functional importance of its catalytic activity [230,234,435]. ASXL1/2 contain two uncharacterized N-terminal domains, ASXN and ASXM, and a C-terminal Plant Homeo Domain (PHD) finger [367,372]. Interestingly, the DUB activity of a BAP1 family member, UCH37, is stimulated by RPN13 (ADRM1) 19S proteasome subunit [441-443], and phylogenetic studies suggest that RPN13 and ASXL1/2 share a conserved domain termed the DEUBiquitinase ADaptor (DEUBAD) domain corresponding to ASXM [378]. This suggests that BAP1/ASXL1/2 might use a similar mechanism of DUB activation as UCH37/RPN13.

The genes encoding ASXL1/2 are involved in chromosomal translocations and are frequently truncated in various cancer types [444]. ASXL1 is frequently mutated in myeloid malignancies. Most of these mutations generate truncated ASXL1 proteins that retain the N-terminal region required for interaction with BAP1 [79]. Although, ASXL1 interaction with BAP1 was initially revealed dispensable for leukemia development [375], it was recently shown

that leukemia-associated mutations of ASXL1, lead to an aberrant enhancement of BAP1 DUB activity [445]. Moreover, expression of these ASXL1 constructs in hematopoietic precursor cell line causes an overall depletion of H2Aub associated with defects in myeloid differentiation [445]. However, the involvement of this interaction in other cancers remains unknown. In addition, the specific contribution of ASXL1 and ASXL2 to BAP1 function remains undefined. Here, we sought to determine how ASXL1/2 modulates the H2A DUB activity of BAP1, and the relevance of these factors for BAP1 tumor suppressor function. We mapped the exact interaction domains and motifs between BAP1 and ASXL1/2 and demonstrated that ASXL1/2 form two mutually exclusive complexes with BAP1, both of which are competent in deubiquitinating H2A. Furthermore, we showed that the loss of BAP1 expression in cancer is concomitant with a destabilization of ASXL2. We also found that the ASXM domain of ASXL1/2 is prerequisite for ubiquitin binding and deubiquitination by BAP1. Moreover, we found that BAP1 catalytic and non-catalytic domains form, along with the ASXM domain, a composite ubiquitin binding interface (CUBI) required for promoting BAP1 DUB activity by ASXL1/2 and coordination of cell proliferation. Finally, we identified a cancer-derived mutation of BAP1 CTD, ΔR606-H609, which results in a selective loss of interaction with ASXL1/2 and inhibition of H2A DUB activity. The ΔR606-H609 mutation also abolishes the ability of BAP1/ASXL2 axis to regulate cell proliferation and cellular senescence, thus providing a link between BAP1 function and mechanisms of tumor suppression.

4.3 EXPERIMENTAL PROCEDURES

4.3.1 Plasmids-Retroviral constructs :

BAP1, pOZ-N-Flag-HA-BAP1 C91S (catalytic dead) and pOZ-N-Flag-HA-BAP1ΔHBM (BAP1 mutant deleted in the NHNY sequence corresponding to the HCF-1 binding motif); constructs to produce recombinant full-length GST-BAP1 and various deleted forms; pET30a+ BAP1 for production of His-tagged BAP1 were previously described [436]. pCDNA3-Flag-H2A was obtained from Moshe Oren [427]. pOZ-N-Flag-HA-BAP1 ΔCTD1 and pOZ-N-Flag-HA-BAP1 ΔCC2 were generated by PCR-based subcloning. Non-tagged

pCDNA3-BAP1 and pCDNA3-BAP1-C91S were generated by subcloning the cDNAs from pOZ-N-Flag-HA-BAP1 and pOZ-N-Flag-HA-BAP1-C91S respectively. siRNA resistant constructs for BAP1, BAP1-C91S, BAP1 ΔCTD, BAP1R666-H669 were generated using gene synthesis (BioBasic) and then subcloned into modified pENTR D-Topo plasmid (Life Technologies). Expression constructs of siRNA resistant BAP1, BAP1 C91S, BAP1 ΔCTD and BAP1 ΔR666-H669 were generated by recombination using LR clonase kit (Life Technologies) into pMSCV-Flag-HA-IRES-Puro or pDEST-Myc constructs [239]. BAP1ΔUCH, BAP1ΔCC1 and BAP1ΔCTD were described [241], and were sub-cloned by PCR into pENTR. Ubiquitin constructs (Ub wild type, Ub VLI (V70A/L8A/I44A), Ub I36A, Ub I44A, Ub D58A) flanked by att-B and att-P recombination sites were generated by gene synthesis (Life technologies) directly into pMK-Rq plasmid and bacterial expression constructs were generated by recombination into pDEST-GST. Other Ubiquitin mutants constructs (Ub TEK (K6A/L11A/T12A/T14A/E34A), Ub Il36 patch (L8A/I36A/L71A/L73A), Ub IL44 patch (L8A/L44A/H68A/V70A), Ub Phe4 patch (Q2A/F4A/T14A), Ub (Q49A/R72A), Ub (R42A/Q49A/D52A/R72A)) flanked by att-B and att-P recombination sites were generated by gene synthesis (Biobasic) directly into pUC57-Kan Vector and bacterial expression constructs were generated by recombination into pDEST-GST. Human cDNA ASXL1 (NCBI: NM_015338.5) and ASXL2 (NCBI: NM_018263.4) were cloned from HeLa total RNA by reverse transcription and inserted into pENTR D-Topo plasmid. BAP1 point mutations constructs were generated by site direct mutagenesis in pENTR D-Topo BAP1 using PfuUltra High-Fidelity DNA Polymerase. Human Myc-ASXL1 ΔASXM and Myc-ASXL2 ΔASXM constructs were generated by PCR-based subcloning of 2 fragments each ligated in frame into pENTR D-Topo. Expression constructs of ASXL1, ASXL2 and corresponding vectors with deletions of ASXM were generated in pDEST-Myc and pDEST-Flag. Other expression constructs for BAP1 and corresponding mutants forms, were generated using LR clonase in pDEST-Myc, pDEST-Flag and bacterial pDEST-His. Full length ASXM1 and ASXM2 and deletions mutants forms of ASXM2 (ASXM2 246-313, ASXM2 300-401, ASXM2 316-401, ASXM2 246-347) were sub-cloned by PCR and inserted into pENTR D-Topo plasmid. ASXM2 point mutations constructs were generated by site direct mutagenesis in pENTR D-Topo ASXM2. Bacterial expression vectors of ASXM1, ASXM2 and respective mutant forms

were generated in pDEST-GST and pDEST-MBP vectors. Human PAR-4 was cloned in-frame with GFP in pCDNA3 using PCR.

4.3.2 Cell culture and cell transfection:

Primary human skin fibroblasts (LF1), BAP1-deficient human lung squamous carcinoma NCI-*H226*, BAP1-deficient human mesothelioma NCI-H28, U2OS osteosarcoma, human embryonic kidney HEK293T (293T), Cervical cancer HeLa, normal Human Lung Fibroblasts (IMR90), phoenix ampho and 293-GPG packaging cells were cultured in Dulbecco's modified Eagle's medium (DMEM) supplemented with foetal bovine serum (FBS), L-glutamine and penicillin/streptomycin. HeLa S3 cells were cultured in Minimum Essential Media (MEM) supplemented with FBS, L-glutamine and penicillin/streptomycin.
293T cells were transfected with the mammalian expressing vectors using polyethylenimine (PEI) (Sigma-Aldrich). Three days post-transfection, cells were harvested for immunoblotting, immunoprecipitation or immunostaining.

Similar numbers of H226 BAP1-null cells stably expressing BAP1, $BAP1^{C91S}$ or $BAP1^{R666\text{-}H669}$ were seeded on the plates and cultured for 5 days. The clonogenic survival assay was essentially done as described before [229].

U2OS or LF1 cells were transfected using Lipofectamine 2000 (Life technologies) with 200 pmol of either ON-TARGET plus Non-targeting pool (D-001810) or ON-TARGET plus SMARTpool BAP1 (L-005791) (Thermo Scientific, Dharmacon) or with a pool of siRNA sequences purchased from Sigma-Aldrich targeting ASXL1 (pool of 4 oligonucleotides, SASI_Hs02_00347642, SASI_Hs01_00200507, SASI_Hs01_00200508, SASI_Hs01_00200509) and ASXL2 (2 pools of 4 oligonucleotides, SASI_Hs01_00202197, SASI_Hs01_00202198, SASI_Hs01_00202199, SASI_Hs01_00202200 and SASI_Hs01_00202197, SASI_Hs01_00202200, SASI_Hs01_00202203, SASI_Hs01_00202201). Four days post-transfection, cells were harvested for immunoblotting.

siRNA DUB screen-HeLa cells were transfected with individual siRNA pool targeting DUBs (ON-TARGETplus® SMARTpool® siRNA Library-Human Deubiquitinating

Enzymes) using Lipofectamine 2000 (Life Technologies). Three days post-transfection, cells were fixed and used for immunostaining with H2Aub antibody and the fluorescence signals were detected with a Fluoroskan Ascent™ Microplate Fluorometer (Thermo Scientific), and the obtained values were used to derive the Z-scores. The screen was done in duplicate and the values of H2Aub signals were normalized to DAPI staining.

qRT-PCR analysis of mRNA expression-Total RNA was used to prepare the cDNAs as described [436]. The cDNAs were analyzed by Real time PCR using SYBR Green detection DNA quantification kit (Life technologies) to determine levels of gene mRNAs. PCR was conducted on an Applied Biosystems® 7500 Real-Time PCR Systems (Life Technologies). To ensure accurate quantification of mRNA, similar amounts of total RNA were spiked with an in vitro synthesized GAL4 mRNA, which was performed following the manufacturer procedure (MAXIscript Kit Procedure, Life Technologies). The transcript was synthesized from pcDNA.3-GAL4 construct with T7 promoter. The primers used are listed below. hASXL2-F: GAATCCAGGTGCGAAAAGTAC and hASXL2-R: GATGGAGACTGGAAAACGAGC and GAL4-F: CAACTGGGAGTGTCGCTACT, and GAL4-R: AATCATGTCAAGGTCTTCTCGA

4.3.3 Immunoblotting and antibodies :

Total cell extracts were used for SDS-PAGE and immunoblotting was done according to standard procedures [436]. The band signals were acquired with a LAS-3000 LCD camera coupled to MultiGauge software (Fuji, Stamford, CT, USA). Anti-FOXK2 rabbit polyclonal antibody was previously described [241]. The rabbit polyclonal antibody anti-ASXL1 was generated using bacteria-expressed fragment (700-950 amino acids of the human protein) with Pacific Immunology. Mouse monoclonal anti-BAP1 (C4, sc-28383), rabbit polyclonal anti-BAP1 (H300, sc-28236), rabbit polyclonal anti-YY1 (H414, sc-1703), rabbit polyclonal anti-OGT (H300, sc-32921), mouse monoclonal anti-CDC6 (180.2, sc-9964), mouse monoclonal anti-MCM6, mouse monoclonal anti-tubulin (B-5-1-2, sc-SC-23948), mouse monoclonal anti-p53 (DO-1, sc-126), mouse monoclonal anti-p16 (JC8, sc-56330), mouse monoclonal anti-MDM2 (SMP14, sc-965), rabbit polyclonal anti-FOXK1 (H-140, sc-134550), and mouse monoclonal anti-PARP1 (F2, sc-8007) were from Santa Cruz. Rabbit polyclonal anti-HCF-1

(A301-400A) and rabbit polyclonal anti-ASXL2 (A302-037A) were from Bethyl Laboratories. Mouse monoclonal anti-p21 (55643) was from BD Pharmigen. Mouse monoclonal anti-Flag (M2) and rabbit polyclonal anti-GST (G7781) were from Sigma-Aldrich. Mouse monoclonal anti-MYC (9E10) was from Covance. Rabbit polyclonal anti-H2Aub K119 (D27C4) rabbit polyclonal anti-H2Bub K120 (D11 XP), mouse monoclonal anti-RB (4H1), rabbit polyclonal anti- pRB (S807/811) and mouse monoclonal (HRP conjugated) anti-MBP (E8038) were from Cell Signaling. Mouse monoclonal anti-H2Bub antibody (NRO3) was from MEDIMABS. Mouse monoclonal anti-Phospho-H2AX (ser139) (clone JBW301, 05-636), Mouse monoclonal anti-H2Bub antibody clone 56 (05-1312), Mouse monoclonal anti-H2Aub K119 antibody clone E6C5 (05-678) and mouse monoclonal anti-β-Actin (MAB1501, clone C4) were from Millipore.

4.3.4 Immunodepletion and Immunoprecipitation :

Immunodepletion experiments were done as described [436]. Reciprocal immunoprecipitation from the BAP1 complexes was conducted essentially as described [241]. Briefly, the purified BAP1 complexes were incubated with the indicated antibodies overnight at 4 ºC. The immuno-depleted complexes were recovered next day with protein G sepharose beads saturated with 1% BSA. Co-immunoprecipitation was conducted as described [436].

4.3.5 Cell lines with stable expression and protein complex purification :

HeLa S3 cell lines stably expressing Flag-HA-BAP1, Flag-HA-BAP1ΔCTD1, or Flag-HA-BAP1R666-H669, H28 cell lines stably expressing Flag-HA-BAP1 and Flag-HA-BAP1C91S, as well as H226 cell lines stably expressing Flag-HA-BAP1, Flag-HA-BAP1C91S and Flag-HA- BAP1R666-H669 were generated following retroviral infection using pOZ-N-Flag-HA-IRES-IL2R retroviral constructs and selection using anti-IL2 magnetic beads (Life Technologies) [436]. U2OS expressing siRNA resistant Flag-HA-BAP1, Flag-HA-BAP1C91S, Flag-HA-BAP1 ΔCTD and Flag-HA- BAP1R666-H669 were generated following retroviral infection using pMSCV-Flag-HA-IRES-Puro based constructs and selection with 3 μg/ml of puromycin. Around 3 X 109 of HeLa S3 cells were used for the immunoaffinity purification of the different BAP1 complexes. The purification was done as

previously described [241]. Eluted complexes were used for silver stain, western blot analysis and in vitro ubiquitin pulldown and DUB assays.

4.3.6 In vitro interaction assays:

Protein interaction pull down assays were conducted as previously described [436].

4.3.7 Ubiquitin pull down interaction assays-GST:

GST-ubiquitin immobilized beads and its corresponding mutant forms were purified using glutathione agarose beads. For the Ubiquitin-Agarose pull down interaction assays, His-BAP1 or the corresponding mutant forms (1.6 µg, 20 nM) were pre-incubated for 30 min to 1 hour with GST-ASXM1 or GST-ASXM2 (2 µg each, 50 nM) or GST-ASXM2 deletion mutant forms at 4 ºC in 50 mM Tris, pH 7.5; 150 mM NaCl; 1% Triton; 1 mM PMSF, protease inhibitors cocktail and 2 mM DTT. The mix was incubated for 3 hours with Ubiquitin-Agarose beads (Boston Biochem) which were then washed 6 times with the same buffer. The associated proteins were eluted in Laemmli buffer and subjected to western blotting. For the GST-Ubiquitin (GST-Ub) pull down interaction assays, His-BAP1 or His-BAP1 C91S or the recombinant BAP1 deletion mutants (1.6 µg, 20 nM) were pre-incubated for 30 min to 1 hour with either MBP-ASM2 or its corresponding mutant forms (2 µg, 30 nM). The mix was then incubated overnight with either GST-Ubiquitin immobilized beads or mutant forms (3 µg, 80 nM). The beads were washed 6 times with the same buffer and the associated proteins were subjected to western blotting. For the GST-Ubiquitin (GST-Ub) pull down interaction assays using MBP-ASXM2 (2 µg, 30 nM) or MBP-CTD (3 µg, 40 nM), the purified proteins were incubated for 16 hours with GST-Ubiquitin immobilized beads (3 µg, 80 nM). The beads were washed 6 times with the same buffer and the associated proteins were subjected to western blotting.

4.3.8 Purification of the nucleosomes and in vitro DUB assay:

Native nucleosomes were purified as described [229]. The purified nucleosomes were used for the in vitro DUB assay using either Flag-HA purified BAP1 complexes or bacteria-purified His-BAP1 (8 ng, 2 pM) with or without bacteria purified GST-ASXM1/2 (10 ng, 4

pM) or MBP-ASXM2 (10 ng, 2,8 pM) as described [229]. The DUB reaction was carried out in the reaction buffer (50 mM Tris-HCl, pH 7.3; 1 mM MgCl2; 50 mM NaCl; 1 mM DTT) for the indicated times at 37°C. The in vitro reaction was stopped by adding Laemmli buffer and analyzed by immunoblotting.

4.3.9 Synchronization and cell cycle analysis:

U2OS cells were synchronized at the G1/S border using the method of thymidine (2 mM) double block and analyzed by flow cytometry as described previously [419]. Immunofluorescence-The immunostaining procedure was carried as previously described [275].

4.3.10 Protein sequence analysis and structure modeling:

Conservation of protein sequences was determined using Geneious 6.1.2 (Biomatters, http://www.geneious.com). The ubiquitin resolved 3D structure PDB file (1UBQ) was downloaded from the PDB database (http://www.rcsb.org/pdb/home/home.do). We used the Chimera software (UCSF Chimera V 1.10) to visualize the 3D structure and to highlight different ubiquitin interfaces.

4.3.11 Statistical Analysis:

Most experiments were conducted at least three times. Quantifications were done for a representative experiment. DUB RNAi screen was conducted once. Cell counts for senescence studies were derived from one representative experiment and are shown as average with standard deviation.

4.4 RESULTS

4.4.1 ASXL1 and ASXL2 compete for their interaction with BAP1.

ASXL1 and ASXL2 factors co-purified with BAP1 [239,436], and mass spectrometry peptide counts suggest that they are associated with BAP1 at similar levels (Fig. 4.1A). BAP1 interaction with ASXL1/2 was not affected by the loss of HCF-1, a major subunit of the BAP1 core complexes associated through its HCF-1 binding motif (HBM). We also note that the

interaction between BAP1 and OGT is strongly reduced in the context of BAP1$^{\Delta HBM}$ complexes, indicating that HCF-1 bridges OGT and BAP1. (Fig.4.1B). We sought to further investigate the functional relationship between these factors. Immunoprecipitation (IP) of ASXL2 from purified BAP1 complexes did not show interaction with ASXL1 (Fig. 4.1C), and ASXL1 and ASXL2 failed to interact with each other following overexpression (Fig. 4.1D). We noted that BAP1 interaction with ASXL2 was reduced following expression of ASXL1 (Fig. 4.1D), suggesting that ASXL1 might compete with ASXL2 for BAP1 binding. To further confirm that ASXL1 and ASXL2 compete for interaction with BAP1, we overexpressed increasing amounts of ASXL1 with constant amounts of BAP1 and ASXL2 in 293T cells and conducted immunoprecipitation. Interestingly, although ASXL2 and BAP1 protein levels also increased following ASXL1 overexpression, we observed that ASXL2 was displaced from BAP1-containing protein complexes (Fig. 4.1E) indicating that ASXL1 and ASXL2 form two distinct complexes with BAP1.

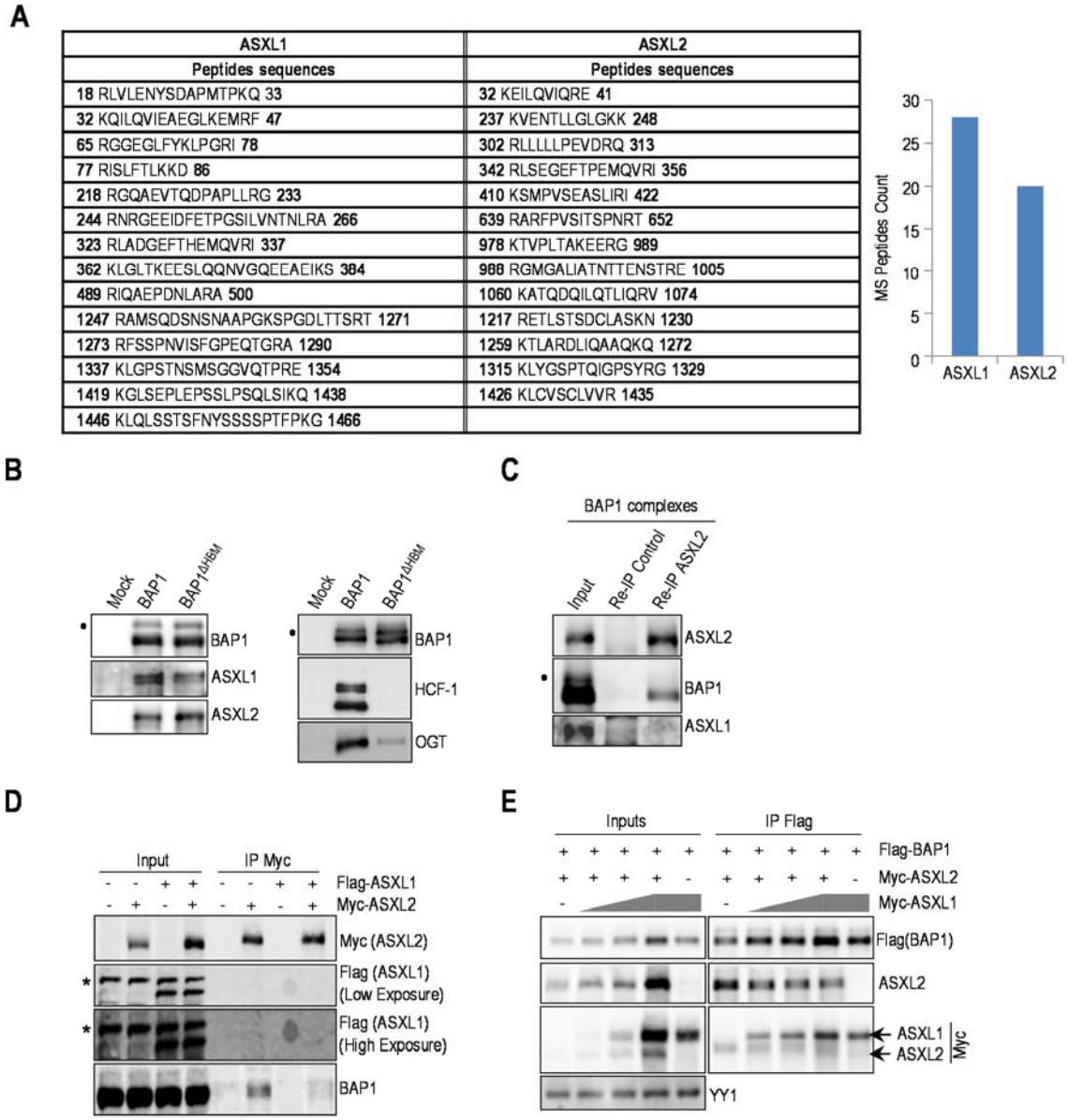

Figure 4.1. BAP1 interacts with either ASXL1 or ASXL2.

A) BAP1 complexes contain relatively similar amounts of ASXL1/2 proteins. ASXL1/2 peptides identified by mass spectrometry following the purification of BAP1 complexes from HeLa S3 cells. The amino acid positions of the peptides are indicated. **B)** HCF-1 is not required to maintain the interaction between BAP1 and ASXL1/2. Purification of BAP1 or BAP1$^{\Delta HBM}$ (lacking the HCF-1-binding motif) complexes and detection of ASXL1/2 and BAP1 by immunoblotting (left panel). The immunopurifed proteins were also analyzed by immunoblotting to detect the two major components of the BAP1 complexes, HCF-1 and OGT (right panel). Note that OGT is greatly reduced in the BAP1$^{\Delta HBM}$ complexes due to the absence of HCF-1. **C**) Reciprocal immunoprecipitation (Re-IP) of

ASXL2 from the purified BAP1 complexes. **D**) 293T cells were transfected with Myc-ASXL2 (6 μg) with or without Flag-ASXL1 (4 μg) expression vectors and harvested, three days later, for IP of Myc (ASXL2). **E)** 293T cells were transfected with Flag-BAP1 (0.1 μg) and Myc-ASXL2 (3 μg) constructs in the presence of increasing amounts of Myc-ASXL1 construct (1, 2 and 5 μg) and harvested, three days later, for IP of BAP1 using anti-Flag. Overexpressed Myc-ASXL2 was detected with anti-ASXL2 and anti-Myc antibodies. ASXL1 was detected with anti-Myc antibody. The difference in M.W. allows discrimination between ASXL1 and ASXL2 bands. YY1 is used as a loading control. Quantification of band intensity for each protein was conducted relative to the lowest amount of transfected plasmid. The dot and the star indicate a monoubiquitinated form of BAP1 [241], and non-specific bands respectively (panels **B**, **C**, **D**).

4.4.2 BAP1 and ASXL1/2 are co-regulated and loss of BAP1 in cancer is concomitant with ASXL2 destabilization.

To further investigate the relevance of ASXL1 and ASXL2 in regulating BAP1 function, we transfected 293T cells with BAP1 and increasing amounts of Myc-tagged ASXL1/2-expressing constructs. We found that BAP1 protein levels increased with ASXL1/2 expression in a dose-dependent manner (Fig. 4.2A). Conversely, ASXL1/2 protein levels were also increased following overexpression of BAP1 (Fig. 4.2B). siRNA knockdown of either ASXL1 or ASXL2 in U2OS osteosarcoma cells or primary human fibroblasts resulted in a significant decrease of BAP1 protein levels (Fig. 4.2C,D), while combined knockdown of ASXL1/2 caused an even stronger decrease of BAP1 levels than depletion of individual proteins (Fig. 4.2C). This indicates that ASXL1/2 are necessary for maintaining proper protein levels of this DUB. We also observed that depletion of ASXL1 resulted in a noticeable decrease of ASXL2, while knockdown of ASXL2 caused an increase of ASXL1 (Fig. 4.2C,D). Knockdown of BAP1 strongly reduced ASXL2 levels. This effect is independent of BAP1 DUB activity, as the decrease of ASXL2 protein in U2OS cells was prevented by re-expression of siRNA-resistant forms of BAP1, either wild type or catalytically dead mutant, $BAP1^{C91S}$ (Fig. 4.2E). The dependency of ASXL2 protein levels on BAP1 abundance suggests that ASXL2/BAP1 may form an obligate complex. Consistently, immunodepletion of endogenous proteins from HeLa nuclear extracts revealed that the majority of ASXL2 is associated with BAP1 (Fig. 4.2F). However, only about half the amount of BAP1 is in complex with ASXL2. PARP1 was used as a control which remained in the flow through fraction. Significantly, ASXL2 was downregulated in BAP1-deficient H28 mesothelioma and H226 lung carcinoma cells, and re-expression of BAP1 or $BAP1^{C91S}$ restored ASXL2 protein

levels in these cells, without affecting its mRNA levels (Fig. 4.2G,H). These data suggest that BAP1/ASXL1/2 interactions are regulated and that loss of BAP1 during cancer development results in concomitant loss of ASXL2 protein and function.

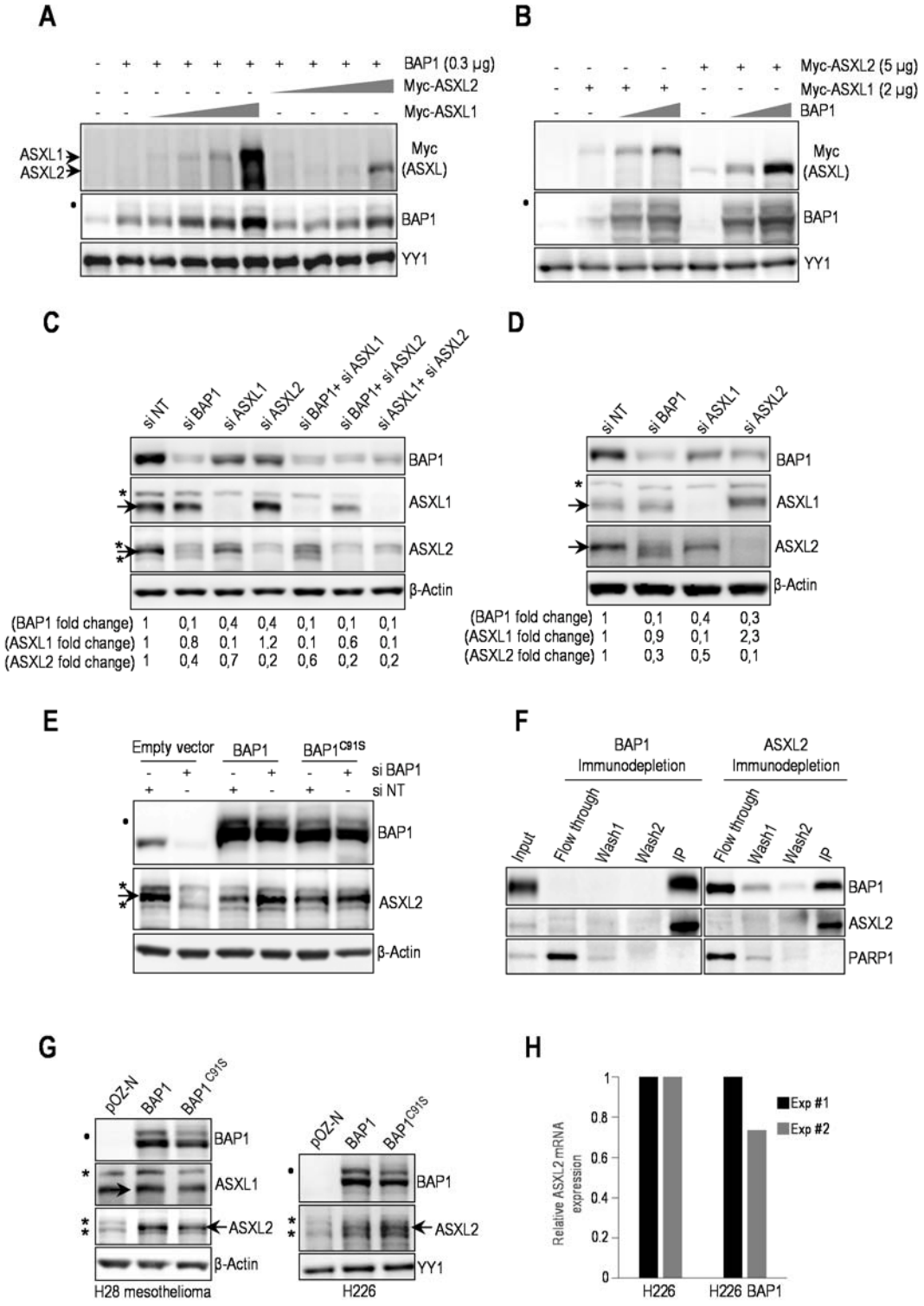
A
BAP1 (0.3 µg)
Myc-ASXL2
Myc-ASXL1
ASXL1
ASXL2
Myc (ASXL)
BAP1
YY1
B
Myc-ASXL2 (5 µg)
Myc-ASXL1 (2 µg)
BAP1
Myc (ASXL)
BAP1
YY1
C
si NT
si BAP1
si ASXL1
si ASXL2
si BAP1+ si ASXL1
si BAP1+ si ASXL2
si ASXL1+ si ASXL2
BAP1
ASXL1
ASXL2
β-Actin
(BAP1 fold change) 1 0,1 0,4 0,4 0,1 0,1 0,1
(ASXL1 fold change) 1 0,8 0,1 1,2 0,1 0,6 0,1
(ASXL2 fold change) 1 0,4 0,7 0,2 0,6 0,2 0,2
D
si NT
si BAP1
si ASXL1
si ASXL2
BAP1
ASXL1
ASXL2
β-Actin
(BAP1 fold change) 1 0,1 0,4 0,3
(ASXL1 fold change) 1 0,9 0,1 2,3
(ASXL2 fold change) 1 0,3 0,5 0,1
E
Empty vector
BAP1
BAP1C91S
si BAP1
si NT
BAP1
ASXL2
β-Actin
F
BAP1 Immunodepletion
ASXL2 Immunodepletion
Input
Flow through
Wash1
Wash2
IP
Flow through
Wash1
Wash2
IP
BAP1
ASXL2
PARP1
G
pOZ-N
BAP1
BAP1 C91S
BAP1
ASXL1
ASXL2
β-Actin
H28 mesothelioma
pOZ-N
BAP1
BAP1C91S
BAP1
ASXL2
YY1
H226
H
Relative ASXL2 mRNA expression
1
0.8
0.6
0.4
0.2
0
Exp #1
Exp #2
H226
H226 BAP1

Figure 4.2. BAP1 and ASXL1/2 are co-regulated and loss of BAP1 in cancer is concomitant with ASXL2 depletion.

A) 293T cells were transfected with BAP1 and increasing amounts of either Myc-ASXL1 (0.5, 1, 2 and 5 μg) or Myc-ASXL2 (0.5, 1, 2 and 5 μg) expression vectors and harvested, three days later, for immunoblotting. **B**) 293T cells were transfected with Myc-ASXL1 or Myc-ASXL2 with increasing amounts of BAP1 (0.3 and 1 μg) vectors and harvested, three days later, for immunoblotting. Quantification of band intensity for each protein was conducted relative to the lowest amount of transfected plasmid (panels, **A, B**). **C)** Protein levels following siRNA depletion of BAP1 and/or ASXL1/2 in U2OS cells. **D**) Protein expression following siRNA depletion of BAP1, ASXL1 and ASXL2 in LF1 human fibroblasts. **E**) Depletion of endogenous BAP1 using siRNA in U2OS cells stably expressing empty vector, siRNA-resistant BAP1 wild-type or siRNA-resistant BAP1 catalytic dead mutant (C91S). Protein levels of BAP1 and ASXL2 were detected by immunoblotting. Quantification of band intensity was conducted relative to the non-target siRNA control (panels **C**, **D**, **E**). **F**) Immunodepletion of BAP1 or ASXL2 from HeLa nuclear extracts. The nuclear DNA damage signaling enzyme, PARP1, was used as a control, which mostly remained in the flow through fraction. **G**) Reconstitution by retroviral infection of H28 mesothelioma and H226 non-small lung carcinoma BAP1-deficient cells with BAP1 or $BAP1^{C91S}$. Protein levels of BAP1 and mutants were detected by immunoblotting. **H**) mRNA of ASXL2 in reconstituted H226 cells was quantified by qPCR. The data represent two independent experiments. β-Actin or YY1 are used as protein loading controls. Quantification of band intensity was conducted relative to BAP1 transfected samples (panels **G**). The dot and stars indicate a monoubiquitinated form of BAP1 [241], and non-specific bands respectively (panels, **A**, **B**, **C**, **D**, **E**, **G**).

4.4.3 The ASXM domain of ASXL1/2 is required for interaction with the CTD of BAP1.

BAP1 was shown to interact with the N-terminal region of ASXL1 (1-337 a.a.) [79]. To identify the exact domain of ASXL1/2 responsible for this interaction, we conducted GST-pull down assays and found that *in vitro*-translated ASXM domain (ASXM1: 253-391 a.a., ASXM2: 253-411 a.a. of ASXL1 and ASXL2 respectively) interacted with GST-BAP1 (Fig. 4.3A, B). To gain insights into the significance of the BAP1/ASXL1/2 interactions, we generated ASXL1/2 expression constructs lacking the BAP1-interacting domain ($ASXL1/2^{\Delta ASXM}$). As expected, following transfection, protein levels of $ASXL2^{\Delta ASXM}$, but not $ASXL1^{\Delta ASXM}$, were reduced in comparison to their wild type counterparts (Fig. 4.3C). Of note, the polypeptides encoded by the ASXL1/2 constructs were essentially nuclear (Fig. 4.3D). GFP-PAR-4 fusion protein which localizes in both the cytoplasm and the nucleus was included as a control [446]. Next, after adjusting the amounts of transfected plasmids to obtain comparable expression of the wild type and mutant forms of ASXL1/2, we found that the

ability of ASXL1/2 mutants, lacking their respective ASXM domain, to interact with BAP1 and to form protein complexes *in vivo* was strongly reduced (Fig. 4.3E).

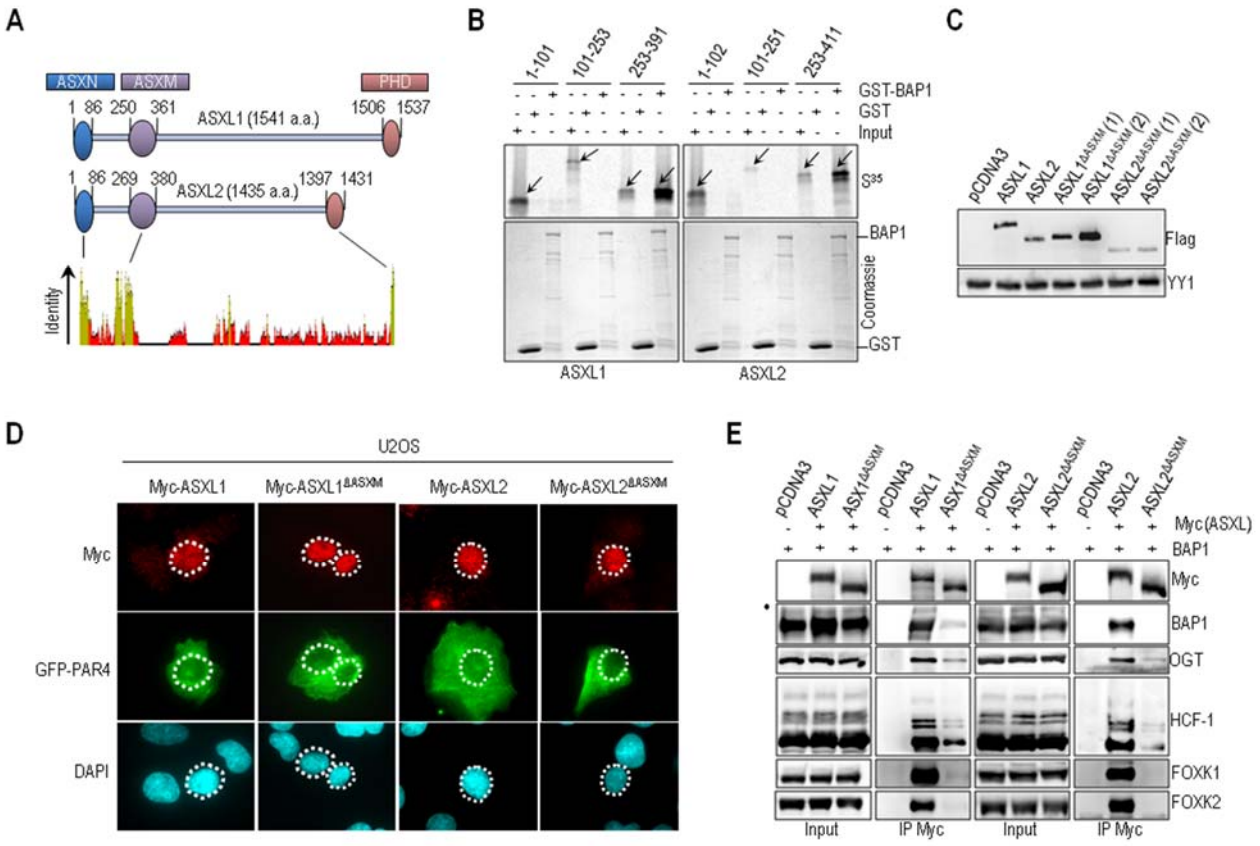

Figure 4.3. ASXM of ASXL1/2 is required for interaction with BAP1.

A) Schematic representation and conservation of ASXL1/2. **B**) GST-pull down assay using GST-BAP1 and methionine S^{35}-labeled ASXL1 or ASXL2 fragments. The arrows indicate the full length forms of the fragments. **C**) ASXM is required for ASXL2, but not ASXL1, stability. Flag-ASXL1/2 and their respective Flag-ASXL1/2 ΔASXM mutants (3 µg each) were transfected in 293T cells which were harvested, three days post-transfection, for immunoblotting. A duplicate of transfection is shown for Flag-ASXL1/2 ΔASXM mutants. **D**) U2OS cells were transfected with either Myc-ASXL1 (4 µg), Myc-ASXL1 ΔASXM (4 µg), Myc-ASXL2 (4 µg), or Myc-ASXL2 ΔASXM (4 µg) along with GFP-PAR4 (0.5 µg). Three days post-transfection, cells were harvested for Immunostaining using the indicated antibodies. The cells overexpressing the different forms of ASXL1/2 were encircled. **E**) 293T cells were transfected with Myc-ASXL1 (4 µg), Myc-ASXL1 ΔASXM (4 µg), Myc-ASXL2 (4 µg), or Myc-ASXL2 ΔASXM (6 µg), along with BAP1 (1 µg) vectors and harvested, three days post-transfection, for IP with anti-Myc. The dot indicates a monoubiquitinated form of BAP1 (panel **E**) [241].

BAP1 contains an Ubiquitin Carboxyl Hydrolase (UCH) catalytic domain and a Coiled-Coil motif (CC1) in the N-terminal region, as well as a C-Terminal Domain (CTD) containing a second Coiled-Coil motif (CC2) [226,234,241] (Fig. 4.4A). This DUB also possesses a big middle region (MR), that contain the HBM and other protein interaction motifs, separating UCH/CC1 from the CTD, [226,234,440,447]. We found that only GST-tagged fragments of BAP1 containing an intact CTD interacted with ASXM domains of ASXL1/2 (Fig. 4.4B). These results indicate that ASXL1/2 use the ASXM domain to interact with the CTD of BAP1. To provide further insights into ASXL1/2/BAP1 interactions, we constructed BAP1 mutants disrupted in the CTD region (Fig. 4.4C). The BAP1$^{\Delta CTD1}$ represents a deletion of CTD except for the KRKKFK putative nuclear localization signal [236]. The BAP1$^{\Delta CTD}$ and BAP1$^{\Delta CC2}$ represent a complete deletion of the CTD and CC2, respectively. Supporting our finding reported above, we noticed that disruption of CTD resulted in decreased BAP1 protein levels (Fig. 4.4D). We also generated HeLa cell lines stably expressing BAP1wild type or its mutant form lacking most of the CTD, BAP1$^{\Delta CTD1}$, and use them for complex purification. To enable meaningful comparisons, the eluted complexes were adjusted by immunoblotting for similar amounts of BAP1 protein prior to silver staining. This revealed that BAP1 and BAP1$^{\Delta CTD1}$ complexes were quite similar in protein composition (Fig. 4.4E). However, immunoblotting analysis showed that the interaction between BAP1$^{\Delta CTD1}$ and ASXL1/2 was abolished (Fig. 4.4E). In contrast, association of BAP1$^{\Delta CTD1}$ with HCF-1/OGT remained unchanged in comparison to the wild type variant. Altogether, these results indicate that CTD and ASXM domains are necessary and sufficient for assembly of BAP1/ASXL1/2 complexes.

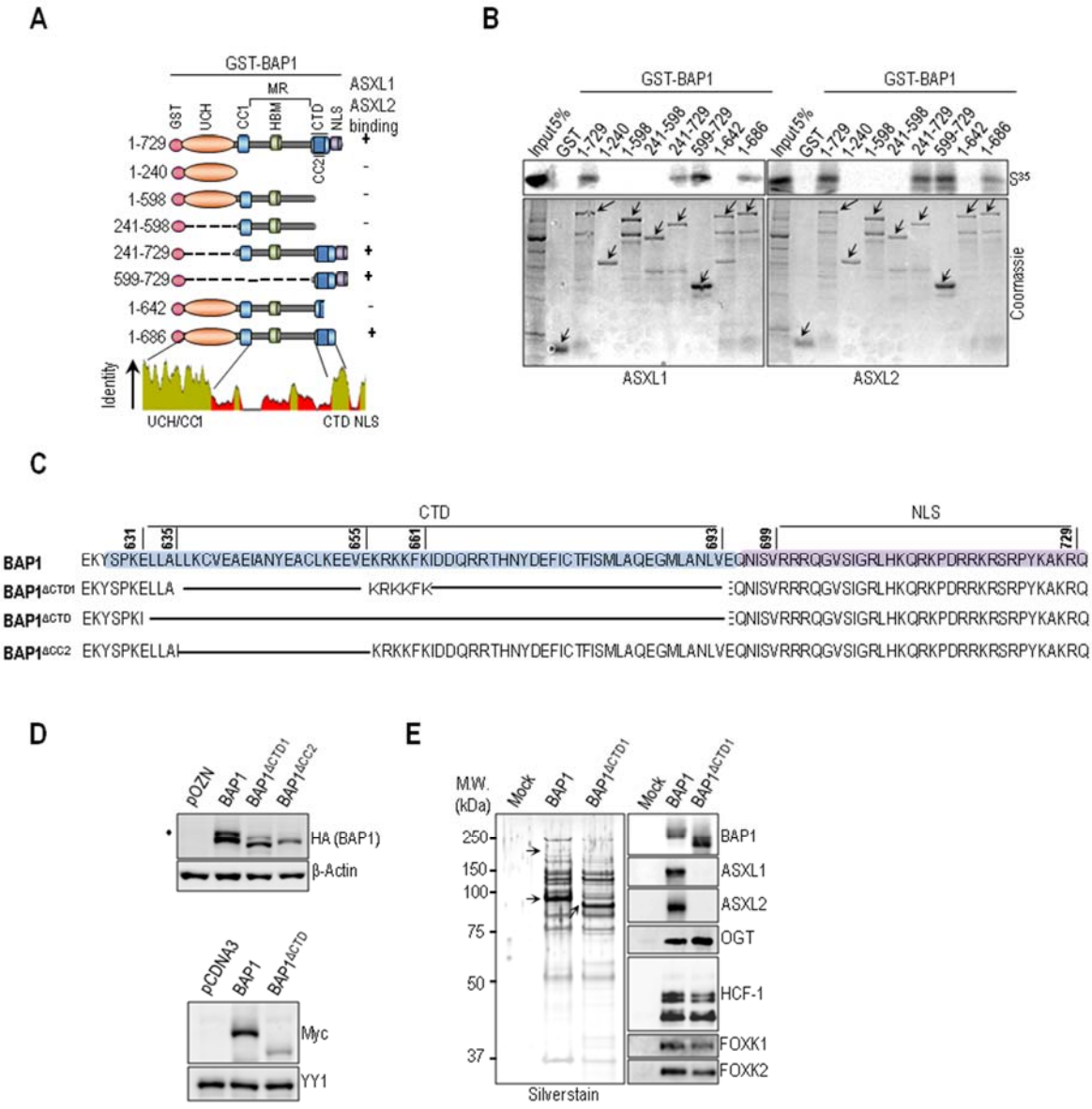

Figure 4.4 BAP1 interacts with ASXL1/2 via its CTD domain.

A) Schematic representation of the BAP1 fragments used for *in vitro* pull down in panel **B. B)** GST-pull down assay using GST-BAP1 fragments and methionine S^{35}-labeled ASXM domains of ASXL1 or ASXL2. The arrows indicate the full length forms of the fragments**. C)** Schema of the different deletions in the CTD domain used to generate BAP1 mutants. $BAP1^{\Delta CTD1}$ represents a deletion of the CTD from 635 up to 693 amino acids except the KRKKFK motif which is suggested to function as an NLS [236]. We also generated a $BAP1^{\Delta CTD}$ which represents a mutant with a deletion of the CTD domain (Δ631-693 amino acids). $BAP1^{\Delta CC2}$ represents a mutant with a smaller deletion within the CTD domain

(Δ635-655 amino acids). **D)** A functional CTD is required for proper protein stability of BAP1. Protein expression levels of BAP1 and its CTD deletion mutant form in stable HeLa S cell lines (Top panel). Myc-BAP1, Myc-BAP1 ΔCTD expression constructs (3 μg each) were transfected in 293T cells, which were harvested, three days post-transfection, for immunoblotting (Bottom panel). **E)** Left panel, silver stain of the immunopurified BAP1 and BAP1$^{\Delta CTD1}$ complexes. Right panel, western blot detection of components of the BAP1 complexes. The high and low arrows indicate the position of ASXL2 and BAP1 (WT and BAP1$^{\Delta CTD1}$) respectively. β-Actin or YY1 are used as protein loading controls. The dot indicates a monoubiquitinated form of BAP1 (panel **D**) [241].

4.4.4 BAP1 is a major DUB for H2Aub K119 and its enzymatic activity is ASXM-dependent.

Several DUBs including BAP1 were reported to target H2Aub K119 in mammals [182,448]. However, the relative contribution of each enzyme in H2A deubiquitination *in vivo* remained unknown. We conducted an siRNA screen using a library that covers the human DUB repertoire by analyzing the global increase of H2Aub using an in-cell western assay. Depletion of BAP1 produced the most significant increase of H2Aub, indicating that this enzyme is a major DUB for this histone modification under normal growth conditions (Fig. 4.5A). To investigate how ASXL1/2 regulate mammalian BAP1 DUB activity *in vivo*, we conducted RNAi-mediated depletion of these factors, and found that neither ASXL1 nor ASXL2 individual knockdown induced noticeable changes in global H2Aub levels (Fig. 4.5B, 4.5C). However, combined knockdown of ASXL1 and ASXL2 resulted in significant increase of H2Aub, similar to the effect induced by BAP1 depletion (Fig. 4.5B). This prompted us to determine the respective contribution of ASXL1 and ASXL2 to the H2A DUB activity of BAP1. A striking BAP1-mediated deubiquitination of H2A was observed upon its co-expression with either ASXL1 or ASXL2, and this effect was dependent on BAP1 catalytic activity (Fig. 4.5D). Consistent with our mapping analysis, ASXL1 and ASXL2 lacking ASXM were unable to stimulate H2A deubiquitination (Fig. 4.5E). In addition, we purified monoubiquitinated nucleosomal Flag-H2A, from 293T cells, that we used for *in vitro* DUB assay and found that ASXM1 or ASXM2, but not GST-CTD used as a control, are sufficient for stimulating BAP1-mediated deubiquitination of H2A (Fig. 4.5F). Based on these results, we concluded that interaction between ASXL1/2 and BAP1 require ASXM, and the latter is necessary and sufficient for promoting BAP1-mediated deubiquitination of its physiological substrate H2Aub K119.

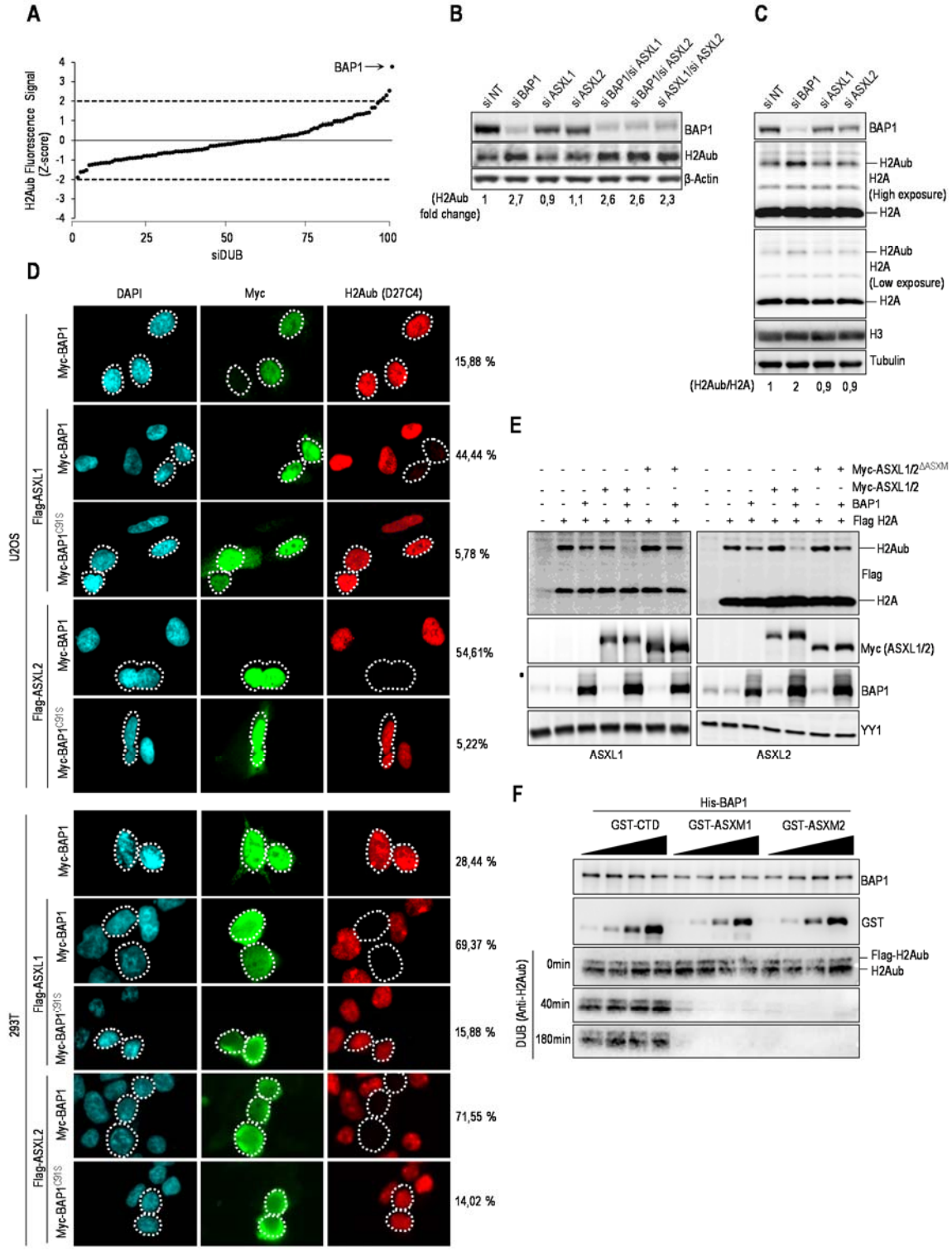
A
BAP1
H2Ub Fluorescence Signal (Z-score)
siDUB
B
si NT
si BAP1
si ASXL1
si ASXL2
si BAP1/si ASXL1
si BAP1/si ASXL2
si ASXL1/si ASXL2
BAP1
H2Aub
β-Actin
(H2Aub fold change) 1 2,7 0,9 1,1 2,6 2,6 2,3
C
si NT
si BAP1
si ASXL1
si ASXL2
BAP1
H2Aub
H2A (High exposure)
H2A
H2Aub
H2A (Low exposure)
H2A
H3
Tubulin
(H2Aub/H2A) 1 2 0,9 0,9
D
DAPI
Myc
H2Ub (D27C4)
U2OS
293T
Myc-BAP1
Flag-ASXL1
Flag-ASXL2
Myc-BAP1C91S
15,88 %
44,44 %
5,78 %
54,61%
5,22%
28,44 %
69,37 %
15,88 %
71,55 %
14,02 %
E
Myc-ASXL1/2ΔASXM
Myc-ASXL1/2
BAP1
Flag H2A
H2Aub
Flag
H2A
Myc (ASXL1/2)
BAP1
YY1
ASXL1
ASXL2
F
His-BAP1
GST-CTD
GST-ASXM1
GST-ASXM2
BAP1
GST
Flag-H2Aub
H2Aub
DUB (Anti-H2Aub)
0min
40min
180min

Figure 4.5. ASXM of ASXL1/2 stimulates BAP1 DUB activity.

A) siRNA screen for DUBs that coordinate H2Aub levels. Following transfection with siRNA DUB library, HeLa cells were fixed and immunostained for H2Aub K119 (H2Aub). The fluorescence signal was determined and the values used to derive the Z-scores. **B)** Knockdown of BAP1 or concomitant Knockdown of ASXL1 and ASXL2 induces a significant increase of the global level of H2Aub. U2OS cells were transfected with siRNA as indicated and harvested four days post-transfection for immunoblotting using the indicated antibodies. Quantification of band intensity for H2Aub was conducted relative to the non-target siRNA control (siNT). **C)** Increase of H2Aub levels following BAP1 depletion is not due to a global increase of H2A. U2OS cells were transfected with siRNA of BAP1, ASXL1 and ASXL2 and harvested, four days post-transfection, for immunoblotting using the respective antibodies. Tubulin was used a loading control for soluble proteins and histone H3 as a loading control for histones levels. Quantification of band intensity for H2Aub was conducted relative to the **non**-modified histone H2A and the values were then normalized to the non-target siRNA control (siNT**). D)** ASXL1/2 promote BAP1 DUB activity toward H2Aub *in vivo*. U2OS cells (top panel) or 293T cells (bottom panel) were transfected with either Myc-BAP1 (0.5 μg) or Myc-BAP1 C91S (0.5 μg) expression constructs in the presence or absence of Flag-ASXL1/2 (4 μg) expression constructs. Three days post-transfection, cells were harvested for Immunostaining using the indicated antibodies. The cells overexpressing BAP1 and $BAP1^{C91S}$ were encircled. Note that the transfections were conducted with plasmid ratios optimized to ensure that most BAP1 transfected cells also express ASXL1 or ASXL2. Cells overexpressing BAP1 were counted for change in H2Aub signal. The percentages at the right of the panel represent the number of cells showing very low signal of H2Aub versus the total number of BAP1 expressing cells. **E)** 293T cells were transfected as indicated using Flag H2A (0.2 μg), BAP1 (1 μg), Myc-ASXL1 (4 μg) or Myc-ASXL1 ΔASXM (4 μg) vectors (left panel); Myc-ASXL2 (4 μg) or Myc-ASXL2 ΔASXM (6 μg) vectors (right panel) and harvested, three days later, for immunoblotting**. F)** *In vitro* DUB assay of nucleosomal H2A using recombinant His-BAP1 (8 ng, 2 pM) in presence of increasing amounts of recombinant GST-CTD, GST-ASXM1 or GST-ASXM2 (0.6 pM, 1.2 pM, 2 pM and 4 pM). β-Actin, Tubulin or YY1 were used as loading controls.

4.4.5 Identifications of domains and motifs in ASXM required for promoting ubiquitin binding and DUB activity towards histone H2A of BAP1.

To further dissect the mechanism of H2A deubiquitination by BAP1, we conducted ubiquitin pull down assays and found that ASXM2 strongly enhanced BAP1 binding to ubiquitin (Fig.4.6A). ASXM2 alone can directly bind ubiquitin, but this interaction was weak as an enrichment of about two-folds above the background was observed (Fig. 4.6A). ASXM1 also promoted BAP1 binding to ubiquitin in a similar manner as ASXM2 (Fig. 4.6B). Since ASXM1 and ASXM2 domains acted similarly in promoting BAP1 binding to ubiquitin and DUB activity, we selected ASXM2 for further studies. Sequence alignment of ASXL proteins indicated that the ASXM domain is highly conserved (Fig. 4.6C). We generated several constructs encompassing several regions and conserved motifs of ASXM2 (Fig. 4.6C). We found that the 246-347 a.a. region interacted with BAP1 as efficiently as the full length

ASXM2 (246-401 a.a.), while no interaction was observed for the 316-401 a.a. region (Fig. 4.6D). The 246-313 a.a. and 300-401 a.a. regions interacted only poorly with BAP1. These results suggest that critical interaction motifs are located within or overlapping with the 300-347 a.a. region (Fig. 4.6D). Only the full length ASXM2 and the 246-347 a.a. fragment, that strongly interacted with BAP1, promoted its binding to ubiquitin and DUB activity. Nonetheless, we noted that the 246-347 a.a. fragment was significantly less competent in promoting BAP1 binding to ubiquitin which could explain its weakness in promoting deubiquitination (Fig. 4.6D,E). Next, we generated discrete mutations of several highly conserved residues of ASXM2 (Fig. 4.6C), and found that ASXM2 interaction with BAP1 and ubiquitin binding are maintained for most mutants except for the LLLL303-306AAAA hydrophobic stretch mutant which essentially lost its interaction with BAP1 (Fig. 4.6F,G). As expected, the LLLL303-306AAAA mutant failed to stimulate DUB activity (Fig. 4.6H). Interestingly, while the L286A and NN328-329AA mutants were essentially equally efficient in promoting BAP1 binding to ubiquitin, their ability to deubiquitinate H2A was significantly different (Fig. 4.6G,H).

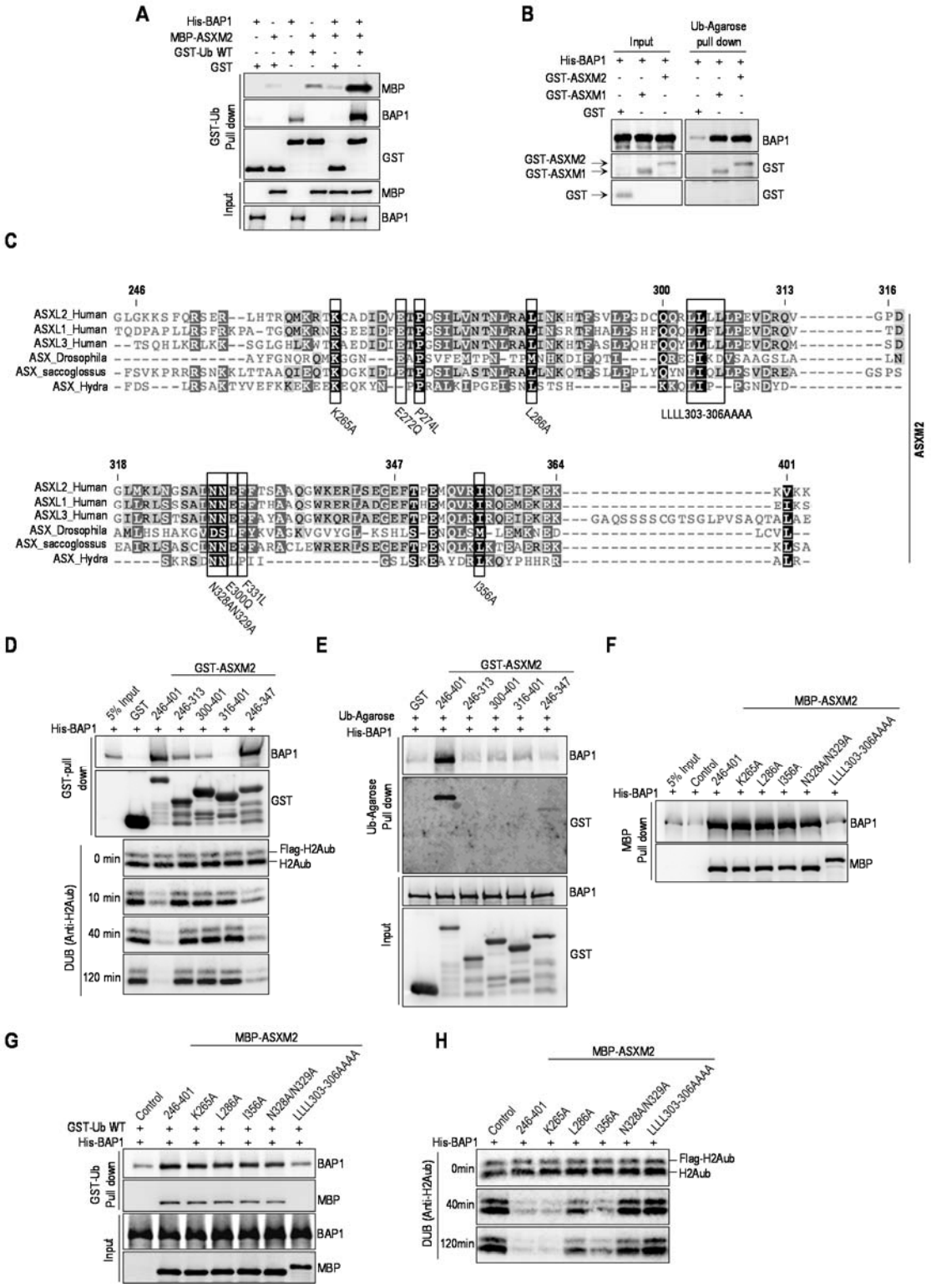
A
His-BAP1
MBP-ASXM2
GST-Ub WT
GST
GST-Ub Pull down
MBP
BAP1
GST
Input
B
Input
Ub-Agarose pull down
His-BAP1
GST-ASXM2
GST-ASXM1
GST
C
ASXL2_Human
ASXL1_Human
ASXL3_Human
ASX_Drosophila
ASX_saccoglossus
ASX_Hydra
K265A
E272Q
P274L
L286A
LLLL303-306AAAA
ASXM2
F331L
E340Q
N328AN329A
I356A
D
GST-ASXM2
5% Input
GST
246-401
246-313
300-401
316-401
246-347
His-BAP1
GST-pull down
Flag-H2Aub
H2Aub
DUB (Anti-H2Aub)
0 min
10 min
40 min
120 min
E
Ub-Agarose
Ub-Agarose Pull down
F
MBP-ASXM2
Control
K265A
L286A
I356A
N328AN329A
LLLL303-306AAAA
MBP Pull down
G
GST-Ub WT
GST-Ub Pull down
H
0min
40min
120min

Figure 4.6. ASXM enhances BAP1 binding to ubiquitin.

A) Recombinant His-BAP1 (1.6 µg, 20 nM) and MBP-ASXM2 (2 µg, 30 nM) were incubated with either GST or GST-Ubiquitin-Agarose beads (3 µg, 80 nM) and the pulled down fractions were analysed by immunoblotting. **B)** Recombinant His-BAP1 (1.6 µg, 20 nM) and GST-ASXM1 or GST-ASXM2 (2 µg, 40 nM) were incubated with ubiquitin-agarose beads and the pulled down fractions were analyzed by immunoblotting. **C)** Multiple sequence alignment between the ASXM domains of human ASXL1/2, Drosophila ASX and other paralogs and orthologs of ASX. The mutants of ASXM2 including the cancer-associated mutants used in panels **F**, **G**, **H** and Fig.**9** are shown. **D)** GST pull down interaction assay and *in vitro* DUB reactions of H2A using His-BAP1 and GST-ASXM2 (full length and deletion mutant forms). For the pull down assay, His-BAP1 (1.6 µg, 20 nM) was incubated with GST-ASXM2 (2 µg, 40 nM) or the different fragment of GST-ASXM2 (2 µg, 50 nM). His-BAP1 (8 ng, 2 pM) and the different recombinant ASXM2 fragments (10 ng, 4 pM) were used for the DUB reactions. **E)** His-BAP1 (1.6 µg, 20 nM) and the different GST-fused fragments of ASXM2 (2 µg, 40 nM) were subjected to ubiquitin-Agarose pull down assay followed by immunoblotting. **F**) MBP-pull down interaction assay using recombinant MBP-ASXM2 (full length and mutant forms) (2 µg, 30 nM) and His-BAP1 (1.6 µg, 20 nM). **G**) GST-Ubiquitin pull down assay using MBP-ASXM2 full length and the different mutant forms with His-BAP1. The pull down was done as in **(A)**. **H**) *In vitro* DUB reactions of H2A using His-BAP1 (8 ng, 2 pM) and the different recombinant MBP-ASXM2 (10 ng, 2,8 pM).

4.4.6 Intramolecular interactions in BAP1 create an ASXM-dependent Composite Ubiquitin Binding Interface (CUBI) and enable DUB activity.

The CTD of BAP1 is necessary and sufficient for the interaction between BAP1 and ASXL1/2 (Fig. 4.4). This domain also engages an intramolecular interaction with both the CC1 and the UCH domains in order to ensure BAP1 auto-deubiquitination and proper nuclear localization [241]. Hence, we sought to test whether this intramolecular interaction in BAP1 is necessary for ASXM stimulation of ubiquitin binding and DUB activity. Indeed, as is the case for $BAP1^{\Delta UCH}$ or $BAP1^{C91S}$, $BAP1^{\Delta CTD}$ was unable to deubiquitinate H2A following incubation with ASXM2 (Fig. 4.7A,B). $BAP1^{\Delta CTD}$ or $BAP1^{\Delta CC2}$ mutants were also incapable of deubiquitinating H2A in the context of BAP1 protein complexes *in vitro* (Fig. 4.7C), As a control, $BAP1^{\Delta HBM}$ complexes were competent in promoting DUB activity (Fig. 4.7D), as previously shown [250]. $BAP1^{\Delta CTD}$ was also unable to promote BAP1 DUB activity *in vivo* when expressed with either ASXL1 or ASXL2 (Fig. 4.7E). In addition, while ASXM2 promoted binding to ubiquitin of both BAP1 and $BAP1^{C91S}$, this domain failed to enhance ubiquitin binding of $BAP1^{\Delta CTD}$ or $BAP1^{\Delta UCH}$ (Fig. 4.7F). ASXM2 only partially promoted $BAP1^{\Delta CC1}$ binding to ubiquitin (Fig. 4.7A,F), and this mutant is completely inactive in H2A

deubiquitination (Fig. 4.7B). Thus, ASXM2 requires intramolecular interactions between multiple domains of BAP1 to promote ubiquitin binding and catalysis.

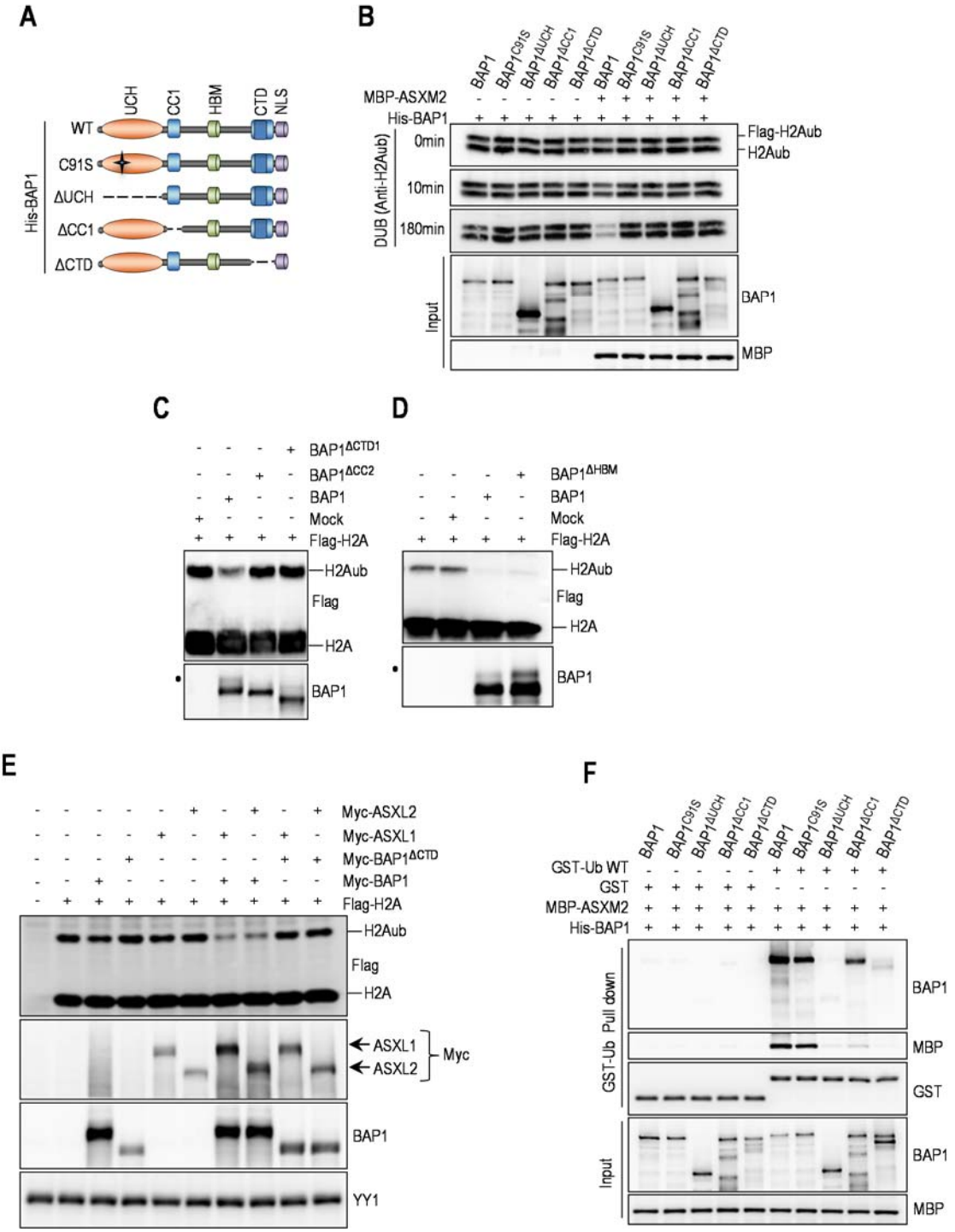

Figure 4.7. Intramolecular interaction in BAP1 is required to create an ASXM-inducible composite ubiquitin binding interface (CUBI).

A) Schematic representation of the different BAP1 mutants generated for *in vitro* experiments done in panel **B**. **B)** *In vitro* DUB reaction of nucleosomal H2A using His-BAP1 or its mutant forms (8 ng, 2 pM) in presence or absence of MBP-ASXM2 (10 ng, 2,8 pM). **C-D)** *In vitro* deubiquitination assay of nucleosomal histone H2A using purified Flag-HA BAP1, BAP1$^{\Delta CTD1}$ or BAP1$^{\Delta CC2}$ complexes. BAP1$^{\Delta HBM}$ was used as a control since HCF-1 is not required for BAP1 DUB activity. **E)** *In vivo* DUB activity of BAP1$^{\Delta CTD}$ is abolished due to the lack of interaction with ASXL1/2. Flag-H2A (0.2 µg) expression construct was co-expressed in 293T cells with either Myc-BAP1 (1 µg) or Myc-BAP1 ΔCTD (1 µg) with or without Myc-ASXL1 (4 µg) or Myc-ASXL2 (6 µg) expression constructs. Three days post-transfection, cells were harvested for immunoblotting. YY1 is used as a loading control. **F)** His-BAP1 mutants (1.6 µg, 20 nM) and MBP-ASXM2 (2 µg, 30 nM) were subjected to GST-Ubiquitin pull down assay followed by immunoblotting.

In contrast to the CC1 and CTD in BAP1, the corresponding domains in UCH37, helix α7 and ULD respectively, are contiguous (Fig. 4.8A, left panel) [449]. Nonetheless, co-crystallization of UCH37 of the worm *Trichinella spiralis* (tsUCH37) with ubiquitin indicated an intramolecular interaction similar to the one observed in BAP1 [449]. In addition, R261 and Y262 a.a. residues of the ULD establish direct contacts with ubiquitin K48 and Q49/R72, respectively [449]. Molecular dynamics simulation suggested that E265 and N272, part of a non-crystalized extension of the ULD, might also bind R42 and D52 of ubiquitin, respectively [449]. R261, Y262, E265 and N272 are essentially conserved in BAP1 and correspond to K659, F660, D663 and N670, respectively (Fig. 4.8A, right panel). Thus, we were prompted to test whether the CTD is sufficient for binding ubiquitin in solution. We found that the CTD weakly interacted with ubiquitin, as a signal above the background was consistently observed (Fig. 4.8B). Importantly, mutation of ubiquitin R42/Q49/D52/R72 residues (we termed the RQDR charged patch), involved in binding the tsUCH37 ULD, reduced this interaction (Fig. 4.8B,C). Moreover, mutation of the RQDR patch also abolished ubiquitin binding by the BAP1/ASXM2 complex (Fig. 4.8D). Also, ubiquitin binding by BAP1/ASXM2 is completely abrogated by mutating the VLI, Ile36 and Il44 hydrophobic patches of ubiquitin, which are involved in binding by the UCH domain [449-451] (Fig. 4.8C,D). These data indicate that the hydrophobic and the charged RQDR patches are necessary to ensure strong ubiquitin binding by the BAP1/ASXM2 complex. Finally, mutation of the TEK box, Phe4 patch or D58 did not

affect ubiquitin binding by BAP1/ASXM2 (Fig. 4.8C,D). We concluded that ASXM induces the assembly of a composite ubiquitin binding interface (CUBI) that requires catalytic and non-catalytic domains of BAP1 and involves multiple patches of ubiquitin.

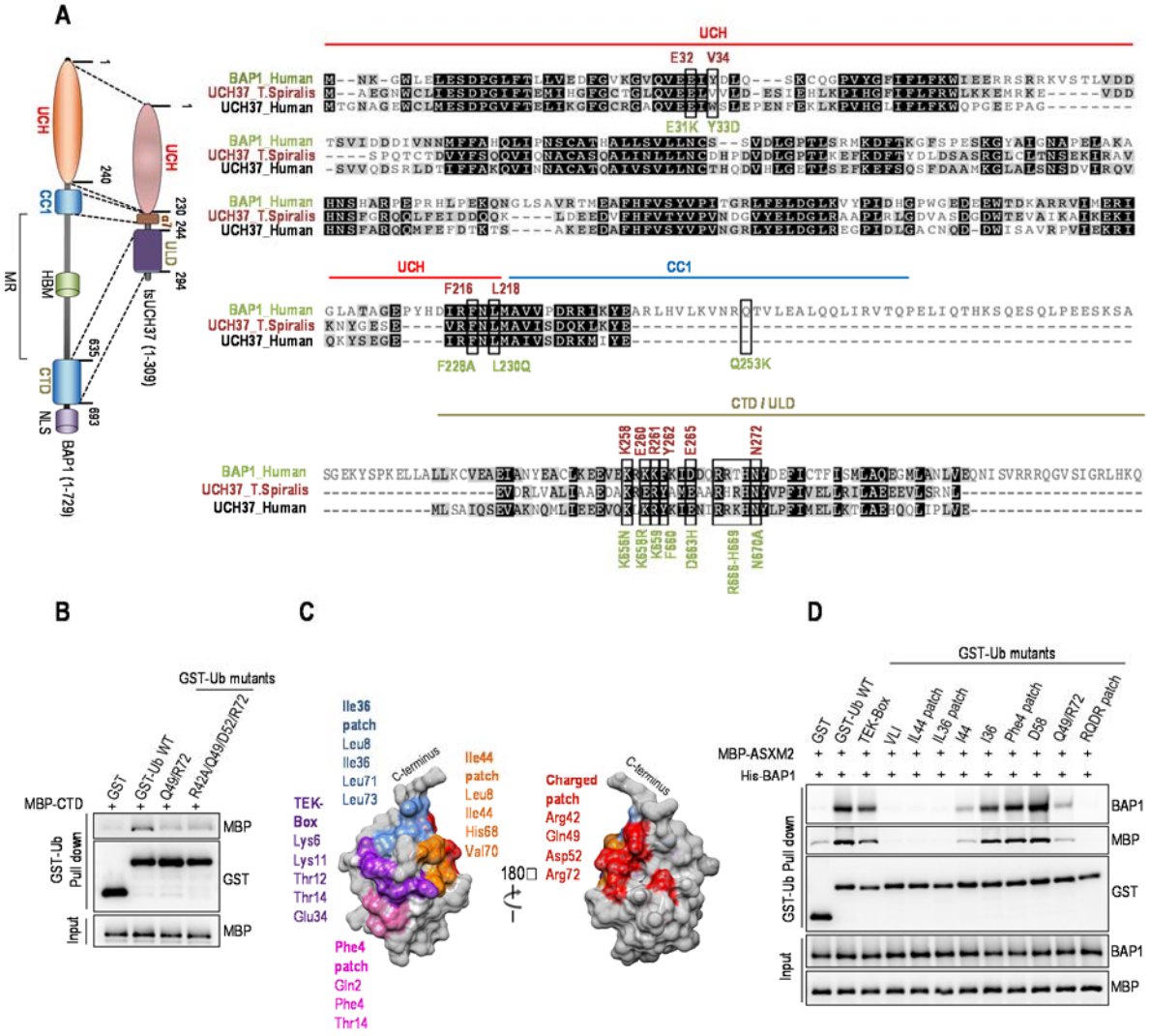

Figure 4.8. BAP1 CTD is an ubiquitin-interacting domain.

A) Comparison between BAP1 and UCH37. tsUCH37 of the worm *Trichinella spiralis* whose crystal structure was recently reported (38), was aligned with human UCH37 and BAP1. The functional conserved domains between BAP1 and tsUCH37 are shown in the left panel. The alignment (right panel) show conserved motifs and residues in the UCH, CC1 and CTD domains. The mutants of BAP1 including the cancer-associated mutants used in **Fig. 9** are shown. Note the presence in the CTD of the cancer mutant BAP1$^{R666\text{-}H669}$ with a deletion of the R666 to H669 amino acids. **B)** MBP-CTD (3 µg, 40

nM) of BAP1 was subjected to GST-Ubiquitin pull down assay using GST-Ubiquitin wild type or its mutant forms (3 μg, 80 nM) (all residues were converted to alanines) and then analysed by immunoblotting. **C)** Ubiquitin structure showing the various interaction interfaces**. D)** GST-Ubiquitin pull down interaction assays using GST-Ubiquitin wild type or its different mutant forms (all residues of each path were converted to alanines) and His-BAP1 with MBP-ASXM2 followed by immunoblotting. The pull down was done as in **Fig. 4.7F**.

4.4.7 Cancer-derived mutations abolish BAP1 interaction with ASXL1/2, ubiquitin binding and DUB activity.

We asked whether tumor-associated mutations of BAP1 result in selective loss of interaction with ASXL1/2 and ubiquitin binding and catalysis. Based on our data and tsUCH37-ubiquitin co-crystal structure [449], we analyzed the previously reported cancer mutation landscape of BAP1 (cBioPortal for Cancer Genomics and COSMIC cancer databases), notably in solid tumors (e.g. uveal melanoma and renal cell carcinoma) and selected several mutations within or near its UCH (E31K, Y33D), CC1 (L230Q, Q253K) and CTD (K656N, K658R, D663H, R666-H669) domains [231,250] (Fig. 4.8A). We also included additional mutations, not found in cancer, but corresponding to highly conserved amino acids in the vicinity of these cancer mutations (F228A, N670A) (Fig. 4.8A). We co-expressed these BAP1 mutants with ASXL2 and found that most mutations did not significantly affect protein interactions except for the R666-H669 mutant whose interaction with ASXL2 is strongly reduced (Fig. 4.9A). It is worth mentioning that although BAP1 and ASXL2 are overexpressed in 293T cells, reduced protein levels of R666-H669 mutant are still observed (Fig. 4.9A). *In vitro* ubiquitin pull down interaction assays revealed that E31K and Y33D mutations in the UCH domain result in a reduced binding of BAP1/ASXM2 to ubiquitin (Fig. 4.9B). Significantly, several mutants in other domains, e.g., F228A, L230Q, K658R and R666-H669 strongly affected BAP1/ASXM2 ability to bind ubiquitin (Fig. 4.9B). Most BAP1 mutants were also significantly disrupted in their ability to deubiquitinate H2A (Fig. 4.9B). Interestingly, the D663H mutant was essentially efficient in binding ASXM2 and ubiquitin but failed to promote efficient DUB activity. Since the deletion of amino acids R666-H669 (hereafter $BAP1^{R666\text{-}H669}$) abolished interaction with ASXL2, ubiquitin binding and DUB activity, we selected this mutant for further biochemical and functional studies. Of note, $BAP1^{R666\text{-}H669}$ is expressed predominantly in the nucleus (Fig. 4.9C). We generated HeLa cells stably expressing Flag-HA-$BAP1^{R666\text{-}H669}$ and conducted immuno-affinity purification of DUB

complexes. After adjusting for similar amounts of immunopurified BAP1 we conducted silver staining of the eluted material. This indicated that R666-H669 mutation did not change the overall composition of BAP1 complexes as compared to the wild type, except for missing ASXL2 band in the purified $BAP1^{R666\text{-}H669}$ complexes (Fig. 4.9D, left panel). ASXL1 co-migrates with other high M.W. proteins, and could not be discerned as a distinct band. Strikingly, western blot analysis of the complexes indicated that $BAP1^{R666\text{-}H669}$ does not interact with ASXL1/2, whereas interaction with HCF-1/OGT were not affected (Fig. 4.9D, right panel). Moreover, the purified $BAP1^{R666\text{-}H669}$ complex was unable to deubiquitinate nucleosomal histone H2A (Fig. 4.9E, left panel), or to bind ubiquitin *in vitro* (Fig. 4.9E, right panel). Concordant with this data, neither full length ASXL1 nor ASXL2 are capable of stimulating DUB activity by $BAP1^{R666\text{-}H669}$ *in vivo* (Fig. 4.9F). To further investigate the disruption of BAP1/ASXL2 DUB activity in cancer, we selected several reported cancer-associated point mutations in ASXM2 (Fig. 4.6C), especially in solid tumors (e.g. breast carcinoma and colorectal adenocarcinoma), and found that these mutations did not disrupt ASXM2 interaction with BAP1 (Fig. 4.9G). The BAP1/ASXM2 complex with P274L mutation showed reduced binding to ubiquitin, while the ability of other mutants to bind ubiquitin was essentially unaffected (Fig. 4.9H). Finally, three of these mutants (P274L, E330Q, F331L) showed reduced DUB activity toward H2A indicating that ASXL2 is also targeted by mutations that inhibit the enzymatic activity of the complex (Fig. 4.9I). Altogether, these results indicate that several cancer-associated mechanisms target the BAP1/ASXL2 complexes inducing loss of ubiquitin binding and DUB activity.

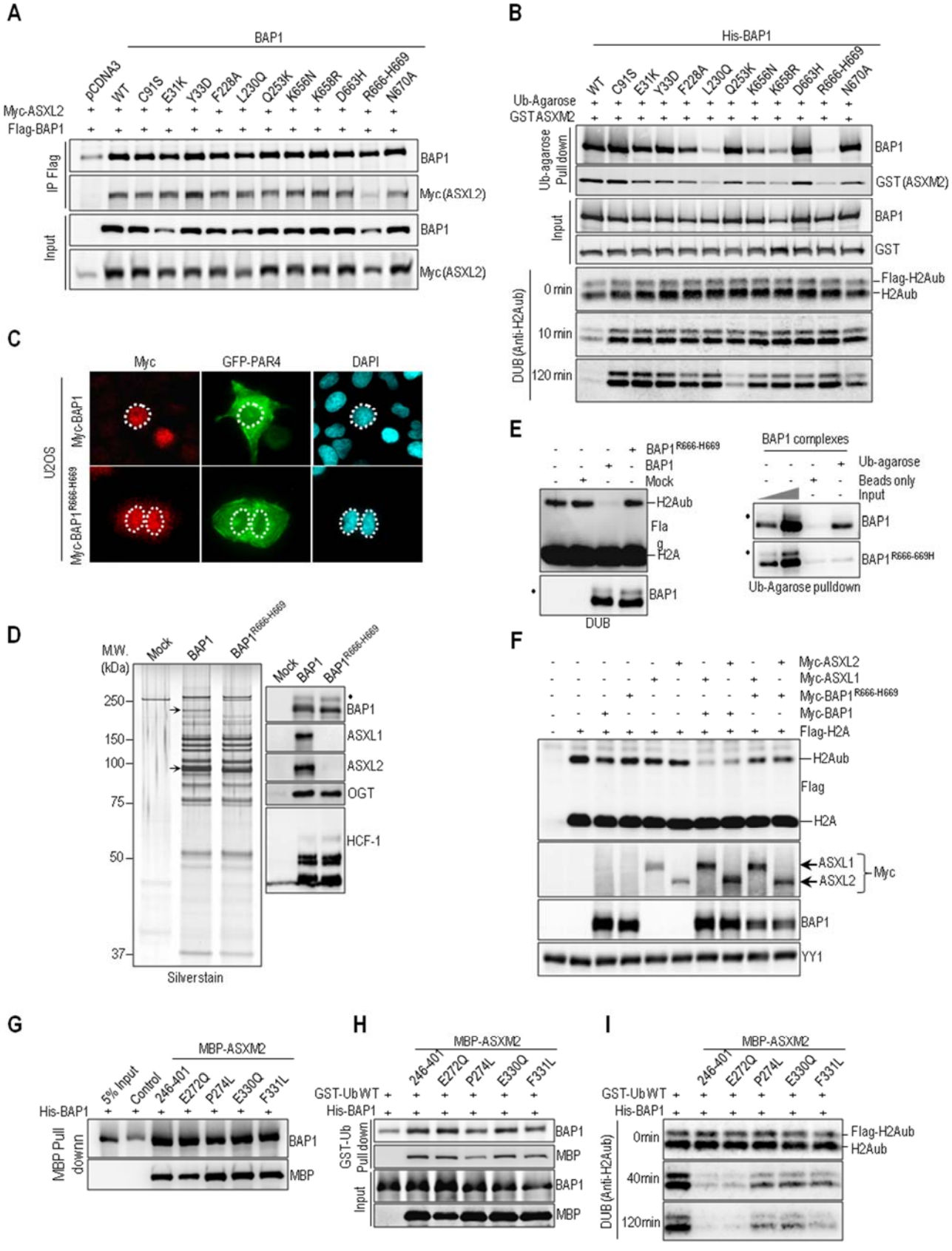
A
BAP1
pCDNA3
WT
C91S
E31K
Y33D
F228A
L230Q
Q253K
K656N
K658R
D663H
R666-H669
N670A
Myc-ASXL2
Flag-BAP1
IP Flag
BAP1
Myc(ASXL2)
Input
BAP1
Myc(ASXL2)
B
His-BAP1
Ub-Agarose
GST ASXM2
Ub-agarose Pull down
BAP1
GST (ASXM2)
Input
BAP1
GST
DUB (Anti-H2Aub)
0 min
10 min
120 min
Flag-H2Aub
H2Aub
C
Myc
GFP-PAR4
DAPI
U2OS
Myc-BAP1
Myc-BAP1R666-H669
D
M.W. (kDa)
Mock
BAP1
BAP1R666-H669
250
150
100
75
50
37
Silverstain
BAP1
ASXL1
ASXL2
OGT
HCF-1
E
BAP1R666-H669
BAP1
Mock
H2Aub
Flag
H2A
BAP1
DUB
BAP1 complexes
Ub-agarose
Beads only
Input
BAP1
BAP1R666-669H
Ub-Agarose pulldown
F
Myc-ASXL2
Myc-ASXL1
Myc-BAP1R666-H669
Myc-BAP1
Flag-H2A
H2Aub
Flag
H2A
ASXL1
ASXL2
Myc
BAP1
YY1
G
MBP-ASXM2
His-BAP1
5% Input
Control
246-401
E272Q
P274L
E330Q
F331L
MBP Pull downn
BAP1
MBP
H
MBP-ASXM2
GST-Ub WT
His-BAP1
246-401
E272Q
P274L
E330Q
F331L
GST-Ub Pull down
BAP1
MBP
Input
BAP1
MBP
I
MBP-ASXM2
GST-Ub WT
His-BAP1
246-401
E272Q
P274L
E330Q
F331L
DUB (Anti-H2Aub)
0min
40min
120min
Flag-H2Aub
H2Aub

Figure 4.9. Disruption of BAP1 ubiquitin binding and DUB activity by cancer-associated mutations of BAP1 and ASXL2.

A) R666-H669 BAP1 cancer mutation abolishes its interaction with ASXL2. Myc-ASXL2 (6 µg) construct was co-transfected in 293T with either Flag-BAP1, Flag-BAP1 C91S or Flag-BAP1 mutants constructs (1 µg) and cells were harvested for Flag IP of BAP1 followed by immunoblotting. **B)** Ubiquitin pull down and *in vitro* DUB assays of nucleosomal H2A using GST-ASXM2 and His-BAP1, His-BAP1^{C91S} or the different recombinant mutant forms of BAP1. The same amounts of recombinant proteins as presented in **Fig. 4.5**, **4.6** and **4.7** were used for the *in vitro* reactions. **C)** U2OS cells were transfected with either Myc-BAP1 (4 µg) or Myc- BAP1 R666-H669 (4 µg) along with GFP-PAR4 (0.5 µg). Three days later, cells were harvested for immunostaining using the indicated antibody. Cells expressing BAP1 or BAP1$^{R666-H669}$ were encircled. **D**) BAP1 complexes were purified from HeLa cells stably expressing Flag-HA-BAP1 or Flag-HA-BAP1$^{R666-H669}$. Left panel, silver stain shows the profiles of the complexes. Right panel, western blot detection of the major components of the BAP1 complexes. The high and low arrows indicate the position of ASXL2 and BAP1 respectively. **E)** *In vitro* DUB assay of nucleosomal H2A (top panel) and Ubiquitin pull down assay (bottom panel) using BAP1 and BAP1$^{R666-H669}$ complexes. **F)** R666-H669 BAP1 cancer mutation results in the abrogation of its DUB activity *in vivo*. Flag-H2A (0.2 µg) construct was co-expressed in 293T cells with either Myc-BAP1 (1 µg) or Myc-BAP1 R666-H669 (1 µg) with or without Myc-ASXL1 (4 µg) or Myc-ASXL2 (6 µg) expression constructs. Three days post-transfection, cells were harvested for immunoblotting. **G)** His-BAP1 (1.6 µg, 20 nM) and MBP-cancer associated mutants forms of ASXM2 (2 µg, 30 nM) were subjected to MBP pull down interaction assays. **H-I)** His-BAP1 and MBP-ASXM2 mutants were subjected as done in **Fig. 4**.**6**, **4.7** and **4.8** to GST-Ubiquitin pull down assay **(H)** and *in vitro* DUB assay using nucleosomal H2A **(I)**. The reactions were analyzed by immunoblotting. YY1 is used as a loading control. The dot indicates a monoubiquitinated form of BAP1 [241] (panels **D**, **E**).

4.4.8 BAP1/ASXL1/2 axis is required for proper cell cycle progression.

We enquired to determine the biological significance of BAP1/ASXL1/2 interactions. Since BAP1 knockdown delays cell proliferation in multiple cell types [227,234,435], we sought to determine whether ASXL1/2 and BAP1 interactions influence cell cycle progression. We generated U2OS cells stably expressing comparable levels of siRNA-resistant BAP1, BAP1^{C91S} or BAP1$^{R666-H669}$ (Fig. 4.10A), and conducted RNAi depletion of endogenous BAP1. Cells were then synchronized in early S phase using double thymidine block and released in the cell cycle. As expected, in the empty vector cells, depletion of endogenous BAP1 delayed S phase progression. While re-expression of BAP1 rescued the defect induced by knockdown of endogenous BAP1, this was not observed with BAP1^{C91S} nor BAP1$^{R666-H669}$ (Fig. 4.10B). In addition, expression of BAP1^{C91S} or BAP1$^{R666-H669}$ significantly affected the ability of U2OS cells to be synchronized (Fig. 4.10B). Similar cell cycle defects were also observed following expression of BAP1 lacking CTD, BAP1$^{\Delta CTD}$ (Fig. 4.10C). The increase of H2Aub levels following knockdown of BAP1, was prevented by re-expression of wild type BAP1, but not

by BAP1$^{R666\text{-}H669}$ or BAP1^{C91S} mutants (Fig. 4.10A). We note that the higher levels of H2Aub in U2OS expressing BAP1^{C91S} might result from a dominant negative effect on endogenous BAP1. Next, re-introduction of BAP1, but not the BAP1$^{R666\text{-}H669}$ nor the BAP1^{C91S} in the BAP1-deficent lung carcinoma cell line H226 promoted substantial H2A deubiquitination (Fig. 4.10D, top panel). In addition, unlike the wild type BAP1, which strongly inhibited cell proliferation as previously observed [236], the BAP1$^{R666\text{-}H669}$ mutant only partially inhibited cell proliferation (Fig. 4.10D, bottom panel). Thus, physical interaction between ASXL1/2 and BAP1 and DUB activity are required for proper coordination of cell cycle progression.

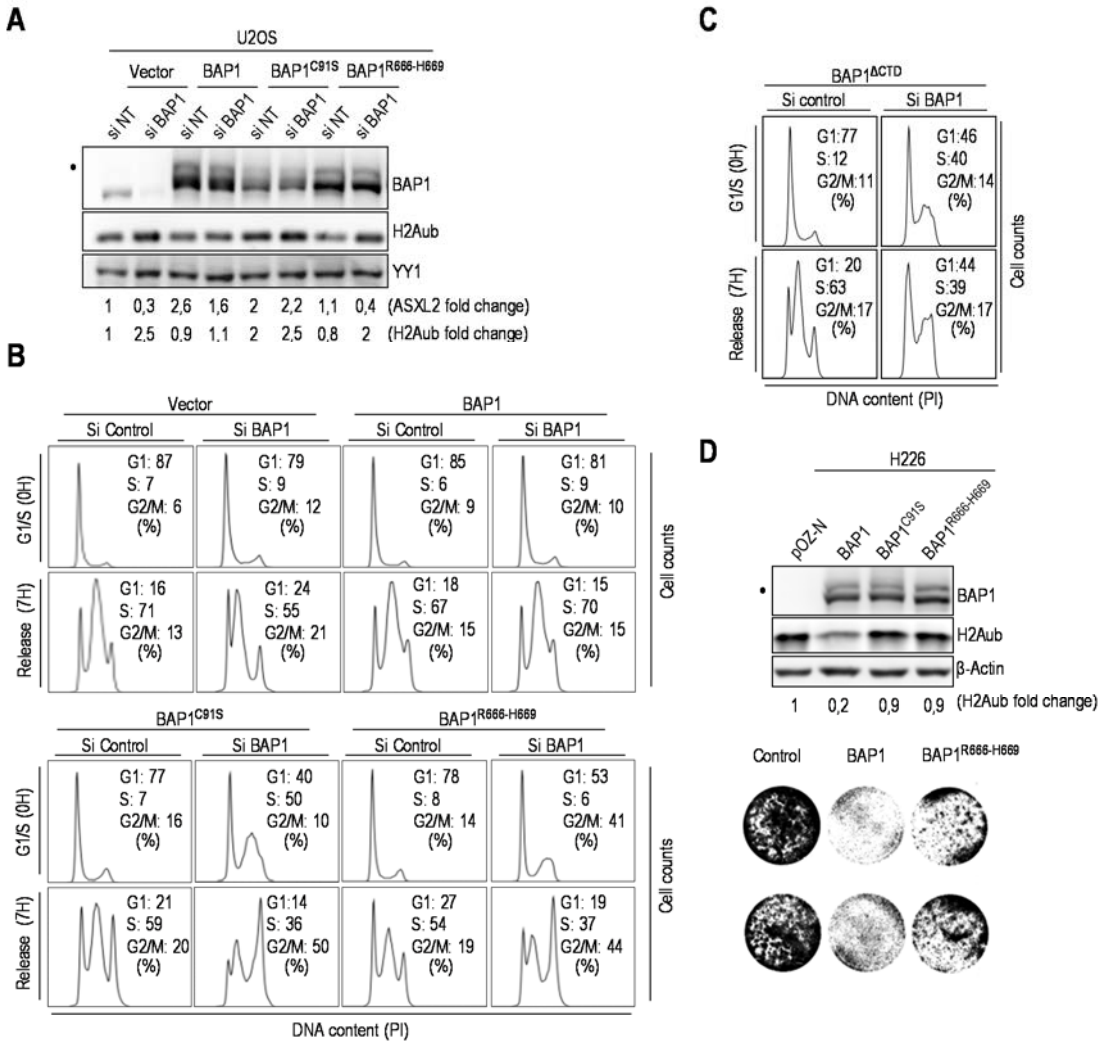

Figure 4.10. BAP1 regulates cell cycle progression in CTD-dependent manner.

A) Protein levels following depletion of endogenous BAP1 using siRNA in U2OS cells stably expressing siRNA-resistant BAP1, $BAP1^{C91S}$ or $BAP1^{R666\text{-}H669}$. **B-C)** Mutations of CTD disrupts BAP1 function in regulating cell proliferation. Following siRNA for endogenous BAP1, U2OS cells stably expressing siRNA-resistant BAP1, $BAP1^{C91S}$, $BAP1^{R666\text{-}H669}$ or $BAP1^{\Delta CTD}$ were synchronized by double thymidine block at the G1/S boundary and released 7 hours to progress through S phase and were then subjected to FACS analysis. **D)** H226 BAP1-null cells stably expressing BAP1, $BAP1^{C91S}$ or $BAP1^{R666\text{-}H669}$ was analysed by immunoblotting (top panel). Similar numbers of cells were plated and cultured for 5 days prior staining with crystal violet dye (bottom panel). YY1 and β-Actin were used as a protein loading controls. The dot indicates a monoubiquitinated form of BAP1 [241] (panels **A**, **D**).

4.4.9 Enforced expression of BAP1 or ASXL2 induce cellular senescence and the p53/p21 tumor suppressor pathway in CTD/ASXM-dependent manner.

Cellular senescence-associated cell cycle exit is a potent tumor suppressor mechanism. Since we established that BAP1 function is coordinated with ASXL1 and ASXL2 in regulating cell cycle progression, we were prompted to determine if BAP1/ASXL1/2 might influence cellular senescence. Of note, PcG proteins, notably BMI1, are known to be involved in senescence [452-454]. Of note, PcG proteins, notably BMI1, are known to be involved in senescence [452-454]. Therefore, we evaluated whether enforced expression of BAP1, trigger senescence in the normal diploid human fibroblasts IMR90 cell line model. Strikingly, retroviral overexpression of BAP1 reduced cell proliferation and induced senescence-associated β-galactosidase (SA-β-gal) activity (Fig. 4.11A,B). Interestingly, overexpression of BAP1C91S mutant also induced senescence with a more pronounced effect than the wild type form (Fig.4.11A,B). To probe whether this effect is due to BAP1 ability to interact with ASXL1/2, we evaluated the effect of BAP1ΔCTD and BAP1R666-H669 on cellular senescence. Indeed, these mutations significantly reduced the ability of BAP1 to induce senescence (Fig 4.11A,B). Similar effects were observed for the double mutants BAP1C91S-ΔCTD, although a complete rescue was observed for BAP1C91S-R666-H669 (Fig. 4.11A,B). On the other hand, overexpression of ASXL2, but not ASXL1, also strongly induced senescence and reduced cell proliferation (Fig. 4.11A,B). Moreover, deletion of ASXM (ASXL2ΔASXM) inhibited the senescence-inducing ability of ASXL2, indicating the importance of ASXL2-BAP1 interaction in coordinating cellular senescence.

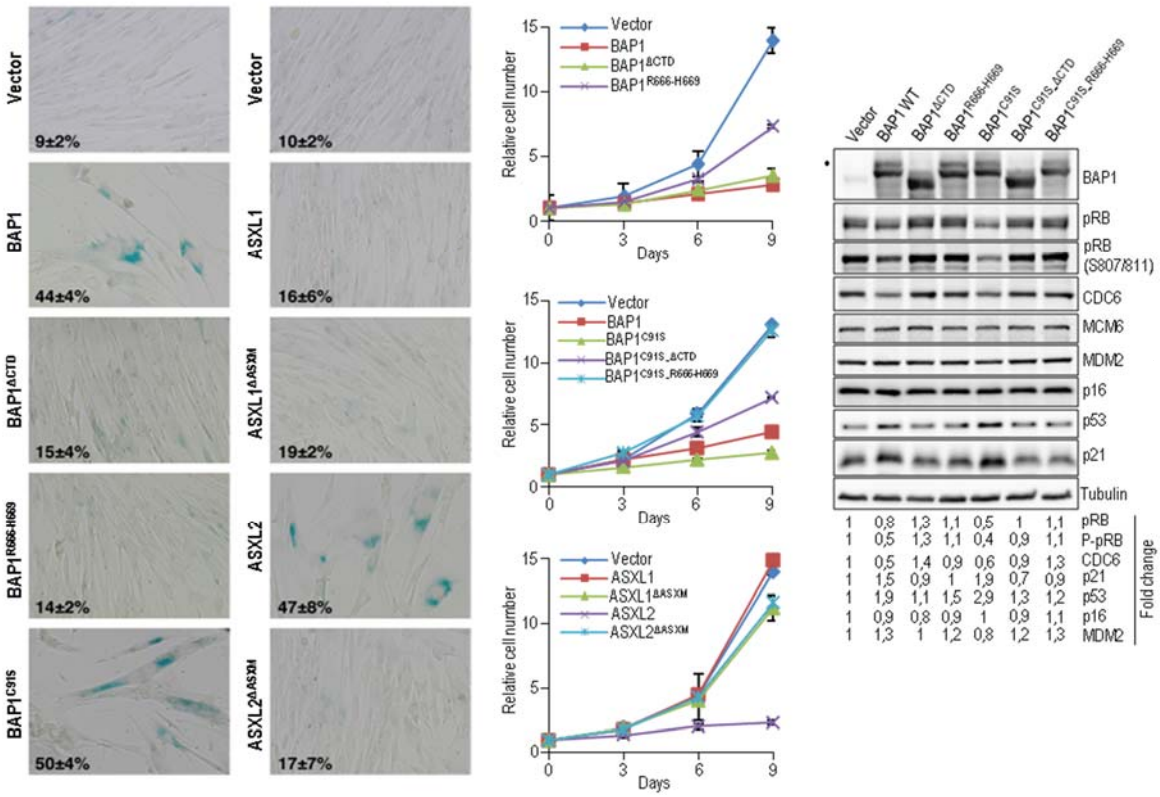

Figure 4.11. ASXL2 and BAP1 overexpression induce senescence in an ASXM- and CTD-dependent manner respectively.

A) IMR90 cells were infected using retroviral expression vectors for BAP1, ASXL1, ASXL2 and their respective mutant forms. Eight days post-selection the cells were fixed for staining of senescence-associated β-galactosidase assay (SA-β-gal). **B)** Cells were also transduced with retroviral expression vectors for BAP1, ASXL1, ASXL2 and their respective mutant forms and counted every three days after selection to follow cell proliferation. 100 cells were counted in triplicate and data presented as percentage of positive cells, average ± SD. **C)** BAP1 overexpression triggers cellular senescence and induces the p53/p21 DNA damage response in ASXL1/2 dependent manner. Eight days post-selection the senescent cells were harvested for immunoblotting. Quantification of band intensity was conducted relative to the empty vector transduced cells. Tubulin was used as a protein loading controls. The dot indicates a monoubiquitinated form of BAP1 [241] (panels **C**).

To provide further insights into the molecular mechanism that orchestrate BAP1/ASXL2-mediated senescence, we evaluated the expression levels of known proteins that induce cellular senescence upon overexpression of BAP1, BAP1^{C91S} and corresponding mutants (Fig. 4.11C). We found that, although the effect of BAP1 was less pronounced than the BAP1^{C91S} form, overexpression of this DUB induced the p53/p21 tumor suppressor pathway. Overexpression of BAP1$^{\Delta CTD}$, BAP1$^{R666\text{-}H669}$, BAP1$^{C91S\text{-}\Delta CTD}$ or BAP1$^{C91S\text{-}R666\text{-}H669}$ did not upregulate p53/p21 indicating the requirement for ASXL1/2 in BAP1-mediated senescence

(Fig. 4.11C). We also observed a concomitant decrease of CDC6 and pRB following overexpression of BAP1 or BAP1^{C91S}, and these effects required interaction with ASXL1/2. In contrast, no significant changes were observed on p16INK4a cell cycle inhibitor and the p53 E3 ligase MDM2.

Altogether, these results indicate that the fine balance between ASXL1/2 complexes and their coordination of BAP1 DUB activity are required for the proper progression of cell cycle and tumor suppression.

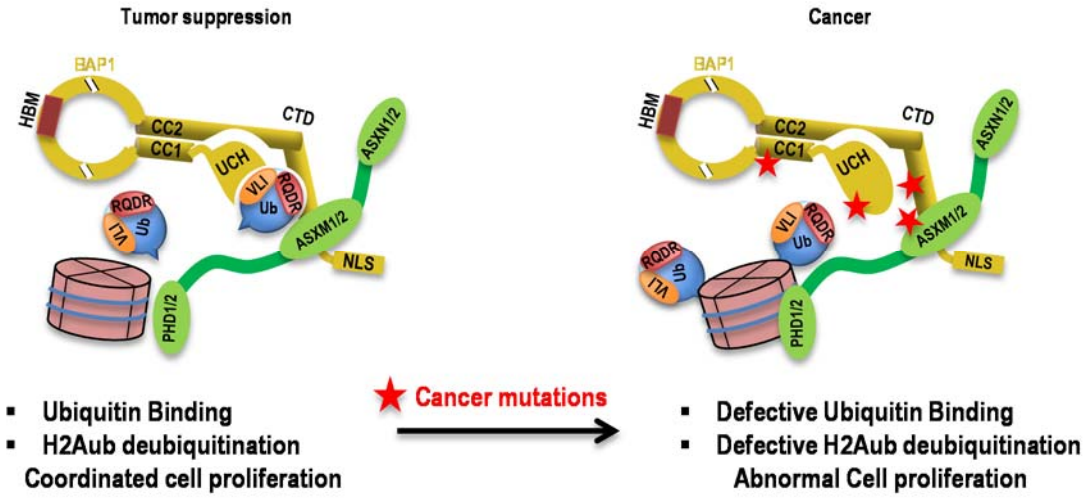

Figure 4.12. Model for the regulation of BAP1-mediated deubiquitination by ASXL1/2.

An intramolecular interaction involving UCH/CC1 and CTD domains of BAP1 creates an ASXM-inducible composite ubiquitin binding interface (CUBI) that facilitates ubiquitin binding and catalysis. The red stars indicate cancer-associated mutations of BAP1 or ASXM that disrupt the CUBI.

4.5 DISCUSSION

We provided novel insights into the mechanisms by which the DUB activity and function of the tumor suppressor BAP1 are coordinated. First, we revealed that BAP1 and ASXL1/2 protein levels are tightly regulated by each other. Notably, BAP1 protein levels are nearly completely reduced following concomitant depletion of ASXL1 and ASXL2. This regulation is highly conserved since, in drosophila, deletion of ASX also destabilized dBAP1/Calypso [79]. The fact that relatively similar protein amounts of ASXL1 and ASXL2 co-purified with mammalian BAP1 and that siRNA depletion of either ASXL1 or ASXL2 reduced BAP1 protein levels by approximately half, it is likely that BAP1/ASXL1 and BAP1/ASXL2 complexes coexist in the cells with a similar abundance. These complexes might exert distinct functions and/or compete for gene regulatory regions. We also found that depletion or loss of BAP1 destabilized ASXL2, but not ASXL1. These findings demonstrate for the first time the importance of complex assembly in maintaining proper protein levels of ASXL2, and hence its function in vivo. Thus, developmental or disease-associated inactivation or loss of expression of one component would result in a profound functional impact on the other partners. Indeed, loss of BAP1 in two tumor types of different histological origins, i.e., mesothelioma and non-small lung carcinoma, caused a severe reduction of ASXL2 protein levels. A survey of mutations in several cancers shows truncating mutations and deletions of BAP1 that would often result in the loss of the CTD and consequently ASXL1/2 interaction. Therefore, loss of ASXL2 function is a prevalent event in cancers with BAP1 mutations.

Similar to other post-translational modifications, ubiquitin recognition plays important roles in ubiquitin-dependent signaling [187]. Often, UBDs involve distinct protein domains that engage interactions with the hydrophobic patches or other surfaces of ubiquitin and act as signal readers [187]. Our study revealed that the CTD domain of BAP1 plays a central role in coordinating ubiquitin binding and catalysis by BAP1/ASXL1/2 complexes. First, the CTD is sufficient for binding a RQDR charged patch of ubiquitin and can be qualified as a bona fide UBD. Second, the CTD interacts with the CC1 and the UCH domains [241], and acts to stabilize the interaction of the ubiquitin with the catalytic domain. Third, the CTD also strongly interacts with ASXM domain, and the latter induces ubiquitin binding by the CUBI and is

required for catalysis. We also found that ASXM itself weakly bind ubiquitin, and hence probably participate in ubiquitin positioning. Thus, our data support a model whereby UCH, CC1, CTD and ASXM domains cooperate in order to generate an interface for stable binding with multiple ubiquitin patches, thus facilitating recruitment and specific substrate deubiquitination (Fig. 12). In support of our findings on BAP1/ASXL1/2, recent crystallography and molecular studies characterized the mechanism of activation of UCH37 by RPN13 [450,451]. The most remarkable similarities with BAP1 are the conserved intramolecular interaction between the DEUBAD of RPN13 and the ULD of UCH37 and the stimulatory effect of RPN13 at the level of substrate binding. Moreover, highly conserved amino acid residues in BAP1 and UCH37, are required for the interaction with the hydrophobic patch of ubiquitin. Finally, similar to ASXM, the DEBUAD of RPN13 also establishes a weak interaction with ubiquitin [450,451]. Thus, BAP1 and UCH37 share a highly conserved mechanism of cofactor-mediated DUB activation. Interestingly, INO80 chromatin remodeling factor also possesses a DEUBAD, and through molecular mimicry, this domain associates with and inhibits UCH37 [450,451]. Of note, BAP1 also interacts with INO80 ATPase, a component of the INO80 chromatin remodeling complex, and promotes its deubiquitination [439]. As INO80G (NFRKB) subunit of the complex inhibits UCHL5 through its DEUBAD, it will be interesting to determine whether, in specific contexts, this factor could also negatively regulate the DUB activity of BAP1.

Our protein complex purification studies indicated that deletion of BAP1 HBM domain does not interfere with BAP1 interaction with ASXL1/2. Conversely, mutation in CTD does not impact the interaction of BAP1 with HCF-1/OGT. Moreover, BAP1 complexes lacking HCF-1/OGT are competent in deubiquitinating nucleosomal histone H2A indicating that these components do not directly participate in ubiquitin binding and catalysis. Taking into account that dBAP1/Calypso does not possess the middle region which was acquired later in vertebrate evolution [79], HCF1/OGT and ASXL1/2 appear to define two functional axes of the BAP1 complexes. Notably, HCF-1 recruits chromatin modifying complexes including MLL family of histone H3K4 methyltransferases and Sin3/HDAC deacetylase complexes at gene regulatory regions [270,288]. Thus, HCF1/OGT and ASXL1/2 exert distinct, but likely concerted,

functions tethered by BAP1. Indeed, similar to HCF-1 interactions with BAP1 [435], ASXL1/2 association with this DUB also regulates cell proliferation.

To establish the significance of BAP1/ASXL1/2 complexes for tumor suppression, we conducted RNAi rescue studies, and showed that cancer-derived mutations that directly target BAP1/ASXL1/2 interaction result in a loss of DUB activity, increased H2Aub levels and deregulation of cell cycle progression. In addition, mutations that directly target the BAP1 catalytic site are frequently found in cancer [77,231,250], and these mutations also result in increased H2Aub levels and deregulation of cell cycle control. These findings highlight the importance of the catalytic activity of BAP1/ASXL1/2 complexes for tumor suppression. Interestingly, overexpression of BAP1 or its catalytically dead form in primary human fibroblasts induced cellular senescence and up regulation of the p53/p21 DNA damage response in CTD-dependent manner, although more pronounced effects were observed for the catalytic inactive form of BAP1. It is currently unclear how both catalytically competent and inactive BAP1 promote cellular senescence. Nonetheless, as the catalytic dead BAP1 binds ubiquitin, it is possible that these effects are associated mostly with BAP1/ASXL1/2 binding to H2Aub rather than catalysis. Deregulation of H2Aub levels or its recognition might cause defects in transcriptional events [436], DNA double strand break repair [229] or replication fork progression [439], all of which could promote the induction of DNA damage and the p53 response and lead to genomic instability and cancer development. While further studies are needed to address these possibilities, our findings, nonetheless, suggest that the proper balance of BAP1/ASXL1/2 complexes and their coordinated binding to ubiquitinated substrates and/or DUB activity are essential for normal control of cell proliferation. Another interesting finding is that, overexpression of ASXL2, but not ASXL1, induces senescence in ASXM-dependent manner. Taking into account that ASXL2 and BAP1 form an obligate complex, our study delineates that ASXL2 plays an important role in regulating BAP1 function in cell proliferation. Moreover, a cancer-derived mutation of BAP1 that abolishes its interaction with ASXL1/2 prevents cellular senescence, further supporting the notion that the BAP1/ASXL2 signaling axis is important for tumor suppression.

Although, we cannot exclude that BAP1/ASXL1/2 target other known substrates such HCF-1 and OGT [230,234], our study and others provide strong support for the role of this DUB in the

regulation of H2Aub levels and tumor suppression. Indeed (i) BAP1 was revealed as a major DUB for H2A in mammalian cells, (ii) several cancer mutations of BAP1 and ASXL2 target the UCH/CC1/CTD/ASXM platform, which is critical for ubiquitin binding and H2A deubiquitination, (iii) BAP1 null cancer cells display high H2Aub levels that could be reduced following reintroduction of BAP1, but not ASXL1/2 interaction-deficient mutants, (iv) both PcG proteins Ring1B and BMI1, two critical components of the PRC1 complex that catalyze H2A ubiquitination, regulate cell proliferation and are overexpressed in cancer [455-457]. Thus, our study provides further insights into the potential involvement of H2Aub in tumorigenes.

4.6 Acknowledgements

We thank Yang Shi for support, Haider Dar, Sarah Hadj-Mimoune, Diana Adjaoud and Marie-Anne Germain for technical assistance.

Conflict of interest

The authors declare that they have no conflicts of interest.

Author contributions

SD, IHM and EBA designed the study. SD, IHM and EBA wrote the paper. SD and IHM performed and analyzed the data presented in Figures 1, 2, 3, 4, 5, 10. SD conducted the experiments related to Figures 8 and 9. SD and NM performed the experiments of Figures 6 and 7. NM realized the experiments of Figure 5A and 5F. HB and NM performed the alignment analysis presented in Figures 6C and 8A respectively. HB conducted the experiments related to Figures 5D and 8C. JG conducted the experiments of Figure 1E and 2H. SD, FAM, AM, JG and NVGI designed and performed the experiments related to Figure 11. HP realized the experiment of Figure 3B. HY performed the experiment of Figure 2F. NSN helped with the construction of mammalian expression vectors for ASXL1, ASXL2, ASXL1 ΔASXM and ASXL2 ΔASXM. SD and NM designed and generated the expression vectors of the different mutant forms of BAP1, ASXM2 and Ubiquitin used for the experiments related to Figures 6, 7, 8 and 9. All the authors reviewed and interpreted the data, and edited the manuscript. All authors reviewed the results and approved the final version of the manuscript.

FOOTNOTES

* This work was supported by grants from the Canadian Institutes of Health Research (CIHR) (MOP-115132) and the Natural Sciences and Engineering Research Council of Canada (355814-2010) to E.B.A, and CIHR to F.A.M (MOP-133442). E.B.A. is a scholar of the Fonds de la Recherche du Québec - Santé (FRQ-S) and the CIHR. H.W. and F.A.M. are Scholars of

the FRQ-S. S.D. had a PhD scholarship from the Islamic Bank for Development. H.Y. had a PhD scholarship from the CIHR. H.B has a PhD scholarship from the Ministry of Higher Education and from Scientific Research of Tunisia and the Cole Foundation. J.G has a M.Sc. scholarship from the FRQ-S. H.Y. had a PhD scholarship from the CIHR.

1To whom correspondence may be addressed: Maisonneuve-Rosemont Hospital Research Center and Department of Medicine, University of Montréal, Montréal H3C 3J7, Québec, Canada.

2The abbreviations used are: DUB, Deubiquitinase; H2Aub, H2A K119 ubiquitination; CTD, C-Terminal domain; CUBI, Composite Ubiquitin Binding Interface; UCH, Ubiquitin Carboxyl Hydrolase; CC1, Coiled Coil motif 1; CC2, Coiled Coil motif 2; ULD, C-Terminal Domain of UCH37; UBD, Ubiquitin Binding domains; PR-DUB, Polycomb Repressive-DUB, PRC1, Polycomb Repressive Complex 1; PcG, Polycomb Group Proteins; TrxG, Trithorax Group Proteins; PHD, Plant Homeo Domain.

CHAPITRE 5

5 DISCUSSION

Nos études révèlent un lien fonctionnel entre le complexe BAP1, le contrôle de la prolifération cellulaire et la tumorigenèse. Comprendre d'avantage comment BAP1 et ses partenaires agissent pour moduler la signalisation cellulaire qui gouverne le système de l'ubiquitine, nous permettrait d'identifier les faiblesses des cellules cancéreuses ayant perdu ce gène suppresseur de tumeurs afin de les cibler avec de nouvelles thérapies personnalisées anti-cancer.

5.1 Relation fonctionnelle entre OGT et HCF-1 :

Dans le but d'investiguer les mécanismes de coopérations fonctionnelles au sein du complexe BAP1, nous avons contribué à élucider un mécanisme unique de régulation entre HCF-1 et OGT. OGT et HCF-1 ont déjà été retrouvées associées au sein de plusieurs complexes de régulation de la chromatine. Récemment, il a été démontré que ces deux facteurs épigénétiques participent avec BAP1 dans le contrôle de la gluconéogenèse[230,250,261].

De manière significative, nous avons retrouvé que HCF-1 et OGT sont étroitement contrôlées l'un par l'autre. Cette co-régulation entre des sous-unités protéiques appartenant à un même complexe est un aspect fréquemment retrouvé au sein de complexes de régulateurs transcriptionnels à savoir le complexe PRC2 (co-régulation entre SUZ12 et EZH2) [36], le complexe PR-DUB (activation de l'activité catalytique entre ASX et Calypso) [79] et même au niveau du complexe BAP1 (stabilisation et activation catalytique entre BAP1/ASXL1/ASXL2) [209]. Du fait que la fonction de HCF-1 est généralement attribuée à l'activation transcriptionnelle, la façon la plus simple de proposer un mécanisme de régulation de OGT, est que le niveau d'expression de celle-ci est modulé au niveau transcriptionnel. Néanmoins, le niveau de mRNA de OGT ne change pas suite à la déplétion de HCF-1 par RNAi, et ce dernier semble être très faiblement recruté sur le promoteur de OGT. Ce qui est très intéressant, est le fait que nous avons pu détecter une mono-et une polyubiquitination de OGT, suggérant que celle-ci est sujette à une régulation protéasomale[275]. De ce fait, en interagissant avec OGT,

HCF-1 pourrait inhiber le recrutement d'une ubiquitine ligase E3 et par conséquent son ciblage par le protéasome.

5.1.1 La O-GlcNAcylation de HCF-1 est requise pour son clivage protéolytique :

L'activation de HCF-1 chez les mammifères requiert sa maturation qui consiste en son clivage protéolytique. Ce type de modifications post-traductionnelles est un mécanisme de signalisation largement adopté au sein des organismes multicellulaires [102,458]. En effet, le clivage protéolytique module la fonction de plusieurs protéines, notamment les régulateurs transcriptionnels. Ainsi, la protéolyse limitée promouvait aussi bien l'activation que l'inactivation des substrats cibles. Nous pouvons citer comme exemple, le clivage protéolytique au sein de la voie de signalisation canonique de Notch. En effet, le récepteur Notch est clivé suite à son activation avec un de ses ligands DSL (Delta-Serrate-LAG2). Cette protéolyse est un évènement crucial qui permet la libération du domaine intracellulaire de Notch (NICD) et sa translocation vers le noyau afin de participer à l'assemblage de complexes transcriptionnels et activer l'expression des gènes cibles [459]. Le clivage protéolytique peut également se présenter sous la forme d'un auto clivage, requis pour l'activation de la protéine. L'activation des caspases suite à l'initiation de la signalisation de l'apoptose conduit à l'induction du processus d'autocatalyse afin d'inciter la dimérisation et l'activation de ces dernières [460,461]. D'autre part, les caspases elles-mêmes catalysent la protéolyse de leurs substrats permettant l'enlèvement de motifs ou régions régulatrices et de ce fait leur activation ou inactivation [462].

Ce qui est d'une importance majeure par rapport à notre caractérisation fonctionnelle entre OGT et HCF-1 est le fait que nous avons révélé pour la première fois que la O-GlcNAcylation de HCF-1 active sa maturation protéolytique. En effet, la déplétion de OGT par siRNA provoque une accumulation importante de la forme précurseur de HCF-1 avec une diminution considérable des produits de clivage[275].

Le HCF-1 humain subit une protéolyse finement contrôlé au sein de son site spécifique de clivage, le PPD [275,279,283,284,463,464]. De manière intéréssante, HCF-1 est une des protéines les plus modifiées par O-GlcNAcylation dans la cellule humaine. On compte plus d'une vingtaine de sites susceptibles à être modifiés. La majorité de ces sites se retrouvent au niveau de la région N-terminale de HCF-1 et plus précisément au sein du domaine Basic [275]. L'implication de ces modifications dans la régulation de la fonction de HCF-1 n'est pas connue. En effet, la O-GlcNAcylation du domaine N-terminale n'est pas requise pour la maturation protéolytique de HCF-1 puisque ce processus n'est pas affecté lorsque la région N-terminale de celui-ci est mutée au niveau de ses sites de O-GlcNAcylation [275]. De plus, des études de protéomiques ont déterminé la présence de plusieurs sites de phosphorylation au niveau de la région N-terminale de HCF-1. Ces sites sont pour la plupart des sites de O-GlcNAcylation [426,465,466]. Il serait intéressant d'investiguer d'avantage comment ces différentes voies de signalisations régulent la fonction biologique de HCF-1 en modifiant son domaine N-terminale. Dans le but d'analyser d'avantage comment la OGT stimule la maturation protéolytique de HCF-1, il a été important de caractériser leur interaction. Lors de la purification de HCF-1N, une quantité significative de OGT a été co-purifiée, démontrant que celle-ci interagie avec la région N-terminale de HCF-1 (HCF-1N) [288]. Afin de d'affiner d'avantage l'interaction entre ces deux protéines nous avons révélé la présence d'un petit fragment nommé OBM (OGT Binding Motif) au sein du domaine Basic comme premier domaine interagissant avec OGT [275,288]. Nous avons également identifié un deuxième motif de liaison de OGT avec HCF-1 qui se localise au niveau du PPD. Ce dernier semble être suffisant pour favoriser l'interaction avec OGT qui elle, admet une affinité beaucoup plus élevée envers le PPD que la région N-terminale. Plus intéressant encore, nous avons montré que la O-GlcNAcylation du PPD stimule directement le clivage de HCF-1. Par conséquent la OGT modifie deux régions différentes du HCF-1 (le domaine N-terminale et le PPD). Il est fort probable que ces évènements de O-GlcNAcylation de HCF-1 possèdent des effets distincts mais complémentaires dans la régulation de la fonction de HCF-1.

5.1.2 OGT est-elle la protéase qui clive HCF-1?:

Le mécanisme de la maturation de HCF-1 est un processus qui s'est développé au cours de l'évolution. En effet, HCF de la *Drosophile* subit un clivage protéolytique catalysé par la Taspase1 au niveau d'un site de clivage différent du PPD de HCF-1 de l'humain [281,282]. Le mécanisme de protéolyse de HCF-1 n'a été dévoilé que très récemment et la signification biologique de ce processus de maturation reste très peu comprise [275,283,284].

L'analyse de la séquence protéique de OGT ne suggère pas qu'elle possède une activité protéase spécifique. De ceci découle l'hypothèse que le clivage de HCF-1 est une signalisation qui nécessite l'implication de plusieurs facteurs notamment, la OGT, l'UDP-GlcNAc et une protéase. Toutefois, des travaux récents du groupe de Herr, sont venus proposer pour la première fois que OGT elle-même pourrait avoir une activité protéolytique envers le PPD de HCF-1. En effet, OGT recombinante purifiée à partir des bactéries était capable de promouvoir de manière partielle le clivage protéolytique du PPD qui lui a été obtenu par traduction *in vitro* [283]. Toutefois, cela n'exclu pas la possibilité d'avoir une contamination par des protéases au niveau des préparations bactériennes, qui pourraient favoriser la protéolyse du PPD. De plus, afin de valoriser d'avantage ces résultats, un autre travail est apparu ultérieurement du groupe de Walker et Herr qui décrit plus en détails le mécanisme de protéolyse du PPD [284]. Ils ont ainsi pu définir par cristallographie, l'interaction de OGT avec le PPD et ont émis un mécanisme biochimique de clivage protéolytique [284]. Le scenario de la maturation de HCF-1 *in vivo* peut être complètement diffèrent de ce qui a été déjà reporté *in vitro*. En effet, des études précédentes par le groupe de Kristie et Herr ont proposée que HCF-1 possède une activité protéolytique autonome, puisqu'une forme recombinante du PPD de HCF-1 purifiée à partir des bactéries était capable de s'auto-cliver en absence de OGT [279,464]. Encore plus intéressant, l'utilisation d'une série d'inhibiteurs de potéases présentaient un effet mineur sur l'inhibition du clivage du PPD suggérant que la O-GlcNAcylation du PPD par OGT engendrerait des changements structurels au niveau des séquences répétitives de protéolyse du PPD facilitant ainsi le processus de l'autocatalyse. Également, la O-GlcNAcylation du PPD pourrait être un signal pour le recrutement d'une nouvelle peptidase.

À la lumière de ces évidences, et afin de caractériser d'avantage le rôle de OGT dans l'induction de la maturation du HCF-1, nous avons démontré que le domaine PPD est faiblement clivé lorsqu'il est surexprimé dans les cellules 293T. Plus spécifiquement, le PPD

(i) se localise de manière similaire au niveau du cytoplasme et du noyau (ii) interagie avec OGT et (iii) permet sa stabilisation et sa séquestration au niveau du cytoplasme sans être efficacement clivé. D'autre part, nous avons révélé que la maturation protéolytique du PPD est grandement augmentée lorsque celui-ci a été fusionné à une séquence codante pour un signal de localisation nucléaire (séquence du *SV40 T-large antigen*) et a donc été ramené massivement au niveau du noyau [275]. Inversement, la diminution du niveau protéique de OGT par shRNA permet une restauration significative du niveau protéique de la forme complète du PPD [275]. Tous ces résultats suggèrent que , *in vivo*, OGT promouvait directement le clivage de HCF-1 et que la O-GlcNAcylation du PPD est un signal d'initiation pour sa protéolyse qui nécessite la localisation nucléaire de OGT et de HCF-1[275,283,284].

5.1.3 Rôle de la maturation de HCF-1 dans le contrôle de sa fonction biologique :

Ce mécanisme intriguant de protéolyse de HCF-1 est indispensable pour assurer le bon fonctionnement de ce cofacteur transcriptionnel. En effet, des travaux antérieurs ont démontré que la sous-unité HCF-1 N (Fragments N-terminaux de HCF-1) est requise et est suffisante pour promouvoir la transition G1/S du cycle cellulaire alors que la sous- unité HCF-1 C (Fragments C-terminaux de HCF-1) permet la progression au cours de la mitose et plus particulièrement, la bonne élaboration de la cytokinèse [266]. Plus spécifiquement, l'utilisation d'une forme mutée de HCF-1 dont le PPD a été éliminé par délétion, ne permet pas de corriger le déficit de la cytokinèse provoqué par la déplétion de HCF-1 par RNAi. Il n'est toujours pas totalement défini comment et pourquoi les fragments N- et C-terminaux de HCF-1 restent associés. Récemment une étude structurale de l'association des domaines SAS avec les domaines FN3-1 est venue soutenir l'idée que le clivage du PPD semble être requis pour assurer l'assemblage de ces deux domaines [257,280]. Également, il a été montré que la surexpression du HCF-1C permet de corriger les effets des aberrations mitotiques observées au niveau de la cytokinèse induites par la déplétion de HCF-1 [257]. Ceci pourrait suggérer que l'interaction SAS/FN3-1 n'est pas requise pour assurer la fonction du HCF-1C mais que l'effet inhibiteur attribué par le HCF-1N pourrait être éliminé par la maturation protéolytique de HCF-1.

En vertu de sa fonction particulière d'induction de la protéolyse de HCF-1, OGT peut assurer le dosage des niveaux de HCF-1 sous forme de précurseur versus ses produits de clivage. Ceci aura pour effet de moduler l'activité de HCF-1 pour la régulation de l'expression des gènes cibles, puisque la déplétion de OGT par RNAi stimule l'expression des gènes IE du *herpes simplex virus-1* (HSV-1) [275]. De plus, Il serait intéressant de definir si la protéolyse limitée du PPD coordonnée par son O-GlcNAcylation serait une signalisation qui favoriserait un gain ou une perte de certaines fonctions spécifiques du HCF-1, évenements importants pour la progression du cycle cellulaire. En effet, la O-GlcNAcylation du HCF-1 pourrait augmenter ou inhiber son interaction avec d'autres protéines puisque le HCF-1 N représente une plateforme pour des interactions avec différents partenaires. Compte tenu que HCF-1 est une protéine très abondante et est impliquée dans le contrôle de plusieurs voies de signalisation cellulaires, il serait intéressant de déterminer comment la O-GlcNAcylation de ce cofacteur transcriptionnel coordonne sa fonction biologique dans différents contextes physiologiques ou même dans des conditions de stress.

5.2 La O-GlcNAcylation fait-elle partie du code des histones?

OGT est un partenaire important du complexe BAP1du fait que (i) OGT régule la fonction de HCF-1 en promouvant son clivage protéolytique, (ii) OGT se retrouve associée en quantité significativement élevée avec HCF-1 au sein du complexe BAP1 suggérant son implication dans la régulation d'autres fonctions de ce complexe (iii) le complexe OGT/HCF-1/BAP1 est un régulateur majeur de la gluconéogenèse et (iiii) la O-GlcNAcylation émerge comme un composant intégral de l'épigénome. De ce fait, nous nous sommes intéressés à vouloir démystifier de plus près le lien entre la O-GlcNAcylation et l'ubiquitination dans la modulation de différents évènements de signalisations liés à la régulation de la chromatine. De manière plus spécifique, la O-GlcNAcylation coordonne plusieurs processus cellulaires comme la prolifération cellulaire, la différentiation, l'homéostasie des cellules souches ainsi que le maintien de l'empreinte génétique [301,303,308,323,328]. Tous ces mécanismes sont finement régulés par les protéines Polycombes et de ce fait, ils sont également la cible du complexe PR-DUB qui est représenté chez l'humain par le complexe BAP1.

Comme il a été mentionné dans l'introduction, la O-GlcNAcylation a été proposée comme étant une nouvelle marque épigénétique[20,357,360,415]. Toutefois, la relation fonctionnelle de cette modification avec d'autres modifications épigénétiques comme la phosphorylation, la méthylation, l'acétylation ou l'ubiquitination est également très peu analysée [21,346,347]. Néanmoins, il a été suggéré qu'il existe une coopération entre la O-GlcNAcylation au niveau des résidus sérines et thréonines qui ont été proposés à être modifiés et d'autres PTMs des histones (phosphorylation de H3S10 et H2B K120ub) pour la régulation de l'expression génique[20,357,360,415]. D'autre part, la majorité des sites de O-GlcNAcylation détectés au niveau des histones se retrouvent dans la région globulaire du nucléosome suggérant que cette modification pourrait influencer la maintenance de la structure ordonnée de la chromatine. Néanmoins, la mutation des résidus des histones qui ont été reportés à être modifiés par O-GlcNAcylation, diminue très faiblement le niveau global de cette modification au niveau de la chromatine soulevant ainsi des doutes quant à l'existence de cette marque épigénétique [21].

Le domaine de l'épigénétique souffre du manque d'outils sensibles et faciles à utiliser pour investiguer différentes voies de signalisation cellulaires gouvernées par la O-GlcNAcylation. Cet obstacle dans l'identification des protéines modifiées par O-GlcNAcylation est principalement dû à deux facteurs qui sont, (1) la stœchiométrie du O-GlcNAc sur les résidus des protéines modifiées qui est très faible et (2) la liaison glycosidique entre la molécule du O-GlcNAc et les résidus sérines et thréonines qui est très instable durant les processus de fragmentation par spectrométrie de masse [467,468]. Différentes techniques ont été entreprises afin de détecter et/ou identifier les mêmes ou de nouveaux résidus au niveau des histones modifiées par O-GlcNAcylation à savoir, l'utilisation d'anticorps dirigés contre le O-GlcNAc (le RL2 et le CTD 110.6), la spectrométrie de masse ou encore des approches chimio enzymatiques comme le marquage des protéines par un analogue du O-GlcNAc, le GlcNAz (*azide-containing GlcNAc analog*) [469-471]. De plus, il est important de noter que l'affinité des deux anticorps, le RL2 et le CTD110.6 envers le O-GlcNAc est relativement faible. Des travaux ont déjà remis en question la spécificité du CTD 110.6. Même si celui-ci a été généré contre le peptide CTD de la polII modifié par O-GlcNAcylation, il admet une affinité assez considérable pour les protéines modifiées par le N-GlcNAc2 ou le O-mannose [395,396].

Durant notre investigation sur la O-GlcNAcylation des histones, nous avons été surpris que n'avons pas été capable de détecter cette modification et ce en adoptant des approches multiples déjà élaborées par différents groupes. De plus nous avons été incapables de valider la relation potentielle entre la O-GlcNAcylation de H2B S112 et l'ubiquitination de H2B K120. Ainsi nos résultats soulèvent des doutes quant à l'occurrence et l'abondance de la O-GlcNAcylation des histones dans les cellules de mammifères. De plus, nous évoquons de multiples enjeux concernant les différentes techniques couramment utilisées pour la détection de cette modification au niveau des histones.

Il est largement admis qu'en général, les anticorps représentent un outil robuste et très spécifique pour tous types d'analyses moléculaires. Ainsi, du fait de la faible spécificité des anticorps contre le O-GlcNAc, il est important de considérer de développer de nouveaux anticorps qui seront spécifiquement dirigés contre des résidus sérines et thréonines modifiés par O-GlcNAcylation au niveau des protéines (il s'agirait d'anticorps qui reconnaitraient le O-GlcNAc dans le contexte d'une séquence peptidique spécifique). Développer ce genre d'outils nous permettrait de (i) mieux comprendre la fonction biologique de la O-GlcNAcylation, (ii) définir de manière beaucoup plus robuste les événements cellulaires liés à la O-GlcNAcylation des régulateurs épigénétiques et ce au cours de processus physiologiques normales (comme la prolifération cellulaire, la différentiation, la reprogrammation cellulaire, la sénescence) ou suite à des conditions de stress (comme la mort cellulaire ou le stress nutritionnel). Il faut toutefois noter qu'en utilisant les anticorps RL2 et anti-H2B S112 O-GlcNAc nous n'avons pas été capable de détecter un signal spécifique de O-GlcNAcylation au niveau des histones aussi bien au cours du cycle cellulaire que dans des conditions de déprivation de nutriments, (iii) comprendre le lien fonctionnel entre la O-GlcNAcylation et les autres marques épigénétiques de la chromatine et (iiii) établir le contexte cellulaire spécifique au cours duquel la O-GlcNAcylation des histones pourrait se produire, si elle existe.

5.3 Rôle de la OGT au sein de complexes protéiques de régulations épigénétiques

Malgré l'apogée de la O-GlcNAcylation dans la modulation de plusieurs processus cellulaires, le lien fonctionnel entre OGT et les différents régulateurs de la chromatine n'est qu'à ses débuts.

La régulation des protéines par O-GlcNAcylation est un processus qui dépend principalement de la disponibilité du O-GlcNAc dans la cellule et de ce fait des différents métabolites énergétiques requis pour la production de ce substrat. Les fluctuations de la balance énergétique dans les cellules auront donc un impact important dans la régulation fonctionnelle des facteurs et cofacteurs transcriptionnels. De manière plus spécifique, du fait que OGT est un partenaire important et majeur du complexe BAP1/HCF-1, l'étude de la fonction biologique de ce complexe aurait une retombée significative sur la compréhension de nombreux mécanismes de régulation transcriptionnelle aussi bien au cours de processus physiologiques normales que dans des conditions d'anomalies métaboliques, neurologiques, de désordres hématologiques et également au cours du développement de différents types de cancers. Ainsi, du fait que le complexe BAP1/HCF-1/OGT est considéré comme un régulateur majeur du métabolisme cellulaire, la modulation du niveau de O-GlcNAcylation de HCF-1 permettrait à celui-ci d'agir comme un senseur métabolique capable de convertir l'état énergétique de la cellule en signaux de régulation de l'expression des gènes. De plus, du moment que HCF-1/OGT s'associent à d'autres complexes enzymatiques de modification de la chromatine à savoir les complexes MLL, les complexes TET2/3, le complexe CLOCK/BMAL1, ces régulateurs épigénétiques favoriseraient ainsi le lien entre l'état métabolique de la cellule et le contrôle de l'expression des gènes au cours de la différentiation, la progression du cycle cellulaire ainsi que la régulation du rythme circadien. La présence particulière de OGT dans les complexes TET2/3 souligne un lien important entre la O-GlcNAcylation et la déméthylation de l'ADN dans la coordination de multiples processus cellulaires.

Depuis quelques années, les altérations métaboliques prennent de plus en plus d'ampleur quant à leur implication dans le développement de plusieurs maladies malignes humaines. Les reprogrammations métaboliques constituent un processus nécessaire pour le passage de l'état prolifératif normal à la croissance incontrôlée spécifique des cellules cancéreuses [333,472-476]. De plus, de nombreux gènes suppresseurs de tumeurs et oncogènes sont des régulateurs du métabolisme. De manière plus spécifique, les niveaux d'expression de la

OGT et la O-GlcNAcylation globale des protéines sont dérégulés dans de nombreux cancers comme le cancer du pancréas, du sein et de la prostate [325,477]. En effet, diverses études ont reportées que les niveaux élevés de O-GlcNAcylation sont à l'origine de l'amplification de la prolifération des cellules cancéreuses, de l'angiogenèse tumorale, de l'état métastatique des tumeurs ainsi que de la maintenance de la signalisation pro-inflammatoire [299,304,327]. Comme il a été proposé que OGT régule négativement la voie de signalisation Akt [318], il serait intéressant d'investiguer si le complexe BAP1/HCF-1/OGT permettrait de lier les voies oncogéniques des récepteurs à activité tyrosine kinases, RTKs (EGFR, HER, Met et VEGFR) à des évènements transcriptionnels.

5.4. Régulation de la déubiquitinase suppressive de tumeurs, BAP1

Les régulations des niveaux d'expression génique et la stabilité protéique constituent des processus indispensables pour le control adéquat des fonctions biologiques des déubiquitinases. Depuis les dix dernières années, les recherches se poursuivent pour élucider les différentes fonctions de ces enzymes. Néanmoins malgré tous ces progrès, les mécanismes de régulations de ces enzymes restent très peu compris.

Le complexe BAP1 contient plusieurs partenaires qui admettent des activités enzymatiques différentes (LSD2, HAT1, OGT et UBE2O) permettant d'intégrer la déméthylation, l'acétylation, la O-GlcNAcylation et l'ubiquitination dans la coordination de la fonction suppressive de tumeurs de BAP1. Plus particulièrement, nous avons révélé très récemment un nouveau mécanisme unique de régulation de BAP1 par son partenaire, l'ubiquitine ligase atypique UBE2O. Nous avons démontré que UBE2O multi-monoubiquitine BAP1 au niveau de son NLS provoquant ainsi sa séquestration dans le cytoplasme. Grâce à son activité d'autodéubiquitination, BAP1 permet de maintenir sa localisation nucléaire [241]. De plus, nous avons trouvé que des mutations de cancer au niveau du domaine CTD de BAP1 inhibent son activité auto-catalytique et provoquent sa rétention dans le cytoplasme [241]. Ces données, décrivent qu'un contrôle harmonieux entre l'ubiquitination et la déubiquitination de BAP1 assure une régulation propre de la fonction biologique de cette DUB **(Voir Annexe 2)**.

5.4.1 Régulation transcriptionnelle par le complexe multi-protéique BAP1

En tenant compte de la composition très particulière du complexe BAP1, nous pouvons suggérer que ce complexe multi-protéique régule différents gènes et ce en fonction de l'interaction de BAP1 avec ses partenaires.

Récemment, nous avons contribué à la détermination de certains aspects des mécanismes d'action de BAP1. Pour démontrer le rôle du complexe BAP1 dans la régulation transcriptionnelle, (i) nous avons déterminé pour la première fois que cette DUB forme principalement un complexe transcriptionnel multi-protéique formé d'une multitude de facteurs et régulateurs transcriptionnels, notamment YY1, HCF-1, FOXK1, FOXK2, ASXL1, ASXL2, (ii) BAP1 est majoritairement associé à HCF-1 qui représente un régulateur transcriptionnel majeur des gènes de contrôle du cycle cellulaire, notamment les gènes cibles de E2F, (iii) BAP1 forme un complexe ternaire avec HCF-1 et YY1 requis pour la régulation transcriptionnelle, (iv) YY1 est requis pour le recrutement de BAP1 et de HCF-1 au niveau des promoteurs des gènes cibles permettant ainsi d'établir un lien direct entre BAP1 et la régulation de la prolifération cellulaire 78, et (v) la déplétion de BAP1 entraine une diminution de l'expression des gènes du cycle cellulaire. D'autre part, notre groupe a également établi un rôle unique de BAP1 comme gène suppresseur de tumeurs dans la réparation des dommages doubles brins de l'ADN par recombinaison homologue. Également, nous présentons dans cette même étude, la première évidence que la phosphorylation de BAP1 après dommage à l'ADN coordonne sa fonction de régulation de la prolifération cellulaire 229 (Voir Annexe 3).

De manière importante, il est maintenant connu que le complexe BAP1 est un complexe Polycombe du fait que cette DUB est associé à plusieurs facteurs qui ont été définis pour être des protéines Polycombes à savoir, YY1478, OGT346,347, ASXL1 et ASXL2361-364. Toutes ces protéines ont été impliquées dans la régulation de l'activation et la répression génique, le développement, la prolifération cellulaire ainsi que la différentiation. De plus, BAP1 catalyse la déubiquitination de la monoubiquitination de H2A, une modification épigénétique requise

pour la progression du cycle cellulaire. De même, la déplétion de Calypso démontre un rôle important de cette DUB dans le développement 79.

La fonction transcriptionnelle de BAP1 aurait évoluée, du fait qu'initialement, Calypso, ne possédait pas le domaine HBM d'interaction avec HCF-1 et n'est en complexe qu'avec ASX. Ce complexe a été caractérisé pour sa capacité à être recruté sur les promoteurs de certains gènes Hox afin de promouvoir leur répression génique et ce en catalysant la déubiquitination de H2Aub 79. Ainsi, au cours de l'évolution, BAP1 aurait acquis la particularité d'interagir avec d'autres facteurs et cofacteurs transcriptionnels et ce afin de pouvoir contrôler un nombre plus large de gènes cible. Ce qui est intéressant est que nous avons démontré que BAP1 s'intègre au sein d'un complexe multi-protéique de 1,6 MDa et que des évidences suggèrent que BAP1 formerait divers sous complexes et ce en fonction des partenaires auxquels il s'associerait 78. En effet, le partenaire majeur de BAP1, HCF-1, interagit à travers le domaine HBM avec plusieurs facteurs transcriptionnels lui permettant d'intégrer plusieurs complexes distincts de régulation de la chromatine. Puisque BAP1 est majoritairement complexé avec HCF-1, nous pouvons suggérer que cette DUB formerait divers complexes de régulation transcriptionnels et ce en s'intégrant de manière différentielle avec les complexes HCF-1/OGT/TET2, HCF-1/MLL1 /OGT, HCF-1/MLL5/OGT, HCF-1/MOF, HCF-1/ LSD1, HCF-1/SETD1A 69,259,268,270,272,285,286 ,287-289. De ce fait, le complexe BAP1 aurait une fonction dynamique dans la régulation d'une multitude de gènes cibles et aurait ainsi un rôle majeur pour le contrôle de nombreux processus cellulaires.

Durant notre investigation sur le rôle transcriptionnel du complexe BAP1, nous avons démontré que cette deubiquitinase admet un rôle majeur plus particulièrement dans la régulation de la prolifération cellulaire 78,209 . En effet, en adoptant une étude d'analyse d'expression globale des gènes couplée à une déplétion de BAP1 par shRNA, nous avons reporté que l'inactivation de BAP1 était à l'origine d'une dérégulation des gènes cibles de E2F 78. Également, HCF-1 est connu d'interagir spécifiquement soit avec des activateurs (comme E2F1) ou des répresseurs (comme E2F4) transcriptionnels afin de contrôler la transition G1/S 266,269,270. De plus, les promoteurs de certains gènes cible de E2F présentent une séquence

de liaison spécifique de YY1, qui lui interagit avec E2F2 et E2F3 pour l'activation de ces gènes 479. Ainsi, le complexe ternaire BAP1/HCF-1/YY1 aurait un rôle majeur pour la régulation de l'activation et la répression génique des gènes cible de E2F. De plus, les résultats d'analyse génomique démontrent aussi que BAP1 régulent l'expression des gènes impliqués dans d'autres processus cellulaires. En effet, la déplétion de BAP1 provoque une dérégulation de l'expression des gènes mitochondriaux et des gènes qui encodent pour des enzymes de régulation du métabolisme 78. De manière plus importante, YY1 est connu pour réguler une panoplie de gènes mitochondriaux 480-482. De même des études récentes ont révélés que HCF-1 émerge comme un nouveau régulateur transcriptionnel de certains gènes du métabolisme cellulaire 274,291. Ainsi, nous avons démontré que le complexe BAP1/HCF-1 est recruté par YY1 pour activer l'expression du gène mitochondriale cox7c 78.

Afin de mieux déterminer le spectre des gènes régulés par le complexe BAP1, il serait important de comprendre d'avantage comment les régulations épigénétiques sont coordonnées au niveau de la chromatine. Étant un complexe à plusieurs activités enzymatiques, la coordination de la fonction de ces facteurs de modification de la chromatine permettrait une régulation hautement contrôlée de l'expression génique.

5.4.2 Dualité fonctionnelle du complexe BAP1 pour la régulation de la prolifération cellulaire

Depuis sa découverte, le mécanisme d'action exact de BAP1 dans la régulation du cycle cellulaire n'est toujours pas élucidé. Néanmoins plusieurs évidences démontrent clairement que BAP1 est un gène suppresseur de tumeurs majeur. Ce qui est à nos jours encore intriguant est qu'aussi bien la déplétion que la surexpression de BAP1 promouvaient l'inhibition de la prolifération de cellules cancéreuses. Ceci, démontre qu'un propre dosage du niveau de BAP1 est important pour maintenir une prolifération harmonieuse des cellules. A présent, une des explications les plus plausibles qui justifie la dérégulation de la prolifération cellulaire est que le changement de l'état d'expression de BAP1 est probablement à l'origine d'une expression non contrôlée des gènes cible de E2F.

Afin de mieux clarifier le mécanisme de régulation du cycle cellulaire par BAP1, il est important de corréler la fonction de cette DUB avec le rôle que peuvent avoir ses partenaires. En effet, HCF-1, OGT et YY1 régulent de manière étroite l'expression des gènes cible de E2F. De plus, l'interaction de BAP1 avec HCF-1 semble être importante pour la régulation de la prolifération cellulaire médiée par BAP1 233. Ainsi, E2F1 requiert HCF-1 afin de favoriser le recrutement de Set1 et MLL sur les gènes cible de E2F 270. YY1 se positionne comme étant un partenaire important pour favoriser le recrutement de BAP1 sur les gènes cibles. Ce facteur de transcription est connu pour jouer le rôle d'un activateur et d'un suppresseur transcriptionnel et ce dépendamment des gènes cibles qu'il régule483. D'autre part, les protéines ASXL1 et ASXL2 semblent être des facteurs importants pour mettre en place une dualité fonctionnelle du complexe BAP1. En effet ces protéines s'intègrent au sein des protéines qui se définissent par avoir aussi bien les caractéristiques fonctionnelles des Polycombes que des Thritorax 361-364. De ce fait nous pouvons suggérer que ASXL1 et ASXL2 gouvernent le changement de régulation transcriptionnel de BAP1 et ce dépendamment de son interaction spécifique avec ASXL1 ou ASXL2. Plus particulièrement, les complexes BAP1/ASXL1 et BAP1/ASXL2 réguleraient plusieurs processus cellulaires incluant la prolifération cellulaire et ce en catalysant l'activation ou la répression génique via la coordination de la deubiquitination de H2Aub avec H3K4me3 et H3K27me3. De plus, il a été reporté que plusieurs partenaires de ASXL1 et ASXL2 régulent directement la transition G1/S du cycle cellulaire 270,479,484. Nous avons récemment démontré que BAP1/ASXL1 et BAP1ASXL2 sont deux complexes protéiques dont leurs fonctions dans la régulation de la prolifération cellulaire est antagoniste 209. Néanmoins, le mécanisme de régulation ainsi que le spectre des gènes régulés par ces complexes restent très peu définis. Toutes ces évidences suggèrent que BAP1/ASXL1 et BAP1/ASXL2 réguleraient les gènes cibles de E2F afin de contrôler la progression du cycle cellulaire au cours de la transition G1/S. Ainsi, une dérégulation des complexes associés à ces protéines serait à l'origine de défauts pouvant conduire à des transformations cellulaires.

Une nouvelle étude a récemment dévoilé un nouveau rôle potentiel de BAP1 dans les cellules cancéreuses du sein. Le rôle de BAP1 comme gène suppresseur de tumeurs semble être beaucoup plus complexe qu'on le pense. Les auteurs ont proposé que BAP1 puisse être

une cible thérapeutique au niveau du cancer du sein et probablement dans d'autres types de cancer 485. Dans cette même investigation, il a été reporté que BAP1 stabilise les niveaux protéiques de KLF5, un facteur transcriptionnel surexprimé au niveau des cellules cancéreuses du sein de type Erα négatives. Également, il a été proposé que KLF5 s'intègre au sein d'un complexe protéique formé principalement de BAP1. HCF-1 et OGT. De ce fait, il a été reporté pour la première fois que BAP1/KLF5 régule l'expression génique de l'inhibiteur du cycle cellulaire, p27 et que cette interaction est requise pour promouvoir la prolifération cellulaire ainsi que l'induction de l'état métastatique des cellules cancéreuses 485.

BAP1 est un gène suppresseur de tumeurs fréquemment muté dans une multitude de cancers. Cependant, BAP1 ne présente pas de mutations identifiées au sein des cellules cancéreuses du sein HCC1806 prise comme modèle au cours de l'étude de l'interaction de BAP1 avec KLF5. Même si les auteurs ont reporté que la déplétion de BAP1 cause une inhibition de la prolifération à la phase S du cycle cellulaire, la surexpression de KLF5 reverse de manière partielle ce défaut cellulaire suggérant que des investigations plus poussées sont nécessaires afin de mieux comprendre le mécanisme d'action de BAP1/KLF5.

La grande majorité des données suggèrent que BAP1 s'incorpore au sein de différents complexes protéiques lui permettant de se procurer une dualité fonctionnelle pour l'exécution de sa fonction suppressive de tumeurs.

5.4.3 Co-stabilisation protéique entre BAP1 et ASXL1/2

Les deux protéines Polycombes ASXL1 et ASXL2 (ASXL1/2) ont suscité notre intérêt du faite de la particularité fonctionnelle qu'elles peuvent ajouter au mécanisme d'action de BAP1. En effet, l'association de cette DUB avec ASXL1/2 souligne son rôle unique comme complexe Polycombe. Nous avons contribué à développer un nouvel aperçu quand au mécanisme par lequel l'activité catalytique de ce gène suppresseur de tumeur est contrôlée 209.

D'abord, nous avons défini le mécanisme d'interaction entre BAP1 et ASXL1/2. De ce fait, nous avons défini le domaine CTD de BAP1 comme région commune requise pour

favoriser son interaction avec ASXL1/2. De même, ASXL1/2 présentent leur domaine ASXM pour interagir avec BAP1. Nous avons présenté qu'il existe une co-régulation protéique entre BAP1 et ASXL1/2. En effet, la déplétion conjointe de ASXL1/2 induit une déstabilisation des niveaux protéiques de BAP1 de manière similaire à la déplétion de BAP1 lui-même par siRNA. Cette régulation de BAP1 par les protéines Polycombes est un processus qui a été conservé au cours de l'évolution puisque la déplétion de ASX chez la Drosophile déstabilise également Calypso (dBAP1) 79. De manière plus spécifique, la déplétion par siRNA de ASXL1 ou de ASXL2 permet de réduire de moitié le niveau protéique de BAP1. Compte tenu de ce qui précède et du fait que le complexe BAP1 admet relativement la même quantité en ASXL1/2, nous proposons que BAP1 forme deux complexes mutuellement exclusifs avec ASXL1 et ASXL2 qui pourraient se retrouver à la même abondance dans les cellules.

Afin de caractériser d'avantage la relation fonctionnelle entre BAP1 et ASXL1/2, nous avons démontré que la déplétion de BAP1 par siRNA affecte plus spécifiquement les niveaux protéiques de ASXL2. De plus, ASXL2 est déstabilisée suite à la perte de BAP1 dans deux types de cellules cancéreuses prises comme modèles dans notre étude à savoir les cellules H28 du mésothéliome et les cellules H226 du cancer du poumon. De plus, suite à des expériences d'immunodéplétion, nous révélons que la majorité de ASXL2 est complexée avec BAP1 alors que la moitié du niveau protéique de ce dernier s'associe avec ASXL2. Ces résultats révèlent pour la première fois une relation fonctionnelle entre BAP1 et ASXL2 et soulignent l'importance de maintenir un complexe BAP1/ASXL2 stable au sein des cellules. L'apparition de mutations au niveau des cancers qui provoquent une inactivation ou une perte de BAP1 ou de ASXL2 seraient à l'origine d'une inactivation fonctionnelle de l'autre partenaire 209.

5.4.4 Rôle de ASXL1/2 dans la coordination de l'activité catalytique de BAP1

Il a été déjà reporté que BAP1 forme un complexe minimal avec la région N-terminale de ASXL1 requis pour initier in vitro l'activité catalytique de cette DUB envers la forme monoubiquitinée de H2A (H2Aub) 79. La déubiquitination de H2Aub in vivo par

BAP1 et d'autres DUBs a été aussi observée 182,448. Néanmoins la contribution de chacune de ces enzymes ainsi que le mécanisme de régulation gouvernant cette déubiquitination n'avait pas été définis. Nous nous sommes donc intéressés à investiguer d'avantage le mécanisme de déubiquitination de H2Aub médié par BAP1 et à étudier l'implication de ASXL1/2 dans l'activation de la catalyse. Tout d'abord, nous avons réalisé un criblage RNAi en traitant des cellules par des siRNA individuels couvrant toutes les DUBs du génome humain. Nos résultats ont révélé que BAP1 est la seule enzyme dont la déplétion a engendré l'augmentation la plus significative du niveau global de H2Aub. Ceci suggère fortement que BAP1 représente la DUB majeure pour cette modification en conditions de proliférations normales.

Par des expériences de perte de fonction et de surexpression, nous avons démontré que ASXL1 et ASXL2 sont tous les deux indispensables pour induire la déubiquitination de H2Aub par BAP1. Plus spécifiquement, le domaine ASXM de ASXL1/2 est suffisant pour stimuler une déubiquitination totale de H2Aub par BAP1. Ainsi, une bonne interaction entre BAP1 et ASXL1/2 est requise pour maintenir l'activité catalytique de BAP1 puisque les mutants de BAP1, BAP1ΔCTD et BAP1ΔR666-H669 sont incapables de déubiquitiner H2Aub in vivo et in vitro. Ces résultats concordent avec le dernier travail de Rao et ses collègues qui ont démontré que des formes tronquées de ASXL1 qui ont perdu la région C-terminale de la protéine, sont capables grâce à la présence du domaine ASXM de stabiliser l'activité catalytique de BAP1 envers H2Aub 445.

D'un point de vue mécanistique, nous avons défini de plus près la liaison de BAP1 à l'ubiquitine ainsi que le rôle majeur que possède ASXL1/2 pour favoriser et stabiliser cette interaction. Plus particulièrement, nous avons défini un modèle unique de liaison des complexes BAP1/ASXLs à l'ubiquitine. En effet, nous présentons que BAP1 en association avec ASXLs permet de créer un domaine composite particulier (CUBI pour Composit Ubiquitin Binding Interface) de liaison à l'ubiquitine qui requiert la participation des domaines ASXM de ASXL1/2 (nommés ASXM1 et ASXM2 pour ASXL1 et ASXL2 respectivement) ainsi que les domaines UCH, CC1 et CTD de BAP1. Plus spécifiquement, ASXM2 admet une affinité faible envers l'ubiquitine mais permet d'augmenter considérablement la liaison de BAP1 sur l'ubiquitine. De plus, nos résultats soulignent un rôle important du domaine CTD dans l'intégration de la liaison à l'ubiquitine avec l'activité catalytique du complexe

BAP1/ASXL1/2. De ce fait le CTD est (i) qualifié comme étant un nouveau domaine de liaison à l'ubiquitine (UBD) qui se lie à un patch chargé au niveau de cette molécule (RQDR charged patch), (ii) permet de maintenir les interactions intramoléculaires avec les domaines UCH et CC1 afin de stabiliser la liaison de BAP1 à l'ubiquitine via son domaine UCH, (iii) interagi fortement avec ASXM ce qui permet la formation du CUBI et de ce fait l'induction de la liaison à l'ubiquitine du complexe BAP1/ASXL1/2 et la stimulation de l'activité catalytique de BAP1. Cette liaison à l'ubiquitine est particulière puisqu'elle nécessite la reconnaissance de différents patchs de l'ubiquitine, le patch hydrophobe et le patch RQDR par l'intermédiaire du UCH et du CTD respectivement 209.

Ce modèle de liaison à l'ubiquitine et d'activation de la catalyse ressemble à celui entrepris par UCH37, une DUB appartenant à la famille des UCH. UCH37 admet des domaines UCH et ULD similaires aux domaines UCH et CTD de BAP1. De manière analogue à BAP1, UCH37 se lie au patch hydrophobe de l'ubiquitine via son domaine UCH grâce à des acides aminés qui sont conservés entre BAP1 et UCH37 436,437. De plus, son affinité envers l'ubiquitine ainsi que son activité catalytique sont significativement stimulé grâce à la sous-unité protéique du protéasome RPN13 (ADRM1) 441-443,450,451. RPN13 possède un domaine DEUBAD (DEUBiquitinase ADaptor) similaire au domaine ASXM de ASXL1/2 378. Il a été de même démontré que RPN13 admet une affinité faible envers l'ubiquitine 450,451. De ce fait nos résultats révèlent pour la première fois que le mécanisme d'activation des DUBs de la famille des UCHs (BAP1 et UCH37) par l'intermédiaire de cofacteurs, est un processus conservé. Un mécanisme de régulation négative de l'activité catalytique de BAP1 peut également être suggéré. En effet, il a été défini que INO80G (NFRKB), un composant du complexe INO80 de remodelage de la chromatine possède aussi un domaine DEUBAD, mais que contrairement à RPN13, inhibe la fonction catalytique de UCH37 450,451. BAP1 est connu pour interagir et déubiquitiner INO80 439. De même, nous avons démontré que de manière similaire à BAP1, INO80 représente un substrat pour UBE2O et sa polyubiquitination induite par cette enzyme provoque sa séquestration dans le cytoplasme 241. UBE2O semble avoir un rôle majeur dans la régulation des voies de signalisation qui gouvernent le transport nucléocytoplasmique. De ce fait, il serait intéressant de déterminer si dans certains contextes

cellulaires spécifiques, l'ubiquitination serait un signal pour favoriser l'interaction de BAP1 avec INO80 au dépend de son interaction avec ASXL1/2 et de ce fait son inhibition.

5.4.5 L'interaction de BAP1 avec ASXL1/2 est requise pour la bonne exécution de sa fonction suppressive de tumeurs

Nous nous sommes demandés si l'interaction de BAP1 avec ASXL1/2, pouvaient influencer la prolifération cellulaire et la fonction suppressive de tumeurs de cette DUB.

Au niveau des cellules de mammifères les rôles fonctionnels de BAP1/ASXL1 et BAP1/ASXL2 sont très peu caractérisés.

ASXL1 semble s'associer à des complexes épigénétiques distincts et ce dépendamment du type cellulaire ou des conditions physiologiques de la cellule. En effet, l'étude du groupe de Levine a démontré que même BAP1 et ASXL1 interagissent dans des cellules leucémiques myéloïdes, mais aucune relation fonctionnelle entre ces deux facteurs épigénétiques n'a été révélée 375. De plus, dans la même étude, il a été reporté qu'ASXL1 s'associe au complexe PRC2 de façon indépendante de son interaction avec BAP1 afin de promouvoir le recrutement de PRC2 au niveau des promoteurs des gènes cibles et la triméthylation de H3K27. D'autre part, le groupe de Rao a décrit que des mutations fréquentes de ASXL1 dans des leucémies myéloïdes ou le syndrome de Bohring–Opitz provoquent la génération de protéines tronquées de ASXL1 qui confèrent un gain de fonction du complexe ASXL1/BAP1 et ce grâce à la présence du domaine ASXM. En effet, la surexpression de ces complexes dans des cellules souches hématopoïétiques induit une déubiquitination globale de H2Aub, une diminution significative de H3K27me3 ainsi qu'une augmentation sélective de H3K4me3 sur certains gènes bivalents dont les promoteurs sont marqués par H2Aub et H3K4me3. Ces évènements épigénétiques qui dépendent de l'activité catalytique de BAP1 sont à l' origine d'une différentiation spontanée des précurseurs hématopoïétiques en mastocytes 445. Notre travail représente la première description qui soulève un lien fonctionnel entre BAP1 et ASXL1/2 dans la régulation de la fonction suppressive de tumeurs de cette DUB. Nos données démontrent que l'interaction de BAP1 avec ASXL/2 est requise

pour maintenir une prolifération harmonieuse des cellules. En effet, par des expériences de perte de fonctions dans des cellules stables exprimant différentes formes de BAP1 résistants aux siRNA, nous avons révélé que la délétion du CTD ainsi que la mutation R666-H669, provoquent une inhibition de l'activité catalytique de BAP1 associée à une incapacité de celui-ci à restaurer l'augmentation du niveau de H2Aub obtenue suite à la déplétion de la forme endogène de BAP1. Ceci a eu pour conséquence une dérégulation du cycle cellulaire. Nos résultats supportent le fait que des mutations de cancer touchant le domaine UCH sont à l'origine d'une augmentation du niveau global de H2Aub dans les cellules cancéreuses et une dérégulation du cycle cellulaire 77,231,250. Encore plus remarquable, la surexpression de BAP1 et de BAP1 catalytique inactif (BAP1 C91S) dans les cellules de fibroblastes primaires IMR90, induit la sénescence cellulaire, un mécanisme de suppression de tumeurs majeur 486-491. Cette réponse cellulaire semble s'intégrer dans la voie de réponse aux dommages à l'ADN de p53/p21. Plus spécifiquement, la sénescence induite par BAP1 est dépendante de son interaction avec ASXL1/2 puisque BAP1ΔCTD et le mutant de cancer de BAP1 (R666-H669) sont incapables de promouvoir la sénescence. Un autre résultat très intéressant, est que contrairement à ASXL1, la surexpression de ASXL2 dans les IMR90 induit la sénescence cellulaire de façon dépendante de l'interaction avec BAP1 du fait que ASXL2 ΔASXM est incapable de promouvoir cette réponse.

La régulation de la sénescence par le complexe BAP1 peut se produire de différents moyens. En effet, du fait que BAP1 interagi avec HCF-1 et YY1 qui eux sont des régulateurs majeurs des gènes cibles de E2F, la surexpression de BAP1/ASXL2 pourrait engendrer un stress réplicatif suite à la surexpression des gènes cibles de E2F comme CDC6 et E2F1, qui stimulerait une ré-réplication de l'ADN et serait à l'origine de l'établissement d'une réponse de dommages de l'ADN et l'induction de la voie oncogénique de la sénescence 492,493. De plus, BAP1/ASXL1/2 pourrait réguler l'expression de gènes encodant pour des inhibiteurs du cycle cellulaire. En effet, l'inhibiteur des kinases dépendantes des cyclines 1A, p21, est étroitement régulé par E2F1 et est impliqué dans l'induction de la sénescence494,495. De plus, différentes composantes des complexes PRC1 ont été identifiées comme jouant un rôle important dans la régulation de la signalisation de la sénescence. En effet, les complexes PRC1 modulent de façon très étroite l'état d'expression du locus INK4b/ARF/INK4α qui code pour

les protéines, p15INK4b, ARF et p16INK4α, acteurs universels de la sénescence 62,452,496-501. Ainsi, la surexpression de protéines du PRC1 incluant les protéines CBX ou la déplétion de BMI1 engendre respectivement une inhibition ou une de-répression de l'expression des protéines ARF et p16. De ce fait, du moment que le complexe BAP1 regroupe plusieurs régulateurs transcriptionnels (facteurs de transcription et facteurs de remodelage de la chromatine), la surexpression de BAP1 pourrait donc agir au niveau de la chromatine en contrecarrant l'action des complexes PRC1. Le rôle de BAP1 dans le contrôle du locus INK4b/ARF/INK4α a été récemment reporté 502. En effet, le complexe BAP1/ASXL1 est recruté au niveau de ce locus afin de permettre l'activation spécifique du gène p15INK4b en réponse à des signalisations oncogéniques et des stimuli externe antiprolifératives. Cette activité de suppression tumorale requiert la deubiquitination de H2Aub 502. Ainsi, il n'est pas à exclure que BAP1/ASXL2, comme c'est le cas pour BAP1/ASXL1, régulerait de manière directe l'expression du INK4b/ARF/INK4α, sachant également que ARF est un gène cible de E2F1.

De plus, compte tenu de la dernière découverte sur le mécanisme de répression génétique par les protéines Polycombes qui peuvent agir de manière indépendante de leurs activité catalytique, nous pouvons penser que BAP1C91S pourrait entreprendre un mécanisme similaire pour catalyser la de-répression des gènes E2F, activer la voie p53/p21 et induire la sénescence. D'autre part, la surexpression d'ASXL2 et de BAP1 pourrait induire un changement structurel de la chromatine qui serait à l'origine de l'apparition de dommages de l'ADN double brins. Des dérégulations dans le contrôle de tous ces mécanismes liés à la chromatine seraient à l'origine de défauts du cycle cellulaire et le développement de cancer. De ce fait, nos résultats démontrent qu'un propre dosage des niveaux protéiques de BAP1 et de ASXL2 dans les cellules ainsi que le maintien du complexe BAP1/ASXL2 sont des facteurs importants pour la régulation de la fonction suppressive de tumeurs de BAP1.

L'étude globale du complexe BAP1 démontre à présent que cette déubiquitinase admet un rôle majeur dans la régulation de la signalisation cellulaire associée à la chromatine et ce en adoptant possiblement plusieurs mécanismes. En effet, le complexe BAP1 pourrait avoir une fonction de (i) ''writer'' et ce grâce à l'action de la OGT qui modifie par O-GlcNAcylation les protéines associées à la chromatine et l'acetyltransferase HAT qui catalyse l'acétylation des

histones, de (ii) ‘‘reader’’ par l’intermédiaire de ASXL1/2 qui se lient au niveau de la chromatine grâce à leur domaines PHD et ASXN (qui probablement va lier l’ADN) et ASXM (qui permettrait au complexe BAP1 de se lier à son substrat physiologique, H2Aub) et de ‘‘eraser’’ et ce grâce à BAP1 lui-même et LSD2 (à travers la déubiquitination et la déméthylation des histones respectivement).

D’autres études seront nécessaires afin compléter notre compréhension des mécanismes d’action et la régulation de cette machine moléculaire, un complexe déubiquitinase requis pour la fonction de la chromatine et la suppression de tumeurs.

RÉFÉRENCES :

1 Margueron, R. & Reinberg, D. Chromatin structure and the inheritance of epigenetic information. *Nat Rev Genet* **11**, 285-296, doi:10.1038/nrg2752 (2010).

2 Probst, A. V., Dunleavy, E. & Almouzni, G. Epigenetic inheritance during the cell cycle. *Nature reviews. Molecular cell biology* **10**, 192-206, doi:10.1038/nrm2640 (2009).

3 Khorasanizadeh, S. The nucleosome: from genomic organization to genomic regulation. *Cell* **116**, 259-272 (2004).

4 Becker, P. B. & Horz, W. ATP-dependent nucleosome remodeling. *Annu Rev Biochem* **71**, 247-273, doi:10.1146/annurev.biochem.71.110601.135400 (2002).

5 Saha, A., Wittmeyer, J. & Cairns, B. R. Chromatin remodelling: the industrial revolution of DNA around histones. *Nature reviews. Molecular cell biology* **7**, 437-447, doi:10.1038/nrm1945 (2006).

6 Kornberg, R. D. Chromatin structure: a repeating unit of histones and DNA. *Science* **184**, 868-871 (1974).

7 Kornberg, R. D. & Thomas, J. O. Chromatin structure; oligomers of the histones. *Science* **184**, 865-868 (1974).

8 Luger, K., Mader, A. W., Richmond, R. K., Sargent, D. F. & Richmond, T. J. Crystal structure of the nucleosome core particle at 2.8 A resolution. *Nature* **389**, 251-260, doi:10.1038/38444 (1997).

9 Caterino, T. L. & Hayes, J. J. Structure of the H1 C-terminal domain and function in chromatin condensation. *Biochem Cell Biol* **89**, 35-44, doi:10.1139/O10-024 (2011).

10 Oudet, P., Gross-Bellard, M. & Chambon, P. Electron microscopic and biochemical evidence that chromatin structure is a repeating unit. *Cell* **4**, 281-300 (1975).

11 Clapier, C. R. & Cairns, B. R. The biology of chromatin remodeling complexes. *Annu Rev Biochem* **78**, 273-304, doi:10.1146/annurev.biochem.77.062706.153223 (2009).

12 Zentner, G. E. & Henikoff, S. Regulation of nucleosome dynamics by histone modifications. *Nature structural & molecular biology* **20**, 259-266, doi:10.1038/nsmb.2470 (2013).

13 Kouzarides, T. Chromatin modifications and their function. *Cell* **128**, 693-705, doi:10.1016/j.cell.2007.02.005 (2007).

14 Campos, E. I. & Reinberg, D. Histones: annotating chromatin. *Annual review of genetics* **43**, 559-599, doi:10.1146/annurev.genet.032608.103928 (2009).

15 Lelli, K. M., Slattery, M. & Mann, R. S. Disentangling the many layers of eukaryotic transcriptional regulation. *Annual review of genetics* **46**, 43-68, doi:10.1146/annurev-genet-110711-155437 (2012).
16 Ruthenburg, A. J., Li, H., Patel, D. J. & Allis, C. D. Multivalent engagement of chromatin modifications by linked binding modules. *Nature reviews. Molecular cell biology* **8**, 983-994, doi:10.1038/nrm2298 (2007).
17 Shilatifard, A. Chromatin modifications by methylation and ubiquitination: implications in the regulation of gene expression. *Annu Rev Biochem* **75**, 243-269, doi:10.1146/annurev.biochem.75.103004.142422 (2006).
18 Chi, P., Allis, C. D. & Wang, G. G. Covalent histone modifications--miswritten, misinterpreted and mis-erased in human cancers. *Nature reviews. Cancer* **10**, 457-469, doi:10.1038/nrc2876 (2010).
19 Strahl, B. D. & Allis, C. D. The language of covalent histone modifications. *Nature* **403**, 41-45, doi:10.1038/47412 (2000).
20 Fujiki, R. *et al.* GlcNAcylation of histone H2B facilitates its monoubiquitination. *Nature* **480**, 557-560, doi:10.1038/nature10656 (2011).
21 Sakabe, K., Wang, Z. & Hart, G. W. Beta-N-acetylglucosamine (O-GlcNAc) is part of the histone code. *Proceedings of the National Academy of Sciences of the United States of America* **107**, 19915-19920, doi:10.1073/pnas.1009023107 (2010).
22 Tan, M. *et al.* Identification of 67 histone marks and histone lysine crotonylation as a new type of histone modification. *Cell* **146**, 1016-1028, doi:10.1016/j.cell.2011.08.008 (2011).
23 Phillips, D. M. The presence of acetyl groups of histones. *The Biochemical journal* **87**, 258-263 (1963).
24 Allfrey, V. G., Faulkner, R. & Mirsky, A. E. Acetylation and Methylation of Histones and Their Possible Role in the Regulation of Rna Synthesis. *Proceedings of the National Academy of Sciences of the United States of America* **51**, 786-794 (1964).
25 Bannister, A. J. & Kouzarides, T. Regulation of chromatin by histone modifications. *Cell Res* **21**, 381-395, doi:10.1038/cr.2011.22 (2011).
26 Bedford, M. T. & Clarke, S. G. Protein arginine methylation in mammals: who, what, and why. *Molecular cell* **33**, 1-13, doi:10.1016/j.molcel.2008.12.013 (2009).
27 Hon, G. C., Hawkins, R. D. & Ren, B. Predictive chromatin signatures in the mammalian genome. *Hum Mol Genet* **18**, R195-201, doi:10.1093/hmg/ddp409 (2009).
28 Mosammaparast, N. & Shi, Y. Reversal of histone methylation: biochemical and molecular mechanisms of histone demethylases. *Annu Rev Biochem* **79**, 155-179, doi:10.1146/annurev.biochem.78.070907.103946 (2010).
29 Roth, S. Y., Denu, J. M. & Allis, C. D. Histone acetyltransferases. *Annu Rev Biochem* **70**, 81-120, doi:10.1146/annurev.biochem.70.1.81 (2001).
30 Shilatifard, A. The COMPASS family of histone H3K4 methylases: mechanisms of regulation in development and disease pathogenesis. *Annu Rev Biochem* **81**, 65-95, doi:10.1146/annurev-biochem-051710-134100 (2012).
31 Steffen, P. A. & Ringrose, L. What are memories made of? How Polycomb and Trithorax proteins mediate epigenetic memory. *Nature reviews. Molecular cell biology* **15**, 340-356, doi:10.1038/nrm3789 (2014).

32 Helin, K. & Dhanak, D. Chromatin proteins and modifications as drug targets. *Nature* **502**, 480-488, doi:10.1038/nature12751 (2013).
33 Schuettengruber, B., Martinez, A. M., Iovino, N. & Cavalli, G. Trithorax group proteins: switching genes on and keeping them active. *Nature reviews. Molecular cell biology* **12**, 799-814, doi:10.1038/nrm3230 (2011).
34 Ringrose, L. & Paro, R. Epigenetic regulation of cellular memory by the Polycomb and Trithorax group proteins. *Annual review of genetics* **38**, 413-443, doi:10.1146/annurev.genet.38.072902.091907 (2004).
35 Cao, R. *et al.* Role of histone H3 lysine 27 methylation in Polycomb-group silencing. *Science* **298**, 1039-1043, doi:10.1126/science.1076997 (2002).
36 Cao, R. & Zhang, Y. SUZ12 is required for both the histone methyltransferase activity and the silencing function of the EED-EZH2 complex. *Molecular cell* **15**, 57-67, doi:10.1016/j.molcel.2004.06.020 (2004).
37 Kuzmichev, A., Nishioka, K., Erdjument-Bromage, H., Tempst, P. & Reinberg, D. Histone methyltransferase activity associated with a human multiprotein complex containing the Enhancer of Zeste protein. *Genes & development* **16**, 2893-2905, doi:10.1101/gad.1035902 (2002).
38 Levine, S. S. *et al.* The core of the polycomb repressive complex is compositionally and functionally conserved in flies and humans. *Molecular and cellular biology* **22**, 6070-6078 (2002).
39 Wang, H. *et al.* Role of histone H2A ubiquitination in Polycomb silencing. *Nature* **431**, 873-878, doi:10.1038/nature02985 (2004).
40 Margueron, R. & Reinberg, D. The Polycomb complex PRC2 and its mark in life. *Nature* **469**, 343-349, doi:10.1038/nature09784 (2011).
41 Ringrose, L. Polycomb comes of age: genome-wide profiling of target sites. *Current opinion in cell biology* **19**, 290-297, doi:10.1016/j.ceb.2007.04.010 (2007).
42 Christophersen, N. S. & Helin, K. Epigenetic control of embryonic stem cell fate. *The Journal of experimental medicine* **207**, 2287-2295, doi:10.1084/jem.20101438 (2010).
43 Dillon, N. Factor mediated gene priming in pluripotent stem cells sets the stage for lineage specification. *BioEssays : news and reviews in molecular, cellular and developmental biology* **34**, 194-204, doi:10.1002/bies.201100137 (2012).
44 Kennison, J. A. Introduction to Trx-G and Pc-G genes. *Methods in enzymology* **377**, 61-70, doi:10.1016/S0076-6879(03)77003-7 (2004).
45 Schumacher, A. & Magnuson, T. Murine Polycomb- and trithorax-group genes regulate homeotic pathways and beyond. *Trends in genetics : TIG* **13**, 167-170 (1997).
46 Akam, M. The molecular basis for metameric pattern in the Drosophila embryo. *Development* **101**, 1-22 (1987).
47 Lewis, E. B. A gene complex controlling segmentation in Drosophila. *Nature* **276**, 565-570 (1978).
48 Ingham, P. W. Differential expression of bithorax complex genes in the absence of the extra sex combs and trithorax genes. *Nature* **306**, 591-593 (1983).

49 Ingham, P. W. trithorax and the regulation of homeotic gene expression in Drosophila: a historical perspective. *The International journal of developmental biology* **42**, 423-429 (1998).
50 Cavalli, G. & Paro, R. Epigenetic inheritance of active chromatin after removal of the main transactivator. *Science* **286**, 955-958 (1999).
51 Kennison, J. A. & Tamkun, J. W. Dosage-dependent modifiers of polycomb and antennapedia mutations in Drosophila. *Proceedings of the National Academy of Sciences of the United States of America* **85**, 8136-8140 (1988).
52 Maeda, R. K. & Karch, F. The ABC of the BX-C: the bithorax complex explained. *Development* **133**, 1413-1422, doi:10.1242/dev.02323 (2006).
53 Soshnikova, N. & Duboule, D. Epigenetic regulation of vertebrate Hox genes: a dynamic equilibrium. *Epigenetics : official journal of the DNA Methylation Society* **4**, 537-540 (2009).
54 Mendenhall, E. M. & Bernstein, B. E. Chromatin state maps: new technologies, new insights. *Current opinion in genetics & development* **18**, 109-115, doi:10.1016/j.gde.2008.01.010 (2008).
55 Eissenberg, J. C. & Shilatifard, A. Histone H3 lysine 4 (H3K4) methylation in development and differentiation. *Developmental biology* **339**, 240-249, doi:10.1016/j.ydbio.2009.08.017 (2010).
56 Ang, Y. S. *et al.* Wdr5 mediates self-renewal and reprogramming via the embryonic stem cell core transcriptional network. *Cell* **145**, 183-197, doi:10.1016/j.cell.2011.03.003 (2011).
57 Bagchi, A. *et al.* CHD5 is a tumor suppressor at human 1p36. *Cell* **128**, 459-475, doi:10.1016/j.cell.2006.11.052 (2007).
58 Pullirsch, D. *et al.* The Trithorax group protein Ash2l and Saf-A are recruited to the inactive X chromosome at the onset of stable X inactivation. *Development* **137**, 935-943, doi:10.1242/dev.035956 (2010).
59 Tyagi, S. & Herr, W. E2F1 mediates DNA damage and apoptosis through HCF-1 and the MLL family of histone methyltransferases. *The EMBO journal* **28**, 3185-3195, doi:10.1038/emboj.2009.258 (2009).
60 Kotake, Y., Zeng, Y. & Xiong, Y. DDB1-CUL4 and MLL1 mediate oncogene-induced p16INK4a activation. *Cancer research* **69**, 1809-1814, doi:10.1158/0008-5472.CAN-08-2739 (2009).
61 Sharpless, N. E. *et al.* Loss of p16Ink4a with retention of p19Arf predisposes mice to tumorigenesis. *Nature* **413**, 86-91, doi:10.1038/35092592 (2001).
62 Bracken, A. P. *et al.* The Polycomb group proteins bind throughout the INK4A-ARF locus and are disassociated in senescent cells. *Genes & development* **21**, 525-530, doi:10.1101/gad.415507 (2007).
63 Kia, S. K., Gorski, M. M., Giannakopoulos, S. & Verrijzer, C. P. SWI/SNF mediates polycomb eviction and epigenetic reprogramming of the INK4b-ARF-INK4a locus. *Molecular and cellular biology* **28**, 3457-3464, doi:10.1128/MCB.02019-07 (2008).
64 Krogan, N. J. *et al.* COMPASS, a histone H3 (Lysine 4) methyltransferase required for telomeric silencing of gene expression. *The Journal of biological chemistry* **277**, 10753-10755, doi:10.1074/jbc.C200023200 (2002).

65 Miller, T. *et al.* COMPASS: a complex of proteins associated with a trithorax-related SET domain protein. *Proceedings of the National Academy of Sciences of the United States of America* **98**, 12902-12907, doi:10.1073/pnas.231473398 (2001).
66 Roguev, A. *et al.* The Saccharomyces cerevisiae Set1 complex includes an Ash2 homologue and methylates histone 3 lysine 4. *The EMBO journal* **20**, 7137-7148, doi:10.1093/emboj/20.24.7137 (2001).
67 Mohan, M., Lin, C., Guest, E. & Shilatifard, A. Licensed to elongate: a molecular mechanism for MLL-based leukaemogenesis. *Nature reviews. Cancer* **10**, 721-728, doi:10.1038/nrc2915 (2010).
68 Ito, S. *et al.* Tet proteins can convert 5-methylcytosine to 5-formylcytosine and 5-carboxylcytosine. *Science* **333**, 1300-1303, doi:10.1126/science.1210597 (2011).
69 Dou, Y. *et al.* Physical association and coordinate function of the H3 K4 methyltransferase MLL1 and the H4 K16 acetyltransferase MOF. *Cell* **121**, 873-885, doi:10.1016/j.cell.2005.04.031 (2005).
70 Goo, Y. H. *et al.* Activating signal cointegrator 2 belongs to a novel steady-state complex that contains a subset of trithorax group proteins. *Molecular and cellular biology* **23**, 140-149 (2003).
71 Lee, S. *et al.* Coactivator as a target gene specificity determinant for histone H3 lysine 4 methyltransferases. *Proceedings of the National Academy of Sciences of the United States of America* **103**, 15392-15397, doi:10.1073/pnas.0607313103 (2006).
72 Wang, L. *et al.* Hierarchical recruitment of polycomb group silencing complexes. *Molecular cell* **14**, 637-646, doi:10.1016/j.molcel.2004.05.009 (2004).
73 Schuettengruber, B., Chourrout, D., Vervoort, M., Leblanc, B. & Cavalli, G. Genome regulation by polycomb and trithorax proteins. *Cell* **128**, 735-745, doi:10.1016/j.cell.2007.02.009 (2007).
74 Klymenko, T. *et al.* A Polycomb group protein complex with sequence-specific DNA-binding and selective methyl-lysine-binding activities. *Genes & development* **20**, 1110-1122, doi:10.1101/gad.377406 (2006).
75 Lagarou, A. *et al.* dKDM2 couples histone H2A ubiquitylation to histone H3 demethylation during Polycomb group silencing. *Genes & development* **22**, 2799-2810, doi:10.1101/gad.484208 (2008).
76 Abdel-Wahab, O. & Dey, A. The ASXL-BAP1 axis: new factors in myelopoiesis, cancer and epigenetics. *Leukemia* **27**, 10-15, doi:10.1038/leu.2012.288 (2013).
77 Carbone, M. *et al.* BAP1 and cancer. *Nature reviews. Cancer* **13**, 153-159 (2013).
78 Yu, H. *et al.* The ubiquitin carboxyl hydrolase BAP1 forms a ternary complex with YY1 and HCF-1 and is a critical regulator of gene expression. *Molecular and cellular biology* **30**, 5071-5085, doi:10.1128/MCB.00396-10 (2010).
79 Scheuermann, J. C. *et al.* Histone H2A deubiquitinase activity of the Polycomb repressive complex PR-DUB. *Nature* **465**, 243-247, doi:10.1038/nature08966 (2010).
80 Muller, J. *et al.* Histone methyltransferase activity of a Drosophila Polycomb group repressor complex. *Cell* **111**, 197-208 (2002).

81 Czermin, B. *et al.* Drosophila enhancer of Zeste/ESC complexes have a histone H3 methyltransferase activity that marks chromosomal Polycomb sites. *Cell* **111**, 185-196 (2002).
82 Margueron, R. *et al.* Role of the polycomb protein EED in the propagation of repressive histone marks. *Nature* **461**, 762-767, doi:10.1038/nature08398 (2009).
83 Chamberlain, S. J., Yee, D. & Magnuson, T. Polycomb repressive complex 2 is dispensable for maintenance of embryonic stem cell pluripotency. *Stem cells* **26**, 1496-1505, doi:10.1634/stemcells.2008-0102 (2008).
84 Cao, Q. *et al.* The central role of EED in the orchestration of polycomb group complexes. *Nature communications* **5**, 3127, doi:10.1038/ncomms4127 (2014).
85 Kuzmichev, A., Jenuwein, T., Tempst, P. & Reinberg, D. Different EZH2-containing complexes target methylation of histone H1 or nucleosomal histone H3. *Molecular cell* **14**, 183-193 (2004).
86 Trojer, P. *et al.* Dynamic Histone H1 Isotype 4 Methylation and Demethylation by Histone Lysine Methyltransferase G9a/KMT1C and the Jumonji Domain-containing JMJD2/KDM4 Proteins. *The Journal of biological chemistry* **284**, 8395-8405, doi:10.1074/jbc.M807818200 (2009).
87 Pasini, D. *et al.* JARID2 regulates binding of the Polycomb repressive complex 2 to target genes in ES cells. *Nature* **464**, 306-310, doi:10.1038/nature08788 (2010).
88 Landeira, D. *et al.* Jarid2 is a PRC2 component in embryonic stem cells required for multi-lineage differentiation and recruitment of PRC1 and RNA Polymerase II to developmental regulators. *Nature cell biology* **12**, 618-624, doi:10.1038/ncb2065 (2010).
89 Shen, X. *et al.* Jumonji modulates polycomb activity and self-renewal versus differentiation of stem cells. *Cell* **139**, 1303-1314, doi:10.1016/j.cell.2009.12.003 (2009).
90 Tong, Z. T. *et al.* EZH2 supports nasopharyngeal carcinoma cell aggressiveness by forming a co-repressor complex with HDAC1/HDAC2 and Snail to inhibit E-cadherin. *Oncogene* **31**, 583-594, doi:10.1038/onc.2011.254 (2012).
91 Gupta, R. A. *et al.* Long non-coding RNA HOTAIR reprograms chromatin state to promote cancer metastasis. *Nature* **464**, 1071-1076, doi:10.1038/nature08975 (2010).
92 Kaneko, S. *et al.* Phosphorylation of the PRC2 component Ezh2 is cell cycle-regulated and up-regulates its binding to ncRNA. *Genes & development* **24**, 2615-2620, doi:10.1101/gad.1983810 (2010).
93 Rinn, J. L. *et al.* Functional demarcation of active and silent chromatin domains in human HOX loci by noncoding RNAs. *Cell* **129**, 1311-1323, doi:10.1016/j.cell.2007.05.022 (2007).
94 Margueron, R. *et al.* Ezh1 and Ezh2 maintain repressive chromatin through different mechanisms. *Molecular cell* **32**, 503-518, doi:10.1016/j.molcel.2008.11.004 (2008).
95 Shen, X. *et al.* EZH1 mediates methylation on histone H3 lysine 27 and complements EZH2 in maintaining stem cell identity and executing pluripotency. *Molecular cell* **32**, 491-502, doi:10.1016/j.molcel.2008.10.016 (2008).

96 He, A. *et al.* PRC2 directly methylates GATA4 and represses its transcriptional activity. *Genes & development* **26**, 37-42, doi:10.1101/gad.173930.111 (2012).
97 Xu, K. *et al.* EZH2 oncogenic activity in castration-resistant prostate cancer cells is Polycomb-independent. *Science* **338**, 1465-1469, doi:10.1126/science.1227604 (2012).
98 Chou, D. M. *et al.* A chromatin localization screen reveals poly (ADP ribose)-regulated recruitment of the repressive polycomb and NuRD complexes to sites of DNA damage. *Proceedings of the National Academy of Sciences of the United States of America* **107**, 18475-18480, doi:10.1073/pnas.1012946107 (2010).
99 Qin, S. & Parthun, M. R. Histone H3 and the histone acetyltransferase Hat1p contribute to DNA double-strand break repair. *Molecular and cellular biology* **22**, 8353-8365 (2002).
100 Yu, Y., Teng, Y., Liu, H., Reed, S. H. & Waters, R. UV irradiation stimulates histone acetylation and chromatin remodeling at a repressed yeast locus. *Proceedings of the National Academy of Sciences of the United States of America* **102**, 8650-8655, doi:10.1073/pnas.0501458102 (2005).
101 Kennison, J. A. The Polycomb and trithorax group proteins of Drosophila: trans-regulators of homeotic gene function. *Annual review of genetics* **29**, 289-303, doi:10.1146/annurev.ge.29.120195.001445 (1995).
102 Shao, Z. *et al.* Stabilization of chromatin structure by PRC1, a Polycomb complex. *Cell* **98**, 37-46, doi:10.1016/S0092-8674(00)80604-2 (1999).
103 Lanzuolo, C. & Orlando, V. Memories from the polycomb group proteins. *Annual review of genetics* **46**, 561-589, doi:10.1146/annurev-genet-110711-155603 (2012).
104 Di Croce, L. & Helin, K. Transcriptional regulation by Polycomb group proteins. *Nature structural & molecular biology* **20**, 1147-1155, doi:10.1038/nsmb.2669 (2013).
105 Cao, R., Tsukada, Y. & Zhang, Y. Role of Bmi-1 and Ring1A in H2A ubiquitylation and Hox gene silencing. *Molecular cell* **20**, 845-854, doi:10.1016/j.molcel.2005.12.002 (2005).
106 Li, Z. *et al.* Structure of a Bmi-1-Ring1B polycomb group ubiquitin ligase complex. *The Journal of biological chemistry* **281**, 20643-20649, doi:10.1074/jbc.M602461200 (2006).
107 Gao, Z. *et al.* PCGF homologs, CBX proteins, and RYBP define functionally distinct PRC1 family complexes. *Molecular cell* **45**, 344-356, doi:10.1016/j.molcel.2012.01.002 (2012).
108 Francis, N. J., Saurin, A. J., Shao, Z. & Kingston, R. E. Reconstitution of a functional core polycomb repressive complex. *Molecular cell* **8**, 545-556 (2001).
109 Francis, N. J., Kingston, R. E. & Woodcock, C. L. Chromatin compaction by a polycomb group protein complex. *Science* **306**, 1574-1577, doi:10.1126/science.1100576 (2004).
110 King, I. F. *et al.* Analysis of a polycomb group protein defines regions that link repressive activity on nucleosomal templates to in vivo function. *Molecular and cellular biology* **25**, 6578-6591, doi:10.1128/MCB.25.15.6578-6591.2005 (2005).

111 Zhou, W. *et al.* Histone H2A monoubiquitination represses transcription by inhibiting RNA polymerase II transcriptional elongation. *Molecular cell* **29**, 69-80, doi:10.1016/j.molcel.2007.11.002 (2008).
112 Joazeiro, C. A. & Weissman, A. M. RING finger proteins: mediators of ubiquitin ligase activity. *Cell* **102**, 549-552 (2000).
113 Bentley, M. L. *et al.* Recognition of UbcH5c and the nucleosome by the Bmi1/Ring1b ubiquitin ligase complex. *The EMBO journal* **30**, 3285-3297, doi:10.1038/emboj.2011.243 (2011).
114 Wei, J., Zhai, L., Xu, J. & Wang, H. Role of Bmi1 in H2A ubiquitylation and Hox gene silencing. *The Journal of biological chemistry* **281**, 22537-22544, doi:10.1074/jbc.M600826200 (2006).
115 Mattiroli, F. *et al.* RNF168 ubiquitinates K13-15 on H2A/H2AX to drive DNA damage signaling. *Cell* **150**, 1182-1195, doi:10.1016/j.cell.2012.08.005 (2012).
116 Bhatnagar, S. *et al.* TRIM37 is a new histone H2A ubiquitin ligase and breast cancer oncoprotein. *Nature* **516**, 116-120, doi:10.1038/nature13955 (2014).
117 Goldknopf, I. L. *et al.* Isolation and characterization of protein A24, a "histone-like" non-histone chromosomal protein. *The Journal of biological chemistry* **250**, 7182-7187 (1975).
118 Nickel, B. E. & Davie, J. R. Structure of polyubiquitinated histone H2A. *Biochemistry* **28**, 964-968 (1989).
119 Bradbury, E. M. Reversible histone modifications and the chromosome cell cycle. *BioEssays : news and reviews in molecular, cellular and developmental biology* **14**, 9-16, doi:10.1002/bies.950140103 (1992).
120 Joo, H. Y. *et al.* Regulation of cell cycle progression and gene expression by H2A deubiquitination. *Nature* **449**, 1068-1072, doi:10.1038/nature06256 (2007).
121 Mueller, R. D., Yasuda, H., Hatch, C. L., Bonner, W. M. & Bradbury, E. M. Identification of ubiquitinated histones 2A and 2B in Physarum polycephalum. Disappearance of these proteins at metaphase and reappearance at anaphase. *The Journal of biological chemistry* **260**, 5147-5153 (1985).
122 Endoh, M. *et al.* Histone H2A mono-ubiquitination is a crucial step to mediate PRC1-dependent repression of developmental genes to maintain ES cell identity. *PLoS genetics* **8**, e1002774, doi:10.1371/journal.pgen.1002774 (2012).
123 Trojer, P. *et al.* L3MBTL2 protein acts in concert with PcG protein-mediated monoubiquitination of H2A to establish a repressive chromatin structure. *Molecular cell* **42**, 438-450, doi:10.1016/j.molcel.2011.04.004 (2011).
124 Nakagawa, T. *et al.* Deubiquitylation of histone H2A activates transcriptional initiation via trans-histone cross-talk with H3K4 di- and trimethylation. *Genes & development* **22**, 37-49, doi:10.1101/gad.1609708 (2008).
125 Stock, J. K. *et al.* Ring1-mediated ubiquitination of H2A restrains poised RNA polymerase II at bivalent genes in mouse ES cells. *Nature cell biology* **9**, 1428-1435, doi:10.1038/ncb1663 (2007).
126 de Napoles, M. *et al.* Polycomb group proteins Ring1A/B link ubiquitylation of histone H2A to heritable gene silencing and X inactivation. *Developmental cell* **7**, 663-676, doi:10.1016/j.devcel.2004.10.005 (2004).

127 Fang, J., Chen, T., Chadwick, B., Li, E. & Zhang, Y. Ring1b-mediated H2A ubiquitination associates with inactive X chromosomes and is involved in initiation of X inactivation. *The Journal of biological chemistry* **279**, 52812-52815, doi:10.1074/jbc.C400493200 (2004).
128 Boyer, L. A. *et al.* Polycomb complexes repress developmental regulators in murine embryonic stem cells. *Nature* **441**, 349-353, doi:10.1038/nature04733 (2006).
129 Schoeftner, S. *et al.* Recruitment of PRC1 function at the initiation of X inactivation independent of PRC2 and silencing. *The EMBO journal* **25**, 3110-3122, doi:10.1038/sj.emboj.7601187 (2006).
130 Tavares, L. *et al.* RYBP-PRC1 complexes mediate H2A ubiquitylation at polycomb target sites independently of PRC2 and H3K27me3. *Cell* **148**, 664-678, doi:10.1016/j.cell.2011.12.029 (2012).
131 Wilkinson, F., Pratt, H. & Atchison, M. L. PcG recruitment by the YY1 REPO domain can be mediated by Yaf2. *Journal of cellular biochemistry* **109**, 478-486, doi:10.1002/jcb.22424 (2010).
132 Sanchez, C. *et al.* Proteomics analysis of Ring1B/Rnf2 interactors identifies a novel complex with the Fbxl10/Jhdm1B histone demethylase and the Bcl6 interacting corepressor. *Molecular & cellular proteomics : MCP* **6**, 820-834, doi:10.1074/mcp.M600275-MCP200 (2007).
133 Wu, X., Johansen, J. V. & Helin, K. Fbxl10/Kdm2b recruits polycomb repressive complex 1 to CpG islands and regulates H2A ubiquitylation. *Molecular cell* **49**, 1134-1146, doi:10.1016/j.molcel.2013.01.016 (2013).
134 Ogawa, H., Ishiguro, K., Gaubatz, S., Livingston, D. M. & Nakatani, Y. A complex with chromatin modifiers that occupies E2F- and Myc-responsive genes in G0 cells. *Science* **296**, 1132-1136, doi:10.1126/science.1069861 (2002).
135 Blackledge, N. P. *et al.* Variant PRC1 complex-dependent H2A ubiquitylation drives PRC2 recruitment and polycomb domain formation. *Cell* **157**, 1445-1459, doi:10.1016/j.cell.2014.05.004 (2014).
136 Cooper, S. *et al.* Targeting polycomb to pericentric heterochromatin in embryonic stem cells reveals a role for H2AK119u1 in PRC2 recruitment. *Cell reports* **7**, 1456-1470, doi:10.1016/j.celrep.2014.04.012 (2014).
137 Kalb, R. *et al.* Histone H2A monoubiquitination promotes histone H3 methylation in Polycomb repression. *Nature structural & molecular biology* **21**, 569-571, doi:10.1038/nsmb.2833 (2014).
138 Bergink, S. *et al.* DNA damage triggers nucleotide excision repair-dependent monoubiquitylation of histone H2A. *Genes & development* **20**, 1343-1352, doi:10.1101/gad.373706 (2006).
139 Gieni, R. S., Ismail, I. H., Campbell, S. & Hendzel, M. J. Polycomb group proteins in the DNA damage response: a link between radiation resistance and "stemness". *Cell cycle* **10**, 883-894 (2011).
140 Ismail, I. H., Andrin, C., McDonald, D. & Hendzel, M. J. BMI1-mediated histone ubiquitylation promotes DNA double-strand break repair. *The Journal of cell biology* **191**, 45-60, doi:10.1083/jcb.201003034 (2010).

141 Eskeland, R. *et al.* Ring1B compacts chromatin structure and represses gene expression independent of histone ubiquitination. *Molecular cell* **38**, 452-464, doi:10.1016/j.molcel.2010.02.032 (2010).
142 Grau, D. J. *et al.* Compaction of chromatin by diverse Polycomb group proteins requires localized regions of high charge. *Genes & development* **25**, 2210-2221, doi:10.1101/gad.17288211 (2011).
143 Pengelly, A. R., Kalb, R., Finkl, K. & Muller, J. Transcriptional repression by PRC1 in the absence of H2A monoubiquitylation. *Genes & development* **29**, 1487-1492, doi:10.1101/gad.265439.115 (2015).
144 Hershko, A. & Ciechanover, A. The ubiquitin system. *Annu Rev Biochem* **67**, 425-479, doi:10.1146/annurev.biochem.67.1.425 (1998).
145 Varshavsky, A. Regulated protein degradation. *Trends in biochemical sciences* **30**, 283-286, doi:10.1016/j.tibs.2005.04.005 (2005).
146 Mukhopadhyay, D. & Riezman, H. Proteasome-independent functions of ubiquitin in endocytosis and signaling. *Science* **315**, 201-205, doi:10.1126/science.1127085 (2007).
147 Grabbe, C., Husnjak, K. & Dikic, I. The spatial and temporal organization of ubiquitin networks. *Nature reviews. Molecular cell biology* **12**, 295-307, doi:10.1038/nrm3099 (2011).
148 Varshavsky, A. The early history of the ubiquitin field. *Protein science : a publication of the Protein Society* **15**, 647-654, doi:10.1110/ps.052012306 (2006).
149 Wilkinson, K. D. The discovery of ubiquitin-dependent proteolysis. *Proceedings of the National Academy of Sciences of the United States of America* **102**, 15280-15282, doi:10.1073/pnas.0504842102 (2005).
150 Wilkinson, K. D., Ventii, K. H., Friedrich, K. L. & Mullally, J. E. The ubiquitin signal: assembly, recognition and termination. Symposium on ubiquitin and signaling. *EMBO Rep* **6**, 815-820, doi:10.1038/sj.embor.7400506 (2005).
151 Vijay-Kumar, S., Bugg, C. E. & Cook, W. J. Structure of ubiquitin refined at 1.8 A resolution. *Journal of molecular biology* **194**, 531-544 (1987).
152 Lange, O. F. *et al.* Recognition dynamics up to microseconds revealed from an RDC-derived ubiquitin ensemble in solution. *Science* **320**, 1471-1475, doi:10.1126/science.1157092 (2008).
153 Pickart, C. M. Mechanisms underlying ubiquitination. *Annu Rev Biochem* **70**, 503-533, doi:10.1146/annurev.biochem.70.1.503 (2001).
154 Komander, D., Clague, M. J. & Urbe, S. Breaking the chains: structure and function of the deubiquitinases. *Nature reviews. Molecular cell biology* **10**, 550-563, doi:10.1038/nrm2731 (2009).
155 Zeng, W. *et al.* Reconstitution of the RIG-I pathway reveals a signaling role of unanchored polyubiquitin chains in innate immunity. *Cell* **141**, 315-330, doi:10.1016/j.cell.2010.03.029 (2010).
156 Xia, Z. P. *et al.* Direct activation of protein kinases by unanchored polyubiquitin chains. *Nature* **461**, 114-119, doi:10.1038/nature08247 (2009).
157 Deshaies, R. J. & Joazeiro, C. A. RING domain E3 ubiquitin ligases. *Annu Rev Biochem* **78**, 399-434, doi:10.1146/annurev.biochem.78.101807.093809 (2009).

158 Schulman, B. A. & Harper, J. W. Ubiquitin-like protein activation by E1 enzymes: the apex for downstream signalling pathways. *Nature reviews. Molecular cell biology* **10**, 319-331, doi:10.1038/nrm2673 (2009).
159 Ye, Y. & Rape, M. Building ubiquitin chains: E2 enzymes at work. *Nature reviews. Molecular cell biology* **10**, 755-764, doi:10.1038/nrm2780 (2009).
160 Lee, I. & Schindelin, H. Structural insights into E1-catalyzed ubiquitin activation and transfer to conjugating enzymes. *Cell* **134**, 268-278, doi:10.1016/j.cell.2008.05.046 (2008).
161 Rotin, D. & Kumar, S. Physiological functions of the HECT family of ubiquitin ligases. *Nature reviews. Molecular cell biology* **10**, 398-409, doi:10.1038/nrm2690 (2009).
162 Jin, J., Li, X., Gygi, S. P. & Harper, J. W. Dual E1 activation systems for ubiquitin differentially regulate E2 enzyme charging. *Nature* **447**, 1135-1138, doi:10.1038/nature05902 (2007).
163 van Wijk, S. J. & Timmers, H. T. The family of ubiquitin-conjugating enzymes (E2s): deciding between life and death of proteins. *FASEB journal : official publication of the Federation of American Societies for Experimental Biology* **24**, 981-993, doi:10.1096/fj.09-136259 (2010).
164 Wu, K., Kovacev, J. & Pan, Z. Q. Priming and extending: a UbcH5/Cdc34 E2 handoff mechanism for polyubiquitination on a SCF substrate. *Molecular cell* **37**, 784-796, doi:10.1016/j.molcel.2010.02.025 (2010).
165 Parker, J. L. & Ulrich, H. D. Mechanistic analysis of PCNA poly-ubiquitylation by the ubiquitin protein ligases Rad18 and Rad5. *The EMBO journal* **28**, 3657-3666, doi:10.1038/emboj.2009.303 (2009).
166 Petroski, M. D. & Deshaies, R. J. Mechanism of lysine 48-linked ubiquitin-chain synthesis by the cullin-RING ubiquitin-ligase complex SCF-Cdc34. *Cell* **123**, 1107-1120, doi:10.1016/j.cell.2005.09.033 (2005).
167 Hofmann, R. M. & Pickart, C. M. Noncanonical MMS2-encoded ubiquitin-conjugating enzyme functions in assembly of novel polyubiquitin chains for DNA repair. *Cell* **96**, 645-653 (1999).
168 Ravid, T. & Hochstrasser, M. Diversity of degradation signals in the ubiquitin-proteasome system. *Nature reviews. Molecular cell biology* **9**, 679-690, doi:10.1038/nrm2468 (2008).
169 van der Veen, A. G. & Ploegh, H. L. Ubiquitin-like proteins. *Annu Rev Biochem* **81**, 323-357, doi:10.1146/annurev-biochem-093010-153308 (2012).
170 Ikeda, F. & Dikic, I. Atypical ubiquitin chains: new molecular signals. 'Protein Modifications: Beyond the Usual Suspects' review series. *EMBO Rep* **9**, 536-542, doi:10.1038/embor.2008.93 (2008).
171 Peng, J. *et al.* A proteomics approach to understanding protein ubiquitination. *Nat Biotechnol* **21**, 921-926, doi:10.1038/nbt849 (2003).
172 Kirisako, T. *et al.* A ubiquitin ligase complex assembles linear polyubiquitin chains. *The EMBO journal* **25**, 4877-4887, doi:10.1038/sj.emboj.7601360 (2006).
173 Tagwerker, C. *et al.* A tandem affinity tag for two-step purification under fully denaturing conditions: application in ubiquitin profiling and protein complex

identification combined with in vivocross-linking. *Molecular & cellular proteomics : MCP* **5**, 737-748, doi:10.1074/mcp.M500368-MCP200 (2006).
174 Kim, H. T. *et al.* Certain pairs of ubiquitin-conjugating enzymes (E2s) and ubiquitin-protein ligases (E3s) synthesize nondegradable forked ubiquitin chains containing all possible isopeptide linkages. *The Journal of biological chemistry* **282**, 17375-17386, doi:10.1074/jbc.M609659200 (2007).
175 Komander, D. & Rape, M. The ubiquitin code. *Annu Rev Biochem* **81**, 203-229, doi:10.1146/annurev-biochem-060310-170328 (2012).
176 Welchman, R. L., Gordon, C. & Mayer, R. J. Ubiquitin and ubiquitin-like proteins as multifunctional signals. *Nature reviews. Molecular cell biology* **6**, 599-609, doi:10.1038/nrm1700 (2005).
177 Dikic, I., Wakatsuki, S. & Walters, K. J. Ubiquitin-binding domains - from structures to functions. *Nature reviews. Molecular cell biology* **10**, 659-671, doi:10.1038/nrm2767 (2009).
178 Varshavsky, A. The ubiquitin system, an immense realm. *Annu Rev Biochem* **81**, 167-176, doi:10.1146/annurev-biochem-051910-094049 (2012).
179 Hoeller, D., Hecker, C. M. & Dikic, I. Ubiquitin and ubiquitin-like proteins in cancer pathogenesis. *Nature reviews. Cancer* **6**, 776-788, doi:10.1038/nrc1994 (2006).
180 Bernassola, F., Karin, M., Ciechanover, A. & Melino, G. The HECT family of E3 ubiquitin ligases: multiple players in cancer development. *Cancer cell* **14**, 10-21, doi:10.1016/j.ccr.2008.06.001 (2008).
181 Kirkin, V. & Dikic, I. Ubiquitin networks in cancer. *Current opinion in genetics & development* **21**, 21-28, doi:10.1016/j.gde.2010.10.004 (2011).
182 Hammond-Martel, I., Yu, H. & Affar el, B. Roles of ubiquitin signaling in transcription regulation. *Cellular signalling* **24**, 410-421, doi:10.1016/j.cellsig.2011.10.009 (2012).
183 Jackson, S. P. & Durocher, D. Regulation of DNA damage responses by ubiquitin and SUMO. *Molecular cell* **49**, 795-807, doi:10.1016/j.molcel.2013.01.017 (2013).
184 Craney, A. & Rape, M. Dynamic regulation of ubiquitin-dependent cell cycle control. *Current opinion in cell biology* **25**, 704-710, doi:10.1016/j.ceb.2013.07.004 (2013).
185 Kulathu, Y. & Komander, D. Atypical ubiquitylation - the unexplored world of polyubiquitin beyond Lys48 and Lys63 linkages. *Nature reviews. Molecular cell biology* **13**, 508-523, doi:10.1038/nrm3394 (2012).
186 Xu, P. *et al.* Quantitative proteomics reveals the function of unconventional ubiquitin chains in proteasomal degradation. *Cell* **137**, 133-145, doi:10.1016/j.cell.2009.01.041 (2009).
187 Husnjak, K. & Dikic, I. Ubiquitin-binding proteins: decoders of ubiquitin-mediated cellular functions. *Annu Rev Biochem* **81**, 291-322, doi:10.1146/annurev-biochem-051810-094654 (2012).
188 Shih, S. C., Sloper-Mould, K. E. & Hicke, L. Monoubiquitin carries a novel internalization signal that is appended to activated receptors. *The EMBO journal* **19**, 187-198, doi:10.1093/emboj/19.2.187 (2000).

189 Sloper-Mould, K. E., Jemc, J. C., Pickart, C. M. & Hicke, L. Distinct functional surface regions on ubiquitin. *The Journal of biological chemistry* **276**, 30483-30489, doi:10.1074/jbc.M103248200 (2001).
190 Kamadurai, H. B. *et al.* Insights into ubiquitin transfer cascades from a structure of a UbcH5B approximately ubiquitin-HECT(NEDD4L) complex. *Molecular cell* **36**, 1095-1102, doi:10.1016/j.molcel.2009.11.010 (2009).
191 Hu, M. *et al.* Crystal structure of a UBP-family deubiquitinating enzyme in isolation and in complex with ubiquitin aldehyde. *Cell* **111**, 1041-1054 (2002).
192 Reyes-Turcu, F. E. *et al.* The ubiquitin binding domain ZnF UBP recognizes the C-terminal diglycine motif of unanchored ubiquitin. *Cell* **124**, 1197-1208, doi:10.1016/j.cell.2006.02.038 (2006).
193 Rahighi, S. *et al.* Specific recognition of linear ubiquitin chains by NEMO is important for NF-kappaB activation. *Cell* **136**, 1098-1109, doi:10.1016/j.cell.2009.03.007 (2009).
194 Cui, J. *et al.* Glutamine deamidation and dysfunction of ubiquitin/NEDD8 induced by a bacterial effector family. *Science* **329**, 1215-1218, doi:10.1126/science.1193844 (2010).
195 Nijman, S. M. *et al.* A genomic and functional inventory of deubiquitinating enzymes. *Cell* **123**, 773-786, doi:10.1016/j.cell.2005.11.007 (2005).
196 Rawlings, N. D., Morton, F. R. & Barrett, A. J. MEROPS: the peptidase database. *Nucleic acids research* **34**, D270-272, doi:10.1093/nar/gkj089 (2006).
197 Quesada, V., Ordonez, G. R., Sanchez, L. M., Puente, X. S. & Lopez-Otin, C. The Degradome database: mammalian proteases and diseases of proteolysis. *Nucleic acids research* **37**, D239-243, doi:10.1093/nar/gkn570 (2009).
198 Reyes-Turcu, F. E., Ventii, K. H. & Wilkinson, K. D. Regulation and cellular roles of ubiquitin-specific deubiquitinating enzymes. *Annu Rev Biochem* **78**, 363-397, doi:10.1146/annurev.biochem.78.082307.091526 (2009).
199 Liang, J. *et al.* MCP-induced protein 1 deubiquitinates TRAF proteins and negatively regulates JNK and NF-kappaB signaling. *The Journal of experimental medicine* **207**, 2959-2973, doi:10.1084/jem.20092641 (2010).
200 Heyninck, K. & Beyaert, R. A20 inhibits NF-kappaB activation by dual ubiquitin-editing functions. *Trends in biochemical sciences* **30**, 1-4, doi:10.1016/j.tibs.2004.11.001 (2005).
201 Song, L. & Rape, M. Reverse the curse--the role of deubiquitination in cell cycle control. *Current opinion in cell biology* **20**, 156-163, doi:10.1016/j.ceb.2008.01.012 (2008).
202 Guterman, A. & Glickman, M. H. Deubiquitinating enzymes are IN/(trinsic to proteasome function). *Curr Protein Pept Sci* **5**, 201-211 (2004).
203 Komada, M. Controlling receptor downregulation by ubiquitination and deubiquitination. *Curr Drug Discov Technol* **5**, 78-84 (2008).
204 Schmidt, M., Hanna, J., Elsasser, S. & Finley, D. Proteasome-associated proteins: regulation of a proteolytic machine. *Biol Chem* **386**, 725-737, doi:10.1515/BC.2005.085 (2005).

205 Daniel, J. A. & Grant, P. A. Multi-tasking on chromatin with the SAGA coactivator complexes. *Mutation research* **618**, 135-148, doi:10.1016/j.mrfmmm.2006.09.008 (2007).
206 Kennedy, R. D. & D'Andrea, A. D. The Fanconi Anemia/BRCA pathway: new faces in the crowd. *Genes & development* **19**, 2925-2940, doi:10.1101/gad.1370505 (2005).
207 Byrne, A. *et al.* Knockdown of human deubiquitinase PSMD14 induces cell cycle arrest and senescence. *Experimental cell research* **316**, 258-271, doi:10.1016/j.yexcr.2009.08.018 (2010).
208 Kato, H. *et al.* Induction of human endometrial cancer cell senescence through modulation of HIF-1alpha activity by EGLN1. *International journal of cancer. Journal international du cancer* **118**, 1144-1153, doi:10.1002/ijc.21488 (2006).
209 Daou, S. *et al.* The BAP1/ASXL2 Histone H2A Deubiquitinase Complex Regulates Cell Proliferation and Is Disrupted in Cancer. *The Journal of biological chemistry* **290**, 28643-28663, doi:10.1074/jbc.M115.661553 (2015).
210 Leonard, N. *et al.* Loss of heterozygosity at cylindromatosis gene locus, CYLD, in sporadic skin adnexal tumours. *Journal of clinical pathology* **54**, 689-692 (2001).
211 Tsou, W. L. *et al.* Ubiquitination regulates the neuroprotective function of the deubiquitinase ataxin-3 in vivo. *The Journal of biological chemistry* **288**, 34460-34469, doi:10.1074/jbc.M113.513903 (2013).
212 Williams, S. A. *et al.* USP1 deubiquitinates ID proteins to preserve a mesenchymal stem cell program in osteosarcoma. *Cell* **146**, 918-930, doi:10.1016/j.cell.2011.07.040 (2011).
213 Reyes-Turcu, F. E. & Wilkinson, K. D. Polyubiquitin binding and disassembly by deubiquitinating enzymes. *Chem Rev* **109**, 1495-1508, doi:10.1021/cr800470j (2009).
214 Sheng, Y. *et al.* Molecular recognition of p53 and MDM2 by USP7/HAUSP. *Nature structural & molecular biology* **13**, 285-291, doi:10.1038/nsmb1067 (2006).
215 Lee, K. K., Florens, L., Swanson, S. K., Washburn, M. P. & Workman, J. L. The deubiquitylation activity of Ubp8 is dependent upon Sgf11 and its association with the SAGA complex. *Molecular and cellular biology* **25**, 1173-1182, doi:10.1128/MCB.25.3.1173-1182.2005 (2005).
216 Ingvarsdottir, K. *et al.* H2B ubiquitin protease Ubp8 and Sgf11 constitute a discrete functional module within the Saccharomyces cerevisiae SAGA complex. *Molecular and cellular biology* **25**, 1162-1172, doi:10.1128/MCB.25.3.1162-1172.2005 (2005).
217 Wyce, A. *et al.* H2B ubiquitylation acts as a barrier to Ctk1 nucleosomal recruitment prior to removal by Ubp8 within a SAGA-related complex. *Molecular cell* **27**, 275-288, doi:10.1016/j.molcel.2007.01.035 (2007).
218 Cooper, E. M. *et al.* K63-specific deubiquitination by two JAMM/MPN+ complexes: BRISC-associated Brcc36 and proteasomal Poh1. *The EMBO journal* **28**, 621-631, doi:10.1038/emboj.2009.27 (2009).
219 Sato, Y. *et al.* Structural basis for specific cleavage of Lys 63-linked polyubiquitin chains. *Nature* **455**, 358-362, doi:10.1038/nature07254 (2008).

220 Hu, M. *et al.* Structure and mechanisms of the proteasome-associated deubiquitinating enzyme USP14. *The EMBO journal* **24**, 3747-3756, doi:10.1038/sj.emboj.7600832 (2005).
221 Mevissen, T. E. *et al.* OTU deubiquitinases reveal mechanisms of linkage specificity and enable ubiquitin chain restriction analysis. *Cell* **154**, 169-184, doi:10.1016/j.cell.2013.05.046 (2013).
222 Johnston, S. C., Riddle, S. M., Cohen, R. E. & Hill, C. P. Structural basis for the specificity of ubiquitin C-terminal hydrolases. *The EMBO journal* **18**, 3877-3887, doi:10.1093/emboj/18.14.3877 (1999).
223 Yang, W. *et al.* The histone H2A deubiquitinase Usp16 regulates embryonic stem cell gene expression and lineage commitment. *Nature communications* **5**, 3818, doi:10.1038/ncomms4818 (2014).
224 Kimura, Y. & Tanaka, K. Regulatory mechanisms involved in the control of ubiquitin homeostasis. *Journal of biochemistry* **147**, 793-798, doi:10.1093/jb/mvq044 (2010).
225 Ye, Y. *et al.* Polyubiquitin binding and cross-reactivity in the USP domain deubiquitinase USP21. *EMBO Rep* **12**, 350-357, doi:10.1038/embor.2011.17 (2011).
226 Jensen, D. E. *et al.* BAP1: a novel ubiquitin hydrolase which binds to the BRCA1 RING finger and enhances BRCA1-mediated cell growth suppression. *Oncogene* **16**, 1097-1112 (1998).
227 Nishikawa, H. *et al.* BRCA1-associated protein 1 interferes with BRCA1/BARD1 RING heterodimer activity. *Cancer research* **69**, 111-119, doi:10.1158/0008-5472.CAN-08-3355 (2009).
228 Ohta, T., Sato, K. & Wu, W. The BRCA1 ubiquitin ligase and homologous recombination repair. *FEBS letters* **585**, 2836-2844, doi:10.1016/j.febslet.2011.05.005 (2011).
229 Yu, H. *et al.* Tumor suppressor and deubiquitinase BAP1 promotes DNA double-strand break repair. *Proceedings of the National Academy of Sciences of the United States of America* **111**, 285-290, doi:10.1073/pnas.1309085110 (2014).
230 Dey, A. *et al.* Loss of the tumor suppressor BAP1 causes myeloid transformation. *Science* **337**, 1541-1546, doi:10.1126/science.1221711 (2012).
231 Harbour, J. W. *et al.* Frequent mutation of BAP1 in metastasizing uveal melanomas. *Science* **330**, 1410-1413, doi:10.1126/science.1194472 (2010).
232 Je, E. M., Lee, S. H. & Yoo, N. J. Somatic mutation of a tumor suppressor gene BAP1 is rare in breast, prostate, gastric and colorectal cancers. *APMIS : acta pathologica, microbiologica, et immunologica Scandinavica* **120**, 855-856, doi:10.1111/j.1600-0463.2012.02909.x (2012).
233 Machida, Y. J., Machida, Y., Vashisht, A. A., Wohlschlegel, J. A. & Dutta, A. The deubiquitinating enzyme BAP1 regulates cell growth via interaction with HCF-1. *The Journal of biological chemistry* **284**, 34179-34188, doi:10.1074/jbc.M109.046755 (2009).
234 Misaghi, S. *et al.* Association of C-terminal ubiquitin hydrolase BRCA1-associated protein 1 with cell cycle regulator host cell factor 1. *Molecular and cellular biology* **29**, 2181-2192, doi:10.1128/MCB.01517-08 (2009).

235 Testa, J. R. *et al.* Germline BAP1 mutations predispose to malignant mesothelioma. *Nature genetics* **43**, 1022-1025, doi:10.1038/ng.912 (2011).
236 Ventii, K. H. *et al.* BRCA1-associated protein-1 is a tumor suppressor that requires deubiquitinating activity and nuclear localization. *Cancer research* **68**, 6953-6962, doi:10.1158/0008-5472.CAN-08-0365 (2008).
237 Eletr, Z. M., Yin, L. & Wilkinson, K. D. BAP1 is phosphorylated at serine 592 in S-phase following DNA damage. *FEBS letters* **587**, 3906-3911, doi:10.1016/j.febslet.2013.10.035 (2013).
238 Ismail, I. H. *et al.* Germline mutations in BAP1 impair its function in DNA double-strand break repair. *Cancer research* **74**, 4282-4294, doi:10.1158/0008-5472.CAN-13-3109 (2014).
239 Sowa, M. E., Bennett, E. J., Gygi, S. P. & Harper, J. W. Defining the human deubiquitinating enzyme interaction landscape. *Cell* **138**, 389-403, doi:10.1016/j.cell.2009.04.042 (2009).
240 Johnston, S. C., Larsen, C. N., Cook, W. J., Wilkinson, K. D. & Hill, C. P. Crystal structure of a deubiquitinating enzyme (human UCH-L3) at 1.8 A resolution. *The EMBO journal* **16**, 3787-3796, doi:10.1093/emboj/16.13.3787 (1997).
241 Mashtalir, N. *et al.* Autodeubiquitination protects the tumor suppressor BAP1 from cytoplasmic sequestration mediated by the atypical ubiquitin ligase UBE2O. *Molecular cell* **54**, 392-406, doi:10.1016/j.molcel.2014.03.002 (2014).
242 Blattler, S. M. *et al.* Yin Yang 1 deficiency in skeletal muscle protects against rapamycin-induced diabetic-like symptoms through activation of insulin/IGF signaling. *Cell metabolism* **15**, 505-517, doi:10.1016/j.cmet.2012.03.008 (2012).
243 Murali, R., Wiesner, T. & Scolyer, R. A. Tumours associated with BAP1 mutations. *Pathology* **45**, 116-126, doi:10.1097/PAT.0b013e32835d0efb (2013).
244 Ji, L., Minna, J. D. & Roth, J. A. 3p21.3 tumor suppressor cluster: prospects for translational applications. *Future oncology* **1**, 79-92, doi:10.1517/14796694.1.1.79 (2005).
245 Angeloni, D. Molecular analysis of deletions in human chromosome 3p21 and the role of resident cancer genes in disease. *Briefings in functional genomics & proteomics* **6**, 19-39, doi:10.1093/bfgp/elm007 (2007).
246 Abdel-Rahman, M. H. *et al.* Germline BAP1 mutation predisposes to uveal melanoma, lung adenocarcinoma, meningioma, and other cancers. *Journal of medical genetics* **48**, 856-859, doi:10.1136/jmedgenet-2011-100156 (2011).
247 Bott, M. *et al.* The nuclear deubiquitinase BAP1 is commonly inactivated by somatic mutations and 3p21.1 losses in malignant pleural mesothelioma. *Nature genetics* **43**, 668-672, doi:10.1038/ng.855 (2011).
248 Goldstein, A. M. Germline BAP1 mutations and tumor susceptibility. *Nature genetics* **43**, 925-926, doi:10.1038/ng.956 (2011).
249 Wiesner, T. *et al.* Germline mutations in BAP1 predispose to melanocytic tumors. *Nature genetics* **43**, 1018-1021, doi:10.1038/ng.910 (2011).
250 Pena-Llopis, S. *et al.* BAP1 loss defines a new class of renal cell carcinoma. *Nature genetics* **44**, 751-759, doi:10.1038/ng.2323 (2012).

251 Carbone, M. *et al.* BAP1 cancer syndrome: malignant mesothelioma, uveal and cutaneous melanoma, and MBAITs. *Journal of translational medicine* **10**, 179, doi:10.1186/1479-5876-10-179 (2012).
252 Nasu, M. *et al.* High Incidence of Somatic BAP1 alterations in sporadic malignant mesothelioma. *Journal of thoracic oncology : official publication of the International Association for the Study of Lung Cancer* **10**, 565-576, doi:10.1097/JTO.0000000000000471 (2015).
253 Yoshikawa, Y. *et al.* Frequent inactivation of the BAP1 gene in epithelioid-type malignant mesothelioma. *Cancer science* **103**, 868-874, doi:10.1111/j.1349-7006.2012.02223.x (2012).
254 Wiesner, T. *et al.* A distinct subset of atypical Spitz tumors is characterized by BRAF mutation and loss of BAP1 expression. *The American journal of surgical pathology* **36**, 818-830, doi:10.1097/PAS.0b013e3182498be5 (2012).
255 Wadt, K. *et al.* A cryptic BAP1 splice mutation in a family with uveal and cutaneous melanoma, and paraganglioma. *Pigment cell & melanoma research* **25**, 815-818, doi:10.1111/pcmr.12006 (2012).
256 Herr, W. The herpes simplex virus VP16-induced complex: mechanisms of combinatorial transcriptional regulation. *Cold Spring Harbor symposia on quantitative biology* **63**, 599-607 (1998).
257 Wilson, A. C., Boutros, M., Johnson, K. M. & Herr, W. HCF-1 amino- and carboxy-terminal subunit association through two separate sets of interaction modules: involvement of fibronectin type 3 repeats. *Molecular and cellular biology* **20**, 6721-6730 (2000).
258 Wilson, A. C., LaMarco, K., Peterson, M. G. & Herr, W. The VP16 accessory protein HCF is a family of polypeptides processed from a large precursor protein. *Cell* **74**, 115-125 (1993).
259 Wysocka, J. & Herr, W. The herpes simplex virus VP16-induced complex: the makings of a regulatory switch. *Trends in biochemical sciences* **28**, 294-304, doi:10.1016/S0968-0004(03)00088-4 (2003).
260 Ajuh, P., Chusainow, J., Ryder, U. & Lamond, A. I. A novel function for human factor C1 (HCF-1), a host protein required for herpes simplex virus infection, in pre-mRNA splicing. *The EMBO journal* **21**, 6590-6602 (2002).
261 Ruan, H. B. *et al.* O-GlcNAc transferase/host cell factor C1 complex regulates gluconeogenesis by modulating PGC-1alpha stability. *Cell metabolism* **16**, 226-237, doi:10.1016/j.cmet.2012.07.006 (2012).
262 Zhang, E. E. *et al.* A genome-wide RNAi screen for modifiers of the circadian clock in human cells. *Cell* **139**, 199-210, doi:10.1016/j.cell.2009.08.031 (2009).
263 Wysocka, J., Reilly, P. T. & Herr, W. Loss of HCF-1-chromatin association precedes temperature-induced growth arrest of tsBN67 cells. *Molecular and cellular biology* **21**, 3820-3829, doi:10.1128/MCB.21.11.3820-3829.2001 (2001).
264 Goto, H. *et al.* A single-point mutation in HCF causes temperature-sensitive cell-cycle arrest and disrupts VP16 function. *Genes & development* **11**, 726-737 (1997).
265 Reilly, P. T., Wysocka, J. & Herr, W. Inactivation of the retinoblastoma protein family can bypass the HCF-1 defect in tsBN67 cell proliferation and cytokinesis. *Molecular and cellular biology* **22**, 6767-6778 (2002).

266 Julien, E. & Herr, W. Proteolytic processing is necessary to separate and ensure proper cell growth and cytokinesis functions of HCF-1. *The EMBO journal* **22**, 2360-2369, doi:10.1093/emboj/cdg242 (2003).
267 Vogel, J. L. & Kristie, T. M. The novel coactivator C1 (HCF) coordinates multiprotein enhancer formation and mediates transcription activation by GABP. *The EMBO journal* **19**, 683-690, doi:10.1093/emboj/19.4.683 (2000).
268 Narayanan, A., Ruyechan, W. T. & Kristie, T. M. The coactivator host cell factor-1 mediates Set1 and MLL1 H3K4 trimethylation at herpesvirus immediate early promoters for initiation of infection. *Proceedings of the National Academy of Sciences of the United States of America* **104**, 10835-10840, doi:10.1073/pnas.0704351104 (2007).
269 Julien, E. & Herr, W. A switch in mitotic histone H4 lysine 20 methylation status is linked to M phase defects upon loss of HCF-1. *Molecular cell* **14**, 713-725, doi:10.1016/j.molcel.2004.06.008 (2004).
270 Tyagi, S., Chabes, A. L., Wysocka, J. & Herr, W. E2F activation of S phase promoters via association with HCF-1 and the MLL family of histone H3K4 methyltransferases. *Molecular cell* **27**, 107-119, doi:10.1016/j.molcel.2007.05.030 (2007).
271 Musarrat, J., Arezina-Wilson, J. & Wani, A. A. Repair of base alkylation damage in targeted restriction endonuclease sequences of plasmid DNA. *Biochimica et biophysica acta* **1263**, 201-211 (1995).
272 Yokoyama, A. *et al.* Leukemia proto-oncoprotein MLL forms a SET1-like histone methyltransferase complex with menin to regulate Hox gene expression. *Molecular and cellular biology* **24**, 5639-5649, doi:10.1128/MCB.24.13.5639-5649.2004 (2004).
273 Kristie, T. M., Liang, Y. & Vogel, J. L. Control of alpha-herpesvirus IE gene expression by HCF-1 coupled chromatin modification activities. *Biochimica et biophysica acta* **1799**, 257-265, doi:10.1016/j.bbagrm.2009.08.003 (2010).
274 Vercauteren, K., Gleyzer, N. & Scarpulla, R. C. PGC-1-related coactivator complexes with HCF-1 and NRF-2beta in mediating NRF-2(GABP)-dependent respiratory gene expression. *The Journal of biological chemistry* **283**, 12102-12111, doi:10.1074/jbc.M710150200 (2008).
275 Daou, S. *et al.* Crosstalk between O-GlcNAcylation and proteolytic cleavage regulates the host cell factor-1 maturation pathway. *Proceedings of the National Academy of Sciences of the United States of America* **108**, 2747-2752, doi:10.1073/pnas.1013822108 (2011).
276 Piluso, D., Bilan, P. & Capone, J. P. Host cell factor-1 interacts with and antagonizes transactivation by the cell cycle regulatory factor Miz-1. *The Journal of biological chemistry* **277**, 46799-46808, doi:10.1074/jbc.M206226200 (2002).
277 Vogel, J. L. & Kristie, T. M. Site-specific proteolysis of the transcriptional coactivator HCF-1 can regulate its interaction with protein cofactors. *Proceedings of the National Academy of Sciences of the United States of America* **103**, 6817-6822, doi:10.1073/pnas.0602109103 (2006).
278 Scarr, R. B. & Sharp, P. A. PDCD2 is a negative regulator of HCF-1 (C1). *Oncogene* **21**, 5245-5254, doi:10.1038/sj.onc.1205647 (2002).

279 Vogel, J. L. & Kristie, T. M. Autocatalytic proteolysis of the transcription factor-coactivator C1 (HCF): a potential role for proteolytic regulation of coactivator function. *Proceedings of the National Academy of Sciences of the United States of America* **97**, 9425-9430, doi:10.1073/pnas.160266697 (2000).
280 Park, J., Lammers, F., Herr, W. & Song, J. J. HCF-1 self-association via an interdigitated Fn3 structure facilitates transcriptional regulatory complex formation. *Proceedings of the National Academy of Sciences of the United States of America* **109**, 17430-17435, doi:10.1073/pnas.1208378109 (2012).
281 Liu, Y., Hengartner, M. O. & Herr, W. Selected elements of herpes simplex virus accessory factor HCF are highly conserved in Caenorhabditis elegans. *Molecular and cellular biology* **19**, 909-915 (1999).
282 Capotosti, F., Hsieh, J. J. & Herr, W. Species selectivity of mixed-lineage leukemia/trithorax and HCF proteolytic maturation pathways. *Molecular and cellular biology* **27**, 7063-7072, doi:10.1128/MCB.00769-07 (2007).
283 Capotosti, F. *et al.* O-GlcNAc transferase catalyzes site-specific proteolysis of HCF-1. *Cell* **144**, 376-388, doi:10.1016/j.cell.2010.12.030 (2011).
284 Lazarus, M. B. *et al.* HCF-1 is cleaved in the active site of O-GlcNAc transferase. *Science* **342**, 1235-1239, doi:10.1126/science.1243990 (2013).
285 Deplus, R. *et al.* TET2 and TET3 regulate GlcNAcylation and H3K4 methylation through OGT and SET1/COMPASS. *The EMBO journal* **32**, 645-655, doi:10.1038/emboj.2012.357 (2013).
286 Fujiki, R. *et al.* GlcNAcylation of a histone methyltransferase in retinoic-acid-induced granulopoiesis. *Nature* **459**, 455-459, doi:10.1038/nature07954 (2009).
287 Cai, Y. *et al.* Subunit composition and substrate specificity of a MOF-containing histone acetyltransferase distinct from the male-specific lethal (MSL) complex. *The Journal of biological chemistry* **285**, 4268-4272, doi:10.1074/jbc.C109.087981 (2010).
288 Wysocka, J., Myers, M. P., Laherty, C. D., Eisenman, R. N. & Herr, W. Human Sin3 deacetylase and trithorax-related Set1/Ash2 histone H3-K4 methyltransferase are tethered together selectively by the cell-proliferation factor HCF-1. *Genes & development* **17**, 896-911, doi:10.1101/gad.252103 (2003).
289 Mazars, R. *et al.* The THAP-zinc finger protein THAP1 associates with coactivator HCF-1 and O-GlcNAc transferase: a link between DYT6 and DYT3 dystonias. *The Journal of biological chemistry* **285**, 13364-13371, doi:10.1074/jbc.M109.072579 (2010).
290 Peng, H., Nogueira, M. L., Vogel, J. L. & Kristie, T. M. Transcriptional coactivator HCF-1 couples the histone chaperone Asf1b to HSV-1 DNA replication components. *Proceedings of the National Academy of Sciences of the United States of America* **107**, 2461-2466, doi:10.1073/pnas.0911128107 (2010).
291 Dejosez, M. *et al.* Ronin/Hcf-1 binds to a hyperconserved enhancer element and regulates genes involved in the growth of embryonic stem cells. *Genes & development* **24**, 1479-1484, doi:10.1101/gad.1935210 (2010).
292 Lewis, B. A. & Hanover, J. A. O-GlcNAc and the epigenetic regulation of gene expression. *The Journal of biological chemistry* **289**, 34440-34448, doi:10.1074/jbc.R114.595439 (2014).

293 Janetzko, J. & Walker, S. The making of a sweet modification: structure and function of O-GlcNAc transferase. *The Journal of biological chemistry* **289**, 34424-34432, doi:10.1074/jbc.R114.604405 (2014).
294 Banerjee, P. J., Woodcock, M. G., Bunce, C., Scott, R. & Charteris, D. G. A pilot study of intraocular use of intensive anti-inflammatory; triamcinolone acetonide to prevent proliferative vitreoretinopathy in eyes undergoing vitreoretinal surgery for open globe trauma; the Adjuncts in Ocular Trauma (AOT) Trial: study protocol for a randomised controlled trial. *Trials* **14**, 42, doi:10.1186/1745-6215-14-42 (2013).
295 Gong, C. X., Liu, F. & Iqbal, K. O-GlcNAc cycling modulates neurodegeneration. *Proceedings of the National Academy of Sciences of the United States of America* **109**, 17319-17320, doi:10.1073/pnas.1215395109 (2012).
296 Torres, C. R. & Hart, G. W. Topography and polypeptide distribution of terminal N-acetylglucosamine residues on the surfaces of intact lymphocytes. Evidence for O-linked GlcNAc. *The Journal of biological chemistry* **259**, 3308-3317 (1984).
297 Holt, G. D. & Hart, G. W. The subcellular distribution of terminal N-acetylglucosamine moieties. Localization of a novel protein-saccharide linkage, O-linked GlcNAc. *The Journal of biological chemistry* **261**, 8049-8057 (1986).
298 Schindler, M., Hogan, M., Miller, R. & DeGaetano, D. A nuclear specific glycoprotein representative of a unique pattern of glycosylation. *The Journal of biological chemistry* **262**, 1254-1260 (1987).
299 Wang, S. *et al.* Extensive crosstalk between O-GlcNAcylation and phosphorylation regulates Akt signaling. *PloS one* **7**, e37427, doi:10.1371/journal.pone.0037427 (2012).
300 Wang, Z. *et al.* Extensive crosstalk between O-GlcNAcylation and phosphorylation regulates cytokinesis. *Science signaling* **3**, ra2, doi:10.1126/scisignal.2000526 (2010).
301 Hart, G. W., Housley, M. P. & Slawson, C. Cycling of O-linked beta-N-acetylglucosamine on nucleocytoplasmic proteins. *Nature* **446**, 1017-1022, doi:10.1038/nature05815 (2007).
302 Ozcan, S., Andrali, S. S. & Cantrell, J. E. Modulation of transcription factor function by O-GlcNAc modification. *Biochimica et biophysica acta* **1799**, 353-364, doi:10.1016/j.bbagrm.2010.02.005 (2010).
303 Love, D. C., Krause, M. W. & Hanover, J. A. O-GlcNAc cycling: emerging roles in development and epigenetics. *Seminars in cell & developmental biology* **21**, 646-654, doi:10.1016/j.semcdb.2010.05.001 (2010).
304 Hart, G. W., Slawson, C., Ramirez-Correa, G. & Lagerlof, O. Cross talk between O-GlcNAcylation and phosphorylation: roles in signaling, transcription, and chronic disease. *Annu Rev Biochem* **80**, 825-858, doi:10.1146/annurev-biochem-060608-102511 (2011).
305 Sakaidani, Y. *et al.* O-linked-N-acetylglucosamine on extracellular protein domains mediates epithelial cell-matrix interactions. *Nature communications* **2**, 583, doi:10.1038/ncomms1591 (2011).
306 Kamemura, K. & Hart, G. W. Dynamic interplay between O-glycosylation and O-phosphorylation of nucleocytoplasmic proteins: a new paradigm for metabolic

control of signal transduction and transcription. *Progress in nucleic acid research and molecular biology* **73**, 107-136 (2003).

307 Butkinaree, C., Park, K. & Hart, G. W. O-linked beta-N-acetylglucosamine (O-GlcNAc): Extensive crosstalk with phosphorylation to regulate signaling and transcription in response to nutrients and stress. *Biochimica et biophysica acta* **1800**, 96-106, doi:10.1016/j.bbagen.2009.07.018 (2010).

308 Slawson, C., Copeland, R. J. & Hart, G. W. O-GlcNAc signaling: a metabolic link between diabetes and cancer? *Trends in biochemical sciences* **35**, 547-555, doi:10.1016/j.tibs.2010.04.005 (2010).

309 Abramowitz, L. K., Olivier-Van Stichelen, S. & Hanover, J. A. Chromosome imbalance as a driver of sex disparity in disease. *Journal of genomics* **2**, 77-88, doi:10.7150/jgen.8123 (2014).

310 Martinez-Fleites, C. *et al.* Structure of an O-GlcNAc transferase homolog provides insight into intracellular glycosylation. *Nature structural & molecular biology* **15**, 764-765, doi:10.1038/nsmb.1443 (2008).

311 Kreppel, L. K., Blomberg, M. A. & Hart, G. W. Dynamic glycosylation of nuclear and cytosolic proteins. Cloning and characterization of a unique O-GlcNAc transferase with multiple tetratricopeptide repeats. *The Journal of biological chemistry* **272**, 9308-9315 (1997).

312 Lubas, W. A., Frank, D. W., Krause, M. & Hanover, J. A. O-Linked GlcNAc transferase is a conserved nucleocytoplasmic protein containing tetratricopeptide repeats. *The Journal of biological chemistry* **272**, 9316-9324 (1997).

313 Jinek, M. *et al.* The superhelical TPR-repeat domain of O-linked GlcNAc transferase exhibits structural similarities to importin alpha. *Nature structural & molecular biology* **11**, 1001-1007, doi:10.1038/nsmb833 (2004).

314 Clarke, A. J. *et al.* Structural insights into mechanism and specificity of O-GlcNAc transferase. *The EMBO journal* **27**, 2780-2788, doi:10.1038/emboj.2008.186 (2008).

315 Iyer, S. P. & Hart, G. W. Roles of the tetratricopeptide repeat domain in O-GlcNAc transferase targeting and protein substrate specificity. *The Journal of biological chemistry* **278**, 24608-24616, doi:10.1074/jbc.M300036200 (2003).

316 Lairson, L. L., Henrissat, B., Davies, G. J. & Withers, S. G. Glycosyltransferases: structures, functions, and mechanisms. *Annu Rev Biochem* **77**, 521-555, doi:10.1146/annurev.biochem.76.061005.092322 (2008).

317 Lazarus, M. B., Nam, Y., Jiang, J., Sliz, P. & Walker, S. Structure of human O-GlcNAc transferase and its complex with a peptide substrate. *Nature* **469**, 564-567, doi:10.1038/nature09638 (2011).

318 Yang, X. *et al.* Phosphoinositide signalling links O-GlcNAc transferase to insulin resistance. *Nature* **451**, 964-969, doi:10.1038/nature06668 (2008).

319 Hanover, J. A., Krause, M. W. & Love, D. C. Bittersweet memories: linking metabolism to epigenetics through O-GlcNAcylation. *Nature reviews. Molecular cell biology* **13**, 312-321, doi:10.1038/nrm3334 (2012).

320 Ruan, H. B., Singh, J. P., Li, M. D., Wu, J. & Yang, X. Cracking the O-GlcNAc code in metabolism. *Trends in endocrinology and metabolism: TEM* **24**, 301-309, doi:10.1016/j.tem.2013.02.002 (2013).

321 Hanover, J. A., Krause, M. W. & Love, D. C. The hexosamine signaling pathway: O-GlcNAc cycling in feast or famine. *Biochimica et biophysica acta* **1800**, 80-95, doi:10.1016/j.bbagen.2009.07.017 (2010).
322 Marshall, S., Bacote, V. & Traxinger, R. R. Discovery of a metabolic pathway mediating glucose-induced desensitization of the glucose transport system. Role of hexosamine biosynthesis in the induction of insulin resistance. *The Journal of biological chemistry* **266**, 4706-4712 (1991).
323 Slawson, C. & Hart, G. W. O-GlcNAc signalling: implications for cancer cell biology. *Nature reviews. Cancer* **11**, 678-684, doi:10.1038/nrc3114 (2011).
324 Akimoto, Y., Kreppel, L. K., Hirano, H. & Hart, G. W. Increased O-GlcNAc transferase in pancreas of rats with streptozotocin-induced diabetes. *Diabetologia* **43**, 1239-1247, doi:10.1007/s001250051519 (2000).
325 Caldwell, S. A. *et al.* Nutrient sensor O-GlcNAc transferase regulates breast cancer tumorigenesis through targeting of the oncogenic transcription factor FoxM1. *Oncogene* **29**, 2831-2842, doi:10.1038/onc.2010.41 (2010).
326 Dias, W. B. & Hart, G. W. O-GlcNAc modification in diabetes and Alzheimer's disease. *Molecular bioSystems* **3**, 766-772, doi:10.1039/b704905f (2007).
327 Ma, Z. & Vosseller, K. O-GlcNAc in cancer biology. *Amino acids* **45**, 719-733, doi:10.1007/s00726-013-1543-8 (2013).
328 Lazarus, B. D., Love, D. C. & Hanover, J. A. O-GlcNAc cycling: implications for neurodegenerative disorders. *The international journal of biochemistry & cell biology* **41**, 2134-2146, doi:10.1016/j.biocel.2009.03.008 (2009).
329 Forma, E., Jozwiak, P., Brys, M. & Krzeslak, A. The potential role of O-GlcNAc modification in cancer epigenetics. *Cellular & molecular biology letters* **19**, 438-460, doi:10.2478/s11658-014-0204-6 (2014).
330 Aumann, S. & Abdel-Wahab, O. Somatic alterations and dysregulation of epigenetic modifiers in cancers. *Biochemical and biophysical research communications* **455**, 24-34, doi:10.1016/j.bbrc.2014.08.004 (2014).
331 Issad, T. & Pagesy, P. [Protein O-GlcNAcylation and regulation of cell signalling: involvement in pathophysiology]. *Biologie aujourd'hui* **208**, 109-117, doi:10.1051/jbio/2014015 (2014).
332 Warburg, O. On respiratory impairment in cancer cells. *Science* **124**, 269-270 (1956).
333 Warburg, O. On the origin of cancer cells. *Science* **123**, 309-314 (1956).
334 Fardini, Y., Dehennaut, V., Lefebvre, T. & Issad, T. O-GlcNAcylation: A New Cancer Hallmark? *Frontiers in endocrinology* **4**, 99, doi:10.3389/fendo.2013.00099 (2013).
335 de Queiroz, R. M., Carvalho, E. & Dias, W. B. O-GlcNAcylation: The Sweet Side of the Cancer. *Frontiers in oncology* **4**, 132, doi:10.3389/fonc.2014.00132 (2014).
336 Gao, Y., Wells, L., Comer, F. I., Parker, G. J. & Hart, G. W. Dynamic O-glycosylation of nuclear and cytosolic proteins: cloning and characterization of a neutral, cytosolic beta-N-acetylglucosaminidase from human brain. *The Journal of biological chemistry* **276**, 9838-9845, doi:10.1074/jbc.M010420200 (2001).

337 Schultz, J. & Pils, B. Prediction of structure and functional residues for O-GlcNAcase, a divergent homologue of acetyltransferases. *FEBS letters* **529**, 179-182 (2002).
338 Toleman, C., Paterson, A. J., Whisenhunt, T. R. & Kudlow, J. E. Characterization of the histone acetyltransferase (HAT) domain of a bifunctional protein with activable O-GlcNAcase and HAT activities. *The Journal of biological chemistry* **279**, 53665-53673, doi:10.1074/jbc.M410406200 (2004).
339 Comtesse, N., Maldener, E. & Meese, E. Identification of a nuclear variant of MGEA5, a cytoplasmic hyaluronidase and a beta-N-acetylglucosaminidase. *Biochemical and biophysical research communications* **283**, 634-640, doi:10.1006/bbrc.2001.4815 (2001).
340 Dehennaut, V., Leprince, D. & Lefebvre, T. O-GlcNAcylation, an Epigenetic Mark. Focus on the Histone Code, TET Family Proteins, and Polycomb Group Proteins. *Frontiers in endocrinology* **5**, 155, doi:10.3389/fendo.2014.00155 (2014).
341 Deng, R. P. *et al.* Global identification of O-GlcNAc transferase (OGT) interactors by a human proteome microarray and the construction of an OGT interactome. *Proteomics* **14**, 1020-1030, doi:10.1002/pmic.201300144 (2014).
342 Chen, J. *et al.* Identifying candidate genes for Type 2 Diabetes Mellitus and obesity through gene expression profiling in multiple tissues or cells. *Journal of diabetes research* **2013**, 970435, doi:10.1155/2013/970435 (2013).
343 Yang, X., Zhang, F. & Kudlow, J. E. Recruitment of O-GlcNAc transferase to promoters by corepressor mSin3A: coupling protein O-GlcNAcylation to transcriptional repression. *Cell* **110**, 69-80 (2002).
344 Amirouchene-Angelozzi, N. *et al.* Establishment of novel cell lines recapitulating the genetic landscape of uveal melanoma and preclinical validation of mTOR as a therapeutic target. *Molecular oncology* **8**, 1508-1520, doi:10.1016/j.molonc.2014.06.004 (2014).
345 Gambetta, M. C., Oktaba, K. & Muller, J. Essential role of the glycosyltransferase sxc/Ogt in polycomb repression. *Science* **325**, 93-96, doi:10.1126/science.1169727 (2009).
346 Sinclair, D. A. *et al.* Drosophila O-GlcNAc transferase (OGT) is encoded by the Polycomb group (PcG) gene, super sex combs (sxc). *Proceedings of the National Academy of Sciences of the United States of America* **106**, 13427-13432, doi:10.1073/pnas.0904638106 (2009).
347 Ingham, P. W. A gene that regulates the bithorax complex differentially in larval and adult cells of Drosophila. *Cell* **37**, 815-823 (1984).
348 Shafi, R. *et al.* The O-GlcNAc transferase gene resides on the X chromosome and is essential for embryonic stem cell viability and mouse ontogeny. *Proceedings of the National Academy of Sciences of the United States of America* **97**, 5735-5739, doi:10.1073/pnas.100471497 (2000).
349 O'Donnell, N., Zachara, N. E., Hart, G. W. & Marth, J. D. Ogt-dependent X-chromosome-linked protein glycosylation is a requisite modification in somatic cell function and embryo viability. *Molecular and cellular biology* **24**, 1680-1690 (2004).

350 Myers, S. A., Panning, B. & Burlingame, A. L. Polycomb repressive complex 2 is necessary for the normal site-specific O-GlcNAc distribution in mouse embryonic stem cells. *Proceedings of the National Academy of Sciences of the United States of America* **108**, 9490-9495, doi:10.1073/pnas.1019289108 (2011).
351 Chen, Q., Chen, Y., Bian, C., Fujiki, R. & Yu, X. TET2 promotes histone O-GlcNAcylation during gene transcription. *Nature* **493**, 561-564, doi:10.1038/nature11742 (2013).
352 Ito, R. *et al.* TET3-OGT interaction increases the stability and the presence of OGT in chromatin. *Genes to cells : devoted to molecular & cellular mechanisms* **19**, 52-65, doi:10.1111/gtc.12107 (2014).
353 Zhang, Q. *et al.* Differential regulation of the ten-eleven translocation (TET) family of dioxygenases by O-linked beta-N-acetylglucosamine transferase (OGT). *The Journal of biological chemistry* **289**, 5986-5996, doi:10.1074/jbc.M113.524140 (2014).
354 Vella, P. *et al.* Tet proteins connect the O-linked N-acetylglucosamine transferase Ogt to chromatin in embryonic stem cells. *Molecular cell* **49**, 645-656, doi:10.1016/j.molcel.2012.12.019 (2013).
355 Shi, F. T. *et al.* Ten-eleven translocation 1 (Tet1) is regulated by O-linked N-acetylglucosamine transferase (Ogt) for target gene repression in mouse embryonic stem cells. *The Journal of biological chemistry* **288**, 20776-20784, doi:10.1074/jbc.M113.460386 (2013).
356 Hanover, J. A. Epigenetics gets sweeter: O-GlcNAc joins the "histone code". *Chem Biol* **17**, 1272-1274, doi:10.1016/j.chembiol.2010.12.001 (2010).
357 Arnaudo, A. M. & Garcia, B. A. Proteomic characterization of novel histone post-translational modifications. *Epigenetics & chromatin* **6**, 24, doi:10.1186/1756-8935-6-24 (2013).
358 Sakabe, K. & Hart, G. W. O-GlcNAc transferase regulates mitotic chromatin dynamics. *The Journal of biological chemistry* **285**, 34460-34468, doi:10.1074/jbc.M110.158170 (2010).
359 Xu, Q. *et al.* AMPK regulates histone H2B O-GlcNAcylation. *Nucleic acids research* **42**, 5594-5604, doi:10.1093/nar/gku236 (2014).
360 Fong, J. J. *et al.* beta-N-Acetylglucosamine (O-GlcNAc) is a novel regulator of mitosis-specific phosphorylations on histone H3. *The Journal of biological chemistry* **287**, 12195-12203, doi:10.1074/jbc.M111.315804 (2012).
361 Sinclair, D. A. *et al.* The Additional sex combs gene of Drosophila encodes a chromatin protein that binds to shared and unique Polycomb group sites on polytene chromosomes. *Development* **125**, 1207-1216 (1998).
362 Sinclair, D. A., Campbell, R. B., Nicholls, F., Slade, E. & Brock, H. W. Genetic analysis of the additional sex combs locus of Drosophila melanogaster. *Genetics* **130**, 817-825 (1992).
363 Simon, J., Chiang, A. & Bender, W. Ten different Polycomb group genes are required for spatial control of the abdA and AbdB homeotic products. *Development* **114**, 493-505 (1992).

364 Breen, T. R. & Duncan, I. M. Maternal expression of genes that regulate the bithorax complex of Drosophila melanogaster. *Developmental biology* **118**, 442-456 (1986).
365 Milne, T. A., Sinclair, D. A. & Brock, H. W. The Additional sex combs gene of Drosophila is required for activation and repression of homeotic loci, and interacts specifically with Polycomb and super sex combs. *Molecular & general genetics : MGG* **261**, 753-761 (1999).
366 Baskind, H. A. *et al.* Functional conservation of Asxl2, a murine homolog for the Drosophila enhancer of trithorax and polycomb group gene Asx. *PloS one* **4**, e4750, doi:10.1371/journal.pone.0004750 (2009).
367 Fisher, C. L., Randazzo, F., Humphries, R. K. & Brock, H. W. Characterization of Asxl1, a murine homolog of Additional sex combs, and analysis of the Asx-like gene family. *Gene* **369**, 109-118, doi:10.1016/j.gene.2005.10.033 (2006).
368 Gildea, J. J., Lopez, R. & Shearn, A. A screen for new trithorax group genes identified little imaginal discs, the Drosophila melanogaster homologue of human retinoblastoma binding protein 2. *Genetics* **156**, 645-663 (2000).
369 Fisher, C. L., Berger, J., Randazzo, F. & Brock, H. W. A human homolog of Additional sex combs, ADDITIONAL SEX COMBS-LIKE 1, maps to chromosome 20q11. *Gene* **306**, 115-126 (2003).
370 Katoh, M. & Katoh, M. Identification and characterization of ASXL2 gene in silico. *International journal of oncology* **23**, 845-850 (2003).
371 Katoh, M. & Katoh, M. Identification and characterization of ASXL3 gene in silico. *International journal of oncology* **24**, 1617-1622 (2004).
372 Cho, Y. S., Kim, E. J., Park, U. H., Sin, H. S. & Um, S. J. Additional sex comb-like 1 (ASXL1), in cooperation with SRC-1, acts as a ligand-dependent coactivator for retinoic acid receptor. *The Journal of biological chemistry* **281**, 17588-17598, doi:10.1074/jbc.M512616200 (2006).
373 Lee, S. W. *et al.* ASXL1 represses retinoic acid receptor-mediated transcription through associating with HP1 and LSD1. *The Journal of biological chemistry* **285**, 18-29, doi:10.1074/jbc.M109.065862 (2010).
374 Park, U. H., Yoon, S. K., Park, T., Kim, E. J. & Um, S. J. Additional sex comb-like (ASXL) proteins 1 and 2 play opposite roles in adipogenesis via reciprocal regulation of peroxisome proliferator-activated receptor {gamma}. *The Journal of biological chemistry* **286**, 1354-1363, doi:10.1074/jbc.M110.177816 (2011).
375 Abdel-Wahab, O. *et al.* ASXL1 mutations promote myeloid transformation through loss of PRC2-mediated gene repression. *Cancer cell* **22**, 180-193, doi:10.1016/j.ccr.2012.06.032 (2012).
376 Izawa, T. *et al.* ASXL2 Regulates Glucose, Lipid, and Skeletal Homeostasis. *Cell reports* **11**, 1625-1637, doi:10.1016/j.celrep.2015.05.019 (2015).
377 Farber, C. R. *et al.* Mouse genome-wide association and systems genetics identify Asxl2 as a regulator of bone mineral density and osteoclastogenesis. *PLoS genetics* **7**, e1002038, doi:10.1371/journal.pgen.1002038 (2011).
378 Sanchez-Pulido, L., Kong, L. & Ponting, C. P. A common ancestry for BAP1 and Uch37 regulators. *Bioinformatics* **28**, 1953-1956, doi:10.1093/bioinformatics/bts319 (2012).

379 Katoh, M., Igarashi, M., Fukuda, H., Nakagama, H. & Katoh, M. Cancer genetics and genomics of human FOX family genes. *Cancer letters* **328**, 198-206, doi:10.1016/j.canlet.2012.09.017 (2013).
380 Sanchez, R. & Zhou, M. M. The PHD finger: a versatile epigenome reader. *Trends in biochemical sciences* **36**, 364-372, doi:10.1016/j.tibs.2011.03.005 (2011).
381 Li, Y. & Li, H. Many keys to push: diversifying the 'readership' of plant homeodomain fingers. *Acta Biochim Biophys Sin (Shanghai)* **44**, 28-39, doi:10.1093/abbs/gmr117 (2012).
382 Liu, L. *et al.* Solution structure of an atypical PHD finger in BRPF2 and its interaction with DNA. *J Struct Biol* **180**, 165-173, doi:10.1016/j.jsb.2012.06.014 (2012).
383 Aasland, R., Gibson, T. J. & Stewart, A. F. The PHD finger: implications for chromatin-mediated transcriptional regulation. *Trends in biochemical sciences* **20**, 56-59 (1995).
384 Musco, G. & Peterson, P. PHD finger of autoimmune regulator: an epigenetic link between the histone modifications and tissue-specific antigen expression in thymus. *Epigenetics : official journal of the DNA Methylation Society* **3**, 310-314 (2008).
385 Musselman, C. A. & Kutateladze, T. G. PHD fingers: epigenetic effectors and potential drug targets. *Mol Interv* **9**, 314-323, doi:10.1124/mi.9.6.7 (2009).
386 Ragvin, A. *et al.* Nucleosome binding by the bromodomain and PHD finger of the transcriptional cofactor p300. *Journal of molecular biology* **337**, 773-788, doi:10.1016/j.jmb.2004.01.051 (2004).
387 Saksouk, N. *et al.* HBO1 HAT complexes target chromatin throughout gene coding regions via multiple PHD finger interactions with histone H3 tail. *Molecular cell* **33**, 257-265, doi:10.1016/j.molcel.2009.01.007 (2009).
388 Shi, X. *et al.* ING2 PHD domain links histone H3 lysine 4 methylation to active gene repression. *Nature* **442**, 96-99, doi:10.1038/nature04835 (2006).
389 Zeng, L. *et al.* Structural insights into human KAP1 PHD finger-bromodomain and its role in gene silencing. *Nature structural & molecular biology* **15**, 626-633, doi:10.1038/nsmb.1416 (2008).
390 Zeng, L. *et al.* Mechanism and regulation of acetylated histone binding by the tandem PHD finger of DPF3b. *Nature* **466**, 258-262, doi:10.1038/nature09139 (2010).
391 Ali, M. *et al.* Tandem PHD fingers of MORF/MOZ acetyltransferases display selectivity for acetylated histone H3 and are required for the association with chromatin. *Journal of molecular biology* **424**, 328-338, doi:10.1016/j.jmb.2012.10.004 (2012).
392 Baker, L. A., Allis, C. D. & Wang, G. G. PHD fingers in human diseases: disorders arising from misinterpreting epigenetic marks. *Mutation research* **647**, 3-12, doi:10.1016/j.mrfmmm.2008.07.004 (2008).
393 Aravind, L. & Iyer, L. M. The HARE-HTH and associated domains: novel modules in the coordination of epigenetic DNA and protein modifications. *Cell cycle* **11**, 119-131, doi:10.4161/cc.11.1.18475 (2012).

394 Gutierrez, L. *et al.* The role of the histone H2A ubiquitinase Sce in Polycomb repression. *Development* **139**, 117-127, doi:10.1242/dev.074450 (2012).
395 Metzeler, K. H. *et al.* ASXL1 mutations identify a high-risk subgroup of older patients with primary cytogenetically normal AML within the ELN Favorable genetic category. *Blood* **118**, 6920-6929, doi:10.1182/blood-2011-08-368225 (2011).
396 Abdel-Wahab, O. *et al.* Concomitant analysis of EZH2 and ASXL1 mutations in myelofibrosis, chronic myelomonocytic leukemia and blast-phase myeloproliferative neoplasms. *Leukemia* **25**, 1200-1202, doi:10.1038/leu.2011.58 (2011).
397 Bejar, R. *et al.* Clinical effect of point mutations in myelodysplastic syndromes. *N Engl J Med* **364**, 2496-2506, doi:10.1056/NEJMoa1013343 (2011).
398 Patel, J. P. *et al.* Prognostic relevance of integrated genetic profiling in acute myeloid leukemia. *N Engl J Med* **366**, 1079-1089, doi:10.1056/NEJMoa1112304 (2012).
399 Thol, F. *et al.* Prognostic significance of ASXL1 mutations in patients with myelodysplastic syndromes. *Journal of clinical oncology : official journal of the American Society of Clinical Oncology* **29**, 2499-2506, doi:10.1200/JCO.2010.33.4938 (2011).
400 Boultwood, J. *et al.* Frequent mutation of the polycomb-associated gene ASXL1 in the myelodysplastic syndromes and in acute myeloid leukemia. *Leukemia* **24**, 1062-1065, doi:10.1038/leu.2010.20 (2010).
401 Hoischen, A. *et al.* De novo nonsense mutations in ASXL1 cause Bohring-Opitz syndrome. *Nature genetics* **43**, 729-731, doi:10.1038/ng.868 (2011).
402 Grasso, C. S. *et al.* The mutational landscape of lethal castration-resistant prostate cancer. *Nature* **487**, 239-243, doi:10.1038/nature11125 (2012).
403 Sjoblom, T. *et al.* The consensus coding sequences of human breast and colorectal cancers. *Science* **314**, 268-274, doi:10.1126/science.1133427 (2006).
404 Gelsi-Boyer, V. *et al.* Mutations of polycomb-associated gene ASXL1 in myelodysplastic syndromes and chronic myelomonocytic leukaemia. *British journal of haematology* **145**, 788-800, doi:10.1111/j.1365-2141.2009.07697.x (2009).
405 Carbuccia, N. *et al.* Mutations of ASXL1 gene in myeloproliferative neoplasms. *Leukemia* **23**, 2183-2186, doi:10.1038/leu.2009.141 (2009).
406 Gelsi-Boyer, V. *et al.* ASXL1 mutation is associated with poor prognosis and acute transformation in chronic myelomonocytic leukaemia. *British journal of haematology* **151**, 365-375, doi:10.1111/j.1365-2141.2010.08381.x (2010).
407 Chou, W. C. *et al.* Distinct clinical and biological features of de novo acute myeloid leukemia with additional sex comb-like 1 (ASXL1) mutations. *Blood* **116**, 4086-4094, doi:10.1182/blood-2010-05-283291 (2010).
408 Gelsi-Boyer, V. *et al.* Mutations in ASXL1 are associated with poor prognosis across the spectrum of malignant myeloid diseases. *J Hematol Oncol* **5**, 12, doi:10.1186/1756-8722-5-12 (2012).

409 Carbuccia, N. *et al.* Mutual exclusion of ASXL1 and NPM1 mutations in a series of acute myeloid leukemias. *Leukemia* **24**, 469-473, doi:10.1038/leu.2009.218 (2010).
410 Szpurka, H. *et al.* Spectrum of mutations in RARS-T patients includes TET2 and ASXL1 mutations. *Leuk Res* **34**, 969-973, doi:10.1016/j.leukres.2010.02.033 (2010).
411 Bullen, J. W. *et al.* Cross-talk between two essential nutrient-sensitive enzymes: O-GlcNAc transferase (OGT) and AMP-activated protein kinase (AMPK). *The Journal of biological chemistry* **289**, 10592-10606, doi:10.1074/jbc.M113.523068 (2014).
412 Nagel, A. K. & Ball, L. E. O-GlcNAc transferase and O-GlcNAcase: achieving target substrate specificity. *Amino acids* **46**, 2305-2316, doi:10.1007/s00726-014-1827-7 (2014).
413 Vocadlo, D. J. O-GlcNAc processing enzymes: catalytic mechanisms, substrate specificity, and enzyme regulation. *Current opinion in chemical biology* **16**, 488-497, doi:10.1016/j.cbpa.2012.10.021 (2012).
414 Harwood, K. R. & Hanover, J. A. Nutrient-driven O-GlcNAc cycling - think globally but act locally. *Journal of cell science* **127**, 1857-1867, doi:10.1242/jcs.113233 (2014).
415 Zhang, S., Roche, K., Nasheuer, H. P. & Lowndes, N. F. Modification of histones by sugar beta-N-acetylglucosamine (GlcNAc) occurs on multiple residues, including histone H3 serine 10, and is cell cycle-regulated. *The Journal of biological chemistry* **286**, 37483-37495, doi:10.1074/jbc.M111.284885 (2011).
416 Jozwiak, P., Forma, E., Brys, M. & Krzeslak, A. O-GlcNAcylation and Metabolic Reprograming in Cancer. *Frontiers in endocrinology* **5**, 145, doi:10.3389/fendo.2014.00145 (2014).
417 Isono, T. O-GlcNAc-specific antibody CTD110.6 cross-reacts with N-GlcNAc2-modified proteins induced under glucose deprivation. *PloS one* **6**, e18959, doi:10.1371/journal.pone.0018959 (2011).
418 Mizuguchi-Hata, C., Ogawa, Y., Oka, M. & Yoneda, Y. Quantitative regulation of nuclear pore complex proteins by O-GlcNAcylation. *Biochimica et biophysica acta* **1833**, 2682-2689, doi:10.1016/j.bbamcr.2013.06.008 (2013).
419 Hammond-Martel, I. *et al.* PI 3 kinase related kinases-independent proteolysis of BRCA1 regulates Rad51 recruitment during genotoxic stress in human cells. *PLoS One* **5**, e14027, doi:10.1371/journal.pone.0014027 (2010).
420 Vassilev, L. T. *et al.* Selective small-molecule inhibitor reveals critical mitotic functions of human CDK1. *Proc Natl Acad Sci U S A* **103**, 10660-10665, doi:10.1073/pnas.0600447103 (2006).
421 Haynes, P. A. & Aebersold, R. Simultaneous detection and identification of O-GlcNAc-modified glycoproteins using liquid chromatography-tandem mass spectrometry. *Anal Chem* **72**, 5402-5410 (2000).
422 Vester-Christensen, M. B. *et al.* Mining the O-mannose glycoproteome reveals cadherins as major O-mannosylated glycoproteins. *Proc Natl Acad Sci U S A* **110**, 21018-21023, doi:10.1073/pnas.1313446110 (2013).
423 Alfaro, J. F. *et al.* Tandem mass spectrometry identifies many mouse brain O-GlcNAcylated proteins including EGF domain-specific O-GlcNAc transferase

targets. *Proceedings of the National Academy of Sciences of the United States of America* **109**, 7280-7285, doi:10.1073/pnas.1200425109 (2012).

424 Vosseller, K. *et al.* O-linked N-acetylglucosamine proteomics of postsynaptic density preparations using lectin weak affinity chromatography and mass spectrometry. *Mol Cell Proteomics* **5**, 923-934, doi:10.1074/mcp.T500040-MCP200 (2006).

425 Trinidad, J. C. *et al.* Global identification and characterization of both O-GlcNAcylation and phosphorylation at the murine synapse. *Mol Cell Proteomics* **11**, 215-229, doi:10.1074/mcp.O112.018366 (2012).

426 Myers, S. A., Daou, S., Affar el, B. & Burlingame, A. Electron transfer dissociation (ETD): the mass spectrometric breakthrough essential for O-GlcNAc protein site assignments-a study of the O-GlcNAcylated protein host cell factor C1. *Proteomics* **13**, 982-991, doi:10.1002/pmic.201200332 (2013).

427 Minsky, N. & Oren, M. The RING domain of Mdm2 mediates histone ubiquitylation and transcriptional repression. *Mol Cell* **16**, 631-639 (2004).

428 Stoscheck, C. M. Quantitation of protein. *Methods Enzymol* **182**, 50-68 (1990).

429 Comer, F. I. & Hart, G. W. Reciprocity between O-GlcNAc and O-phosphate on the carboxyl terminal domain of RNA polymerase II. *Biochemistry* **40**, 7845-7852 (2001).

430 MacGurn, J. A., Hsu, P. C. & Emr, S. D. Ubiquitin and membrane protein turnover: from cradle to grave. *Annual review of biochemistry* **81**, 231-259, doi:10.1146/annurev-biochem-060210-093619 (2012).

431 Nakayama, K. I. & Nakayama, K. Ubiquitin ligases: cell-cycle control and cancer. *Nature reviews. Cancer* **6**, 369-381 (2006).

432 Metzger, M. B., Hristova, V. A. & Weissman, A. M. HECT and RING finger families of E3 ubiquitin ligases at a glance. *Journal of cell science* **125**, 531-537, doi:125/3/531 [pii]

10.1242/jcs.091777 (2012).

433 Eletr, Z. M. & Wilkinson, K. D. Regulation of proteolysis by human deubiquitinating enzymes. *Biochimica et biophysica acta* **1843**, 114-128, doi:10.1016/j.bbamcr.2013.06.027 (2014).

434 Abdel-Rahman, M. H. *et al.* Germline BAP1 mutation predisposes to uveal melanoma, lung adenocarcinoma, meningioma, and other cancers. *J Med Genet*, doi:jmedgenet-2011-100156 [pii]

10.1136/jmedgenet-2011-100156 (2011).

435 Machida, Y. J., Machida, Y., Vashisht, A. A., Wohlschlegel, J. A. & Dutta, A. The deubiquitinating enzyme BAP1 regulates cell growth via interaction with HCF-1. *The Journal of biological chemistry* (2009).

436 Yu, H. *et al.* The Ubiquitin Carboxyl Hydrolase BAP1 Forms a Ternary Complex with YY1 and HCF-1 and is a Critical Regulator of Gene Expression. *Molecular and cellular biology*, doi:MCB.00396-10 [pii]

10.1128/MCB.00396-10 (2010).

437 Pan, H. *et al.* BAP1 regulates cell cycle progression through E2F1 target genes and mediates transcriptional silencing via H2A monoubiquitination in uveal melanoma cells. *The international journal of biochemistry & cell biology* **60C**, 176-184, doi:10.1016/j.biocel.2015.01.001 (2015).
438 Ismail, I. H. *et al.* Germ-line Mutations in BAP1 Impair its Function in DNA Double-Strand break Repair. *Cancer research*, doi:10.1158/0008-5472.CAN-13-3109 (2014).
439 Lee, H. S., Lee, S. A., Hur, S. K., Seo, J. W. & Kwon, J. Stabilization and targeting of INO80 to replication forks by BAP1 during normal DNA synthesis. *Nature communications* **5**, 5128, doi:10.1038/ncomms6128 (2014).
440 Okino, Y., Machida, Y., Frankland-Searby, S. & Machida, Y. J. BRCA1-associated protein 1 (BAP1) deubiquitinase antagonizes the ubiquitin-mediated activation of FoxK2 target genes. *The Journal of biological chemistry* **290**, 1580-1591, doi:10.1074/jbc.M114.609834 (2015).
441 Yao, T. *et al.* Proteasome recruitment and activation of the Uch37 deubiquitinating enzyme by Adrm1. *Nature cell biology* (2006).
442 Qiu, X. B. *et al.* hRpn13/ADRM1/GP110 is a novel proteasome subunit that binds the deubiquitinating enzyme, UCH37. *EMBO J* **25**, 5742-5753, doi:10.1038/sj.emboj.7601450 (2006).
443 Hamazaki, J. *et al.* A novel proteasome interacting protein recruits the deubiquitinating enzyme UCH37 to 26S proteasomes. *The EMBO journal* **25**, 4524-4536, doi:10.1038/sj.emboj.7601338 (2006).
444 Katoh, M. Functional and cancer genomics of ASXL family members. *British journal of cancer*, doi:bjc2013281 [pii]

10.1038/bjc.2013.281 (2013).
445 Balasubramani, A. *et al.* Cancer-associated ASXL1 mutations may act as gain-of-function mutations of the ASXL1-BAP1 complex. *Nature communications* **6**, 7307, doi:10.1038/ncomms8307 (2015).
446 Lee, J. W. *et al.* Protein expression and intracellular localization of prostate apoptosis response-4 (Par-4) are associated with apoptosis induction in nasopharyngeal carcinoma cell lines. *Cancer letters* **257**, 252-262, doi:10.1016/j.canlet.2007.08.004 (2007).
447 Ji, Z. *et al.* The forkhead transcription factor FOXK2 acts as a chromatin targeting factor for the BAP1-containing histone deubiquitinase complex. *Nucleic acids research* **42**, 6232-6242, doi:10.1093/nar/gku274 (2014).
448 Belle, J. I. & Nijnik, A. H2A-DUBbing the mammalian epigenome: expanding frontiers for histone H2A deubiquitinating enzymes in cell biology and physiology. *The international journal of biochemistry & cell biology* **50**, 161-174, doi:10.1016/j.biocel.2014.03.004 (2014).
449 Morrow, M. E. *et al.* Stabilization of an unusual salt bridge in ubiquitin by the extra C-terminal domain of the proteasome-associated deubiquitinase UCH37 as a mechanism of its exo specificity. *Biochemistry* **52**, 3564-3578, doi:10.1021/bi4003106 (2013).

450 Sahtoe, D. D. *et al.* Mechanism of UCH-L5 activation and inhibition by DEUBAD domains in RPN13 and INO80G. *Molecular cell* **57**, 887-900, doi:10.1016/j.molcel.2014.12.039 (2015).
451 VanderLinden, R. T. *et al.* Structural basis for the activation and inhibition of the UCH37 deubiquitylase. *Molecular cell* **57**, 901-911, doi:10.1016/j.molcel.2015.01.016 (2015).
452 Jacobs, J. J., Kieboom, K., Marino, S., DePinho, R. A. & van Lohuizen, M. The oncogene and Polycomb-group gene bmi-1 regulates cell proliferation and senescence through the ink4a locus. *Nature* **397**, 164-168, doi:10.1038/16476 (1999).
453 Dietrich, N. *et al.* Bypass of senescence by the polycomb group protein CBX8 through direct binding to the INK4A-ARF locus. *The EMBO journal* **26**, 1637-1648, doi:10.1038/sj.emboj.7601632 (2007).
454 Luis, N. M. *et al.* Regulation of human epidermal stem cell proliferation and senescence requires polycomb- dependent and -independent functions of Cbx4. *Cell stem cell* **9**, 233-246, doi:10.1016/j.stem.2011.07.013 (2011).
455 Leung, C. *et al.* Bmi1 is essential for cerebellar development and is overexpressed in human medulloblastomas. *Nature* **428**, 337-341, doi:10.1038/nature02385 (2004).
456 Xu, F. *et al.* Overexpression of the EZH2, RING1 and BMI1 genes is common in myelodysplastic syndromes: relation to adverse epigenetic alteration and poor prognostic scoring. *Annals of hematology* **90**, 643-653, doi:10.1007/s00277-010-1128-5 (2011).
457 Bosch, A. *et al.* The Polycomb group protein RING1B is overexpressed in ductal breast carcinoma and is required to sustain FAK steady state levels in breast cancer epithelial cells. *Oncotarget* **5**, 2065-2076 (2014).
458 Lopez-Otin, C. & Overall, C. M. Protease degradomics: a new challenge for proteomics. *Nature reviews. Molecular cell biology* **3**, 509-519, doi:10.1038/nrm858 (2002).
459 Guruharsha, K. G., Kankel, M. W. & Artavanis-Tsakonas, S. The Notch signalling system: recent insights into the complexity of a conserved pathway. *Nat Rev Genet* **13**, 654-666, doi:10.1038/nrg3272 (2012).
460 Raina, D. *et al.* c-Abl tyrosine kinase regulates caspase-9 autocleavage in the apoptotic response to DNA damage. *The Journal of biological chemistry* **280**, 11147-11151, doi:10.1074/jbc.M413787200 (2005).
461 Renatus, M., Stennicke, H. R., Scott, F. L., Liddington, R. C. & Salvesen, G. S. Dimer formation drives the activation of the cell death protease caspase 9. *Proceedings of the National Academy of Sciences of the United States of America* **98**, 14250-14255, doi:10.1073/pnas.231465798 (2001).
462 Affar, E. B. *et al.* Caspase-3-mediated processing of poly(ADP-ribose) glycohydrolase during apoptosis. *The Journal of biological chemistry* **276**, 2935-2942, doi:10.1074/jbc.M007269200 (2001).
463 Kristie, T. M. & Sharp, P. A. Purification of the cellular C1 factor required for the stable recognition of the Oct-1 homeodomain by the herpes simplex virus alpha-

trans-induction factor (VP16). *The Journal of biological chemistry* **268**, 6525-6534 (1993).
464 Wilson, A. C., Peterson, M. G. & Herr, W. The HCF repeat is an unusual proteolytic cleavage signal. *Genes & development* **9**, 2445-2458 (1995).
465 Huttlin, E. L. *et al.* A tissue-specific atlas of mouse protein phosphorylation and expression. *Cell* **143**, 1174-1189, doi:10.1016/j.cell.2010.12.001 (2010).
466 Olsen, J. V. *et al.* Quantitative phosphoproteomics reveals widespread full phosphorylation site occupancy during mitosis. *Science signaling* **3**, ra3, doi:10.1126/scisignal.2000475 (2010).
467 Boyce, M. *et al.* Metabolic cross-talk allows labeling of O-linked beta-N-acetylglucosamine-modified proteins via the N-acetylgalactosamine salvage pathway. *Proceedings of the National Academy of Sciences of the United States of America* **108**, 3141-3146, doi:10.1073/pnas.1010045108 (2011).
468 Chuh, K. N., Zaro, B. W., Piller, F., Piller, V. & Pratt, M. R. Changes in metabolic chemical reporter structure yield a selective probe of O-GlcNAc modification. *Journal of the American Chemical Society* **136**, 12283-12295, doi:10.1021/ja504063c (2014).
469 Wang, S. *et al.* Proteomic approaches for site-specific O-GlcNAcylation analysis. *Bioanalysis* **6**, 2571-2580, doi:10.4155/bio.14.239 (2014).
470 Rexach, J. E. *et al.* Quantification of O-glycosylation stoichiometry and dynamics using resolvable mass tags. *Nature chemical biology* **6**, 645-651, doi:10.1038/nchembio.412 (2010).
471 Kim, E. J. Chemical arsenal for the study of O-GlcNAc. *Molecules* **16**, 1987-2022, doi:10.3390/molecules16031987 (2011).
472 Ward, P. S. & Thompson, C. B. Metabolic reprogramming: a cancer hallmark even warburg did not anticipate. *Cancer cell* **21**, 297-308, doi:10.1016/j.ccr.2012.02.014 (2012).
473 Hanahan, D. & Weinberg, R. A. Hallmarks of cancer: the next generation. *Cell* **144**, 646-674, doi:10.1016/j.cell.2011.02.013 (2011).
474 DeBerardinis, R. J., Lum, J. J., Hatzivassiliou, G. & Thompson, C. B. The biology of cancer: metabolic reprogramming fuels cell growth and proliferation. *Cell metabolism* **7**, 11-20, doi:10.1016/j.cmet.2007.10.002 (2008).
475 Vander Heiden, M. G., Cantley, L. C. & Thompson, C. B. Understanding the Warburg effect: the metabolic requirements of cell proliferation. *Science* **324**, 1029-1033, doi:10.1126/science.1160809 (2009).
476 Phan, L. M., Yeung, S. C. & Lee, M. H. Cancer metabolic reprogramming: importance, main features, and potentials for precise targeted anti-cancer therapies. *Cancer Biol Med* **11**, 1-19, doi:10.7497/j.issn.2095-3941.2014.01.001 (2014).
477 Huang, X. *et al.* O-GlcNAcylation of cofilin promotes breast cancer cell invasion. *The Journal of biological chemistry* **288**, 36418-36425, doi:10.1074/jbc.M113.495713 (2013).
478 Brown, J. L., Fritsch, C., Mueller, J. & Kassis, J. A. The Drosophila pho-like gene encodes a YY1-related DNA binding protein that is redundant with pleiohomeotic in homeotic gene silencing. *Development* **130**, 285-294 (2003).

479 Schlisio, S., Halperin, T., Vidal, M. & Nevins, J. R. Interaction of YY1 with E2Fs, mediated by RYBP, provides a mechanism for specificity of E2F function. *Embo J* **21**, 5775-5786 (2002).
480 Xi, H. *et al.* Analysis of overrepresented motifs in human core promoters reveals dual regulatory roles of YY1. *Genome Res* **17**, 798-806 (2007).
481 van Waveren, C. & Moraes, C. T. Transcriptional co-expression and co-regulation of genes coding for components of the oxidative phosphorylation system. *BMC Genomics* **9**, 18 (2008).
482 Cunningham, J. T. *et al.* mTOR controls mitochondrial oxidative function through a YY1-PGC-1alpha transcriptional complex. *Nature* **450**, 736-740 (2007).
483 Hyde-DeRuyscher, R. P., Jennings, E. & Shenk, T. DNA binding sites for the transcriptional activator/repressor YY1. *Nucleic acids research* **23**, 4457-4465 (1995).
484 Affar, E. B. *et al.* Essential dosage-dependent functions of the transcription factor Yin Yang 1 in late embryonic development and cell cycle progression. *Mol. Cell Biol.* **26**, 3565-3581 (2006).
485 Qin, J. *et al.* BAP1 promotes breast cancer cell proliferation and metastasis by deubiquitinating KLF5. *Nature communications* **6**, 8471, doi:10.1038/ncomms9471 (2015).
486 Hayflick, L. & Moorhead, P. S. The serial cultivation of human diploid cell strains. *Experimental cell research* **25**, 585-621 (1961).
487 Hayflick, L. The Limited in Vitro Lifetime of Human Diploid Cell Strains. *Experimental cell research* **37**, 614-636 (1965).
488 Bodnar, A. G. *et al.* Extension of life-span by introduction of telomerase into normal human cells. *Science* **279**, 349-352 (1998).
489 Serrano, M., Lin, A. W., McCurrach, M. E., Beach, D. & Lowe, S. W. Oncogenic ras provokes premature cell senescence associated with accumulation of p53 and p16INK4a. *Cell* **88**, 593-602 (1997).
490 Lin, A. W. *et al.* Premature senescence involving p53 and p16 is activated in response to constitutive MEK/MAPK mitogenic signaling. *Genes & development* **12**, 3008-3019 (1998).
491 Zhu, J., Woods, D., McMahon, M. & Bishop, J. M. Senescence of human fibroblasts induced by oncogenic Raf. *Genes & development* **12**, 2997-3007 (1998).
492 Bartkova, J. *et al.* Oncogene-induced senescence is part of the tumorigenesis barrier imposed by DNA damage checkpoints. *Nature* **444**, 633-637, doi:10.1038/nature05268 (2006).
493 Di Micco, R. *et al.* Oncogene-induced senescence is a DNA damage response triggered by DNA hyper-replication. *Nature* **444**, 638-642, doi:10.1038/nature05327 (2006).
494 Shi, X. *et al.* Rb protein is essential to the senescence-associated heterochromatic foci formation induced by HMGA2 in primary WI38 cells. *J Genet Genomics* **40**, 391-398, doi:10.1016/j.jgg.2013.05.007 (2013).
495 Moiseeva, O., Bourdeau, V., Vernier, M., Dabauvalle, M. C. & Ferbeyre, G. Retinoblastoma-independent regulation of cell proliferation and senescence by

the p53-p21 axis in lamin A /C-depleted cells. *Aging cell* **10**, 789-797, doi:10.1111/j.1474-9726.2011.00719.x (2011).

496 Jacobs, J. J. *et al.* Bmi-1 collaborates with c-Myc in tumorigenesis by inhibiting c-Myc-induced apoptosis via INK4a/ARF. *Genes & development* **13**, 2678-2690 (1999).

497 Itahana, K. *et al.* Control of the replicative life span of human fibroblasts by p16 and the polycomb protein Bmi-1. *Molecular and cellular biology* **23**, 389-401 (2003).

498 Guo, W. J., Datta, S., Band, V. & Dimri, G. P. Mel-18, a polycomb group protein, regulates cell proliferation and senescence via transcriptional repression of Bmi-1 and c-Myc oncoproteins. *Molecular biology of the cell* **18**, 536-546, doi:10.1091/mbc.E06-05-0447 (2007).

499 Guo, W. J. *et al.* Mel-18 acts as a tumor suppressor by repressing Bmi-1 expression and down-regulating Akt activity in breast cancer cells. *Cancer research* **67**, 5083-5089, doi:10.1158/0008-5472.CAN-06-4368 (2007).

500 Yap, K. L. *et al.* Molecular interplay of the noncoding RNA ANRIL and methylated histone H3 lysine 27 by polycomb CBX7 in transcriptional silencing of INK4a. *Molecular cell* **38**, 662-674, doi:10.1016/j.molcel.2010.03.021 (2010).

501 Gil, J., Bernard, D., Martinez, D. & Beach, D. Polycomb CBX7 has a unifying role in cellular lifespan. *Nature cell biology* **6**, 67-72, doi:10.1038/ncb1077 (2004).

502 Wu, X. *et al.* Tumor suppressor ASXL1 is essential for the activation of INK4B expression in response to oncogene activity and anti-proliferative signals. *Cell Res* **25**, 1205-1218, doi:10.1038/cr.2015.121 (2015).

ANNEXES

Annexe 1 Article: The Ubiquitin Carboxyl Hydrolase BAP1 Forms a Ternary Complex with YY1 and HCF-1 and is a Critical Regulator of Gene Expression.

Helen Yu[1], Nazar Mashtalir[1], Salima Daou[1], Ian Hammond-Martel[1], Julie Ross[1], Guangchao Sui[2], Gerald W. Hart[3], Frank J. Rauscher III[4], Elliot Drobetsky[1], Eric Milot[1], Yang Shi[5] and El Bachir Affar[1],[6]

1 Maisonneuve-Rosemont Hospital Research Center, Department of Medicine and Department of Biochemistry, University of Montréal, Montréal, Canada

2 Wake Forest University School of Medicine, Winston-Salem, NC, USA.

John Hopkins University School of Medicine, Baltimore, MD, USA

4 The Wistar Institute, Philadelphia, PA, USA

5 Department of Pathology, Harvard Medical School and Division of New Born Medicine, Department of Medicine, Children's Hospital Boston, MA, USA

Running title: BAP1 is a transcription co-activator

Publié dans: MCB ,2010 Nov,30 (21):5071-85

Abstract

The candidate tumor suppressor BAP1 is a deubiquitinating enzyme (DUB) involved in the regulation of cell proliferation, although the molecular mechanisms governing its function remain poorly defined. BAP1 was recently shown to interact with, and deubiquitinate the transcriptional regulator Host Cell Factor-1 (HCF-1). Here, we show that BAP1 assembles multi-protein complexes containing numerous transcription factors and cofactors including HCF-1 and the transcription factor Yin Yang 1 (YY1). Through its coiled coil motif, BAP1 directly interacts with the zinc fingers of YY1. Moreover, HCF-1 interacts with the middle region of YY1 encompassing the glycine-lysine-rich domain and is essential for the formation of a ternary complex with YY1 and BAP1 *in vivo*. BAP1 activates transcription in an enzymatic activity-dependent manner and regulates the expression of a variety of genes involved in numerous cellular processes. We further show that BAP1 and HCF-1 are recruited by YY1 to the promoter of *cox7c* gene, which encodes a mitochondrial protein used here as a model of BAP1-activated gene expression. Our findings (i) establish a direct link between BAP1 and transcriptional control of genes regulating cell growth and proliferation and (ii) shed light on a novel mechanism of transcription regulation involving ubiquitin signaling.

Introduction

Post-translational modification of proteins with ubiquitin plays a central role in a wide variety of biological processes in eukaryotic cells (44, 64). Depending on the nature of the modification (e.g. poly- vs. mono-ubiquitination), modified substrates can be either degraded by the proteasome or regulated at the level of their activity and function (4, 45). Ubiquitination is reversible and a significant repertoire of proteases, termed deubiquitinating enzymes (DUBs), are emerging as critical regulators of ubiquitin signaling (40, 46).

BAP1 (BRCA1-Associated Protein1) was originally isolated as a nuclear DUB that interacts with, and enhances the growth suppressive effect of, the tumor suppressor BRCA1 (19). BAP1 also acts in a BRCA1-independent manner, as its overexpression in cells lacking BRCA1 was shown to inhibit cell proliferation and tumor growth (60). Interestingly, recent studies indicate that RNAi-mediated depletion of BAP1 can also exert an inhibitory effect on cell proliferation (31, 36, 41). Although the exact molecular mechanisms are largely unknown, the above data suggest

that BAP1 controls cell cycle progression. In further support of this notion, homozygous inactivating mutations in *BAP1* have been found in subsets of lung carcinoma and breast cancer cell lines suggesting that this DUB is a tumor suppressor (19, 67).

BAP1 is a member of the UCH family including UCH-L1, UCH-L3 and UCH-L5 (UCH37), all of which possess a conserved catalytic domain containing an invariant histidine, cysteine, and aspartic acid catalytic triad (20). Although UCH family members were initially associated with the maturation and turnover of ubiquitin, these enzymes possess isopeptidase activity and thus might selectively regulate protein stability or activity (32, 35, 41). Remarkably BAP1 possesses a large C-terminal domain, not present in other UCH members, which is predicted to play an important role in regulating and coordinating its DUB activity through selective association with potential substrates or regulatory components.

Host cell factor 1 (HCF-1) is a chromatin-associated protein initially identified as part of a multi-protein complex comprising the viral co-activator VP16 and the POU domain transcription factor Oct-1 (23). During herpes simplex virus infection, this complex is recruited to the enhancer/promoter of the immediate early gene to activate viral gene expression (23). HCF-1 was further shown to interact, often through a tetrapeptide sequence termed the HCF-1 binding motif (HBM), with specific members of diverse classes of transcription factors including E2F1, Krox20, Sp1, and GABP. This suggests a crucial role for HCF-1 in regulating the expression of a plethora of genes involved in diverse cellular processes (7, 10, 16, 22, 28-30, 34, 58, 62). HCF-1 also associates with chromatin modifying enzymes, most notably methyltransferases (Set1, MLL1, MLL5), acetyltransferases (hMOF) and deacetylases (HDAC1, HDAC2) (8, 11, 39, 58, 68, 72). Most recently HCF-1 was shown to recruit LSD1 to demethylate the repressive mark histone H3 lysine 9, and to promote the trimethylation of histone H3 lysine 4 by Set1, a mark associated with active genes (26). Although HCF-1 has been mostly associated with transcription activation, this regulator is also involved in transcription repression (6, 58, 68). It is thought that sequence-specific DNA-binding transcription factors are responsible for the differential recruitment of distinct HCF-1 complexes to either positively or negatively regulate target gene expression. For instance HCF-1 was shown to regulate the G1/S transition of cell cycle through specific interaction with either E2F4 or E2F1 which, respectively, represses or activates E2F target genes (58). Despite the above findings, the manner in which HCF-1 is selectively recruited to coordinate the assembly of diverse

chromatin modifying complexes that tightly regulate gene expression remains an area of active investigation.

BAP1 was recently shown to interact, through a NHNY sequence (HBM) located in its middle region, with the kelch motif of HCF-1; moreover this interaction appears to be required for cell proliferation (31, 36). Ectopic expression studies indicate that BAP1 can deubiquitinate HCF-1 (31, 36), although the significance of this event remains to be elucidated. Additional proteins identified by virtue of their co-purification with BAP1 have also been recently reported, most of which are involved in regulation of chromatin-associated processes particularly transcription (31, 54). These include the forkhead transcription factors FOXK1 and FOXK2, the histone acetyltransferase HAT1, the human homolog of additional sex combs ASXL1 and ASXL2, the histone lysine demethylase KDM1B (LSD2), and the ubiquitin conjugating E2 enzyme UBE20. Interestingly, very recently, the drosophila polycomb group protein Calypso was found to be the orthologue of BAP1. Calypso associates with ASX to form the transcription complex PR-DUB that in turn deubiquitinates histone H2A and regulates hox gene expression (47). However it should be noted that the association of human BAP1 with several additional partners as described above suggests a substantially more complex network of functional interactions.

Here, we establish that mammalian BAP1 is assembled into high molecular weight multi-protein complexes containing transcription factors and cofactors including HCF-1. We reveal novel BAP1-interacting partners including the transcription factor Yin Yang 1 (YY1), a zinc finger protein that possesses dual functionality by either activating or repressing gene expression depending upon its association with specific transcription co-activators or co-repressors at specific target gene promoters (see reviews (13, 51)). We show that BAP1 directly interacts with YY1, and HCF-1 is required for this interaction *in vivo*. Finally, in providing a model for BAP1-mediated control of gene expression, we demonstrate that this DUB is a direct co-activator of *cox7c*, a nuclear gene encoding a component of the mitochondrial respiratory chain. Our data provide novel molecular insight into the involvement of deubiquitination in the control of gene expression.

Materials And Methods

Plasmids and Antibodies

Retroviral constructs that express N-terminal Flag-HA-tagged wildtype or mutant forms of human BAP1 were generated by subcloning the cDNA into the POZ-N plasmid provided by Y. Nakatani (38). The catalytically inactive BAP1, POZ-BAP1 (C91S) was generated by site-directed mutagenesis. The BAP1 mutant deleted in the NHNY sequence corresponding the HCF-1 binding domain (ΔHBD) was generated by PCR-based subcloning of 2 fragments ligated in frame into POZ-N. The Gal4-BAP1 and Gal4-BAP1 catalytically inactive (C91S) constructs were generated by PCR amplification of the Gal4 DNA binding sequence and ligation in frame into pCDNA.3 BAP1. The Gal4-BAP1 ΔHBM was generated by subcloning BAP1 ΔHBM in frame into pCDNA.3 containing Gal4 DNA binding sequence. shRNAs for hBAP1 (#1 and #2) and hHCF-1 were generated as previously described (57). The targeted sequences of these shRNAs are listed in the supplemental information. The constructs used to produce recombinant full length GST-YY1 and various deletion fragments have been described (25). Constructs to produce recombinant full length GST-BAP1 and various deleted forms were obtained by PCR-amplification of various fragments, which were cloned into pGEX4T1. The construct for producing recombinant human His-tagged YY1 has been described (56). A construct to produce recombinant human His-tagged BAP1 was generated by subcloning BAP1 cDNA into pET30a+. The shRNA construct for YY1 and non-target sequence have been described (56). The pCGN-HCF-1 vector (65) was used for subcloning HCF-1 into the pcDNA.3/HA vector.

Monoclonal anti-BAP1 (C4) and anti-YY1 (H10), polyclonal anti-BAP1 (H300) and anti-TFIID (N12) were from Santa Cruz. Monoclonal anti-HCF-1 (M2) (66) and polyclonal anti-HCF-1 (N18) (14) have been used. Polyclonal anti-HCF-1 (A301-400A) was from Bethyl laboratories. Monoclonal anti-RNA Polymerase II (H14) was from Covance. Polyclonal anti-Histone H3 (06-755), polyclonal anti-Histone H3 trimethylated at lysine 27 (H3 K27 me3) (17-622) and monoclonal anti-βactin (MAB1501) were from Millipore. The antibodies used as controls for IP and ChIP were the polyclonal anti-GFP (FL), anti-HA (Y-11) and rabbit IgG (sc-2027), and were from Santa Cruz.

Cell culture, RNAi and immunoblotting

HeLa cervical cancer, U2OS osteosarcoma and PhenixA virus-producing cells were cultured in Dulbecco's modified Eagle's medium (DMEM) supplemented with 10% fetal bovine serum and penicillin/streptomycin. Cells were transfected with either a non-targeting control or BAP1 RNA interference (RNAi) plasmid using Lipofectamine 2000 (Invitrogen). For transient RNAi experiments, shRNA vectors were mixed with the pBABE puromycin resistance-encoding vector, and transfected cells were selected by adding 2 μg/ml of puromycin for 2 days as described (1). U2OS cells with stable depletion of BAP1 were generated by co-transfection of RNAi vectors with pCDNA.3 neomycin resistance-encoding vector, and independent clones were isolated following G418 selection (1.5 mg/ml) and tested for BAP1 knockdown by western blotting. The siRNA smart pools for human HCF-1, BAP1 and a non-target control were from Dharmacon (Thermo Scientific) and were transfected into HeLa or U2OS cells using Lipofectamine 2000.

Total cell extracts were prepared in lysis buffer (50 mM Tris-HCl, pH 7.3; 5 mM EDTA; 50 mM KCl; 0.1% NP-40; 1 mM phenylmethylsulfonyl fluoride (PMSF); 1 mM dithiothreitol and protease inhibitors cocktail (Sigma)), and protein concentration determined by Bradford assay. SDS-PAGE and western blotting were conducted according to standard procedures.

Purification of BAP1-associated proteins and co-immunoprecipitation

HeLa and U2OS cell lines stably expressing Flag-HA-BAP1 (WT, C91S or ΔHBD) were generated following retroviral transduction and 4 rounds of selection using magnetic beads coupled to IL2 receptor antibody as previously described (38). HeLa (~9 X 10^9 cells) or U2OS (~0.5 X 10^9 cells) were used for purification of BAP1-associated proteins, essentially as previously described (38). Standard co-immunoprecipitations using appropriate antibodies were conducted as previously described (56)**.**

Immunodepletion was conducted on HeLa nuclear extracts (~100 μg of proteins) by overnight incubation at 4 ºC with 2 μg of anti-HCF-1 or anti-BAP1 polyclonal antibody in IP buffer (50 mM Tris, pH 7.3; 150 mM NaCl; 5 mM EDTA; 10 mM NaF; 1% Triton X-100; 1 mM PMSF and protease inhibitors cocktail (Sigma)). The anti-HA (Y-11) polyclonal antibody was used as control. The immuno-complexes were incubated for 7 hours at 4 ºC with protein G agarose beads (Sigma) which were saturated with 1% BSA in IP buffer. After centrifugation, the flow

through and bead fractions were collected. The immuno-complexes were washed once with the IP buffer supplemented with 1% BSA. Bound proteins were eluted from the beads with Laemmli buffer and subjected, along with the flow through fractions, to western blotting.

Preparation of chromatin fractions and digestion with Micrococcal nuclease (MNase) were conducted as previously described (15). Briefly, the nuclear pellet was resuspended in 20 mM Tris-HCl (pH 7.5), 100 mM KCl, 2 mM $MgCl_2$, 1 mM $CaCl_2$, 0.3 M sucrose, 0.1% Triton X-100, and protease inhibitor cocktail. Following MNase treatment (3 U/ml for 10 min), the reaction was ended with 5 mM each EGTA and EDTA. The samples were then centrifuged at 13,000 g for 10 min at 4°C to obtain the soluble chromatin fraction.

Glycerol gradient and gel filtration analysis

Molecular mass separation of native BAP1 complexes from nuclear extract was conduced using a 10-40 % glycerol gradient prepared in 20 mM Tris-HCl, pH 7.9; 100 mM KCl; 5 mM $MgCl_2$; 1 mM PMSF; 0.1% NP40 and 10 mM 2-mercaptoethanol. The samples were centrifuged for 12 h at 50,000 RPM (SW55Ti rotor, Beckman,) at 4 ºC. Individual fractions were then collected from top to bottom and analyzed by western blotting. The CtBP co-repressor complex estimated to have a molecular mass of 1.3-1.5 MDa was used as reference (52).

Gel filtration analysis of purified BAP1 complexes was conducted using a Superose6 HR gel exclusion chromatography column. Eluted fractions were analysed by silver staining and western blotting. The native molecular weight markers used for column calibration were thyroglobulin (669 KDa), ferritin (440 KDa), catalase (232 KDa), lactate dehydrogenase (140 KDa) and albumin (66 KDa) (obtained from GE Healthcare).

Deubiquitination assay on Ub-AMC

Deubiquitination assay on Ub-AMC was conducted as previously described (32) with the following modifications. Purified BAP1 complexes (WT, C91S and ΔHBM) and recombinant His-BAP1 were adjusted to the same amount of BAP1 protein (125 ng; 1.5 pmol) and incubated individually with 37.5 pmol of Ub-AMC (Boston Biochem) in 100 µl of assay buffer (50 mM Tris pH 7.3, 0.25 mM EDTA, 10% DMSO and 1 mM DTT) for 1200 sec. Fluorescence was measured using a fluorimeter (Cytofluor, PerSeptive Biosystems) at excitation and emission wavelengths of 380 nm and 460 nm, respectively.

In vitro interaction assays

Recombinant GST fusion proteins were purified using glutathione agarose beads (Sigma) and 2 to 3 µg of beads containing bound proteins were incubated with 10 µl of *in vitro* translated *methionine-S35* labeled HCF-1 (*TNT*® T7 Quick Coupled Transcription/Translation System, Promega), 1 µg His-YY1, or 1 µg His-BAP1 for 6 to 8 hours at 4 ºC in 50 mM Tris, pH 7.5; 50 mM NaCl; 0.02% Tween 20; 1 mM PMSF and 500 µM dithiothreitol). The beads were extensively washed with the same buffer, and bound proteins eluted in Laemmli buffer and subjected to autoradiography or western blotting.

Immunofluorescence

Cells were fixed for 20 min using 3 % paraformaldehyde prepared in phosphate-buffered saline (PBS). Cells were then permeabilized with 0.5% NP-40 in PBS for 20 min and washed with PBS containing 0.1% NP-40. Cells were further incubated in blocking solution (PBS containing 0.1% NP-40 and 10% FBS) and stained with a monoclonal anti-BAP1 antibody. Anti-mouse Alexa Fluor® 594 (Invitrogen) was used as secondary antibody. Nuclei were stained with 4',6-diamidino-2-phenylindole (DAPI). Z-stacks were acquired using Leica DMRE microscope, HCX PL APO 63X/ 1.32-0.6 OIL CS objective and Retiga Ex (Qimaging) camera and deconvoluted with the Openlab 3.1.1 program. RGB profiles were generated by WCIF-ImageJ program (NIH).

Cell synchronization and cell cycle analysis

U2OS cells were synchronized at the G1/S border using a thymidine double block protocol (17). The DNA content of cells was analyzed essentially as described (1). Briefly, cells were harvested by trypsinization and fixed with 70 % ethanol. After one wash with PBS, cells were treated with 100 µg/ml RNase A (Sigma-Aldrich) for 30 min at 37°C, stained with 50 µg/ml propidium iodide (Sigma-Aldrich), and analyzed using a FACScan flow cytometer equipped with Cellquest software (Becton Dickinson).

Genome-wide gene expression analysis and qRT-PCR analysis of individual mRNAs

U2OS cells, transfected with a non-target control shRNA or shRNAs targeting BAP1, were selected with puromycin containing medium and then synchronized at the G1/S border to allow comparative analysis of gene expression. RNA was prepared using Trizol reagent (Invitrogen) and

the RNeasy kit (QIAGEN). The generation of cDNA and biotinylated cRNA and hybridization to Human genome Hu133 plus 2.0 arrays (Affymetrix; containing 47,000 transcripts and transcripts variants) were conducted following the One-Cycle target Labeling Protocol of the GeneChip ® Expression Analysis Technical Manual from Affymetri*x* (Genome Québec Innovation Centre, Montréal, Canada). Gene expression levels from shControl and shRNAs were subjected to comparative analysis using the expression analysis software Flex Array V1.1. A functional analysis of genes deregulated following BAP1 depletion was conducted using Ingenuity Pathways Analysis Version 8.5 (3). The gene expression data for both shRNAs are deposited in the Gene Expression Omnibus (GEO) NCBI database.

Levels of individual mRNAs in BAP1 depleted cells were determined by RT-PCR. Total mRNA (prepared as described above) was used for reverse transcription using the Superscript III reverse transcriptase and oligo(dT)$_{12\text{-}18}$ primers (Invitrogen). The obtained cDNAs were subjected to PCR amplification with the primer sets described in Supplemental Information. The mRNA levels were normalized to GAPDH expression.

Chromatin immunoprecipitation analysis

Chromatin immunoprecipitation (ChIP) experiments were conducted essentially as previously described (2) with the following modifications. U2OS cells (5 X 10^6) were cross-linked with 1% formaldehyde in PBS at room temperature for 10 min with prior incubation in 1.5 mM EGS (ethylene glycolbis [succnimidyl succinate]; Sigma-Aldrich) in PBS for 30 min at room temperature as described (42, 73). Following quenching with glycine (125 mM) for 5 min, cells were scraped in cold PBS. The cells were first washed with buffer A (50 mM Tris-HCl, pH 8.0; 0.1% NP40; 2 mM EDTA; 10% glycerol; 1 mM PMSF and protease inhibitors cocktail (Sigma)) and then sonicated in Buffer B (50 mM Tris-HCL, pH 8.0; 1% SDS; 10 mM EDTA; 1 mM PMSF and protease inhibitors cocktail) to generate 300-600 bp fragments. After centrifugation and pre-clearing for 1 hour, the suspension was incubated overnight with polyclonal anti-HCF-1, anti-BAP1, anti-YY1 or a non-relevant antibody used as control. Immunocomplexes were recovered with protein A agarose beads (Millipore) and the DNA was purified after decrosslinking with phenol-chloroform extraction. Real time PCR was conducted using SYBR green reaction and detection kit (Invitrogen) on an iCycler iQ apparatus (Bio-Rad). Quantification was conducted using the $2^{-\Delta\Delta CT}$ method, where $\Delta\Delta$CT is calculated as follows: (ChIP CT– input CT of the control

antibody) – (ChIP CT – input CT of the target antibody). The results are shown as a ratio of target gene promoter versus reference gene promoter. The amplification efficiency of all primer sets was verified before qPCR analysis. All experiments were done at least 3 times and the data shown are results of a representative experiment. The primer sets used are described in the Supplemental Information.

Luciferase reporter assays

HeLa cells were transfected with various amounts of Gal4-BAP1, Gal4-BAP (C91S), BAP1 or Gal4 expression plasmids along with 500 ng Gal4-TK-Luciferase or 500 ng TK-luciferase reporter plasmids. pEGFP-N2 construct (10 ng) was also included to ensure equal transfection efficiency between the different conditions. Luciferase activity was measured 2 days post-transfection using a luciferase assay (Promega).

Results

BAP1 is assembled into high molecular weight multi-protein complexes and interacts with the transcription factor YY1.

HeLa nuclear extracts were prepared wherein nearly all nuclear BAP1 protein was recovered (Figure 1A, top panel). Glycerol density gradient fractionation of these extracts showed that most of the endogenous protein is detected as a peak in the high molecular weight fractions (~ 1.3 to1.8 MDa), suggesting that BAP1 is assembled into multi-protein complexes (Figure 1A, bottom panel). To identify these potential complexes, we generated a stable HeLa cell line expressing Flag-HA-BAP1 and conducted a large-scale double immunopurification of the protein using anti-Flag and anti-HA columns. Silver stain of the eluted material revealed that several polypeptides co-purify with BAP1 (Figure 1B). These proteins are specific since no apparent protein bands were detected in the HA elution from the mock purification. Of note, most of the proteins co-purifying with BAP1 were readily detectable following the anti-Flag purification step. Nonetheless, to ensure high specificity, the HA-eluted material was used for mass spectrometry analysis to identify BAP1-interacting partners. Several recently reported as well as novel BAP1-interacting proteins were recovered (Table S1). As reflected by the protein sequence coverage and the number of identified peptides for each protein, the most abundant polypeptides identified include the transcriptional regulator HCF-1, the forkhead transcription factors FOXK1 and FOXK2, the O-linked N-acetyl glucosamine transferase (OGT), the human homolog of additional sex combs ASXL1 and ASXL2, the ETS-related transcription factors ELF-1 and ELF-2, and the E2 enzyme UBE20. Less abundant BAP1-interacting proteins comprise specific transcription factors and cofactors such as YY1, ZNF131, PRDM10, and the histone H3 K4 demethylase KDM1B. To validate these results, we also established a U2OS osteosarcoma cell line stably expressing Flag-HA-BAP1. Using this model cell type, we found that, although a small-scale cell preparation was used, most of the major BAP1-associated proteins were recovered following purification (Table S2).

Stoichiometric amounts of HCF-1 co-purify with BAP1, as a large number of peptides were obtained following mass spectrometry analysis and the intensities of the silver stained bands were similar for the two proteins (Figure 1B and Table S1). Since the majority of endogenous BAP1 protein migrates within a high molecular weight fraction (Figure 1A), we reasoned that all of the

cellular BAP1 might be complexed with HCF-1. In fact, nearly all BAP1 protein could be immunodepleted from nuclear extracts using an excess of HCF-1 antibody (Figure 1C, top panel). As expected, virtually all HCF-1 protein was recovered in the bead fraction. As negative control, the nuclear protein PARP1 was shown to remain in the extracts. Next, we immunodepleted BAP1 using a specific antibody and observed that although nearly all BAP1 was recovered, only a minor fraction of HCF-1 was depleted (Figure 1C, bottom panel). This indicates that (i) HCF-1 is highly abundant relative to BAP1, and (ii) essentially all cellular BAP1 is complexed with HCF-1. Thus, HCF-1 could be a major scaffold protein for BAP1 and might play a critical role in coordinating the association of this DUB with other partners to form specific transcription regulatory complexes.

To provide insight into the potential role of BAP1 as a gene-specific transcription regulator, we focused in this study on characterizing the interaction of BAP1/HCF-1 with YY1. The anti-HA eluted material was fractionated using size exclusion chromatography, which revealed that BAP1 is assembled into ~1.3-1.8 MDa multi-protein complexes (Figure 1D). These complexes contain the transcription factor YY1 and HCF-1, and very likely additional components. Next, the anti-Flag purified BAP1 material was used as input for immunoprecipitation using anti-HCF-1 antibody, and both YY1 and BAP1 were co-immunoprecipitated (Figure 1E). These results strongly suggest the existence of at least one complex simultaneously containing BAP1, HCF-1 and YY1. Moreover, the interactions of endogenous YY1 with HCF-1 and BAP1 were also confirmed (Figure 1F).

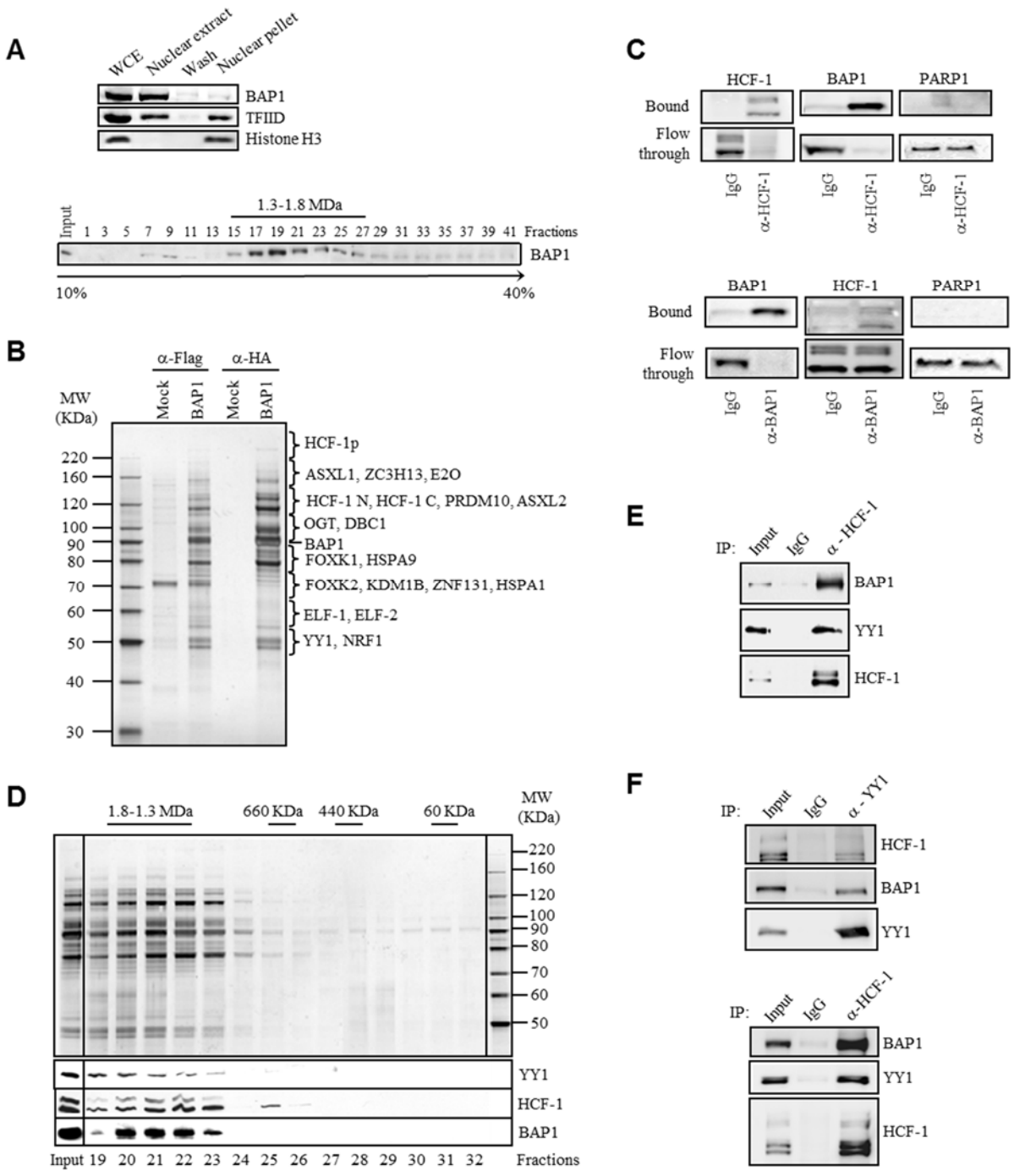

Figure 1. BAP1 assembles high molecular weight multi-protein complexes containing YY1 transcription factor. (**A**) Top panel, extraction of cellular BAP1 protein. HeLa nuclei isolated with hypotonic buffer were extracted with 300 mM of KCl for 30 min to obtain the nuclear extract and the chromatin/nuclear matrix pellet fractions. The nuclear pellet was washed once. All fractions were resuspended in the same volume and used for to the immunodetection of BAP1. TFIID was detected as a marker for the transcriptional machinery and Histone H3 as a marker for chromatin.WCE, whole cell extract. Bottom panel, endogenous BAP1 migrates in high molecular weight fractions. HeLa nuclear extract was fractionated using glycerol density gradient ultracentrifugation. Fractions

collected from the top to the bottom were subsequently used for immunodetection of BAP1. The gradient was calibrated with the previously purified CtBP complex whose estimated molecular weight is ~1.3-1.5 MDa. (**B**) Purification of BAP1-associated proteins. A HeLa cell line stably expressing Flag-HA-BAP1 was used for sequential double immunopurification using anti-Flag antibody and anti-HA antibody columns. The Flag- or HA-eluted proteins were separated by SDS-PAGE and detected by silver staining. The mock purification was conducted using a stable cell line generated with the empty vector. Several regions were cut from the gel and the polypeptides were identified by mass spectrometry. (**C**) Immunodepletion of HCF-1 (top panel) or BAP1 (bottom panel) from nuclear extracts using an excess of anti-HCF-1 or anti-BAP1 polyclonal antibodies. A non-relevant anti-HA polyclonal antibody was used as a control IgG. BAP1 and HCF-1 were immunodetected in the beads and the flow through fractions. The nuclear protein PARP1 was detected as a negative control. (**D**) BAP1 forms high molecular weight multi-protein complexes. Fractionation of the BAP1 purified material using a Superose6 HR gel filtration column. The eluted complexes were detected with silver stain. BAP1, HCF-1 and YY1 were detected by immunoblotting. (**E**) Reciprocal immunoprecipitation. The Flag purified BAP1 material was used as input for additional immunoprecipitations using a polyclonal antibody against HCF-1 or a non-relevant anti-GFP antibody (IgG control). The immunocomplexes were extensively washed and YY1, HCF-1 and BAP1 were detected by immunoblotting. (**F**) Interaction of endogenous HCF-1, BAP1 and YY1. HeLa nuclear extract was used for immunoprecipitation using a polyclonal antibody against YY1 (top panel), a polyclonal antibody against HCF-1 (bottom panel) or a non-relevant anti-GFP antibody (IgG control). The immunocomplexes were washed and YY1, HCF-1 and BAP1 were detected by immunoblotting.

The DUB activity is not required for BAP1 complexes formation.

It was recently shown that BAP1 can disassemble K48 ubiquitin chains on HCF-1 suggesting that this DUB might regulate the stability of HCF-1 and possibly other substrates (31, 36). In addition, ubiquitin peptides were detected following mass spectrometry analysis of BAP1-associated proteins suggesting that some polypeptides were ubiquitinated (Table S1). Thus, we first tested whether loss of BAP1 function affects the stability of YY1. Knockdown of BAP1 using two shRNAs resulted in its substantial depletion, whereas no significant changes were observed in steady state levels of YY1 or HCF-1 (Figure 2A, left panel). These results were confirmed using a pool of 4 different siRNAs targeting BAP1 (Figure 2A, right panel). Next, we sought to determine whether DUB activity is required for assembly of BAP1 complexes. For this purpose, a stable cell line expressing BAP1 mutated in the catalytic cysteine (C91S) was generated. As BAP1 wildtype or C91S are not highly expressed, we did not observe a significant difference in cell proliferation between these two conditions (data not shown). Importantly, the purified complexes containing either BAP1, or its catalytically inactive form, are essentially indistinguishable (Figure 2B, left panel). These results were confirmed by immunoblotting for some of the associated components i.e., YY1 and HCF-1 (Figure 2B, right panel).

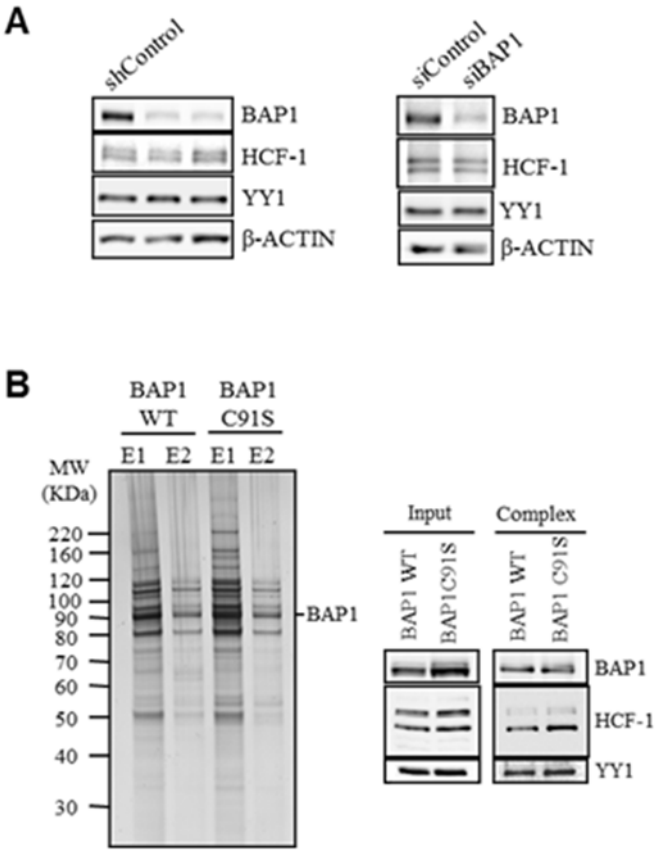

Figure 2. The DUB activity is not required for the assembly of BAP1 complexes or YY1 stability.
(**A**) Depletion of BAP1 does not affect the steady-state levels of YY1 and HCF-1. Left panel, HeLa cells were transfected with either non-targeting control or BAP1 shRNA plasmids along with the pBABE puromycin resistance-encoding vector, and transfected cells were selected by adding puromycin for 2 days prior to harvesting for western blotting using the indicated antibodies. Right panel, the siRNA smart pools for human BAP1, or a non-target control, were transfected into U2OS cells and expressed for 3 days prior to harvesting for western blotting using the indicated antibodies. (**B**) BAP1 catalytic activity is not required for BAP1 complexes formation. A HeLa cell line stably expressing Flag-HA-BAP1 catalytic inactive mutant (C91S) was used along with the wildtype control cells for double immuno-purification of BAP1 complexes. Silver staining was conducted on fractions from two elutions (E1 and

BAP1 directly interacts with YY1 in vitro and HCF-1 is required for complex formation in vivo.

recombinant proteins including various deletion mutants and conducted *in vitro* GST pulldown assays. We found that BAP1 directly interacts with YY1. The C-terminus region of BAP1 (aa 599-729), encompassing the coiled coil domain, is necessary and sufficient for this interaction (Figure 3A, top right panel). We used smaller GST-BAP1 deletion fragments within the 599-729 aa region and identified the coiled coil domain as the interacting motif (Figure 3A, bottom right panel). Thus, BAP1 could simultaneously bind YY1 and HCF-1. Next, we demonstrated that *in vitro* translated full length ^{35}S Met-HCF-1 interacts directly with YY1 and the central region of the latter (aa 142-260), which contains the GA/GK rich domain, is required for this interaction (Figure 3B, bottom left panel). Finally, we determined that the zinc fingers region of YY1 (aa 313-414) is necessary and sufficient for interaction with BAP1 (Figure 3B, bottom right panel). Taken together the above data indicate that BAP1, HCF-1 and YY1 interact using non-overlapping domains, and thus can form a ternary complex involving binary binding for each protein.

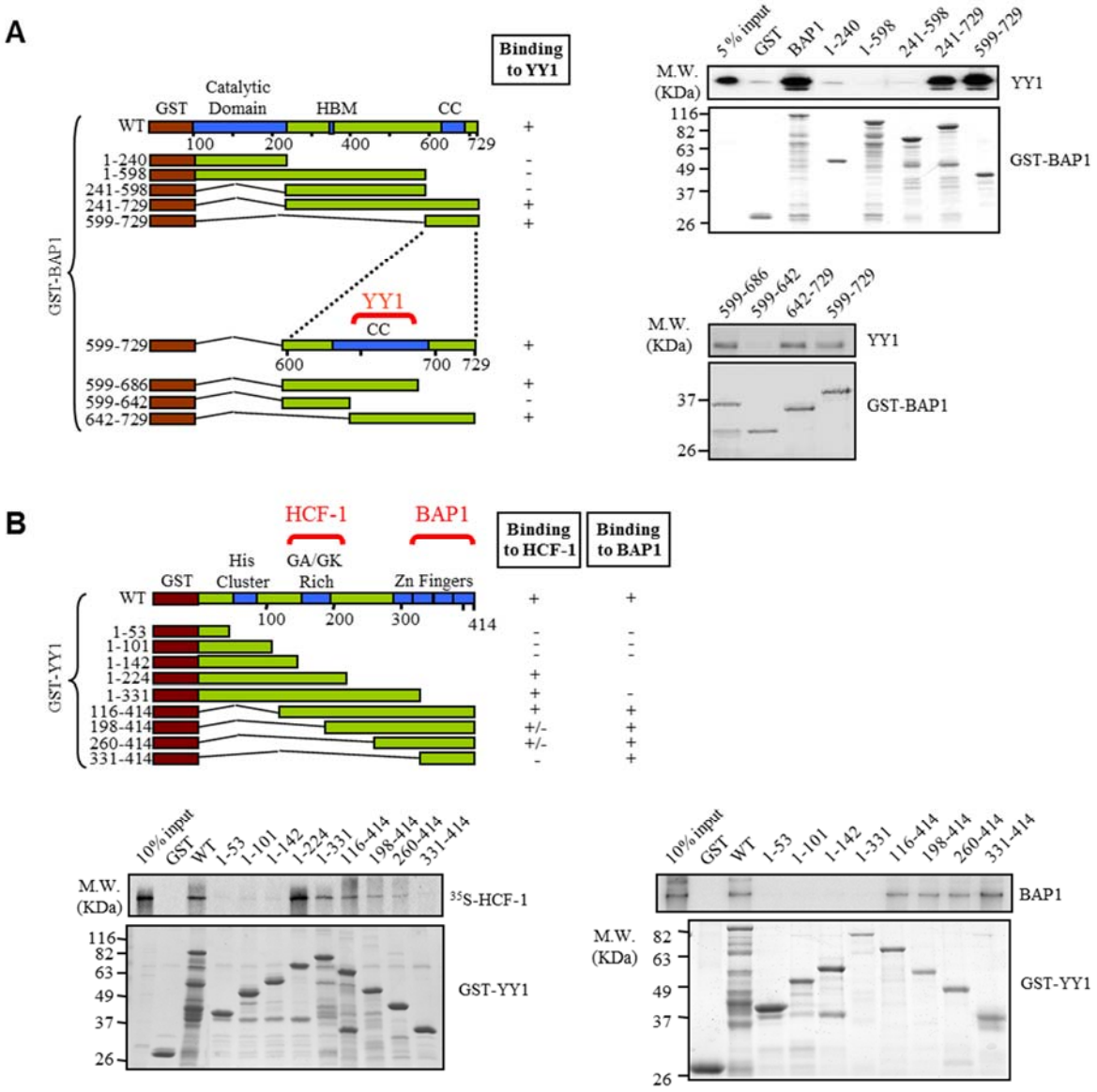

Figure 3. HCF-1 is required for ternary complex formation with YY1 and BAP1.

(**A**) Interaction *in vitro* between YY1 and BAP1 mutants. Various GST deletion fragments of BAP1 bound to GSH beads were incubated with His-YY1 for 8 hours and, following extensive washes, the bead-associated complexes were analyzed by coomassie blue staining for GST-BAP1 fragments and western blotting for YY1. HBM, HCF-1 Binding Motif; CC, coiled-coil domain. (**B**) Interaction *in vitro* between HCF-1 or BAP1 and various YY1 mutants. Bottom left panel, interaction *in vitro* between YY1 and HCF-1. Various GST deletion fragments of YY1 bound to GSH beads were incubated with *in vitro* translated ^{35}S labeled-HCF-1 for 8 hours and following purification, HCF-1 was analyzed by autoradiography. Bottom right panel, identification of the YY1 domain required for interaction with BAP1. Various GST deletion fragments of YY1 were incubated with His-BAP1 for 8 hours and the bead-associated complexes were analyzed by coomassie blue staining and western blotting for BAP1.

To further characterize these interactions *in vivo*, a stable cell line expressing BAP1 lacking the HBM was generated and used for the double immunopurification of BAP1-associated proteins. Silver staining of the eluted proteins reveals that while some polypeptide bands appear similar between wildtype and mutant, several other bands were absent or substantially reduced in the elution of the mutant BAP1 (Figure 4A, left panel). As expected, HCF-1 was not detected in the elution of the mutant BAP1 (31, 36) (Figure 4A, right panel). Significantly, BAP1 interaction with YY1 was dramatically reduced between the wildtype and the mutant lacking HBM, suggesting that HCF-1 is required for optimal interaction between YY1 and BAP1 *in vivo*. Of note neither YY1 nor HCF-1 levels were changed upon expression of BAP1 lacking HBM. Next, we depleted HCF-1 using shRNA and immunopurified BAP1. As expected, substantially reduced levels of HCF-1 were observed following the BAP1 purification (Figure 4B), and the interaction of BAP1 with YY1 was again reduced. Altogether, these data indicate that BAP1, HCF-1, and YY1 form a ternary complex *in vivo*, strongly suggesting a functional link between these proteins. We then sought to determine whether the DUB activity of BAP1 is modulated by its interacting partners using similar amounts of BAP1, either recombinant or assembled into complexes, i.e., WT, ΔHBM and C91S (Figure 4C, left panel). Deubiquitination assays toward the substrate ubiquitin-AMC (Figure 4C, right panel) were conducted. As expected, no activity could be detected for the catalytic inactive BAP1 used as control. However recombinant BAP1 and BAP1 complexes (wildype or ΔHBM) exhibited similar DUB activities.

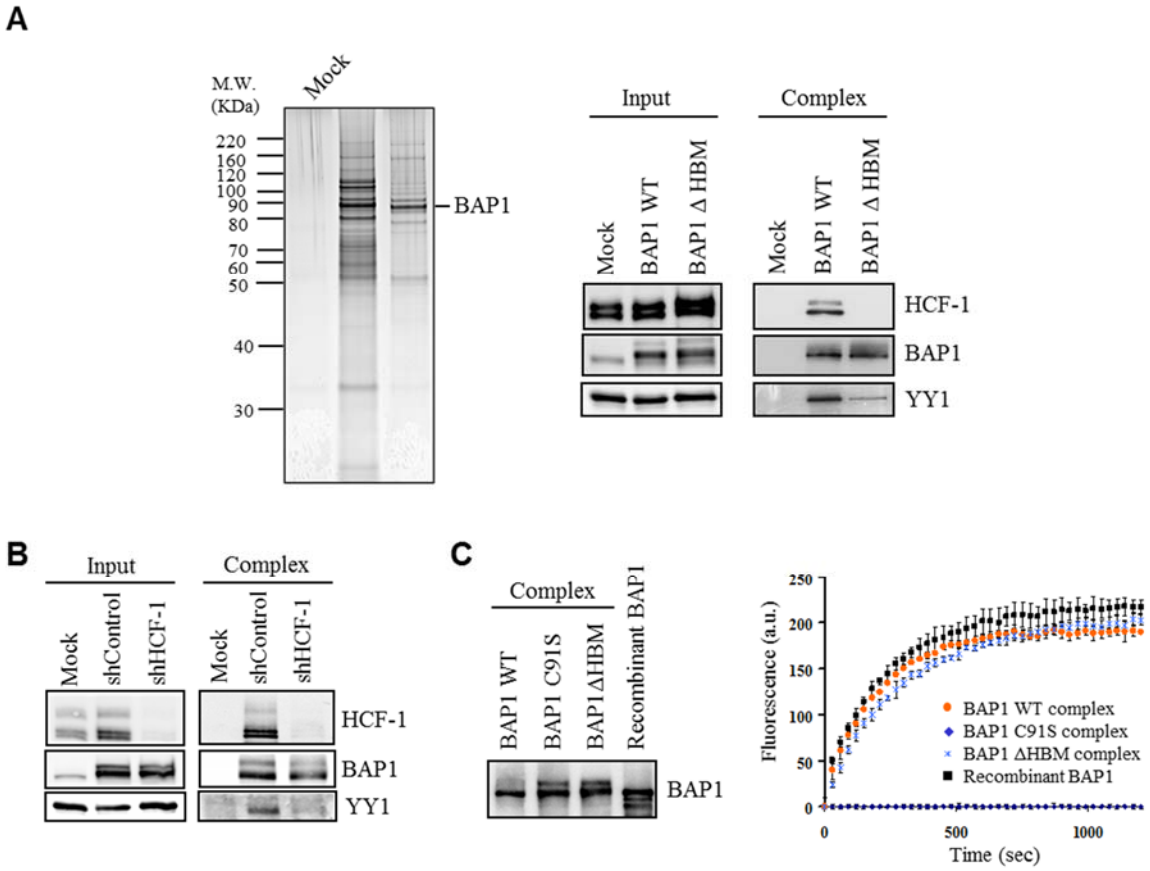

Figure 4. HCF-1 is required for ternary complex formation with BAP1 and YY1 *in vivo.*

(**A**) HCF-1 is required for proper assembly of BAP1 complexes. A HeLa cell line stably expressing Flag-HA-BAP1 lacking the HBM was used for immunopurification using anti-Flag and anti-HA antibodies. The eluted material was used for SDS-PAGE and silver stain (left panel). Immunoblotting detection of BAP1, HCF-1 and YY1 (right panel). The BAP1 wildtype (WT) was used as a control. (**B**) Depletion of HCF-1 destabilizes BAP1 interaction with YY1. A HeLa cell line stably expressing Flag-HA-BAP1 was transfected with either a non-targeting control or HCF-1 shRNA plasmid along with the pBABE puromycin resistance-encoding vector, and transfected cells were selected by adding puromycin for 2 days prior harvesting for double immunopurification of BAP1. The eluted proteins were detected by western blotting using the indicated antibodies.**(C)** Cleavage of Ub-AMC by various BAP1 complexes (WT, C91S and ΔHBM) and recombinant BAP1. Left panel, equal quantities of BAP1 were used for deubiquitination reactions with 37.5 pmol of Ub-AMC. Right panel, release of AMC was monitored by fluorescence spectroscopy (Excitation: 380 nm and Emission: 460 nm). All experiments were repeated at least 3 times and the data are presented as mean ± SD. a.u., arbitrary units.

BAP1 is associated with transcriptionally active chromatin.

Most of the BAP1-interacting proteins are known to be involved in chromatin-associated processes suggesting a role for BAP1 in regulating gene expression. BAP1 was shown to associate with chromatin (31). In our study, we found that this protein is mostly excluded from heterochromatic regions as indicated by the nearly mutually exclusive staining between BAP1 and the highly packed chromatin, i.e., regions strongly stained with DAPI (Figure 5A). Thus, we set out to determine whether BAP1 is associated with transcriptionally active regions by isolating the chromatin fraction and conducting short-term incubations with micrococcal nuclease (MNase) to release accessible nucleosomes. Nearly all BAP1 was recovered in the soluble fraction (Figure 5B). As expected, the basal transcription factor TFIID and RNA pol II were also recovered predominantly in the soluble fraction. HCF-1 and YY1 were found in this fraction as well, but to a lesser extent than BAP1 or RNA pol II. Histone H3 was only partially recovered indicating that a fraction less accessible to MNase, the heterochromatin, remained in the pellet. Consistent with this, histone H3 trimethylated at lysine 27, which is associated with transcriptional repression and compacted chromatin (49), was found predominantly in the pellet. These results suggest that BAP1 is associated with actively transcribed regions where it might form complexes with HCF-1, YY1 and other regulators to control gene expression. Although, BAP1/HCF-1 and YY1 were found on chromatin, the possibility remained that these proteins coexist in different complexes. To determine whether BAP1/HCF-1/YY1 indeed form a complex on chromatin, we immunopurified BAP1 from the chromatin fraction following digestion with MNase. We found that BAP1 immunoprecipitated both HCF-1 and YY1 from this fraction (Figure 5C, right panel). Of note, MNase digestion was nearly complete as indicated by the release of mononucleosomes (Figure 5C, left panel).

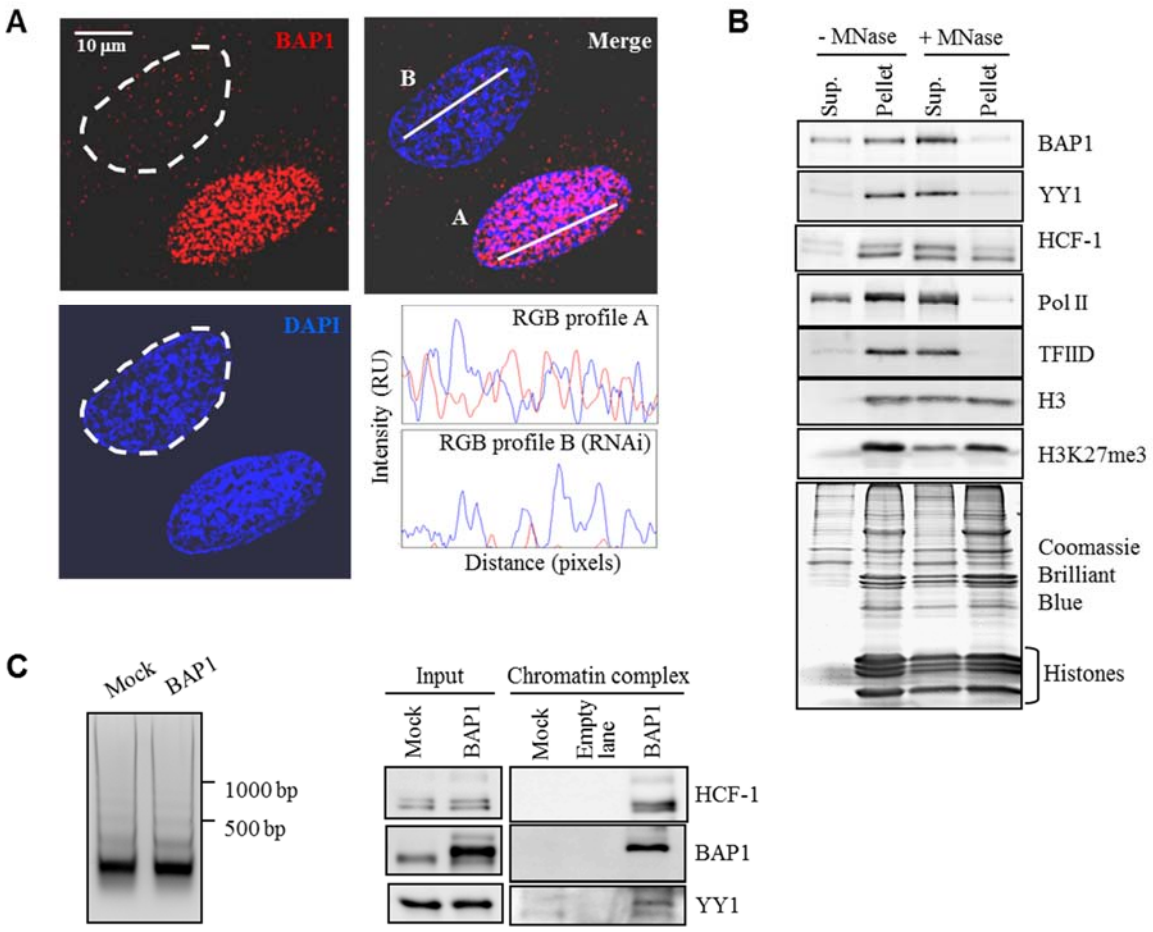

Figure 5. A BAP1/HCF-1/YY1 complex is associated with euchromatin regions.

(**A**) Immunolocalization of BAP1 in U2OS cells, indicating that this DUB is mostly excluded from heterochromatic regions. To ensure the specificity of immunostaining, U2OS cells were transiently transfected with siRNA against BAP1 and at three days post-transfection cells were used for immunostaining employing a BAP1 monoclonal antibody. Following Z-stacks image acquisition, RGB profiles were generated by WCIF-ImageJ program (NIH). Although most of the cells are depeleted of BAP1, some were not transfected and show normal BAP1 expression. In the image shown, the cell delimited with the discontinuous line has been RNAi-depleted for BAP1. The other cell shown in the image presumably did not receive the siRNA and expresses normal levels of BAP1. The intensity of fluorescence signals for BAP1 (red) and DNA (blue) at the indicated bars are shown in relative units (bottom right panel). (**B**) BAP1 as well as other components of the BAP1 complexes are associated with euchromatin. The chromatin/nuclear matrix fraction was treated with micrococcal nuclease (MNase) to release nucleosomes. Proteins were detected in the soluble and pellet fractions by immunoblotting or coomassie blue staining. (**C**) Purification of BAP1/HCF-1/YY1 from chromatin fraction. Chromatin fraction of HeLa cells stably expressing Flag-HA-BAP1 was digested with MNase (3U/ml) for 10 min. Following centrifugation at 13,000 g/10 min, an aliquot was used for phenol-chloroform extraction of DNA and agarose gel analysis (left panel). Immunopurification of BAP1 was conducted with the prepared chromatin fraction. The eluted proteins were detected using BAP1, YY1 and HCF-1 antibodies (right panel).

BAP1 is a transcriptional co-activator and regulates the expression of genes involved in numerous cellular processes.

To elucidate the role of BAP1 in transcription regulation, a well-established transcription reporter assay was used (24). This consists of targeting a protein of interest, fused in frame with the GAL4 DNA binding domain, to the luciferase reporter driven by a promoter containing GAL4 binding sites and the thymidine kinase promoter (Figure 6A). A fusion between the DNA binding domain of Gal4 (1-147aa) and BAP1 was generated and expressed in HeLa cells by transient transfection (Figure 6B, bottom panel). Gal4-BAP1 activated transcription of the reporter gene by 3 to 4 fold (Figure 6B, top panel). This effect was not observed following expression of BAP1 alone, the Gal4 domain alone, or Gal4-BAP1 along with a thymidine kinase reporter lacking Gal4 binding sites. Altogether, these results suggest that transcription activation by Gal4-BAP1 requires DNA binding and is not an indirect effect. A Gal4-BAP1 mutant lacking the HBM, expressed at the same levels as the wildtype (Figure 6C, right panel), also activated transcription although less efficiently than the wildtype form (Figure 6C, left panel). Importantly, a Gal4-BAP1 catalytic inactive mutant (C91S) was unable to activate transcription suggesting that BAP1 regulates gene expression in a DUB activity-dependent manner (Figure 6D, top panel). We note that although BAP1 C91S was expressed at lower levels than the wildtype for the same quantity of transfected DNA (Figure 6D, bottom panel), no reporter activation was observed with C91S over a wide range of plasmid concentrations.

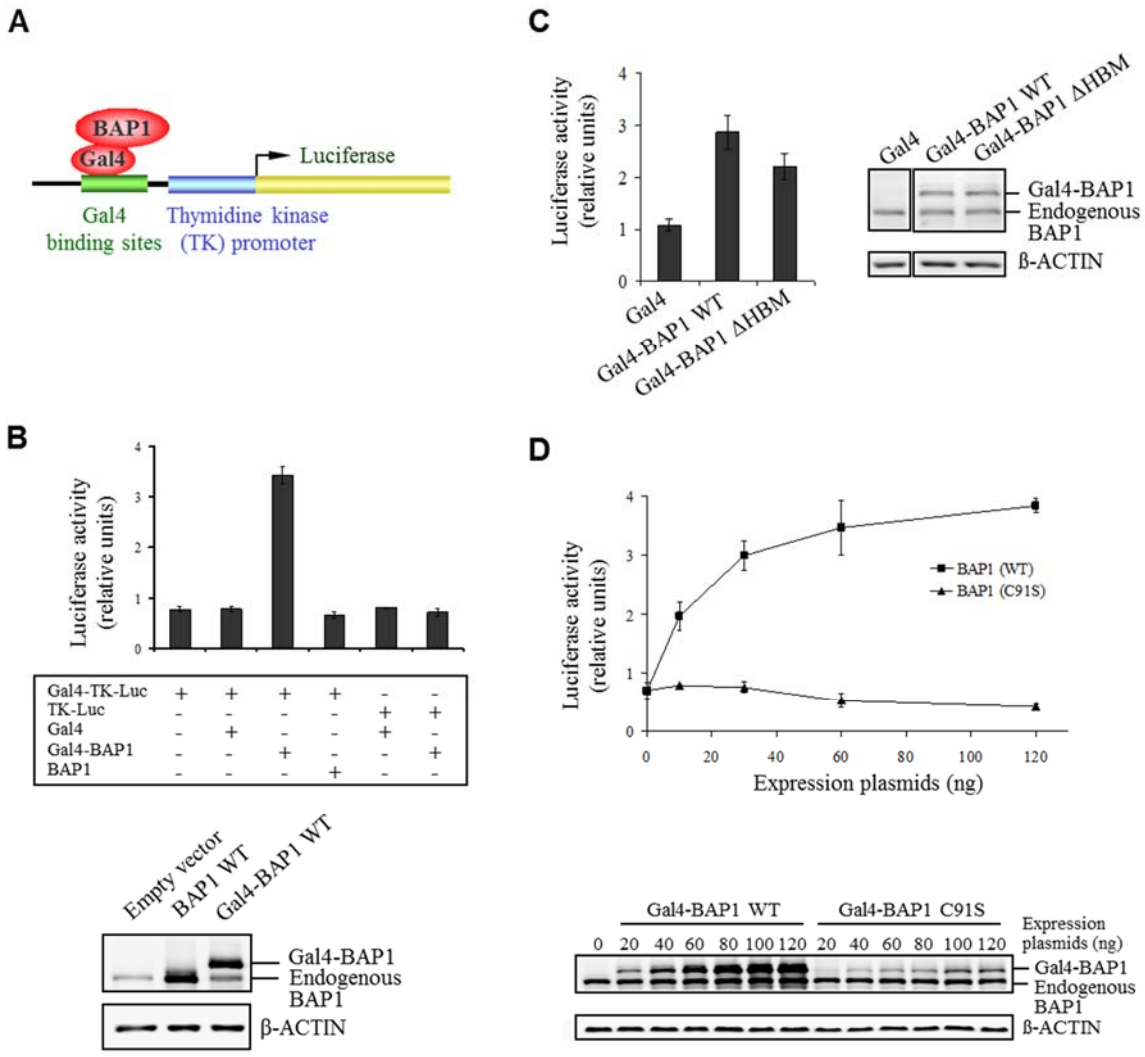

Figure 6. BAP1 activates transcription in a DUB-activity dependent manner.
(**A**) Schematic representation of the Gal4 transcription system. A transcription reporter assay was conducted by targeting BAP1 to the Gal4-TK-luciferase using Gal4-BAP1 fusion protein. This consists of targeting a protein of interest, fused in frame to the GAL4 DNA binding domain, to the luciferase reporter driven by a promoter containing GAL4 binding sites and the thymidine kinase proximal promoter. (**B**) Gal4-BAP1 activates transcription. HeLa cells were transfected with 100 ng of Gal4-BAP1, BAP1 or Gal4 expression plasmids along with 500 ng Gal4-TK-Luciferase or 500 ng TK-Luciferase reporter plasmids. Equal expression of various BAP1 constructs was confirmed by western blotting using anti-BAP1 (bottom panel) and luciferase activity was measured (top panel) at 2 days post-transfection. **(C)** HCF-1 is essentially dispensable for Gal4-BAP1 transcriptional activity. The Gal4 reporter assay was conducted using 500 ng Gal4-TK-Luciferase and equal amount of Gal4-BAP1 WT and Gal4-BAP1 ΔHBM. The expression of BAP1 constructs was monitored by western blotting (right panel) and luciferase activity was measured (left panel) at 2 days post-transfection. (**D**) The BAP1 catalytic activity is required for transcription activation. The Gal4 reporter assay was conducted using 500 ng Gal4-TK-Luciferase and various amounts of Gal4-BAP1 WT or the catalytic inactive mutant (C91S). The expression of BAP1 constructs was monitored by western blotting (bottom panel) and luciferase activity was measured (top panel) at 2 days post-transfection. All experiments were repeated at least 3 times and the results shown are from a representative experiment. Data are presented as mean ± SD.

In order to identify potential BAP1 target genes, global mRNA expression profiling using microarrays was conducted following BAP1 depletion in U2OS cells using two shRNA constructs and a non-targeting shRNA as a control. The gene expression data for both shRNAs are deposited in the Gene Expression Omnibus (GEO) NCBI database. Using the cut-off of two-fold difference relative to the control, we found that BAP1 depletion resulted in significantly elevated or decreased expression of about 249 genes (137 up-regulated and 112 down-regulated). Among these genes, several are associated with cell cycle progression, DNA damage signaling/repair, as well as survival and metabolism, suggesting that BAP1 participates in a diverse cellular processes (Figure 7A and Table 1). Interestingly, several E2F target genes including *skp2*, *p107, cdc2, cdc25a* were downregulated. The effect of BAP1 knockdown on the expression of some of these genes and others was further validated by RT-PCR (Figure 7B).

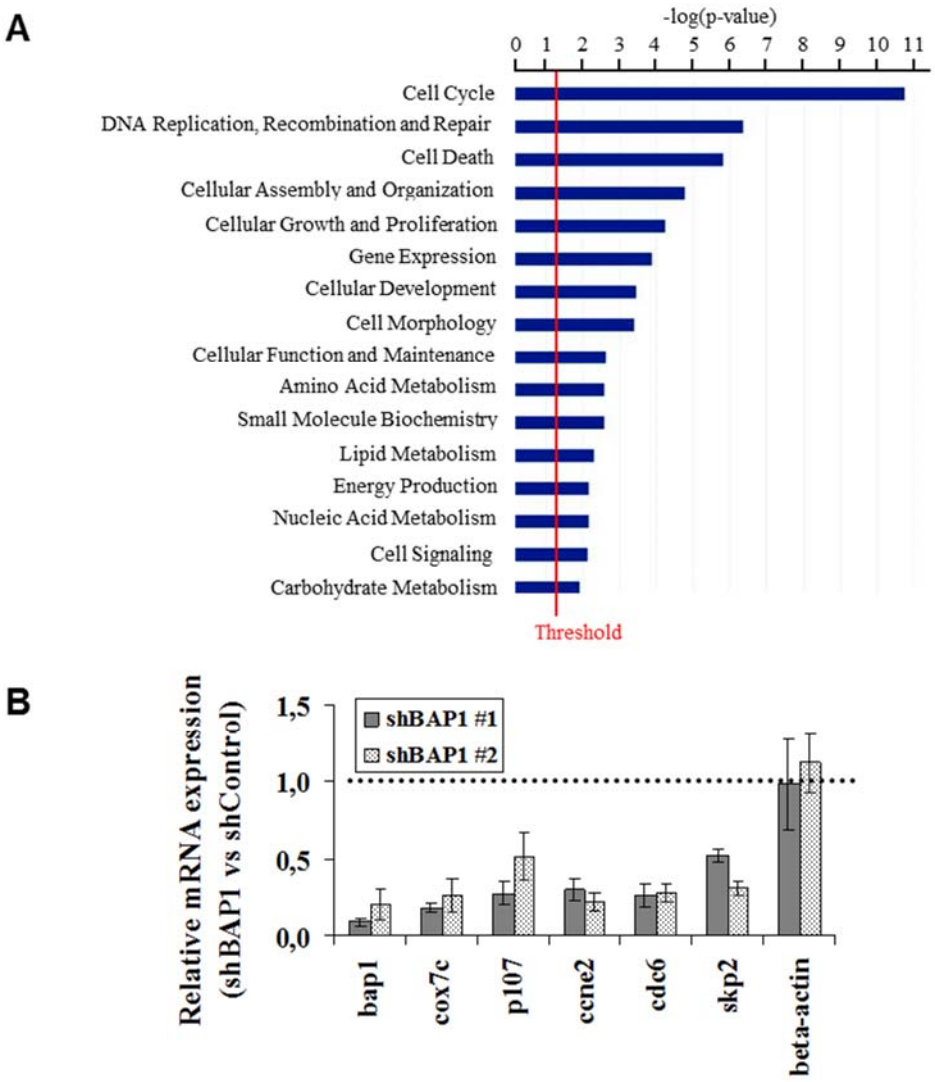

Figure 7. BAP1 regulates the expression of genes involved in numerous cellular processes.
(**A**) Functional analysis of genes deregulated following BAP1 depletion. The bar chart was generated by Ingenuity Pathways Analysis Version 8.5 using 1244 genes deregulated for both shBAP1s (Fold change: less than 0.7 and more than 1.5). The p value is calculated using the Fisher Exact Test. The smaller the p-value the less likely that the association is random. The line denotes the cutoff for significance (p value of 0.05). (**B**) RT-PCR analysis of selected genes. U2OS cells were transfected with either a non-targeting control or BAP1 shRNA plasmids along with the pBABE puromycin resistance-encoding vector, and transfected cells were selected by adding puromycin for 24 hours prior to synchronization at the G1/S border by the method of double thymidine block. mRNA quantification was conducted by real time RT-PCR analysis. All experiments were repeated at least 3 times and the data are presented as mean ± SD.

BAP1 is recruited by YY1 to regulate *cox7c* gene expression.

It is not known whether BAP1 assembles complexes that can be recruited to specific promoters to activate transcription. In light of our data, we reasoned that BAP1 might be recruited by YY1 to regulate gene expression. To investigate this possibility, we selected *cox7c,* one of the most downregulated genes based on our microarrays data. *cox7c* encodes a subunit of the holoenzyme that mediates the terminal step of the mitochondrial electron transport chain. The bovine *cox7c* promoter has been shown to contain two YY1 binding sites, mutations in which abrogate most of the promoter activity (50). These sites are highly conserved in mouse and human (Figure 8A). First, we confirmed that COX7C protein levels were also downregulated following BAP1 depletion in U2OS and HeLa cells (Figures 8B). Moreover, similar results were obtained following knockdown of HCF-1 (Figures 8B). Interestingly, depletion of YY1 induces a significant increase of COX7C expression in both HeLa and U2OS cells (Figure 8B). To determine whether BAP1 regulates *cox7c* expression in a DUB activity-dependent manner, we transducded U2OS cells with retroviral particles to overexpress either BAP1 or C91S mutant (Figure 8C). BAP1 C91S significantly inhibited the expression of COX7C protein, an effect not observed with the wildtype form. Of note, BAP1 C91S is a *bona fide* dominant negative mutant since it competes with wildtype BAP1 for assembly of the same multi-protein complexes (Figure 2B). To further characterize the role of the BAP1/HCF-1/YY1 complex in regulating gene expression, we conducted ChIP assays and found that these proteins are all enriched on the promoter region of *cox7c,* but not on the *β-globin* promoter (Figure 8D, left panel). Moreover, YY1 depletion by shRNA significantly decreased the enrichment of BAP1 and HCF-1 on the *cox7c* promoter indicating an essential role of YY1 in targeting BAP1/HCF-1 to specific gene regulatory regions (Figure 8D, left panel). Of note, shRNA-mediated depletion of YY1 did not affect either HCF-1 or BAP1 levels (Figure 8D, right panel).

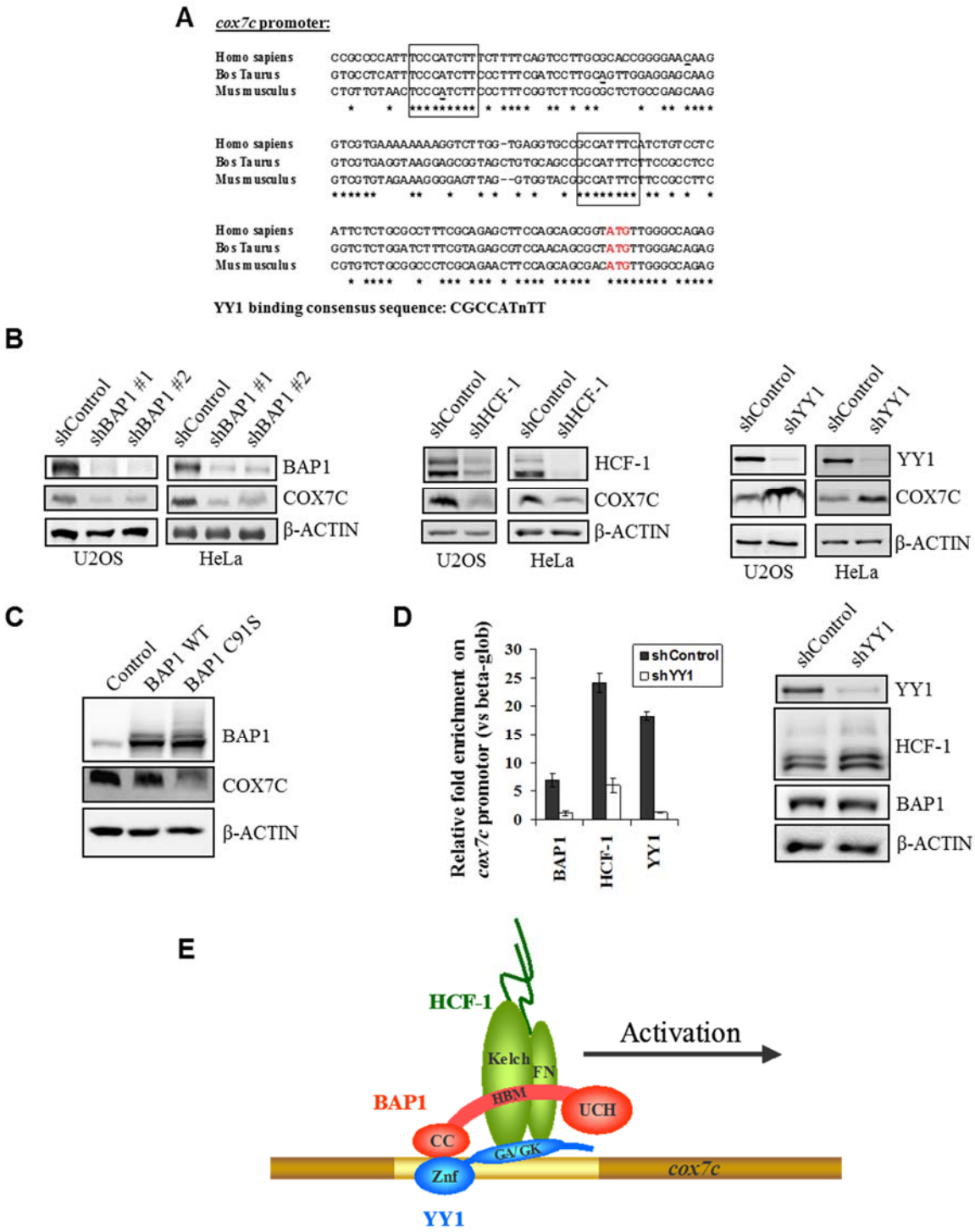

Figure 8. YY1 recruits BAP1 to co-activate *cox7c* expression.

(**A**) Alignment of *cox7c* promoter sequences from various mammalian species, *Homo Sapiens*, NC000005.9; *Bos Taurus*, NC007305.3; *Mus Musculus* NC000079.5. The YY1 binding sites are framed. The TSS is underlined. (**B**) Expression of COX7C following depletion of BAP1, HCF-1 or YY1. COX7C protein levels following transfection with BAP1 (left panel), HCF-1 (middle panel), YY1 (right panel) or non-target control shRNAs in U2OS or HeLa cells. Following transfection and selection with puromycin for 2 days, cells were harvested for immunoblotting. (**C**)

Downregulation of COX7C following expression of catalytic inactive BAP1. U2OS cells were transduced with retroviral particles to overexpress either BAP1 or its catalytic inactive form (C91S). Following 3 days, cells were harvested for western blotting using the indicated antibodies. (**D**) *cox7c* promoter occupancy by YY1, BAP1, and HCF-1. YY1 shRNA was expressed in U2OS cells by transfection and selection with puromycin for 2 days before harvesting for ChIP (left panel) or western blotting (right panel). ChIP was conducted using polyclonal antibodies against BAP1, HCF-1 or YY1. An IgG was used as control. The enrichment of factors was calculated versus *βglobin* promoter used as a control. All experiments were repeated at least 3 times and the results shown are from a representative experiment. Data are presented as mean ± SD. (**E**) Model representing the recruitment of BAP1 and HCF-1 to the *cox7c* promoter by the transcription factor YY1.

Discussion

In this study, we identified novel BAP1-interacting proteins and showed that nearly all cellular BAP1 forms high molecular weight multi-protein complexes with several transcription factors and cofactors. The associated partners are likely to play critical roles in targeting BAP1 to potential substrates, thereby regulating its function. Based on the relative abundance of BAP1-associated proteins purified from HeLa or U2OS cells, and on data from other studies (31, 36, 54), it appears that HCF-1, ASXL1 and/or ASXL2, OGT, FOXK1 and/or FOXK2 might form a BAP1 core complex. This minimal complex may selectively associate with additional regulators or transcription factors to form specific functional complexes in a cell type- and/or promoter-dependent manner. Indeed. sub-stoichiometric levels of several transcription factors co-purified with BAP1. These factors are involved a wide range of cellular processes, suggesting that BAP1 might exert a much broader role in regulating cell function than previously appreciated. Consistent with this notion, BAP1 depletion by RNAi induced profound changes in the expression of genes mediating and/or controlling numerous cellular pathways. Further studies will be needed to investigate how BAP1, via selective interactions with specific transcription factors and cofactors, regulates specific biological responses.

We provided strong evidence that BAP1 is a transcriptional co-activator: i) BAP1 associates with transcriptionally active chromatin. ii) BAP1 acts as an activator, in a DUB activity-dependent manner when targeted to a promoter using the Gal4 system. iii) Genome wide expression analysis reveals a considerable number of genes downregulated following BAP1 depletion. iv) BAP1 directly occupies the *cox7c* promoter, and depletion of BAP1 results in downregulation of this gene. It is also possible that BAP1 possesses dual co-activator/co-repressor functions, depending upon its association with specific transcription factors and cofactors on the

regulatory elements of target genes. In agreement with this latter hypothesis, some BAP1-interacting proteins including HCF-1, YY1, OGT and ASXL are known to interact with both co-activators and co-repressors (5, 9, 12, 43, 53, 68, 70, 71). In addition, a significant number of genes were up-regulated following depletion of BAP1. This suggests that BAP1 might exert a repressive effect on their promoters although these genes could constitute indirect targets, i.e., their up-regulation results from secondary changes induced by BAP1 depletion.

Using YY1 as a model for sequence-specific transcription factors that interact with BAP1/HCF-1, we demonstrated that these three proteins form a ternary complex *in vivo* which can associate with chromatin. Moreover, we found that BAP1 and HCF-1 are recruited by YY1 to co-activate *cox7c*, a gene previously reported to depend on YY1 binding sites for transcriptional activation (50). While depletion of BAP1 or HCF-1 reduces expression of *cox7c*, in contrast depletion of YY1 induces an increase in expression of this gene. These results suggest that YY1 possesses a dual function of both repressor and activator of *cox7c*, depending on its association with the HCF-1/BAP1 co-activator complex. A similar repression/activation mechanism by YY1 has been previously shown for the murine beta interferon promoter (37, 63). Consistent with this model, YY1 interacts with HCF-1 through the central region containing a GA/GK rich domain, previously shown to be involved in interactions with HDACs (70). This suggests that the association of YY1 with HCF-1/BAP1 is mutually exclusive with respect to its interaction with HDAC co-repressive complexes. With respect to *cox7c* expression, it is well-known that nuclear-encoded mitochondrial genes including components of the cytochrome C oxidase complex are not constitutively expressed, but rather subject to tight regulation by several transcription factors and cofactors depending on the state of cell growth, energy balance and other tissues-specific needs (18). Therefore, such genes are expected to oscillate between activation and repression states.

It is not clear at the present time whether BAP1 might regulate all YY1 target genes. It is possible that it might regulate only a subset of these targets, perhaps those on which YY1 acts as an activator only or on which it might exert dual activator/repressor function. Other transcription factors might dictate the specificity via interaction with YY1. Indeed YY1 is well known to interact with numerous transcription factors such as SP1, C-myc, and E2Fs (25, 48, 74). HCF-1, via additional interactions, might also contribute to the selectivity of recruitment of BAP1 to specific YY1-target genes. In this respect it is not surprising that Gal4-BAP1 lacking HBM is only slightly

impaired in transcription activation, suggesting that the interaction between HCF-1 and BAP1 might be mostly involved in recruitment of the latter to specific promoters.

Precisely how the assembled BAP1/HCF-1/YY1 complex acts to induce activation of *cox7c* or other target genes remains to be established. Nonetheless, the data suggest that the molecular mechanism involves ubiquitin signaling and deubiquitination of specific substrates on target promoters. BAP1 might be continuously needed to prevent degradation of HCF-1 (31, 36). Although the stability of the total cellular pool of HCF-1 is not significantly affected by BAP1 depletion, it is nonetheless possible that BAP1 stabilizes HCF-1 only on specific promoters following recruitment by YY1 or other transcription factors. Consistent with this, a BAP1 catalytic inactive mutant exerts a dominant negative effect on *cox7c* expression. It is also plausible that HCF-1 association with BAP1 and YY1 targets the DUB activity to deubiquitinate histones, specific transcription factors, or components of the general transcription machinery. Consistent with this, the drosophila BAP1 Calyposo deubiquitinates H2A, a histone mark associated with gene repression (47). However, Calyposo does not possess HBM and thus the mammalian BAP1 appears to selectively associate with HCF-1 and numerous other proteins not found with Calypso. In addition, in contrast to Calypso whose activity on ubiquitin AMC is very low when not associated with ASX, the recombinant mammalian BAP1 appears to have the same activity as complexed BAP1. We note that although BAP1 partners do not affect its DUB activity on ubiquitin-AMC, this does not exclude the possibility of their effect in the context of a physiological substrate *in vivo*.

Our results also shed light on the biological function of BAP1. This DUB was previously shown to be required for proper cell cycle progression, particularly the G1/S transition (31, 41), Moreover we observed similar effects in U2OS (data not shown), the cell type used here for global gene expression analysis. We also provided molecular insight linking BAP1 to the control of cell cycle genes including subsets of E2F targets. In addition HCF-1 is known to be required for normal G1/S transition, and was recently shown to play a major role in regulating the expression of E2F target genes by promoting histone H3 K4 trimethylation (21, 58). Thus, BAP1 might play a pivotal role in regulating the G1/S transition under normal and possibly stress conditions. Supporting this view, BAP1 is phosphorylated on an ATM/ATR consensus motif in response to DNA damage (33,

55), suggesting that these critical DNA damage-responsive checkpoint kinases might regulate BAP1 DUB activity and thus its function in controlling expression of cell cycle genes.

BAP1 might also participate in transcriptional regulatory programs that coordinate cell growth with cell cycle. For instance, in addition to *cox7c*, the expression of several mitochondrial and general metabolism genes are shown here to be deregulated upon BAP1 knockdown. Interestingly, recent bioinformatics and genome-wide promoter occupancy studies indicated that YY1 binding sites are enriched in the promoter regions of nuclear genes that encode mitochondrial proteins (59, 69). Moreover, NRF1, a major regulator of mitochondrial respiration, co-purifies with BAP1 (Table S1); and both YY1 and NRF1 binding sites are frequently found in close proximity in a large number of promoters of genes encoding mitochondrial proteins (59, 69). Furthermore HCF-1 has been found to interact with, and increase the transcriptional activity of, peroxisome proliferator-activated receptor gamma co-activator-1 (PGC-1), a major transcriptional regulator of mitochondrial biogenesis (27, 61). Thus BAP1 might play an important role in dynamically controlling transcriptional responses that coordinate mitochondrial function. Such responses in turn could constitute targets of stress signaling pathways (e.g., induced by DNA damage) that orchestrate adaptative metabolic responses.

In summary, our work indicates that BAP1 associates with several transcription factors and co-factors and is a gene-specific transcription regulator. As such, our findings establish a framework for further studies to (i) delineate the exact role of BAP1 in regulating the expression of genes involved in cell cycle progression, and (ii) define how deregulation of BAP1 function contributes to tumorigenesis.

Acknowledgements

This work was supported by grants to E.B.A. from the Terry Fox Foundation (grant#018144) and to Y.S from NIH (grant#GM053874). E.B.A. is a scholar of Le Fonds de la Recherche en Santé du Québec (FRSQ). H.Y. is a scholar of the Cole Foundation. We are grateful to Winship Herr for his generous gift of HCF-1 construct and antibodies.

Appendixes

Contains Supplemental Table 1, 2 & 3

References

1. Affar, E. B., F. Gay, Y. Shi, H. Liu, M. Huarte, S. Wu, C. Tucker, E. Li, and Y. Shi. 2006. Essential dosage-dependent functions of the transcription factor Yin Yang 1 in late embryonic development and cell cycle progression. Mol. Cell Biol. 26:3565-3581.

2. Bottardi, S., J. Ross, V. Bourgoin, N. Fotouhi-Ardakani, B. Affar el, M. Trudel, and E. Milot. 2009. Ikaros and GATA-1 combinatorial effect is required for silencing of human gamma-globin genes. Mol Cell Biol 29:1526-37.

3. Calvano, S. E., W. Xiao, D. R. Richards, R. M. Felciano, H. V. Baker, R. J. Cho, R. O. Chen, B. H. Brownstein, J. P. Cobb, S. K. Tschoeke, C. Miller-Graziano, L. L. Moldawer, M. N. Mindrinos, R. W. Davis, R. G. Tompkins, and S. F. Lowry. 2005. A network-based analysis of systemic inflammation in humans. Nature 437:1032-7.

4. Chen, Z. J., and L. J. Sun. 2009. Nonproteolytic functions of ubiquitin in cell signaling. Mol Cell 33:275-86.

5. Cho, Y. S., E. J. Kim, U. H. Park, H. S. Sin, and S. J. Um. 2006. Additional sex comb-like 1 (ASXL1), in cooperation with SRC-1, acts as a ligand-dependent coactivator for retinoic acid receptor. J Biol Chem 281:17588-98.

6. Dejosez, M., J. S. Krumenacker, L. J. Zitur, M. Passeri, L. F. Chu, Z. Songyang, J. A. Thomson, and T. P. Zwaka. 2008. Ronin is essential for embryogenesis and the pluripotency of mouse embryonic stem cells. Cell 133:1162-74.

7. Delehouzee, S., T. Yoshikawa, C. Sawa, J. Sawada, T. Ito, M. Omori, T. Wada, Y. Yamaguchi, Y. Kabe, and H. Handa. 2005. GABP, HCF-1 and YY1 are involved in Rb gene expression during myogenesis. Genes Cells 10:717-31.

8. Dou, Y., T. A. Milne, A. J. Tackett, E. R. Smith, A. Fukuda, J. Wysocka, C. D. Allis, B. T. Chait, J. L. Hess, and R. G. Roeder. 2005. Physical association and coordinate function of the H3 K4 methyltransferase MLL1 and the H4 K16 acetyltransferase MOF. Cell 121:873-85.

9. Fisher, C. L., I. Lee, S. Bloyer, S. Bozza, J. Chevalier, A. Dahl, C. Bodner, C. D. Helgason, J. L. Hess, R. K. Humphries, and H. W. Brock. 2010. Additional sex combs-like 1 belongs to the enhancer of trithorax and polycomb group and genetically interacts with Cbx2 in mice. Dev Biol 337:9-15.

10. Freiman, R. N., and W. Herr. 1997. Viral mimicry: common mode of association with HCF by VP16 and the cellular protein LZIP. Genes Dev 11:3122-7.

11. Fujiki, R., T. Chikanishi, W. Hashiba, H. Ito, I. Takada, R. G. Roeder, H. Kitagawa, and S. Kato. 2009. GlcNAcylation of a histone methyltransferase in retinoic-acid-induced granulopoiesis. Nature 459:455-9.

12. Gambetta, M. C., K. Oktaba, and J. Muller. 2009. Essential role of the glycosyltransferase sxc/Ogt in polycomb repression. Science 325:93-6.

13. Gordon, S., G. Akopyan, H. Garban, and B. Bonavida. 2006. Transcription factor YY1: structure, function, and therapeutic implications in cancer biology. Oncogene 25:1125-42.

14. Goto, H., S. Motomura, A. C. Wilson, R. N. Freiman, Y. Nakabeppu, K. Fukushima, M. Fujishima, W. Herr, and T. Nishimoto. 1997. A single-point mutation in HCF causes temperature-sensitive cell-cycle arrest and disrupts VP16 function. Genes Dev 11:726-37.

15. Groisman, R., J. Polanowska, I. Kuraoka, J. Sawada, M. Saijo, R. Drapkin, A. F. Kisselev, K. Tanaka, and Y. Nakatani. 2003. The ubiquitin ligase activity in the DDB2 and CSA complexes is differentially regulated by the COP9 signalosome in response to DNA damage. Cell 113:357-67.

16. Gunther, M., M. Laithier, and O. Brison. 2000. A set of proteins interacting with transcription factor Sp1 identified in a two-hybrid screening. Mol Cell Biochem 210:131-42.

17. Harper, J. V. 2005. Synchronization of cell populations in G1/S and G2/M phases of the cell cycle. Methods Mol Biol 296:157-66.

18. Hock, M. B., and A. Kralli. 2009. Transcriptional control of mitochondrial biogenesis and function. Annu Rev Physiol 71:177-203.

19. Jensen, D. E., M. Proctor, S. T. Marquis, H. P. Gardner, S. I. Ha, L. A. Chodosh, A. M. Ishov, N. Tommerup, H. Vissing, Y. Sekido, J. Minna, A. Borodovsky, D. C. Schultz, K. D. Wilkinson, G. G. Maul, N. Barlev, S. L. Berger, G. C. Prendergast, and F. J. Rauscher, 3rd. 1998. BAP1: a novel ubiquitin hydrolase which binds to the BRCA1 RING finger and enhances BRCA1-mediated cell growth suppression. Oncogene 16:1097-1112.

20. Johnston, S. C., C. N. Larsen, W. J. Cook, K. D. Wilkinson, and C. P. Hill. 1997. Crystal structure of a deubiquitinating enzyme (human UCH-L3) at 1.8 A resolution. Embo J 16:3787-96.

21. Julien, E., and W. Herr. 2003. Proteolytic processing is necessary to separate and ensure proper cell growth and cytokinesis functions of HCF-1. Embo J 22:2360-9.

22. Knez, J., D. Piluso, P. Bilan, and J. P. Capone. 2006. Host cell factor-1 and E2F4 interact via multiple determinants in each protein. Mol Cell Biochem 288:79-90.

23. Kristie, T. M., Y. Liang, and J. L. Vogel. 2009. Control of alpha-herpesvirus IE gene expression by HCF-1 coupled chromatin modification activities. Biochim Biophys Acta 1799:257-65.

24. Lee, J. S., K. M. Galvin, R. H. See, R. Eckner, D. Livingston, E. Moran, and Y. Shi. 1995. Relief of YY1 transcriptional repression by adenovirus E1A is mediated by E1A-associated protein p300. Genes Dev 9:1188-98.

25. Lee, J. S., K. M. Galvin, and Y. Shi. 1993. Evidence for physical interaction between the zinc-finger transcription factors YY1 and Sp1. Proc Natl Acad Sci U S A 90:6145-9.

26. Liang, Y., J. L. Vogel, A. Narayanan, H. Peng, and T. M. Kristie. 2009. Inhibition of the histone demethylase LSD1 blocks alpha-herpesvirus lytic replication and reactivation from latency. Nat Med 15:1312-7.

27. Lin, J., P. Puigserver, J. Donovan, P. Tarr, and B. M. Spiegelman. 2002. Peroxisome proliferator-activated receptor gamma coactivator 1beta (PGC-1beta), a novel PGC-1-related transcription coactivator associated with host cell factor. J Biol Chem 277:1645-8.

28. Lu, R., P. Yang, S. Padmakumar, and V. Misra. 1998. The herpesvirus transactivator VP16 mimics a human basic domain leucine zipper protein, luman, in its interaction with HCF. J Virol 72:6291-7.

29. Luciano, R. L., and A. C. Wilson. 2003. HCF-1 functions as a coactivator for the zinc finger protein Krox20. J Biol Chem 278:51116-24.

30. Luciano, R. L., and A. C. Wilson. 2000. N-terminal transcriptional activation domain of LZIP comprises two LxxLL motifs and the host cell factor-1 binding motif. Proc Natl Acad Sci U S A 97:10757-62.

31. Machida, Y. J., Y. Machida, A. A. Vashisht, J. A. Wohlschlegel, and A. Dutta. 2009. The deubiquitinating enzyme BAP1 regulates cell growth via interaction with HCF-1. J Biol Chem.

32. Mason, D. E., J. Ek, E. C. Peters, and J. L. Harris. 2004. Substrate profiling of deubiquitin hydrolases with a positional scanning library and mass spectrometry. Biochemistry 43:6535-44.

33. Matsuoka, S., B. A. Ballif, A. Smogorzewska, E. R. McDonald, 3rd, K. E. Hurov, J. Luo, C. E. Bakalarski, Z. Zhao, N. Solimini, Y. Lerenthal, Y. Shiloh, S. P. Gygi, and S. J. Elledge. 2007. ATM and ATR substrate analysis reveals extensive protein networks responsive to DNA damage. Science 316:1160-6.

34. Mazars, R., A. Gonzalez-de-Peredo, C. Cayrol, A. C. Lavigne, J. L. Vogel, N. Ortega, C. Lacroix, V. Gautier, G. Huet, A. Ray, B. Monsarrat, T. M. Kristie, and J. P. Girard. 2010. The thap-zinc finger protein thap1 associates with coactivator HCF-1 and O-GLcNAc transferase: A link between DYT6 and DYT3 dystonias. J Biol Chem.

35. Misaghi, S., P. J. Galardy, W. J. Meester, H. Ovaa, H. L. Ploegh, and R. Gaudet. 2005. Structure of the ubiquitin hydrolase UCH-L3 complexed with a suicide substrate. J Biol Chem 280:1512-20.

36. Misaghi, S., S. Ottosen, A. Izrael-Tomasevic, D. Arnott, M. Lamkanfi, J. Lee, J. Liu, K. O'Rourke, V. M. Dixit, and A. C. Wilson. 2009. Association of C-terminal ubiquitin hydrolase BRCA1-associated protein 1 with cell cycle regulator host cell factor 1. Mol Cell Biol 29:2181-92.

37. Mokrani, H., O. Sharaf el Dein, Z. Mansuroglu, and E. Bonnefoy. 2006. Binding of YY1 to the proximal region of the murine beta interferon promoter is essential to allow CBP recruitment and K8H4/K14H3 acetylation on the promoter region after virus infection. Mol Cell Biol 26:8551-61.

38. Nakatani, Y., and V. Ogryzko. 2003. Immunoaffinity purification of mammalian protein complexes. Methods Enzymol 370:430-44.

39. Narayanan, A., W. T. Ruyechan, and T. M. Kristie. 2007. The coactivator host cell factor-1 mediates Set1 and MLL1 H3K4 trimethylation at herpesvirus immediate early promoters for initiation of infection. Proc Natl Acad Sci U S A 104:10835-40.

40. Nijman, S. M., M. P. Luna-Vargas, A. Velds, T. R. Brummelkamp, A. M. Dirac, T. K. Sixma, and R. Bernards. 2005. A genomic and functional inventory of deubiquitinating enzymes. Cell 123:773-786.

41. Nishikawa, H., W. Wu, A. Koike, R. Kojima, H. Gomi, M. Fukuda, and T. Ohta. 2009. BRCA1-associated protein 1 interferes with BRCA1/BARD1 RING heterodimer activity. Cancer Res 69:111-9.

42. Nowak, D. E., B. Tian, and A. R. Brasier. 2005. Two-step cross-linking method for identification of NF-kappaB gene network by chromatin immunoprecipitation. Biotechniques 39:715-25.

43. Ozcan, S., S. S. Andrali, and J. E. Cantrell. 2010. Modulation of transcription factor function by O-GlcNAc modification. Biochim Biophys Acta.

44. Pickart, C. M., and M. J. Eddins. 2004. Ubiquitin: structures, functions, mechanisms. Biochim. Biophys. Acta 1695:55-72.

45. Pickart, C. M., and D. Fushman. 2004. Polyubiquitin chains: polymeric protein signals. Curr Opin Chem Biol 8:610-6.

46. Reyes-Turcu, F. E., K. H. Ventii, and K. D. Wilkinson. 2009. Regulation and cellular roles of ubiquitin-specific deubiquitinating enzymes. Annu Rev Biochem 78:363-97.

47. Scheuermann, J. C., A. G. de Ayala Alonso, K. Oktaba, N. Ly-Hartig, R. K. McGinty, S. Fraterman, M. Wilm, T. W. Muir, and J. Muller. 2010. Histone H2A deubiquitinase activity of the Polycomb repressive complex PR-DUB. Nature 465:243-7.

48. Schlisio, S., T. Halperin, M. Vidal, and J. R. Nevins. 2002. Interaction of YY1 with E2Fs, mediated by RYBP, provides a mechanism for specificity of E2F function. Embo J 21:5775-86.

49. Schuettengruber, B., D. Chourrout, M. Vervoort, B. Leblanc, and G. Cavalli. 2007. Genome regulation by polycomb and trithorax proteins. Cell 128:735-45.

50. Seelan, R. S., and L. I. Grossman. 1997. Structural organization and promoter analysis of the bovine cytochrome c oxidase subunit VIIc gene. A functional role for YY1. J Biol Chem 272:10175-81.

51. Shi, Y., J. S. Lee, and K. M. Galvin. 1997. Everything you have ever wanted to know about Yin Yang 1. Biochim Biophys Acta 1332:F49-66.

52. Shi, Y., J. Sawada, G. Sui, B. Affar el, J. R. Whetstine, F. Lan, H. Ogawa, M. P. Luke, and Y. Nakatani. 2003. Coordinated histone modifications mediated by a CtBP co-repressor complex. Nature 422:735-8.

53. Sinclair, D. A., M. Syrzycka, M. S. Macauley, T. Rastgardani, I. Komljenovic, D. J. Vocadlo, H. W. Brock, and B. M. Honda. 2009. Drosophila O-GlcNAc transferase (OGT) is encoded by the Polycomb group (PcG) gene, super sex combs (sxc). Proc Natl Acad Sci U S A 106:13427-32.

54. Sowa, M. E., E. J. Bennett, S. P. Gygi, and J. W. Harper. 2009. Defining the human deubiquitinating enzyme interaction landscape. Cell 138:389-403.

55. Stokes, M. P., J. Rush, J. Macneill, J. M. Ren, K. Sprott, J. Nardone, V. Yang, S. A. Beausoleil, S. P. Gygi, M. Livingstone, H. Zhang, R. D. Polakiewicz, and M. J. Comb. 2007. Profiling of UV-induced ATM/ATR signaling pathways. Proc Natl Acad Sci U S A 104:19855-60.

56. Sui, G., B. Affar el, Y. Shi, C. Brignone, N. R. Wall, P. Yin, M. Donohoe, M. P. Luke, D. Calvo, S. R. Grossman, and Y. Shi. 2004. Yin Yang 1 is a negative regulator of p53. Cell 117:859-872.

57. Sui, G., C. Soohoo, B. Affar el, F. Gay, Y. Shi, W. C. Forrester, and Y. Shi. 2002. A DNA vector-based RNAi technology to suppress gene expression in mammalian cells. Proc. Natl. Acad. Sci. U. S. A. 99:5515-5520.

58. Tyagi, S., A. L. Chabes, J. Wysocka, and W. Herr. 2007. E2F activation of S phase promoters via association with HCF-1 and the MLL family of histone H3K4 methyltransferases. Mol Cell 27:107-19.

59. van Waveren, C., and C. T. Moraes. 2008. Transcriptional co-expression and co-regulation of genes coding for components of the oxidative phosphorylation system. BMC Genomics 9:18.

60. Ventii, K. H., N. S. Devi, K. L. Friedrich, T. A. Chernova, M. Tighiouart, E. G. Van Meir, and K. D. Wilkinson. 2008. BRCA1-associated protein-1 is a tumor suppressor that requires deubiquitinating activity and nuclear localization. Cancer Res 68:6953-62.

61. Vercauteren, K., N. Gleyzer, and R. C. Scarpulla. 2008. PGC-1-related coactivator complexes with HCF-1 and NRF-2beta in mediating NRF-2(GABP)-dependent respiratory gene expression. J Biol Chem 283:12102-11.

62. Vogel, J. L., and T. M. Kristie. 2000. The novel coactivator C1 (HCF) coordinates multiprotein enhancer formation and mediates transcription activation by GABP. Embo J 19:683-90.

63. Weill, L., E. Shestakova, and E. Bonnefoy. 2003. Transcription factor YY1 binds to the murine beta interferon promoter and regulates its transcriptional capacity with a dual activator/repressor role. J Virol 77:2903-14.

64. Welchman, R. L., C. Gordon, and R. J. Mayer. 2005. Ubiquitin and ubiquitin-like proteins as multifunctional signals. Nat. Rev. Mol. Cell Biol. 6:599-609.

65. Wilson, A. C., K. LaMarco, M. G. Peterson, and W. Herr. 1993. The VP16 accessory protein HCF is a family of polypeptides processed from a large precursor protein. Cell 74:115-25.

66. Wilson, A. C., J. E. Parrish, H. F. Massa, D. L. Nelson, B. J. Trask, and W. Herr. 1995. The gene encoding the VP16-accessory protein HCF (HCFC1) resides in human Xq28 and is highly expressed in fetal tissues and the adult kidney. Genomics 25:462-8.

67. Wood, L. D., D. W. Parsons, S. Jones, J. Lin, T. Sjoblom, R. J. Leary, D. Shen, S. M. Boca, T. Barber, J. Ptak, N. Silliman, S. Szabo, Z. Dezso, V. Ustyanksky, T. Nikolskaya, Y. Nikolsky, R. Karchin, P. A. Wilson, J. S. Kaminker, Z. Zhang, R. Croshaw, J. Willis, D. Dawson, M. Shipitsin, J. K. Willson, S. Sukumar, K. Polyak, B. H. Park, C. L. Pethiyagoda, P. V. Pant, D. G. Ballinger, A. B. Sparks, J. Hartigan, D. R. Smith, E. Suh, N. Papadopoulos, P. Buckhaults, S. D. Markowitz, G. Parmigiani, K. W. Kinzler, V. E. Velculescu, and B. Vogelstein. 2007. The genomic landscapes of human breast and colorectal cancers. Science 318:1108-13.

68. Wysocka, J., M. P. Myers, C. D. Laherty, R. N. Eisenman, and W. Herr. 2003. Human Sin3 deacetylase and trithorax-related Set1/Ash2 histone H3-K4 methyltransferase are tethered together selectively by the cell-proliferation factor HCF-1. Genes Dev 17:896-911.

69. Xi, H., Y. Yu, Y. Fu, J. Foley, A. Halees, and Z. Weng. 2007. Analysis of overrepresented motifs in human core promoters reveals dual regulatory roles of YY1. Genome Res 17:798-806.

70. Yang, W. M., C. Inouye, Y. Zeng, D. Bearss, and E. Seto. 1996. Transcriptional repression by YY1 is mediated by interaction with a mammalian homolog of the yeast global regulator RPD3. Proc Natl Acad Sci U S A 93:12845-50.

71. Yang, X., F. Zhang, and J. E. Kudlow. 2002. Recruitment of O-GlcNAc transferase to promoters by corepressor mSin3A: coupling protein O-GlcNAcylation to transcriptional repression. Cell 110:69-80.

72. Yokoyama, A., Z. Wang, J. Wysocka, M. Sanyal, D. J. Aufiero, I. Kitabayashi, W. Herr, and M. L. Cleary. 2004. Leukemia proto-oncoprotein MLL forms a SET1-like histone methyltransferase complex with menin to regulate Hox gene expression. Mol Cell Biol 24:5639-49.

73. Zeng, P. Y., C. R. Vakoc, Z. C. Chen, G. A. Blobel, and S. L. Berger. 2006. In vivo dual cross-linking for identification of indirect DNA-associated proteins by chromatin immunoprecipitation. Biotechniques 41:694, 696, 698.

74. Zhao, J. H., T. Inoue, W. Shoji, Y. Nemoto, and M. Obinata. 1998. Direct association of YY-1 with c-Myc and the E-box binding protein in regulation of glycophorin gene expression. Oncogene 17:1009-17.

Annexe 2 Article: Autodeubiquitination protects the tumor suppressor BAP1 from cytoplasmic sequestration mediated by the atypical ubiquitin ligase UBE2O

Nazar Mashtalir[1], Salima Daou[1], Haithem Barbour[1], Nadine N Sen[1], Jessica Gagnon[1], Ian Hammond-Martel[1], Haider H Dar[1], Marc Therrien[2] and El Bachir Affar[1],[3]

1Maisonneuve-Rosemont Hospital Research Center, Department of Medicine, University of Montréal, QC, Montréal, H1T 2M4, Canada

2Institute for Research in Immunology and Cancer, Laboratory of Intracellular Signaling, University of Montréal, Montréal, QC, H3T 1J4, Canada

Running title: UBE2O ligase regulates the tumor suppressor BAP1.

Publié dans: Molecular Cell, 2014, 2014,54(3)392-406.

Summary

The tumor suppressor BAP1 interacts with chromatin-associated proteins and regulates cell proliferation, but its mechanism of action and regulation remain poorly defined. We show that the ubiquitin conjugating enzyme UBE2O multi-mono-ubiquitinates the nuclear localization signal of BAP1, thereby inducing its cytoplasmic sequestration. This activity is counteracted by BAP1 auto-deubiquitination through intramolecular interactions. Significantly, we identified cancer-derived BAP1 mutations that abrogate auto-deubiquitination and promote its cytoplasmic retention, indicating that BAP1 auto-deubiquitination ensures tumor suppression. The antagonistic relationship between UBE2O and BAP1 is also observed during adipogenesis, whereby UBE2O promotes differentiation and cytoplasmic localization of BAP1. Finally, we established a putative targeting consensus sequence of UBE2O and identified numerous chromatin remodeling factors as potential targets, several of which tested positive for UBE2O-mediated ubiquitination. Thus, UBE2O defines an atypical ubiquitin-signaling pathway that coordinates the function of BAP1 and establishes a paradigm for regulation of nuclear trafficking of chromatin-associated proteins.

Highlights

- UBE2O ubiquitinates BAP1 on its NLS, and regulates its subcellular localization
- The mechanism of BAP1 auto-deubiquitination is disrupted in cancer
- UBE2O and BAP1 have antagonistic roles in cell cycle regulation and differentiation
- UBE2O targets itself and a subset of chromatin regulators

Introduction

The covalent attachment of ubiquitin to target proteins, i.e., ubiquitination, regulates both protein stability and function, and is fundamental to diverse biological processes (Hammond-Martel et al., 2012; Jackson and Durocher, 2013). The deubiquitinase (DUB) BAP1 is a transcriptional regulator required for mammalian development (Dey et al., 2012; Yu et al., 2010). BAP1 is also a tumor suppressor inactivated in various cancers, and reconstitution studies in cancer cells harboring BAP1 mutations indicated that both BAP1 catalytic activity and nuclear localization are required for its growth suppressive properties (Carbone et al., 2013; Ventii et al., 2008). Moreover, RNAi-mediated depletion of BAP1 also induces defects in cell cycle progression indicating that this protein is a key regulator of cell proliferation (Machida et al., 2009). At the molecular level, BAP1 assembles a large multi-protein complex consisting of numerous transcription factors and chromatin-associated proteins including the Host Cell Factor-1 (HCF-1), the Polycomb Group (PcG) proteins Additional Sex Combs Like 1 and 2 (ASXL1/2), the histone demethylase KDM1B, the O-linked N-acetylglucosamine transferase (OGT), the forkhead transcription factors FOXK1/FOXK2, and the zinc finger transcription factor Yin Yang1 (YY1) (Machida et al., 2009; Misaghi et al., 2009; Sowa et al., 2009; Yu et al., 2010).

The *Drosophila* BAP1, Calypso, is a PcG protein that interacts with Additional Sex Combs (ASX), localizes at PcG-target gene regulatory regions, and represses HOX gene expression. Calypso/ASX heterodimer, termed PR-DUB (Polycomb repressive DUB), deubiquitinates histone H2A (Scheuermann et al., 2010), a chromatin modification involved in chromatin remodeling and gene silencing (Lanzuolo and Orlando, 2012).

We and others previously identified the ubiquitin conjugating enzyme UBE2O as a substoichiometric factor that co-purifies with the human BAP1 (Machida et al., 2009; Sowa et al., 2009; Yu et al., 2010), suggesting that it might be involved in the coordination of BAP1 function. UBE2O belongs to the E2 family of ubiquitin-conjugating enzymes, although, unlike most members of this family, it is unusually large (140 kDa) (van Wijk and Timmers, 2010). Pioneering studies from Pickart's group suggested that UBE2O might function as an E2/E3 hybrid (Berleth and Pickart, 1996; Klemperer et al., 1989). This was essentially based on the observation that UBE2O can ubiquitinate free histones *in vitro*, in the presence of E1 enzyme only. It has been proposed that ubiquitination by UBE2O involves an intramolecular thioester relay mechanism

since this enzyme is inhibited by phenylarsine oxide (PAO) which can crosslink adjacent cysteines (Klemperer et al., 1989). Otherwise, the physiological substrates of UBE2O are largely unknown. Nonetheless, it was recently shown that UBE2O regulates TRAF6-dependent NF-κB in a catalytic activity-independent manner (Zhang et al., 2013b), monoubiquitinates SMAD6 during bone morphogenetic protein signaling (Zhang et al., 2013a), and coordinates endosomal protein trafficking (Hao et al., 2013) thus implicating UBE2O in numerous cellular processes. In this study, we uncover a novel ubiquitin-signaling pathway, mediated by UBE2O, that has important implications for chromatin-associated processes.

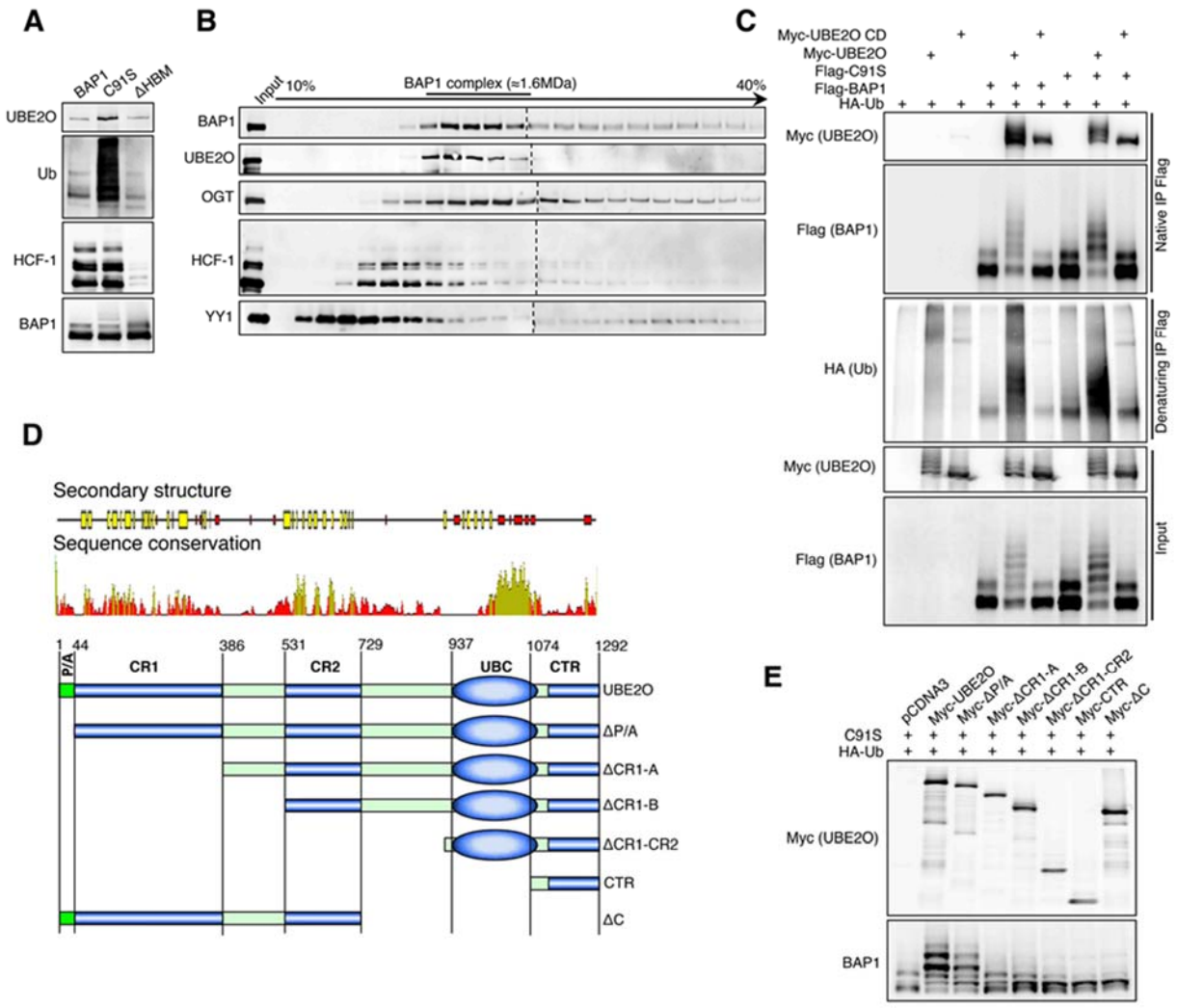

Figure 1. UBE2O interacts with and ubiquitinates BAP1 and this effect is actively counteracted by BAP1 auto-deubiquitination. (See also Figure S1). A) Purified BAP1 complexes were used for western blot. **B)** HeLa nuclear extract was resolved by glycerol gradient, and used for western blot. **C)** 293T cells were co-transfected with 2 µg of HA-Ub, 2 µg of Myc-UBE2O (wild type or **CD**), and 1 µg of Flag-BAP1 (wild type or C91S) expression vectors, and cell extracts were used for immunoprecipitation. **D)** Top, schema representing the human UBE2O with secondary structure prediction (alpha helixes are in red and beta strands are in yellow). The main predicted domains are indicated as CR1 (conserved region 1), CR2 (conserved region 2), UBC (ubiquitin conjugating) and CTR (C-terminal region). Bottom, schema representing UBE2O deletion mutants used for the ubiquitination assay. **E)** 293T cells were co-transfected with 2 µg of HA-Ub, 2 µg of Myc-UBE2O fragments, and 1 µg of C91S expression vectors, and cell extracts were used for western blot.

Results

The ubiquitin conjugating enzyme UBE2O interacts with and ubiquitinates BAP1

We previously described the purification of complexes formed by wild type and catalytic dead BAP1 (C91S) (Yu et al., 2010). The complexes were essentially identical, although when probed with an anti-ubiquitin antibody, the C91S complex exhibited a dramatic increase in signal (Figure 1A). We also routinely observed mono-ubiquitination of BAP1 in transfected cells, independently of its DUB activity (Figure 1A and Figure S1A-E). This suggests that BAP1 might be functionally regulated by distinct ubiquitination events in DUB activity-dependent and -independent manner. To identify E3 ligases responsible for the ubiquitination of BAP1, we initially considered UBE2O which was more abundant in the C91S versus the wild type BAP1 complex (Figure 1A). The UBE2O association with BAP1 was not affected by mutation of the HCF-1 Binding Motif (HBM) which eliminates HCF-1, a major component of the complex (Figure 1A). Glycerol density gradient fractionation of nuclear extracts indicated that UBE2O co-sediments with the BAP1 complex (Figure 1B). Next, we co-transfected BAP1 or C91S with UBE2O or its catalytic dead mutant C1040S (hereafter UBE2O CD) and ubiquitin into 293T cells. Strikingly, UBE2O ubiquitinates BAP1, and modified forms were more abundant in the C91S mutant (Figure 1C). Incubation of UBE2O-modified BAP1 C91S with an excess of USP2 DUB catalytic domain resulted in its complete deubiquitination further demonstrating ubiquitin conjugation (Figure S1F). Of note, deletion of the UCH catalytic domain results in the abolishment of the constitutive mono-ubiquitination (Figure S1G). On the other hand, a similar UBE2O-dependent ubiquitination pattern could be observed for BAP1 C91S or BAP1 ΔUCH indicating that UBE2O-mediated ubiquitination is distinct from its constitutive mono-ubiquitination.

To control for the specificity of UBE2O-mediated BAP1 ubiquitination, we evaluated other E2s and none was able to ubiquitinate BAP1 (Figure S1H,I). We also tested two known H2A DUBs, i.e., USP16 and MYSM1, as well as the SUMO protease SENP2, and no UBE2O-mediated ubiquitination could be observed (Figure S1J). Using multiple sequence alignment, we identified three main conserved regions in UBE2O namely CR1 (conserved region 1), CR2 (conserved region 2) and UBC (Ubiquitin conjugating) (Figure 1D, Figure S1K). Secondary structure prediction analysis revealed all-β domains within CR1 and CR2 and the typical α/β UBC fold. Deletion of either N- (ΔCR1-CR2) or C-terminal (ΔC) regions of UBE2O completely disrupted BAP1 ubiquitination (Figure 1D, E). Moreover, deletion of only the N-terminal CR1 region

(ΔCR1-A) was sufficient to abolish UBE2O catalytic activity. Hence, the integrity of multiple domains of UBE2O is required for ubiquitination of BAP1.

UBE2O catalyzes the multi-mono-ubiquitination of BAP1

To determine the mechanism of UBE2O action on BAP1, we established an *in vitro* assay for BAP1 ubiquitination using wild type and C91S complexes immobilized on the beads (Figure S2A). UBE2O-mediated ubiquitination appears to be highly specific for the C91S mutant as no modified forms were observed for other BAP1 partners (Figure 2A). Moreover, ubiquitination of the C91S mutant did not disrupt complex integrity, since none of the complex components was released into the soluble fraction in a UBE2O-dependent manner (Figure 2A). Notably, we did not detect ubiquitination of wild type BAP1 as opposed to C91S, and this ubiquitination was completely abolished by the UBE2O inhibitor PAO (Figure 2A, Figure S2B). We note that UBE2O, purified from HeLa cells under high or low salt conditions or from bacteria, ubiquitinates C91S to similar extents (Figure S2C,D). Importantly, although less efficient, ubiquitination was also observed using bacteria-purified BAP1 and UBE2O (Figure S2E). Therefore UBE2O is an atypical E2/E3 enzyme with substrate binding and ubiquitin conjugating functions.

To further confirm that auto-deubiquitination prevents accumulation of ubiquitin on BAP1, the beads-bound wild type complex was pretreated with N-ethylmaleimide (NEM), which resulted in a significant ubiquitination of BAP1 by UBE2O (Figure S2A, Figure 2B). Next, we used methylated ubiquitin, which is unable to form poly-ubiquitin or linear chains in the *in vitro* reaction (Figure 2C). The reaction with methylated ubiquitin was as efficient as with the unmodified ubiquitin and resulted in a similar ubiquitination pattern, indicating that UBE2O multi-mono-ubiquitinates BAP1. The same observation was made *in vivo* when a K0 ubiquitin mutant, incapable of chain formation, was used for co-transfection of 293T cells with the C91S mutant and UBE2O (Figure 2D). Next, 293T cells were co-transfected with wild type BAP1 or C91S mutant and UBE2O, and then treated with the proteasome inhibitor MG132 (Figure 2E). The typical multi-mono-ubiquitination pattern of BAP1 was unchanged after proteasome inhibition, indicating that UBE2O is unable to directly catalyze poly-ubiquitin chain elongation with subsequent degradation of BAP1. Immunodetection of endogenous CDC25A was conducted as a control for proteasome inhibition. Next, we tested several E3s that interact with either UBE2O or BAP1 and no further chain elongation was observed (Figure S2F-I). To further confirm that the stability of BAP1 is not

directly regulated by UBE2O, we performed siRNA knockdown of UBE2O in MCF7 cells, which express high protein levels of this enzyme, followed by treatment with cycloheximide (CHX) (Figure 2F). Endogenous BAP1 appears to be highly stable and UBE2O knockdown did not significantly change BAP1 protein levels. We concluded that UBE2O catalyzes BAP1 multi-mono-ubiquitination without directly promoting its proteasomal degradation under normal growth conditions. Of note, UBE2O depletion also did not affect the constitutive mono-ubiquitination of BAP1 observed in cells transfected with this DUB (Figure S2J).

The NLS of BAP1 is required for UBE2O-mediated ubiquitination

Using a GST pull down assay, we found that the BAP1 C-terminal region (598-729 aa), which includes the C-terminal domain (CTD) and NLS, is necessary and sufficient for UBE2O binding (Figure 3A). Surprisingly, co-expression of UBE2O with CTD-NLS promoted the latter's degradation by the proteasome, since it could be reversed by MG132 (Figure 3B, left panel and Figure S3A, B). Immunoprecipitation of the CTD-NLS revealed an ubiquitination pattern similar to that of the full length BAP1 (4-5 sites of multi-mono-ubiquitination), although some high molecular weight smears were also detected (Figure 3B, right panel). Next, we found that both wild type and K0 ubiquitin mutants promoted UBE2O-mediated multi-mono-ubiquitination and degradation of the CTD-NLS (Figure S3C). Moreover, knockdown of endogenous UBE2O rescued the degradation of CTD-NLS (Figure 3C). These results confirm that the CTD-NLS represents both the interaction and ubiquitination region for UBE2O. The degradation of CTD-NLS can be explained by the small size of this region (only 101aa), in line with a recent discovery by Ciechanover's group indicating that monoubiquitinated substrates of less than 150 aa can be degraded without further ubiquitin chain formation (Shabek et al., 2012). Next, we purified the complex of the BAP1ΔCTD mutant that possesses a large deletion of aa 631-693 leaving only the NLS region intact (aa 699-729) (Figure 3D). The abundance of UBE2O was nearly unchanged between the wild type and the mutant indicating that UBE2O binds the NLS region.

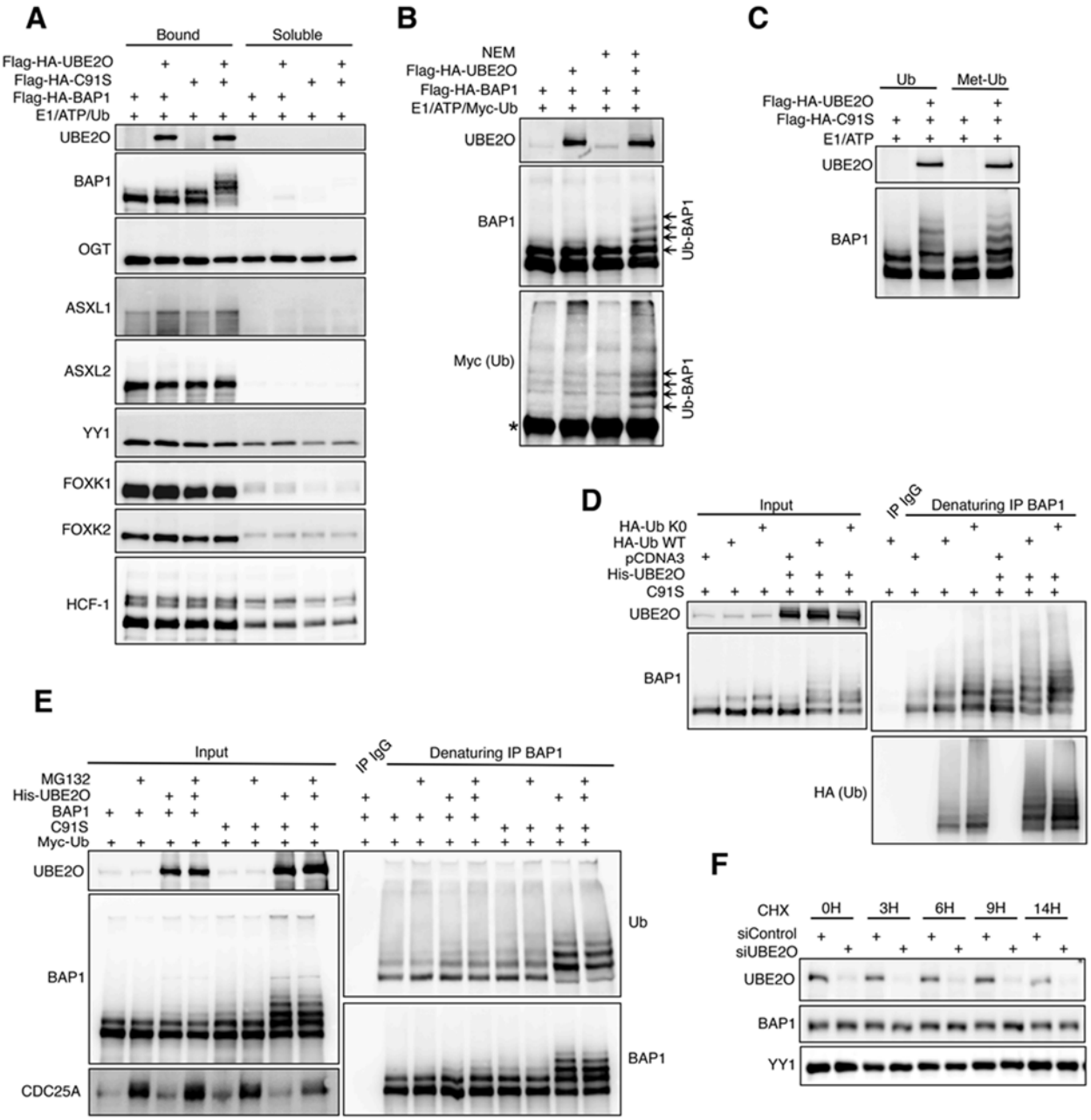

Figure 2. Characterization of UBE2O mediated ubiquitination of BAP1. (See also Figure S2).
A) In vitro ubiquitination reaction with beads-immobilized BAP1 or C91S complexes incubated with immunopurified UBE2O. Fractions were used for western blot detection of components of the BAP1 complex. **B)** In vitro ubiquitination reaction using the BAP1 complex inhibited with NEM. **C)** The C91S complex was used for in vitro reaction with UBE2O and either unmodified or methylated ubiquitin. **D)** 293T cells were co-transfected with 2 µg of wild type ubiquitin or K0 mutant ubiquitin, 1 µg of BAP1 or C91S and 2 µg of empty vector or His-UBE2O expression vectors, and cell lysates were used for immunoprecipitation. **E)** 293T cells were co-transfected with 1 µg of HA-Ub, 2 µg of BAP1 or C91S and 1 µg of His-UBE2O expression vectors. Cells were treated with DMSO or 20 µM MG132 for 8 hours before immunoprecipitation. **F)** MCF7 cells were transfected with non-targeting or UBE2O siRNA for 96 hours, treated with 20 µg/ml of cycloheximide and analyzed by western blot. *indicates non-specific bands.

BAP1 possesses a complex NLS region (Figure S3D,E). We designed a set of BAP1 NLS mutants in the C91S background to render the ubiquitination analysis more sensitive. We found that both C91SΔ688-716 and C91SΔ711-729 mutants were unable to bind and to be ubiquitinated by UBE2O (Figure 3E). Therefore, the NLS region that includes the RRR (aa 699-701) site, the hydrophobic GVSIGRL patch (aa 703-709) as well as the basic amino acid stretch RRKRSRPYKAKRQ (aa 717-729) is required for binding and ubiquitination by UBE2O. The region of basic amino acids RRKRSR (aa 717-722) is strictly required for binding and ubiquitination by UBE2O (Figures 3E, Figure S3F-G). Thus, multiple determinants of this composite and highly conserved NLS are required for UBE2O-mediated ubiquitination of BAP1 (Figure S3H).

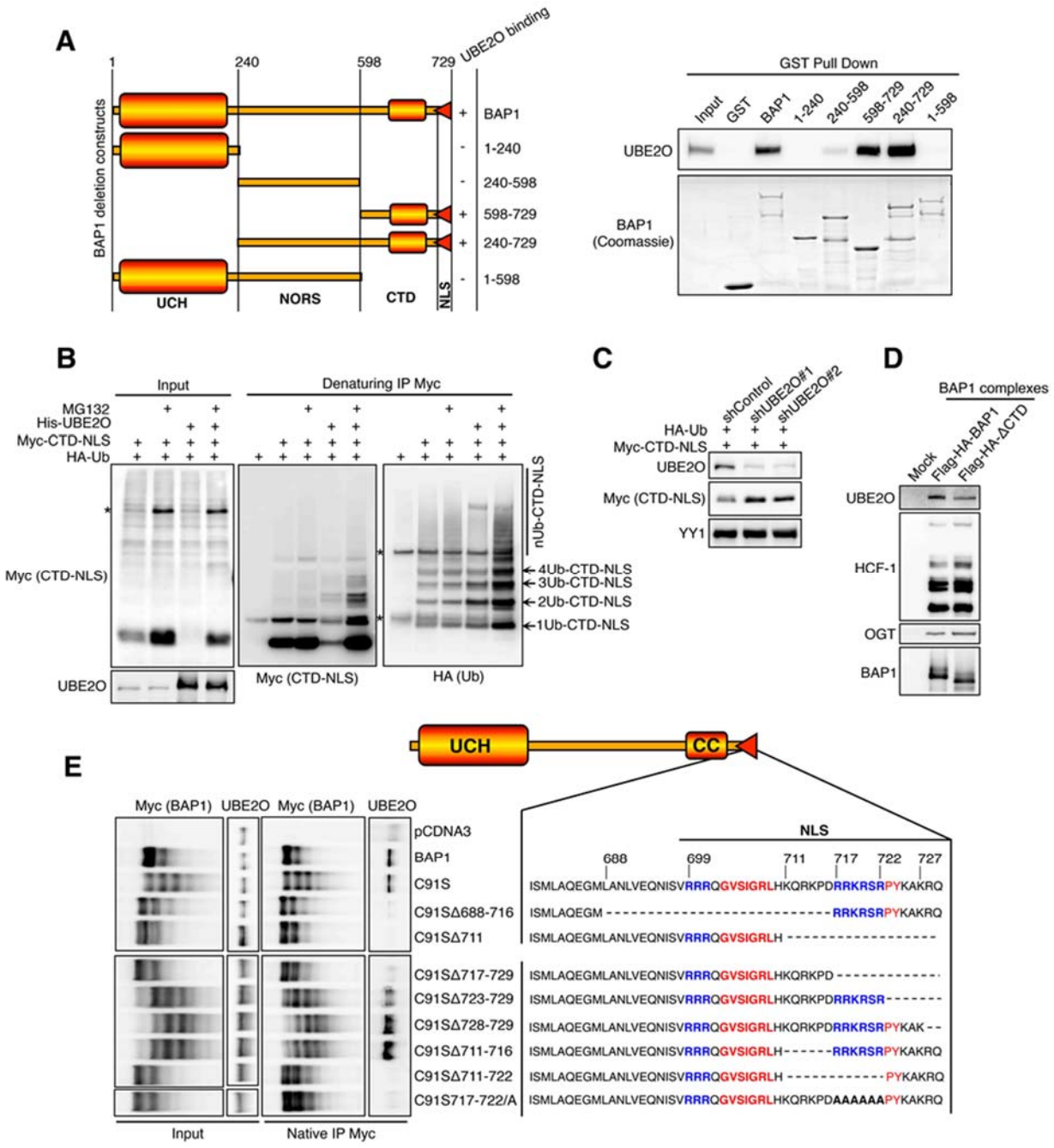

Figure 3. BAP1 NLS is required for its ubiquitination by UBE2O. (See also Figure S3).
A) Schematic representation of GST-BAP1 fragments used for pull-down assay with His-UBE2O. **B)** 293T cells were co-transfected with 2 µg of HA-Ub, 2 µg of His-UBE2O, and 1 µg of Myc-CTD-NLS expression vectors, and cell extracts were used for immunoprecipitation. **C)** U2OS cells were co-transfected with 2 µg of shControl, shUBE2O#1 or shUBE2O#2 and 1 µg of HA-Ub and 0,5 µg of Myc-CTD-NLS expression vectors, and cell extracts were used for western blot. **D)** Purified complexes of BAP1 or BAP1 ΔCTD were used for western blot detection of components of BAP1 complex. **E)** 293T cells were co-transfected with 2 µg of HA-Ub, 2 µg of His-UBE2O, and 1 µg of Myc-BAP1 mutants expression vectors, and cell extracts were used for immunoprecipitation. * indicates non-specific bands.

UBE2O ubiquitinates the NLS of BAP1 and regulates its subcellular localization

To identify the UBE2O ubiquitination sites on BAP1, we performed an anti-Flag affinity purification of C91S co-transfected with ubiquitin and UBE2O (Figure 4A). MS peptide analysis revealed 14 unique ubiquitination sites in BAP1, 9 of which were detected more than once (Figure 4B). Analysis of all ubiquitination events revealed that 50 % are located in the area of NLS, which represents only 4 % of the protein. Next, we introduced a series of lysine to arginine mutations in the CTD-NLS region (12 K/R) or in the NLS alone (5 K/R) of C91S (Figure 4C). Mutation of all lysine sites in the CTD-NLS (12 K/R) strongly reduced C91S ubiquitination; moreover, mutation of lysines in the NLS (5 K/R) region had an identical effect on C91S ubiquitination compared with the 12 K/R mutant. Interestingly, the binding of UBE2O to either mutants of C91S was unchanged indicating that K/R mutations do not significantly affect UBE2O binding affinity. Taken together, these results indicate that UBE2O ubiquitinates primarily the NLS of BAP1.

Ubiquitination was reported to promote nuclear export of proteins (Groulx and Lee, 2002; Li et al., 2003). Therefore, we evaluated whether the ubiquitination of BAP1 affects its subcellular localization. BAP1 is prominently nuclear, but displayed strong cytoplasmic staining when co-expressed with UBE2O. This effect depends on the catalytic activity of UBE2O. Notably, the effect of UBE2O on the C91S mutant was more pronounced with almost all cells showing cytoplasmic or nucleo-cytoplasmic localization (Figure 4D). In addition, the C91S mutant usually displayed a more pronounced cytoplasmic localization compared to the wild type BAP1. Of note, overexpression of UBE2O, but not its catalytic dead form, also promoted cytoplasmic localization of endogenous BAP1 (Figure S4). To probe whether this effect is due to its inability to deubiquitinate its NLS, we compared the nuclear localization of BAP1 and C91S (5 K/R) mutants (Figure 4E). Remarkably, the K/R mutation rescued the C91S mutant from the cytoplasmic sequestration, thus supporting the notion that NLS auto-deubiquitination is involved in the regulation of BAP1 nuclear import/export.

Intramolecular interaction in BAP1 is required for efficient NLS auto-deubiquitination

UCH37 is highly similar to BAP1 and its crystal structure suggests that an intramolecular interaction occurs between the UCH and the CTD (Figure S5A) (Burgie et al., 2011). Since catalytically dead UCH37 C88A is also strongly ubiquitinated by an unknown E3 ligase (Figure S5B), we reasoned that both BAP1 and UCH37 might use their respective CTD regions for

interaction with the UCH domain (Figure S5C). Examination of CTD and UCH flanking sequences of BAP1 revealed putative coiled coil motifs that can engage in intramolecular interactions (Figure S4D). Next, we used the crystal structure of UCH37 to generate a superimposed model of BAP1 (Figure 5A). This model suggests that the CTD region (containing the CC2) forms an interaction interface with the CC1 and the UCH domain. We note that this model cannot predict the structure of the NLS and NORS regions, which are not present in UCH37. To validate our computational prediction, we designed a series of deletion mutants in the N- terminus of BAP1 including the UCH domain alone and a larger fragment that includes CC1 (UCH-CC1) (Figure 5B). Co-IP between the fragments revealed that both UCH and UCH-CC1 interact with CTD-NLS (Figure 5C). To test whether this interaction can promote deubiquitination of CTD-NLS, we took advantage of the earlier observation that CTD-NLS can be degraded as a result of ubiquitination by UBE2O. We designed a complementation/rescue system in which the degradation of CTD-NLS would be counteracted by the N-terminus of BAP1. Indeed, the degradation of CTD-NLS was efficiently rescued only by UCH-CC1 but not by UCH alone, and this was dependent on the catalytic activity of BAP1 (Figure 5D). This suggests that despite direct CC2/UCH interaction, the CC1/CC2 interface plays an important role in NLS deubiquitination. To further test the requirement of the CC1/CC2 in the context of the full-length protein, CC1 and CTD deletion mutants were used (Figure 5B). Deletion of the CTD (ΔCTD) or CC2 (ΔCC2) almost completely blocked the auto-deubiquitination activity of BAP1 despite the presence of a catalytically proficient UCH domain (Figure 5E). The CC1 deletion mutant had a less pronounced auto-deubiquitination defect consistent with the fact that CC2 interacts with both CC1 and UCH. To test whether the deficiency in the ability of BAP1 to auto-deubiquitinate the NLS affects its localization, cell lines stably expressing the wild type or mutants BAP1 were generated. IF analysis revealed that the wild type BAP1 displayed a typical nuclear localization, whereas the ΔCTD and ΔCC2 mutants had a stronger cytoplasmic localization similar to the C91S mutant (Figure 5J). Notably the ΔHBM mutant displayed normal localization similar to wild type BAP1. Thus BAP1 auto-deubiquitination depends on an intramolecular binding between CC2 and UCH-CC1 and is important to counteract the E3 ligase activity of UBE2O towards the NLS.

BAP1 NLS auto-deubiquitination is disrupted by cancer-associated mutations of CTD

Our results suggest that disruption of auto-deubiquitination leads to improper BAP1 localization. We thus searched for cancer mutations in BAP1 that may target the UCH-CC1 interaction interface with CC2. We first tested G13V and F660A mutations and none had a noticeable effect on BAP1 auto-deubiquitination (Figure S5E,F). Next, we considered two small in frame deletions of CC2 (ΔE631-A634 and ΔK637-C638InsN) (Harbour et al., 2010) (Figure 5B). We conducted complex purification of BAP1, ΔE631-A634 and ΔK637-C638InsN, and strikingly observed in both mutants an intense band around 230 kDa that corresponds to UBE2O (Figure 5F). Other major components of the complex such as OGT and HCF-1 showed no apparent differences (Figure 5F). The CC2 directly interacts with UCH, so mutations in this region may interfere with the catalytic activity of BAP1. To test this, we used an *in vitro* deubiquitination assay using a BAP1 natural substrate, i.e., the nucleosomal histone H2A ubiquitinated at position K119 (Figure S5G, H, I). The activities of both cancer mutants were very similar to BAP1, whereas the control C91S failed to deubiquitinate H2A (Figure 5G).

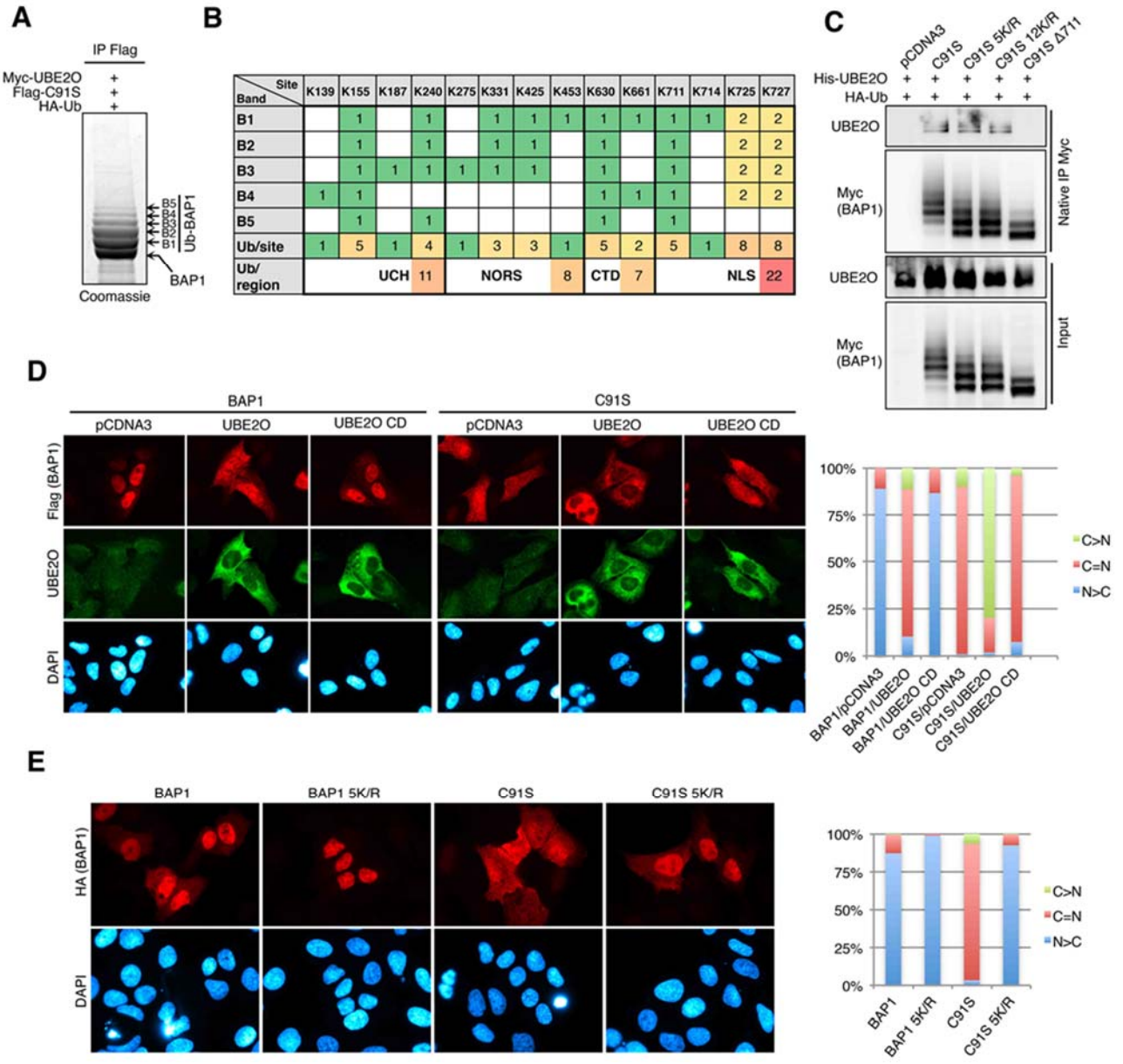

Figure 4. Ubiquitination of BAP1 NLS by UBE2O promotes its cytoplasmic sequestration. (See also Figure S4). **A)** 293T cells were co-transfected with 2 µg of HA-Ub, 2 µg of Myc-UBE2O, and 1 µg of Flag-C91S, and cell extracts were used for Flag immunoprecipitation. The indicated bands were excised for MS analysis. **B)** Table of ubiquitination events detected by MS. **C)** Cells were co-transfected with 2 µg of HA-Ub, 2 µg of His-UBE2O, and 1 µg of Myc-tagged BAP1 mutants expression vectors, and cell extracts were used for immunoprecipitation. **D)** U2OS cells were co-transfected with either 2 µg of empty vector, Myc-UBE2O or Myc-UBE2O CD and 3 µg of either Flag-HA-BAP1 or Flag-HA-C91S expression vectors and were used for immunofluorescence analysis. Representative cell counts for BAP1 subcellular localization are shown. C, cytoplasmic; N, Nuclear. **E)** U2OS cells were transfected with Flag-HA-BAP1 mutants expression vectors and used for immunofluorescence analysis in panel **D**.

Next, to evaluate whether these cancer mutations affect the auto-deubiquitination activity of BAP1, we exploited the UCH/CTD rescue system and the ability of UBE2O to promote degradation of the BAP1 CTD-NLS. We cloned the CTD-NLS region of ΔK637-C638InsN mutant, and a mutant with a large internal deletion in CC2 (Δ636-655) as a control (Figure 5B). Remarkably, complementation with UCH-CC1 rescued the wild type CTD-NLS, but not the ΔK637-C638InsN and Δ635-655 (Figure 5H). Next, we sought to investigate these mutations in the context of the full-length protein. The effect of UBE2O on the cancer mutants was almost as dramatic as on the C91S despite their catalytic proficiency (Figure 5I). Finally, ΔE631-A634 and ΔK637-C638InsN mutants displayed increased cytoplasmic localization similar to the C91S mutant (Figure 5J).

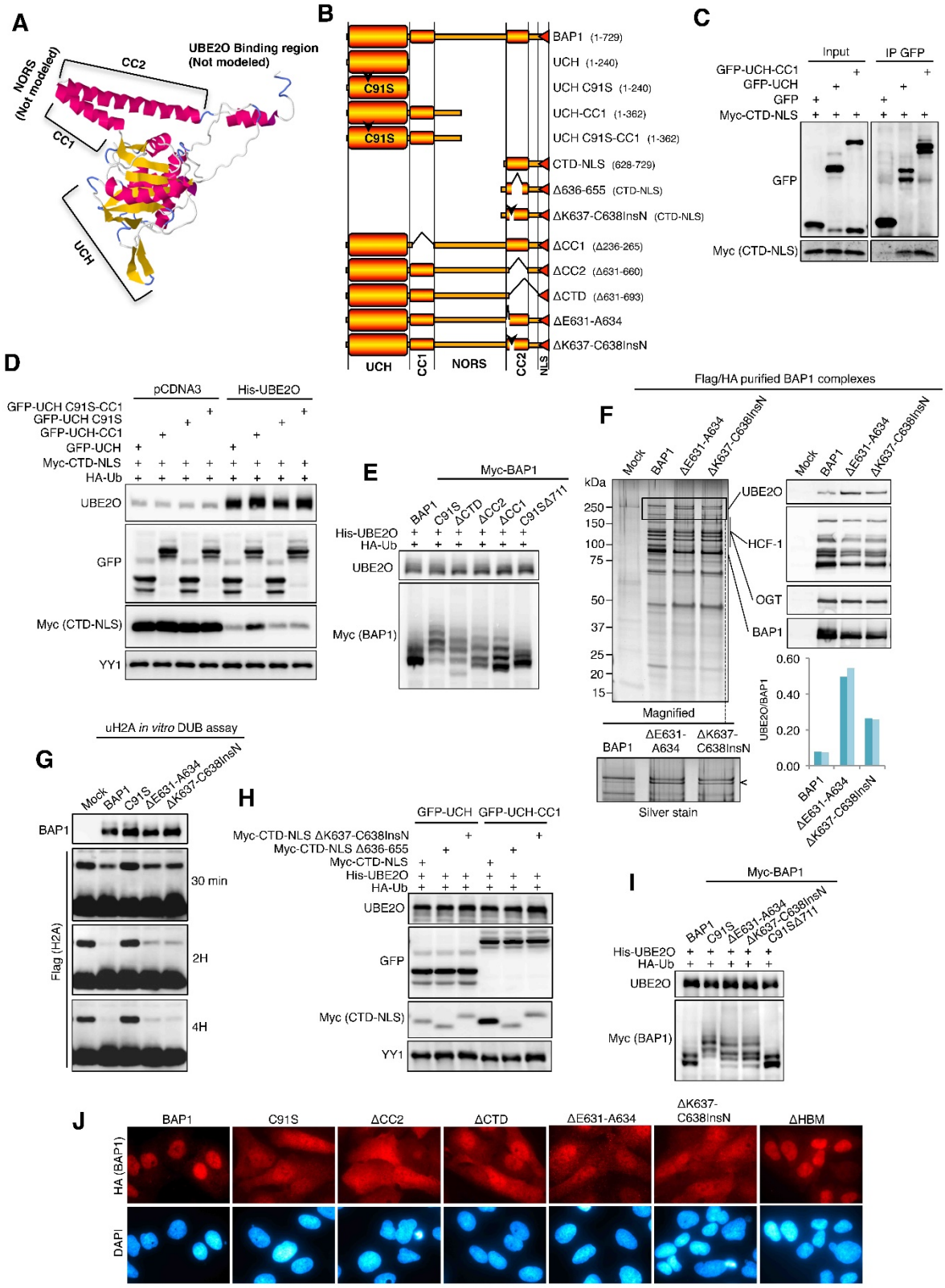

Figure 5. BAP1 intramolecular interaction promotes auto-deubiquitination, a mechanism disrupted by cancer mutations. (See also Figure S5). A) Predicted model of BAP1 UCH/CTD interface based on UCH37 crystal structure (PDB: 3IHR). Note that NLS and NORS are not present in UCH37, and thus not included in the model. **B)** Schematic

representation of the mutants used for the complementation assay and the deletion mutants used in the context of full length BAP1. **C)** 293T cells were co-transfected with 2 µg of the indicated GFP fusion constructs and 2 µg of Myc-CTD-NLS expression vectors, and cell extracts were used for immunoprecipitation. **D)** 293T cells were co-transfected with 2 µg of HA-Ub and either 2 µg of empty vector or His-UBE2O, 1 µg of the indicated GFP fusion constructs and 1 µg of Myc-CTD-NLS expression vectors. **E)** 293T cells were co-transfected with 2 µg of HA-Ub, 2 µg of His-UBE2O, and 1 µg of Myc-BAP1 mutants expression vectors. **F**) Purified BAP1 complexes were analyzed by silver stain and western blotting. Densitometric ratios between UBE2O and BAP1 indicate its relative abundance in the complexes. The histogram shows two independent experiments. **G)** *In vitro* nucleosome deubiquitination reaction with purified BAP1 complexes. Samples were incubated at 37°C for the indicated times. **H)** 293T cells were co-transfected with 2 µg of HA-Ub, 2 µg of His-UBE2O expression vectors, 1 µg of indicated GFP fusion constructs and 1 µg of Myc-tagged constructs. **I)** 293T cells were co-transfected with 2 µg of HA-Ub, 2 µg of His-UBE2O, and 1 µg of Myc-tagged BAP1 mutants expression vectors. **J)** U2OS cell lines stably expressing Flag-HA-BAP1 and its mutant forms were used for immunofluorescence analysis.

UBE2O is regulated by active nucleo-cytoplasmic transport mechanisms and promotes BAP1 cytoplasmic localization during adipocyte differentiation

UBE2O possesses two functional NLS motifs, but the full-length enzyme displayed predominant cytoplasmic localization (Figure S6A-E). Next, purification of UBE2O-associated proteins followed by MS analysis revealed numerous components of the nuclear import/export machinery as well as several kinases that might coordinate its nuclear trafficking (Figure S6F). Taking into account that UBE2O is a heavily phosphorylated enzyme (Figure S6G), we sought to determine the impact of kinase inhibition on UBE2O localization. We treated cells with a panel of kinase inhibitors of various specificities and observed a nuclear translocation of UBE2O with the CDK-inhibitors Purvalanol A and RO-3306 (Figure 6A,B). Interestingly, UBE2O catalytic dead form was strongly retained in the nucleus indicating the importance of catalytic activity in coordinating its nucleo-cytoplasmic transport. Consistent with its potential role in negatively regulating BAP1 function, siRNA-depletion of UBE2O increased cell proliferation whereas siRNA-depletion of BAP1 resulted in decreased cell proliferation (Figure 6C). Of note, no noticeable changes in UBE2O or BAP1 localization were observed in unperturbed cycling cells (Data not shown), suggesting that only very limited pools of UBE2O or BAP1 might be imported or exported respectively. Taking into account that BAP1 tightly coordinate cell proliferation, we reasoned that a substantial change in BAP1 localization might be observed during permanent cell cycle exit. Since UBE2O was implicated in promoting adipocyte differentiation in the mouse embryo cell line C3H10T1/2, we recapitulated this effect using the 3T3-L1 cellular model of adipocyte differentiation as determined by immunoblotting for aP2 and Perilipin (PLIN) adipogenic markers and Oil Red O staining (Figure 6D,E). Significantly, a fraction of BAP1 become excluded from the nucleus as 3T3-L1 cells differentiate into adipocytes (Figure 6F). In

addition, mutation of the UBE2O-ubiquitination sites in BAP1 resulted in a substantial retention of this DUB in the nucleus. Since BAP1 5K/R mutant still interact with UBE2O and is ubiquitinated on other sites, we also replaced the NLS region of BAP1, containing the UBE2O-interacting motif, with T-large antigen NLS which prominently prevented the cytoplasmic localization of this DUB during differentiation.

UBE2O targets a subset of bipartite NLS-containing transcription regulators

UBE2O displays prominent UBC-dependent auto-catalytic activity *in vitro* and *in vivo* (Figure 7A and Figure 1C), which is inhibited by PAO (Figure S2B, Figure 7A). In addition, a nuclear retention of UBE2O, more pronounced for the catalytic dead form was observed following treatment with CDK inhibitors (Figure 6A,B). Thus, we sought to determine if NLS sequences within UBE2O may constitute auto-ubiquitination sites. Strikingly the NLS1/A mutant was completely auto-ubiquitination-deficient similar to UBE2O CD, whereas mutation of NLS2 had no significant effect on UBE2O auto-ubiquitination (Figure S6A, Figure 7B). In addition, the bipartite NLS regions of UBE2O and BAP1 contain a highly conserved patch of aliphatic hydrophobic amino acids (VLI patch) between the minor and major NLS sites (linker region) (Figure 7C). Mutation of the VLI patch disrupted auto-ubiquitination (Figure S7A). Of note, the NLS1 architecture is highly conserved between most UBE2O orthologs (Figure S6E). These results prompted us to search whether this subtype of bipartite NLS may serve as a specific signal for UBE2O recognition and ubiquitination in other proteins. Several candidates were identified, notably chromatin-associated proteins, suggesting that UBE2O might exert extensive control over nuclear signaling pathways (Figure S7F). We selected four proteins, i.e., p400, CDT1, INO80 and CXXC1, predicted as potential UBE2O substrates. INO80 and p400 are members of SWI/SNF family of chromatin-remodeling ATPases (Jin et al., 2005; Vassilev et al., 1998) containing the predicted NLS sequences (Figure 7C). CXXC1 is the CpG island binding protein and component of the SET1 complex (Lee and Skalnik, 2005) that contains two predicted NLS sequences with NLS2 containing the putative UBE2O binding motif.

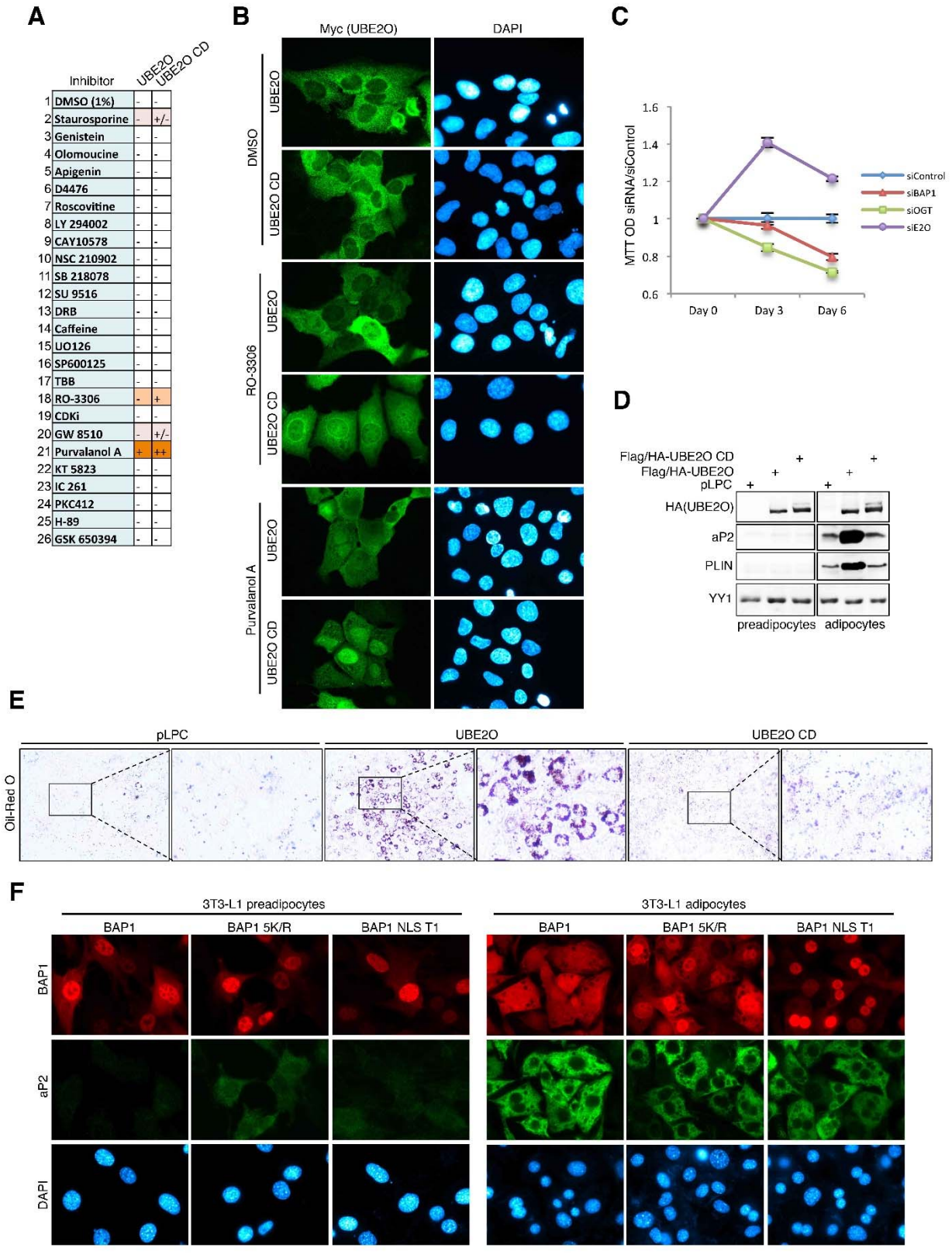
A
Inhibitor
UBE2O
UBE2O CD
1 DMSO (1%) - -
2 Staurosporine - +/-
3 Genistein - -
4 Olomoucine - -
5 Apigenin - -
6 D4476 - -
7 Roscovitine - -
8 LY 294002 - -
9 CAY10578 - -
10 NSC 210902 - -
11 SB 218078 - -
12 SU 9516 - -
13 DRB - -
14 Caffeine - -
15 UO126 - -
16 SP600125 - -
17 TBB - -
18 RO-3306 - +
19 CDKi - -
20 GW 8510 - +/-
21 Purvalanol A + ++
22 KT 5823 - -
23 IC 261 - -
24 PKC412 - -
25 H-89 - -
26 GSK 650394 - -
B
Myc (UBE2O)
DAPI
DMSO
RO-3306
Purvalanol A
UBE2O
UBE2O CD
C
MTT OD siRNA/siControl
1.6
1.4
1.2
1
0.8
0.6
Day 0
Day 3
Day 6
siControl
siBAP1
siOGT
siE2O
D
Flag/HA-UBE2O CD
Flag/HA-UBE2O
pLPC
HA(UBE2O)
aP2
PLIN
YY1
preadipocytes
adipocytes
E
pLPC
UBE2O
UBE2O CD
Oil-Red O
F
3T3-L1 preadipocytes
3T3-L1 adipocytes
BAP1
BAP1 5K/R
BAP1 NLS T1
aP2
DAPI

Figure 6. UBE2O shuttles between the nucleus and cytoplasm and promotes BAP1 cytoplasmic localization during adipocyte differentiation. (See also Figure S6). A) Effect of kinase inhibition on nuclear localization of UBE2O. U2OS cells were transfected with 4 µg Myc-UBE2O or Myc-UBE2O CD expression vectors and then treated with a panel of kinase inhibitors for 24 hours prior harvesting for IF. + and - Indicate the relative intensity in the nuclear staining of UBE2O. **B)** Representative images of UBE2O localization in U2OS cells treated with CDK inhibitors. **C**) Effects of siRNA-depletion of UBE2O, BAP1 on cell proliferation, determined by MTT assay. siRNA for OGT is used as a control of decreased proliferation. Note that the values are relative to the non-target control siRNA for each time point. **D,E)** Effects of overexpression of UBE2O wild type or catalytic dead form on the differentiation of 3T3L1. Immunodetection of differentiation markers (E) and Oil-Red O staining (F). YY1 is used as a loading control. **F)** Localization of BAP1 and mutants during adipocyte differentiation. The BAP1 NLST1 corresponds to a mutant in which the NLS region of BAP1 which includes the UBE2O-binding motif is replaced with the T large antigen NLS. The BAP1 K/R mutant is mutated in the UBE2O-ubiquitination sites of the NLS.

The DNA replication factor CDT1 also harbors a potential binding and ubiquitination site for UBE2O (Nishitani et al., 2000). INO80, p400 and CDT1 were degraded following co-expression with UBE2O in a catalytic-activity dependent manner, ostensibly as a result of ubiquitin chain extension by unknown E3 ligases (Figure 7D, Figure S7B). CXXC1 showed several slow migrating bands suggesting its ubiquitination without degradation (Figure 7D, right panel). Next, we selected INO80 and CXXC1 as two contrasting examples of UBE2O action for further characterization of their ubiquitination by UBE2O (Figure 7D). When the immunoprecipitated INO80 was loaded in equal amounts, the ubiquitin blot showed a typical polyubiquitin smear in the stacking gel (Figure 7D, left panel). The ubiquitination profile of CXXC1 was similar to that of BAP1 and UBE2O with several distinct multi-mono-ubiquitin bands (Figure 7D, right panel). Ubiquitination of INO80 and CXXC1 by UBE2O had a pronounced effect on their subcellular localization, as both proteins displayed stronger cytoplasmic localization following co-expression of wild type but not UBE2O CD mutant (Figure 7E). We also found a potential UBE2O binding consensus in ALC1, another nuclear SWI/SNF family chromatin-remodeling enzyme (Ahel et al., 2009), but UBE2O had no effect on ALC1 ubiquitination and localization (Figure S7C,D,E). This can be explained by the absence of the major NLS stretch in the vicinity of the consensus and/or the location of the consensus in the masked fold of its Macro domain. Therefore, UBE2O targets a subset of chromatin remodeling and modifying factors containing a bipartite NLS with a specific VLI patch in the linker region with the exception of CDT1, which contains the major NLS stretch upstream of the UBE2O consensus. Thus, substrate ubiquitination by UBE2O can induce cytoplasmic localization, which might be accompanied by further proteasomal degradation as a consequence of ubiquitin chain extension by other E3 ligases.

Discussion

Regulation of BAP1 by UBE2O-mediated ubiquitination

Here, we define a regulatory mechanism involving the E2/E3 hybrid UBE2O which multi-mono-ubiquitinates BAP1 in the NLS region. Under normal growth conditions, BAP1 is predominantly nuclear whereas UBE2O is mainly cytoplasmic suggesting that BAP1 ubiquitination is highly regulated. In particular, this compartmentalization raises the question regarding the cellular compartment where the ubiquitination actually occurs. UBE2O could be imported into the nucleus to ubiquitinate BAP1 and promote its ubiquitin-mediated nuclear export as observed for other proteins (Groulx and Lee, 2002; Li et al., 2003). Since we did not observe a noticeable accumulation of endogenous UBE2O in the nucleus, it is possible that only a small fraction of UBE2O is imported into this compartiment at any given time. Controling UBE2O import itself would provide another level of regulation for the fine-tuning of BAP1 ubiquitination. Indeed, (i) BAP1 and UBE2O exert antagonistic functions during cell proliferation, (ii) CDK inhibitors promoted UBE2O nuclear localization with a stronger effect towards its catalytic dead form, (iii) UBE2O exhibits an auto-ubiquitination activity towards its own NLS, and (iv) two recent studies revealed that the K521 residue (K516 in mouse), part of UBE2O NLS1, is ubiquitinated *in vivo* (Figure S6G)**.** Our data do not exclude the possibility that, under specific conditions, BAP1 might be exported to the cytoplasm prior to its ubiquitination, although we did not identify any export signal in BAP1. Further studies are needed to dissect the possible mechanisms of UBE2O nucleocytoplasmic transport including its regulation.

On the other hand, since ubiquitination of BAP1 is counteracted by auto-deubiquitination, one can predict that a yet to be identified signal is needed to inactivate BAP1 catalytic activity. This initiating event would render this DUB susceptible to ubiquitination by UBE2O. BAP1 could be modified by other post-translational modifications that inhibit its auto-deubiquitination. In fact, several phosphorylation and ubiquitination sites of BAP1 were identified in proteomics studies (Figure S6H), and in this study we identified several ubiquitination sites on UCH, some of which might result from the action of other E3 ligases. Under normal cell growth conditions, UBE2O-mediated ubiquitination of BAP1 might not necessarily lead to a net accumulation of BAP1 in the cytoplasm, since this could be a protracted process that is concomitant with both *de novo* synthesis of BAP1 and further degradation or re-import of this DUB. We speculate that this could be an

editing mechanism that might coordinate the transcriptional competency of BAP1. In contrast, during adipocyte differentiation, we observed a net cytoplasmic redistribution BAP1 that would drastically impact its transcriptional activity. It is also possible that BAP1 might exert cytoplasmic functions in terminally differentiated adipocytes. We note that, since our conclusion is based on ectopically expressed BAP1, further work is needed to establish this regulation for the endogenous enzyme and to provide insights into the possible concerted action of post-translational modifications in regulating the trafficking and function of this DUB.

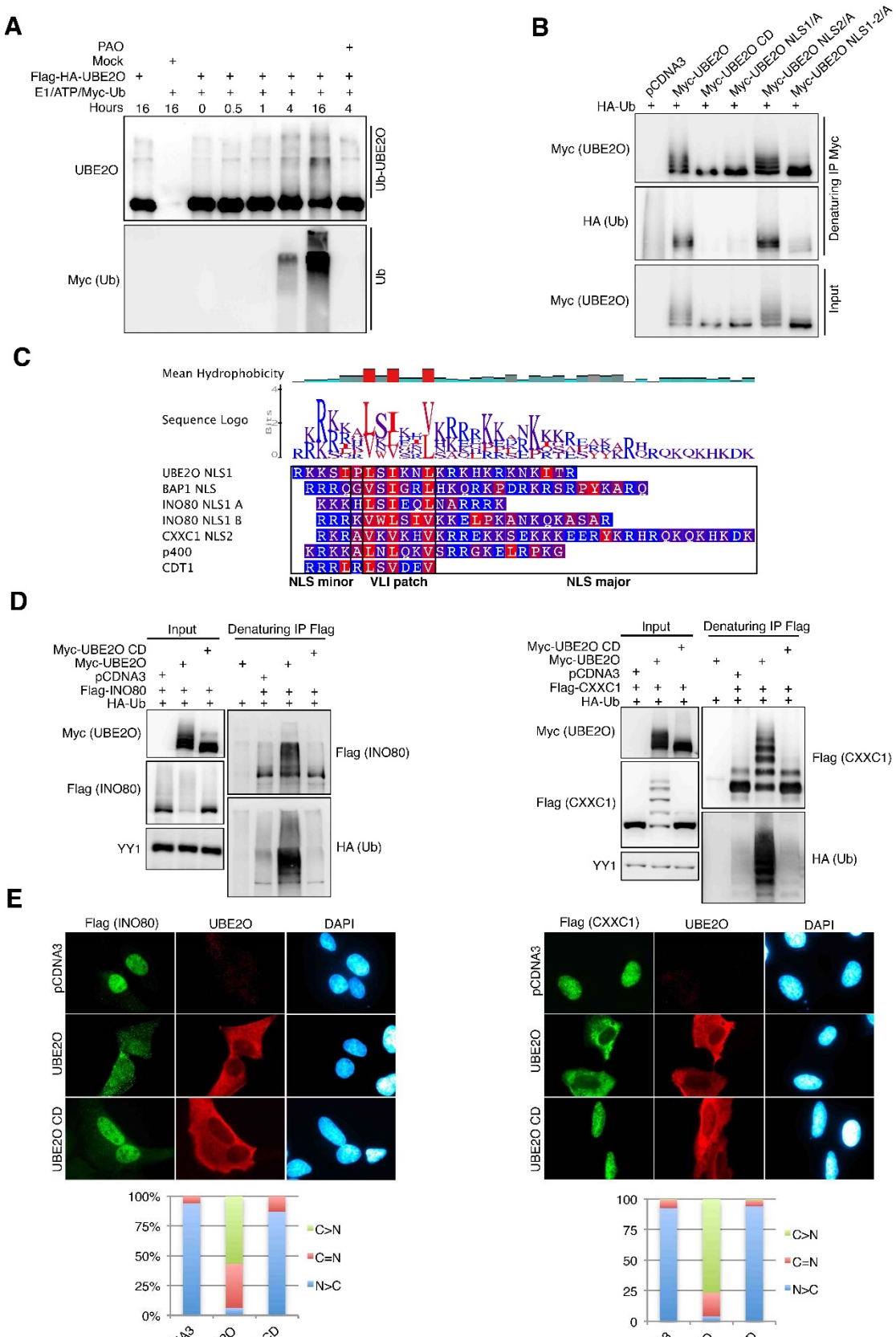
A
PAO
Mock
Flag-HA-UBE2O
E1/ATP/Myc-Ub
Hours 16 16 0 0.5 1 4 16 4
UBE2O
Myc (Ub)
Ub-UBE2O
Ub
B
pCDNA3
Myc-UBE2O
Myc-UBE2O CD
Myc-UBE2O NLS1/A
Myc-UBE2O NLS2/A
Myc-UBE2O NLS1-2/A
HA-Ub
Myc (UBE2O)
HA (Ub)
Myc (UBE2O)
Denaturing IP Myc
Input
C
Mean Hydrophobicity
Sequence Logo
Bits
UBE2O NLS1
BAP1 NLS
INO80 NLS1 A
INO80 NLS1 B
CXXC1 NLS2
p400
CDT1
RKKSIPLSIKNLKRKHKRKNKITR
RRRQGVSIGRLHKQRKPDRKRSRPYKARQ
KKKHLSIEQLNARRRK
RRRKVWLSIVKKELPKANKQKASAR
RKRAVKVKHVKRREKKSEKKKEERYKRHRQKQKHKDK
KRKKALNLQKVSRRGKELRPKG
RRRLRLSVDEV
NLS minor
VLI patch
NLS major
D
Input
Denaturing IP Flag
Myc-UBE2O CD
Myc-UBE2O
pCDNA3
Flag-INO80
Flag-CXXC1
HA-Ub
Myc (UBE2O)
Flag (INO80)
YY1
HA (Ub)
Flag (CXXC1)
E
Flag (INO80)
UBE2O
DAPI
Flag (CXXC1)
pCDNA3
UBE2O
UBE2O CD
100%
75%
50%
25%
0%
C>N
C=N
N>C
INO80/pCDNA3
INO80/UBE2O
INO80/UBE2O CD
100
75
50
25
0
CXXC1/pCDNA3
CXXC1/UBE2O
CXXC1/UBE2O CD

Figure 7. UBE2O targets a subset of chromatin-associated proteins. (See also Figure S7). A) *In vitro* ubiquitination reaction with the purified UBE2O. Samples were incubated for the indicated times. **B)** 293T cells were co-transfected with 2 µg of HA-Ub and 2 µg of indicated Myc-UBE2O mutants, and cell extracts were used for immunoprecipitation. **C)** Sequence alignment between the UBE2O/BAP1 NLS and a subset of identified UBE2O substrates. Hydrophobic amino acids are in red and polar amino acids are in blue. A large N-terminal extension containing the NLS of CDT1 is not shown. **D)** 293T cells were co-transfected with 2 µg of HA-Ub and 1 µg of Flag-CXXC1 or 2 µg of Flag-INO80, and either 2 µg of empty vector, Myc-UBE2O or Myc-UBE2O CD expression vectors, and cell extracts were used for immunoprecipitation. **E)** U2OS cells were co-transfected with 0,5 µg of HA-Ub and either 1 µg of empty vector, Myc-UBE2O, Myc-UBE2O CD and 1 µg of either Flag-INO80 or Flag-CXXC1 expression vectors and used for immunofluorescence analysis. Representative cell counts are shown.

Auto-deubiquitination of BAP1 and its disruption in cancer

Auto-deubiquitination of DUBs was previously observed for UCH-L1, which was able to counteract its own ubiquitination by an unknown E3 ligase (Meray and Lansbury, 2007). Interestingly, in our study, we noticed a similar mechanism regulating UCH37. We also note that UCH37 and BAP1 share a common ancestry. Although vertebrate BAP1 acquired the long NORS region, which contains the HCF-1 interaction motif, the intramolecular interaction between the amino and carboxy termini seems to be evolutionary conserved. It is possible that DUB auto-deubiquitination might constitute a regulatory mechanism, which is more widely used than currently appreciated.

Cancer-associated mutations in BAP1 disrupt its function by multiple means. Large deletions in the BAP1 gene result in dysfunctional proteins. Point mutations in the UCH domain of BAP1 often target the catalytic site or its immediate environment resulting in disruption of catalytic activity. The cancer-derived mutations of BAP1 in the catalytic site are predicted to impact both auto-deubiquitination as well as DUB activity towards other substrates. Histone H2A is a substrate of BAP1 (Scheuermann et al., 2010; Yu et al., 2014), and other substrates such as HCF-1 and OGT were previously also described (Machida et al., 2009; Misaghi et al., 2009; Ruan et al., 2012). In this study, we identified two cancer-mutations in the coiled-coil motif of the C-terminal region that remarkably did not compromise BAP1 complex assembly, but instead promoted UBE2O association with this DUB. It would be interesting to further determine whether this is a result of structural changes in BAP1 that facilitate UBE2O binding, or rather is a consequence of increased cytoplasmic sequestration of BAP1. Importantly, the two cancer-derived mutations selectively compromised the auto-deubiquitination activity of BAP1 without affecting its H2A DUB activity. These cancer-derived mutations also revealed that auto-deubiquitination function of the enzyme is important for its proper nuclear localization. Thus, by separating the two

activities of BAP1, we provide a biochemical paradigm for testing the involvement of other ubiquitin signaling cascades in regulating BAP1 function.

UBE2O acts as an atypical E2/E3 that ubiquitinates a subset of NLS-containing proteins

The evolution of protein conjugation pathways can be traced back to prokaryotic and archea cells. In eukaryotes, this system diversified resulting in establishment of the classical E1/E2/E3/substrate ubiquitin transfer cascade (Burroughs et al., 2012; Hochstrasser, 2009). UBE2O is highly conserved in plants and animals suggesting that it evolved from a common ancestor at least 1.6 billion years ago, when the prototypic animal and plant cell types were evolving (Meyerowitz, 2002). UBE2O seems to employ the properties of both E2 and E3 enzymes suggesting that it might recognize a limited number of substrates. In our study, we discovered that UBE2O specifically binds and ubiquitinates a subset of bipartite NLS that contain a VLI patch in their linker. Based on the consensus between two identified UBE2O substrates, i.e. BAP1 and UBE2O itself, we were able to predict the substrate specificity of the enzyme in turn allowing us to identify more putative UBE2O substrates including proteins involved in RNA processing, transcription, DNA replication, and chromatin remodelling. Thus, UBE2O might be involved in coordinating major signaling pathways in the cytoplasm, organelles, and nucleus that orchestrate cell function during proliferation and differentiation or in response to extracellular stimuli. Although we were able to detect UBE2O expression in multiple cultured cell lines, its expression seems to be highly regulated. UBE2O levels were previously reported to increase during erythroid differentiation (Wefes et al., 1995). Chromatin of differentiating cells is subjected to multiple epigenetic and structural changes, requiring specific ubiquitin signaling pathways to promote the displacement of chromatin-associated regulators to activate or repress gene expression (Geng et al., 2012). Indeed, UBE2O promotes adipocyte differentiation and is also highly expressed in brain, heart, and skeletal muscle (Nagase et al., 2000; Yokota et al., 2001; Zhang et al., 2013a), all of which comprise post-mitotic cells that must finely coordinate gene expression programs to fulfill metabolically demanding requirements.

Materials and methods

Cell culture, transfections and western blot

Cells were cultured according to standard protocols. siRNA and plasmids were transfected using Lipofectamine or PEI. Total cell lysates were used for western blotting. Differentiation of 3T3L1 and additional details are provided in the supplemental text.

Imunoprecipitation of BAP1 and UBE2O

Cell lines stably expressing BAP1, ΔE631-A634, ΔK637-C638InsN, ΔCTD, ΔCC1 or UBE2O were generated following retroviral transduction and used for immunoprecipitation under native or denaturing conditions as indicated in **the supplemental text.**

Glycerol gradient fractionation

Molecular mass fractionation of nuclear extract was conduced using a 10-40 % glycerol gradient as indicated in **the supplemental text.**

In vitro interaction assays

Recombinant GST-BAP1 fusion proteins were purified using glutathione agarose beads and incubated with His-UBE2O. The beads were extensively washed and bound proteins eluted in Laemmli buffer and subjected to western blotting. **Additional details are described in the supplemental text.**

In vitro and in vivo ubiquitination assay

In vitro ubiquitination reactions were conducted using, human recombinant UBE1, BAP1 and UBE2O complexes or bacteria-purified enzymes. **Additional details and Mass spectrometry analysis of ubiquitination sites was done as described in the supplemental text.**

In vitro nucleosome deubiquitination assays

Preparation of chromatin fractions from Flag-H2A transfected 293T cells and digestion with Micrococcal nuclease (MNase) were conducted with modification of the original protocol (Groisman et al., 2003). The procedure is described in the supplemental text.

Immunofluorescence

The procedure was carried out as previously described (Daou et al., 2011) with additional details provided in the supplemental text.

Protein sequence analysis, and structure modeling

Protein sequences were analyzed using Geneious 6.1.2 created by Biomatters, available from http://www.geneious.com. Other bioinformatics tools are described in the supplemental text.

Acknowledgments

We thank Elliot Drobetsky, Eric Milot, Dindial Ramotar and Hugo Wurtele for the critical reading of the manuscript. We thank Diana Adjaoud for technical assistance. This work was supported by grants from the Canadian Institute of Health Research (CIHR) to EBA (MOP115132) and MT (MOP-93654). EBA is a scholar of the CIHR and Le Fonds de la Recherche en Santé du Québec. MT holds a Tier 1 Canada Research Chair in Intracellular Signaling. NM was supported by a PhD scholarship from the Fonds Québécois de la Recherche sur la Nature et les Technologies. The authors would like to dedicate this paper to the memory of Cecile M. Pickart for her original work that guided us to demonstrate that UBE2O is indeed an E2/E3 hybrid.

References

Ahel, D., Horejsi, Z., Wiechens, N., Polo, S.E., Garcia-Wilson, E., Ahel, I., Flynn, H., Skehel, M., West, S.C., Jackson, S.P*., et al.* (2009). Poly(ADP-ribose)-dependent regulation of DNA repair by the chromatin remodeling enzyme ALC1. Science *325*, 1240-1243.

Berleth, E.S., and Pickart, C.M. (1996). Mechanism of ubiquitin conjugating enzyme E2-230K: catalysis involving a thiol relay? Biochemistry *35*, 1664-1671.

Burgie, S.E., Bingman, C.A., Soni, A.B., and Phillips, G.N., Jr. (2011). Structural characterization of human Uch37. Proteins.

Burroughs, A.M., Iyer, L.M., and Aravind, L. (2012). The natural history of ubiquitin and ubiquitin-related domains. Frontiers in bioscience : a journal and virtual library *17*, 1433-1460.

Carbone, M., Yang, H., Pass, H.I., Krausz, T., Testa, J.R., and Gaudino, G. (2013). BAP1 and cancer. Nature reviews. Cancer *13*, 153-159.

Daou, S., Mashtalir, N., Hammond-Martel, I., Pak, H., Yu, H., Sui, G., Vogel, J.L., Kristie, T.M., and Affar el, B. (2011). Crosstalk between O-GlcNAcylation and proteolytic cleavage regulates the host cell factor-1 maturation pathway. Proceedings of the National Academy of Sciences of the United States of America *108*, 2747-2752.

Dey, A., Seshasayee, D., Noubade, R., French, D.M., Liu, J., Chaurushiya, M.S., Kirkpatrick, D.S., Pham, V.C., Lill, J.R., Bakalarski, C.E*., et al.* (2012). Loss of the tumor suppressor BAP1 causes myeloid transformation. Science *337*, 1541-1546.

Geng, F., Wenzel, S., and Tansey, W.P. (2012). Ubiquitin and proteasomes in transcription. Annual review of biochemistry *81*, 177-201.

Groisman, R., Polanowska, J., Kuraoka, I., Sawada, J., Saijo, M., Drapkin, R., Kisselev, A.F., Tanaka, K., and Nakatani, Y. (2003). The ubiquitin ligase activity in the DDB2 and CSA complexes is differentially regulated by the COP9 signalosome in response to DNA damage. Cell *113*, 357-367.

Groulx, I., and Lee, S. (2002). Oxygen-dependent ubiquitination and degradation of hypoxia-inducible factor requires nuclear-cytoplasmic trafficking of the von Hippel-Lindau tumor suppressor protein. Molecular and cellular biology *22*, 5319-5336.

Hammond-Martel, I., Yu, H., and Affar el, B. (2012). Roles of ubiquitin signaling in transcription regulation. Cellular signalling *24*, 410-421.

Hao, Y.H., Doyle, J.M., Ramanathan, S., Gomez, T.S., Jia, D., Xu, M., Chen, Z.J., Billadeau, D.D., Rosen, M.K., and Potts, P.R. (2013). Regulation of WASH-Dependent Actin Polymerization and Protein Trafficking by Ubiquitination. Cell *152*, 1051-1064.

Harbour, J.W., Onken, M.D., Roberson, E.D., Duan, S., Cao, L., Worley, L.A., Council, M.L., Matatall, K.A., Helms, C., and Bowcock, A.M. (2010). Frequent mutation of BAP1 in metastasizing uveal melanomas. Science *330*, 1410-1413.

Hochstrasser, M. (2009). Origin and function of ubiquitin-like proteins. Nature *458*, 422-429.
Jackson, S.P., and Durocher, D. (2013). Regulation of DNA Damage Responses by Ubiquitin and SUMO. Molecular cell *49*, 795-807.

Jin, J., Cai, Y., Yao, T., Gottschalk, A.J., Florens, L., Swanson, S.K., Gutierrez, J.L., Coleman, M.K., Workman, J.L., Mushegian, A.*, et al.* (2005). A mammalian chromatin remodeling complex with similarities to the yeast INO80 complex. The Journal of biological chemistry *280*, 41207-41212.

Klemperer, N.S., Berleth, E.S., and Pickart, C.M. (1989). A novel, arsenite-sensitive E2 of the ubiquitin pathway: purification and properties. Biochemistry *28*, 6035-6041.

Lanzuolo, C., and Orlando, V. (2012). Memories from the polycomb group proteins. Annual review of genetics *46*, 561-589.

Lee, J.H., and Skalnik, D.G. (2005). CpG-binding protein (CXXC finger protein 1) is a component of the mammalian Set1 histone H3-Lys4 methyltransferase complex, the analogue of the yeast Set1/COMPASS complex. The Journal of biological chemistry *280*, 41725-41731.

Li, M., Brooks, C.L., Wu-Baer, F., Chen, D., Baer, R., and Gu, W. (2003). Mono- versus polyubiquitination: differential control of p53 fate by Mdm2. Science *302*, 1972-1975.

Machida, Y.J., Machida, Y., Vashisht, A.A., Wohlschlegel, J.A., and Dutta, A. (2009). The deubiquitinating enzyme BAP1 regulates cell growth via interaction with HCF-1. The Journal of biological chemistry *284*, 34179-34188.

Meray, R.K., and Lansbury, P.T., Jr. (2007). Reversible monoubiquitination regulates the Parkinson disease-associated ubiquitin hydrolase UCH-L1. The Journal of biological chemistry *282*, 10567-10575.

Meyerowitz, E.M. (2002). Plants compared to animals: the broadest comparative study of development. Science *295*, 1482-1485.

Misaghi, S., Ottosen, S., Izrael-Tomasevic, A., Arnott, D., Lamkanfi, M., Lee, J., Liu, J., O'Rourke, K., Dixit, V.M., and Wilson, A.C. (2009). Association of C-terminal ubiquitin hydrolase BRCA1-associated protein 1 with cell cycle regulator host cell factor 1. Molecular and cellular biology *29*, 2181-2192.

Nagase, T., Kikuno, R., Hattori, A., Kondo, Y., Okumura, K., and Ohara, O. (2000). Prediction of the coding sequences of unidentified human genes. XIX. The complete sequences of 100 new cDNA clones from brain which code for large proteins in vitro. DNA research : an international journal for rapid publication of reports on genes and genomes *7*, 347-355.

Nishitani, H., Lygerou, Z., Nishimoto, T., and Nurse, P. (2000). The Cdt1 protein is required to license DNA for replication in fission yeast. Nature *404*, 625-628.

Ruan, H.B., Han, X., Li, M.D., Singh, J.P., Qian, K., Azarhoush, S., Zhao, L., Bennett, A.M., Samuel, V.T., Wu, J.*, et al.* (2012). O-GlcNAc transferase/host cell factor C1 complex regulates gluconeogenesis by modulating PGC-1alpha stability. Cell metabolism *16*, 226-237.

Scheuermann, J.C., de Ayala Alonso, A.G., Oktaba, K., Ly-Hartig, N., McGinty, R.K., Fraterman, S., Wilm, M., Muir, T.W., and Muller, J. (2010). Histone H2A deubiquitinase activity of the Polycomb repressive complex PR-DUB. Nature *465*, 243-247.

Shabek, N., Herman-Bachinsky, Y., Buchsbaum, S., Lewinson, O., Haj-Yahya, M., Hejjaoui, M., Lashuel, H.A., Sommer, T., Brik, A., and Ciechanover, A. (2012). The size of the proteasomal substrate determines whether its degradation will be mediated by mono- or polyubiquitylation. Molecular cell *48*, 87-97.

Sowa, M.E., Bennett, E.J., Gygi, S.P., and Harper, J.W. (2009). Defining the human deubiquitinating enzyme interaction landscape. Cell *138*, 389-403.

van Wijk, S.J., and Timmers, H.T. (2010). The family of ubiquitin-conjugating enzymes (E2s): deciding between life and death of proteins. FASEB journal : official publication of the Federation of American Societies for Experimental Biology *24*, 981-993.

Vassilev, A., Yamauchi, J., Kotani, T., Prives, C., Avantaggiati, M.L., Qin, J., and Nakatani, Y. (1998). The 400 kDa subunit of the PCAF histone acetylase complex belongs to the ATM superfamily. Molecular cell *2*, 869-875.

Ventii, K.H., Devi, N.S., Friedrich, K.L., Chernova, T.A., Tighiouart, M., Van Meir, E.G., and Wilkinson, K.D. (2008). BRCA1-associated protein-1 is a tumor suppressor that requires deubiquitinating activity and nuclear localization. Cancer research *68*, 6953-6962.

Wefes, I., Mastrandrea, L.D., Haldeman, M., Koury, S.T., Tamburlin, J., Pickart, C.M., and Finley, D. (1995). Induction of ubiquitin-conjugating enzymes during terminal erythroid differentiation. Proceedings of the National Academy of Sciences of the United States of America *92*, 4982-4986.

Yokota, T., Nagai, H., Harada, H., Mine, N., Terada, Y., Fujiwara, H., Yabe, A., Miyazaki, K., and Emi, M. (2001). Identification, tissue expression, and chromosomal position of a novel gene encoding human ubiquitin-conjugating enzyme E2-230k. Gene *267*, 95-100.

Yu, H., Mashtalir, N., Daou, S., Hammond-Martel, I., Ross, J., Sui, G., Hart, G.W., Rauscher, F.J., 3rd, Drobetsky, E., Milot, E.*, et al.* (2010). The ubiquitin carboxyl hydrolase BAP1 forms a ternary complex with YY1 and HCF-1 and is a critical regulator of gene expression. Molecular and cellular biology *30*, 5071-5085.

Yu, H., Pak, H., Hammond-Martel, I., Ghram, M., Rodrigue, A., Daou, S., Barbour, H., Corbeil, L., Hebert, J., Drobetsky, E.*, et al.* (2014). Tumor suppressor and deubiquitinase BAP1 promotes DNA double-strand break repair. Proceedings of the National Academy of Sciences of the United States of America *111*, 285-290.

Zhang, X., Zhang, J., Bauer, A., Zhang, L., Selinger, D.W., Lu, C.X., and Ten Dijke, P. (2013a). Fine-tuning BMP7 signalling in adipogenesis by UBE2O/E2-230K-mediated monoubiquitination of SMAD6. The EMBO journal *32*, 996-1007.

Zhang, X., Zhang, J., Zhang, L., van Dam, H., and Ten Dijke, P. (2013b). UBE2O negatively regulates TRAF6-mediated NF-kappaB activation by inhibiting TRAF6 polyubiquitination. Cell research *23*, 366-377.

Supplemental information inventory

Figure S1. Related to Figure 1.

Contains the initial characterization of the UBE2O-independent BAP1 monoubiquitination, the comparison of UBE2O with other E2s, the *in vivo* ubiquitination controls for UBE2O specificity and UBE2O sequence conservation.

Figure S2. Related to Figure 2.

Contains schema of the protein purifications, the *in vitro* ubiquitination reactions and characterization of the effects of other E3 ligases on UBE2O-mediated ubiquitination of BAP1.

Figure S3. Related to Figure 3.

Contains the information about the degradation of CTD-NLS, the characterization of BAP1 NLS, the alanine mutagenesis screen in BAP1 NLS and the alignment of NLS regions of BAP1 orthologs.

Figure S4. Related to Figure 4.

Contains immunostaining of UBE2O overexpression and its effects on the localization of endogenous BAP1, YY1 and HCF-1.

Figure S5. Related to Figure 5.

Contains the characterization of UCH37 in respect to its auto-deubiquitination activity, the alignment of UCH37 and BAP1 C-terminal regions, crystal structure of UCH37, the characterization of the effect of the G13V mutation on BAP1 auto-deubiquitination activity and the establishment of the *in vitro* H2A DUB assay on nucleosomes.

Figure S6. Related to Figure 6.

Contains the mapping and characterization of UBE2O NLS regions, purification of UBE2O-associated proteins and schema of UBE2O and BAP1 post-translational modifications.

Figure S7. Related to Figure 7.

Contains the effects of the mutation in the VLI patch which disrupts UBE2O auto-catalytic activity, the effects of UBE2O on the degradation of p400 and CDT1 following expression of UBE2O, the characterization of the predicted UBE2O substrate ALC1 which tested negative for UBE2O-mediated ubiquitination and the list of the predicted UBE2O nuclear substrates based on the *[KR][KR][KR]-X(1,3)-[VLI]-X-[VLI]-X-X-[VLI]* consensus.

Supplemental Figures

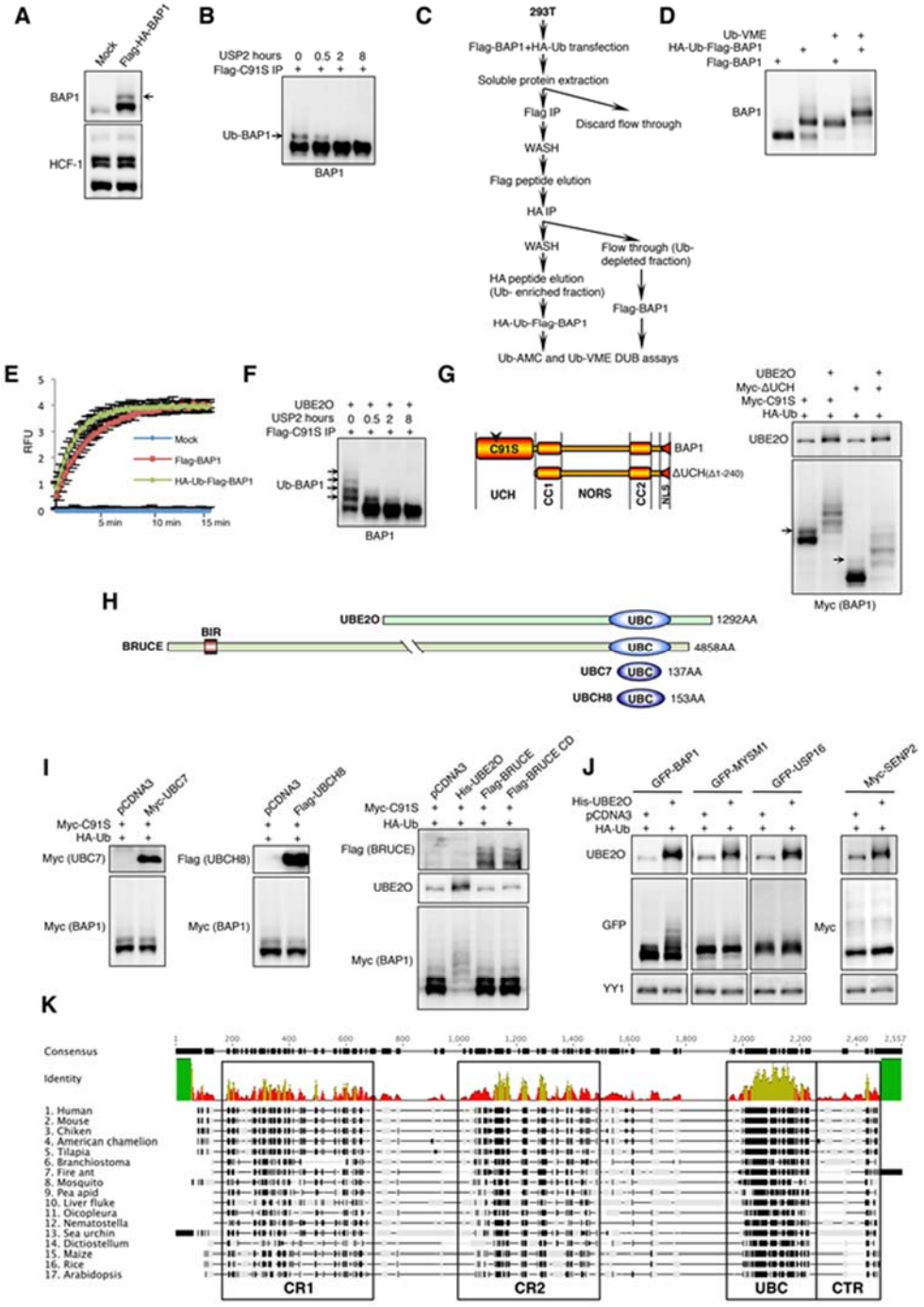

Figure S1 (Related to Figure 1).
Characterization of the UBE2O-independent mono-ubiquitination of BAP1.
A) Detection of the modified form of BAP1 in U2OS cells stably expressing Flag-HA-BAP1. U2OS cells were transduced with empty pOZ-N vector or pOZ-N-BAP1, selected with anti-IL2 receptor-coupled magnetic beads (4 rounds of selection), as previously described (Yu et al., 2010), and cell lysates were subjected to western blotting with the indicated antibodies. **B)** 293T cells were transfected with 3 µg of Flag-BAP1 C91S and harvested three days-post-transfection for immunoprecipitation. Anti-Flag column-purified C91S was incubated with 200 nM of recombinant USP2 catalytic domain and collected for western blotting at the indicated time points. Note the decrease of the constitutive ubiquitin modification. **C)** Schema of the double column purification strategy of ubiquitin-depleted and -enriched fractions of BAP1. **D)** Analysis of the anti-HA beads-bound and the flow through fractions revealed that the slower migrating band was enriched in the HA-bound fraction and depleted in the flow through fraction proving the monoubiquitination nature of the modification. Monoubiquitination of BAP1 does not influence its ability to incorporate the ubiquitin vinylmethylester (Ub-VME) suicide substrate. HA-Ub-Flag-BAP1 and unmodified Flag-BAP1 fractions where incubated with 1 µM of Ub-VME probe and analyzed by western blot as recently described (Yu et al., 2014). Note the similar efficiency of Ub-VME incorporation that corresponds to the slower migrating form of BAP1. **E)** Fluorometric analysis of the BAP1 activity towards the Ub-AMC DUB substrate. Adjusted amounts of the HA-Ub-Flag-BAP1 and unmodified Flag-BAP1 fractions where incubated with 100 nM of the Ub-AMC and fluorescence was analyzed in real time. Data are represented as mean +/- SD. Note that the modified form of BAP1 displays a similar DUB activity as the modified form towards this model substrate. **F)** The ubiquitinated forms of C91S can be efficiently deubiquitinated by USP2. The procedure was carried out essentially as in panel B except that UBE2O was included in the co-transfection. **G)** Similar UBE2O-mediated multi-mono-ubiquitination of BAP1 C91S or ΔUCH. 293T cells were co-transfected with 1 µg of Myc-C91S or Myc-BAP1 ΔUCH, 2 µg of HA-Ub and 2 µg of either empty vector or UBE2O. Three days later, cell lysates were used for western blotting and probed with the indicated antibodies. Note the decrease of the constitutive BAP1 mono-ubiquitination upon the deletion of the UCH domain indicating that distinct activities modify BAP1.
Characterization of UBE2O specificity towards BAP1.
H) Comparison of several members of class I and IV ubiquitin carrier enzymes. **I)** To control for specificity, we evaluated other E2s (van Wijk and Timmers, 2010) including BRUCE, the closest evolutionary relative of UBE2O which was previously shown to act as an E2/E3 hybrid on other substrates (Bartke et al., 2004; Hao et al., 2004).
293T cells were co-transfected with 1 µg of Myc-C91S, 2 µg of HA-Ub and either 2 µg of empty vector, Myc-UBC7, Flag-UBCH8, 5 µg of Flag-BRUCE or 5 µg Flag-BRUCE CD (C4654S) expression vectors. Three days later, cell lysates were used for western blotting. **J)** We also tested two known H2A DUBs, i.e., USP16 and MYSM1 (Joo et al., 2007; Zhu et al., 2007), as well as the SUMO protease SENP2 (Kim et al., 2000). 293T cells were co-transfected with 2 µg of HA-Ub and either 2 µg of empty vector or 2 µg of His-UBE2O and either 1 µg of GFP-BAP1, GFP-MYSM1, GFP-USP16 or Myc-SENP2 expression vectors. Three days later, cell lysates were used for western blotting. **K)** Multiple sequence alignment of UBE2O orthologs, conserved regions are highlighted.

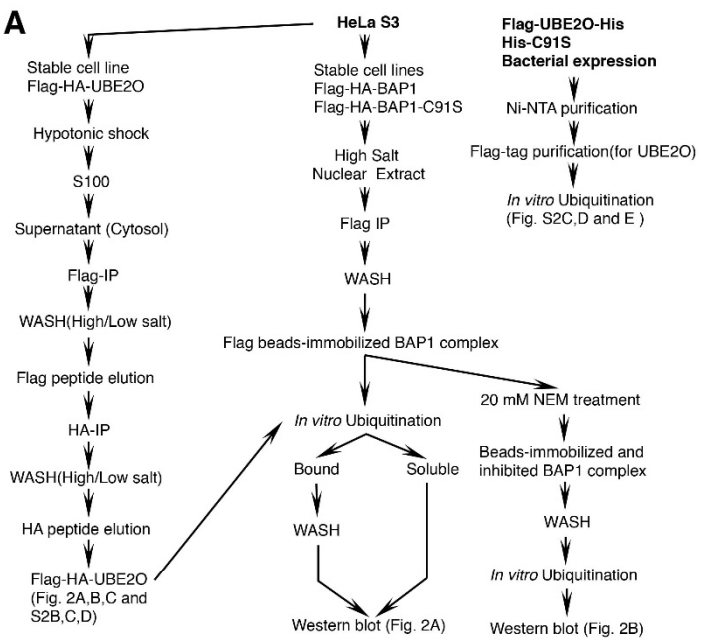

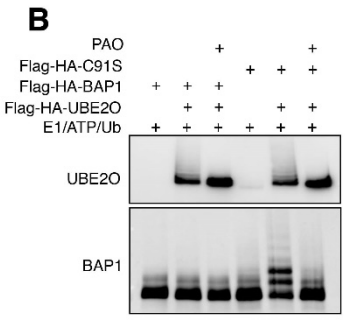

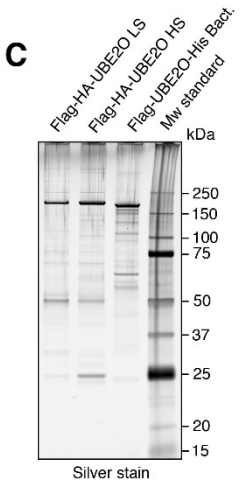

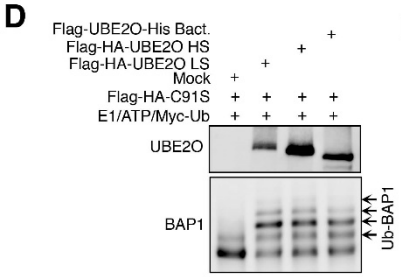

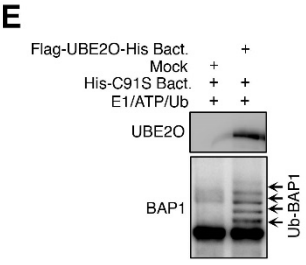

F

UBE2O		BAP1	
this study (MS)	other sources	this study (MS)	other sources
TRIM28 (12 peptides)	**TRIM27**(Markson.,2009; Hao et al., 2013)	**TRIM28** (1 peptide)	**BARD1** (Nishikawa., 2009)
RNF219 (5 peptides)	**RNF10** (Markson., 2009)	**RNF219** (2 peptides)	**BRCA1** (Jensen et al., 1998)
HUWE1 (28 peptides)		**BARD1** (1 peptide)	**HUWE1** (Sowa et al., 2009)

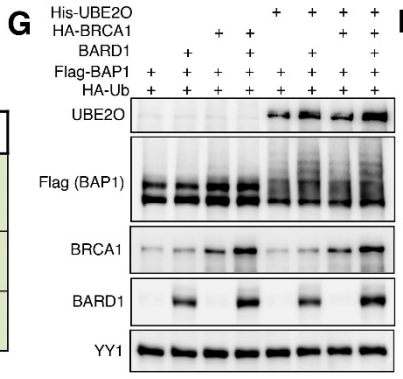

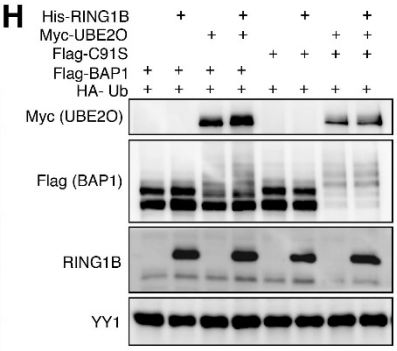

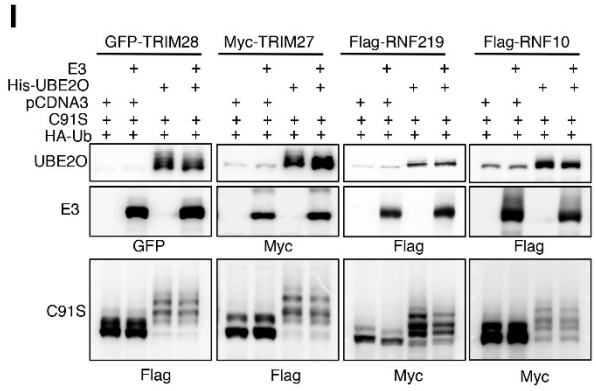

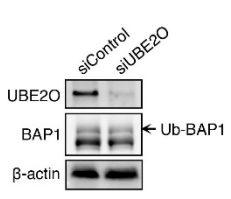

Figure S2 (Related to Figure 2).
Set up of the *in vitro* ubiquitination reaction.
A) Schema of protein purification and *in vitro* ubiquitination reactions for figure 2A, 2B, S2B, S2D and S2E. **B)** Purified BAP1 or C91S complexes were incubated with immunopurified UBE2O in an *in vitro* ubiquitination reaction. Samples were treated with 100 μM PAO as indicated. **C)** Mammalian Flag/HA or bacterial His/Flag purified UBE2O was loaded on a 4-12% gel and used for silver staining. **D)** Purified C91S complexes were incubated with UBE2O, purified from human cells or bacteria, in an *in vitro* ubiquitination reaction. Note that UBE2O maintains similar activity towards C91S independently of its origin and method of purification. HS and LS represent high salt and low salt washes, respectively. **E)** Ubiquitination with recombinant enzymes. His-C91S was purified from bacteria and used for *in vitro* reaction with bacteria purified Flag-UBE2O-His.
UBE2O- and BAP1-interacting ubiquitin ligases do not influence UBE2O ubiquitination activity towards BAP1.
F) Summary of potential UBE2O- and BAP1-interacting ubiquitin ligases. Our purification and mass spectrometry analysis of UBE2O- or BAP1-interacting proteins revealed additional substoichiometric E3 ligases that might participate in UBE2O-dependent or –independent ubiquitination of BAP1. Other E3 ligases previously reported as potential UBE2O- or BAP1-interacting enzymes are also included. **G)** 293T cells were transfected with 2 μg of HA-Ub, 1 μg of HA-BRCA1 and/or 0,5 μg of HA-BARD1, 1 μg of BAP1 and either 2 μg of empty vector or Myc-UBE2O expression vectors. Three days later, cell lysates were used for western blotting with the indicated antibodies. We note that BAP1 was described as a partner of the tumor suppressor and RING E3 ligase complex BRCA1/BARD1 that may perform ubiquitin chain elongation (Jensen et al., 1998; Wu-Baer et al., 2003). Nonetheless co-transfection with BRCA1/BARD1 did not significantly affect the pattern of BAP1 ubiquitination by UBE2O. **H)** Cells were transfected with 2 μg of HA-Ub, 1 μg of His-RING1B, 1 μg of BAP1 or C91S and either 2 μg of empty vector or Myc-UBE2O expression vectors. Three days later, cell lysates were used for western blotting with the indicated antibodies. BAP1 acts in concert with the RING1B E3 ligase to regulate H2A ubiquitination (Carbone et al., 2013; Scheuermann et al., 2010). However, no direct ubiquitination of BAP1 or cooperation between RING1B and UBE2O were observed. **I)** Cells were transfected with 2 μg of HA-Ub, 0.5 μg of C91S, 2 μg of empty vector or His-UBE2O and 3 μg of GFP-TRIM28, Myc-TRIM27, Flag-RNF219 or Flag-RNF10 expression vectors. Three days later, cell lysates were used for western blotting with the indicated antibodies. Note the similar pattern of the C91S ubiquitination independently of the ubiquitin ligase co-expression. We were unable to express significant levels of HUWE1 (~500 kDa). Thus, we did not conclude about its potential effect alone or on UBE2O-mediated ubiquitination of BAP1. **J)** U2OS cell line stably expressing Flag-HA-BAP1 was transfected with control siRNA or siUBE2O. Three days later, cell lysates were used for western blotting with the indicated antibodies. Note that the knockdown of UBE2O has no effect on the constitutive monoubiquitination of BAP1 (described in Figure S1A-E, G).

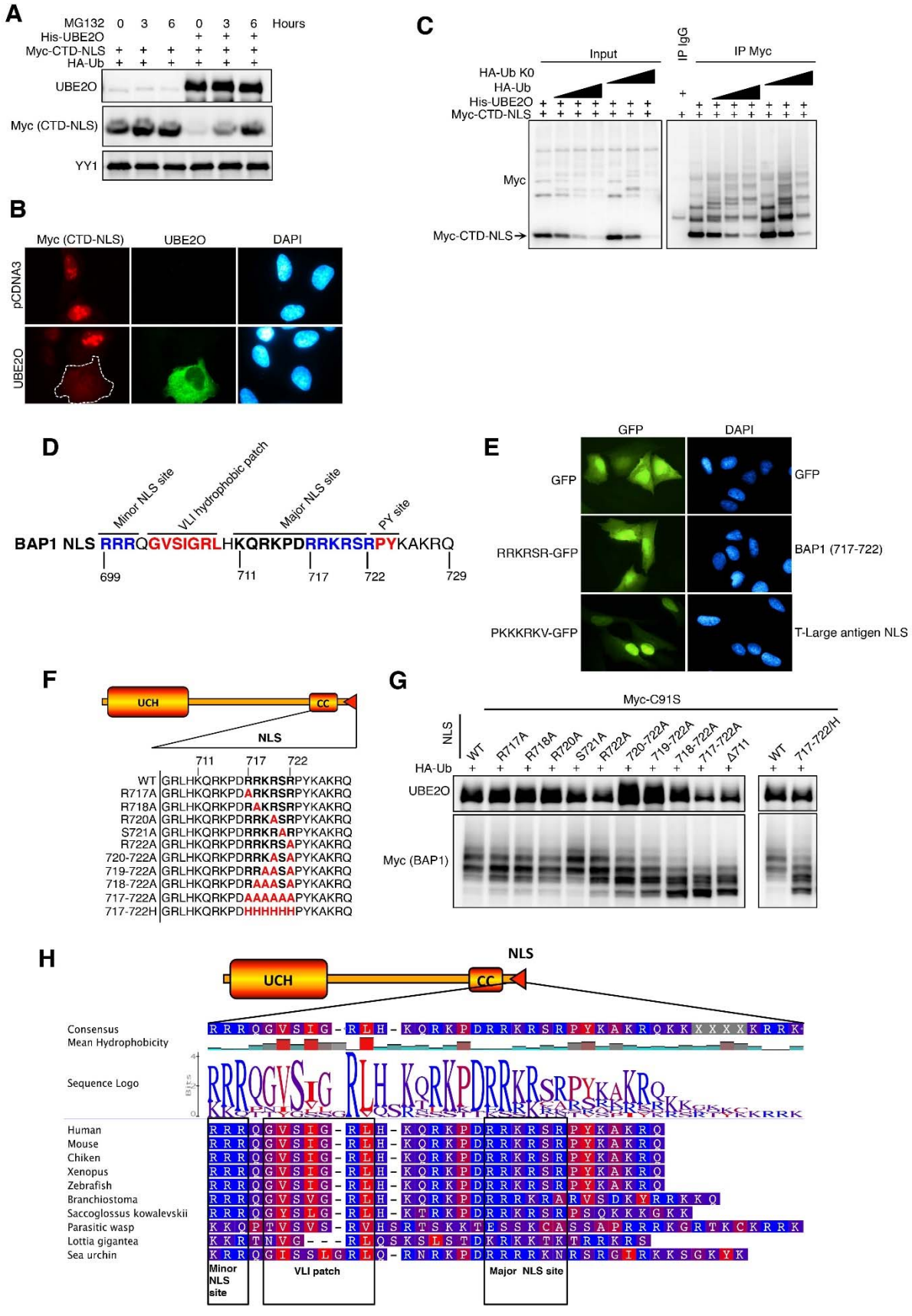
A
MG132 0 3 6 0 3 6 Hours
His-UBE2O
Myc-CTD-NLS
HA-Ub
UBE2O
Myc (CTD-NLS)
YY1
B
Myc (CTD-NLS)
UBE2O
DAPI
pCDNA3
UBE2O
C
Input
IP IgG
IP Myc
HA-Ub K0
HA-Ub
His-UBE2O
Myc-CTD-NLS
Myc
Myc-CTD-NLS
D
Minor NLS site
VLI hydrophobic patch
Major NLS site
PY site
BAP1 NLS RRRQGVSIGRLHKQRKPDRRKRSRPYKAKRQ
699
711
717
722
729
E
GFP
DAPI
GFP
RRKRSR-GFP
PKKKRKV-GFP
BAP1 (717-722)
T-Large antigen NLS
F
UCH
CC
NLS
711 717 722
WT GRLHKQRKPDRRKRSRPYKAKRQ
R717A GRLHKQRKPDARKRSRPYKAKRQ
R718A GRLHKQRKPDRAKRSRPYKAKRQ
R720A GRLHKQRKPDRRKASRPYKAKRQ
S721A GRLHKQRKPDRRKRARPYKAKRQ
R722A GRLHKQRKPDRRKRSAPYKAKRQ
720-722A GRLHKQRKPDRRKASAPYKAKRQ
719-722A GRLHKQRKPDRRAASAPYKAKRQ
718-722A GRLHKQRKPDRAAASAPYKAKRQ
717-722A GRLHKQRKPDAAAAAAPYKAKRQ
717-722H GRLHKQRKPDHHHHHHPYKAKRQ
G
Myc-C91S
NLS
WT R717A R718A R720A S721A R722A 720-722A 719-722A 718-722A 717-722A Δ711
WT 717-722/H
HA-Ub
UBE2O
Myc (BAP1)
H
UCH
CC
NLS
Consensus
Mean Hydrophobicity
Sequence Logo
Bits
Human
Mouse
Chiken
Xenopus
Zebrafish
Branchiostoma
Saccoglossus kowalevskii
Parasitic wasp
Lottia gigantea
Sea urchin
Minor NLS site
VLI patch
Major NLS site

Figure S3 (Related to Figure 3).

UBE2O promotes degradation of BAP1 CTD-NLS.

A) 293T cells were co-transfected with 2 µg of HA-Ub, 2 µg of His-UBE2O, and 1 µg of Myc-CTD-NLS expression vectors. Three days later, cells were treated with 20 µM of MG132 for the indicated time points and harvested for western blotting. **B)** U2OS cells were co-transfected with 0,5 µg of HA-Ub, 1 µg of His-UBE2O and 1 µg of Myc-CTD-NLS expression vectors and plated on coverslips. Three days later, cells were fixed and used for immunofluorescence. **C)** 293T cells were co-transfected with increasing amounts of HA-Ub or HA-Ub K0 (0.5 µg, 1.5 µg or 4 µg), 2 µg of His-UBE2O, and 1 µg of Myc-CTD-NLS expression vectors. Three days later, cells extracts were analyzed by western blotting. Note that UBE2O promotes the Myc-CTD-NLS degradation in ubiquitin-dependent manner, and a similar degradation profile is obtained with either wild type or K0 ubiquitin mutant.

Characterization of the BAP1 NLS region.

D) Representation of the predicted BAP1 NLS. The basic regions are in blue and hydrophobic regions are in red. BAP1 possesses a complex NLS region that shares similarities with classical monopartite (Conti et al., 1998), bipartite (Robbins et al., 1991) and the atypical hydrophobic/basic PY NLS (Lee et al., 2006). **E)** U2OS cells were transfected with 0,5 µg of the indicated GFP fusion NLS. Three days later, cells were fixed and used for fluorescence microscope imaging. The region spanning a short stretch of basic amino acids RRKRSR (aa 717-722) is necessary for proper nuclear localization of BAP1 (Ventii et al., 2008). However, when fused to GFP, this motif was not sufficient to promote nuclear localization, i.e., additional sequences are required for NLS function. Therefore, we considered the entire aa 699-729 region as BAP1 NLS for further characterization.

Requirement of the major NLS site of BAP1 for UBE2O-mediated ubiquitination.

F) Schematic representation of the alanine screen mutants, mutations are indicated in red. **G)** 293T cells were co-transfected with 2 µg of HA-Ub, 2 µg of His-UBE2O, and 1 µg of Myc-C91S mutants expression vectors. Three days later, cell extracts were used for western blotting and probed with the indicated antibodies. Single point mutations in the region did not cause significant reduction of C91S ubiquitination, but cumulative alanine mutations were able to gradually decrease the efficiency of ubiquitination. The substitution of RRKRSR to a similarly positively charged histidine stretch also strongly reduced the ubiquitination by UBE2O indicating that the arginine/lysine residues are critical

Sequence comparison of the NLS region from different BAP1 orthologs.

H) Multiple sequence alignment of the NLS regions of BAP1 from metazoan species using the Geneious tool, polar amino acids are in blue, hydrophobic amino acids are in red.

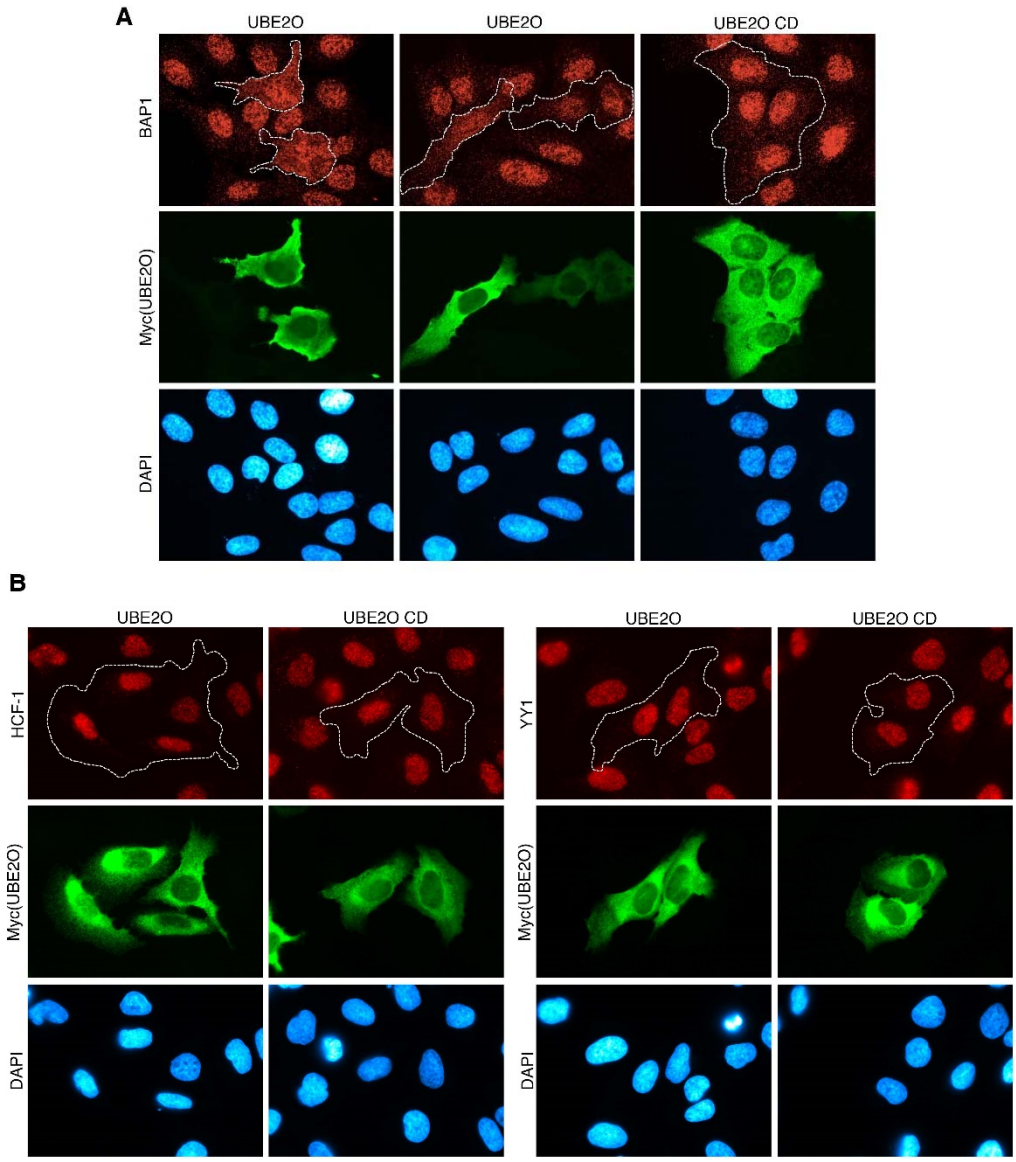

Figure S4 (Related to Figure 4).
Overexpression of UBE2O promotes cytoplasmic localization of endogenous BAP1.
U2OS cells were transfected with 4 µg of the Myc-UBE2O or Myc-UBE2O CD. Three days later, cells were fixed and used for Immunofluorescence for BAP1 **(A)** or HCF-1 and YY1 **(B).** UBE2O promoted cytoplasmic localization of BAP1 but had no visible effect on YY1 and HCF-1.

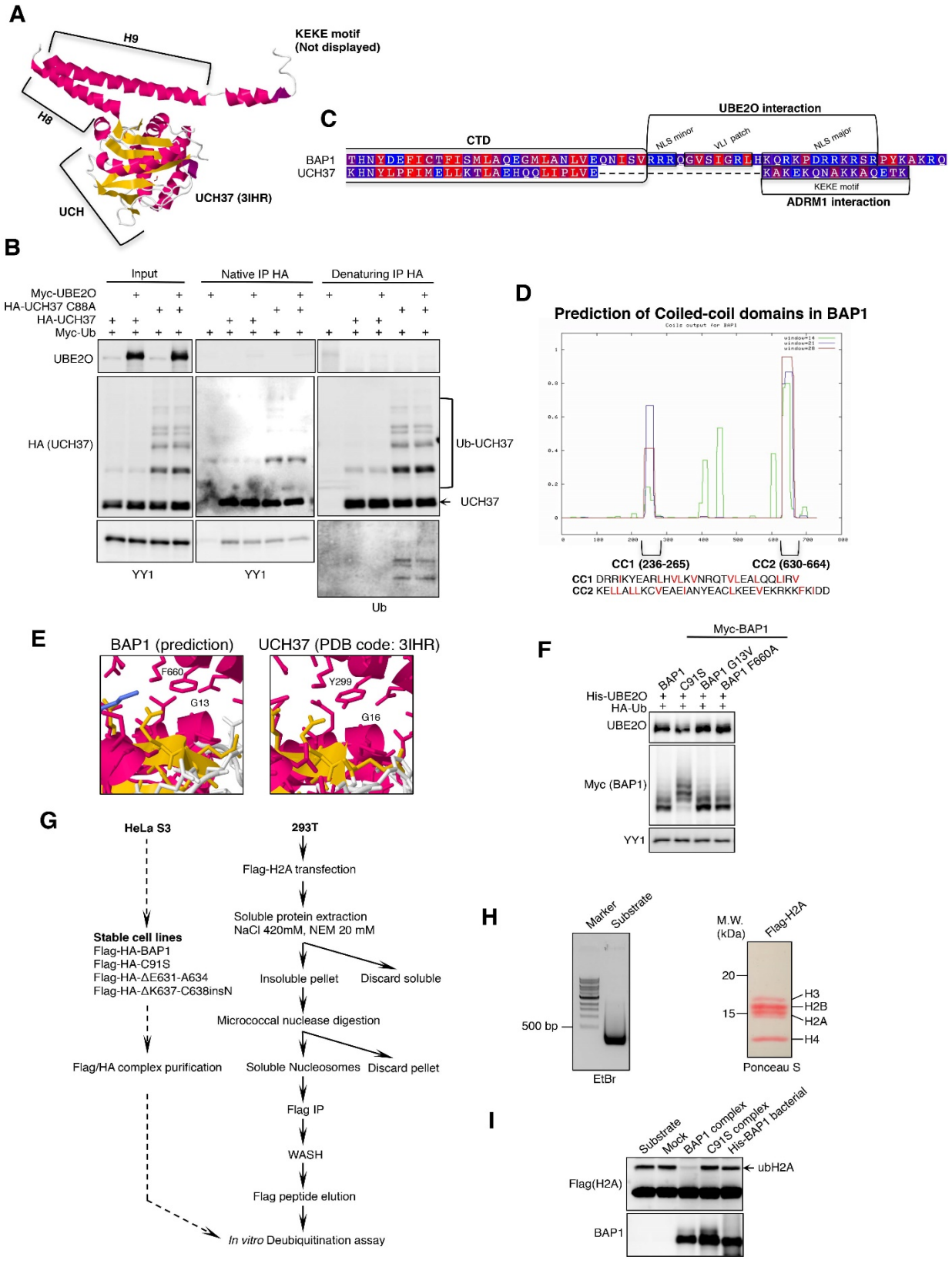
A
H9
KEKE motif
(Not displayed)
H8
UCH37 (3IHR)
UCH
C
UBE2O interaction
CTD
NLS minor
VLI patch
NLS major
BAP1
UCH37
KEKE motif
ADRM1 interaction
B
Input
Native IP HA
Denaturing IP HA
Myc-UBE2O
HA-UCH37 C88A
HA-UCH37
Myc-Ub
UBE2O
HA (UCH37)
Ub-UCH37
UCH37
YY1
YY1
Ub
D
Prediction of Coiled-coil domains in BAP1
CC1 (236-265)
CC2 (630-664)
CC1 DRRIKYEARLHVLKVNRQTVLEALQQLIRV
CC2 KELLALLKCVEAEIANYEACLKEEVEKRKKFKIDD
E
BAP1 (prediction)
UCH37 (PDB code: 3IHR)
F660
G13
Y299
G16
F
Myc-BAP1
BAP1
C91S
BAP1 G13V
BAP1 F660A
His-UBE2O
HA-Ub
UBE2O
Myc (BAP1)
YY1
G
HeLa S3
293T
Flag-H2A transfection
Soluble protein extraction
NaCl 420mM, NEM 20 mM
Stable cell lines
Flag-HA-BAP1
Flag-HA-C91S
Flag-HA-ΔE631-A634
Flag-HA-ΔK637-C638insN
Insoluble pellet
Discard soluble
Micrococcal nuclease digestion
Flag/HA complex purification
Soluble Nucleosomes
Discard pellet
Flag IP
WASH
Flag peptide elution
In vitro Deubiquitination assay
H
Marker
Substrate
500 bp
EtBr
M.W.
(kDa)
Flag-H2A
20
15
H3
H2B
H2A
H4
Ponceau S
I
Substrate
Mock
BAP1 complex
C91S complex
His-BAP1 bacterial
Flag(H2A)
ubH2A
BAP1

Figure S5 (Related to Figure 5).

BAP1 and UCH37 may employ a similar auto-deubiquitination mechanism.

A) Crystal structure of UCH37 (3IHR) (Burgie et al., 2011). **B)** UCH37 (UCHL5) is highly similar to BAP1 with respect to domain architecture (Sanchez-Pulido et al., 2012). Crystal structure of UCH37 suggests that an intramolecular interaction occurs between the UCH and the CTD. Therefore, we evaluated the possibility that UCH37 might also be regulated by UBE2O. 293T cells were co-transfected with 1 μg of Myc-Ub, 1 μg of HA-UCH37 wild type or HA-UCH37 C88A and either 2 μg of empty vector or Myc-UBE2O expression vectors. Three days later, cells lysates were used for IP with HA antibodies under native or denaturing conditions. Western blots were probed with the indicated antibodies. We detected ubiquitination of UCH37, which was more pronounced for its catalytic dead mutant (C88A), but this effect was independent of UBE2O. UCH37 also failed to interact with UBE2O in co-IP. Nonetheless, this result suggests that UCH37 may employ the same auto-deubiquitination mechanism as BAP1 to counteract the action of another, yet to be identified E3 ligase. Note that UCH37 co-immunoprecipitates endogenous YY1 providing an indication of IP validity (Yao et al., 2008). **C)** Alignment of human BAP1 and human UCH37 C-terminal regions, polar amino acids are in blue, hydrophobic amino acids are in red. Note the difference in the C-terminal region of both proteins, NLS in BAP1 and ADRM1-interacting region (KEKE) in UCH37 (Hamazaki et al., 2006; Yao et al., 2006). **D)** Prediction of coiled-coil domains in BAP1 using COILS program (Lupas et al., 1991). The amino acid sequences of CC1 and CC2 are presented. The hydrophobic amino acids are indicated in red.

G13V cancer mutant of BAP1 does not impair auto-deubiquitination of NLS.

We initially tested the G13V mutation recently described in renal carcinoma (Pena-Llopis et al., 2012). **E)** Prediction for the G13/F660 intra-molecular interaction (left) based on the crystal structure of UCH37 (3IHR)(right). **F)** 293T Cells were co-transfected with 2 μg of HA-Ub, 2 μg of His-UBE2O, and 1 μg of Myc-BAP1 expression vectors. Three days later, samples were used for western blotting and probed with the indicated antibodies. The G13 residue in UCH is predicted to interact with the F660 residue of the CC2; nonetheless G13V and F660A mutations did not have a noticeable effect on the auto-deubiquitination activity of BAP1.

Establishment of the *in vitro* nucleosome deubiquitination assay.

G) Schema representing the steps for the preparation of nucleosomes containing H2A mono-ubiquitinated on lysine 119 and the *in vitro* DUB assays. **H)** DNA from nucleosomal Flag elution was purified using phenol/chloroform separation and loaded on EtBr agarose gel (left). The Ponceau S staining of the nucleosomal Flag elution indicates the presence of all four histone types (right panel). **I)** *In vitro* nucleosome deubiquitination reaction with purified BAP1 complexes and bacteria purified BAP1. Samples were incubated at 37°C for 4 hours, reactions were stopped with 2X Laemmli buffer, and used for western blot with the indicated antibodies. Note that recombinant BAP1 (not assembled into its complex) does not deubiquitinate H2A .

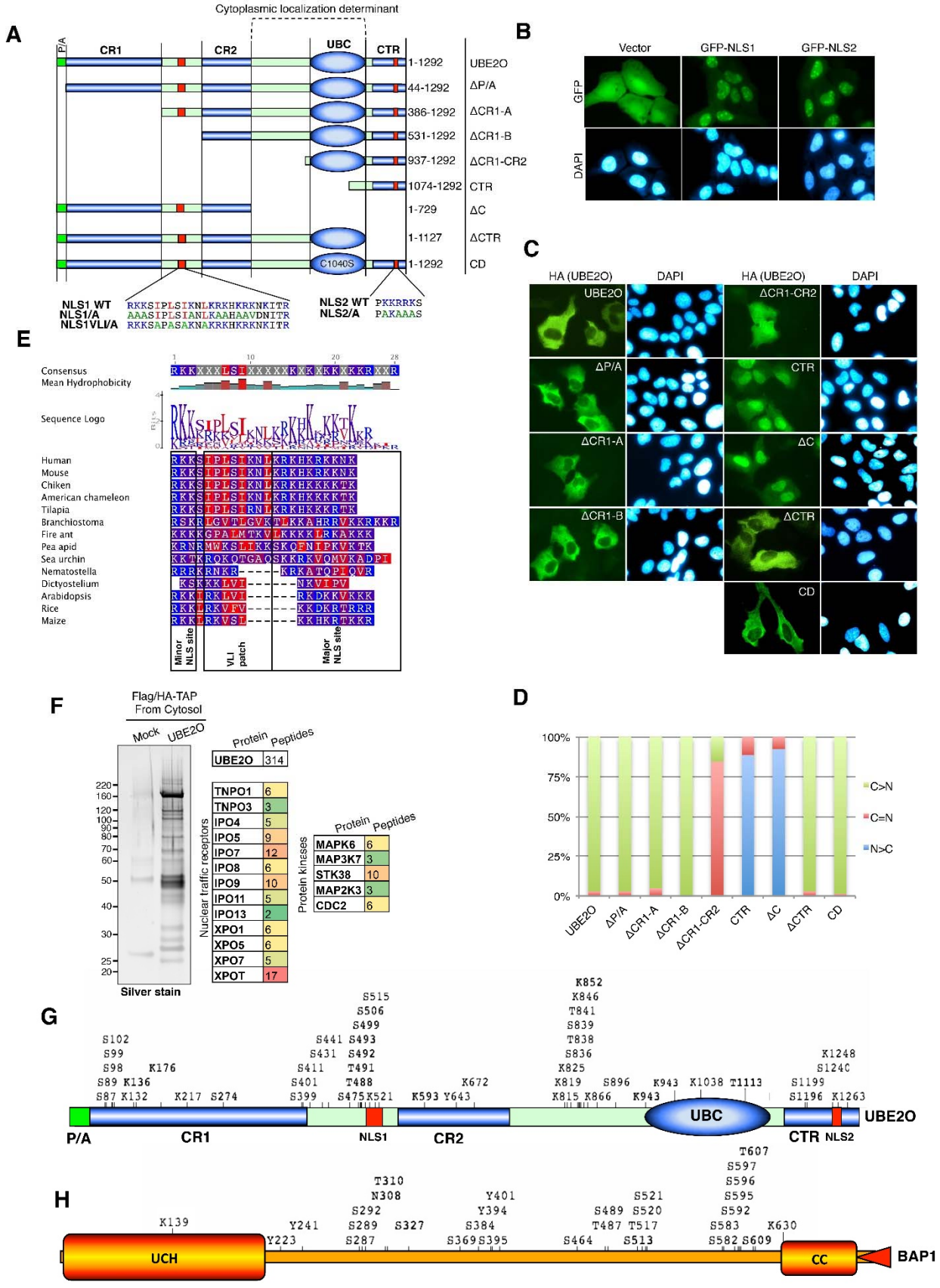
A
Cytoplasmic localization determinant
P/A
CR1
CR2
UBC
CTR
1-1292 UBE2O
44-1292 ΔP/A
386-1292 ΔCR1-A
531-1292 ΔCR1-B
937-1292 ΔCR1-CR2
1074-1292 CTR
1-729 ΔC
1-1127 ΔCTR
1-1292 CD
C1040S
NLS1 WT RKKSIPLSIKNLKRKHKRKNKITR
NLS1/A AAASIPLSIANLKAAHAAVDNITR
NLS1VLI/A RKKSAPASAKNAKRKHKRKNKITR
NLS2 WT PKKRRKS
NLS2/A PAKAAAS
B
Vector
GFP-NLS1
GFP-NLS2
GFP
DAPI
C
HA (UBE2O)
DAPI
UBE2O
ΔCR1-CR2
ΔP/A
CTR
ΔCR1-A
ΔC
ΔCR1-B
ΔCTR
CD
E
Consensus
Mean Hydrophobicity
Sequence Logo
Human
Mouse
Chiken
American chameleon
Tilapia
Branchiostoma
Fire ant
Pea apid
Sea urchin
Nematostella
Dictyostelium
Arabidopsis
Rice
Maize
Minor NLS site
VLI patch
Major NLS site
F
Flag/HA-TAP
From Cytosol
Mock
UBE2O
Silver stain
Protein
Peptides
UBE2O 314
Nuclear traffic receptors
TNPO1 6
TNPO3 3
IPO4 5
IPO5 9
IPO7 12
IPO8 6
IPO9 10
IPO11 5
IPO13 2
XPO1 6
XPO5 6
XPO7 5
XPOT 17
Protein kinases
MAPK6 6
MAP3K7 3
STK38 10
MAP2K3 3
CDC2 6
D
100%
75%
50%
25%
0%
C>N
C=N
N>C
UBE2O
ΔP/A
ΔCR1-A
ΔCR1-B
ΔCR1-CR2
CTR
ΔC
ΔCTR
CD
G
P/A
CR1
NLS1
CR2
UBC
CTR
NLS2
UBE2O
H
UCH
CC
BAP1

Figure S6 (Related to Figure 6).

Subcellular localization of UBE2O deletion mutants reveals nuclear and cytoplasmic targeting regions.

A) Schema of UBE2O mutants used to study its subcellular localization**. B)** U2OS cells were transfected with 1 µg of GFP fusion expression vectors of UBE2O NLS regions or empty vector and plated on coverslips. Two day later, cells were fixed and used for fluorescence microscopy analysis. **C)** U2OS cells were transfected with 3 µg of Flag-HA tagged expression vectors of UBE2O mutants and plated on coverslips. Two days later, cells were fixed and used for the immunofluorescence analysis with HA antibody. **D)** Representative cell counts for UBE2O subcellular localization are shown.

Multiple sequence alignment of NLS1 region from different UBE2O orthologs.

E) Multiple sequence alignment of NLS regions in UBE2O orthologs, polar amino acids are in blue, hydrophobic amino acids are in red.

F) Tandem affinity purification of UBE2O-associated proteins from HeLa cells followed by MS analysis. The regulators of nuclear traffic and protein kinases are presented

Post-translational modifications of UBE2O and BAP1.

G) Schema of known UBE2O phosphorylation and ubiquitination sites (modified from http://www.phosphosite.org/)

H) Schema of known BAP1 phosphorylation and ubiquitination sites (modified from http://www.phosphosite.org/)

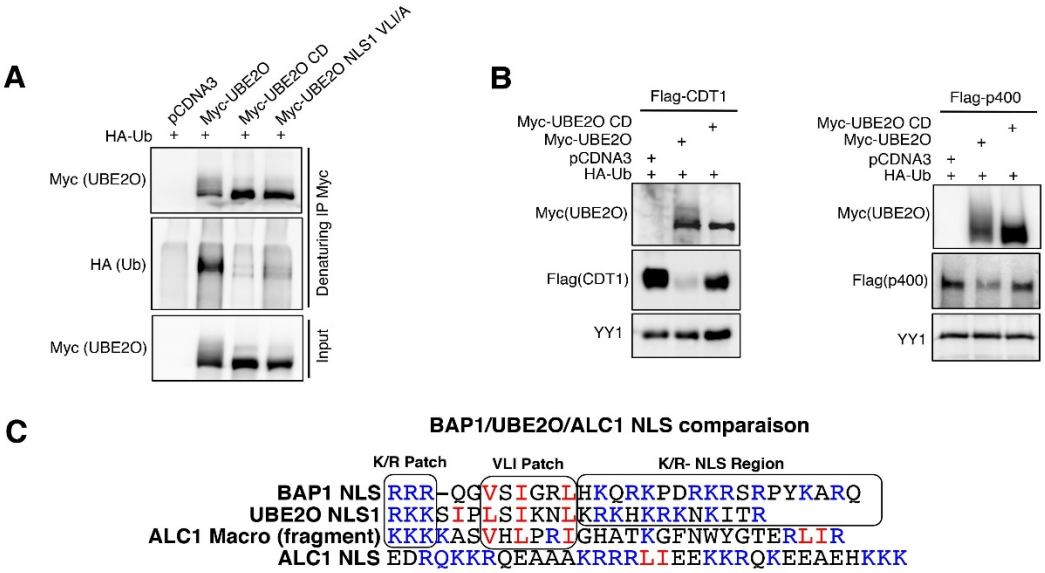

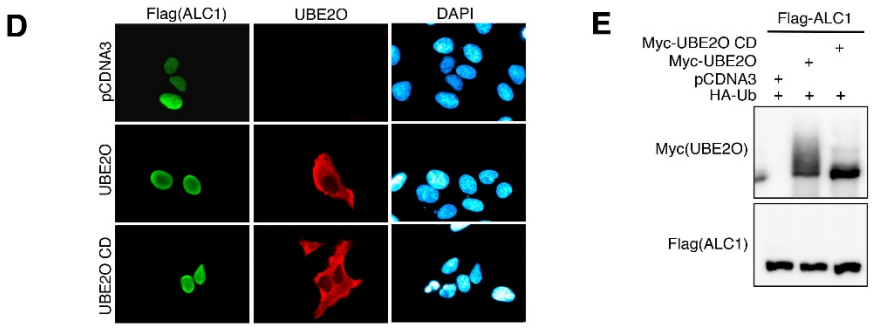

F

UniProt ID[a]	Name[b]	position[c]	Consensus sequence[d]	UBE2O substrate[e]
Q92560	**BAP1**	699-709	RRRqgVsIgrL	Yes
Q9C0C9	**UBE2O**	512-523	RKKsipLsIknL	Yes
Q9ULG1	**INO80**	264 - 273; 276 - 285	KKKh.LsIeqL; RRRk.VwLsiV	Yes
Q9H211	**CDT1**	67 - 77	RRRlrLsVdeV	Yes
Q9NS56	**TOPORS**	859 - 870	KRKtrsLsVeiV	unknown
Q9BRD0	**BUD13**	469 - 478	RKRn.LkLerL	unknown
Q5T5N4	**C6orf118**	172 - 182	RRReeLrLpdL	unknown
Q86WJ1	**ALC1**	833 - 843	KKKasVhLprI	NO
O43889	**CREB3**	192 - 202	RRKkkVyVggL	unknown
Q9P0U4	**CXXC1**	321 - 330	RKRa.VkVkhV	Yes
Q96L91	**EP400**	899 - 909	KRKkaLnLqkV	Yes
Q9NSI2	**FAM207A**	134 - 144	RRRatVvVgdL	unknown
O94915	**FRYL**	974 - 984	RRRdiLrVqlV	unknown
P5419	**HIRA**	628 - 638	KRKleLeVetV	unknown
Q32MZ4	**LRRF1**	578 - 588	KKKspVpVetL	unknown
O60942	**MCE1**	221 - 231	RRKerLkLgaI	unknown
O00566	**MPP10**	669 - 679	KKRqdIsVhkL	unknown
P35228	**NOS2**	509 - 518	KRRe.IpLkvL	unknown
Q86V59	**PNMAL1**	362 - 372	RKKkkVsLgpV	unknown
O60216	**RAD21**	319 - 329	KRKrkLiVdsV	unknown
P62979	**RS27A**	94 - 103	KRKk.VkLavL	unknown
P15822	**ZEP1**	1280 - 1289	KKKr.LrLaeI	unknown
Q9NQ69	**LHX9**	220 - 231	KRKspaLgVdiV	unknown
Q96NK8	**NEUROD6**	81 - 92	KKKttkLrLerV	unknown
Q96C28	**ZNF707**	166 - 177	RRKqraVeLsfI	unknown

Figure S7 (Related to Figure 7).

NLS1 hydrophobic VLI patch is required for auto-catalytic UBE2O targeting.

A) 293T cells were co-transfected with 2 µg of HA-Ub and 2 µg of indicated Myc-tagged UBE2O mutants, and cell extracts were used for immunoprecipitation.

UBE2O promotes degradation of p400 and CDT1.

B) 293T cells were co-transfected with 2 µg of HA-Ub and 2 µg of empty vector, Myc-UBE2O or Myc-UBE2O CD and either 1 µg of Flag-CDT1 or 5 µg Flag-p400 expression vectors. Three days later, samples were used for western blotting and probed with the indicated antibodies.

UBE2O does not ubiquitinate or promote localization change of ALC1, protein with unrelated NLS and the predicted consensus within Macro domain.

C) Sequence alignment between the UBE2O/BAP1 in comparison to ALC1 NLS. VLI patch is in red, and basic amino acids are in blue. Note that the K/R NLS region is absent downstream of the UBE2O consensus found in ALC1. The previously defined NLS sequence of ALC1 does not show similarities with the UBE2O consensus (Cheng et al., 2013). **D)** U2OS cells were co-transfected with 0,5 µg of HA-Ub and either 1 µg of empty vector, Myc-UBE2O or Myc-UBE2O CD and 1 µg of Flag-ALC1 expression vectors and plated on coverslips. Three days later, cells were fixed and used for immunofluorescence analysis with the indicated antibodies. **E)** 293T cells were co-transfected with 2 µg of HA-Ub and 2 µg of empty vector, Myc-UBE2O or Myc-UBE2O CD and 1µg of Flag-ALC1 expression vectors. Three days later, samples were used for western blotting and probed with the indicated antibodies.

Identification of potential UBE2O substrates

F) Prediction of UBE2O substrates based on BAP1/UBE2O NLS consensus

[a]UniProt accession number.

[b]protein name.

[c]protein positions of the *[KR][KR][KR]-X(1,3)-[VLI]-X-[VLI]-X-X-[VLI]* UBE2O binding consensus.

[d]consensus sequence (consensus-defined amino acids are capital).

[e]experimental evidence for the predicted UBE2O-mediated substrate ubiquitination (see Figures 7 and figure S7).

Extended Experimental Procedures

Plasmids and Antibodies

UBE2O and RING1B were cloned from HeLa total RNA by reverse transcription and inserted into pENTR D-Topo plasmid (Life Technologies). MYSM1 and USP16 were cloned from HeLa total RNA by reverse transcription and inserted into pEGFP-C1 plasmid. Human RNF10 and RNF219 were cloned from U2OS total RNA by reverse transcription and inserted into p3XFLAG-CMV™-7 expression vector (Sigma-Aldrich). UBE2O expression constructs were generated using LR clonase kit (Life Technologies) in pDEST-Myc, pDEST-His or retroviral pMSCV-Flag/HA-IRES-Puro (Sowa et al., 2009).

For bacterial expression, the UBE2O cDNA was cloned into pET-30a+ vector (Novagen), to generate N-terminal Flag- and the C- terminal His-tags for the double column purification.

The catalytically inactive UBE2O was generated by site-directed mutagenesis. Non-tagged pCDNA3-BAP1 and C91S were generated by subcloning the cDNA from pOZ-N BAP1 and pOZ-N C91S respectively. BAP1 cancer mutants ΔE631-A634, ΔK637-C638InsN, ΔCC2 and ΔCTD and UBE2O NLS mutants were generated using gene synthesis (BioBasic) and then subcloned into modified pENTR D-Topo plasmid.

BAP1 NLS mutants were generated by subcloning of annealed short adapters containing corresponding mutations in pENTR D-Topo BAP1 and/or C91S. NLS-GFP were generated by subcloning of annealed short adapters containing corresponding BAP1 or UBE2O NLS sequences in pOD35 plasmid provided by Dr. Paul Maddox (Institute for Research in Immunology and Cancer, Canada). All constructs were sequenced.

shRNAs for human UBE2O were from Sigma (#1 NM022066x814s1c1 and #2 NM022066x4103s1c1). The constructs used to produce recombinant full length GST-BAP1 and various deletion fragments, and BAP1 mutant deleted in the NHNY sequence corresponding to the HCF-1 binding domain (ΔHBM) and BAP1 catalytic dead C91S were described (Yu et al., 2010).

Flag-INO80 expression vector was provided by Dr. Yang Shi (Harvard Medical School, USA) (Wu et al., 2007). Flag-p400 was provided by Dr. David M. Livingston (Harvard Medical School, USA) (Chan et al., 2005). Flag-CXXC1 expression vector was provided by Dr. David Skalnik (Indiana University-Purdue University Indianapolis, USA) (Tate et al., 2009). Flag-CDT1 expression vector was provided by Dr. Kevin Struhl (Harvard Medical School, USA) (Miotto and Struhl, 2011). Flag-ALC1 expression vector was provided by Dr. Simon Boulton (London

Research Institute, UK) (Ahel et al., 2009). Flag-BRUCE and Flag-BRUCE CD expression vectors were from Dr. Stefan Jentsch (Max Planck Institute of Biochemistry, Germany) (Bartke et al., 2004). HA-UCH37 and HA-UCH37 C88A expression vectors were from Dr. Joan Conaway (Stowers Institute for Medical Research, USA) (Yao et al., 2008). Myc-UBC7 expression vector was provided by Dr. Allan M. Weissman (Center for Cancer Research National Cancer Institute, USA) (Tiwari and Weissman, 2001). Flag-UBCH8 expression vector was provided by Dr. Dong-Er Zhang (UC San Diego, USA) (Kim et al., 2004). GFP-TRIM28 expression vector was provided by Dr. Fanxiu Zhu (Florida State University USA) (Liang et al., 2011). Myc-TRIM27 expression vector was provided by Dr. Patrick R. Potts (UT Southwestern Dallas, USA) (Hao et al., 2013). HA-BRCA1 was generated by subcloning from the GFP-BRCA1 plasmid previously described (Hammond-Martel et al., 2010) into pCDNA3 plasmid. BARD1 expression vector was from Origene (SC119847). HA-wild type and K0 Ub expression vectors were from Dr. Ted Dawson (John Hopkins University, USA) (Lim et al., 2005).

The siRNA ON-TARGETplus® smart pool for human UBE2O and a non-target control were from Dharmacon (Thermo Scientific).

Rabbit polyclonal anti-UBE2O was from Novus Biologicals (NBP-03336). Mouse monoclonal anti-BAP1 (C4), rabbit polyclonal anti-BAP1 (H300), rabbit polyclonal anti-YY1 (H414), rabbit polyclonal anti-OGT (H300), mouse monoclonal anti-GFP (B2), rabbit polyclonal anti-GFP (FL), mouse monoclonal anti-RING1B (N-32), mouse monoclonal anti-BRCA1 (D-9), mouse monoclonal anti-BARD1 (2059c4a), mouse monoclonal anti-CDC25A (F6), mouse monoclonal anti-Ubiquitin (P4D1) were from Santa Cruz. Rabbit polyclonal anti-HCF-1 (A301-400A) and rabbit polyclonal anti-ASXL2 (A302-037A) were from Bethyl Laboratories. Mouse monoclonal anti-Flag (M2) was from Sigma. Mouse monoclonal anti-Myc (9E10) and mouse monoclonal anti-HA (HA11) were from Covance. Rabbit polyclonal anti-HA (ab9110) was from Abcam. Rabbit monoclonal anti-Perilipin (PLIN) was from New England BioLabs (D1D8) XP®). Rabbit polyclonal anti-aP2 (FABP4) was from Cayman Chemicals. Mouse polyclonal anti-FOXK1 was provided by Dr. Xiao-Hua Li from Southwestern University of Texas. A rabbit polyclonal anti-FOXK2 was generated using a recombinant fragment of human FOXK2 by Pacific Immunology.

Chemicals and reagents

UBE1, USP2 CD, Ub-VME, Ub-AMC, recombinant Myc-Ub and Ub were from Boston Biochem. Cycloheximide (CHX), N-methylmaleimide (NEM), Phenylarsine oxide (PAO), MG132, Micrococcal nuclease (MNase) where from Sigma. Casein kinase II (CKII) inhibitor TBB (100 μM), Casein kinase I (CKI) inhibitor IC261 (10 μM), protein kinase G inhibitor KT5823 (10 μM), CDK1 inhibitor RO-3306 (10 μM) where purchased from Millipore. The CDK1, CDK2 and CDK5 inhibitor Roscovitine (10 μM), MEK1/2 inhibitor UO126 (20 μM) and the protein kinase A (PKA) inhibitor H-89 (20 μM) were purchased from Cell Signaling. The CDK2 inhibitor Purvalanol A (50 μM) was purchased from Abcam. Protein kinase C inhibitor PKC412 (20 μM) and STK inhibitor GSK 650394 (20 μM) were from Santa Cruz. The PI3-Kinase inhibitor caffeine (10 mM), CDK inhibitor CDKi (100 μM), CDK2 inhibitor GW8510 (20 μM) and JNK inhibitor SP600125 (30 μM) were from Sigma. SU 9516 (5 μM), Chk1 inhibitor SB 218078 (1 μM). Broad spectrum kinase inhibitor Staurosporine (100 nM), tyrosine kinase inhibitor Genistein (20 μM), CDK inhibitor Olomoucine (30 μM), CKII inhibitor Apigenin (20 μM), CKII and CDK inhibitor DRB (50 μM), PI3-Kinase inhibitor LY294002 (20 μM), CKII inhibitor NSC 210902 (15 μM), CKI inhibitor D 4476 (25 μM) and CKII inhibitor CAY10578 (15 μM) where from Cayman chemical.

Cell culture, transfections and western blot

HeLa S3 cervical cancer, MCF7 breast cancer, U2OS osteosarcoma, human embryonic kidney 293T, 293GPG virus-producing cells and 3T3-L1 mouse preadipocytes and human primary lung fibroblasts LF-1 were cultured in Dulbecco's modified Eagle's medium (DMEM) supplemented with 10% fetal bovine serum and penicillin/streptomycin.

siRNA and plasmid DNA were transfected in MCF7 and U2OS cells, respectively, using Lipofectamine 2000 (Life Technologies). HEK293T (293T) cells were transfected using PEI (Sigma).

Total cell lysates were prepared in buffer containing 25 mM Tris-HCl pH 7.5 and 1% SDS, samples were immediately boiled at 95°C for 10 min and sonicated to break down DNA. Samples were diluted using 2X or 4X Laemmli buffer (Laemmli, 1970). SDS-PAGE and western blotting were conducted according to standard procedures. Images were acquired using ImageQuant™ LAS 4000 biomolecular imager (GE Healthcare, USA). Densitometry quantification of western blot bands was performed using Gel-Pro Analyzer 3.1 (Media Cybernetics).

Stable cell lines

HeLa S3 cell lines stably expressing Flag-HA-BAP1, Flag-HA-C91S, Flag-HA-ΔE631-A634, Flag-HA-ΔK637-C638InsN, Flag-HA-ΔCTD, Flag-HA-ΔCC1 were generated following retroviral transduction using pOZ-N-based retroviral constructs and selected using anti-IL2 magnetic beads (Life Technologies) as previously described (Yu et al., 2010).

U2OS cell lines stably expressing Flag-HA-BAP1, Flag-HA-C91S, Flag-HA-ΔE631-A634, Flag-HA-ΔK637-C638InsN, Flag-HA-ΔCTD, Flag-HA-ΔCC1 were generated following retroviral transduction of pMSCV-Flag/HA-IRES-Puro based constructs and selected with 3 μg/ml of puromycin.

3T3-L1 cell lines stably expressing Flag-HA-BAP1, Flag-HA-BAP1 5 K/R, Flag-HA-BAP1 NLS T1, Flag-HA-UBE2O and Flag-HA-UBE2O CD were generated following retroviral transduction of pMSCV-Flag/HA-IRES-Puro based constructs and selected with 3 μg/ml of puromycin.

Stable HeLa S3 Flag-HA-UBE2O cell line was generated following retroviral transduction of pMSCV-Flag/HA UBE2O-IRES-Puro and selected with 2 μg/ml of puromycin.

Purification of BAP1 complexes and UBE2O-interacting proteins

HeLa S3 (~12 X 10^9) cells stably expressing Flag-HA-BAP1, Flag-HA-C91S, Flag-HA-ΔE631-A634, Flag-HA-ΔK637-C638InsN, Flag-HA-ΔCTD and Flag-HA-UBE2O were grown in spinner flasks. The cytosolic fraction was used for the purification of UBE2O with Flag and HA immunoaffinity columns essentially as previously described (Groisman et al., 2003) the Flag and HA columns were washed with either low salt buffer containing 100 mM KCl (Flag-HA-UBE2O LS) or 300 mM NaCl (Flag-HA-UBE2O HS) (Figure S2A, C, D)). The BAP1 protein complexes were purified from total soluble protein extracts in EBcom (50 mM Tris-HCl pH 7.5, 150 mM NaCl, 0,5% NP-40, 50 mM NaF, 10 mM β-glycerophosphat, 1 mM Na_3VO_4 1 mM DTT, 1 mM EDTA, 1 mM PMSF and protease inhibitors cocktail (Sigma)). The extracts were clarified by centrifugation at 30,000g for 1 hour, with subsequent filtration of supernatants through a 0,45 μm pore filter. The extracts were incubated with the anti-Flag M2 resin overnight and extensively washed with EBcom. The resin was eluted three times with EBcom containing 200 ng/ml of Flag peptide. The eluted fractions were incubated with anti-HA resin overnight, and the procedure was repeated as for the previous column. The HA eluted fractions were used for silver stain, western blot and in vitro DUB assay. Mass spectrometric identification of UBE2O-interacting proteins was

done at the Taplin Mass Spectrometry facility (Harvard, USA). Identification of additional BAP1-interacting proteins was done at the Proteomics Platform of the Quebec Genomics Center (CHUQ, Laval University, Canada).

Immunoprecipitation

Cells were lysed in buffer EB150 (50 mM Tris-HCl pH 7.5, 150 mM NaCl, 1% NP-40, 10 mM β-mercaptoethanol, 1 mM PMSF and protease inhibitors cocktail (Sigma)) and the lysates were clarified by centrifugation at 21,000 g for 30 min. The supernatants were incubated with indicated antibodies for 3 hours and then protein-G beads were added and incubated for an additional hour. The samples were extensively washed with EB150 and re-suspended in 2X Laemmli buffer. For an IP under denaturing conditions, the cells were harvested as described for western blot, and diluted in EB300 (50 mM Tris-HCl pH 7.5, 300 mM NaCl, 1% NP-40, 10 mM β-mercaptoethanol). The lysates were incubated overnight with antibody and protein-G beads. The beads were washed several times with EB300 and resuspended in 2X Laemmli buffer.

Mass spectrometric identification of ubiquitination sites

293T (~1 X 10^9) cells were transfected with HA-Ub, Flag-C91S, and His-UBE2O expression vectors. 96 hours later, the cells were lysed in EB300 containing 20 mM NEM and protease inhibitor cocktail. The extracts were clarified by centrifugation at 30,000g for 1 hour. The extracts were incubated with the anti-Flag M2 resin overnight and extensively washed with EB300. The resin was eluted three times with EB300 containing 200 ng/ml of Flag peptide. The eluted fractions were combined and concentrated using TCA (trichloroacetic acid) precipitation and loaded on the NuPAGE® Bis-Tris Precast Gel (Life Technologies). The gel was stained with Coomassie G-250 and the modified C91S bands were excised and sent for MS analysis at Taplin Mass Spectrometry facility (Harvard, USA).

Glycerol gradient

Molecular mass fractionation of nuclear extract was conduced using a 10-40 % glycerol gradient prepared in 20 mM Tris-HCl, pH 7.9; 100 mM KCl; 5 mM $MgCl_2$; 1 mM PMSF; 0.1% NP40 and 10 mM β-mercaptoethanol. The samples were centrifuged for 12 hours at 50,000 RPM (SW55Ti rotor, Beckman,) at 4 ºC. Individual fractions were then collected from top to bottom

and analyzed by western blotting. The BAP1 complex is estimated to have a molecular mass of 1.6 MDa.

In vitro interaction assays

Recombinant GST-BAP1 fusion proteins were purified from bacteria using glutathione agarose beads (Sigma) and 2 to 3 μg of bound proteins were incubated with His-UBE2O for 6 to 8 hours at 4 ºC in pull down buffer (50 mM Tris-HCl, pH 7.5; 50 mM NaCl; 0.02% Tween 20; 1 mM PMSF and 500 μM dithiothreitol). The beads were extensively washed with the same buffer, and bound proteins eluted in 2X Laemmli buffer and subjected to western blotting.

In vitro ubiquitination assay

Ubiquitination reactions were conducted in a total volume of 30 μl containing 25 mM Tris-HCl pH 7.5, 10 mM $MgCl_2$, 5 mM ATP, 50 ng/μl Ub, 250 ng of human recombinant UBE1 and 1 mM β-mercaptoethanol. Purified Flag-HA-BAP1, Flag-HA-C91S, His-C91S (bacterial recombinant), Flag-UBE2O-His (bacterial recombinant) and Flag-HA-UBE2O were added as indicated.

Reaction on the beads-immobilized complexes was performed when indicated. Briefly, the anti-Flag M2 beads were incubated with high salt nuclear extracts from HeLa S3 Flag-HA-BAP1 or Flag-HA-C91S for 5 hour and washed 8 times with buffer containing 20 mM Tris-HCl pH 7.5, 100 mM KCl, 1 mM $MgCl_2$, 5 mM EDTA, 0.1% Triton X-100 and 1 mM PMSF. The last wash was performed using buffer containing 25 mM Tris-HCl pH 7.5 and 10 mM $MgCl_2$. The beads-bound complexes (25 μl) were used for the reaction essentially in the same conditions as for the reaction in solution. Reactions were incubated at 37ºC with constant shaking overnight. Met-Ub was previously described (Kirisako et al., 2006)

Purification of the nucleosomes and *In vitro* nucleosome DUB assay

Preparation of chromatin fractions and digestion with Micrococcal nuclease (MNase Sigma) were conducted as previously described (Groisman et al., 2003), with some modifications. The 293T cellular pellet was resuspended in EB420 (50 mM Tris-HCl pH 7.5, 420 mM NaCl, 1% NP-40, 10 mM β-mercaptoethanol, 20 mM NEM and protease inhibitor cocktail). The soluble fraction was discarded and the pellet was extensively washed with MNase buffer (20 mM Tris-HCl pH 7.5, 100 mM KCl, 2 mM $MgCl_2$, 1 mM $CaCl_2$, 0.3 M sucrose, 0.1% NP-40, and protease inhibitor cocktail). Following MNase treatment (3 U/ml for 10 min at room temperature), the reaction was quenched with 5 mM of EGTA and 5 mM of EDTA. The samples were then centrifuged at 20,000g

for 10 minutes at 4°C to obtain the soluble chromatin fraction. The extract was incubated with anti-Flag M2 resin overnight and washed with EB300 buffer. The beads then were eluted with EB300 containing 200 ng/ml of Flag peptide.

The eluted soluble chromatin fraction was incubated with the indicated Flag/HA purified BAP1 complexes and used for western blotting.

Immunofluorescence

The procedure was carried over essentially as previously described (Daou et al., 2011). Briefly cells were fixed in 3% PFA-PBS and permeabilized using PBS 0.1% NP-40. Anti-mouse Alexa Fluor® 594 and Anti-mouse Alexa Fluor® 488 (Life Technologies) were used as secondary antibodies. Nuclei were stained with 4',6-diamidino-2-phenylindole (DAPI).

Images were acquired using Zeiss. Z2 microscope and Plan Apochrmat 40X/0.95 Korr, Plan Apochrmat 63X/1.4 Oil DIC and Plan Apochrmat 100X/1.4 Oil DIC objectives and AxioCam MRm camera. Images were processed using WCIF-ImageJ program (NIH).

Adipogenic differentiation of 3T3-L1 preadipocytes.

3T3-L1 cell lines stably expressing BAP1 or UBE2O were plated at the same density, upon reaching of confluency the growth media was changed to induction media containing 10% fetal bovine serum, penicillin/streptomycin, 1 μM dexamethasone, 1 μg/ml insulin and 500 μM IBMX (Sigma). Two days post-induction, the media was changed to maintenance media containing 10 % fetal bovine serum, penicillin/streptomycin, 1 μg/ml insulin. The cells were fixed with PFA or harvested for western blotting two to three days post-induction. Lipid droplet content was evaluated using Oil-Red O lipid stain (Sigma).

Protein sequence analysis, and structure modelin

Protein sequences were analyzed and aligned using Geneious 6.1.2 created by Biomatters, available from http://www.geneious.com. NLS consensus were analyzed using ProSite (Sigrist et al., 2013) and NLStradamus (Nguyen Ba et al., 2009). Coiled-coil regions were predicted using COILS (Lupas et al., 1991). BAP1 3D structure modeling was performed using SWISS-MODEL (Arnold et al., 2006) and crystal structure of UCH37 (Burgie et al., 2011) (PDB code: 3IHR).

Supplemental References

Ahel, D., Horejsi, Z., Wiechens, N., Polo, S.E., Garcia-Wilson, E., Ahel, I., Flynn, H., Skehel, M., West, S.C., Jackson, S.P., *et al.* (2009). Poly(ADP-ribose)-dependent regulation of DNA repair by the chromatin remodeling enzyme ALC1. Science *325*, 1240-1243.

Arnold, K., Bordoli, L., Kopp, J., and Schwede, T. (2006). The SWISS-MODEL workspace: a web-based environment for protein structure homology modelling. Bioinformatics *22*, 195-201.

Bartke, T., Pohl, C., Pyrowolakis, G., and Jentsch, S. (2004). Dual role of BRUCE as an antiapoptotic IAP and a chimeric E2/E3 ubiquitin ligase. Molecular cell *14*, 801-811.

Burgie, S.E., Bingman, C.A., Soni, A.B., and Phillips, G.N., Jr. (2011). Structural characterization of human Uch37. Proteins.

Carbone, M., Yang, H., Pass, H.I., Krausz, T., Testa, J.R., and Gaudino, G. (2013). BAP1 and cancer. Nature reviews. Cancer *13*, 153-159.

Chan, H.M., Narita, M., Lowe, S.W., and Livingston, D.M. (2005). The p400 E1A-associated protein is a novel component of the p53 --> p21 senescence pathway. Genes & development *19*, 196-201.

Cheng, W., Su, Y., and Xu, F. (2013). CHD1L: a novel oncogene. Molecular cancer *12*, 170.

Conti, E., Uy, M., Leighton, L., Blobel, G., and Kuriyan, J. (1998). Crystallographic analysis of the recognition of a nuclear localization signal by the nuclear import factor karyopherin alpha. Cell *94*, 193-204.

Daou, S., Mashtalir, N., Hammond-Martel, I., Pak, H., Yu, H., Sui, G., Vogel, J.L., Kristie, T.M., and Affar el, B. (2011). Crosstalk between O-GlcNAcylation and proteolytic cleavage regulates the host cell factor-1 maturation pathway. Proceedings of the National Academy of Sciences of the United States of America *108*, 2747-2752.

Groisman, R., Polanowska, J., Kuraoka, I., Sawada, J., Saijo, M., Drapkin, R., Kisselev, A.F., Tanaka, K., and Nakatani, Y. (2003). The ubiquitin ligase activity in the DDB2 and CSA complexes is differentially regulated by the COP9 signalosome in response to DNA damage. Cell *113*, 357-367.

Hamazaki, J., Iemura, S., Natsume, T., Yashiroda, H., Tanaka, K., and Murata, S. (2006). A novel proteasome interacting protein recruits the deubiquitinating enzyme UCH37 to 26S proteasomes. The EMBO journal *25*, 4524-4536.

Hammond-Martel, I., Pak, H., Yu, H., Rouget, R., Horwitz, A.A., Parvin, J.D., Drobetsky, E.A., and Affar el, B. (2010). PI 3 kinase related kinases-independent proteolysis of BRCA1 regulates Rad51 recruitment during genotoxic stress in human cells. PloS one *5*, e14027.

Hao, Y., Sekine, K., Kawabata, A., Nakamura, H., Ishioka, T., Ohata, H., Katayama, R., Hashimoto, C., Zhang, X., Noda, T.*, et al.* (2004). Apollon ubiquitinates SMAC and caspase-9, and has an essential cytoprotection function. Nature cell biology *6*, 849-860.

Hao, Y.H., Doyle, J.M., Ramanathan, S., Gomez, T.S., Jia, D., Xu, M., Chen, Z.J., Billadeau, D.D., Rosen, M.K., and Potts, P.R. (2013). Regulation of WASH-Dependent Actin Polymerization and Protein Trafficking by Ubiquitination. Cell *152*, 1051-1064.

Jensen, D.E., Proctor, M., Marquis, S.T., Gardner, H.P., Ha, S.I., Chodosh, L.A., Ishov, A.M., Tommerup, N., Vissing, H., Sekido, Y.*, et al.* (1998). BAP1: a novel ubiquitin hydrolase which binds to the BRCA1 RING finger and enhances BRCA1-mediated cell growth suppression. Oncogene *16*, 1097-1112.

Joo, H.Y., Zhai, L., Yang, C., Nie, S., Erdjument-Bromage, H., Tempst, P., Chang, C., and Wang, H. (2007). Regulation of cell cycle progression and gene expression by H2A deubiquitination. Nature *449*, 1068-1072.

Kim, K.I., Baek, S.H., Jeon, Y.J., Nishimori, S., Suzuki, T., Uchida, S., Shimbara, N., Saitoh, H., Tanaka, K., and Chung, C.H. (2000). A new SUMO-1-specific protease, SUSP1, that is highly expressed in reproductive organs. The Journal of biological chemistry *275*, 14102-14106.

Kim, K.I., Giannakopoulos, N.V., Virgin, H.W., and Zhang, D.E. (2004). Interferon-inducible ubiquitin E2, Ubc8, is a conjugating enzyme for protein ISGylation. Molecular and cellular biology *24*, 9592-9600.

Kirisako, T., Kamei, K., Murata, S., Kato, M., Fukumoto, H., Kanie, M., Sano, S., Tokunaga, F., Tanaka, K., and Iwai, K. (2006). A ubiquitin ligase complex assembles linear polyubiquitin chains. The EMBO journal *25*, 4877-4887.

Laemmli, U.K. (1970). Cleavage of structural proteins during the assembly of the head of bacteriophage T4. Nature *227*, 680-685.

Lee, B.J., Cansizoglu, A.E., Suel, K.E., Louis, T.H., Zhang, Z., and Chook, Y.M. (2006). Rules for nuclear localization sequence recognition by karyopherin beta 2. Cell *126*, 543-558.

Liang, Q., Deng, H., Li, X., Wu, X., Tang, Q., Chang, T.H., Peng, H., Rauscher, F.J., 3rd, Ozato, K., and Zhu, F. (2011). Tripartite motif-containing protein 28 is a small ubiquitin-related modifier E3 ligase and negative regulator of IFN regulatory factor 7. Journal of immunology *187*, 4754-4763.

Lim, K.L., Chew, K.C., Tan, J.M., Wang, C., Chung, K.K., Zhang, Y., Tanaka, Y., Smith, W., Engelender, S., Ross, C.A.*, et al.* (2005). Parkin mediates nonclassical, proteasomal-independent ubiquitination of synphilin-1: implications for Lewy body formation. The Journal of neuroscience : the official journal of the Society for Neuroscience *25*, 2002-2009.

Lupas, A., Van Dyke, M., and Stock, J. (1991). Predicting coiled coils from protein sequences. Science *252*, 1162-1164.

Miotto, B., and Struhl, K. (2011). JNK1 phosphorylation of Cdt1 inhibits recruitment of HBO1 histone acetylase and blocks replication licensing in response to stress. Molecular cell *44*, 62-71.

Nguyen Ba, A.N., Pogoutse, A., Provart, N., and Moses, A.M. (2009). NLStradamus: a simple Hidden Markov Model for nuclear localization signal prediction. BMC bioinformatics *10*, 202.

Pena-Llopis, S., Vega-Rubin-de-Celis, S., Liao, A., Leng, N., Pavia-Jimenez, A., Wang, S., Yamasaki, T., Zhrebker, L., Sivanand, S., Spence, P.*, et al.* (2012). BAP1 loss defines a new class of renal cell carcinoma. Nature genetics *44*, 751-759.

Robbins, J., Dilworth, S.M., Laskey, R.A., and Dingwall, C. (1991). Two interdependent basic domains in nucleoplasmin nuclear targeting sequence: identification of a class of bipartite nuclear targeting sequence. Cell *64*, 615-623.

Sanchez-Pulido, L., Kong, L., and Ponting, C.P. (2012). A common ancestry for BAP1 and Uch37 regulators. Bioinformatics *28*, 1953-1956.

Scheuermann, J.C., de Ayala Alonso, A.G., Oktaba, K., Ly-Hartig, N., McGinty, R.K., Fraterman, S., Wilm, M., Muir, T.W., and Muller, J. (2010). Histone H2A deubiquitinase activity of the Polycomb repressive complex PR-DUB. Nature *465*, 243-247.

Sigrist, C.J., de Castro, E., Cerutti, L., Cuche, B.A., Hulo, N., Bridge, A., Bougueleret, L., and Xenarios, I. (2013). New and continuing developments at PROSITE. Nucleic acids research *41*, D344-347.

Sowa, M.E., Bennett, E.J., Gygi, S.P., and Harper, J.W. (2009). Defining the human deubiquitinating enzyme interaction landscape. Cell *138*, 389-403.

Tate, C.M., Lee, J.H., and Skalnik, D.G. (2009). CXXC finger protein 1 contains redundant functional domains that support embryonic stem cell cytosine methylation, histone methylation, and differentiation. Molecular and cellular biology *29*, 3817-3831.

Tiwari, S., and Weissman, A.M. (2001). Endoplasmic reticulum (ER)-associated degradation of T cell receptor subunits. Involvement of ER-associated ubiquitin-conjugating enzymes (E2s). The Journal of biological chemistry *276*, 16193-16200.

van Wijk, S.J., and Timmers, H.T. (2010). The family of ubiquitin-conjugating enzymes (E2s): deciding between life and death of proteins. FASEB journal : official publication of the Federation of American Societies for Experimental Biology *24*, 981-993.

Ventii, K.H., Devi, N.S., Friedrich, K.L., Chernova, T.A., Tighiouart, M., Van Meir, E.G., and Wilkinson, K.D. (2008). BRCA1-associated protein-1 is a tumor suppressor that requires deubiquitinating activity and nuclear localization. Cancer research *68*, 6953-6962.

Wu, S., Shi, Y., Mulligan, P., Gay, F., Landry, J., Liu, H., Lu, J., Qi, H.H., Wang, W., Nickoloff, J.A.*, et al.* (2007). A YY1-INO80 complex regulates genomic stability through homologous recombination-based repair. Nature structural & molecular biology *14*, 1165-1172.

Wu-Baer, F., Lagrazon, K., Yuan, W., and Baer, R. (2003). The BRCA1/BARD1 heterodimer assembles polyubiquitin chains through an unconventional linkage involving lysine residue K6 of ubiquitin. The Journal of biological chemistry *278*, 34743-34746.

Yao, T., Song, L., Jin, J., Cai, Y., Takahashi, H., Swanson, S.K., Washburn, M.P., Florens, L., Conaway, R.C., Cohen, R.E.*, et al.* (2008). Distinct modes of regulation of the Uch37 deubiquitinating enzyme in the proteasome and in the Ino80 chromatin-remodeling complex. Molecular cell *31*, 909-917.

Yao, T., Song, L., Xu, W., DeMartino, G.N., Florens, L., Swanson, S.K., Washburn, M.P., Conaway, R.C., Conaway, J.W., and Cohen, R.E. (2006). Proteasome recruitment and activation of the Uch37 deubiquitinating enzyme by Adrm1. Nature cell biology *8*, 994-1002.

Yu, H., Mashtalir, N., Daou, S., Hammond-Martel, I., Ross, J., Sui, G., Hart, G.W., Rauscher, F.J., 3rd, Drobetsky, E., Milot, E.*, et al.* (2010). The ubiquitin carboxyl hydrolase BAP1 forms a ternary complex with YY1 and HCF-1 and is a critical regulator of gene expression. Molecular and cellular biology *30*, 5071-5085.

Yu, H., Pak, H., Hammond-Martel, I., Ghram, M., Rodrigue, A., Daou, S., Barbour, H., Corbeil, L., Hebert, J., Drobetsky, E.*, et al.* (2014). Tumor suppressor and deubiquitinase BAP1 promotes DNA double-strand break repair. Proceedings of the National Academy of Sciences of the United States of America *111*, 285-290.

Zhu, P., Zhou, W., Wang, J., Puc, J., Ohgi, K.A., Erdjument-Bromage, H., Tempst, P., Glass, C.K., and Rosenfeld, M.G. (2007). A histone H2A deubiquitinase complex coordinating histone acetylation and H1 dissociation in transcriptional regulation. Molecular cell *27*, 609-621.

Annexe3 Article: The Tumor Suppressor and Deubiquitinase BAP1 Promotes DNA Double-Strand Breaks Repair

Helen Yu, [a,1], Helen Pak [a,1], Ian Hammond-Marte [a], Mehdi Ghram[a], Amélie Rodrigue[b], Salima Daou[a], Haithem Barbour[a], Luc Corbeil[a], Josée Hébert[a], Elliot Drobetsky[a], Jean Yves Masson[b], Javier M Di Noia[c] and El Bachir Affar[a,2]

a Maisonneuve-Rosemont Hospital Research Center, Department of Medicine, Université de Montréal, Montréal, PQ, H1T 2M4, Canada.

b Genome Stability Laboratory, Laval University Cancer Research Center, Hôtel-Dieu de Québec (Centre Hospitalier Universitaire de Québec), Québec, PQ, G1R 2J6, Canada.

c Research Unit in Mechanisms of Genetic Diversity, Institut de Recherches Cliniques de Montréal, Department of Medicine, Université de Montréal, Montréal, PQ, H2W 1R7, Canada.

Running title: BAP1 promotes homologous recombination repair.

1 Equal contribution

Publié dans: PNAS 2014, 111(1):285-90

Summary

The cellular response to highly genotoxic DNA double-strand breaks (DSBs) involves the exquisite coordination of multiple signaling and repair factors. Here, we conducted a functional RNAi screen and identified BAP1 as a DUB required for efficient assembly of the homologous recombination (HR) factors BRCA1 and RAD51 at ionizing radiation (IR)-induced foci (IRIF). BAP1 is a chromatin-associated protein frequently inactivated in cancers of various tissues. To further investigate the role of BAP1 in DSB repair, we used a gene targeting approach to knock out this DUB in chicken DT40 cells. We demonstrate that BAP1-deficient cells are (i) sensitive to IR and other agents that induce DSBs, (ii) defective in HR-mediated immunoglobulin gene conversion and (iii) exhibit an increased frequency of chromosomal breaks following IR treatment. We also show that BAP1 is recruited to chromatin in the proximity of a single site-specific I-SceI-induced DSB. Finally, we identified six IR-induced phosphorylation sites in BAP1 and demonstrated that mutation of these residues inhibits BAP1 recruitment to DSB site. We also found that both BAP1 catalytic activity and its phosphorylation are critical for promoting DNA repair and cellular recovery from DNA damage. Our data reveal a novel role for BAP1 in DSB repair by HR, thereby providing a possible molecular basis for its tumor suppressor function.

Significance Statement

BAP1 is a deubiquitinase of histone H2A involved in chromatin remodeling. Several studies identified BAP1 as major tumor suppressor inactivated in various cancers. Nonetheless, the manner in which BAP1 protects against cancer development remains enigmatic. We now demonstrate that BAP1 is recruited to double strand DNA break sites and promotes error-free repair of these lesions. We also provide the first evidence that phosphorylation coordinates the function of BAP1 in promoting cellular recovery from DNA damage. Thus, our study represents a significant advance in the field of ubiquitin signaling in the context of cancer development.

Introduction

Following induction of DSBs, a convoluted ubiquitin-mediated signaling cascade culminates in the assembly of multiple repair proteins at the site of DNA damage (1). These early ubiquitin signaling events involve, most notably, the recruitment of the RING finger E3 ligases RNF8/RNF168. RNF168 catalyzes K63-linked ubiquitin chains formation on histones H2A/H2AX, which is required for the recruitment of key downstream factors including 53BP1, BRCA1, and RAD51 (2). 53BP1 and BRCA1/RAD51 promote, in a cell cycle-dependent manner, DSB repair via non-homologous end joining (NHEJ) and homologous recombination (HR) respectively (3). In parallel, another ubiquitin signaling pathway, involving the Polycomb group complex PRC1, also contributes to coordinate the DSB response. PRC1 catalyzes the monoubiquitination of H2A on K119 residue (H2Aub), a critical chromatin modification involved in regulating gene expression and DNA damage/repair responses (4). It was proposed that H2Aub promotes silencing of transcription in chromatin regions flanking the DSBs, thus facilitating DNA repair (5, 6).

Several deubiquitinases (DUBs) have also been linked to DSB signaling and growing evidence suggests that deubiquitination might exert an extensive control on the recruitment and/or disassembly of proteins at the site of DNA damage. For instance, BRCC36, a K63 chain-specific DUB, regulates the recruitment of repair proteins by modulating the level of ubiquitin chains (7, 8). POH1/rpn11/PSMD14, a regulatory subunit of the 19S proteasome, deconjugates ubiquitin chains at DSB sites and promotes the recruitment of RAD51 (9). USP3 and OTUB1 have also been reported to be important for DSB signaling and repair (10, 11).

The DUB BAP1 is a tumor suppressor inactivated in various types of cancer (12). BAP1 forms multi-protein complexes with several chromatin associated-proteins notably the host cell factor 1 (HCF-1) and regulates transcription (13). The *Drosophila* BAP1, Calypso was shown to deubiquitinate H2Aub (14). Thus BAP1 might be involved in the DNA damage response by coordinating H2A ubiquitination. Notably, proteomic studies revealed BAP1 among phosphorylated proteins during DNA damage (15). Nonetheless, the role of BAP1 in DNA damage response, and more generally the mechanism of tumor suppression exerted by this DUB, remain unclear. In the current study, we identify BAP1 as a novel regulator of DSB repair, which in turn may elucidate the molecular underpinnings of its to date poorly understood tumor suppressor function.

Results

A DUB RNAi screen reveals novel regulators of HR proteins assembly at IRIF.

We sought to identify novel DUBs required for the recruitment or the dispersion of repair proteins at IRIF. A human DUB RNAi library was used to screen for DUBs whose depletion affect the number of RAD51 or BRCA1 foci at DSB sites (Fig. 1A). A twenty-four hours time point post-IR was selected for our studies, time at which 50-60 % of cells still exhibit DSB foci, thus facilitating detection of any potential increase or decrease of foci formation (Fig. 1B). Several DUBs were identified in this manner as associated with either increased, or more often decreased, RAD51 and/or BRCA1 foci (Fig. 1C, Table S1). As a proof of validity, we also identified BRCC36, USP3 and PSMD14, which have been previously reported to regulate DSB signaling by impacting RAD51 and/or BRCA1 foci formation (9, 10, 16). The novel DUB candidates whose knockdown induced a decrease in BRCA1/RAD51 foci formation include BAP1, DUB3, STAMBP, STAMBPL1 and COPS5 (Fig. 1C). We also identified candidate DUBs whose knockdown result in increased BRCA1/RAD51 foci formation, notably ZRANB1 (Fig. 1C). Immunostainings of BRCA1 and RAD51 foci following depletion of the known DSB regulator PSMD14 and the novel candidate BAP1 are shown (Fig. 1D).

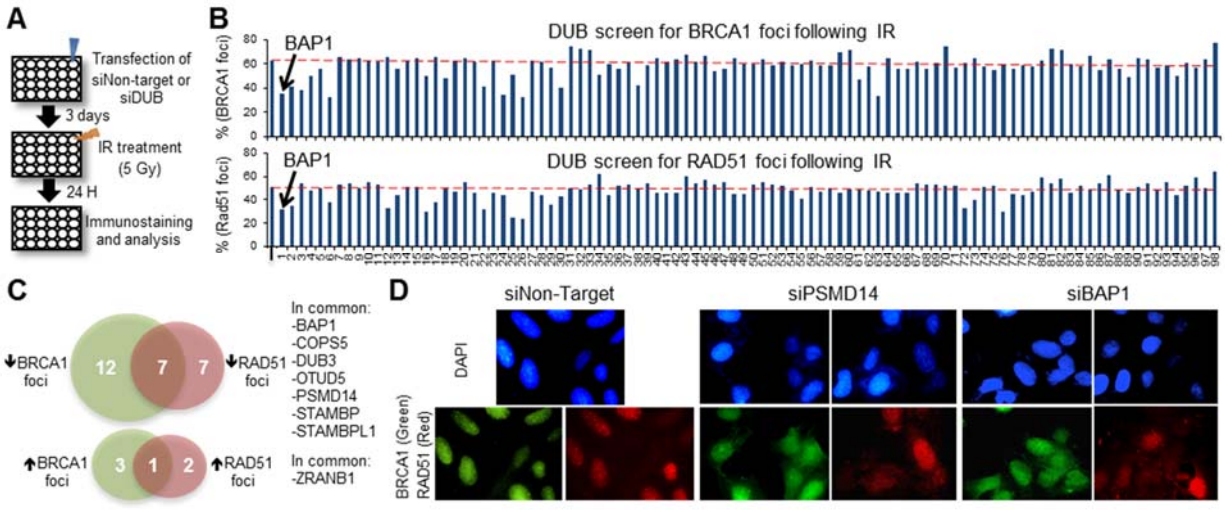

Figure 1. DUB screen identifies novel regulators of HR protein assembly at IRIF. A) Schematic representation of DUB loss-of-function screen for IRIF regulators. U2OS cells were transfected with individual siRNA pool targeting DUBs, exposed to IR and collected for staining. **B)** Graphs represent the percentage of cells with more than 10 foci of BRCA1 or RAD51. Dashed red line shows the percentage of cells with protein foci for the control sample. **C)** Venn diagrams showing DUBs associated with reduced or increased percentage of cells with foci. DUBs having the same phenotype with both BRCA1 and RAD51 foci are indicated. **D)** Representative staining of BRCA1 and RAD51 foci in PSMD14- and BAP1- depleted cells.

BAP1 promotes the recruitment of HR proteins at IRIF.

We focused on further characterization of BAP1 in the DNA damage signaling/repair processes. We used two additional shRNA constructs targeting BAP1 and found that in each case both BRCA1 and RAD51 foci were significantly reduced (Fig. S1A). Next, we monitored the dynamics of IRIF formation for several key proteins in BAP1-depleted cells. Primary human fibroblasts (LF1) were transfected either with control or BAP1 siRNA constructs, irradiated and analyzed at different time points post-damage (Fig. 2A,B and Fig. S1B). Relative to control cells, the majority of BAP1-depleted cells exhibited less than 10 BRCA1 and RAD51 foci per cell at all time points, although γH2AX focus formation was similar. It is known that 53BP1 inhibits BRCA1-mediated HR and promotes NHEJ during the G1 phase (17). However, cell cycle analysis did not reveal any substantial accumulation of cells in the G1 phase (Fig. S2A). In addition, we did not observe any significant increase in 53BP1 foci either prior to, or post, IR treatment (Fig. 2A,B). Consistent with these results, staining for foci containing auto-phosphorylated DNA-PK, a kinase required for NHEJ (18), did not reveal significant differences between BAP1-depleted and control cells (Fig. 2A,B). Interestingly, constitutive BRCA1 foci, that are distinct from IRIF, were also reduced in BAP1-depleted cells indicating that this DUB might be involved in coordinating

BRCA1 association with chromatin under normal growth conditions. Of note, BRCA1/RAD51 protein expression were not significantly different following BAP1 depletion (Fig. 2C). We note that IR-induced accumulation of the p53 tumor suppressor was essentially similar in control vs. BAP1-depleted cells (Fig. S2B). As expected, BAP1-depleted cells manifested a global increase of H2Aub (Fig. 2C and Fig. S2C).

BAP1 does not distinctly accumulate at IRIF (Fig. S1A), but might be transiently and dynamically recruited to DSBs. To assess the potential recruitment of BAP1 to DNA breaks, we fractionated cellular extracts from untreated vs. IR-treated cells and observed a consistent increase of BAP1 in the chromatin fraction in response to IR (Fig. 2D). As expected, accumulation of RAD51 and BRCA1 on chromatin was readily observed. Of note, no obvious change of global H2Aub was observed in the chromatin fractions suggesting that DNA damage-induced H2A ubiquitination marginally contribute to the global H2Aub signal. We further probed whether BAP1 is indeed recruited to DSB sites by chromatin immunoprecipitation (ChIP) (Fig. 2E). Real-time PCR quantification of immunoprecipitated chromatin by BAP1 in the vicinity of a unique DSB created by I-SceI *in vivo* indicated that BAP1 is enriched near the DSB site. Importantly, at the break site, H2Aub levels were inversely correlated with BAP1 recruitment. In contrast, no recruitment of BAP1 was detected distal to the break, where high levels of H2Aub were observed.

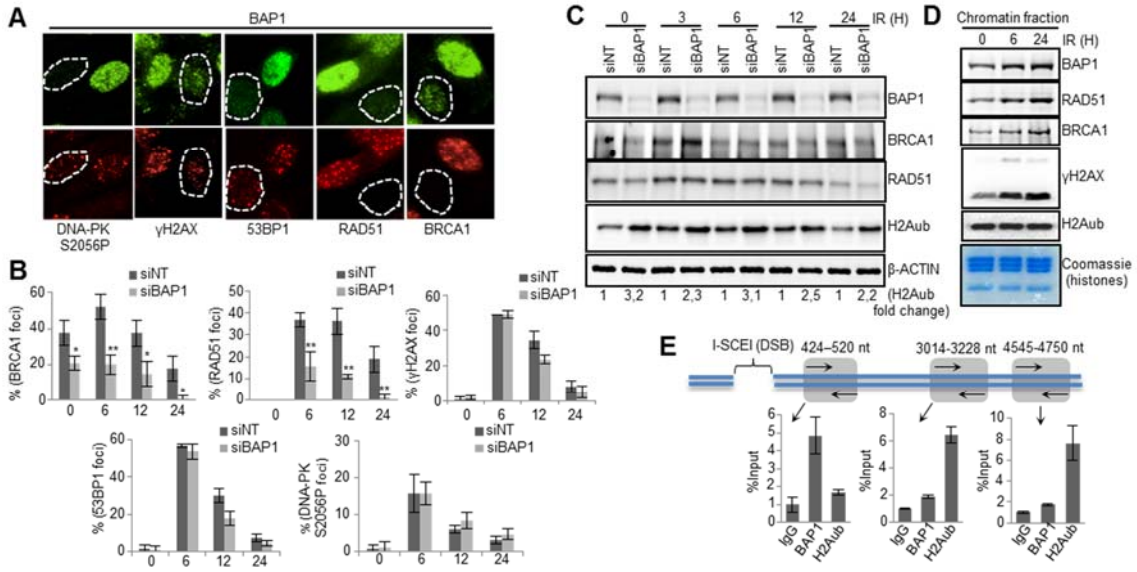

Figure 2. BAP1 promotes IRIF formation and is recruited to the site of double strand breaks (DSBs). LF1 cells were transfected with either control or BAP1 siRNA. Three days following transfection, control and BAP1 RNAi cells were combined (1:1) and treated with IR (7.5 Gy). Cells were fixed and stained for IRIF proteins in BAP1-depleted cells. Representative staining of cells at 12 hours post-IR treatment are shown in **A)** and the data are presented as mean ± SD in **B)**. Dashed white line encircles cells with effectively reduced BAP1 expression**.** Statistical analysis was performed using Student's t-test, $*P < 0.05$, $**P < 0.01$. **C)** Protein levels of BRCA1, RAD51 and other proteins were determined by western blotting. **D)** BAP1 is recruited to chromatin after DNA damage. HeLa cells were treated with IR (15 Gy) and chromatin was isolated and analyzed for the indicated proteins. **E)** BAP1 is recruited at the proximity of a single DSB in MCF7 cells carrying an I-SceI site. Top, schematic representation of the DSB created by I-SceI and the position of the primers used for the ChIP assay. Bottom, enrichment of endogenous BAP1 and H2Aub on regions at proximity to the DSB was determined by ChIP and calculated as percentage of the input. Experiments were repeated 2 times independently and real-time PCR was performed 3 times for each experiment. Data are presented as mean ± SEM.

BAP1 KO DT40 cells are sensitive to DSB-inducing agents and defective in HR-mediated sIgM gene conversion.

To further investigate the function of BAP1 in HR, we generated a conditional BAP1 KO chicken B lymphoma DT40 cells (Fig. 3A). BAP1 is highly conserved between human and chicken (Fig. S3A). Southern blot analysis indicated that both alleles were ablated (Fig. 3B). Targeting of one allele included an expression cassette with the human BAP1 cDNA flanked by two loxP sites allowing Cre-mediated excision. The DT40 Cre-1 cell line used for the KO generation stably expresses a tamoxifen inducible Cre recombinase (19). Thus, following tamoxifen treatment, >95% of the cells lose BAP1 expression (Fig. S3B). To obtain cell populations that are completely

BAP1-deficient, we isolated two single cell KO clones with complete absence of BAP1 expression (Fig. 3C). BAP1-deficient DT40 cells show, as expected, a global increase of H2Aub (Fig. 3C). Cell proliferation was also delayed in BAP1 KO cells (Fig. S4).

To assess the role of BAP1 in DSB repair, we conducted survival assays with BAP1 KO DT40 cells treated with DNA damaging agents that induce DSBs. Since BAP1 KO cells proliferate slower than WT cells (Fig. S4), cell numbers were adjusted before treatment to compensate for any potential bias that could be introduced as a consequence of unequal cell proliferation. We observed that the BAP1-/- cells are more sensitive to IR than WT cells (Fig. 3D). BAP1 KO sensitivity to IR is accompanied by an elevated level of chromosome aberrations (Fig. 3E, S5). HR-deficient cells, such as cancer cells harboring inactivating mutations in BRCA1 or BRCA2, are hypersensitive to poly (ADP-ribose) polymerase (PARP) inhibition (20). We analyzed the response of BAP1 -/- cells to the PARP inhibitor, Olaparib. Indeed, BAP1 -/- cells are strikingly sensitive to PARP inhibition relative to BAP1 +/+ and +/- cells (Fig. 3D). The high sensitivity of BAP1 KO cells to IR and Olaparib is consistent with the recently reported sensitivity of renal carcinoma-derived BAP1-deficient cells to DSB-inducing agents (21).

In order to confirm a role for BAP1 in HR, we took advantage of the fact that DT40 cells constitutively diversify their immunoglobulin loci by gene conversion (22). The DT40 Cre-1 cell line harbors a frameshift in the rearranged V segment of the Ig light chain gene (IgL), which results in a surface IgM negative (sIgM-) phenotype. This frameshift can be repaired by HR-based gene conversion in a fraction of the cells, leading to the re-expression of sIgM (Fig. 3F). Thus, the proportion of sIgM+ revertants in the population can be used to quantify gene conversion efficiency. sIgM- cells were sorted and expanded to allow gene reversion for the same number of population doublings. While approximately 8 % of BAP1 +/+ cells reverted, both BAP1 -/- clones were relatively defective (1 % and 0.5 %) whereas BAP1 +/- cells showed an intermediate phenotype (5 %) (Fig. 3F).

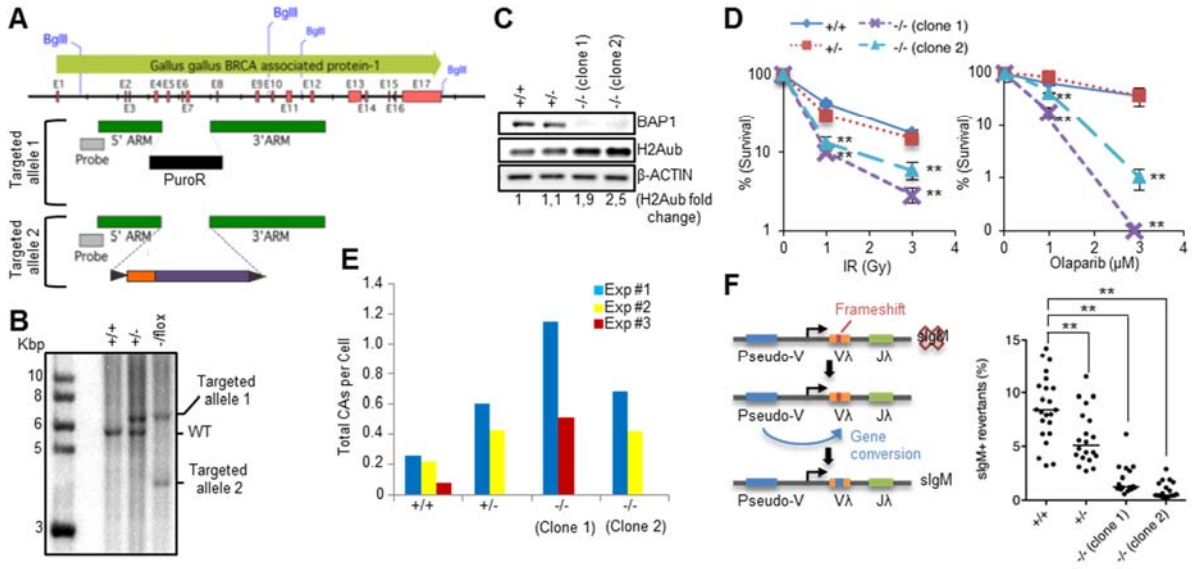

Figure 3. BAP1 KO DT40 cells are sensitive to DNA damaging agents and defective in HR-mediated gene conversion at sIgM locus. A) Schematic for the strategy used to generate BAP1 KO in DT40 cells. **B)** Southern blot confirming BAP1 targeted alleles. **C)** DT40 BAP1 KO clones 1 and 2, isolated after Cre-mediated excision of BAP1. **D)** Clonogenic survival of BAP1 KO DT40 cells treated with IR or Olaparib. Statistical analysis was performed using Student's t-test, $^{**}P < 0.01$. **E)** BAP1 KO DT40 cells have increased chromosome breaks after DNA damage. Cells were treated with IR (2 Gy) and fixed after 3.5 hours. Three independent experiments were done and chromosome aberrations (isochromatid/ chromatid gaps and breaks and radial figures) were scored in 100 cells for each experiment. Results are reported as total aberrations per cell. **F)** Left, schema representing the mechanism of sIgM reversion in DT40 cells by gene conversion. Right, sIgM- cells, isolated by flow cytometry, were expanded for 90 generations and the proportion of sIgM+ revertant cells of each sub-population was determined. The experiment was done 2 times independently and the graph compiles the results of both experiments with medians indicated by horizontal lines. Statistical analysis was performed using Student's t-test, $^{**}P < 0.01$.

Phosphorylation of BAP1 following IR treatment promotes DNA repair and cellular recovery from DNA damage.

In global proteomics studies, BAP1 was reported to be phosphorylated on S592 (ATM/ATR SQ motif) following IR treatment (15). We conducted a large-scale immunopurification of BAP1 post-IR from HeLa cells followed by mass spectrometry analysis. We identified another SQ phosphosite (S276) and novel IR-induced phosphorylation sites two of which are conserved between human and chicken (Fig 4A. Fig. S6A-C).

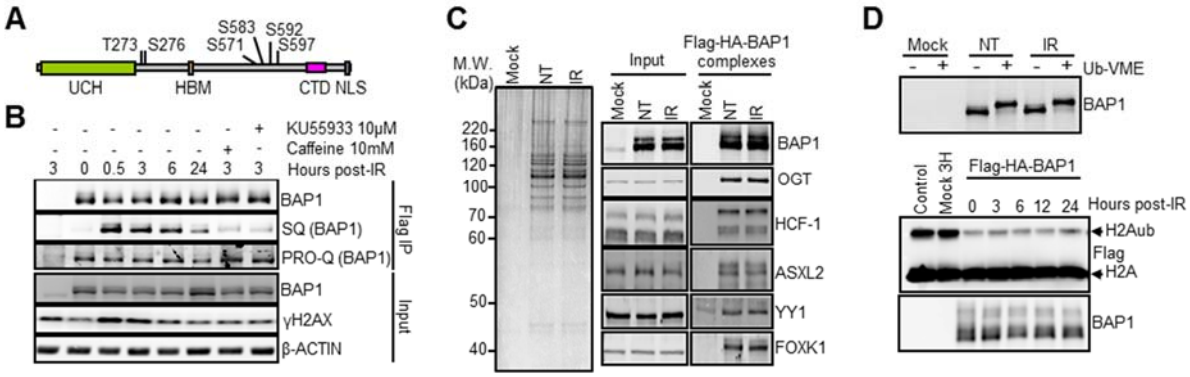

Figure 4. BAP1 is phosphorylated following DNA damage on multiple sites. A) Schematic representation of BAP1 showing its main domains and motifs: ubiquitin C-terminal hydrolase (UCH), HCF-1 binding motif (HBM), C-Terminal Domain (CTD) and nuclear localization signal (NLS) along with the identified phosphorylation sites. **B**) ATM is required for phosphorylation of BAP1. HeLa cells expressing Flag-HA-BAP1 were incubated with ATM inhibitors and then treated with IR (7.5 Gy). Immunoprecipitated BAP1 was subjected to immunoblotting or PRO-Q stain. **C**) BAP1 complexes were purified at 3 hours post-IR and subjected to silver staining (left) and western blot analysis (right). **D)** Top, purified BAP1 complexes were incubated with or without the Ub-VME probe for 2 hours and analyzed by western blot. Bottom, *in vitro* deubiquitination assay of nucleosomal H2Aub using purified BAP1 complexes. Flag-HA-BAP1 complexes were isolated at different times post-IR and incubated with nucleosomes for 4 hours.

Using an anti-pSQ(G) antibody, expected to recognize S592, we found that mutation of S592, indeed abolished the phosphorylation of BAP1 on this site (Fig S7A). Next, using this antibody, we found that inhibition of ATM with caffeine or KU-55933 resulted in decreased phosphorylation of BAP1 S592 (Fig 4B). However, ATR inhibition only resulted in a slight decrease of the S592 phosphorylation signal, while ATR-mediated CHK1 phosphorylation was abrogated (Fig. S7B). Using DNA-PK-deficient cells, we found that this kinase is not responsible for phosphorylation of BAP1 S592 following IR (Fig. S7C). Of note, HCF-1 is not required for BAP1 phosphorylation by ATM since the S592 phosphorylation signal on BAP1 lacking HBM is not decreased following IR treatment (Fig. S7D). CDKs are involved in DSB repair (23, 24), and might in concert with ATM, phosphorylate BAP1 in order to coordinate its function. Using chemical inhibitors in conjunction with the anti-pSQ(G) antibody, we did not observe a requirement of CDKs for BAP1 phosphorylation by ATM (Fig.S7E). Using the PRO-Q phosphostain, we found that the global phosphorylation state of BAP1 did not significantly change following IR treatment or CDK inhibition (Fig. S7E), likely due to the high level of constitutive phosphorylation of BAP1.

Next, we found that the stable components of the BAP1 complexes are unaffected by IR treatment (Fig. 4C and Fig. S6D). We then used an activity-directed ubiquitin probe that binds to the catalytic site of cysteine protease DUBs, and found that the probe labeled purified BAP1 from untreated and IR-treated cells with similar efficiency (Fig. 4D, top panel). Similar results were observed for endogenous BAP1 in HeLa or U2OS cells (Fig. S6E). Next, we evaluated BAP1 DUB activity toward H2A using purified nucleosomes incubated with BAP1 complexes isolated from untreated vs. IR-treated cells (Fig. 4D, bottom panel) and no significant difference was observed. Therefore, we sought to determine the importance of the IR-specific phosphosites of BAP1 for its DNA damage function in vivo. We generated a set of BAP1 phospho-mutants including the conserved residues S/T273/A and S276A, the SQ sites (S276A/S592A, SQ-MUT), and all IR-phosphorylated residues of BAP1 (6 phosphosites converted to alanines, P-MUT). These mutants were used, along with the BAP1 ΔHBM, and the BAP1 catalytically dead (C91S), to stably reconstitute the BAP1-deficient lung carcinoma cell line H226 (Fig. 5A). As previously shown (25), expression of BAP1 WT, but not the catalytic dead mutant, induced a delay in H226 cell proliferation (Fig. 5B). BAP1-deficient in interaction with HCF-1 did not affect cell proliferation. Interestingly, the BAP1 P-MUT also failed to reduce cell proliferation. To further determine the sensitivity of these cells to IR, clonogenic survival assay was performed. To exclude any potential bias that can be introduced by the unequal cell proliferation of the BAP1 stable cell lines, survival rates were normalized to untreated cells. Thus, although H226 cells expressing BAP1 WT proliferate relatively slowly, they were more resistant to IR compared to H226 cells expressing the empty vector. The BAP1 C91S, BAP1 ΔHBM and BAP1 P-MUT were the most sensitive to IR (Fig. 5C). Based on the above, we concluded that phosphorylation of BAP1 on multiple sites as well as catalytic activity are required for promoting cell survival following IR. Of note, no overt apoptosis is induced following IR treatment of H226 expressing the WT or mutant forms of BAP1 (Fig. S8B). Next, we conducted ChIP analysis and found that while the recruitment of BAP1 SQ-MUT to the site of DSB was partially decreased, the recruitment BAP1 P-MUT, was totally abolished (Fig. 5D). Of note, similar to the WT BAP1, the P-MUT assembled protein complexes (Fig S7F, G) and efficiently deubiquitinated nucleosomal H2A in vitro (Fig S7H). To directly analyze DSB repair, we determined the levels of γH2AX in H226 stably expressing BAP1 WT or mutants following IR treatment (Fig. 5E). We found that the WT BAP1, but not the C91S or the P-MUT reduced both the constitutive and IR-induced accumulation γH2AX. BAP1, but not

the C91S mutant, promoted a strong deubiquitination of H2A. Interestingly, while expression of BAP1 P-MUT also significantly promoted deubiquitination of H2A, the remaining levels of H2Aub were consistently twice higher in cells expressing the BAP1 P-MUT than the cells expressing the WT form (Fig. 5E).

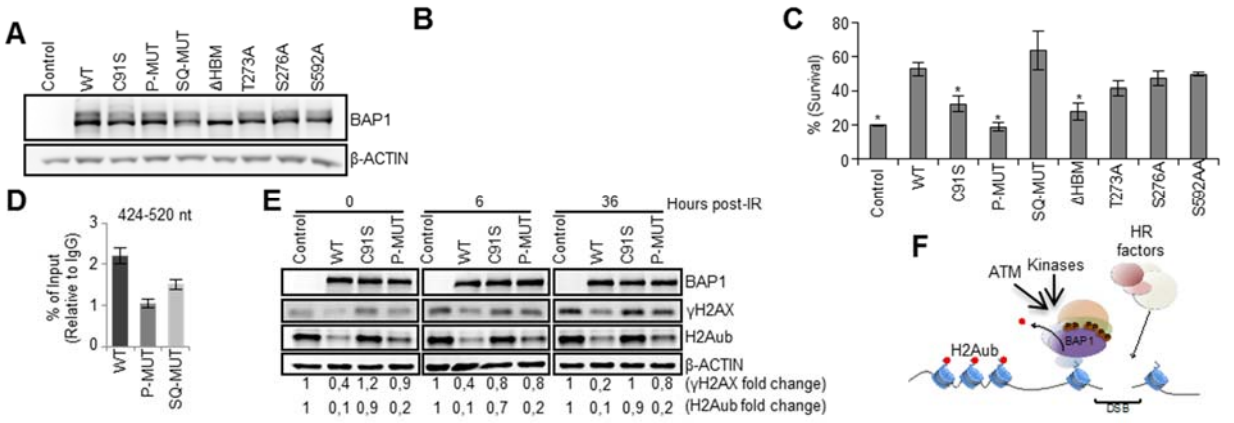

Figure 5. Phosphorylation of BAP1 following IR promotes cellular recovery from DNA damage
A) Generation of H226 cells stably expressing BAP1 WT and mutants. **B)** Effects of BAP1 WT and mutant forms on H226 cells proliferation. The same number of cells was seeded and allowed for colony formation visualized by crystal violet staining. Experiment was done at least three times. **C)** H226 cell lines were treated with IR (20 Gy) and surviving colonies were quantified by crystal violet staining and normalized to the untreated controls. Experiment was done 3 times and data are presented as mean ± SD. Statistical analysis was performed using Student's t-test, $^{**}P < 0.01$. **D)** ChIP analysis of the recruitment of phosphorylation-deficient mutants of BAP1 at the proximity of DSB in MCF7 cells carrying an I-SceI site. Experiment was repeated 2 times independently and real-time PCR was performed 3 times for each experiment. Data are presented as mean ± SEM. **E)** H226 BAP1-deficient cells that express BAP1 WT or mutant forms were treated with IR (15 Gy) and harvested for western blotting. **F)** Model for the role of BAP1 in the DSB response. BAP1 is phosphorylated after DNA damage, thus promoting its recruitment to the DSB site for H2A deubiquitination allowing the recruitment of downstream DSB signaling and repair proteins.

Discussion

We report the identification of DUB candidates that might play important roles in the cellular response to DSBs. Notably, STAMBP and COPS5 appear to be interesting candidates. These DUBs are zinc-dependent metalloproteases of the JAMM/MPN+ family which have intrinsic specificity toward K63-linked ubiquitin chains (26). Since K63 chains are highly involved in the DSB response, it is possible that these DUBs regulate DSB repair. Notably, we also identify BAP1 as a novel regulator of HR. Consistently, BAP1 KO phenocopies BRCA1 KO and RAD51

KO in DT40 cells, being both hypersensitive to DSB-inducing agents accompanied with high levels of chromosome breaks (27, 28). We emphasize that BAP1 heterozygous clones also exhibit chromosomal defects and decreased HR-mediated sIgM reversion. This suggests that BAP1 dosage is critical, which may reflect the fact that all nuclear BAP1 is contained within multi-protein complexes (13). Indeed, BAP1 heterozygous mutations are found in human tumors (29).

Several mechanisms, not necessarily mutually exclusive, might explain how BAP1 regulates HR proteins. First BAP1 depletion decreases the assembly of constitutive BRCA1 foci, which are associated with replication of heterochromatin (30). Thus, it is plausible that BAP1 depletion affects the expression of genes involved in BRCA1 recruitment on chromatin. It is also possible that the effects of BAP1 on the recruitment of HR proteins might be directly linked to its previously reported interaction with BRCA1/BARD1 (31, 32). Although our studies failed to reveal BRCA1/BARD1 as stable components of the BAP1 complexes (13), and BAP1 exerts BRCA1-independent effects on cell proliferation (25), it is possible that BRCA1 interaction with BAP1 is transient and associated with DNA damage-dependent and -independent events. Thus, the implication of BAP1 in HR revealed herein provides impetus for future studies to determine the exact significance of the interaction between BAP1 and BRCA1/BARD1.

On the other hand, to facilitate DNA repair, transcription appears to be blocked at DSB by PRC1-mediated H2A ubiquitination (5). Accordingly, DUBs that remove H2Aub at DSBs are expected to inhibit HR. However, we observed the opposite effect, i.e., the H2A DUB BAP1 promotes HR. In fact, the BAP1 complex might act in concert with the PRC1 complex to promote dynamic ubiquitination/deubiquitination of H2A thereby ensuring the proper dosage of this modification at the site of DSB. Based on our ChIP analysis for BAP1 and H2Aub near the DSB site, it is possible that BAP1 deubiquitinates H2A in the proximity of the DSB site to increase chromatin accessibility at this specific region to allow, e.g., DNA resection during HR. Thus, BAP1 depletion causing an increase of H2Aub might interfere with specific chromatin and/or histone modifications events at DSBs, which might explain the observed defect in HR. Moreover, it is possible that more than one H2A DUB is involved in the signaling at DSBs. Some DUBs might assist in chromatin organization to promote DNA repair, whereas others could play a role in foci resolution. Consistent with this model, it was reported that another H2A DUB, USP16, regulates the level of this histone modification to control the derepression of transcription at DSB sites (6).

In support of BAP1 function in the cellular response to DSBs, we showed that its phosphorylation is required for promoting survival after IR. Since BAP1 phosphorylation does not directly impact intrinsic BAP1 DUB activity, it is possible that it rather promotes BAP1 interaction with other factors to facilitate the recruitment to DSBs where it regulates H2Aub levels. Indeed, the residual levels of H2Aub are consistently higher in H226 cells expressing the BAP1 P-MUT than the WT form, probably reflecting an inability of the mutant to deubiquitinate the small pool of H2Aub associated with DSBs. We also note that several sites of BAP1 are phosphorylated following IR treatment, including SQ and non-SQ sites indicating that BAP1 is phosphorylated by multiple DNA damage-responsive kinases. Thus, BAP1 involvement in the DNA damage response might be more complex than anticipated. Indeed, the use of BAP1 P-MUT to reconstitute BAP1-deficient H226 cells indicated that the decrease of cell proliferation following re-introduction of WT BAP1 depends on its phosphorylation, even in the absence of exogenously inflicted DNA damage. The effect of BAP1 phosphorylation on cell proliferation likely reflects a role of this DUB in DNA damage-induced checkpoint responses. In fact, normally growing H226 cells have elevated levels of γH2AX and a severe genomic instability (Fig. S8C,D), indicative of high rates of spontaneous DNA damage in these BAP1-deficient cells. These cancer cells must necessarily harbor defects in DNA damage checkpoints that allow them to proliferate under such genomic instability. Therefore, the expression of BAP1 WT in H226 cells might re-activate certain DNA damage checkpoints thus causing decreased cell proliferation.

In summary, we provide strong evidence indicating that BAP1 is a DNA damage signaling and repair enzyme (Fig. 5F). Loss of BAP1 is expected to decrease HR, an error free repair mechanism. Under such conditions, cells might become much more reliant on NHEJ, an error-prone repair mechanism, resulting in the net accumulation of mutations and chromosomal aberrations that cause genomic instability. Moreover, as a consequence of BAP1 inactivation, defects in checkpoint(s) signaling could promote the survival of cells harboring damaged DNA, thus driving neoplastic transformation.

Materials And Methods

RNAi, **gene targeting and phenotypic analysis.**

Cells were transfected with siRNA or shRNA targeting DUBs or non-target control and harvested as indicated. The DT40 Cre-1 cell line was used to generate the BAP1 KO. Clonogenic

survival assay, cytogenetic analysis, sIgM gene conversion assay, preparation of cell extracts and chromatin fraction for western blotting were done as described in the SI text.

Immunofluorescence and flow cytometry analysis.

Cells were immunostained as previously described (33). Flow cytometry determination of DNA content, BAP1, phospho histone H3 serine 10, and BrdU incorporation were conducted using LSRII flow cytometer and data were processed with FlowJo V887 software.

Chromatin immunoprecipitation on I-SceI-induced double strand break (DSB).

Induction of a single DSB following I-SceI expression, ChIP experiments and real-time PCR were done as described in the SI text.

Purification of BAP1 complexes and identification of phosphorylation sites.

HeLa S3 cells expressing stably Flag-HA-BAP1 or the empty vector were treated with IR and used for immunopurification and Mass spectrometry. Additional details are provided in the SI text.

Deubiquitination assays.

Ubiquitin-Vinyl Methyl Ester (Ub-VME) probe labeling and *In vitro* H2Aub deubiquitination assay were done as described in the SI text.

Acknowledgements. This work was supported by grants from the Cancer Research Society to EBA, the Canadian Institutes of Health Research (CIHR) to JYM, the Canadian Cancer Society Research Institute (grant #700348) to JMDN, and the Natural Sciences and Engineering Research Council of Canada to ED. EBA is a scholar of the CIHR and Le Fonds de la Recherche en Santé du Québec (FRSQ). JYM is a FRSQ National investigator. JMDN is supported by a Canada research chair tier 2. HY was supported by a PhD scholarship from the Cole foundation and the CIHR. We want to thank Huib Ovaa for kindly providing us the DUB probe and Sylvie Lavallée for cytogenetic analysis.

References

1. HARPER JW & ELLEDGE SJ (2007) THE DNA DAMAGE RESPONSE: TEN YEARS AFTER. *MOL CELL* 28(5):739-745.
2. PRICE BD & D'ANDREA AD (2013) CHROMATIN REMODELING AT DNA DOUBLE-STRAND BREAKS. *CELL* 152(6):1344-1354.
3. CHAPMAN JR, TAYLOR MR, & BOULTON SJ (2012) PLAYING THE END GAME: DNA DOUBLE-STRAND BREAK REPAIR PATHWAY CHOICE. *MOL CELL* 47(4):497-510.
4. ZHOU W, WANG X, & ROSENFELD MG (2009) HISTONE H2A UBIQUITINATION IN TRANSCRIPTIONAL REGULATION AND DNA DAMAGE REPAIR. *INT J BIOCHEM CELL BIOL* 41(1):12-15.
5. CHAGRAOUI J, HEBERT J, GIRARD S, & SAUVAGEAU G (2011) AN ANTICLASTOGENIC FUNCTION FOR THE POLYCOMB GROUP GENE BMI1. *PROC NATL ACAD SCI U S A* 108(13):5284-5289.
6. SHANBHAG NM, RAFALSKA-METCALF IU, BALANE-BOLIVAR C, JANICKI SM, & GREENBERG RA (2010) ATM-DEPENDENT CHROMATIN CHANGES SILENCE TRANSCRIPTION IN CIS TO DNA DOUBLE-STRAND BREAKS. *CELL* 141(6):970-981.
7. SHAO G*, ET AL.* (2009) THE RAP80-BRCC36 DE-UBIQUITINATING ENZYME COMPLEX ANTAGONIZES RNF8-UBC13-DEPENDENT UBIQUITINATION EVENTS AT DNA DOUBLE STRAND BREAKS. *PROC NATL ACAD SCI U S A* 106(9):3166-3171.
8. COOPER EM*, ET AL.* (2009) K63-SPECIFIC DEUBIQUITINATION BY TWO JAMM/MPN+ COMPLEXES: BRISC-ASSOCIATED BRCC36 AND PROTEASOMAL POH1. *EMBO J*.
9. BUTLER LR*, ET AL.* (2012) THE PROTEASOMAL DE-UBIQUITINATING ENZYME POH1 PROMOTES THE DOUBLE-STRAND DNA BREAK RESPONSE. *EMBO J* 31(19):3918-3934.
10. NICASSIO F*, ET AL.* (2007) HUMAN USP3 IS A CHROMATIN MODIFIER REQUIRED FOR S PHASE PROGRESSION AND GENOME STABILITY. *CURR BIOL* 17(22):1972-1977.
11. NAKADA S*, ET AL.* (2010) NON-CANONICAL INHIBITION OF DNA DAMAGE-DEPENDENT UBIQUITINATION BY OTUB1. *NATURE* 466(7309):941-946.
12. CARBONE M*, ET AL.* (2013) BAP1 AND CANCER. *NAT REV CANCER* 13(3):153-159.
13. YU H*, ET AL.* (2010) THE UBIQUITIN CARBOXYL HYDROLASE BAP1 FORMS A TERNARY COMPLEX WITH YY1 AND HCF-1 AND IS A CRITICAL REGULATOR OF GENE EXPRESSION. *MOL CELL BIOL*. 30, 5071-5085.
14. SCHEUERMANN JC*, ET AL.* (2010) HISTONE H2A DEUBIQUITINASE ACTIVITY OF THE POLYCOMB REPRESSIVE COMPLEX PR-DUB. *NATURE* 465(7295):243-247.

15. STOKES MP, *ET AL.* (2007) PROFILING OF UV-INDUCED ATM/ATR SIGNALING PATHWAYS. *PROC NATL ACAD SCI U S A* 104(50):19855-19860.
16. CHEN X, ARCIERO CA, WANG C, BROCCOLI D, & GODWIN AK (2006) BRCC36 IS ESSENTIAL FOR IONIZING RADIATION-INDUCED BRCA1 PHOSPHORYLATION AND NUCLEAR FOCI FORMATION. *CANCER RES* 66(10):5039-5046.
17. ESCRIBANO-DIAZ C, *ET AL.* (2013) A CELL CYCLE-DEPENDENT REGULATORY CIRCUIT COMPOSED OF 53BP1-RIF1 AND BRCA1-CTIP CONTROLS DNA REPAIR PATHWAY CHOICE. *MOL CELL* 49(5):872-883.
18. CHEN BP, *ET AL.* (2005) CELL CYCLE DEPENDENCE OF DNA-DEPENDENT PROTEIN KINASE PHOSPHORYLATION IN RESPONSE TO DNA DOUBLE STRAND BREAKS. *J BIOL CHEM* 280(15):14709-14715.
19. ARAKAWA H, LODYGIN D, & BUERSTEDDE JM (2001) MUTANT LOXP VECTORS FOR SELECTABLE MARKER RECYCLE AND CONDITIONAL KNOCK-OUTS. *BMC BIOTECHNOL* 1:7.
20. BRYANT HE, *ET AL.* (2005) SPECIFIC KILLING OF BRCA2-DEFICIENT TUMOURS WITH INHIBITORS OF POLY(ADP-RIBOSE) POLYMERASE. *NATURE* 434(7035):913-917.
21. PENA-LLOPIS S, *ET AL.* (2012) BAP1 LOSS DEFINES A NEW CLASS OF RENAL CELL CARCINOMA. *NAT GENET* 44(7):751-759.
22. WINDING P & BERCHTOLD MW (2001) THE CHICKEN B CELL LINE DT40: A NOVEL TOOL FOR GENE DISRUPTION EXPERIMENTS. *J IMMUNOL METHODS* 249(1-2):1-16.
23. HUERTAS P, CORTES-LEDESMA F, SARTORI AA, AGUILERA A, & JACKSON SP (2008) CDK TARGETS SAE2 TO CONTROL DNA-END RESECTION AND HOMOLOGOUS RECOMBINATION. *NATURE* 455(7213):689-692.
24. JOHNSON N, *ET AL.* (2009) CDK1 PARTICIPATES IN BRCA1-DEPENDENT S PHASE CHECKPOINT CONTROL IN RESPONSE TO DNA DAMAGE. *MOL CELL* 35(3):327-339.
25. VENTII KH, *ET AL.* (2008) BRCA1-ASSOCIATED PROTEIN-1 IS A TUMOR SUPPRESSOR THAT REQUIRES DEUBIQUITINATING ACTIVITY AND NUCLEAR LOCALIZATION. *CANCER RES* 68(17):6953-6962.
26. KOMANDER D, CLAGUE MJ, & URBE S (2009) BREAKING THE CHAINS: STRUCTURE AND FUNCTION OF THE DEUBIQUITINASES. *NAT REV MOL CELL BIOL* 10(8):550-563.
27. VANDENBERG CJ, *ET AL.* (2003) BRCA1-INDEPENDENT UBIQUITINATION OF FANCD2. *MOL CELL* 12(1):247-254.
28. SONODA E, *ET AL.* (1998) RAD51-DEFICIENT VERTEBRATE CELLS ACCUMULATE CHROMOSOMAL BREAKS PRIOR TO CELL DEATH. *EMBO J* 17(2):598-608.

29. DEY A, *ET AL.* (2012) LOSS OF THE TUMOR SUPPRESSOR BAP1 CAUSES MYELOID TRANSFORMATION. *SCIENCE* 337(6101):1541-1546.
30. PAGEAU GJ & LAWRENCE JB (2006) BRCA1 FOCI IN NORMAL S-PHASE NUCLEI ARE LINKED TO INTERPHASE CENTROMERES AND REPLICATION OF PERICENTRIC HETEROCHROMATIN. *J CELL BIOL* 175(5):693-701.
31. JENSEN DE, *ET AL.* (1998) BAP1: A NOVEL UBIQUITIN HYDROLASE WHICH BINDS TO THE BRCA1 RING FINGER AND ENHANCES BRCA1-MEDIATED CELL GROWTH SUPPRESSION. *ONCOGENE* 16(9):1097-1112.
32. NISHIKAWA H, *ET AL.* (2009) BRCA1-ASSOCIATED PROTEIN 1 INTERFERES WITH BRCA1/BARD1 RING HETERODIMER ACTIVITY. *CANCER RES* 69(1):111-119.
33. HAMMOND-MARTEL I, *ET AL.* (2010) PI 3 KINASE RELATED KINASES-INDEPENDENT PROTEOLYSIS OF BRCA1 REGULATES RAD51 RECRUITMENT DURING GENOTOXIC STRESS IN HUMAN CELLS. *PLOS ONE* 5(11):E14027.

Supplemental Materials And Methods

Cell culture, plasmids, antibodies and chemicals

Primary human lung fibroblasts LF1, BAP1-deficient human lung squamous carcinoma NCI-H226, cervical cancer HeLa, osteosarcoma U2OS, breast cancer MCF7 carrying an I-SceI cassette and HEK293T cells were cultured in Dulbecco's modified Eagle's medium (DMEM) supplemented with 10 % fetal bovine serum (FBS) and penicillin/streptomycin (Pen/Strep) in 5% CO_2 at 37ºC. Chicken bursa lymphoma DT40 Cre-1 (1) were cultured in Roswell Park Memorial Institute (RPMI) medium supplemented with 10% FBS, 1% chicken serum, 100 μM β-mercaptoethanol and Pen/Strep in 5% CO_2 at 40 ºC. Cervical cancer HeLa S3 cells used for complex purification were cultured in Minimum Essential Media (MEM) supplemented with 5% FBS/ Pen/Strep in 5% CO_2 at 37 ºC.

Cloning of human BAP1 WT and C91S were described (2). BAP1 mutant in phosphorylation sites (P-MUT: T273A, S276A, S571A, S583A, S592A and S597A) was generated using gene synthesis (BioBasic). Other mutants of BAP1 were generated by site directed mutagenesis. BAP1 (WT and mutants) were then subcloned into pENTR D-Topo plasmid (Life Technologies) and recombined into pMSCV-Flag/HA-IRES-Puro. The targeted sequences of shBAP1 #1 and #2 are GGCTGAGATTGCAAACTATGAG and GGTTTCAGCCCTGAGAGCAAAG respectively (2). pCDNA.3 Flag-H2A plasmid was described (3).

Monoclonal anti-BAP1 (C4), polyclonal anti-BAP1 (H300), monoclonal anti-BRCA1 (D9), polyclonal anti-RAD51 (D92), polyclonal anti-53BP1 (H300), polyclonal anti-YY1 (H414), monoclonal anti-p53 (DO.1), polyclonal anti-OGT (H300) antibodies were purchased from Santa Cruz. Polyclonal anti-ubiquityl-histone H2A lysine 119 (#8240), polyclonal anti-phospho histone H3 serine 10 (#3377), Anti-pSQ (#6966), pCHK1 S345 (#2348) and normal rabbit IgG (2729) are from Cell Signaling. Monoclonal anti-phospho-H2A.X serine 139 (05-636) and monoclonal anti-β-actin (C4) antibodies were purchased from Millipore. Polyclonal anti-HCF-1 (A301-400A) and polyclonal anti-ASXL2 (A302-037A) were purchased from Bethyl laboratories. Monoclonal anti-p21 (556431) was purchased from BD Pharmingen. Monoclonal anti-Flag (M2) was purchased from Sigma and monoclonal anti-HA (HA11) was purchased from Covance. Polyclonal anti-phospho DNA-PK S2056 (ab18192) is from Abcam. Mouse polyclonal anti-FOXK1 antibody was kindly provided by Dr. Xiao-Hua Li (Southwestern University of Texas). Fluorophore-coupled

secondary antibodies anti-mouse/anti-rabbit Alexa Fluor 488 and Alexa Fluor 596 were purchased from Life Technologies. The PI3-Kinase inhibitor caffeine (4), was purchased from Sigma-Aldrich. The ATM inhibitor KU-55933 (5), was purchased from Selleck Chemicals. The ATR inhibitor VE-821 (6), was purchased from Selleck Chemicals. The CDK1 inhibitor RO-3306 (7), was purchased from Calbiochem. The CDK1, CDK2 and CDK5 inhibitor Roscovitine (8), was purchased from Cell Signaling. The CDK2 inhibitor Purvalanol A (9) and GW8510 (10), were purchased from Abcam and Sigma-Aldrich respectively. The CDK2, CDK1 and and CDK4 inhibitor SU9516 (11), was purchased from Tocris Bioscience

siDUB screen

U2OS cells were transfected with individual siRNA pool (consisting of 4 pooled siRNA oligonucleotides) targeting DUBs (ON-TARGETplus® SMARTpool® siRNA Library - Human Deubiquitinating Enzymes) or the non-target control from Dharmacon (G-104705, Lot 10138) using Lipofectamine 2000 (Life Technologies). Three days post-transfection, cells were exposed to 5 Gy of ionizing radiation (IR) and collected 24 hours later for immunostaining. Approximately 100 cells were counted for each condition and cells with more than 10 DNA damage foci were considered as positives.

RNAi and immunoblotting

For siRNA experiments, we used ON-TARGETplus® SMARTpool® siRNA against human BAP1 and non-target control (Dharmacon, Thermo Scientific). Transfections of siRNA or shRNA constructs were done using Lipofectamine 2000 (Life Technologies).

Total cell extracts were prepared in lysis buffer (25 mM Tris-HCl, 1% SDS) and protein concentration was determined by bicinchoninic acid (BCA) assay. SDS-PAGE and western blotting were conducted according to standard procedures. The band signals were acquired using the LAS-3000 LCD camera coupled to the MultiGauge software (Fuji, Standford, CT)

BAP1 gene targeting

The DT40 Cre-1 cell line harboring the fusion protein of Cre and the hormone-binding domain of the mutated estrogen receptor (Mer) (1) was used to generate the BAP1 conditional KO. Gene targeting and southern blotting were done essentially as previously described (12). The targeting constructs were assembled in pBluescript II. The first BAP1 allele was targeted with a puromycin resistance cassette. The second allele was replaced by an insert flanked with two loxP sites that contained the human *BAP1* gene under the chicken beta-actin promoter and a blasticidin

S resistance cassette. Antibiotic resistance cassettes were previously described (1). Positive clones were screened by southern blot on BglII digested genomic DNA with probes generated by PCR with the following primers: TCCCGCTCAACTGAAGTTCT and CCACAAATGCTCTGAGTGGA. To excise the human *BAP1* gene from the conditional BAP1 KO cells, cells were treated with 50 nM of 4-hydroxytamoxifen for 4 days. Cells were then sub-cloned to isolate BAP1 constitutive KO clones.

Clonogenic survival assay

DT40 cells were seeded on plates containing DMEM with 1.5% methylcellulose, 10% FBS, 1% chicken serum, 100 μM β-mercaptoethanol and Pen/Strep. For the IR treatment, the cells were exposed to a cesium-137 source (Gamma Cell; Atomic Energy Canada) at the indicated doses prior seeding. For the Olaparib treatment, cells were seeded in the methylcellulose media containing the indicated concentrations of Olaparib (Selleck chemical). Cells were incubated at 40 ^{o}C for 20-30 days to allow colony formation.

H226 stable cell lines expressing Flag-HA-BAP1 WT, C91S or P-MUT were treated with indicated doses of IR and incubated for 5-7 days. The surviving colonies were washed with phosphate-buffered saline (PBS) and fixed with 3 % paraformaldehyde for 20 minutes. Cells were then stained with 0.2 % crystal violet for 10 minutes followed by several washes with PBS. Retained staining was then extracted with 10 % acetic acid and the optical density (OD) of the extracted dye was determined by spectrophotometry at 540 nm. The population survival rate is determined by the average ratio between the OD of the treated sample and the untreated control sample.

Chromosome aberrations analysis

DT40 cells were treated with 2 Gy of IR and fixed after 3.5 hours. To enrich cells in metaphase, cells were treated with 100 ng/mL of colcemid for 2 hours prior fixation, metaphase spreading and Giemsa staining. Analysis was performed on 100 metaphases of each population. Chromosome abnormalities (isochromatid/ chromatid gaps and breaks and radial figures) were scored.

sIgM phenotype conversion assay

After 20 min incubation with anti-chicken IgM-FITC (Bethyl #A30-102F, 1:800) in phosphate-buffered saline (PBS) containing 2% bovine serum albumin (BSA), DT40 cells were sorted by flow cytometry to obtain homogeneous sIgM negative (sIgM-) populations. Multiple cell populations were cultured in 24-well plates (100 000 cells per well) for 90 doubling times (splitting 1:2 every 1 or 2 days). Their sIgM phenotype is determined by flow cytometry with the same staining procedure used for cell sorting.

Immunofluorescence

Cells were immunostained as previously described (2). The nuclei were stained with 4',6-diamidino-2-phenylindole (DAPI). Images were acquired using the Zeiss Axio Imager Z.2 microscope, Zeiss Acroplan/N-Acroplan 40X/0.65 -0.17 objective and AxioCAM MRm camera.

Flow cytometry analysis

DNA content of cells was analyzed essentially as described (13). Briefly, cells were harvested by trypsinization and fixed with 70 % ethanol. After PBS wash, cells were treated with 100 µg/ml RNase A for 30 min at 37 °C and stained with 50 µg/ml propidium iodide.

DT40 cells intracellular staining for anti-BAP1 (monoclonal) and anti-phospho histone H3 serine 10 was done as follows. Around $1X10^6$ cells were fixed with 70 % of ethanol, blocked with 1 % BSA in PBS and incubated with the indicated primary antibody for 1.5 hours followed by incubation with Alexa Fluor 488-coupled secondary antibody for 1 hour. Between the antibodies incubation, cells were washed with PBS and PBS containing 1 % BSA. DNA was co-stained as described above.

BrdU incorporation in DT40 cells was determined using $1X10^6$ fixed cells following incubation with 20 µM of BrdU for 30 min. DNA of the fixed cells was denatured using HCl 4N/ Triton 0.5 % for 30 min and neutralized by 100 mM Borax pH 8.5. Cells were then blocked with 1 % BSA in PBS followed by incubation with anti-BrdU antibody coupled to Alexa 488 (clone MoBU-1, 1:200, Life Technologies) for 1 hour. DNA was co-stained as described above.

Cells were analyzed using a LSRII flow cytometer (Becton Dickinson) and data were processed with FlowJo V887 software (Tree Star, Inc.).

Chromatin immunoprecipitation on I-SceI-induced double strand break (DSB)

Induction of a single DSB following I-SceI expression, ChIP experiments and real-time PCR were done essentially as previously described (14). Polyclonal anti-BAP1 (H300), polyclonal anti-ubiquitinated histone H2A lysine 119 (DC27C4) and normal rabbit IgG (2729) were used for ChIP experiments. Primers for ChIP experiments were described earlier (15). ChIP on ectopically expressed Flag-HA-BAP1 or mutants was conducted using anti-Flag antibody. First BAP1 constructs were transfected using X-tremeGENE 9 (Roche, #06365779001), then electroporated 24 hours later with the pCAG-ISCEI plasmid before harvesting. Values were calculated as percentage of the input relative to the IgG control, which is set to 1.

Chromatin fractionation

Chromatin fraction was obtained as previously described (16). Briefly, HeLa cells were treated with 15 Gy of IR and fractionated with 50 mM Tris-HCl pH 7.3, 50 mM NaCl, 0.5% Triton, 5 mM EDTA, 50 mM NaF, 10 mM beta-glycerophosphate, 1 mM Na_3VO_4, 10 mM 2-mercaptoethanol, 1 mM phenylmethylsulfonyl fluoride (PMSF) and anti-protease cocktail (Sigma). The pellet fraction (the chromatin) was washed several times with the fractionation buffer before sonication. Proteins were quantified and used for western blotting.

Purification of BAP1-associated proteins following DNA damage and identification of phosphorylation sites

Around 3 X 10^9 HeLa S3 cells expressing stably Flag-HA-BAP1 or the empty vector (2) were treated with 10 Gy of IR. Total extracts were prepared 3 hours post-treatment by lysing cells with 50 mM Tris-HCl pH 7.3, 50 mM NaCl, 0.5% NP-40, 50 mM NaF, 10 mM beta-glycerophosphate, 1 mM Na_3VO_4, 10 mM 2-mercaptoethanol, 1 mM PMSF and anti-protease cocktail (Sigma). Lysates were clarified by centrifugation at 20 000g for 30 min and filtration through 0.45 μM filter. Tandem purification (Flag-HA) was done essentially as previously described (17). Mass spectrometry analysis was provided by the Taplin facility at Harvard Medical School (Boston). PRO-Q Diamond phosphoprotein gel stain was purchased from Life Technologies. The polyacrylamide gel was fixed and stained according to the manufacturer's protocol.

Ub-VME hybridization assay

Ubiquitin-Vinyl Methyl Ester (Ub-VME) probe purification and hybridization assay was done as previously described (18). Purified BAP1 complexes or total cell extract were incubated with Ub-VME for 2 hours at room temperature. Reactions were stopped by adding Laemmli buffer and analysed by western blotting.

In vitro ubH2A deubiquitination assay

Native nucleosomes were isolated from HEK293T cells transfected with pCDNA.3 Flag-H2A. As previously described with some modifications, soluble chromatin fraction was obtained by nucleosomes digestion with micrococcal nuclease (MNase, Sigma) (19). Cells were lysed in 420 buffer (50 mM Tris-HCl pH 7.3, 420 mM NaCl, 1% NP-40, 1 mM PMSF, protease inhibitor cocktail (Sigma), and 20 mM of N-ethylmaleimide (NEM) to block any DUB activity associated with chromatin. After centrifugation, the chromatin pellet was washed twice with the same buffer followed by two washes using MNase buffer (20 mM Tris-HCl pH 7.3, 100 mM KCl, 2 mM $MgCl_2$, 1 mM $CaCl_2$, 0.3 M sucrose, 0.1% NP-40, 1 mM PMSF and protease inhibitor cocktail). Chromatin was then treated with 3 U/ml MNase for 10 min at room temperature and the reaction was stopped with 5 mM EDTA. Following high-speed centrifugation, the soluble chromatin fraction was incubated overnight at 4 °C with Flag M2 agarose beads (Sigma). Beads were then washed several times with EB 300 buffer (50 mM Tris-HCl pH 7.3; 5 mM EDTA; 300 mM NaCl; 10 mM NaF; 1% NP-40; 1 mM PMSF; 1 mM dithiothreitol (DTT); protease inhibitors cocktail (Sigma)) containing 20 mM NEM, followed by several washes with EB 300 buffer without NEM. Beads bound nucleosomes were then eluted with Flag peptides (0.2 μg/ml). The isolated nucleosomes were used for the *in vitro* deubiquitination assay with Flag-HA BAP1 complexes purified at different times post-IR treatment (5 Gy). The DUB reaction was carried in (50 mM Tris-HCl, pH 7.3; 1mM MgCl2; 50 mM NaCl; 1 mM DTT) for 4 hours at 37°C, stopped by adding 2X Laemmli buffer and analyzed by western blotting.

Supporting Information

Table S1: List of DUBs associated with decreased or increased IRIF formation.

BRCA1 foci		RAD51 foci	
DUB name[a]	% cells with foci	DUB name[a]	% cells with foci
Control	63	Control	51
BAP1	35	BAP1	32
COPS5	41	COPS5	35
CXORF53 (BRCC36)	38	DUB3	38
CYLD	50	OTUB1	33
DUB3	33	OTUD5	30
OTUD5	50	OTUD6B	38
OTUD7	48	PSMD14	31
PSMD14	41	STAMBP	25
SENP2	34	STAMBPL1	23
STAMBP	51	UBL4	36
STAMBPL1	32	USP24	41
UBL5	40	USP4	33
UCHL1	51	USP40	40
UEVLD	42	USP43	30
USP15	53		
USP3	47		
USP31	33		
USP6	49		
C13ORF22	50		
DUB name[b]	% cells with foci	DUB name[b]	% cells with foci
Control	63	Control	51
UBR1	75	UCHL1	62
UBTD1	73	USP53	61
USP38	75	ZRANB1	64
ZRANB1	78		

Only DUBs associated with a decrease[a] (BRCA1 foci ≤ 53%, RAD51 foci ≤ 41%) or increase[b] (BRCA1 foci ≥ 73%, RAD51 foci ≥ 61%) of at least 10% of cells with foci compared to the control are considered. The 10% cut-off was chosen to maximize chances of hit identification, taking in account that transfection efficiency was not determined due to lack of specific antibodies for all DUBs. Cells with more than 10 foci of the indicated protein were counted.

Supplemental Figures

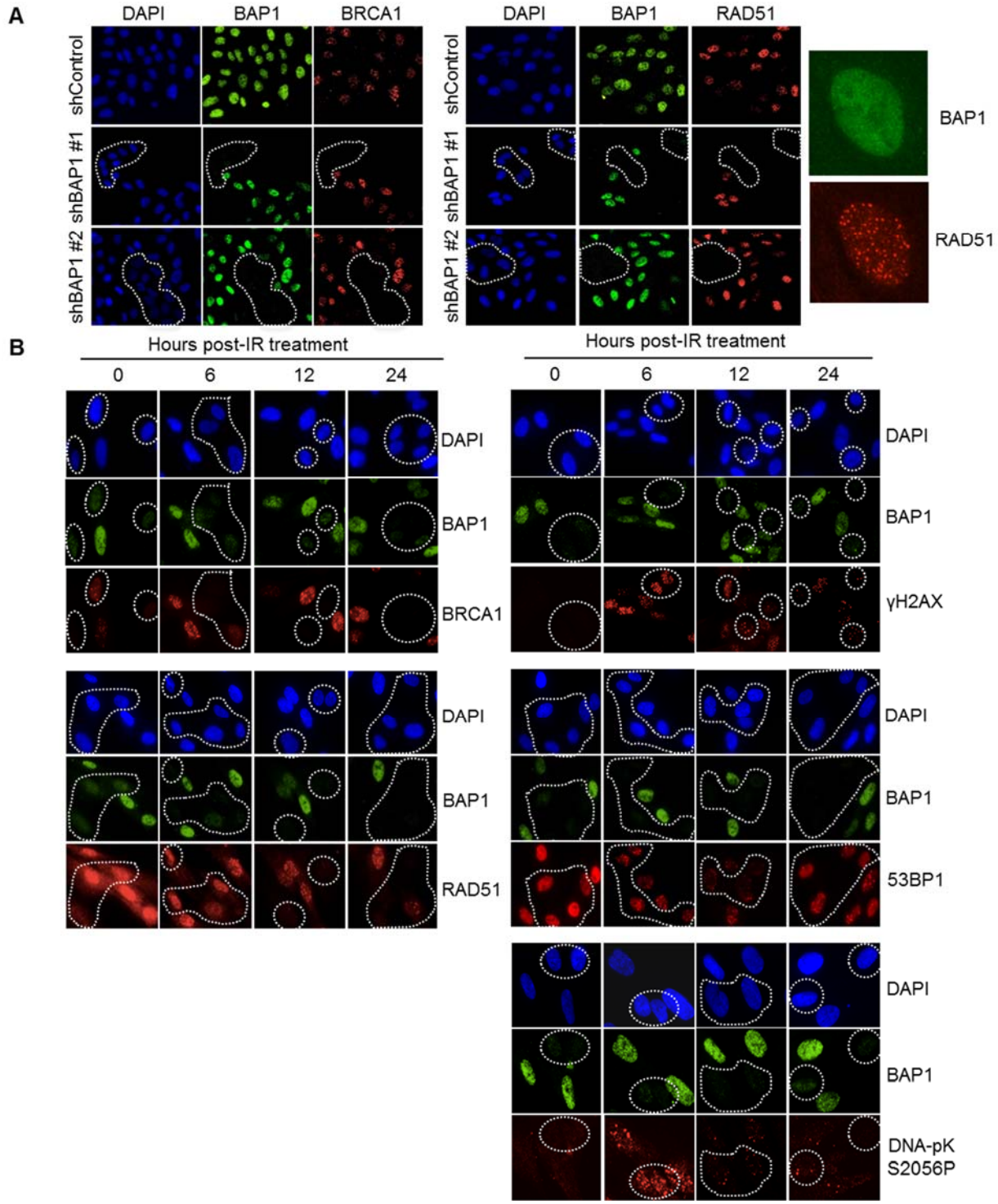

Figure S1. A) BAP1 depletion using shRNA constructs impairs IRIF formation. U2OS cells were transfected with two different shRNA constructs against BAP1 (shBAP1 #1 and shBAP1 #2) and treated with IR (7.5 Gy). 16 hours post-treatment, cells were fixed for immunostaining of the indicated proteins. Representative images of the experiment are shown. White dashed lines encircle the BAP1-depleted cells. **B) BAP1 promotes homologous recombination foci (BRCA1 and RAD51) formation after DNA damage.** Original images of Figure 2A are shown. Human fibroblast LF1 cells transfected with control or BAP1 siRNA constructs were combined (1:1) and treated with IR (7.5 Gy). Cells were fixed at different time points post-IR (0h, 6h, 12h and 24h) and subjected to immunostaining of the indicated proteins. BAP1-depleted cells were identified by decreased BAP1 signal and are encircled by white dashed lines. Note that BAP1 RNAi-treated cells were mixed with the control RNAi-treated cells in these immunofluorescence experiments to facilitate the comparison.

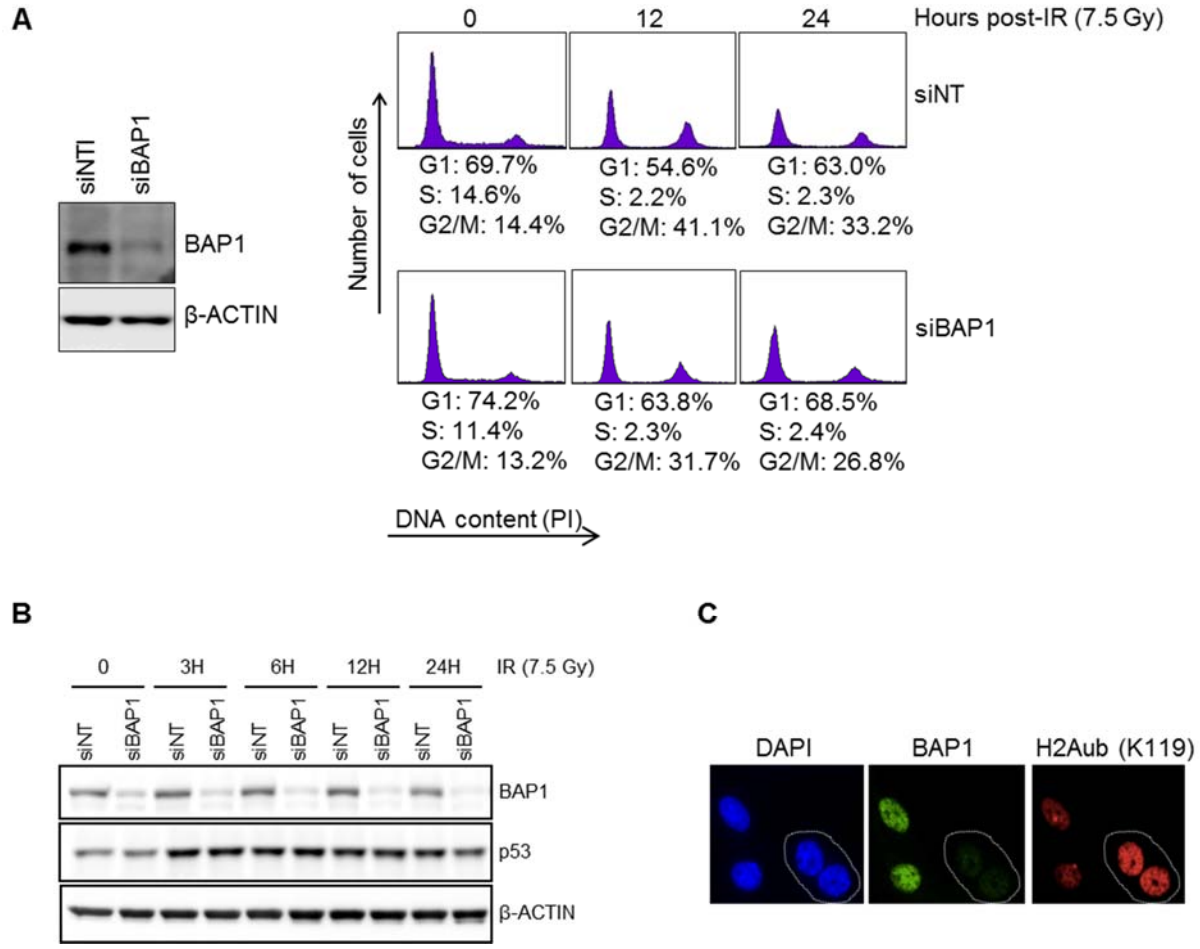

Figure S2. A) Depletion of BAP1 does not cause major defects in cell cycle. Human fibroblast LF1 cells were BAP1-depleted by siRNA and subjected for western blotting of the indicated proteins (left panel) and cell cycle profile analysis by flow cytometry using propidium iodide (right panel). Percentage of cell population at each cell cycle phase is shown. **B) Depletion of BAP1 does not induce stabilization of p53.** LF1 cells were BAP1-depleted using siRNA and treated with IR (7.5 Gy). Cells were collected at different time points following IR treatment and proteins were analyzed by western blot for the indicated proteins. **C) BAP1-depleted cells have increased H2A ubiquitination.** LF1 cells were treated with siControl (siNT) or siBAP1 and combined (1:1) before fixation and immunostaining of the indicated proteins. Representative images of the stainings are shown. BAP1-depleted cells were identified by decreased BAP1 signal and are encircled by white dashed lines.

Figure S2. A) Depletion of BAP1 does not cause major defects in cell cycle. Human fibroblast LF1 cells were BAP1-depleted by siRNA and subjected for western blotting of the indicated proteins (left panel) and cell cycle profile analysis by flow cytometry using propidium iodide (right panel). Percentage of cell population at each cell cycle phase is shown. **B) Depletion of BAP1 does not induce stabilization of p53.** LF1 cells were BAP1-depleted using siRNA and treated with IR (7.5 Gy). Cells were collected at different time points following IR treatment and proteins were analyzed by western blot for the indicated proteins. **C) BAP1-depleted cells have increased H2A ubiquitination.** LF1 cells were treated with siControl (siNT) or siBAP1 and combined (1:1) before fixation and immunostaining of the indicated proteins. Representative images of the stainings are shown. BAP1-depleted cells were identified by decreased BAP1 signal and are encircled by white dashed lines.

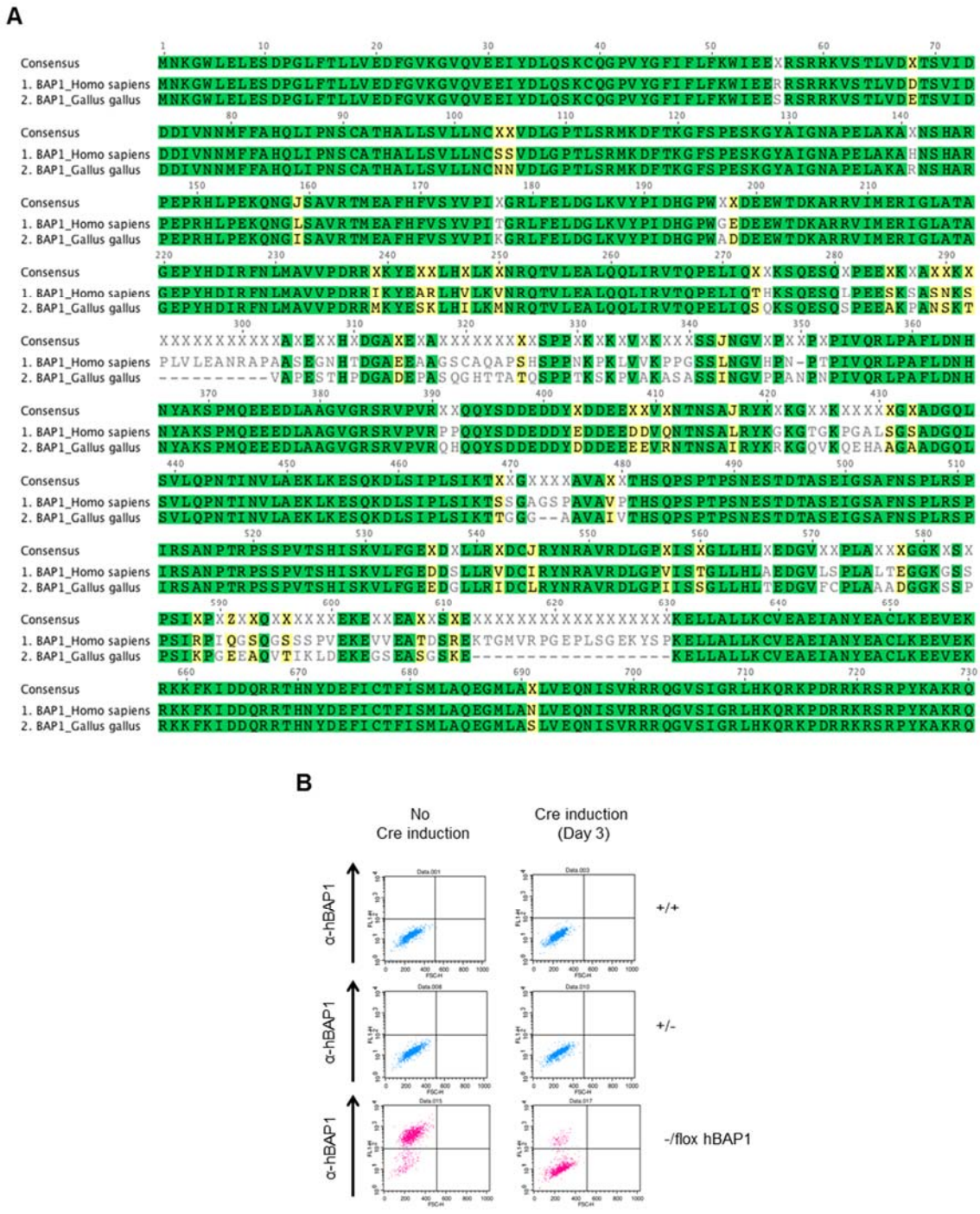

Figure S3. A) BAP1 is highly conserved between human and chicken. Alignment of Gallus gallus (NP_001025761.1) and Homo sapiens (NP_004647.1) BAP1 with ClustalW2 and visualized with Geneious software R6.1.4. Identical amino acids (a.a.) are highlighted in green, similar a.a. are highlighted in yellow and not similar a.a. are in gray. **B) Human BAP1 inserted in chicken bap1 locus can be excised by Cre induction.** Excision following 3 days of Cre induction was analyzed by flow cytometry using an anti-human BAP1 antibody.

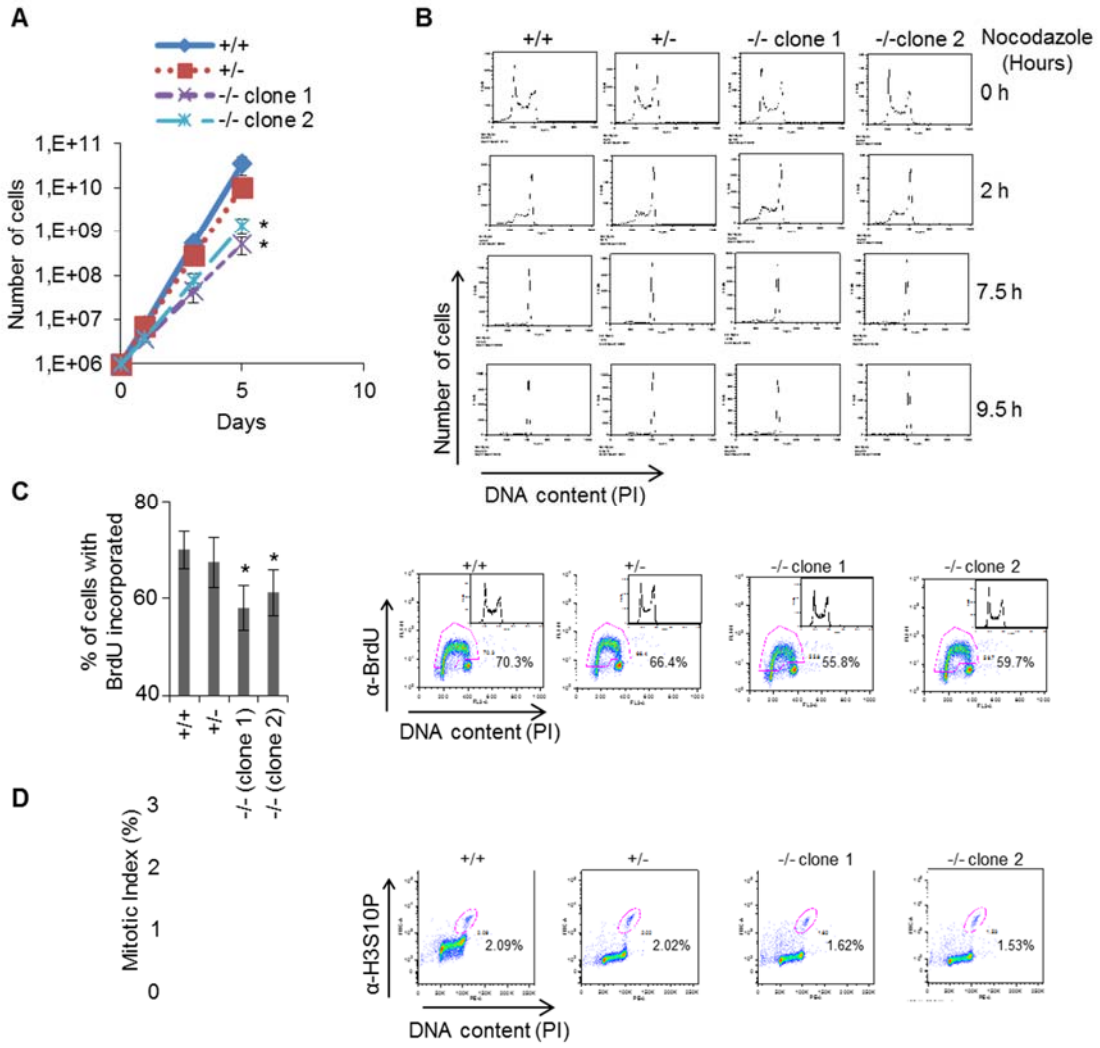

Figure S4. A) BAP1 KO cells proliferate at slower rates. Cells were seeded at the same number at day 0 and counted at days 1, 3 and 5. The experiment was repeated 3 times. Data are presented as mean ± SD. Statistical analysis was performed using Student's t-test, *P < 0.05. **B) BAP1 KO cells did not shown any major defect in G1 phase progression**. BAP1 KO DT40 cells were incubated with 200 ng/ml of nocodazole to arrest the cells in M phase. Different times after the addition of the drug, cells were fixed and subjected to cell cycle profile analysis by flow cytometry using propidium iodide. **C) BAP1 KO cells have a slightly decreased S phase population as revealed by BrdU incorporation.** Cells were incubated with BrdU for 30 min prior fixation and co-stained with anti-BrdU antibody and propidium iodide. Cell cycle profile and BrdU uptake were analyzed by flow cytometry. The experiment was repeated 3 times. Data are presented as mean of BrdU positive cells ± SD. Statistical analysis was performed using Student's t-test, *P < 0.05. Representative results of the experiment are shown on the right. **D) BAP1 KO cells have similar number of mitotic cells than BAP1 WT cells.** Asynchronous cells were fixed and co-stained with anti-phosphorylated H3S10 antibody and propidium iodide. Mitotic population was analyzed by flow cytometry . The experiment was performed 3 times. Data are presented as mean of phosphorylated H3S10 positive cells ± SD. Representative results of the experiment are shown on the right.

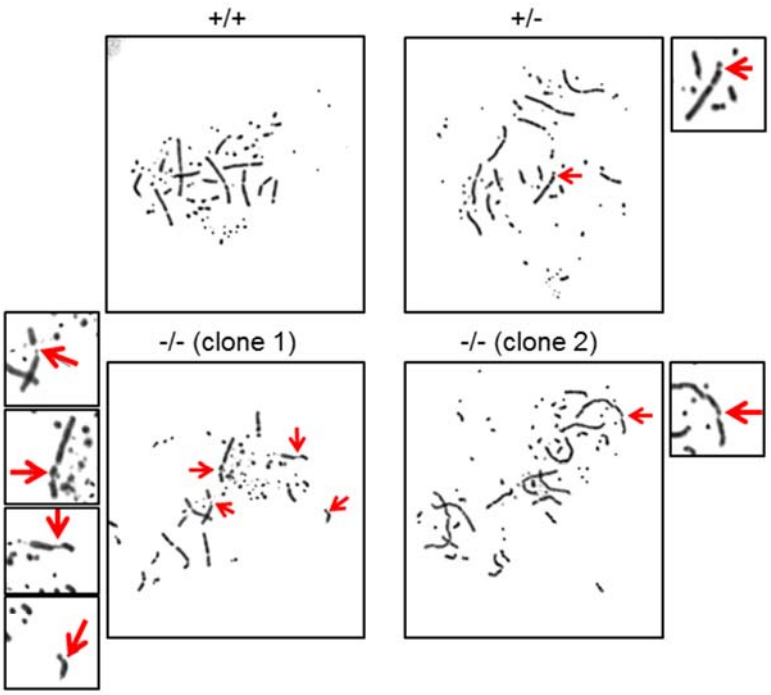

Genotype	Isochromatid		Chromatid		Radial figures	Total aberrations (per cell)	
	Breaks	Gaps	Breaks	Gaps		With chromatid gaps	Without chromatid gaps
+/+	(6) (0) (0)	(10) (10) (3)	(4) (9) (5)	(5) (3) (0)	(1) (0) (0)	(0.26) (0.22) (0.08)	(0.22) (0.19) (0.08)
+/-	(3) (5)	(11) (9)	(21) (38)	(8) (9)	(0) (0)	(0.43) (0.60)	(0.35) (0.51)
-/- (clone 1)	(1) (8)	(10) (26)	(25) (73)	(15) (6)	(0) (0)	(0.51) (1.15)	(0.35) (1.09)
-/- (clone 2)	(9) (2)	(21) (12)	(25) (24)	(11) (4)	(1) (0)	(0.68) (0.42)	(0.57) (0.38)

Figure S5. BAP1 KO DT40 cells have increased chromosome breaks following DNA damage. BAP1 KO DT40 cells were treated with 2 Gy of IR and fixed after 3.5 hours. Colcemid was added to the cells for 2 hours prior fixation to enrich mitotic cells. **A)** Representative images of metaphase spreads of each population are shown. Red arrows indicate chromosomal aberrations. **B)** At least two independent experiments were done and chromosome aberrations of 100 cells were counted in each experiment. Cumulative results of all experiments are shown in Figure 3E.

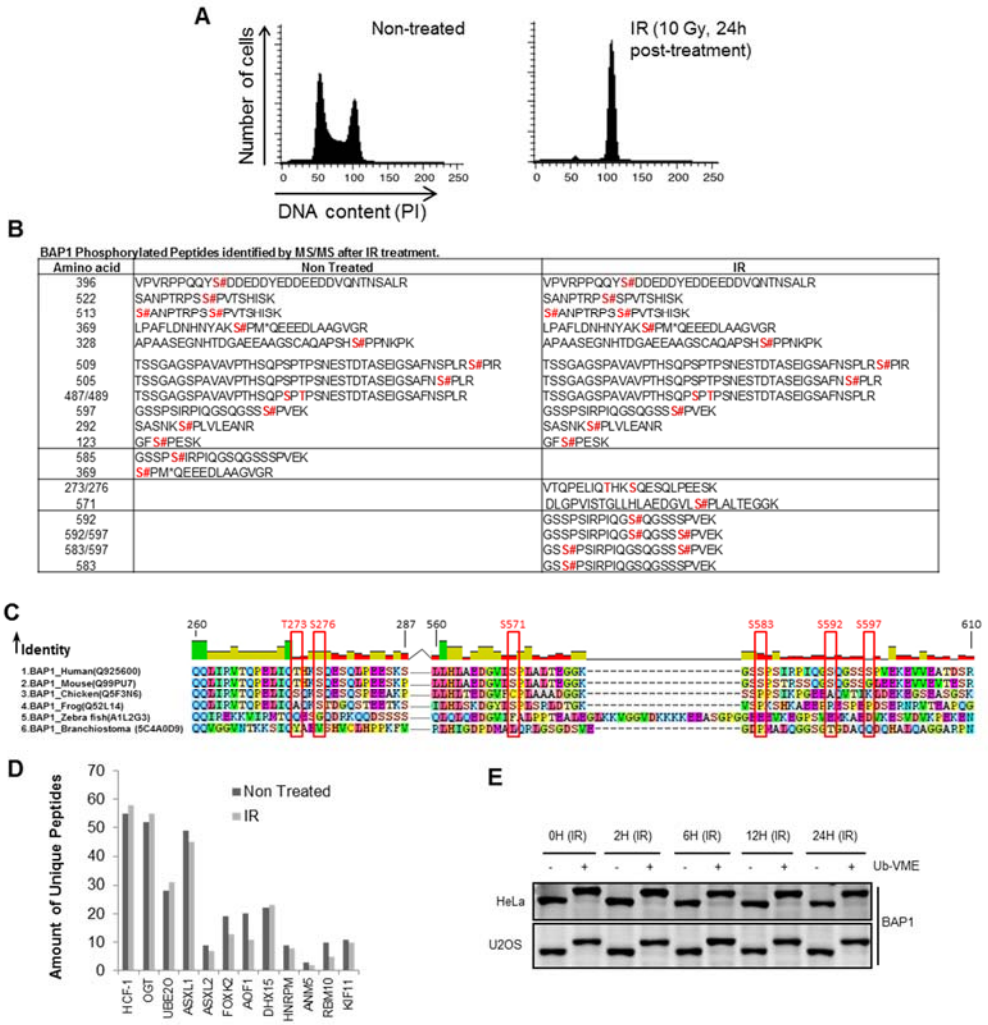

Figure S6. Phosphorylation of BAP1 following IR treatment. A) G2/M checkpoint was induced by IR treatment in the HeLa S3 cells used for BAP1 complexes purification. Cells were treated with IR (10 Gy) and fixed 24h post-treatment for cell cycle profile analysis by flow cytometry using propidium iodide. This assay was conducted to control for the efficiency of the IR treatment in our large scale complexes purification. **B) BAP1 is phosphorylated on specific residues following IR.** BAP1 phosphorylated peptide sequences identified by mass spectrometry are shown. Phospho-residues are colored in red and their position in BAP1 sequence are indicated. **C) Two BAP1 IR-specific phospho-sites are conserved**. Alignment of BAP1 amino acid sequence from different species using Geneious software R6.1.4. Accession numbers are shown. BAP1 IR-specific phospho-residues are squared in red. **D) IR treatment does not affect the assembly of major components of the BAP1 complexes**. Quantification of protein peptides by MS/MS revealed that the composition of the BAP1 core complex does not change following IR. E) BAP1 DUB activity is not affected by IR. DUB activity was revealed by Ubiquitin-VME (Ub-VME) probe labeling assay. IR-treated HeLa and U2OS total cell extracts were incubated with Ub-VME probe for 2 hours and analyzed by western blot using BAP1 antibody. The shifted-up BAP1 bands are indicative of probe labeling.

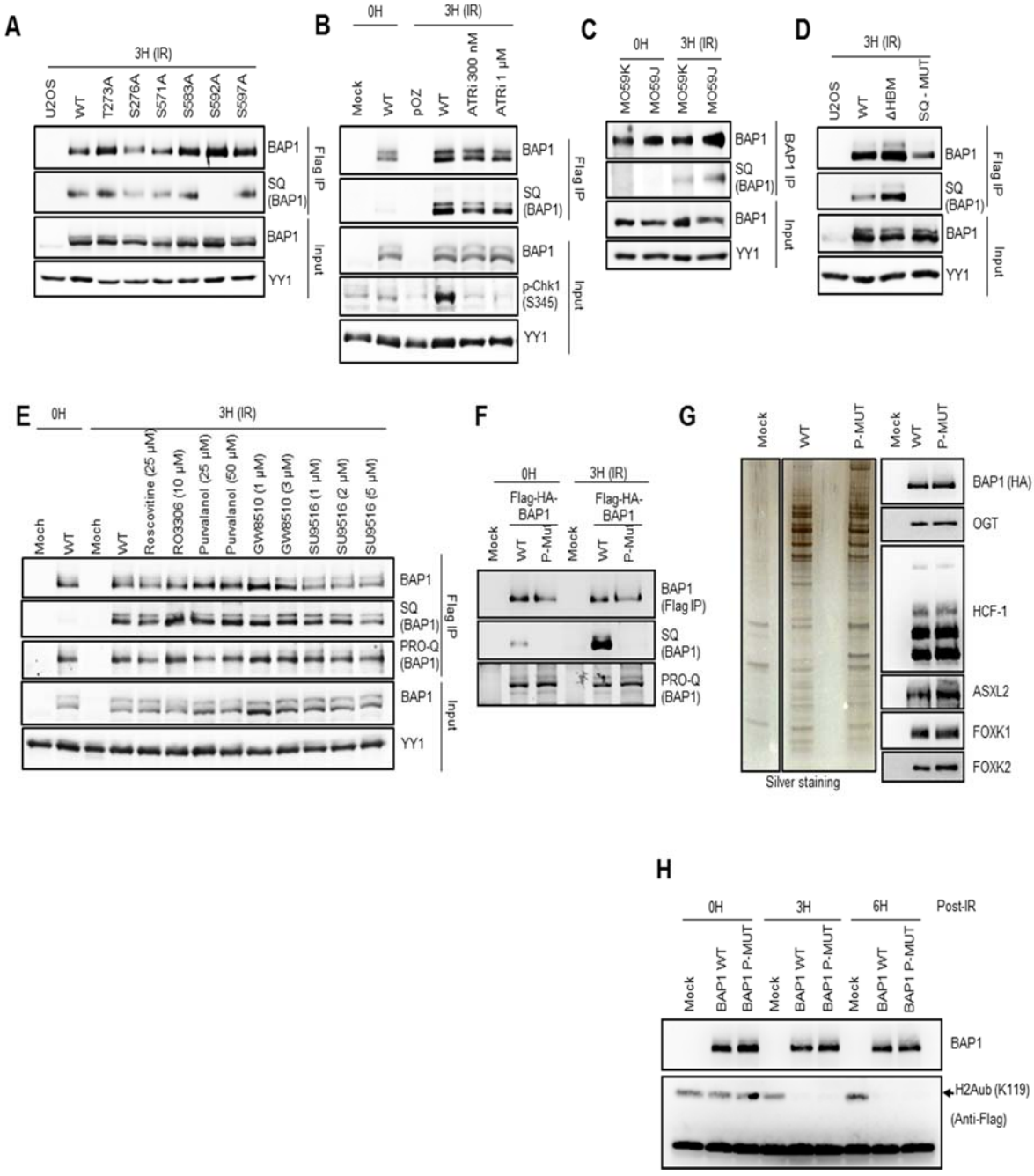
A
3H (IR)
U2OS
WT
T273A
S276A
S571A
S583A
S592A
S597A
BAP1
SQ (BAP1)
BAP1
YY1
Flag IP
Input
B
0H
3H (IR)
Mock
WT
pOZ
WT
ATRi 300 nM
ATRi 1 μM
BAP1
SQ (BAP1)
BAP1
p-Chk1 (S345)
YY1
Flag IP
Input
C
0H
3H (IR)
MO59K
MO59J
MO59K
MO59J
BAP1
SQ (BAP1)
BAP1
YY1
BAP1 IP
Input
D
3H (IR)
U2OS
WT
ΔHBM
SQ - MUT
BAP1
SQ (BAP1)
BAP1
YY1
Flag IP
Input
E
0H
3H (IR)
Moch
WT
Moch
WT
Roscovitine (25 μM)
RO3306 (10 μM)
Purvalanol (25 μM)
Purvalanol (50 μM)
GW8510 (1 μM)
GW8510 (3 μM)
SU9516 (1 μM)
SU9516 (2 μM)
SU9516 (5 μM)
BAP1
SQ (BAP1)
PRO-Q (BAP1)
BAP1
YY1
Flag IP
Input
F
0H
3H (IR)
Flag-HA-BAP1
Flag-HA-BAP1
Mock
WT
P-Mut
Mock
WT
P-Mut
BAP1 (Flag IP)
SQ (BAP1)
PRO-Q (BAP1)
G
Mock
WT
P-MUT
Mock
WT
P-MUT
BAP1 (HA)
OGT
HCF-1
ASXL2
FOXK1
FOXK2
Silver staining
H
0H
3H
6H
Post-IR
Mock
BAP1 WT
BAP1 P-MUT
Mock
BAP1 WT
BAP1 P-MUT
Mock
BAP1 WT
BAP1 P-MUT
BAP1
H2Aub (K119)
(Anti-Flag)

Figure S7. Characterization of BAP1 phosphorylation following DNA damage. A) Mutation of BAP1 phosphorylation sites. U2OS cells stably expressing Flag-HA-BAP1 mutants were treated with IR (7.5 Gy) for 3 hours and used for immunoprecipitation using anti-Flag beads. The samples were subjected to western blotting using an anti-pSQ. YY1 was used as a loading control. Note that mutation of the S276 site (also an SQ motif) does not decrease the signal detected with this anti-pSQ (compare the pSQ signal versus BAP1 signal in the immunoprecipitation). This antibody recognizes pS/TQ(G) found at the position 592 of BAP1. **B) The role of ATR in the phosphorylation of BAP1.** HeLa cells stably expressing Flag-HA-BAP1 were pretreated with the ATR inhibitor VE-821 for 1 hour and then with IR (7.5 Gy) for 3 hours and used for immunoprecipitation using anti-Flag beads. **C) DNA-PK is not required for the phosphorylation of BAP1.** Immunoprecipitation of BAP1 from DNA-PK-deficient and proficient cells, MO59J and MO59K, respectively before and after IR (7.5 Gy) treatment. **D) HCF-1 is not required for phosphorylation of BAP1**. U2OS cells stably expressing Flag-HA-BAP1 WT, ΔHBM or SQ-MUT were treated with IR (7.5 Gy) for 3 hours and used for immunoprecipitation of BAP1 using anti-Flag beads. **E) The inhibition of CDKs does not affect BAP1 phosphorylation.** HeLa cells stably expressing the empty vector or Flag-HA-BAP1 WT were pretreated with the indicated CDK inhibitors for 1 hour and then with IR (7.5 Gy) for 3 hours and used for immunoprecipitation using anti-Flag beads. The immunoprecipitated BAP1 samples were immunoblotted against anti-pSQ or stained with PRO-Q. **F) Characterization of BAP1 P-MUT following IR treatment.** HeLa cells stably expressing the empty vector, Flag-HA-BAP1 WT or P-MUT were treated with IR (7.5 Gy). Following immunoprecipitation using anti-Flag beads, the samples were subjected to immunoblotting using anti-SQ or stained with PRO-Q. **G) The BAP1 P-MUT does not lose interaction with the major partners of BAP1.** HeLa S3 cells stably expressing the empty vector, Flag-HA-BAP1 WT or P-MUT were subjected for immuno-purification using anti-Flag and anti-HA beads followed by silver staining. The major components of the BAP1 complexes were detected by western blot. **H) BAP1 P-MUT exhibits H2A DUB activity in vitro.** Flag-HA-BAP1 WT or P-MUT complexes were incubated with purified nucleosomes for the indicated time points. H2A deubiquitination was analysed by western blotting.

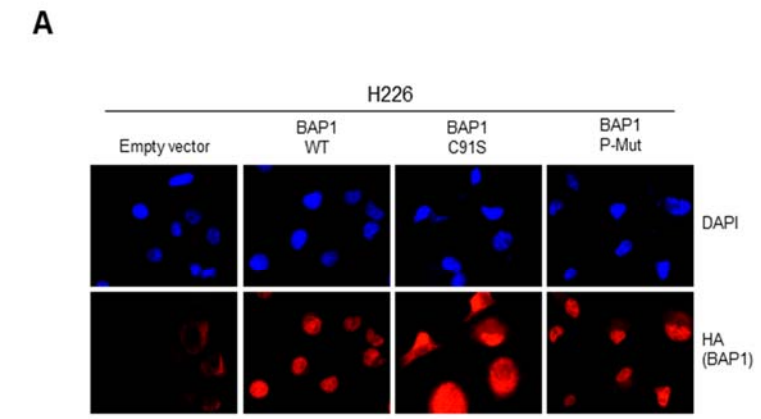

B

		%cells in Sub-G1
0H	Control	0.53
	WT	0.46
	C91S	0.25
	P-MUT	0.66
	SQ-MUT	1.83
	Delta HBM	1.41
	T273A	1.39
	S276A	3.43
	S592A	0.96
24H	Control	0.52
	WT	1.52
	C91S	0.7
	P-MUT	1.12
	SQ-MUT	2.1
	Delta HBM	0.57
	T273A	1.93
	S276A	3
	S592A	1.97
48H	Control	2.44
	WT	2.94
	C91S	3.3
	P-MUT	1.67
	SQ-MUT	2.48
	Delta HBM	2.9
	T273A	3.3
	S276A	4.65
	S592A	2.2

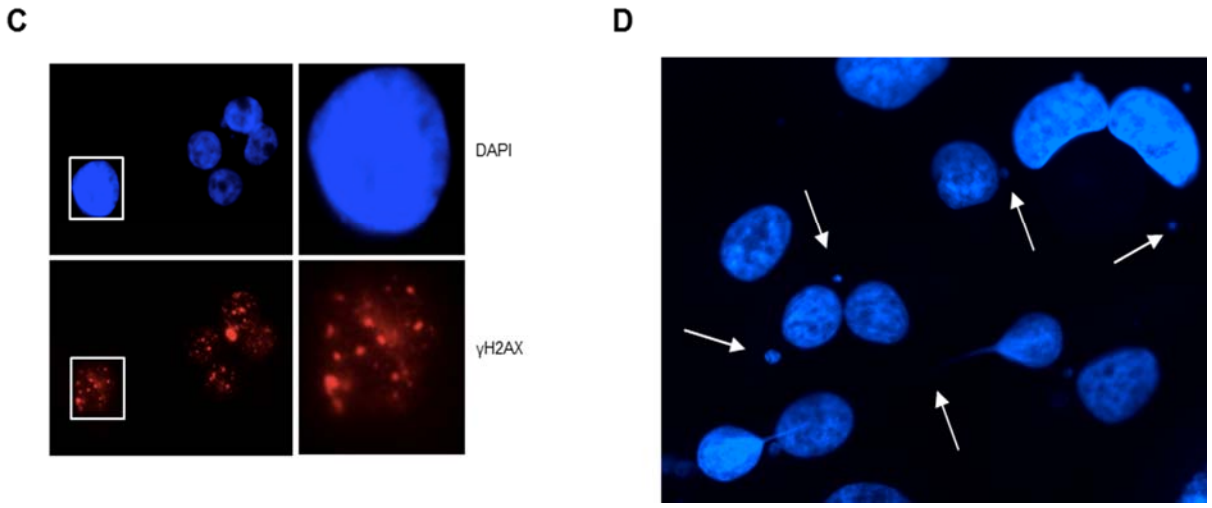

Figure S8. H226 BAP1-deficient cells reconstituted with BAP1 WT, catalytic inactive (C91S) or phospho-mutant (P-MUT). A) H226 cells stably expressing different Flag-HA-BAP1 mutants were fixed and stained with anti-HA antibody and DAPI. **B)** Cells were treated with IR (15 Gy) for the indicated time points and harvested for the analysis of apoptosis. The samples were fixed with ethanol, stained with propidium iodide and analyzed by flow cytometry for the sub G1 population**. C-D) H226 BAP1-deficient cells harbor intrinsic DNA damage foci and exhibit genomic instability. C)** H226 cells were immunostained for γH2AX and DNA was stained with DAPI. H226 cells showed constitutive γH2AX foci. **D)** Chromosome instability in H226 cells was visualized by DAPI-stained DNA. Presence of micronuclei and inter-nuclear bridges are indicated by the white arrows.

Supplemetal References

1. Arakawa H, Lodygin D, & Buerstedde JM (2001) Mutant loxP vectors for selectable marker recycle and conditional knock-outs. (Translated from eng) *BMC Biotechnol* 1:7 (in eng).
2. Yu H, *et al.* (2010) The Ubiquitin Carboxyl Hydrolase BAP1 Forms a Ternary Complex with YY1 and HCF-1 and is a Critical Regulator of Gene Expression. (Translated from Eng) *Mol Cell Biol* (in Eng).
3. Minsky N & Oren M (2004) The RING domain of Mdm2 mediates histone ubiquitylation and transcriptional repression. *Mol Cell* 16(4):631-639.
4. Sarkaria JN, *et al.* (1999) Inhibition of ATM and ATR kinase activities by the radiosensitizing agent, caffeine. *Cancer Res* 59(17):4375-4382.
5. Hickson I, *et al.* (2004) Identification and characterization of a novel and specific inhibitor of the ataxia-telangiectasia mutated kinase ATM. *Cancer Res* 64(24):9152-9159.
6. Charrier JD, *et al.* (2011) Discovery of potent and selective inhibitors of ataxia telangiectasia mutated and Rad3 related (ATR) protein kinase as potential anticancer agents. (Translated from eng) *J Med Chem* 54(7):2320-2330 (in eng).
7. Johnson N, *et al.* (2009) Cdk1 participates in BRCA1-dependent S phase checkpoint control in response to DNA damage. *Mol Cell* 35(3):327-339.
8. Meijer L, *et al.* (1997) Biochemical and cellular effects of roscovitine, a potent and selective inhibitor of the cyclin-dependent kinases cdc2, cdk2 and cdk5. (Translated from eng) *Eur J Biochem* 243(1-2):527-536 (in eng).
9. Villerbu N, Gaben AM, Redeuilh G, & Mester J (2002) Cellular effects of purvalanol A: a specific inhibitor of cyclin-dependent kinase activities. (Translated from eng) *Int J Cancer* 97(6):761-769 (in eng).
10. Johnson K, *et al.* (2005) Inhibition of neuronal apoptosis by the cyclin-dependent kinase inhibitor GW8510: identification of 3' substituted indolones as a scaffold for the development of neuroprotective drugs. (Translated from eng) *J Neurochem* 93(3):538-548 (in eng).
11. Lane ME, *et al.* (2001) A novel cdk2-selective inhibitor, SU9516, induces apoptosis in colon carcinoma cells. (Translated from eng) *Cancer Res* 61(16):6170-6177 (in eng).

12. Campo VA, *et al.* (2013) MSH6- or PMS2-deficiency causes re-replication in DT40 B cells, but it has little effect on immunoglobulin gene conversion or on repair of AID-generated uracils. (Translated from eng) *Nucleic acids research* 41(5):3032-3046 (in eng).
13. Affar EB, *et al.* (2006) Essential dosage-dependent functions of the transcription factor Yin Yang 1 in late embryonic development and cell cycle progression. *Mol. Cell Biol.* 26(9):3565-3581.
14. Rodrigue A, *et al.* (2006) Interplay between human DNA repair proteins at a unique double-strand break in vivo. (Translated from eng) *EMBO J* 25(1):222-231 (in eng).
15. Krietsch J, *et al.* (2012) PARP activation regulates the RNA-binding protein NONO in the DNA damage response to DNA double-strand breaks. (Translated from eng) *Nucleic acids research* 40(20):10287-10301 (in eng).
16. Daou S, *et al.* (2011) Crosstalk between O-GlcNAcylation and proteolytic cleavage regulates the host cell factor-1 maturation pathway. (Translated from eng) *Proc Natl Acad Sci U S A* 108(7):2747-2752 (in eng).
17. Nakatani Y & Ogryzko V (2003) Immunoaffinity purification of mammalian protein complexes. *Methods Enzymol* 370:430-444.
18. Borodovsky A, *et al.* (2002) Chemistry-based functional proteomics reveals novel members of the deubiquitinating enzyme family. *Chem Biol* 9(10):1149-1159.
19. Groisman R, *et al.* (2003) The ubiquitin ligase activity in the DDB2 and CSA complexes is differentially regulated by the COP9 signalosome in response to DNA damage. *Cell* 113(3):357-367.